PHYTOCHEMICAL AND PHARMACOLOGICAL INVESTIGATION OF FOUR TANZANIAN MEDICINAL PLANTS FOR ANTI-PROTOZOAL ACTIVITY

By

HAMISI MASANJA MALEBO

Dip. Ed (Sc.) Mkwawa, B.Sc.(Hons), M.Sc.(Dar es Salaam)

Reg. No: I84/7056/2003

Department of Chemistry

A THESIS SUBMITTED IN FULFILLMENT OF THE AWARD OF THE DEGREE OF DOCTOR OF PHILOSOPHY IN MEDICINAL PHYTOCHEMISTRY IN THE SCHOOL OF PURE AND APPLIED SCIENCES OF KENYATTA UNIVERSITY

S E P T E M B E R , 2 0 0 9

DECLARATION

AND

COPYRIGHT

Declaration by Candidate

I, **Hamisi Masanja Malebo** hereby declare that this thesis is my original work and, to my knowledge, has not been submitted for the award of any degree in another university.

Signature----------Date----------

Hamisi Masanja Malebo

Reg. No: I84/7056/2003

Department of Chemistry,

School of Pure and Applied Sciences,

Kenyatta University, Kenya.

Copyright

This thesis is a copyright material protected under the Berne Convention and other International and National Enactments, in that behalf, on intellectual property rights. No part of this thesis may be reproduced, stored in any retrieval system, or transmitted in any form or by any means, in full or in part, without written permission of the School of Graduate Studies, on behalf of both the author and Kenyatta University.

CERTIFICATION

Certification by Supervisors

We, the undersigned certify that the work reported in this thesis was carried out by the candidate under our supervision; and that we have read and hereby recommend for the award of PhD degree in Medicinal Phytochemistry of Kenyatta University.

Signature----------Date----------

Prof. Isaiah Omolo Ndiege

Department of Chemistry, Kenyatta University, Kenya.

Signature----------Date----------

Dr. Sauda Swaleh

Department of Chemistry, Kenyatta University, Kenya.

Signature----------Date----------

Prof. Ahmed Hassanali

Department of Chemistry, Kenyatta University, Kenya.

Signature----------Date----------

Prof. Dr. Matthias Hamburger

Institute of Pharmaceutical Biology, University of Basel, Switzerland.

Signature----------Date----------

Prof. Dr. Reto Brun

Swiss Tropical Institute, University of Basel, Switzerland.

D E D I C A T I O N

This thesis is dedicated to my parents: my mother Lemi Nzinza Mhangwa; my late father Michael Malaba Malebo, for their prayers, moral, academic and financial support in the formative years which set an effective background for building to this level; my dear wife Leah Malebo; and my son Samwel Masanja Malebo, for their understanding on the long absence from home and prayers which contributed to my success in completing the research and this thesis.

ACKNOWLEDGEMENTS

My sincere gratitude to my supervisors: Prof. Isaiah O. Ndiege, Dr. Sauda Swaleh, Prof. Ahmed Hasannali, Prof. Urs Séquin, Prof. Matthias Hamburger and Prof. Reto Brun for their thorough supervision, guidance and persistent support throughout the course, without which this work could not have been accomplished.

I would like to express my sincere gratitude to Dr. Petur Dalsgaad and Dr. Ollivier Potterat both of the Institute of Pharmaceutical Biology and Dr. Sigmund Gunzenhauser of the Institute of Organic Chemistry, both of the University of Basel in Switzerland, for the training and guidance they gave me on the use of MPLC, HPLC, LC-MS, HSCCC and Sepacore chromatographic machines. The University of Botswana through NABSA is thanked for running some ^{1}H and ^{13}C NMR spectral measurements reported in this thesis. The assistance of Dr. Klaus Kulicke, Dr. Daniel Haüssinger and Dr. Heinz Nadig of the Institute of Organic Chemistry, University of Basel, Switzerland in providing spectroscopic facilities which enabled the characterization of all compounds reported in this thesis is highly appreciated. Similarly the assistance of Mr. Marcel Kaiser, Dr. Sergio Wittilin, Ms. Nina Schild, Ms. Wenzler Tanja, Ms. Monica Cal and Mr. Michael Oberle all of the Parasite Chemotherapy Unit, Swiss Tropical Institute, Basel, Switzerland in providing training and guidance on anti-protozoal and cytotoxicity assays is acknowledged. Heartfelt acknowledgements go to Mr. Leonard B. Mwasumbi (Botanist, University of Dar es Salaam) and Mr. Simon Mathenge of the Herbarium in the Department of Botany, University of Nairobi for the identification and location of all plants which were investigated.

I appreciate the support of my fellow postgraduate students during the whole period of my research: in the Natural Products Research Laboratories: Dr. Jolivet Benoit and Dr. Martin Senn at the Institute of Organic Chemistry, University of Basel, Switzerland; Dr. Thobias Mohn and Dr. Nivan Moodley at the Institute of Pharmaceutical Biology, University of Basel, Switzerland; Dr. Maurice O. Omolo, Mr. Peter G. Kirira, Mr. Isaac Onyango, Mr. Fred Sawenja, Mr. Paul N. Maina, Mr. Erasto Mwangi, Ms. Ruth Omole and Dr. Margaret M. Ng'ang'a at the Department of Chemistry, Kenyatta University in Kenya; and at the STI: Dr. Valentine Pflueger, Dr. Lucy Ochola, Ms. Oyindamola Oduola-Abiodun, Dr. Naomi Maina, Dr. Kefas Mugittu, Dr. Joseph P. Mugasa, Dr. Dorothy Yeboah and Ms. Angela Dillip.

The German Academic Exchange Program (DAAD), Basel Stipend Commission, Swiss Tropical Institute (STI), Institute of Organic Chemistry (UNIBAS), Institute of Pharmaceutical Biology (UNIBAS), National Institute for Medical Research (NIMR) and the Department of Chemistry (KU) are gratefully acknowledged for financial and material support.

Special thanks go to my wife Mrs. Leah Malebo and my son Samwel Masanja Malebo for their understanding and prayers during the whole period of my study. I also extend my special heartfelt thanks to members of my family, especially my parents; my father Mr. Michael M. Malebo who died at a critical phase of my PhD program and my mother Mrs. Lemi M. Malebo. I thank my brothers and sisters, for their good wishes and prayers during my struggle to attain this level of learning.

Ultimately but not least, I would not have made to this level if it would not have been the hand and Will of God. I thank the almighty God for the gift of good health, strength, endurance and inquisitive mind.

TABLE OF CONTENTS

DECLARATION AND COPYRIGHT……..... **ii**
CERTIFICATION…….. **iii**
DEDICATION……. **iv**
ACKNOWLEDGEMENTS…… **v**
LIST OF TABLES……..... **x**
LIST OF FIGURES……. **xii**
LIST OF PLATES…… **xiii**
LIST OF SCHEMES…… **xiv**
LIST OF APPENDICES……. **xv**
ACRONYMS AND ABBREVIATIONS……..... **xviii**
ABSTRACT…….. **xix**
1
CHAPTER ONE: INTRODUCTION…….....
1.0 Malaria, leishmaniasis and trypanosomiasis……..... 1
1.1 Malaria……..... 1
1.2 Trypanosomiasis……..... 4
1.3 Leishmaniasis……..... 8
1.4 Medicinal plants: a foundation of modern medicine……..... 11
1.5 Natural products in drug discovery……..... 11
1.6 Natural products as potential sources of anti-parasitic agents……..... 13
1.6.1 Alkaloids……..... 13
1.6.2 Terpenes……..... 16
1.6.3 Flavonoids……..... 18
1.6.4 Xanthones……..... 20
1.6.5 Naphthoquinones…….. 20
1.6.6 Sulfur containing aliphatics…….. 21
1.7 Statement of the problems……..... 23
1.8 Hypothesis……..... 23
1.9 Research objectives……..... 23
1.9.1 General objective…… 23
1.9.2 Specific objectives…… 23
1.10 Justification…… 24

CHAPTER TWO: ANTI-PROTOZOAL CONSTITUENTS OF ANNONACEAE AND MALPIGHIACEAE…… **25**
2.1 Annonaceae…… 25
2.1.1 Description……..... 25
2.1.1.1 Alkaloids…… 25
2.1.1.2 Annonaceous acetogenins……. 26
2.1.1.3 Flavonoid……..... 27
2.1.1.4 Cyclohexane epoxides……..... 28
2.1.2 *Annickia kummeriae* (Engl. & Diels) Setten & Maas (Annonaceae)……..... 29
2.1.2.1 Botanical Description…… 29
2.1.2.2 Ethnomedical use……..... 30
2.1.2.3 Previous phytochemical and anti-protozoal reports……..... 30
2.2 Malpighiaceae……. 31

2.2.1 Description…….. 31
2.2.1.1 Flavonoids……... 31
2.2.1.2 Naphthoquinones……... 33
2.2.1.3 Triterpenes……..... 34
2.2.1.4 Alkaloids…… 34
2.2.2 *Acridocarpus chloropterus* Oliver (Malipighiaceae)…….. 35
2.2.2.1 Occurrence and botanical description…… 35
2.2.2.2 Ethnomedical use…….. 36
2.3 Bioassay-guided isolation…… 38

CHAPTER THREE: PHARMACOLOGICAL INVESTIGATION OF SELECTED TANZANIAN ANTI-PROTOZOAL PLANTS…….. 39
3.1 Crude plant extracts……..... 39
3.2 Anti-protozoal assays……. 39
3.2.1 Anti-plasmodial activity…….. 39
3.2.2 Anti-trypanosomal activity…….. 41
3.2.3 Anti-leishmanial activity…… 42
3.3 Cytotoxicity…… 43
3.3.1 Cytotoxicity activity (CC_{50})……. 43
3.3.2 Selectivity indices……..... 44
3.4 Selection of a bioactive crude extract for the isolation of anti-plasmodial compounds…….. 45

CHAPTER FOUR: IDENTIFICATION OF ANTI-PROTOZOAL CONSTITUENTS OF *ANNICKIA KUMMERIAE* (ENGL. & DIELS) SETTEN & MAAS…… 49
4.1 Isolation and identification……. 49
4.1.1 Lysicamine (**127**)……. 49
4.1.2 Trivalvone (**128**)……... 52
4.1.3 Annickine (**129**)……..... 57
4.1.4 Palmatine (**82**)……. 61
4.1.5 Jatrorrhizine (**83**)……. 66
4.1.6 Mixture of jatrorrhizine (**83**) and columbamine (**130**)……..... 70
4.1.7 Mixture of palmatine (**82**) and (–)-tetrahydropalmatine (**131**)…… 74
4.2 Anti-parasitic activity and cytotoxicity of compounds isolated from *Annickia kummeriae*…….. 79

CHAPTER FIVE: IDENTIFICATION OF ANTI-PROTOZOAL CONSTITUENTS OF *ACRIDOCARPUS CHLOROPTERUS* OLIVER……..... 83
5.1 Isolation and identification……. 83
5.1.1 β-Sitosterol (**132**)……. 83
5.1.2 Stigmasterol (**133**)……..... 87
5.1.3 Friedelin (**134**)…….. 91
5.1.4 Oleanolic acid (**124**)……..... 95
5.1.5 Ursolic acid (**123**)……. 100
5.1.6 Apigenin (4′, 5, 7-trihydroxyflavone) (**135**)…… 105
5.1.7 Luteolin (3′, 4′, 5, 7-tetrahydroxyflavone) (**136**)…… 107
5.1.8 Vitexin (8-glucopyranosyl-4′, 5, 7-trihydroxyflavone) (**137**)……..... 111

5.1.9 Kaempferol (3, 4′, 5, 7-tetrahydroxyflavone) (**138**)……..... 114
5.1.10 Quercetin (3, 3′, 4′, 5, 7-pentahydroxyflavone) (**139**)……..... 116
5.2 Antiparasitic activity and cytotoxicity of compounds from *Acridocarpus chloropterus*……..…… 120

CHAPTER SIX: EXPERIMENTAL……. 127
6.1 Reagents, equipment and materials……. 127
6.1.2.1 Solvent evaporation……... 127
6.1.2.2 Chromatography…… 127
6.1.3 Spectroscopy……. 129
6.1.4 Melting points……... 130
6.1.5 Bioassay equipment……..... 130
6.2 Plant material……... 133
6.2.1 Collection and identification…… 133
6.2.2 Extraction…… 134
6.3 Biological assays……. 134
6.3.1 Anti-plasmodial screening: *in vitro Plasmodium falciparum* assay…… 134
6.3.2 *In vitro* assay for African trypanosomes (Alamar blue assay)…… 136
6.3.3 *In vitro* leishmanicidal assay…… 137
6.3.4 Cytotoxicity assay…… 138
6.4 Isolation of compounds……... 139
6.4.1 Extraction and bioassay-guided isolation of compounds from *Annickia kummeriae*…… 139
6.4.2 Extraction and isolation of compounds from *Acridocarpus chloropterus*……. 142

CHAPTER SEVEN: CONCLUSION AND RECOMMENDATION……. 146
7.1 Conclusions……. 146
7.2 Recommendations……... 148
REFERENCES……. 149
APPENDICES…… 165
MANUSCRIPTS FOR PUBLICATION
Anti-plasmodial, anti-trypanosomal, anti-leishmanial and cytotoxicity activity of selected Tanzanian medicinal plants **286**
Antiplasmodial, antitrypanosomal and antileishmanial aporphine and protoberberine alkaloids from *Annickia kummeriae* (Engl. & Diels) Setten & Maas (Annonaceae) **298**

LIST OF TABLES

Table	Title	
1	Yields of solvent extracts of selected anti-protozoal plants……	39
2	Anti-plasmodial activity (IC_{50}) of extracts of selected Tanzanian medicinal plants……	39
3	Comparison of the anti-plasmodial activity (IC_{50}) of solvent extracts of Tanzanian medicinal plants with chloroquine and artemisinin……	40
4	Anti-trypanosomal activity (IC_{50}) of extracts of selected Tanzanian medicinal plants…	41
5	Comparison of anti-trypanosomal (IC_{50}) of extracts of selected Tanzanian medicinal plants with Melarsoprol……	41
6	Antileishmanial activity (IC_{50}) of extracts of selected Tanzanian medicinal plants……	42
7	Comparison of anti-leishmanial activity (IC_{50}) of extracts of selected Tanzanian medicinal plants with Miltefosine……	43
8	Cytotoxicity (CC_{50}) of extracts of selected Tanzanian medicinal plants……	43
9	Comparison of cytotoxicity (CC_{50}) of extracts of selected Tanzanian medicinal plants with podophyllotoxin……	44
10	Antiprotozoal activity, cytotoxicity and selectivity indices of extracts of selected Tanzanian medicinal plants……	44
11	Anti-plasmodial activity (IC_{50}) and cytotoxicity (CC_{50}) of HSCCC fractions of Annickia kummeriae methanolic leaf extract……	46
12	Anti-plasmodial activity (IC_{50}) and cytotoxicity (CC_{50}) of fractions AKLM 2 ……	47
13	1D and 2D ^{1}H NMR (600 MHz, CD_3OD) data of lysicamine (**127**)……	49
14	1D and 2D ^{13}C NMR (600 MHz, CD_3OD) data for lysicamine (**127**)……	50
15	1D and 2D ^{1}H NMR (500 MHz, $CDCl_3$) data for trivalvone (**128**)……	52
16	1D and 2D ^{13}C NMR (500 MHz, $CDCl_3$) data for trivalvone (**128**)……	53
17	1D and 2D ^{1}H NMR (600 MHz, $CDCl_3$) data for annickine (**129**)……	57
18	1D and 2D ^{13}C NMR (600 MHz, $CDCl_3$) data for annickine (**129**)……	58
19	1D and 2D 1H NMR (500 MHz, CD_3OD) data for palmatine (**82**)……	61
20	1D and 2D ^{13}C NMR (500 MHz, CD_3OD) data for palmatine (**82**)……	62
21	1D and 2D ^{1}H NMR (600 MHz, $CDCl_3$) data for jatrorrhizine (**83**)……	66
22	1D and 2D ^{13}C NMR (600 MHz, $CDCl_3$) data for jatrorrhizine (**83**)……	67
23	1D and 2D ^{1}H NMR (600 MHz, $CDCl_3$) data for columbamine (**130**)……	70
24	1D and 2D NMR data (600 MHz, $CDCl_3$) data for Columbamine (**130**)……	71
25	1D and 2D ^{1}H NMR (600 MHz, CD_3OD) for (–)-tetrahydropalmatine (**131**)……	74
26	1D and 2D ^{13}C NMR (600 MHz, CD_3OD) of (–)-tetrahydropalmatine (**131**)……	75
27	Anti-protozoal activity (IC_{50}) and cytotoxicity (CC_{50}) data for compounds isolated from *A. kummeriae* ……	79
28	Comparison of anti-protozoal activity (IC_{50}) and cytotoxicity (CC_{50}) of isolated compounds with standard drugs……	80
29	1D and 2D ^{1}H NMR and COSY (500 MHz, $CDCl_3$) for β-sitosterol (**132**)……	84
30	1D and 2D ^{13}C NMR (500 MHz, $CDCl_3$) data for β-sitosterol (**132**)……	86
31	1D and 2D ^{1}H NMR (500 MHz, $CDCl_3$) data for stigmasterol (**133**)……	89
32	1D and 2D NMR (500 MHz, $CDCl_3$) data for stigmasterol (**133**)……	90
33	1D and 2D 1H NMR (500 MHz, $CDCl_3$) data for friedelin (**134**)……	93
34	1D and 2D NMR (500 MHz, $CDCl_3$) data for stigmasterol (**133**)……	94
35	1D and 2D ^{1}H NMR (500 MHz, $CDCl_3$) data for oleanolic acid (**124**)……	97
36	1D and 2D ^{13}C NMR (500 MHz, $CDCl_3$) data for oleanolic acid (**124**)……	98
37	1D and 2D ^{1}H NMR (600 MHz, DMSO) data for ursolic acid (**123**)……	101
38	1D and 2D ^{13}C NMR (500 MHz, $CDCl_3$) data for ursolic acid (**123**)……	102
39	1D and 2D ^{1}H NMR (500 MHz, DMSO) data for apigenin (**135**)……	105
40	1D and 2D NMR (500 MHz, $CDCl_3$) data for apigenin (**135**)……	105
41	1D and 2D ^{1}H NMR (500 MHz, DMSO) data for luteolin (**136**)……	108
42	1D and 2D ^{13}C NMR (500 MHz, $CDCl_3$) data for luteolin (**136**)……	108
43	1D and 2D ^{1}H NMR (500 MHz, DMSO) data for vitexin. (**137**)……	111
44	1D and 2D NMR (500 MHz, $CDCl_3$) data for vitexin (**137**)……	112
45	1D and 2D ^{1}H NMR (500 MHz, DMSO) data for kaempferol (**138**)……	114
46	1D and 2D NMR (500 MHz, $CDCl_3$) data for kaempefrol (**138**)……	114

47 1D and 2D ^{1}H NMR (500 MHz, DMSO) data for quercetin (**139**)…….. 117
48 1D and 2D ^{13}C NMR (500 MHz, $CDCl_3$) data for quercetin (**139**)…… 117
49 Anti-protozoal activity (IC_{50}) and cytotoxicity (CC_{50}) data of compounds isolated from *Acridocarpus chloropterus*…… 120
50 Plant species collected from Tanga, Coast and Kagera regions in Tanzania…… 133

LIST OF FIGURES

Figure	Title	
1	Distribution of drug resistant malaria in the world……....	2
2	Distribution of human African trypanosomiasis……..	4
3	Distribution of chagas disease……..	6
4	Distribution of leishmaniasis……	9
5	Distribution of leishmaniasis/HIV co-infection……	9
6	Important 2D correlations for lysicamine (**127**)……...	51
7	Important COSY interactions for trivalvone (**128**)……..	54
8	Important HMBCs for trivalvone (**128**)……	54
9	Partial structure of trivalvone (**128**)…….	55
10	Partial structure of trivalvone (**128**)……..	55
11	Important COSYs and HMBCs of annickine (**129**)……..	59
12	MS fragmentation of annickine (**129**) …….	60
13	Important HMBCs for palmatine (**82**)……..	62
14	COSYs and NOESYs for palmatine (**82**)…….	62
15	Diagnostic MS fragments of palmatine (**82**)……	64
16	Important HMBCs for jatrorrhizine (**83**)……..	68
17	Important COSYs and NOESYs for jatrorrhizine (**83**)……	68
18	Important HMBCs for columbamine (**130**)……..	71
19	Important COSYs and NOESYs for columbamine (**130**)…….	72
20	Important HMBCs for (–)-tetrahydropalmatine (**131**)……	76
21	Important COSYs and NOESYs for (–)-tetrahydropalmatine (**131**)……	76
22	Structure-activity-relationships of palmatine (**82**) and jatrorrhizine (**83**)……	81
23	Comparison of anti-protozoal activity of palmatine (**82**), jatrorrhizine (**83**) and columbamine (**130**) plus jatrorrhizine (**83**) mixture……..	81
24	Comparison of anti-protozoal activity of palmatine (**82**) and (–)-tetrahydropalmatine (**131**) plus palmatine (**82**) mixture……	82
25	Important HMBCs for β-sitosterol (**132**)……..	85
26	Important MS fragmentations for β-sitosterol (**132**)…….	87
27	Important HMBCs for stigmasterol (**133**)……	88
28	Important MS fragmentations for stigmasterol (**133**)……..	91
29	Important HMBCs for friedelin (**134**)…… ….	92
30	Important MS fragmentations for friedelin (**134**)…….	95
31	Selected HMBCs of oleanolic acid (**124**)…….	97
32	Important MS fragmentations for oleanolic acid (**124**)……	99
33	Important HMBCs for ursolic acid (**123**)…….	103
34	Important NOESYs for ursolic acid (**123**)……	103
35	Important MS fragmentations for ursolic acid (**123**)……	104
36	Selected HMBCs and COSYs for apigenin (**135**)……	106
37	Diagnostic MS fragments for apigenin (**135**)……...	107
38	Selected HMBCs and COSYs for luteolin (**136**)……..	109
39	Diagnostic MS fragments for luteolin (**136**)…….	110
40	Selected HMBCs and COSYs for vitexin (**137**)……...	112
41	Diagnostic MS fragments for vitexin (**137**)……..	113
42	Selected HMBCs and COSYs for kaempefrol (**138**)……	115
43	Diagnostic MS fragments for kaempferol (**138**)……...	116
44	Selected HMBCs and COSYs for quercetin (**139**)……...	118
45	Diagnostic MS fragments for quercetin (**139**)……..	119
46	Structure-activity-relationship between β-sitosterol (**132**) and stigmasterol (**133**)……..	121
47	Structure-activity-relationship: friedelin (**134**), oleanolic acid (**124**) & ursolic acid (**123**)..	122
48	Structure-activity-relationship between apigenin (**135**) and related flavonoids……...	123

LIST OF PLATES

Plate	Title	
1	Photograph of *Annickia kummeriae* leaves……..	29
2	Photograph of *Acridocarpus chloropterus* Oliver leaves……	35
3	Photograph of medium pressure liquid chromatography Büchi B-680 system……	128
4	Photograph of preparative high speed counter-current chromatograph……...	129
5	Diagram of a biological safety cabinet…….	131
6	Photograph of biological safety cabinet……...	131
7	Photograph of Betaplate liquid scintillation counter……	132
8	Photograph of Spectramax micro-plate fluorometer……	133
9	Diagrammatic representation of a Costar™ 96-well micro-titre plate…….	135

LIST OF SCHEMES

Scheme

1 Isolation of anti-protozoal compounds from the leaves of *Annickia kummeriae* leaves……. 139
2 Isolation of antiprotozoal compounds from the stem bark of *Acridocarpus chloropterus*…….. 142

LIST OF APPENDICES

Appendix	Type of spectral data	
1a	^{1}H NMR spectrum of lysicamine (**127**)……	165
1b	HMQC spectrum of lysicamine (**127**)……	166
1c	COSY spectrum of lysicamine (**127**)……	167
1d	NOESY spectrum of lysicamine (**127**)……	168
1e	HMBC spectrum of lysicamine (**127**)……	169
1f	MS spectrum of lysicamine (**127**)……	170
2a	^{1}H NMR spectrum of trivalvone (**128**)……	171
2b	^{13}C NMR spectrum of trivalvone (**128**)……	172
2c	DEPT 135 spectrum of trivalvone (**128**)……	173
2d	HMQC spectrum of trivalvone (**128**)……	174
2e	COSY spectrum of trivalvone (**128**)……	175
2f	HMBC spectrum of trivalvone (**128**)……	176
2g	MS spectrum of trivalvone (**128**)……	177
3a	^{1}H NMR spectrum of annickine (**129**)……..	178
3b	HMQC spectrum of annickine (**129**)……	179
3c	NOESY spectrum of annickine (**129**)……	180
3d	COSY spectrum of annickine (**129**)……	181
3e	HMBC spectrum of annickine (**129**)……	182
3f	MS spectrum of annickine (**129**)……	183
4a	^{1}H NMR spectrum of palmatine (**82**)……	184
4b	^{13}C NMR spectrum of palmatine (**82**)……	185
4c	DEPT 135 spectrum of palmatine (**82**)……	186
4d	HMQC spectrum 1 of palmatine (**82**)……	187
4d	HMQC spectrum 2 of palmatine (**82**)……	188
4e	COSY spectrum of palmatine (**82**)……	189
4f	HMBC spectrum of palmatine (**82**)……	190
4g	IR spectrum of palmatine (**82**)……	191
4h	MS spectrum of palmatine (**82**)……	192
5a	^{1}H NMR spectrum of jatrorrhizine (**83**)……	193
5b	^{13}C NMR spectrum of jatrorrhizine (**83**)……..	194
5c	HMQC spectrum of jatrorrhizine (**83**)…….	195
5d	COSY spectrum of jatrorrhizine (**83**)……	196
5e	HMBC spectrum of jatrorrhizine (**83**)…….	197
5f	NOESY spectrum 1 of jatrorrhizine (**83**)…….	198
5f	NOESY spectrum 2 of jatrorrhizine (**83**)…….	199
5g	IR spectrum of jatrorrhizine (**83**)…….	200
5h	MS spectrum of jatrorrhizine (**83**)……	201
6a	^{1}H NMR spectrum of mixture of jatrorrhizine (**83**)/columbamine (**130**)……..	202
6b	HMQC spectrum of mixture of jatrorrhizine (**83**)/columbamine (**130**)…….	203
6c	COSY spectrum of mixture of jatrorrhizine (**83**)/columbamine (**130**)……..	204
6d	NOESY spectrum of mixture of jatrorrhizine (**83**)/columbamine (**130**)……	205
6e	HMBC spectrum of mixture of jatrorrhizine (**83**)/columbamine (**130**)…….	206
6f	MS spectrum of mixture of jatrorrhizine (**83**)/columbamine (**130**)……	207
7a	^{1}H NMR spectrum of mixture of palmatine (**82**)/(–)-tetrahydropalmatine (**131**)…	208
7b	HMQC spectrum of mixture of palmatine (**82**)/(–)-tetrahydropalmatine (**131**)…	209
7c	COSY spectrum of mixture of palmatine (**82**)/(–)-tetrahydropalmatine (**131**)……	210
7d	NOESY spectrum of mixture of palmatine (**82**)/(–)-tetrahydropalmatine (**131**)…	211
7e	HMBC spectrum of mixture of palmatine (**82**)/(–)-tetrahydropalmatine (**131**)…..	212
7f	MS spectrum of mixture of palmatine (**82**)/(–)-tetrahydropalmatine (**131**)……	213
8a	^{1}H NMR spectrum of β-sitosterol (**132**)……	214
8b	^{13}C NMR spectrum of β-sitosterol (**132**)…….	215
8c	DEPT 135 spectrum of β-sitosterol (**132**)……	216

8d	HMQC spectrum of β-sitosterol (**132**).....	217
8e	HMBC spectrum of β-sitosterol (**132**).....	218
8f	COSY spectrum of β-sitosterol (**132**).....	219
8g	MS spectrum of β-sitosterol (**132**).....	220
9a	^{1}H NMR spectrum of stigmasterol (**133**).....	221
9b	^{13}C NMR spectrum of stigmasterol (**133**).....	222
9c	DEPT 135 spectrum of stigmasterol (**133**).....	223
9d	HMQC spectrum of stigmasterol (**133**).....	224
9e	HMBC spectrum of stigmasterol (**133**).....	225
9f	COSY spectrum of stigmasterol (**133**).....	226
9g	MS spectrum of stigmasterol (**133**).....	227
10a	^{1}H NMR spectrum of friedelin (**134**).....	228
10b	^{13}C NMR spectrum of friedelin (**134**).....	229
10c	DEPT 135 spectrum of friedelin (**134**).....	230
10d	HMQC spectrum of friedelin (**134**).....	231
10e	HMBC spectrum of friedelin (**134**).....	232
10f	COSY spectrumof friedelin (**134**).....	233
10g	TOCSY spectrum of friedelin (**134**).....	234
10h	IR spectrum of friedelin (**134**).....	235
10i	MS spectrum of friedelin (**134**).....	236
11a	^{1}H NMR spectrum of oleanolic acid (**124**).....	237
11b	^{13}C NMR spectrum of oleanolic acid (**124**).....	238
11c	DEPT 135 spectrum of oleanolic acid (**124**).....	239
11d	HMQC spectrum of oleanolic acid (**124**).....	240
11e	HMBC spectrum of oleanolic acid (**124**).....	241
11f	COSY spectrum of oleanolic acid (**124**).....	242
11g	MS spectrum of oleanolic acid (**124**).....	243
12a	^{1}H NMR spectrum of ursolic acid (**123**).....	244
12b	^{13}C NMR spectrum of ursolic acid (**123**).....	245
12c	HMQC spectrum of ursolic acid (**123**).....	246
12d	HMBC spectrum of ursolic acid (**123**).....	247
12e	COSY spectrum of ursolic acid (**123**).....	248
12f	NOESY spectrum of ursolic acid (**123**).....	249
12g	MS spectrum of ursolic acid (**123**).....	250
13a	^{1}H NMR spectrum of apigenin (**135**).....	251
13b	^{13}C NMR spectrum of apigenin (**135**).....	252
13c	DEPT 135 spectrum of apigenin (**135**).....	253
13d	HMQC spectrum of apigenin (**135**).....	254
13e	HMBC spectrum of apigenin (**135**).....	255
13f	COSY spectrum of apigenin (**135**).....	256
13g	MS spectrum of apigenin (**135**).....	257
14a	^{1}H NMR spectrum of luteolin (**136**).....	258
14b	^{13}C NMR spectrum of luteolin (**136**).....	259
14c	DEPT 135 spectrum of luteolin (**136**).....	260
14d	HMQC spectrum of luteolin (**136**).....	261
14e	HMBC spectrum of luteolin (**136**).....	262
14f	COSY spectrum of luteolin (**136**).....	263
14g	MS spectrum of luteolin (**136**).....	264
15a	^{1}H NMR spectrum of vitexin (**137**).....	265
15b	^{13}C NMR spectrum of vitexin (**137**).....	266
15c	DEPT 135 spectrum of vitexin (**137**).....	267
15d	HMQC spectrum of vitexin (**137**).....	268
15e	HMBC spectrum of vitexin (**137**).....	269
15f	COSY spectrum of vitexin (**137**).....	270
15g	MS spectrum of vitexin (**137**).....	271
16a	^{1}H NMR spectrum of kaempferol (**138**).....	272

16b	^{13}C NMR spectrum of kaempferol (**138**)……	273
16c	DEPT 135 spectrum of kaempferol (**138**)……	274
16d	HMQC spectrum of kaempferol (**138**)…….	275
16e	HMBC spectrum of kaempferol (**138**)…….	276
16f	COSY spectrum of kaempferol (**138**)…….	277
16g	MS spectrum of kaempferol (**138**)……..	278
17a	^{1}H NMR spectrum of quercetin (**139**)…….	279
17b	^{13}C NMR spectrum of quercetin (**139**)……	280
17c	DEPT 135 spectrum of quercetin (**139**)……..	281
17d	HMQC spectrum of quercetin (**139**)……	282
17e	HMBC spectrum of quercetin (**139**)……	283
17f	COSY spectrum of quercetin (**139**)…….	284
17g	MS spectrum of quercetin (**139**)……..	285

ACRONMYS AND ABBREVIATIONS

AQ	Amodiaquine
CC	Column chromatography
DBE	Double bond equivalent
$CDCl_3$	Deuterated chloroform
CD_3OD	Deuterated methanol
CH_2Cl_2	Dichloromethane
$CHCl_3$	Chloroform
COSY	Correlation spectroscopy
^{13}C NMR	Carbon 13 nuclear magnetic resonance
^{1}H NMR	Proton nuclear magnetic resonance
CQ	Chloroquine
DEPT	Distortionless enhancement by polarization transfer
DMSO	Dimethyl sulphoxide
EC	Effective concentration
ED	Effective dose
EIMS	Electron impact mass spectra
EtOAc	Ethyl acetate
FABMS	Fast atomic bombardment mass spectra
HEPA	High efficiency particulate air
HEPES	*N*-2-hydroxyethylpiperazine-*N*-2-ethanesulfonic acid
HMBC	Heteronuclear multiple bond correlation
HMQC	Heteronuclear multiple quantum correlation
HPLC	High performance liquid chromatography
HSCCC	High speed counter-current chromatography
Hz	Hertz
IC	Inhibitory concentration
IR	Infrared
LD	Lethal dose
LREIMS	Low resolution electron impact mass spectra
MeOH	Methanol
MEM	Minimum essential media
MP	Melting point
MPLC	Medium pressure liquid chromatography
MQ	Mefloquine
MS	Mass spectroscopy
n-C_6H_{14}	Normal hexane
NMR	Nuclear magnetic resonance
NOESY	Nuclear over-hauser effect spectroscopy
PABA	*p*-aminobenzoic acid
PPM	Parts per million
PTLC	Preparative thin layer chromatography
RBC	Red blood cells
RPMI	Rosewell Park Memorial Institute
SI	Selectivity index
SiO_2	Silicon dioxide (Silica gel)
SP	Sulfadoxine-pyrimethamine
TI	Therapeutic index
TLC	Thin layer chromatography
TOCSY	Total correlation spectroscopy
WHO	World Health Organization

ABSTRACT

Protozoal diseases like malaria, trypanosomiasis and leishmaniasis, caused by *Plasmodium*, *Trypanosoma* and *Leishmania*, respectively, have overwhelming impact on public health in developing regions. Due to their prevalence, virulence and drug resistance, they are the most serious and widespread parasitic diseases encountered by mankind. The inadequate armory of drugs, high cost and lack of new drugs are the major limiting factors in the fight against the three diseases. Consequently, there is continuing need of research on the discovery and development of new effective and safe anti-protozoal drugs. In this work, solvent extracts from four Tanzanian medicinal plants: *Annickia kummeriae*, *Pseudospondias microcarpa*, *Drypetes natalensis* and *Acridocarpus chloropterus*, were tested for anti-protozoal activity. Anti-protozoal bioassays revealed 14 solvent extracts with strong to moderate *in vitro* anti-plasmodial activity (IC_{50} 0.12±0.01-5.50±0.27 μg/ml), 6 with moderate anti-trypanosomal activity (IC_{50} 2.3±0.43-5.40±0.64 μg/ml) and only 3 with mild anti-leishmanial activity (IC_{50} 9.25±0.54-9.79±2.5 μg/ml). *Annickia kummeriae*, *P. microcarpa* and *D. natalensis* solvent extracts exhibited good anti-plasmodial activity and favourable selectivity (SI 29.2-2,250). The strong anti-plasmodial, moderate anti-trypanosomal and mild anti-leishmanial activity of the methanolic extract of *A. kummeriae* leaves encouraged the isolation of anti-protozoal compounds. Bioassay-guided chromatographic fractionation led to isolation and identification of fractions with stronger anti-plasmodial activity and more favourable selectivity than the solvent extracts. Seven anti-protozoal alkaloids: palmatine (**82**), jatrorrhizine (**83**), lysicamine (**127**), trivalvone (**128**), annickine (**129**), columbamine (**130**) and (-)-tetrahydropalmatine (**131**), were identified by spectroscopic methods and subjected to *in vitro* anti-protozoal assays. The isolated alkaloids showed good selectivity and strong to moderate anti-plasmodial activity (IC_{50} 0.08±0.001-2.3±0.44 μg/ml), mild to weak anti-trypanosomal (IC_{50} 3.2±0.01-14.30±0.1 μg/ml) and anti-leishmanial activity (IC_{50} 2.7±0.1-20.4±0.1 μg/ml). Chromatography of *A. chloropterus* extract led to the isolation and identification of 5 triterpenes: β-sitosterol (**132**), stigmasterol (**133**), friedelin (**134**), oleanolic acid (**124**), ursolic acid (**123**); and 5 flavonoids: apigenin (**135**), luteolin (**136**), vitexin (**137**), kaempferol (**138**) and quercetin (**139**). Quercetin (**139**) exhibited moderate *in vitro* anti-plasmodial activity (IC_{50} 2.6±0.05 μg/ml) while the rest of compounds were inactive. Mild to weak *in vitro* anti-trypanosomal activity was observed in quercetin (**139**) (IC_{50} 3.60±0.1 μg/ml), ursolic acid (**123**) (IC_{50} 7.80±0.1 μg/ml) and apigenin (**135**) (IC_{50} 9.0±0.1 μg/ml). Good *in vitro* anti-leishmanial activity (IC_{50} 0.80±0.001, 2.10±0.1, 2.20±0.1, 5.90± 0.1 and 3.5±0.2 μg/ml) and favourable selectivity were observed with ursolic acid (**123**), quercetin (**139**), kaempferol (**138**), apigenin (**135**) and oleanolic acid (**124**), respectively. Chemical structure-biological activity relationship comparisons confirmed that, the methoxyl groups at C-2, C-3 (ring A) and C-9, C-10 (ring D) together with the quaternary nitrogen atom in position 7 are the structural moeties required for strong anti-plasmodial activity in protoberberine alkaloids. Structure-activity-relationship (SAR) comparisons in the isolated triterpenoids confirmed that, the hydroxyl group at C-3 with methyl groups at C-23, C-25, C-26 and C-30, C-12/C-13 double bond, the carboxylic acid group at C-28, and hydrogen at C-20 in the molecular framework of ursolic acid (**123**) are the structural moeties responsible for the strong anti-leishmanial activity whereas in the isolated flavonoids, the hydroxyl groups at C-3 and C-3′ in the apigenin (**135**) molecular framework are the structural moeties responsible for the strong anti-protozoal activity observed. The alkaloids with strong anti-plasmodial and moderate anti-trypanosomal activity may provide lead compounds for the development of drugs for malaria and trypanosomiasis. Similarly, the strong to moderate anti-leishmanial activity of the isolated triterpenes and flavonoids render them good candidates as molecular templates for new drug development.

CHAPTER ONE

INTRODUCTION

1.0 Malaria, leishmaniasis and trypanosomiasis

Protozoal diseases like malaria, trypanosomiasis and leishmaniasis caused by *Plasmodium*, *Trypanosoma* and *Leishmania*, respectively, are still a threat to mankind in the 21st century and have overwhelming impact on public health in developing regions (WHO, 2002). Due to their prevalence, virulence and drug resistance, they are the most serious and widespread parasitic diseases encountered by mankind. Lack of effective anti-protozoal vaccines, and the alarming decrease in effective anti-protozoal drugs due to the development of drug resistance, emphasizes the need for new prophylactic and therapeutic agents.

1.1 Malaria

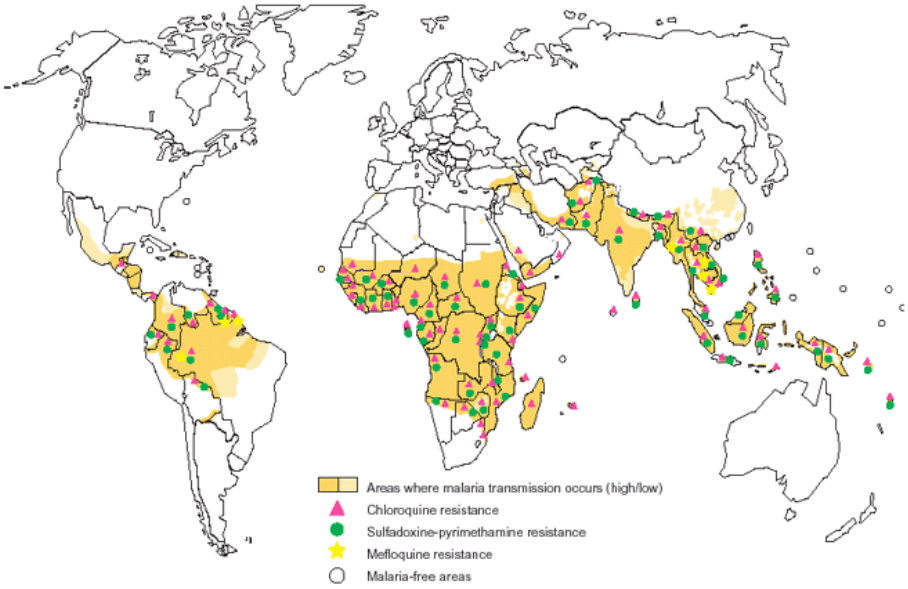
1.1.1 Malaria epidemiology

Malaria is caused by the parasites in the genus *Plasmodium* which are transmitted to humans through bites by female mosquitoes of the genus *Anopheles.* Of the four *Plasmodium* species (*falciparum, vivax, malariae* and *ovale*) that affect humans, *P. falciparum* causes the most severe and sometimes fatal malaria fevers, which accounts for about 90% of all cases and deaths world-wide (WHO, 2002).

Over 2.4 billion people in 102 countries (Fig. 1) live in areas where the disease is endemic and are at risk of being infected. Each year, there are about 500 million people who are afflicted and about 2.7 million people die from malaria (Olliaro & Cattani, 1996; WHO, 2002; WHO, 2005). Approximately 85% of global malaria cases and about 90% of the deaths occur in Africa, the majority being children under five and pregnant women (Olliaro & Cattani, 1996; WHO, 2002; WHO, 2005).

The current urban population explosion, the associated sociological and ecological changes have resulted in a complex epidemiological malaria situation in many African cities.

Figure 1: Distribution of drug resistant malaria in the world (WHO, 2005)



1.1.2 Malaria control strategies

Malaria control strategies are divided into two major groups depending as to whether targeting the vectors (*Anopheles* mosquitoes) or the parasite (*Plasmodium* species).

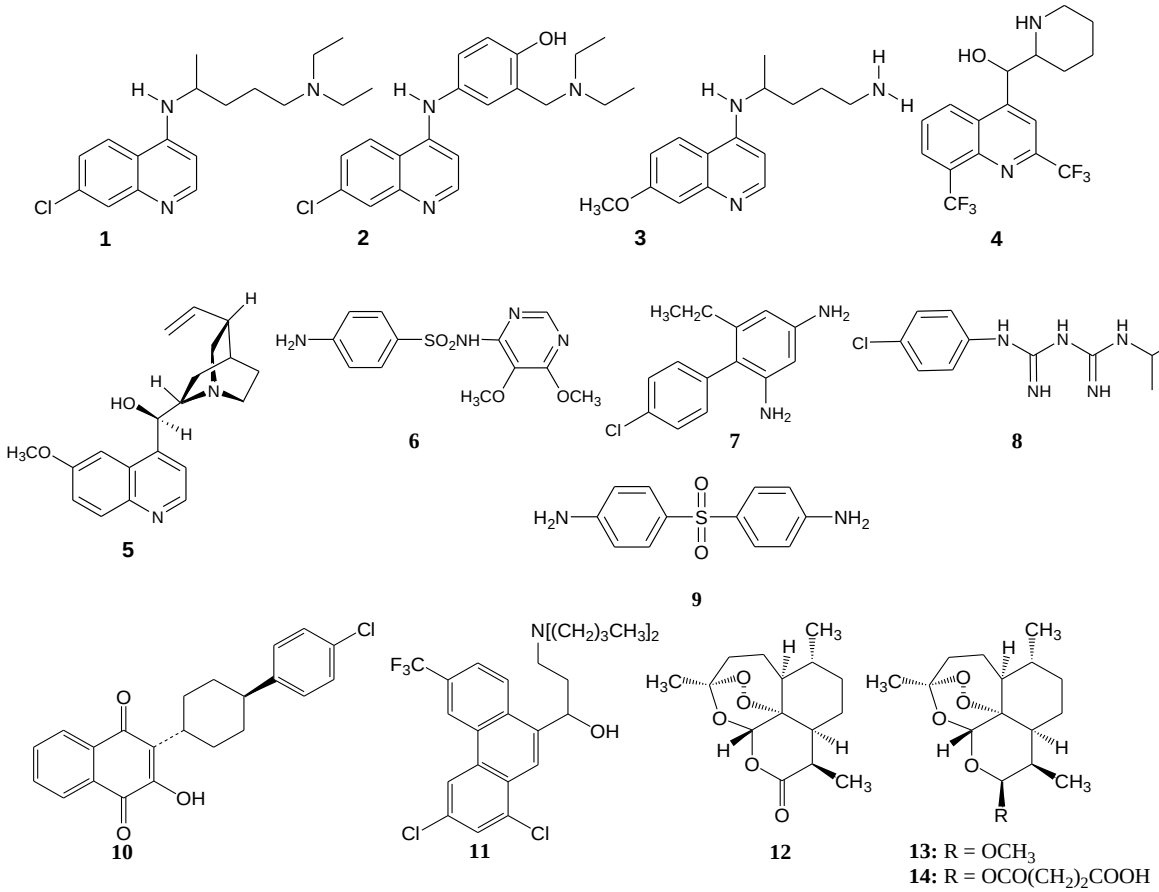
1.1.2.1 Malaria vector control

Malaria control strategy targeting the vector includes chemical as well as non-chemical control methods. Chemical control method includes the application of insecticides (Curtis, 1990; Marbiah *et al*., 1998), larvicides (WHO, 1996; Collins & Paskewitz, 1995), traps baited with semio-chemicals (attractants and pheromones), insecticides treated nets (ITNs), insect growth regulators (IGRs) (Katinka, 1999) and repellents (WHO, 1984; Trigg, 1996). Non-chemical control methods include environmental management (Githeko, 2000; Martens *et al*., 1997), biological control (Lu, 1996; Neri-Barbosa *et al*., 1997) and genetically modified mosquitoes (Cutkomp, 1967; Mshinda *et al*., 2004). Presently, vector control is thought of as one of the best approaches in the war against malaria, especially in the protection of human targets from infective mosquito bites, reduction of mosquito population density and possible elimination of the vector.

1.1.2.2 Malaria parasite control

Malaria control strategy targeting the parasite includes chemotherapy, chemo-prophylaxis and immuno-prophylaxis (vaccine). Prompt, appropriate and adequate chemotherapy is a potentially life saving measure in treating patients with falciparum malaria (WHO, 1986;

Howard, 1987; Kain, 1995). Chemo-prophylaxis when used helps pregnant women, infants and travelers from non-malarious areas against contracting the disease. Currently, there is no vaccine that offers adequate protection against malaria. Chemotherapy in malaria currently depends on seven key drugs and combinations: chloroquine (**1**), amodiaquine (**2**), primaquine (**3**), mefloquine (**4**), quinine (**5**), sulphadoxine (**6**), pyrimethamine (**7**), proguanil (**8**), dapsone (**9**), atovaquone (**10**), halofantrine (halfan) (**11**), artemisinin (**12**) and its derivatives; artemether (**13**) and sodium artesunate (**14**) (WHO, 1986; Wright & Phillipson, 1990; Kain, 1995).



The availability of these drugs considerably improved the treatment of malaria. Unfortunately, two decades ago *Plasmodium falciparum* malaria parasites were shown to have acquired resistance to some of the commonly used clinical anti-plasmodialdrugs such as chloroquine (Kain, 1995). The incidence of drug-resistant *P. falciparum* malaria has been increasing at a rate that exceeds new drug development. Thus, parasites have developed resistance rapidly even to the new synthetic anti-plasmodial drugs, including mefloquine (**4**), amodiaquine (**2**), sulphadoxine (**6**)-pyrimethamine (**7**) (SP) and halofantrine (**11**). The capacity of *P. falciparum* to develop resistance to anti-plasmodial drugs rapidly and the growing evidence that other species such as *Plasmodium vivax* and *Plasmodium malariae*

are also evolving resistance is sufficient reason for an urgent need to discover and develop alternative drugs to combat the disease (Howard, 1987; Kain, 1995). Such drugs should preferably have different modes of action from those of the existing ones. Given the inexorable spread of drug resistance, the search for effective, safe, and affordable drugs for resistant malaria is one of the most pressing health priorities worldwide.

1.2 Trypanosomiasis

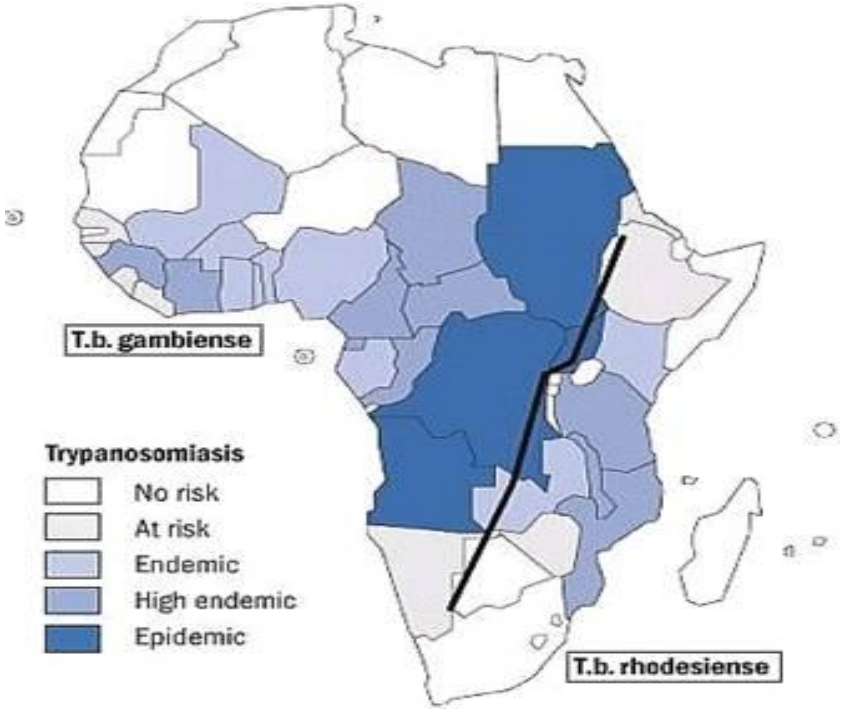
1.2.1 Epidemiology of human trypanosomiasis

Trypanosomiasis is caused by parasites in the genus *Trapanosoma.* It is a highly disabling, mostly severe and fatal disease. There are two forms of trypanosomiasis: the human African trypanosomiasis (HAT) and the American trypanosomiasis (Chagas' disease).

1.2.1.1 Human African trypanosomiasis (HAT)

One form of trypanosomiasis, the human African trypanosomiasis (HAT), also known as sleeping sickness, is found only in Africa (Fig. 2), where about 50,000 new cases are reported annually (Kuzoe, 1993; Molyneux *et al.,* 1996). Sleeping sickness is caused by *Trypanosoma brucei rhodensiense* in eastern Africa and *Trypanosoma brucei gambiense* in western Africa, with some overlaps between the two forms in central Africa.

Figure 2: Distribution of human African trypanosomiasis (HAT) (WHO, 1995)



HAT is transmitted by tsetse flies belonging to the genus *Glossina*. Both male and female tse-tse flies suck blood and can therefore transmit the disease. *Glossina* are responsible for cyclical transmission of the parasitic protozoan between numerous vertebrate hosts (Hoet *et al.,* 2004; Kuzoe, 1993; Molyneux *et al.,* 1996). Of the 31 species of tsetse flies in Africa, 11 are important for transmitting the trypanosomes to humans. Trypanosomes are extracellular organisms, both in the mammalian and insect host. *Trypanosoma brucei gambiense* and *T. b. rhodesiense* are morphologically indistinguishable, measuring 25-40 μm in length but have drastically different epidemiological features. There are two stages to sleeping sickness: the early stage responsible for the haemolymphatic infection and the late stage responsible for the central nervous system (CNS) infection. Infection in the human host begins when the infective stage (metacyclic stage) is injected into the host intra-dermally by an infected tsetse fly. The metacyclic stage rapidly transforms into blood-stage (trypomastigotes) which are long and slender forms that divide by binary fission in the interstitial spaces at the site of the bitten wound. The buildup of metabolic wastes and cell debris leads to the formation of a chancre.

Both forms of trypanosomiasis (sleeping sickness and nagana) affect the central nervous system. The development of late stage sleeping sickness takes decades to occur in West African sleeping sickness and a patient may only suffer from mild fatigue due to the occasional increases in parasite load in the blood. The term “sleeping sickness” is derived from the West African form of trypanosomiasis, primarily because invasion of the cerebrospinal fluid and brain after infection of the blood is often delayed, resulting in symptoms of extreme fatigue that can last for several years before the severe phase of the disease manifested as toxemia, coma and death sets in. In contrast, the typical East African sleeping sickness is far more virulent and can develop into late stage sleeping sickness within weeks and untreated patients can die within weeks or months of infection (Hoet *et al.,* 2004; Kuzoe, 1993; Molyneux *et al.,* 1996). Although symptoms and signs associated with nervous system involvement are varied for both East and West African sleeping sickness, advanced disease epileptic attacks, maniacal behavior, somnolence and coma are some typical late stage symptoms (Dumas & Bisser, 1999). Both treatment options and survival rates are drastically reduced once the trypanosomes infect the CNS (Molyneaux & Ashford, 1983).

The chancre, a tender swelling at the site of the bite, is usually the first symptom of the disease for *T. b. rhodensiense*. Within weeks, infected people start to experience irregular intermittent fevers associated with waves of parasitaemia that are characteristic of *T. b. rhodensiense* infections. For *T. b. gambiense*, lymphoadenopathy occurs more frequently. Oedema of the face is the frequent sign of infection (Molyneaux & Ashford, 1983; Dumas & Bisser, 1999). HAT is a major public health problem in sub-Saharan Africa where over 60 million people in 36 countries are at risk of becoming infected (Hoet *et al.*, 2004; Kuzoe, 1993; Molyneux *et al.*, 1996). It ranks among the top contenders for title of neglected human disease. The disease was largely controlled in the 1960s, but it re-emerged in the 1980s as demonstrated by the 36,000 cases reported in 1998 (Hoet *et al.*, 2004).

1.2.1.2 American trypanosomiasis (Chagas' disease)

The other form of human trypanosomiasis, the American trypanosomiasis (Chagas' disease) occurs mainly in Latin America (Fig. 3), where about 20 million people are infected annually and more than 100 million people are at risk (Marsden, 1996; WHO, 1997). Chagas' disease is caused by *Trypanosoma cruzi*, which is transmitted by reduviid bugs (*Rhodnius* spp. and *Triatoma* spp). The disease is zoonotic and afflicts a large variety of small mammals. Human infection occurs when the reduviid bugs invade human dwellings. The disease can be fatal due to cardiac and nervous complications (Marsden, 1996).

Figure 3: Distribution of Chagas disease
(http://pathmicro.med.sc.edu/parasitology/chagmap1.jpg)



1.2.1.3 Trypanosomiasis control strategies

Trypanosomiasis control strategies are divided into two major methods depending as to whether they are targeting the vectors or the parasites.

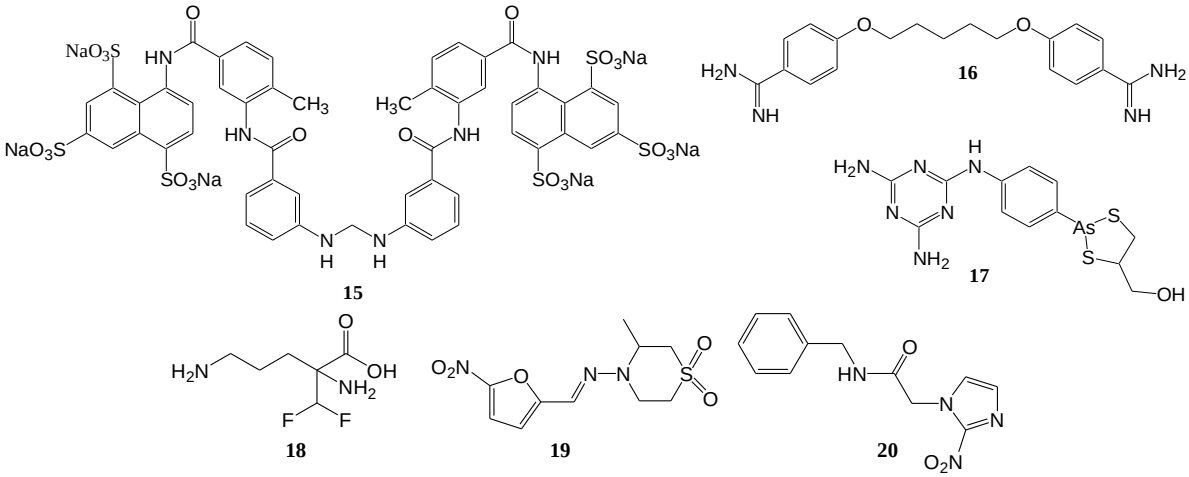
1.2.1.3.1 Trypanosomiasis vector control

Trypanosomiasis control strategy targeting the vector includes both chemical and non-chemical control methods. A wide range of techniques targeting tsetse flies are available (WHO, 1984; Maudlin *et al*., 2004). Insecticides spraying from the ground applied targeting known fly resting sites or at ultra-low volume from the air, are effective in killing all flies initially present and thereafter to kill each generation of newly emerging flies. It is useful against epidemic outbreaks of sleeping sickness, where a rapid cessation in contact between humans and tsetse flies is needed. Tsetse flies are also controlled by using traps and targets. Targets are combinations of cloth and netting baited with an odour attractant and impregnated with a pyrethroid insecticide (Kuzoe & Schofield, 2005). The sterile insect technique involving mass release of sterilized male tsetse flies, which compete with local males to mate with females. Because female tsetse flies generally mate only once, the result is infertile offspring and a decline of the wild tsetse population. A combination of insecticide spraying and trap deployment followed by the sterile insect technique has been successfully used to eliminate *Glossina austeni* from Zanzibar in Tanzania (Vreysen *et al*., 2000).

Even though available techniques to control tsetse flies are highly effective (WHO, 1984; Maudlin *et al*., 2004), all are constrained by the difficulties of applying them on a large enough scale for long enough to achieve sustainable results. Insecticide spraying is efficient but is difficult to sustain because of logistical constraints and high costs. Targets and traps are effective, but their deployment is difficult to sustain for long periods, and implementation through community participation requires constant motivation and supervision to remain effective (WHO, 1984; Maudlin *et al*., 2004). The sterile insect technique is expensive, because it requires large-scale rearing of flies, and it is only recommended for use once the wild tsetse population has been suppressed to low levels using other techniques (Vreysen *et al*., 2000).

1.2.1.3.2 Trypanosomiasis parasite control

Trypanosomiasis control strategy targeting the parasite is mainly through chemotherapy. Prompt, appropriate and adequate chemotherapy is a potentially life saving measure in treating patients suffering from trypanosomiasis. Currently, there is no effective vaccine for protecting humans from trypanosomiasis. The treatment of African trypanosomiasis is based on suramin (**15**), pentamidine (**16**), melarsoprol (**17**) and eflornithine (difluoromethylornithine, DFMO) (**18**) (Kuzoe, 1993; Molyneux *et al.*, 1996; WHO, 1997). The use of these drugs is limited by their marginal efficacy, severe toxicity and the emerging drug resistance (Kuzoe, 1993; WHO, 1997; Hoet *et al.*, 2004). Consequently, newer, safer and more effective drugs are needed. Chemotherapy of American trypanosomiasis is based on two main drugs, nifurtimox (**19**) and benznidazole (**20**) (Marsden, 1996; WHO, 1997). However, there is a controversy over the ability of these drugs to completely cure patients with chronic infections. The long treatment period (60-120 days respectively) provoke adverse reactions in most patients (Marsden, 1996; WHO, 1997).



1.3 Leishmaniasis

1.3.1 Epidemiology of leishmaniasis

Leishmaniasis is caused by obligate intracellular parasites of mononuclear phagocytes of the genus *Leishmania* which are transmitted to humans through bites by sand flies in the genus *Phlebotomous* in the Old World and *Lutzomyia* in the New World (Fig. 4) (Bodley *et al.*, 1995b; Bryceson, 1996; Ho *et al.*, 1994; WHO, 1994; Breman, 1997; Chan-Bacab & Peña Rodríguez, 2001; WHO, 2001). The disease has a wide spectrum of clinical manifestations including cutaneous, mucosal and visceral forms, ranging from destructive and disfiguring sores to *Kala azar*, which destroys internal organs (Bodley *et al.*, 1995b; Bryceson, 1996). Leishmaniasis afflicts large areas of Africa, Asia, Mediterranean and Latin

America (Ho *et al.,* 1994; Bodley *et al.,* 1995b; Bryceson, 1996; Herwaldt, 1999). According to WHO, there are 2 million new cases of leishmaniasis each year (WHO, 1994; Herwaldt, 1999; Chan-Bacab & Peña-Rodríguez, 2001; Croft & Coombs, 2003). With the advent of HIV/AIDS, which currently afflicts more than 30 million people in geographical locations largely overlapping with leishmaniasis (Fig. 5), the nature of the disease has changed considerably, and visceral leishmaniasis is now considered a genuine AIDS-related opportunistic infection largely due to reactivation of latent infections by immunosuppression (Alvar *et al.,* 1997).

Figure 4: Distribution of leishmaniasis
(http://www.wehi.edu.au/media/images/handman/world_map.jpg)

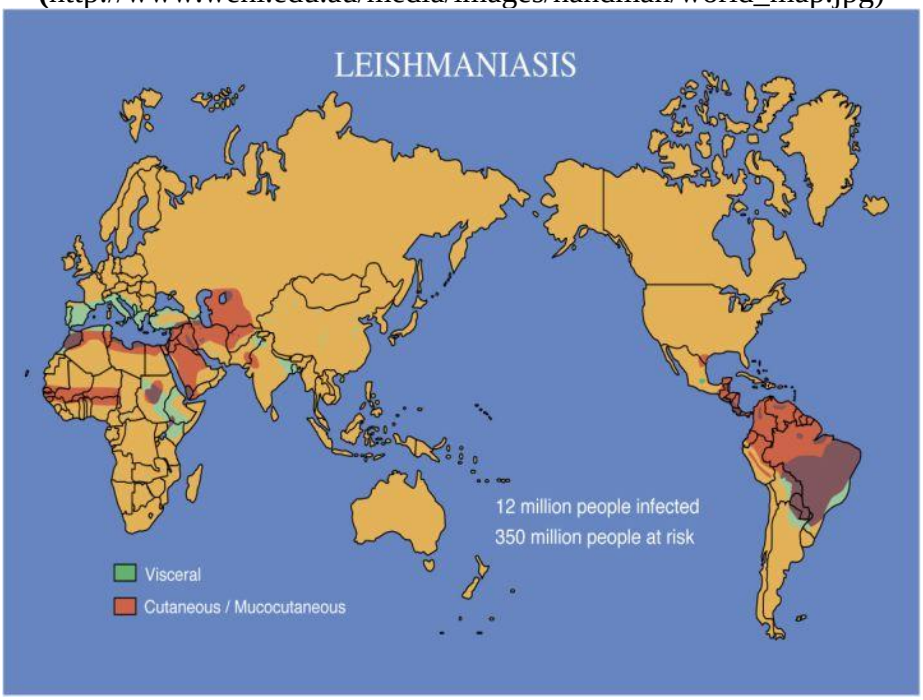
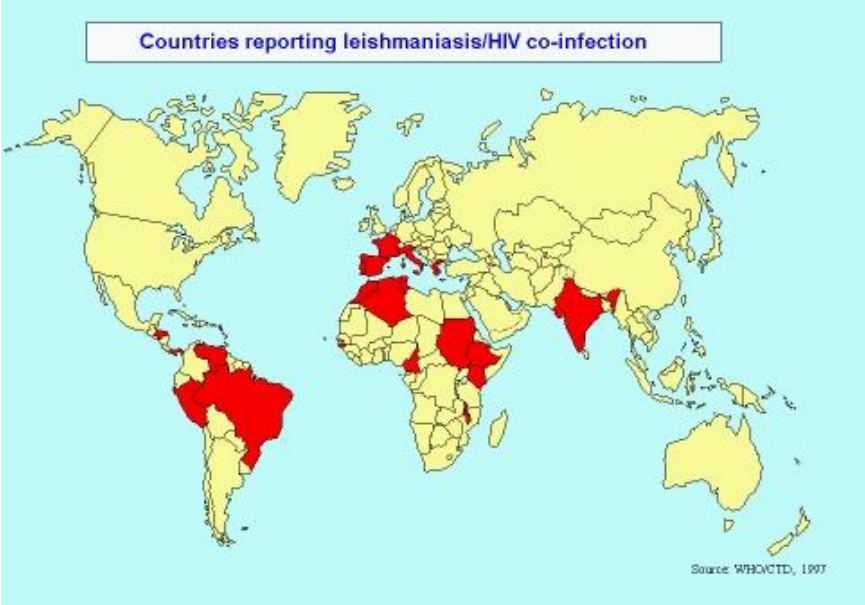


Figure 5: Distribution of leishmaniasis/HIV co-infection
(http://www.mpibpc.mpg.de/groups/eibl/pressrelease/leismap3.jpg)



1.3.2 Leishmaniasis control strategies

Leishmaniasis control is based primarily on diagnosis and treatment of cases coupled with vector control, and in some zoonotic foci, control of animal reservoirs (Desjeux, 1996). Currently, there is no any vaccine proved to be effective in preventing humans from leishmaniasis infection.

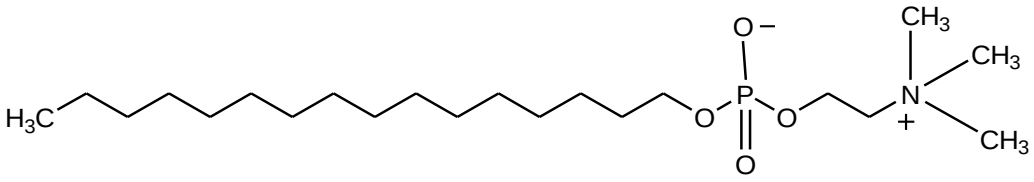
1.3.2.1 Leishmaniasis vector control

Control of domestic and peri-domestic sand-fly vectors is done through indoor residual spraying using pyrethroid insecticides and insecticide-treated nets (Alten *et al*., 2003). In areas where dogs are among the main reservoir hosts, increased use of insecticide-treated dog collars reduces the likelihood of new infections in dogs, and the risk of transmission from dogs to humans. Rodent reservoirs are controlled by using poisoned bait and environmental management, including physical destruction of rodent burrows (Mazloumi *et al*., 2002).

1.3.2.2 Leishmaniasis parasite control

Leishmaniasis treatment failures as a result of antimonial resistance are increasing. Pentamidine (**16**) is used for the treatment of antimonial resistant leishmaniasis though limited in clinical application due to the adverse and toxic side effects (Howard, 1987; Wright & Phillipson, 1990; Ho, 1994; Herwaldt, 1999; Croft & Coombs, 2003). Consequently, there is an urgent need to develop safe and effective anti-leishmanial drugs.

Miltefosine (hexadecylphosphocholine) (**21**) a synthetic alkylphosphocholine analogue that failed clinically as an anti-neoplastic drug, is active against visceral leishmaniasis. Although the biochemical mechanism remains unclear, miltefosine has good efficacy against leishmania *in vitro* when orally administered in animals (Croft *et al.,* 1987; Kuhlencord *et al.,* 1992; Lux *et al.,* 2000; Croft & Coombs, 2003). Clinical trials carried out have confirmed miltefosine (**21**) to be the first effective oral drug for leishmaniasis, as demonstrated by 97% cure rate (29 of 30 patients) with 100 mg/day miltefosine (2.5 mg/kg/day) for 28 days (Sundar *et al.,* 2002). Miltefosine (**21**) has negligible side effects, does not require refrigeration for storage, and has been used successfully to treat antimonial resistant leishmaniasis (Sundar *et al.,* 2002; Croft & Coombs, 2003). Since the drug can be administered orally, it has the potential for use as simple, affordable and effective public health tool at the community level and even during epidemics.



21

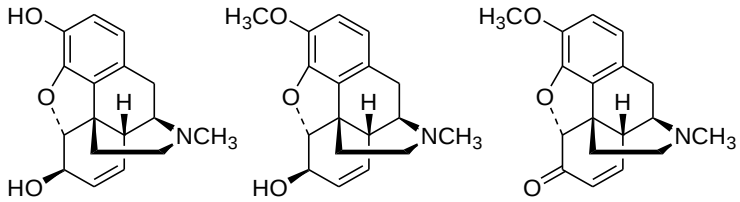
1.4 Medicinal plants: a foundation of modern medicine

Plants have been the major source of medicines for thousands of years. Research in natural products from higher plants represents a major strategy for the discovery and development of new drugs. Historically, natural products from plants and micro-organisms have been the most promising sources of drugs, and they have continued to avail new drugs. Between 1981 and 2002 natural products and derived medicines comprised 61% of all the new drugs launched into the market of which 24% were synthetic or natural mimic compounds, discovered by structure-activity-relationship (SAR) studies (Kinghorn, 1994; Newman *et al*., 2000; Newman *et al*., 2003; Butler, 2004; Balunas & Kinghorn, 2005). About 61% of all the anti-cancer drugs approved by the Food and Drug Administration in the United States of America between 1983 and 1994 were natural products or their derivatives (Cragg *et al*., 1997). A recent review of medicines that are used against human ailments revealed that natural products and related drugs are used for the treatment of 87% (48/55) of all ailments including bacterial, cancer, coagulant, parasitic and viral diseases, among others (Newman *et al.,* 2003). This account strongly suggests that natural products are potential sources of new medicines and lead compounds for drug development.

1.5 Natural products in drug discovery

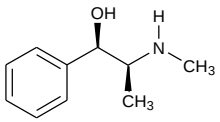
Historical experiences with natural products from traditional medicinal plants as therapeutic tools enabled the introduction of single chemical entities in modern medicine (Kitua & Malebo, 2004). Plants, especially those with ethno-pharmacological uses, have been the primary sources of medicines for drug discovery. Life saving and essential drugs from medicinal plants were introduced into modern therapeutics several centuries ago (Kitua & Malebo, 2004).

Although morphine (**22**) was not isolated until 1806 and commercially manufactured 20 years later, the use of opium poppy (*Papaver somniferum*) as a drug dates back many centuries to the time when monks observerd the anaesthetic and pain-relieving properties (Grabley & Thiericke, 1999). Opium poppy, one of the oldest medicinal plants in recorded history, is the source of many analgesic drugs [morphine (**22**), codeine (**23**) and hydrocodone (**24**)] used for pain and cough relief (Sneader, 1985; Benyhe, 1994; Foye *et al*., 1995). Currently, there are numerous cough remedies in clinical use that contain morphine (**22**), codeine (**23**) or hydrocodone (**24**).

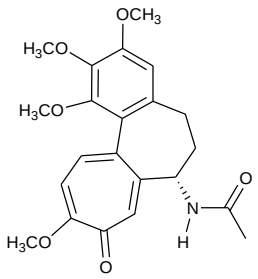


22 **23** **24**

Ephedrine (**25**), the anti-asthmatic drug that was isolated from a Chinese plant (*Ephedra sinica*) is one of the oldest classical cases of drugs developed based on their use in traditional medicine (Huang *et al.,* 1992). It is still in clinical use as a decongestant widely administered for relieving asthma. Similarly, colchicine (**26**), a natural anti-inflammatory alkaloid isolated from a historical medicinal plant (*Colchicium autumnale*) is still in clinical use as the drug of choice for the treatment of gout (Sneader, 1985).

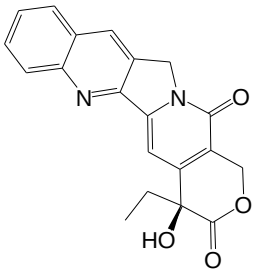


25

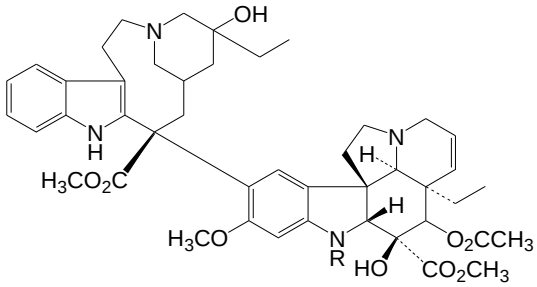


26

Camptothecin (**27**), a pyrrolo[3, 4-*b*]-quinoline alkaloid isolated from the Chinese tree (*Camptotheca acuminate*) is known for its anti-cancer activity (Wall *et al.,* 1966). It is used as an anti-tumour agent against lung, colorectal, ovarian and cervical cancers. Vinblastine (**28**) and vincristine (**29**) are two powerful anti-tumor alkaloids isolated from the Madagascan periwinkle (*Catharanthus roseus*) (Wedge, 2000). Vinblastine (Velban®) (**28**) is the most potent drug used in the treatment of testicular cancer, Hodgkin's disease, carcinoma of the breast, lung, bladder and other organs whereas vincristine (Oncovine®) (**29)** is particularly more effective in treating childhood and lymphocytic leukemia (Wedge, 2000).

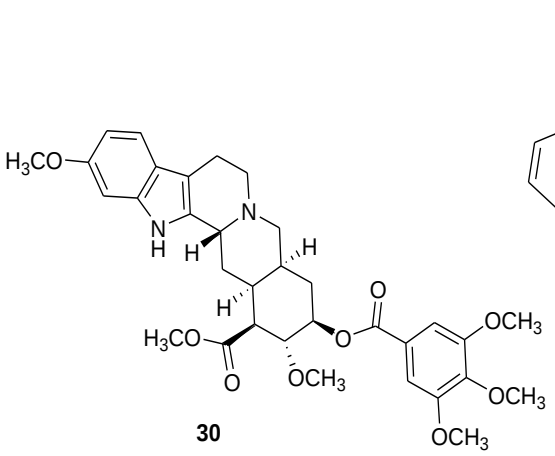


27

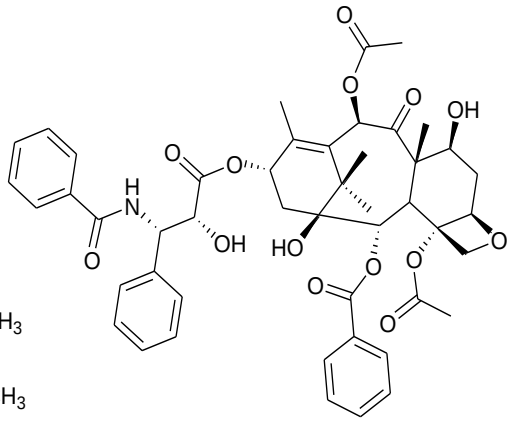


28: R = CH_3 **29**: R = CHO

Rauwolfia serpentina is the source of reserpine (**30**), an important drug for high blood pressure (Sneader, 1985; Miller & Gereau, 2000; Wedge, 2000). Taxol (Paclitaxel®) (**31**), a cytotoxic diterpene alkaloid, first isolated from the bark of the Pacific yew tree (*Taxus brevifolia*) in the late 1960s has been approved as a useful drug for the treatment of refractory, ovarian, breast and lung cancer (Wani *et al.,* 1971; Appendino, 1993). The discovery process involved the screening for anti-cancer bioactivity of over 110,000 compounds from 35,000 different plants by the National Cancer Institute over a 22-year period (Appendino, 1993).



30

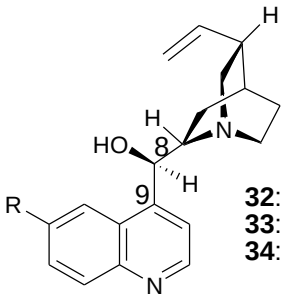


31

1.6 Natural products as potential sources of anti-parasitic agents

1.6.1 Alkaloids

Alkaloids have served as a potential source of new pharmaceutical products and inexpensive starting materials for the synthesis of many known drugs. Among them is quinine (**5**) which was isolated from *Cinchona succirubra* (Rubiaceae) in 1820 (Wright & Phillipson, 1990; Nkunya, 1992; Brogger-Christensen & Kharazmi, 2001) and is the oldest anti-plasmodial drug but still in use. Quinine (**5**) has perhaps saved more lives than any other drug in recorded history (Brogger-Christensen & Kharazmi, 2001; Kayser *et al*., 2003). It is effective against chloroquine resistant cerebral malaria. The molecular framework has been used as a lead template for the development of other effective aminoquinoline based anti-plasmodial analogues, such as chloroquine (**1**), amodiaquine (**2**), primaquine (**3**) and mefloquine (**4**). Quinine (**5**) and other quinoline alkaloids: quinidine (**32**), cinchonine (**33**) and cinchonidine (**34**), from the *Cinchona* bark, have also shown significant anti-trypanosomal activity against *T. b. brucei* (IC_{50} 4.9, 0.8, 1.2 and 7.1 μM, respectively) *in vitro*. Subsequently, quinidine (**32**) and cinchonine (**33**) exhibited good selectivity indices (SI 200) (Hoet *et al.*, 2004), indicating the high potential of these alkaloids for further anti-trypanosomal drug development.

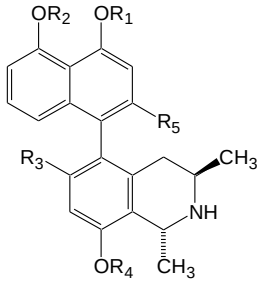


32: R = OMe 8*R*, 9*S*
33: R = H 8*R*, 9*S*
34: R = H 8*S*, 9*R*

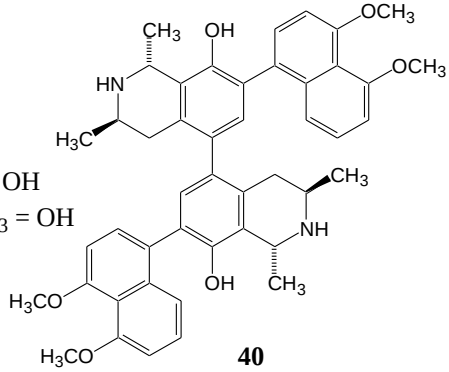
Naphthylisoquinoline alkaloids isolated from tropical lianas form a unique class of new promising anti-protozoal natural products. These compounds consist of naphthalene and an isoquinoline moiety joined by a biaryl axis. Due to a high steric demand of the two halves,

the restricted rotation leads to atropisomerism and axial chirality (Hallock *et al.,* 1994; Bringmann, 1996). The West African liana, *Triphyophyllum peltatum* (Dioncophyllaceae), yielded anti-parasitic naphthylisoquinoline alkaloids [dioncophylline C (**35**) and dioncopeltine A (**36**)] with high *in vitro* anti-plasmodial activity against chloroquine-resistant *P. falciparum* strain (IC_{50} 0.014 and 0.021 µg/ml, respectively). Dioncophylline C (**35**) cured *Plasmodium berghei* infected mice completely after oral treatment with 50 mg/kg per day for 4 days without noticeable toxic-effects, while dioncopeltine A (**36**) suppressed parasitaemia almost totally. Further analysis of the dose-response curve for dioncophylline C (**35**) revealed good anti-plasmodial activity (ED_{50} of 10.71 mg/kg/day) (Hallock *et al.,* 1994; Bringmann, 1996).

Korupensamines A (**37**) and B (**38**) isolated from another Cameroonian liana (*Ancistrocladus korupensis*) exhibited high anti-plasmodial activity (IC_{50} 0.31 and 0.17 µg/ml, respectively) (Hallock *et al.,* 1994; Bringmann, 1996). Dioncophylline A (**39**) exhibited mild activity against chloroquine-resistant strains of *P. falciparum* (IC_{50} 13.6 µg/ml) *in vitro* (Hallock *et al.,* 1994; Bringmann, 1996). Some of the dimers of bioactive principles showed improved bioactivity. Jozimine A (**40**), the dimer of dioncophylline A (**39**) also exhibited strong anti-plasmodial activity (IC_{50} 0.075 µg/ml) (Hallock *et al.,* 1994; Bringmann, 1996). The activity of some of the naphthylisoquinoline alkaloids are higher than chloroquine (IC_{50} 0.12 µg/ml) *in vitro*. The compounds constitute promising novel lead structures for the development of new anti-protozoal agents.



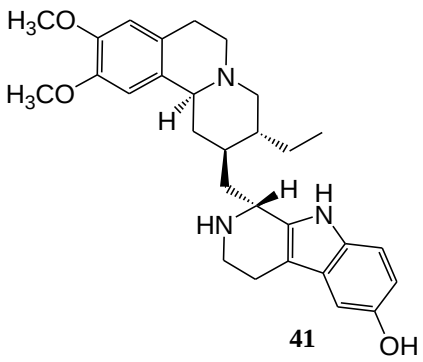
35: $R_1 = R_5 = CH_3$, $R_2 = R_3 = R_4 = H$
36: $R_1 = R_3 = R_4 = R_5 = H$, $R_2 = CH_3$
37: $R_1 = R_2 = R_5 = CH_3$, $R_3 = R_4 = H$
38: $R_1 = R_5 = CH_3$, $R_2 = R_4 = H$, $R_3 = OH$
39: $R_1 = R_5 = cis\ CH_3$, $R_2 = R_4 = H$, $R_3 = OH$



40

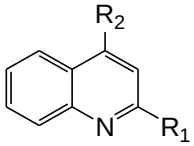
Tubulosine (**41**), which was isolated from *Pogonopus tubulosis* which is a Bolivian plant used by traditional healers in the treatment of malaria, exhibited high anti-malarial activity on CQ-sensitive and resistant strains of *P. falciparum* (IC_{50} 0.006 and 0.011 µg/ml, respectively) (Schwikkard & Van Heerden, 2000). When tested for toxicity against 9KB cells it was more toxic to malaria parasites than to mammalian cells. *In vivo* tests against *Plasmodium vinckei petteri* and *Plasmodium berghei* in mice revealed higher anti-

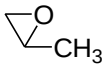
plasmodial activity at lower concentrations than the lethal dose in both cases (Schwikkard & Van Heerden, 2002).

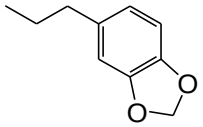


41

Ethno-pharmacologically directed search for new anti-leishmanial drugs has led to the selection of *Galipea longiflora* (Rutaceae) which yielded 2-*n*-propylquinoline (**42**), chimanine B (**43**), chimanine D (**44**), 2-*n*-pentylquinoline (**45**), 4-methoxy-2-phenylquinoline (**46**) and 2-(3, 4-methylenedioxyphenyl)- quinoline (**47**). These compounds exhibited anti-leishmanial activity against *L. donovani* (EC_{50} 25-50 μg/ml) *in vitro*. Only chimanine B (**43**) was active (95% clearance of *Leishmania* parasite load at 50 mg/kg in BALB/c mice when given orally twice a day in four days) *in vivo* (Chan-Bacab & Peňa-Rodríguez, 2001; Kayser *et al*., 2003).



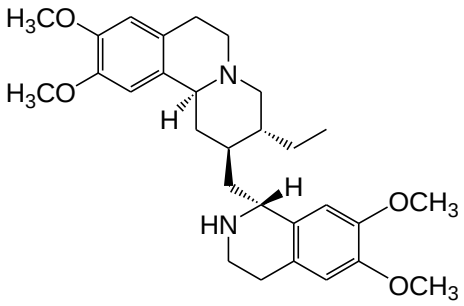
42: $R_1 = C_3H_7$, $R_2 = H$
43: $R_1 = CH{=}CH{-}CH_3$, $R_2 = H$
44: R_1 =  $R_2 = H$

45: $R_1 = C_5H_{11}$, $R_2 = H$
46: R_1 = phenyl, $R_2 = OCH_3$
47: R_1 =  $R_2 = H$

Camptothecin (**27**), an anti-neoplastic and a topoisomerase I inhibitor isoquinoline alkaloid isolated from *Camptotheca acuminata*, showed anti-leishmanial activity against *L. donovani* (EC_{50} 1.5 μM). It also showed anti-trypanosomal activity against *T. brucei* and *T. cruzi* (EC_{50} 3.6 and 1.6 μM, respectively) (Bodley *et al.*, 1995a; Bodley & Shapiro, 1995). For *Leishmania* and *Trypanosoma* parasites, camptothecin (**27**) is an important lead compound for structure-activity relationship (SAR) studies for the much needed new drugs.

Emetine (**48**), an isoquinoline alkaloid isolated from *Cephaelis ipecacuanha* (Rubiaceae) which has for a long time used as a traditional remedy for amoebiasis, showed high *in vitro* anti-trypanosomal activity (IC_{50} 0.039 and 0.43 μM against *T. b. brucei* and *T. congolense*,

respectively). It also exhibited high cytotoxicity level with no selectivity to normal mammalian cells (Hoet *et al.,* 2004).

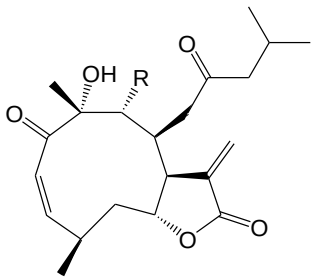


48

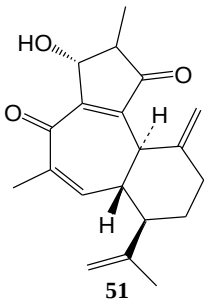
1.6.2 Terpenes

The anti-protozoal potential of sesquiterpenes is well established since artemisinin (**12**) was identified as a new anti-plasmodial drug and lead with high clinical relevance. It is an unusual endoperoxysesquiterpene lactone isolated from a Chinese anti-plasmodial plant, *Artemisia annua* (Asteraceae), and is currently the most potent and safe plant-derived anti-plasmodial drug which is particularly effective in combating cerebral malaria (Klayman, 1985; Van Agtmael *et al*., 1999; Graul, 2001). Useful derivatives include artemether (**13**) and sodium artesunate (**14**) (WHO, 1986; Wright & Phillipson, 1990; Kain, 1995). Artemisinin is also effective against *Leishmania* promastigotes (ED_{50} $7.5x10^{-7}$M) *in vitro*. Both artemisinin and its derivative, artemether (**13**) have strong leishmanicidal activity (ED_{50} $3x10^{-5}$ and $3x10^{-6}$ M, respectively) for amastigotes *in vitro* (Nkunya, 1992).

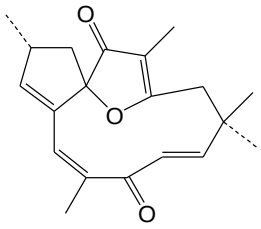
The germanocrenolide sesquiterpenes, neurolenin A (**49**) and neurolenin B (**50**) from *Neurolaena lobata* (Asteraceae), a medicinal plant used in Guatemala for the treatment of malaria, exhibited strong anti-protozoal activity against *Leishmania* promastigotes and *Trypanosoma* epimastigotes (EC_{50} 0.92 and 0.62 µM, respectively) *in vitro* (Chan-Bacab & Peňa-Rodríguez, 2001). Jatrogrossidione (**51**) and jatrophone (**52**), isolated from *Jatropha grossidentata* and *Jatropha isabelli* (Euphorbiaceae) respectively, showed significant activity against *Leishmania* promastigotes (EC_{50} 0.75 and 5.0 µg/ml, respectively) *in vitro*. Jatrophone (**52**) reduced *L. amazonesis* amastigotes *in vivo* at a dose of 25 mg/kg/day (Kayser *et al*., 2003).



49: R = H
50: R = OAc



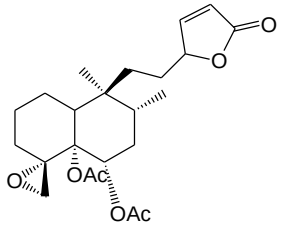
51



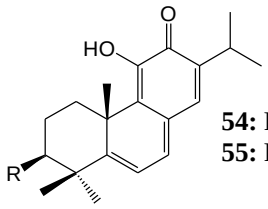
52

Ajuga remota is widely used as anti-malarial remedy (Kuria *et al*, 2002). Several compounds including ajugarin (**53**), a diterpene from *Ajuga remota* that is a commonly occurring medicinal plant in Kenya, constitute novel structures with anti-plasmodial activity. Ajugarin (**53**) is mildly active against *P. falciparum* (IC_{50} 23 µg/ml) *in vitro* (Kuria *et al*, 2002).

Hoslundia opposita (Labiatae) is commonly used in East and West Africa for the treatment of malaria. The hexane crude extract of the root bark exhibited good anti-plasmodial activity against *P. falciparum* multi-drug resistant K1 strain (IC_{50} 5.6 µg/ml) *in vitro* (Nkunya, 1992). Bioassay-guided fractionation yielded abietane-type diterpenes 3-*O*-benzoylhosloppone (**54**) and 3-*O*-cinnamoylhosloppone (**55**) which exhibited strong anti-plasmodial activity against *P. falciparum* multi-drug resistant K1 strain (IC_{50} 0.42 and 0.38 µg/ml, respectively) *in vitro* (Nkunya, 1992).

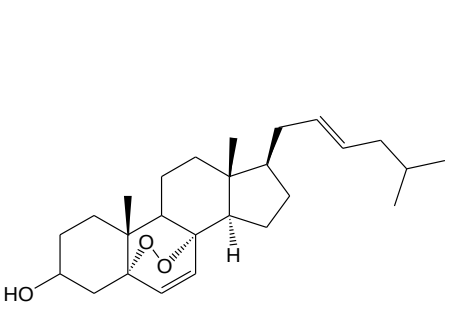


53

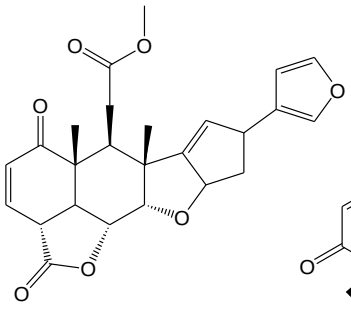


54: R = C_6H_5-COO-
55: R = C_6H_5-CH_2CH_2COO-

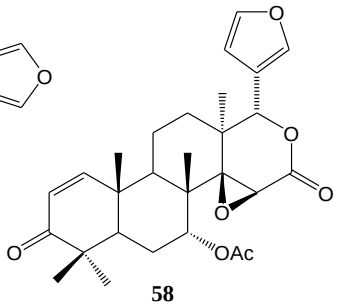
A triterpene endoperoxide, ergosterol-5, 8-endoperoxide (**56**) from *Ajuga remota* is mildly active against *P. falciparum* (IC_{50} 8.2 µg/ml) *in vitro* (Kuria *et al*, 2002). Bitter triterpenoids, commonly known as limonoids, are produced by several species of Meliaceae and Rutaceae. Several limonoids from Meliaceae exhibit anti-plasmodial activity. The neem tree, *Azadirachta indica* (Meliaceae), is widely used as an anti-plasmodial remedy in Africa and Asia. Gedunin (**57**) and nimbolide (**58**) are the most active limonoids against *P. falciparum* (IC_{50} 0.02 and 0.09 µg/ml respectively) *in vitro* so far isolated from *A. indica* (MacKinnon *et al*, 1997).



56



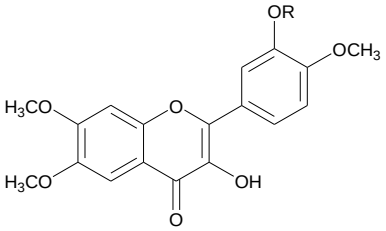
57



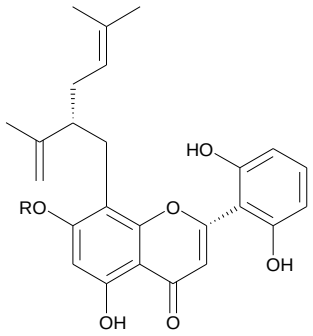
58

1.6.3 Flavonoids

Flavonoids are widespread in the plant kingdom (Schwikkard & Van Heerden, 2002). Before 1986, there were no evidence for their bioactivity against *Plasmodium*, *Leishmania* and *Trypanosoma* parasites. The discovery of two anti-plasmodial flavonoids: artemetin (**59**) and casticin (**60**) from *Artemisia annua* (Asteraceae) resulted in renewed interest in anti-protozoal activity of flavonoids. Subsequently, exiguaflavanone A (**61**) and B (**62**) isolated from *Artemisia indica* (Asteraceae) exhibited activity against *P. falciparum* (EC_{50} 4.6 and 7.1 µg/ml, respectively) *in vitro* (Schwikkard & Van Heerden, 2002; Kayser *et al*., 2003).

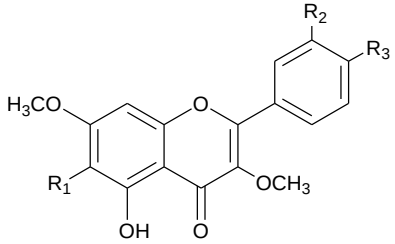


59: R = CH_3
60: R = H



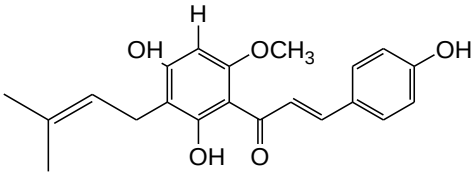
61: R = H
62: R = CH_3

Four anti-trypanosomal methoxylated flavones: chrysosplenetin (**63**) (IC_{50} 2.9 µM), chrysosplenol D (**64**) (IC_{50} 4.7 µM), retusin (**65**) (IC_{50} 14.2 µM), and artemetin (**59**) (IC_{50} 189 µM), were isolated from the leaves of *Ehretia amoena* (Boraginaceae), a plant used traditionally in Uganda for the treatment of sleeping sickness (Hoet *et al*., 2004).

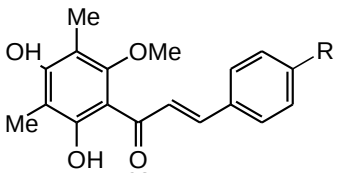


63: $R_1 = R_2 = OCH_3$, $R_3 = OH$
64: $R_1 = OCH_3$, $R_2 = R_3 = OH$
65: $R_1 = H$, $R_2 = R_3 = OCH_3$

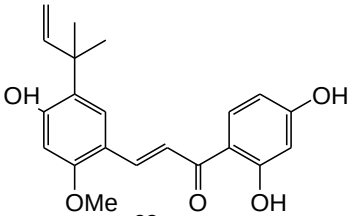
Chalcones, the 1, 3-diaryl-2-propen-1-ones compounds belonging to the flavonoid class of natural products, possess a broad spectrum of biological activity, including anti-protozoal properties (Zhai *et al*., 1999; Frölich *et al*., 2005; Salem & Werbovetz, 2005). Xanthohumol (**66**), which is the major *Humulus lupulus* chalcone constituent, demonstrated anti-plasmodial activity against chloroquine sensitive and multi-drug resistant strains of *P. falciparum* (IC_{50} 8.2 and 24.0 μM, respectively) *in vitro* (Frölich *et al*., 2005). 2′, 4′-Dihydroxy-6′-methoxy-3′, 5′-dimethylchalcone (**67**) and 2, 2′, 4′-trihydroxy-6′-methoxy-3′, 5′-dimethylchalcone (**68**) isolated from *Psorothamnus polydenius* exhibited leishmanicidal (IC_{50} 5.0 and 7.5 μg/ml, respectively) and trypanocidal (IC_{50} 6.3 and 6.8 μg/ml, respectively) activity *in vitro* (Salem & Werbovetz, 2005). Licochalcone A (**69**), isolated from Chinese licorice (*Glycorrhiza glabra*) roots, was found to inhibit the growth of *Leishmania donovani* promastigotes (IC_{50} 4.0 μM) *in vitro* (Zhai *et al*., 1999).



66



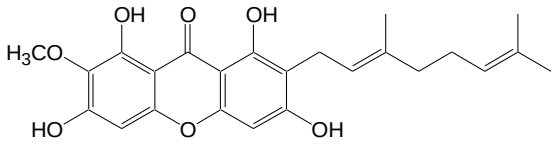
67: R = H **68**: R = OH



69

1.6.4 Xanthones

Anti-plasmodial xanthones have been isolated from *Garcinia cowa* (Guttiferae). Cowaxanthone (**70**) demonstrated significant activity against *P. falciparum* (EC_{50} 1.5 μg/ml) and is comparable to pyrimethamine (EC_{50} 2.8 μg/ml) *in vitro* (Schwikkard & Van Heerden, 2002).

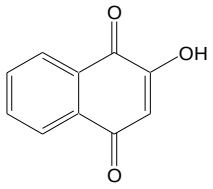


70

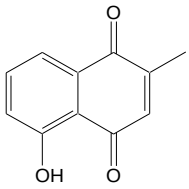
1.6.5 Naphthoquinones

Naphthoquinones and the related quinoid compounds form a major group of anti-protozoal natural products with significant biological activity against *Plasmodium*, *Leishmania* and *Trypanosoma* parasites. Hydrolapachol (**71**) exhibited activity against *Plasmodium lophurae* in ducks in the 1940s, an observation that stimulated the synthesis of hundreds of analogues including atovaquone (**10**) which is currently combined with proguanil (**8**)

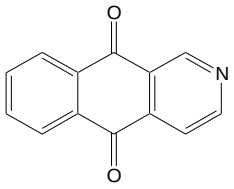
(Malarone®) for the treatment of CQ-resistant malaria. Plumbagin (**72**), isolated from *Plumbago zeylenica*, also exhibits anti-plasmodial activity on chloroquine sensitive and resistant strains (IC_{50} 0.18 and 0.19 µg/ml, respectively). Cytotoxicity assays on KB cell lines indicated that *P. zeylenica* extract was moderately selective (SI 5.0) for CQ-sensitive and resistant strains of *P. falciparum* (Obua *et al*., 2002). Besides the synthetics, new structurally interesting naphthoquinones have been isolated. Benzisoquinoline-5, 10-dione (**73**) from *Psychotria camponutans* (Rubiaceae), exhibited strong activity against CQ-resistant strain of *P. falciparum* (EC_{50} 0.84 µg/ml) *in vitro* but was associated with significant cytotoxicity against mammalian KB cell lines (CC_{50} 1.62 µg/ml) (Schwikkard & Van Heerden, 2002).



71



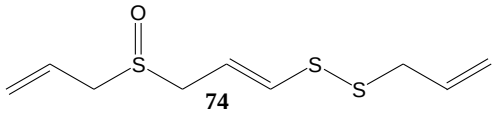
72



73

1.6.6 Sulfur containing aliphatics

Sulfur containing aliphatics were initially isolated from garlic (*Allium sativum*, Liliaceae), and have been shown to exhibit anti-plasmodial and anti-trypanosomal activity. Ajoene (**74**) from garlic, showed significant suppression of *Trypanosoma cruzi* parasitaemia *in vivo* with daily doses of 50 mg/kg over 12 days (Schwikkard & Van Heerden, 2002). It has been shown to affect thiol metabolism by acting as a covalent inhibitor as well as a substrate of human glutathione reductase (GR) and *T. cruzi* trypanothione reductase (TR). The interactions between TR and ajoene (**74**) have been shown to lead to increased oxidative stress of the parasite cell. Ajoene (**74**) also inhibits *de novo* synthesis of neutral lipids and sterols in *T. cruzi* epimastigotes (Schwikkard & Van Heerden, 2002; Kayser *et al*., 2003).



74

Local herbal remedies for malaria, leishmaniasis and trypanosomiasis exist and are widely used by communities in most of developing countries. Considering the great diversity of natural products from plants that have shown strong *in vitro* activity against *Plasmodium*, *Leishmania* and *Trypanosoma* parasites (Nkunya, 1992; Chan-Bacab & Peňa-Rodríguez, 2001; Schwikkard & Van Heerden, 2002; Muregi *et al*, 2003; Kayser *et al*., 2003; Hoet *et al*., 2004; Muregi *et al*, 2004; Kirira *et al*., 2006) and the high selectivity of these

compounds, further scientific investigation seems to be a logical step in exploiting the anti-protozoal compounds, which may be present in plants. This will facilitate selection of extracts and bioactive compounds for further research and drug development programs.

The realm of drugs obtained from plants is vast and rich source of natural products. They are the basis for the traditional medicinal philosophies and practices in Africa and other parts of the world. The large proportion of natural products in drug discovery has originated from the immense and wide-spectrum of chemical structural diversity of and the intricate skeletons of natural compounds. Since natural products have been biosynthesized within living systems, they are evolutionary optimized as drug-like molecules, biologically validated and are more friendly than synthetic molecules, making them good candidates for further drug research and development (Kayser *et al*., 2003; Koehn & Carter, 2005; Balunas & Kinghorn, 2005; Drahl *et al.*, 2005). The discovery of bioactive natural products from traditional medicinal plants has availed important templates for the synthesis and development of a series of natural product analogues with improved solubility, biological activity and reduced side-effects. Out of 300,000–500,000 known plant species (Hammond, 1995), only 20,000-55,000 of species are being used in traditional medicine (Penso, 1976; Schippmann et al., 2002). However, only a small portion of these has been investigated for medicinal properties. Furthermore, only 15,000 (6%) and 37,500 (15%) plant species have been screened for biological activity and phytochemicals, respectively (Fabricant & Farnsworth, 2001). These include plant species that produce important drugs such as artemisinin (**12**), morphine (**22**), ephedrine (**25**), colchicine (**26**), camptothecin (**27**), vinblastine (**28**), vincristine (**29**), reserpine (**30**), taxol (**31**), quinine (**5**), among many other therapeutic compounds.

By 1985 a total of 122 of natural product based drugs were derived from 94 (0.04%) plant species (Farnsworth *et al.,* 1985), leaving one wondering on the abundance of useful and highly needed drugs remaining to be discovered in the uninvestigated species. A large number of crude extracts from several medicinal and non-medicinal plants have been screened and shown to exhibit varying levels of anti-protozoal activity, *in vitro*, implying that a large pool of medicinal plants with promising anti-parasitic activity exists (Nkunya, 1992; Chan-Bacab & Peňa-Rodríguez, 2001; Schwikkard & Van Heerden, 2002; Muregi *et al*, 2003; Kayser *et al*., 2003; Hoet *et al*., 2004; Muregi *et al*, 2004; Kirira *et al*., 2006). Consequently, plants continue to represent a significant pool of raw materials for the discovery of new drugs. Obviously, plants have had quite an effect on the science and

technology of drug discovery and development, and the role of the phytochemist has become important in the isolation, structure elucidation, and synthesis of bioactive compounds. Four questions in the current drug discovery efforts are: (i) which plant species produce bioactive compounds?; (ii) what is the structure of the bioactive molecules?; (iii) how safe and efficacious are the bioactive compounds?; and (iv) can safety and efficacy be improved through structure activity relationship studies?

The selection of plant species for the investigation was based on information obtained from published ethno-botanical and pharmacological reports on the anti-plasmodialand anti-trypanosomal activity of medicinal plants from Tanzania and other parts of the world. The investigation targeted medicinal plants and their chemotaxonomically related species which are used traditionally as remedies against malaria and trypanosomiasis: *Annickia kummeriae* (Engl. & Diels) Setten & Maas, *Drypetes natalensis, Acridocarpus chloropterus* and *Pseudospondias microcarpa* (Ghazanfar & Al-Sabahi, 1993; Moody *et al*., 1995; Gessler, 1995; Muhie, 1996; Freiburghaus *et al*., 1997). *Annickia kummeriae, D. natalensis* and *P. microcarpa* are well known and widely used in traditional medicinal preparations for the treatment of malaria, trypanosomiasis and other ailments in Tanzania and other parts of East and Central Africa (Ghazanfar & Al-Sabahi, 1993; Moody *et al*., 1995; Gessler, 1995; Gessler *et al*., 1995; Muhie, 1996; Freiburghaus *et al*., 1997a, b).

1.7 Statement of the problem

African medicinal plants used for the treatment of protozoal diseases have not been validated and the bioactive chemical principles have not been isolated, characterized and assessed for safety to allow drug development process.

1.8 Hypotheses

The four plant species: *Annickia kummeriae* (Annonaceae)*, Pseudospondias microcarpa (Anacardiaceae), Drypetes natalensis* (Euphorbiaceae) *and Acridocarpus chloropterus* (Malpighiaceae) used in traditional medicine in Tanzania contain novel natural products with unique chemical structures that exhibit significant anti-protozoal activity.

1.9 Research objectives

1.9.1 Objectives

The general objective of the investigations was to evaluate four Tanzanian medicinal plants used in traditional therapy against malaria, sleeping sickness plus leishmaniasis and identify

the molecular basis of anti-protozoal activity.

1.9.2 Specific Objectives

The specific objectives were:

1. To determine the *in vitro* activity of the extracts, fractions and pure compounds of 4 Tanzanian medicinal plants against *Plasmodium falciparum, Trypanosoma brucei rhodesience* and *Leishmania donovani.*
2. To isolate and establish molecular structures of the bioactive chemical constituents of the leaves, stem and root barks of *Annickia kummeriae* (Annonaceae), *Pseudospondias microcarpa (Anacardiaceae), Drypetes natalensis* (Euphorbiaceae) and *Acridocarpus chloropterus* (Malpighiaceae).
3. To evaluate the *in vitro* anti-protozoal activity of pure compounds isolated from the bioactive extracts and fractions of the 4 Tanzanian medicinal plants.
4. To assess the *in vitro* cytotoxicity of the anti-parasitic extracts, fractions and pure compounds from the 4 Tanzanian medicinal plants.

1.10 Justification

Tropical rain forests in Tanzania constitute a rich but largely untapped reservoir of secondary metabolites as sources of lead compounds in drug development. Out of the estimated 10,000-15,000 plant species occurring in Tanzania, a good number of plant species are used as sources of medicines. However, there is no clear record on the actual number of plant species which are used as remedies for various ailments (Senn, 2006). Although various plants Tanzania are used as remedies, only a small number of these plants have been botanically identified (Gessler, 1995; Senn, 2006). Furthermore, only a small percentage has been investigated phytochemically while only a smaller fraction of these have been screened pharmacologically (Nkunya, 1992; Gessler, 1995; Malebo, 2000; Nkunya, 2005; Senn, 2006). Some Tanzanian medicinal plants have been screened for antiprotozoal activity and the active plant extracts investigated phytochemically (Nkunya, 1992; Gessler, 1995; Malebo, 2000; Nkunya, 2005; Senn, 2006). Annonaceae and Malpighiaceae are largely untapped reservoirs of natural products. These families can offer chemotherapeutically important lead compounds for the development of new anti-parasitic agents. Several plant species from Annonaceae and all in family Malpighiaceae found in Tanzania, have not been investigated either phytochemically or pharmacologically.

CHAPTER TWO

ANTI-PROTOZOAL CONSTITUENTS OF ANNONACEAE AND MALPIGHIACEAE

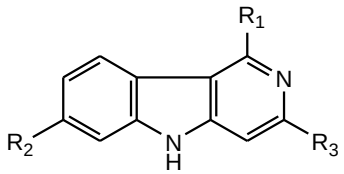
2.1 Annonaceae

2.1.1 Description

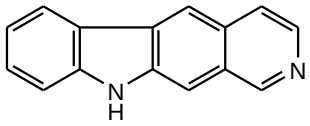
Annonaceae is a relatively large plant family comprising aromatic trees, shrubs, climbers or strugglers that occur in tropical and sub-tropical regions. It is constituted of about 130 genera and more than 2,300 species (Leboeuf *et al.*, 1982) mostly sources of edible fruits and oils, non edible oils and wood for the production of alcohol and fragrances for perfumery among other uses. Many annonaceous plants are used in traditional medicine as remedies for various ailments (Leboeuf *et al.*, 1982). They are known to contain alkaloidal and non-alkaloidal compounds which have peculiar structures, some of which are unique to this family.

2.1.1.1 Alkaloids

Alkaloidal constituents of Annonaceae include protoberberines, aporphines, indoles, isoprenylindoles and sesquiterpenylindoles. Pharmacologically important annonaceous alkaloids include harmine (**75**), an indole alkaloid isolated from *Picrasma javanica,* which exhibits trypanocidal activity against *T. cruzi* epimastigotes (IC_{50} 5 µg/ml) *in vitro*. 4-Methoxy-1-vinyl-β-carboline (**76**), also from the same plant, is active against *P. falciparum* (IC_{50} 1.9 µg/ml) *in vitro* (Pavanand *et al.,* 1988). Ellipticine (**77**), the planar tetracyclic alkaloid isolated from *Ochrosia elliptica*, exhibited strong anti-plasmodial activity against *P. falciparum* K1 strain (IC_{50} 0.018 µg/ml) *in vitro* (Andrade-Neto *et al.,* 2007).



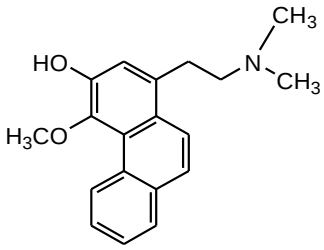
75: R_1 = H, R_2 = OCH_3, R_3 = CH_3
76: R_1 = OCH_3, R_2 = H, R_3 = $CHCH_2$



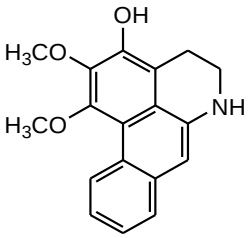
77

Guatteria foliosa, among other annonaceous plants, contains several aporphine alkaloids

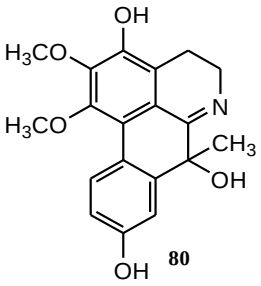
which exhibited significant *in vitro* trypanocidal activity against *T. cruzi*: argentine (**78**) (IC_{50} ≥ 250 µM), (-)-3-hydroxynornuciferine (**79**) (IC_{50} ≥ 250 µM), and (-)-isoguattouregidine (**80**) (IC_{50} ≥ 250 µM) (Mahiou *et al.*, 1994: Kayser *et al.*, 2003).



78

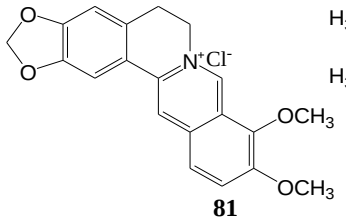


79

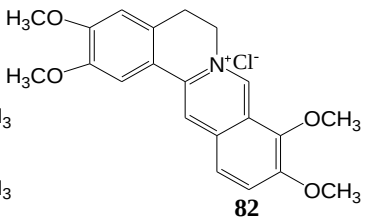


80

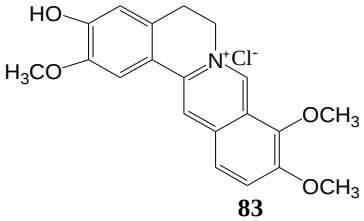
Protoberberine alkaloids commonly occur in higher plants, especially those in Annonaceae, Berberidaceae, Fumariaceae, Magnoliaceae, Menispermaceae, Papaveraceae, Ranunculaceae, Rhamnaceae, Rubiaceae and Rutaceae. Plants which contain these alkaloids have been reported to be used traditionally as remedies against tropical diseases, such as malaria and cutaneous leishmaniasis (Vennerstrom & Klayman, 1988; Phillipson & Wright, 1991). Consequently, the three naturally occurring protoberberines have been found to exhibit significant anti-plasmodial activity against CQ-sensitive and resistant strains of *P. falciparum* at a level similar to that of quinine (**5**): berberine (**81**) (IC_{50} 0.14 and 0.15 µg/ml, respectively), palmatine (**82**) (IC_{50} 0.27 and 0.16 µg/ml, respectively) and jatrorrhizine (**83**) (IC_{50} 42 and 1.61 µg/ml, respectively) *in vitro* (Vennerstrom & Klayman, 1988; Phillipson & Wright, 1991).



81



82



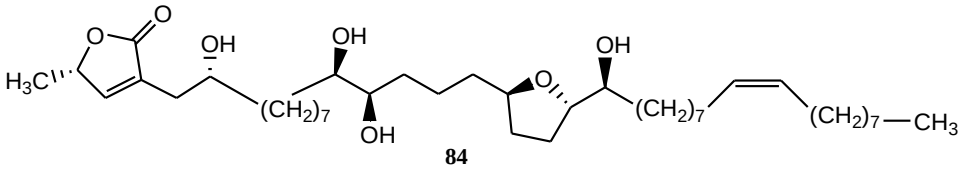
83

2.1.1.2 Annonaceous acetogenins

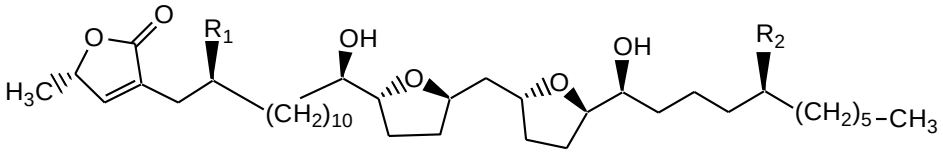
Acetogenis are a particular class of unusual series of polyketides which have so far only been found in plants belonging to the family Annonaceae. These compounds are characterized by the presence of one or two adjacent or isolated tetrahydrofuran rings, with the main functional groups along the C_{35}-C_{38} chain (saturated or unsaturated) as acetoxyl, hydroxyl or ketone and a terminal γ-lactone moiety. Annonaceous acetogenins exhibit a broad spectrum of bio-activity, including anti-leishmanial and anti-trypanosomal properties (Zafra-Polo *et al.*, 1996).

A number of acetogenins including senegalene (**84**) and squamocin (**85**) isolated from *Annona senegalensis*, a commonly occurring medicinal plant in Tanzania. Senegalene (**84**) and squamocin (**85**) were active against promastigotes of *L. major* and *L. donovani* parasites with a minimum effective concentration (MEC) value of 25□ and 50 µg/ml, respectively (Sahpaz *et al.*, 1994; Chan-Bacab & Peña Rodríguez, 2001). Senegalene also showed mild trypanocidal activity against *T. b. rhodesiense* (IC_{50} 50 µg/ml). Crude and partially purified aqueous extracts of the leaves of *A. senegalensis* completely cured experimental *T. b. brucei* infection in mice at 200 µg/kg body weight per day. Sub-inoculation of blood and cerebrospinal fluid drawn from the cured mice into healthy mice failed to produce any infection within 60 days of post-inoculation (Sahpaz *et al.*, 1994; Hoet *et al*., 2004).

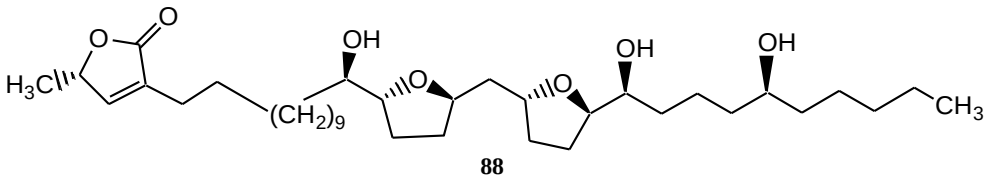
Three acetogenins from *Rollinia sylvastica* and *Rollinia emarginta* were identified to exhibit anti-protozoal and pesticidal activity. Rolliniastatin-2 (**86**) exhibited mild activity against *L. major* and *L. donovani* (IC_{50} 5-10 µg/ml) while asmicin (**87**) exhibited potent larvicidal activity against mosquito larvae as well as pesticidal activity against aphids, mites, the Mexican bean beetle, nematodes and spiders (Chan-Bacab & Peña Rodríguez, 2001). Ophrypetalin (**88**), a trihydroxylated *bis*-tetrahydrofuranlactonyl acetogenin from *Ophrypetalum odoratum*, showed anti-trypanosomal activity against *T. b. rhodesiense* (IC_{50} 0.4 µg/ml) *in vitro* (Sung'hwa, 1996).



84



85: R_1 = H, R_2 = OH: *erythro*, **86**: R_1 = OH, R_2 = H: *erythro* **87**: R_1 = OH, R_2 = H : *threo*



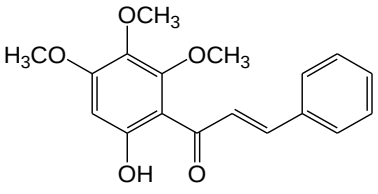
88

2.1.1.3 Flavonoids

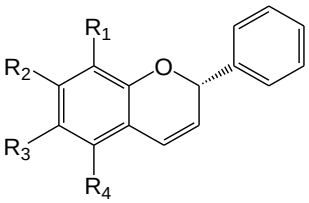
A number of flavonoids have been isolated from several genera in the family: *Monanthotaxis*, *Popowia*, *Sphaerocoryne*, *Uvaria* and *Xylopia* in the family Annonaceae. A

distinctive characteristic observed in the isolated flavonoids, with some few exceptions, is the absence of substitution in ring B, a structural feature which is thought to have potential taxonomic significance (Waterman & Pootakaham, 1979; Leboeuf *et al.*, 1982). Although flavanones and chalcones are widespread in higher plants, the addition of benzyl groups is quite unique and seems to be restricted to these specific genera in Annonaceae. These compounds exhibit a broad spectrum of bioactivity, including anti-inflammatory, anti-tumour, anti-bacterial and anti-plasmodial properties (Panichpol & Waterman, 1978; Waterman & Pootakaham, 1979; Leboeuf *et al.*, 1982).

Recent phytochemical investigations of several Tanzanian medicinal plants have yielded compounds with anti-protozoal activity and other efficacies. Thus, the Tanzanian liana *Uvaria dependens* (Annonaceae) yielded several flavonoids, which exhibited anti-plasmodial activity against chloroquine-resistant *P. falciparum* K1 strain *in vitro.* These include: 6'-hydroxy-2', 3', 4'-trimethoxychalcone (**89**) (IC_{50} 2.0 µg/ml), 5, 6, 7-trimethoxyflav-3-ene (**90**) (IC_{50} 9.0 µg/ml) and 5, 7, 8-trimethoxyflav-3-ene (**91**) (IC_{50} 5.0 µg/ml) (Malebo, 2000).



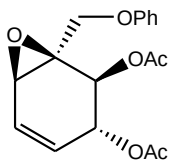
89



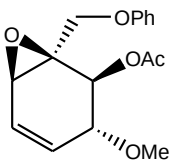
90: R_1 = H, R_2 = R_3 = R_4 = OCH_3
91: R_1 = R_2 = R_3 = OCH_3, R_4 = H

2.1.1.4 Cyclohexane epoxides

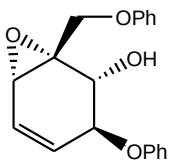
Anti-plasmodial cyclohexane epoxides containing benzoyloxymethylene unit have been isolated from Annonaceae species. *Uvaria pandensis* (Annonaceae) from coastal areas of Tanzania, yielded several cyclohexane epoxides, which exhibited mild *in vitro* anti-plasmodial activity against chloroquine-resistant *P. falciparum* K1 strain. These include: (+)-β-senepoxide (**92**), (+)-pandoxide (**93**) and (–)-pipoxide (**94**) (Nkunya, 2005).



92



93



94

2.1.2 *Annickia kummeriae* (Engl. & Diels) Setten & Maas (Annonaceae)

2.1.2.1 Botanical Description

Annickia kummeriae (Engl. & Diels) Setten & Maas formerly known as *Enantia kummeriae* (Engl. & Diels) is a tree, 25-30 m tall found in the dense humid sub-montane forest in between 800 and 1000 m above sea level in East Usambara Mountains in Tanzania. It belongs to the family Annonaceae. Until recently this species was known to occur only in the East Usambara Mountains in Tanzania. Fallen fruits have now been found in the Mwanihana Forest, Udzungwa Mountains in southern Tanzania, where the species is considered to be rare. *Annickia kummeriae* is not known to occur elsewhere outside Tanzania. It is locally known as muaka/ng'waka (Sambaa) and zonozono (Bondei). The specimen of *A. kummeriae* leaves is shown in plate 2.1.

Plate 1: Photograph of *Annickia kummeriae* leaves



The wood is bright yellow, straight grained and splits easily. The sap is also bright yellow; indumentum composed of simple fasciculate or stellate hairs. The flowers are hermaphrodite, solitary, extra-axillary on the leafy shoots, shortly stalked while buds are 3-angled; bracteoles 1–2, mostly deciduous. The sepals are green, triangular, 7 mm long, cohering together, lanceolate, and mostly smaller than the petals. The petals are green, oblong-elliptic, but broadened at the base into a kind of claw to form an area which encloses the stamens and carpels. The receptacle is convex while the stamens are numerous, linear-

oblong; filaments almost obsolete. The anther-cells are lateral, connective-prolongation ovoid and truncate-capitate. The carpels are numerous, free, cylindrical, with 1 basal ovule, pubescent while the style is short. The stigma is linear and capitate. Monocarps are indehiscent, oblong-ellipsoid, distinctly stipitate and one-seeded. The seed is vertical, oblong-ellipsoid and often with raised ridge. The projections of inner layer of testa entering the endosperm are spinous and not lamelliform (Verdcourt, 1971).

2.1.2.2 Ethnomedical use

A. kummeriae is used traditionally by the Sambaa and Bondei tribes in Tanzania for the treatment of malaria (Muhie, 1996; Freiburghaus et al., 1997a,b).

2.1.2.3 Previous phytochemical and anti-protozoal reports

Crude extract from *A. kummeriae* was previously screened for its anti-trypanosomal activity against *T. b. rhodesiense* and shown to be potent (IC_{50} 0.7 μg/ml) (Freiburghaus *et al.*, 1997a). Previous phytochemical screening of *A. kummeriae* resulted in the isolation of two protoberberine alkaloids: palmatine (**82**) and jatrorrhizine (**83**) (Muhie, 1996). Ethnomedical information shows the genus *Annickia* (formerly *Enantia*) is used for malaria and other ailments. Consequently, *A. kummeriae* was chosen for bioassay-guided phytochemical isolation of anti-protozoal compounds as leads and/or candidates for drug development.

Literature search for previous phytochemical investigations on this genus revealed phytochemical and pharmacological information on *Enantia chlorantha* and *Enantia polycarpa* (Wafo *et al*., 1999). *Enantia polycarpa* is used in West Africa for the treatment of malaria. The stem bark extract of *Enantia polycarpa* showed high *in vitro* anti-plasmodial activity against *Plasmodium falciparum* K1 strain (IC_{50} 0.126 μg/ml) and favourable selectivity (SI 616) (Atindehou *et al*., 2004). It is fascinating to note that another species of the same genus, *Enantia chlorantha,* exhibited *in vivo* activity against *Plasmodium yoelii* in experimentally infected mice (Kimbi *et al*., 1988; Agbaje & Onabanjo, 1991).

The chemistry of *Enantia chlorantha* and *Enantia polycarpa* has been extensively studied (Leboeuf & Cave, 1972; Jössang *et al*, 1977a & b; Wafo *et al*., 1999). The bark and the leaves of *Enantia chlorantha* and *Enantia polycarpa* contain many biologically active alkaloids that are structurally closely related. Protoberberine alkaloids have been reported to occur in *E. chlorantha*, and among these berberine (**81**) was found to exhibit the highest

anti-plasmodialactivity against *P. falciparaum* (IC_{50} 0.14 µg/ml) *in vitro*. Palmatine (**82**) and jatrorrhizine (**83**) exhibited lower anti-plasmodial activity (IC_{50} 0.51 and 0.36 µg/ml, respectively) (Phillipson & Wright, 1991; Moody *et al*., 1995). The majority of *Enantia* alkaloids like palmatine (**82**) and the numerous protoberberines have isoquinoline structure.

Quinoline and isoquinoline alkaloids: quinine (**5**) and quinidine (**32**) have been isolated from *Enantia polycarpa* (Buzas *et al*., 1959, 1965). Quinidine (**32**) the stereoisomer of quinine (**5**) is as potent as quinine against malaria, which explains the extensive use of the barks of *Enantia polycarpa* as an anti-plasmodial remedy in West Africa.

Absence of previous exhaustive phytochemical investigation on *A. kummeriae* prompted us to investigate this plant for the presence of more anti-malarial, trypanocidal and leishmanicidal compounds.

2.2 Malpighiaceae

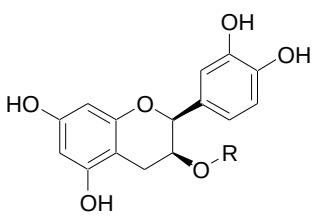
2.2.1 Description

Malpighiaceae is a large family of about 60 genera and 800 species, mainly found in the tropics, extending into the sub-tropics and most abundant in the New World (Milne-Redhead & Polhill, 1968). All species are perennial scramblers, climbers, trees, shrubs, or rarely shrublets. Plant species in this family are known to contain alkaloidal and non-alkaloidal compounds.

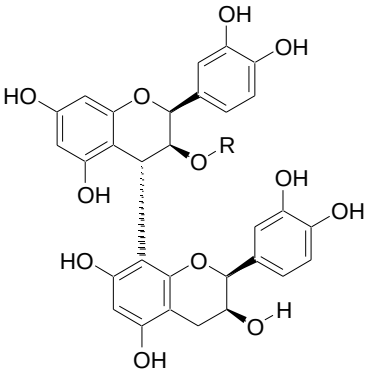
2.2.1.1 Flavonoids

The Oxaca Mexican Indians use the bark of *Byrsonima crassifolia* (Malpighiaceae) to treat fever and gastro-intestinal disorders (Geiss *et al.*, 1995). Subsequently, the crude extracts from *B. crassifolia* have been shown to inhibit *T. cruzi* trypomastigotes *in vitro*. The water infusions of the bark and the leaves of *B. crassifolia* inhibited *T. cruzi* trypomastigotes (IC_{90} 420.9 and 442.3 µg/ml, respectively) *in vitro*. Furthermore, the hexane and the ethanol extracts of the leaves also inhibited *T. cruzi* trypomastigotes (IC_{90} 580.1 and 376.3 µg/ml, respectively) *in vitro* (Berger *et al.*, 1998). A number of proanthocyanidins from *B. crassifolia* including 3-*O*-galloyl-(+)-epicatechin (**95**), 3-*O*-galloyl-(+)-epicatechin-[4α→8]- (+)-epicatechin (**96**), 3-*O*-galloyl-(+)-epicatechin-[4α→8]-3-*O*-galloyl-(+)-epicatechin (**97**), (+)-epicatechin-[4α→8]-3-*O*-galloyl-(+)-epicatechin (**98**), (+)-epicatechin-

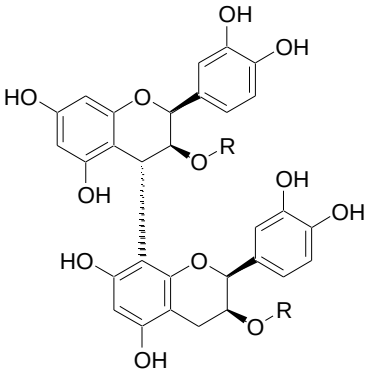
[4α→6]- (+)-epicatechin (**99**), 3-*O*-galloyl-(+)-epicatechin-[4α→8]-3-*O*-galloyl-(+)-epicatechin-[4α→8]-(+)-epicatechin (**100**) and 3-*O*-galloyl-(-)-epicatechin-[4β→8]-3-*O*-galloyl-(+)-epicatechin-[4α→8]-(+)-epicatechin (**101**), have been isolated (Geiss *et al*., 1995).



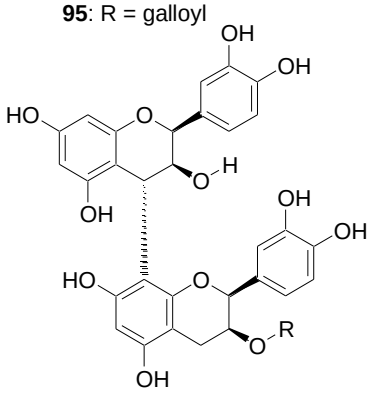
95: R = galloyl



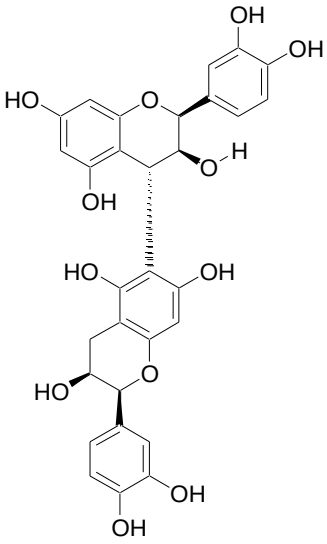
96: R = galloyl



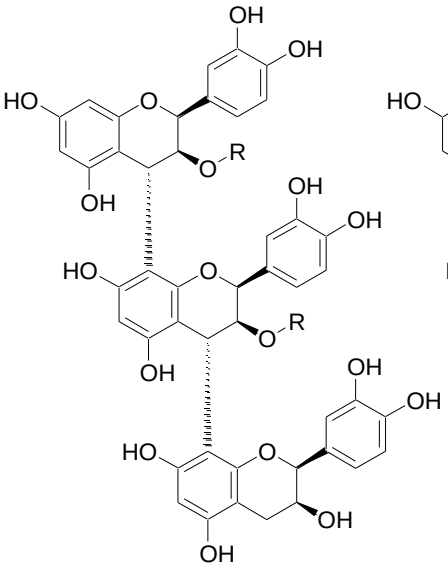
97: R = galloyl



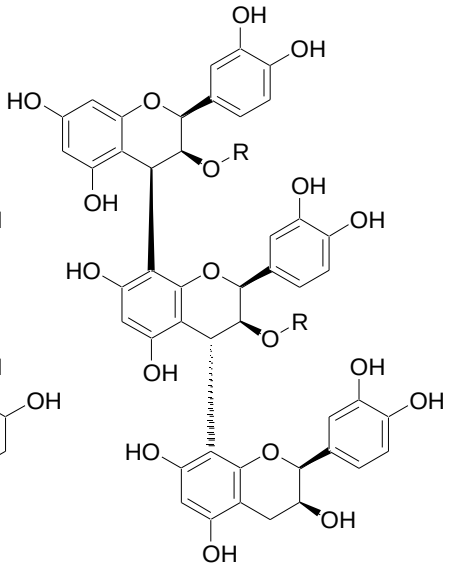
98: R = galloyl



99

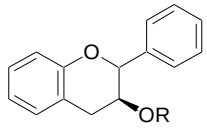


100: R = galloyl

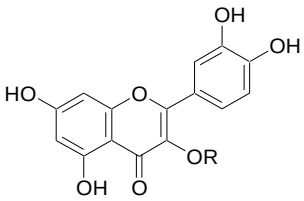


101: R = galloyl

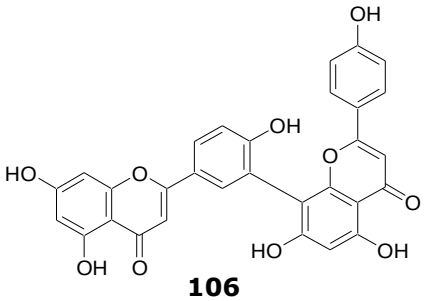
In Brazil, *Byrsonima crassa* is used for the treatment of gastro-intestinal disorders in folk medicine (Sannomiya *et al*, 2005). A number of anti-leishmanial flavonoids have been isolated from *B. crassa* including (+)-catechin (**102**), (-)-epicatechin (**103**), quercetin-3-*O*-β-*D*-galactopyranoside (**104**), quercetin-3-*O*-α-*L*-arabinopyranoside (**105**) and amentoflavone (**106**).



102: (2*R*,3*S*), R = H
103: (2*R*,3*R*), R = H



104: R = ß-*D*-galactopyranoside
105: R = a-*L*-arabinopyranoside

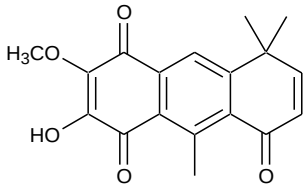


106

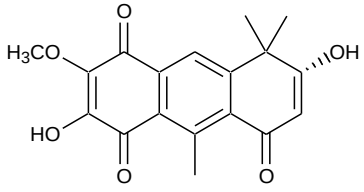
(+)-Catechin (**102**) and (-)-epicatechin (**103**) exhibited mild *in vitro* anti-trypanosomal activity against *T. b. rhodesiense* (IC_{50} 14.5 µg/ml and 21.2 µg/ml, respectively) *in vitro* (Tasdemir et *al.*, 2006). Quercetin-3-*O*-β-*D*-galactopyranoside (**104**) showed moderate anti-leishmanial activity against *L. major*, *L. donovani* and *L. amazonensis* amastigotes (IC_{50} 3.9, 3.0 and 3.6 µg/ml, respectively) *in vitro*. Quercetin-3-*O*-α-L-arabinopyranoside (**105**) also exhibited moderate anti-leishmanial activity against amastigotes of *L. major*, *L. donovani* and *L. amazonensis* (IC_{50} 2.8, 2.5 and 15.0 µg/ml, respectively) *in vitro* (Ercil *et al*, 2005).). Amentoflavone (**106**) showed weaker anti-leishmanial activity against amastigotes of *L. donovani* (IC_{50} 6.0 µg/ml) *in vitro*, mild anti-trypanosomal activity against *T. b. rhodesiense* (IC_{50} 22.7 µg/ml) but was inactive against *T. cruzi* (Tasdemir et *al.*, 2006).

2.2.1.2 Naphthoquinones

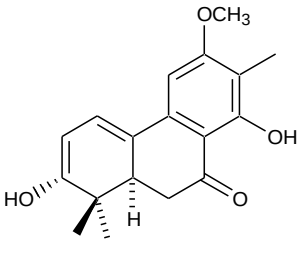
Naphthoquinones constitute a major natural product group with significant activity against *Leishmania*, *Plasmodium* and *Trypanosoma* due to their ability to induce oxidative stress in the parasite cells (Hoet *et al*, 2004). Novel but unusual naphthoquinones have recently been isolated from the bark of *Byrsonima microphylla* (Malpighiaceae) which is used traditionally for the treatment of fever and asthma (Aguiar *et al*., 2005). These include 3-hydroxy-2-methoxy-8, 8, 10-trimethyl-8H-antracen-1, 4, 5-trione (**107**), 3, 7-dihydroxy-2-methoxy-8, 8, 10-trimethyl-7, 8-dihydro-6H-antracen-1, 4, 5-trione (**108**) and (2*S*, 10a*R*)-2, 8-dihydroxy-6-methoxy-1, 1, 7-trimethyl-2, 3, 10, 10a-tetrahydro-1H-fenantren-9-one (**109**) (Aguiar *et al*., 2005) that have not been tested for their anti-protozoal activity.



107



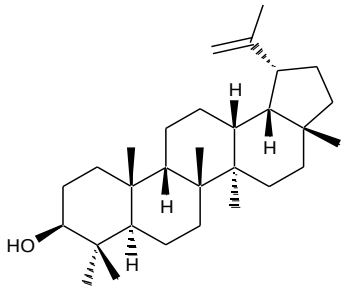
108



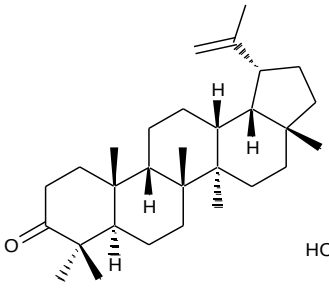
109

2.2.1.3 Triterpenes

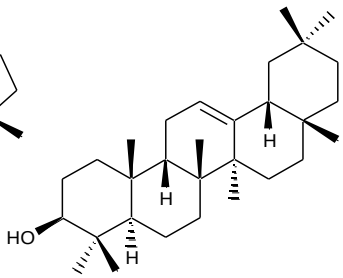
Several triterpenes have been isolated from the anti-prozoal stem bark extract of the *B. microphylla* and *B. crassifolia* (Malpighiaceae), which are used in traditional herbal medicine to treat fever and asthma (Aguiar *et al.*, 2005). These include lupeol (**110**), lupenone (**111**), β-amyrin (**112**), betulin (**113**) and betulinic acid (**114**) (Berger *et al*, 1998). Lupeol (**110**) exhibited 45% suppression of *P. berghei* parasitaemia in experimentally infected mice at 25 µg/ml while lupenone (**111**) was inactive (De Almeida Alves *et al.*, 1997). Betulinic acid (**114**) showed mild anti-plasmodial activity against *P. falciparum* K1 strain (EC_{50} 10.46 µg/ml) *in vitro* (Bringmann *et al.*, 1997).



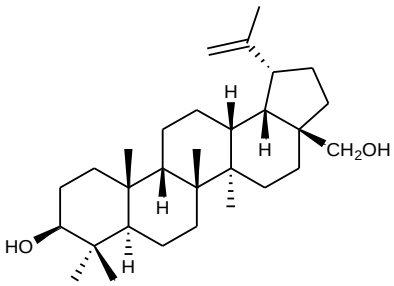
110



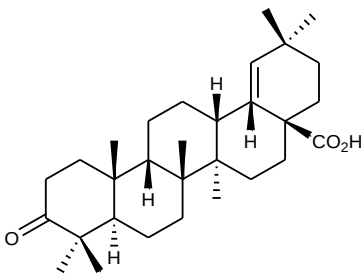
111



112



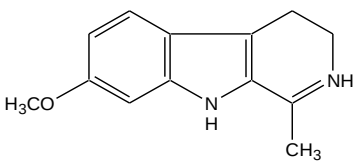
113



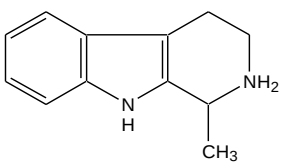
114

2.2.1.4 Alkaloids

Various Malpighiaceae plant species, used as traditional remedies against tropical parasitic diseases, contain *ß*-carboline alkaloids: harmine (**75**), harmaline (**115**) and tetrahydroharmine (**116**) (Lutomski *et al*., 1975; Allen & Holmstedt, 1980; Bruneton, 1999). *In vitro* test against *T. cruzi* epimastigotes revealed that harmine (**75**) from *Banisteriopsis caapi* (Malpighiaceae) reduced parasitaemia by more than 90% at 50 µg/ml. Similarly, significant anti-leishmanial activity (IC_{50} 5.0 µg/ml) against *L. donovani* promastigotes was noted *in vitro* (Cavin *et al*., 1987).



115



116

2.2.2 *Acridocarpus chloropterus* Oliver (Malpighiaceae)

2.2.2.1 Occurrence and botanical description

Acridocarpus chloropterus Oliver (Syn: *Anomalopterus chloroptera*) occurs in Ulanga District near the confluence of Ulanga and Luwegu rivers, in Newala District within the vicinity of the Ruvuma River and also in Pugu Forest Reserve near Dar-es-Salaam in Tanzania (Dalziel, 1937). The specimen of *A. chloropterus* leaves is shown in plate 2.2.

Plate 2: Photograph of *Acridocarpus chloropterus* Oliver leaves



Acridocarpus chloropterus is a scandent shrub or tall woody climber with branches up to 15 m. in length, younger ones ± densely rusty pubescent, older ones quite glabrous, lenticellate. Leaf-lamina 7-15 (19) × 2·5-5·5 (7) cm, oblong or oblong-elliptic, apex acute to sub-obtuse or acuminate, base rounded or rarely sub-cordate or broadly cuneate, coriaceous, usually with one pair of glands near the insertion of the petiole beneath and with 7-13 pairs of prominent lateral nerves, ferrugineous-tomentose (more densely underneath) when young, later usually glabrescent except usually beside the midrib underneath; petiole 2-6 mm. long, stout, canaliculate, pubescent or glabrescent.

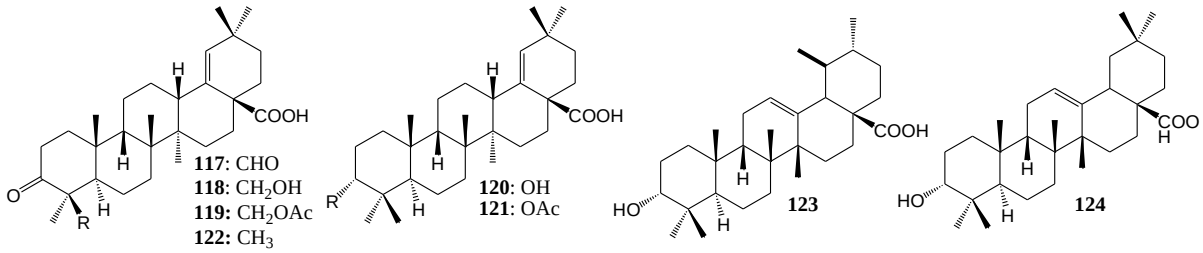
Inflorescences (5) 8–15 (25) cm. long, usually racemes terminating leafy branches, sometimes axillary, many-flowered, pyramidal in outline; bracts 1-2 mm. long, triangular-lanceolate, densely ferrugineous-tomentose, eglandular; bracteoles very small, eglandular. Flowers c. 2·25 cm. in diam. Calyx with 2-3 circular glands; sepals 3-3·5 × ± 2·5 mm,

ovate, sericeous or glabrescent outside. Petals up to 11 × 8 mm., elliptic to ovate, unguiculate, yellow. Stamens with anthers c. 4 mm. long, oblong-ovate, glabrous; filaments ± 1·5 mm. long, thick, ± ligulate. Ovary densely ferrugineous-tomentose; styles 2, 8-10 mm long, stout, terete, curved inwards. Samara with wing 3-4 (5) × 1·5-2·3 cm, obliquely obovate, sometimes somewhat constricted in the lower half, often distally oblique-truncate or obtuse, not clasping the nut, often purplish, usually glabrous (Launert, 1968).

2.2.2.2 Ethnomedical use

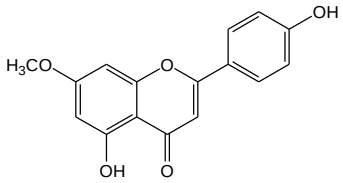
Acridocarpus chloropterus has not been reported as a traditional medicinal plant in Tanzania. However, ethnobotanical information from other countries reveal that plant species in the genus are used as remedies for African trypanosomiasis, gastro-intestinal disorders, paralysis and pemphigus (Bennet & Alarcon, 1994; Dalziel, 1937; Watt & Breyer-Brandwijk, 1962; Ghazanfar & Al-Sabahi, 1993). Consequently, leaves of *Acridocarpus orientalis* are used in Oman as a topical application for the treatment of paralysis (Bennet & Alarcon, 1994). The Tsonga and Shangana of South Africa use the powdered root of *Acridocarpus natalitius* as a purgative for colic pains, constipation and as an ointment in treating pemphigus (Dalziel, 1937). A decoction of the roots of *Acridocarpus plagiopterus* is used in Conakry, Guinea as a vermifuge and as a remedy for sleeping sickness (Ghazanfar & Al-Sabahi, 1993).

There are no previous phytochemical or pharmacological investigations reported on *A. chloropterus*. Literature search for previous phytochemical investigations on the genus only revealed phytochemical and pharmacological information on *Acridocarpus vivy.* Recently, bioassay-guided fractionation of the cytotoxic methanolic stem bark extract from *A. vivy* led to the isolation of 8 cytotoxic triterpenes together with 2 non-cytotoxic flavonoids (Cao *et al*, 2004).

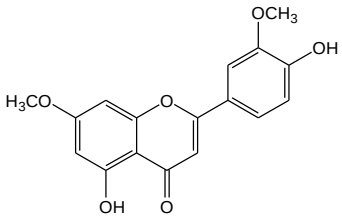


Acridocarpusic acid C (**117**) showed the highest cytotoxic activity against the A2780 human ovarian cancer cell line (CC_{50} 0.7 µg/ml) *in vitro*. The remaining seven triterpenes

showed mild cytotoxic activity (CC_{50} 5.9-15.9 µg/ml). The compounds isolated include acridocarpusic acid A (**118**) (CC_{50} 15.9 µg/ml), acridocarpusic acid B (**119**) (CC_{50} 11.6 µg/ml), acridocarpusic acid D (**120**) (CC_{50} 5.9 µg/ml), acridocarpusic acid E (**121**) (CC_{50} 15.3 µg/ml), moronic acid (**122**) (CC_{50} 13.1 µg/ml), ursolic acid (**123**) (CC_{50} 9.2 µg/ml) and oleanolic acid (**124**) (CC_{50} 8.0 µg/ml) plus the two inactive flavonoids, 4', 5-dihydroxy-7-methoxyflavone (genkwanin) (**125**) and 4', 5-dihydroxy-3', 7-methoxyflavone (diosmetin) (**126**), were inactive (Cao *et al*, 2004).



125



126

Ursolic acid (**123**) exhibits anti-plasmodial activity with 34-97% suppression of parasitaemia in *P. berghei* experimentally infected mice at 15-16 mg/kg/day (Amusan *et al.*, 1996). Oleanolic acid (**124**) exhibits anti-leishmanial activity against *L. donovani* promastigotes (IC_{50} 18.8 µM) (Chan-Bacab & Peña Rodríguez, 2001). 4', 5-Dihydroxy-7-methoxyflavone (genkwanin) (**125**) and 4', 5-dihydroxy-3', 7-methoxyflavone (diosmetin) (**126**) exhibited *in vitro* anti-protozoal activity against *L. donovani*, *T. b. rhodesiense* and *T. cruzi*. (Tasdemir *et al.*, 2006). Genkwanin (**125**) showed mild anti-leishmanial activity against *L. donovani* amastigotes (IC_{50} 9.4 µg/ml), mild anti-trypanosomal activity against *T. b. rhodesiense* (IC_{50} 8.0 µg/ml) *in vitro* but was inactive against *T. cruzi* (IC_{50} >30 µg/ml). Similarly, diosmetin (**126**) exhibited mild anti-leishmanial activity against *L. donovani* amastigotes (IC_{50} 7.1 µg/ml), mild anti-trypanosomal activity against *T. b. rhodesiense* (IC_{50} 6.1 µg/ml) *in vitro* but was inactive against *T. cruzi* (IC_{50} >30 µg/ml) (Tasdemir *et al.*, 2006).

Acridocarpus chloropterus was chosen for phytochemical investigations due to the use of plants belonging to the genus *Acridocarpus* in traditional folk medicine for various ailments including the African trypanosomiasis and lack of previous phytochemical reports. To our knowledge, there were no previous phytochemical investigations reported on *Acridocarpus* species by the time this project was initiated.

2.3 Bioassay-guided isolation

Contemporary drug discovery strategy from plants has mainly relied on bioactivity-guided isolation methods. Bioassay-guided isolation integrates the processes of separation of compounds in a mixture, using various analytical methods, directed by results obtained from biological testing. Succinctly, the initial steps in the process necessitate that many crude plant extracts are evaluated in a biological assay or panel of assays (a screen), and those exhibiting good *in vitro* activity ($IC_{50} \leq 1.0$ μg/ml) and favourable selectivity indices (SI) are moved to the next step which involves chromatographic fractionations and biological testing until the bioactive compound is isolated. Bioactivity-guided isolation methods have led to the discovery of many important drugs including the anti-cancer agents: taxol (**29**) from *Taxus brevifolia* and camptothecin (**25**) from *Camptotheca acuminata* (Wani *et al.*, 1971; Wall *et al.*, 1996; Kinghorn, 1994).

CHAPTER THREE

PHARMACOLOGICAL INVESTIGATION OF SELECTED TANZANIAN ANTI-PROTOZOAL PLANTS

3.1 Crude plant extracts

The yields of plant extracts from sequential solvent extractions are summarized in table 1.

Table 1: Yields of the solvent of selected anti-protozoal plants

Plant species	Plant part	Amount (kg)	Crude extract (g)		
			PE	CH_2Cl_2	MeOH
Annickia kummeriae	L	1.12	19.32	62.38	82.54
	ST	1.55	18.49	82.55	160.15
	RT	1.77	50.02	174.25	249.92
Acridocarpus chloropterus	L	0.88	43.81	69.19	102.25
	ST	1.25	42.12	49.29	67.33
	RT	1.46	18.90	37.50	71.54
Pseudospondias microcarpa	ST	0.80			42.17
	RT	0.61			38.65
Drypetes natalensis	ST	1.20			64.79
	RT	0.99			67.15

L – leaves, ST – stem bark, RT – root bark, PE – petroleum ether, CH_2Cl_2 – dichloromethane, MeOH - methanol

3.2 Anti-protozoal assays

3.2.1 Anti-plasmodial activity

Table 2 summarizes the *in vitro* anti-plasmodial activity of extracts against the multi-drug resistant *P. falciparum* K1 strain.

Table 2: Anti-plasmodial activity (IC_{50}) of extracts of selected Tanzanian medicinal plants

Plant species	Plant part	$IC_{50} \pm$ S.E (µg/ml)		
		PE	CH_2Cl_2	MeOH
Annickia kummeriae	L	4.65 ± 0.15	6.70±1.53	0.12±0.01
	ST	1.85 ± 0.55	0.31±0.05	0.31±0.04
	RT	2.51 ± 0.11	0.36±0.06	0.35±0.04
Acridocarpus chloropterus	L	15.87±1.28	5.50±2.7	15.43±1.42
	ST	16.68±0.10	7.23±1.45	N.D
	RT	10.81±0.38	5.06±0.92	43.83±1.27
Pseudospondias microcarpa	ST	N.D	N.D	1.13±0.16
	RT	N.D	N.D	4.33±1.44
Drypetes natalensis	ST	N.D	N.D	1.42±0.54
	RT	N.D	N.D	1.06 ± 0.20

L – leaves, ST – stem bark, RT – root bark, PE – petroleum ether, CH_2Cl_2 – dichloromethane, MeOH – methanol, N.D – not determined, IC_{50} 0.063±0.03 and 0.002 ± 0.0001 µg/ml for chloroquine and artemisinin, respectively.

The definition of the anti-plasmodial activity used: IC_{50} < 0.5 µg/ml - strong activity; 0.5-5.0 µg/ml – moderate activity; 5.0-10 µg/ml – mild activity and IC_{50} > 10 µg/ml – inactive. CQ and artemisinin (IC_{50} 0.063±0.03 µg/ml and 0.002±0.0001 µg/ml, respectively) were used as standards. Of the 21 plant extracts tested, 5 (23.8%), from the leaves, stem and root bark of *A. kummeriae* (Annonaceae) showed strong activity (IC_{50} 0.12±0.01-0.36±0.06 µg/ml). Seven (33.3%) extracts revealed moderate anti-plasmodial activity (IC_{50} 1.06±0.20–4.65±0.15 µg/ml) against *P. falciparum* K1 strain, while 4 (19.1%) were mildly active (IC_{50} 5.06±0.92 and 7.23±1.45 µg/ml). The remaining 5 (23.8%) extracts were inactive against *P. falciparum* K1 strain (IC_{50} 10.81±0.38 - 43.83±1.27 µg/ml). The leaves, stem and root bark of *A. kummeriae* (Annonaceae) (IC_{50} 0.12±0.01 - 0.36±0.06 µg/ml), the stem and root bark of *D. natalensis* (Euphorbiaceae) (IC_{50} 1.42±0.54 and 1.06±0.20 µg/ml, respectively) and the stem root bark of *P. microcarpa* (Anacardiaceae) (IC_{50} 1.13±0.16 µg/ml) had the best anti-plasmodial activity. The IC_{50} of the most active extracts were compared with that of CQ (IC_{50} 0.063±0.03 µg/ml) and artemisinin (IC_{50} 0.002±0.00 µg/ml). The methanolic extract of *A. kummeriae* leaves (1.9 fold and 60.0 fold lower activities than CQ and artemisinin, respectively) was the most promising. The rest were far less active than the standard drugs (Table 3).

Table 3: Comparison of the anti-plasmodial activity (IC_{50}) of solvent extracts of selected Tanzanian medicinal plants with chloroquine and artemisinin

Plant species	Part	Extract	$\frac{IC_{50}\text{ extract}}{IC_{50}\text{ CQ}}$	$\frac{IC_{50}\text{ extract}}{IC_{50}\text{ Art}}$
Annickia kummeriae	L	MeOH	1.9	60.0
	ST	CH_2Cl_2	4.9	155.0
	ST	MeOH	4.9	155.0
	RT	CH_2Cl_2	5.7	180.0
	RT	MeOH	5.6	175.0
Pseudospondias microcarpa	ST	MeOH	17.9	565.0
Drypetes natalensis	ST	MeOH	22.5	710.0
	RT	MeOH	16.8	530.0

L – leaves, ST – stem bark, RT – root bark, PE – petroleum ether, CH_2Cl_2 – dichloromethane, MeOH – methanol, CQ – chloroquine, Art - artemisinin

The extracts of leaves, stem and root bark of *A. kummeriae* were of particular interest due to the strong anti-plasmodial activity which rendered them good candidates for further scientific investigations.

3.2.2 Anti-trypanosomal activity

Table 4 summarizes the *in vitro* anti-trypanosomal activity of the extracts of selected Tanzanian medicinal plants against *T. b. rhodesiense* STIB 900 strain.

Table 4: Anti-trypanosomal activity (IC_{50}) of extracts of Tanzanian medicinal plants

Plant species	Part	$IC_{50} \pm$ S.E (µg/ml)		
		PE	CH_2Cl_2	MeOH
Annickia kummeriae	L	21.70±3.47	23.50±1.90	2.50±0.19
	ST	7.40±0.53	2.50±0.24	2.50±0.10
	RT	14.10±0.45	2.80±0.23	2.30±0.43
Acridocarpus chloropterus	L	47.40±1.51	29.40±1.90	42.90±1.30
	ST	46.40±0.94	35.80±1.46	N.D
	RT	40.20±2.42	28.30±0.8	68.20±0.80
Pseudospondias microcarpa	ST	N.D	N.D	11.60±1.74
	RT	N.D	N.D	5.40±0.64
Drypetes natalensis	ST	N.D	N.D	10.70±1.99
	RT	N.D	N.D	12.10±0.38

L – leaves, ST – stem bark, RT – root bark, PE – petroleum ether, CH_2Cl_2 – dichloromethane, MeOH – methanol, N.D – not determined, IC_{50} 0.002±0.0001 µg/ml for melarsoprol

The definition of the antitrypanosomal activity used: IC_{50} < 1.0 µg/ml – strong activity, 1.0-5.0 µg/ml – moderate activity, 5.0-10 µg/ml mild activity, and IC_{50} > 10 µg/ml – inactive. Melarsoprol (IC_{50} 0.002±0.0001 µg/ml) was used as the standard drug. Of the 21 plant extracts tested, 14 (66.7%) were inactive against *T. b. rhodesiense* (IC_{50} 10.70±1.99 - 68.20±0.80 µg/ml) while 2 (9.5%) were mildly active (IC_{50} 5.40±0.64 – 7.40±0.53 µg/ml). Five extracts (23.8%) showed moderate activity (IC_{50} 2.30±0.43 - 2.80±0.23 µg/ml). The anti-trypanosomal activity (IC_{50}) of the six most active extracts were compared with melarsoprol (IC_{50} 0.002±0.0001 µg/ml) revealing much lower activity (862.07 and 1,862.07 fold lower than melarsoprol) (Table 5).

Table 5: Comparison of anti-trypanosomal (IC_{50}) of extracts of selected Tanzanian medicinal plants with Melarsoprol

Plant species	Part	Extract	$\frac{IC_{50}\ extract}{IC_{50}\ Mel}$
Annickia kummeriae	L	MeOH	862.07
	ST	CH_2Cl_2	862.07
	ST	MeOH	862.07
	RT	$CHCl_3$	965.52
	RT	MeOH	793.10
Pseudospondias microcarpa	RT	MeOH	1,862.07

L – leaves, ST – stem bark, RT – root bark, PE – petroleum ether, CH_2Cl_2 – dichloromethane, MeOH – methanol, Mel - melarsoprol

Five extracts (23.8%): leaves, stem and root bark of *A. kummeriae* (Annonaceae) (IC_{50} 2.30±0.43-2.80±0.23 µg/ml) were of particular interest due to the moderate anti-trypanosomal activity which rendered them good candidates for further scientific investigations.

3.2.3 Anti-leishmanial activity

Table 6 summarizes the *in vitro* anti-leishmanial activity of plant extracts against *L. donovani* axenic MHOM-ET-67/82 strain.

Table 6: Anti-leishmanial activity (IC_{50}) of extracts of selected Tanzanian medicinal plants

Plant species	Part	IC_{50} ± S.E (µg/ml)		
		PE	CH_2Cl_2	MeOH
Annickia kummeriae	L	>30.0	>30.0	9.25±0.54
	ST	9.74±1.82	18.00±0.42	19.41±1.66
	RT	14.55±1.1	9.79±2.5	12.38±1.12
Acridocarpus chloropterus	L	>30.0	11.66±1.51	28.80±1.21
	ST	>30.0	14.57±1.36	N.D
	RT	>30.0	>30.0	>30.0
Pseudospondias microcarpa	ST	N.D	N.D	29.9±4.19
	RT	N.D	N.D	>30.0
Drypetes natalensis	ST	N.D	N.D	19.00±3.27
	RT	N.D	N.D	29.70±3.52

L – leaves, ST – stem bark, RT – root bark, PE – petroleum ether, CH_2Cl_2 – dichloromethane, MeOH – methanol, N.D – not determined, IC_{50} 0.11±0.001 µg/ml for miltefosine

The definition of the anti-leishmanial activity used: IC_{50} < 1.0 µg/ml – strong activity; 1.0 - 5.0 µg/ml – moderate activity; 5.0 - 10.0 µg/ml – mild activity; and IC_{50} > 10 µg/ml – inactive. Miltefosine (IC_{50} 0.11±0.001 µg/ml) was used as the standard drug.

Eighteen (85.7%) out of the 21 extracts tested were inactive against axenic *L. donovani* amastigotes (IC_{50} 11.66±1.51->30 µg/ml) while 3 (14.3%) exhibited mild anti-leishmanial activity (IC_{50} 9.25±0.54-9.79±2.5 µg/ml). *Annickia kummeriae* leaves (IC_{50} 9.25±0.54 µg/ml), stem bark (IC_{50} 9.74±1.82 µg/ml) and root bark (IC_{50} 9.79±2.5 µg/ml) were the most active extracts. The anti-leishmanial activity (IC_{50}) of the most active extracts were compared with miltefosine (IC_{50} 0.11±0.001 µg/ml) revealing very low potential (77.08 and 81.58 fold lower than miltefosine) (Table 7).

Table 7: Comparison of anti-leishmanial activity (IC_{50}) of extracts of selected Tanzanian medicinal plants with Miltefosine

Plant species	Plant part	Extract	$\frac{IC_{50}\ extract}{IC_{50}\ Milt}$
Annickia kummeriae	L	MeOH	77.08
	ST	PE	81.17
	RT	CH_2Cl_2	81.58

L – leaves, ST – stem bark, RT – root bark, PE – petroleum ether, CH_2Cl_2 – dichloromethane, MeOH – methanol, Milt - miltefosine

3.3 Cytotoxicity

3.3.1 Cytotoxicity activity (CC_{50})

Table 8 shows the *in vitro* cytotoxicity of extracts of selected Tanzanian medicinal plants against rat skeletal myoblast cells (L-6).

Table 8: Cytotoxicity (CC_{50}) of extracts of selected Tanzanian medicinal plants

Plant species	Part	$CC_{50} \pm$ S.E (µg/ml)		
		PE	CH_2Cl_2	MeOH
Annickia kummeriae	L	72.0±3.10	70.60±2.56	30±0.74
	ST	22.0±3.00	58.20±2.80	53.80±2.40
	RT	34.10±3.20	10.50±0.62	61.40±3.97
Acridocarpus chloropterus	L	>90	77.30±2.82	80.80±4.03
	ST	88.10±1.90	82.50±4.20	ND
	RT	>90	64.70±6.90	>90
Pseudospondias microcarpa	ST	ND	ND	>90
	RT	ND	ND	>90
Drypetes natalensis	ST	ND	ND	88.90±1.1
	RT	ND	ND	19.0±0.38

L – leaves, ST – stem bark, RT – root bark, PE – petroleum ether, CH_2Cl_2 – dichloromethane, MeOH – methanol, N.D – not determined, CC_{50} 0.009 ± 0.00001 µg/ml for podophyllotoxin

The definition of the cytotoxicity used: CC_{50} < 1.0 µg/ml – high toxicity; CC_{50} 1.0-10.0 µg/ml – moderate; CC_{50} 10.0-30.0 µg/ml – mild toxicity; and CC_{50} > 30 µg/ml – non toxic. Podophyllotoxin (CC_{50} 0.009±0.00003 µg/ml) was used as standard toxin.

None of the extracts tested showed high cytotoxic activity. Seventeen (81.0%) out of the 21 extracts tested exhibited low or non-cytotoxicity against rat skeletal myoblast cells (L-6) (CC_{50} 34.10±3.20 - >90 µg/ml) while 4 (19.0%) of the extracts were mildly cytotoxic (CC_{50} 10.50±0.62 – 22.0±3.00 µg/ml). The cytotoxicity (CC_{50}) of the four most toxic extracts were compared with podophyllotoxin (CC_{50} 0.009±0.0003 µg/ml) revealing high potential (1,166.7-2,444.4 fold lower than podophyllotoxin (Table 9).

Table 9: Comparison of cytotoxicity (CC_{50}) of extracts of selected Tanzanian medicinal plants with podophyllotoxin

Plant species	Part	Extract	$\frac{IC_{50}\ extract}{IC_{50}\ Pdx}$
Annickia kummeriae	L	MeOH	2,444.4
	ST	PE	1,733.3
	RT	CH_2Cl_2	1,166.7
Drypetes natalensis	RT	MeOH	2,111.1

L – leaves, ST – stem bark, RT – root bark, PE – petroleum ether, CH_2Cl_2 – dichloromethane, MeOH – methanol, Pdx - podophyllotoxin

3.3.2 Selectivity indices

Selectivity indices (SI) were calculated using the formula:

$$SI = \frac{CC_{50}}{IC_{50}}$$

Table 10 is a summary of the *in vitro* anti-protozoal activity, cytotoxicity and selectivity indices (SI) of extracts of selected Tanzanian medicinal plants.

Table 10: Anti-protozoal activity, cytotoxicity and selectivity indices of extracts of selected Tanzanian medicinal plants

	P. falciparum K1		*T.b. rhodesiense*		*L. donovani*	
Plant species, part & extract	IC_{50} (µg/ml)	SI	IC_{50} (µg/ml)	SI	IC_{50} (µg/ml)	SI
A. kummeriae						
L (PE)	4.65±0.15	15.48	21.70±3.47	3.32	>30	>2.40
L (DCM)	6.70±1.53	10.54	23.50±1.90	3.00	>30	>2.35
L (MeOH)	0.12±0.01	250.00	2.50±0.19	12.00	9.25±0.54	3.2
ST (PE)	1.85±0.55	11.89	7.40±0.53	2.97	9.74±1.82	2.26
ST (DCM)	0.31±0.05	187.74	2.50±0.24	23.28	18.00±0.42	3.23
ST (MeOH)	0.31±0.04	173.55	2.50±0.10	21.52	19.41±1.66	2.77
RT (PE)	2.51±0.11	13.59	14.10±0.45	2.42	14.55±1.1	2.34
RT (DCM)	0.36±0.06	29.17	2.80±0.23	3.75	9.79±2.5	1.07
RT (MeOH)	0.35±0.04	175.43	2.30±0.43	26.70	12.38±1.12	4.94
A. chloropterus						
L (PE)	15.87±1.28	>5.67	47.40±1.51	>1.9	>30	>3.00
L (DCM)	5.50±2.7	14.05	29.40±1.90	2.63	11.66±1.51	6.63
L (MeOH)	15.43±1.42	5.23	42.90±1.30	1.88	28.80±1.21	2.81
ST (PE)	16.68±0.10	5.28	46.40±0.94	1.90	>30	>2.94
ST (DCM)	7.23±1.45	11.41	35.80±1.46	2.30	14.57±1.36	5.66
RT (PE)	10.81±0.38	8.33	40.20±2.42	2.24	>30	>3.00
RT (DCM)	5.06±0.92	12.79	28.30±0.80	2.29	>30	>2.16
RT (MeOH)	43.83±1.27	2.05	68.20±0.80	1.32	>30	>3.00
P. microcarpa						
ST (MeOH)	4.33±1.44	20.79	5.40±0.64	7.26	29.9±4.19	>3.00
RT (MeOH)	1.13±0.16	79.65	11.60±1.74	7.38	>30	>5.45
D. natalensis						
ST (MeOH)	1.42±0.54	62.61	10.70±1.99	16.46	19.00±3.27	2.9
RT (MeOH)	1.06±0.20	17.92	12.10±0.38	1.64	29.7±3.52	0.64

L – leaves, ST – stem bark, RT – root bark, PE – petroleum ether, DCM – dichloromethane, MeOH – methanol, IC_{50} 0.063±0.03 and 0.002 ± 0.0001 µg/ml for chloroquine and artemisinin, respectively.

The extracts with anti-plasmodial activity exhibited wide selectivity range (SI 10.54-250.0) while narrow ranges were observed for anti-trypanosomal activity (SI 1.32-26.70) and anti-leishmanial activity (SI 0.64-6.63). Of the 21 extracts tested, 5 (28.6%) exhibited promising anti-plasmodial activity against *P. falciparum* K1 strain (IC_{50} < 1.0 µg/ml, SI 29.17-250.0). Methanolic leaf extract (IC_{50} 0.12±0.01 µg/ml, SI 250.0), dichloromethane stem bark (IC_{50} 0.31 ± 0.05 µg/ml, SI 187.7), methanolic stem bark extract (IC_{50} 0.31±0.04 µg/ml, SI 173.6), dichloromethane root bark (IC_{50} 0.36 ± 0.06 µg/ml, SI 29.20) and methanolic root bark (IC_{50} 0.35±0.04 µg/ml, SI 170.60) extracts of *A. kummeriae* (Annonaceae) are the most active followed by methanolic root bark extract of *P. microcarpa* (IC_{50} 1.13±0.16 µg/ml, SI 79.6) plus methanolic root bark and stem bark extract of *Drypetes natalensis* (IC_{50} 1.06±0.20 µg/ml and 1.42±0.54 µg/ml; SI 17.9 and 63.3) were of particular interest due to the high anti-plasmodial activity. It is interesting to note that the activity (IC_{50}) of the methanolic leaf extract of *A. kummeriae* is comparable to chloroquine (IC_{50} 0.063±0.03 µg/ml) and artemisinin (IC_{50} 0.002±0.00001 µg/ml), and is 1.9 and 60.00 fold lower, respectively.

Five out of 9 extracts of *A. kummeriae* exhibited moderate anti-trypanosomal activity against *T. b. rhodesiense* (IC_{50} <3.0 µg/ml) and favourable selectivity indices (42.9-68.2). These include: dichloromethane root bark (IC_{50} 2.80±0.23 µg/ml, SI 3.75), methanolic stem bark (IC_{50} 2.50 µg/ml, SI 21.52), dichloromethane stem bark (IC_{50} 2.50±0.24 µg/ml, SI 23.28) methanolic root bark (IC_{50} 2.30±0.43 µg/ml, SI 26.70) and methanolic leaf (IC_{50} 2.50±0.19 µg/ml, SI 12.0) extracts.

3.4 Selection of a bioactive crude extract for the isolation of anti-plasmodial compounds

Plant extracts from the leaves, stem and root-bark of *A. kummeriae* (Annonaceae) (IC_{50} 0.12±0.01-0.36±0.06 µg/ml), stem and root bark of *D. natalensis* (Euphorbiaceae) (IC_{50} 1.06±0.20-1.42±0.54 µg/ml), root bark of *P. microcarpa* (Anacardiaceae) (IC_{50} 1.13±0.16 µg/ml) showed promising anti-plasmodial activity (Table 10). Due to the need to isolate compounds with greater probability for the discovery of drug candidates or leads, selections were made based on the level of anti-plasmodial activity and selectivity indices. Therefore the methanolic extract of *A. kummeriae* leaves was selected for further investigation based on the following reasons:

1. Highest *in vitro* anti-plasmodial activity (IC_{50} 0.12±0.01 µg/ml) against multiple drug resistant *P. falciparum* K1 strain.

2. Low cytotoxicity activity (CC_{50} 30±0.74 µg/ml) hence good selectivity (SI 250.0).
3. Absence of exhaustive phytochemical reports on *A. kummeriae*: only two compounds isolated previously (Muhie, 1996).

The methanolic extract of *A. kummeriae* leaves (15.0 g) was fractionated using a stepwise elution by high speed counter-current chromatography (HSCCC) in a biphasic solvent system ($CHCl_3$-MeOH-0.2 M HCl 7:3:4). Seventeen HSCCC fractions were obtained of which eight (47.1%) exhibited strong anti-plasmodial activity against *P. falciparum* K1 strain (IC_{50} 0.05±0.01-0.13±0.02 µg/ml) and excellent selectivity (SI 933.3-1,800.0 (Table 11). Three HSCCC fractions (17.6%) showed good activity (IC_{50} 0.45±0.15-0.87±0.1 µg/ml) and satisfactory selectivity (SI 22.9-145.2) while the remaining 6 (35.3%) exhibited moderate anti-plasmodial activity (IC_{50} 1.0±0.22-5.0±0.31 µg/ml) and moderate selectivity (SI 18.0-90.0).

Table 11: Anti-plasmodial activity (IC_{50}) and cytotoxicity (CC_{50}) of HSCCC fractions of *Annickia kummeriae* methanolic leaf extract

Fraction	Wt (mg)	IC_{50} (µg/ml)	CC_{50} (µg/ml)	SI	$\frac{IC_{50}\ fr.}{IC_{50}\ CQ}$	$\frac{IC_{50}\ fr.}{IC_{50}\ Art}$	$\frac{IC_{50}\ fr.}{IC_{50}\ Pdx}$
AKLM	15,000	0.12±0.01	30.0±0.8	250	1.9	60	3,333
AKLM 1	562	5.0±0.31	>90.0	>18	79.4	2500	>10,000
AKLM 2	2,999	0.87±0.1	20.0±3.3	23	13.8	435	2,222
AKLM 3	1,534	3.01±0.81	78.0±5.4	26	47.8	1,505	8,667
AKLM 4	157	1.34±0.33	76.0±1.44	57	21.3	670	8,444
AKLM 5	249	3.6±0.2	>90.0	>25	57.1	1,800	>10,000
AKLM 6	427	0.45±0.15	59.0±1.5	131	7.1	225	6,556
AKLM 7	165	0.11±0.02	>90.0	>818	1.7	55	>10,000
AKLM 8	221	0.09±0.04	>90.0	>1,000	1.4	45	>10,000
AKLM 9	680	0.06±0.02	>90.0	>1,500	1.0	30	>10,000
AKLM 10	1,295	0.05±0.02	>90.0	>1,800	0.8	25	>10,000
AKLM 11	1,679	0.05±0.01	>90.0	>1,800	0.8	25	>10,000
AKLM 12	1,056	0.06±0.03	>90.0	>1,500	1.0	30	>10,000
AKLM 13	878	0.62±0.4	>90.0	>145	9.8	310	>10,000
AKLM 14	948	1.0±0.22	>90.0	>90	15.9	500	>10,000
AKLM 15	1,232	0.13±0.02	>90.0	>692	2.1	65	>10,000
AKLM 16	416	0.09±0.03	84.0±3.91	933	1.4	45	9,333
AKLM 17	498	1.67±0.43	>90.0	>54	26.5	835	>10,000

AKLM - *Annickia kummeriae* leaves methanolic extract, *P. falciparum* K1 used for anti-plasmodial assays, fr – fraction, rat myoblast L-6 cells used for cytotoxicity assays, CQ - chloroquine (IC_{50} 0.063 ± 0.034 µg/ml), Art - artemisinin (IC_{50} 0.002 ± 0.00001 µg/ml), Pdx - podophyllotoxin (IC_{50} 0.009 ± 0.003 µg/ml).

The anti-plasmodial activity (IC_{50}) and cytotoxicity (CC_{50}) of the seventeen fractions were compared with the standard drugs: chloroquine (IC_{50} 0.063±0.034 µg/ml), artemisinin (IC_{50} 0.002±0.00001 µg/ml) and podophyllotoxin (IC_{50} 0.009±0.003 µg/ml). Fractions AKLM 8-

12 (IC_{50} 0.05±0.01-0.09±0.04 µg/ml, SI 1,000.0-1,800.0) were of particular interest since the anti-plasmodial activity was 0.8-1.4 and 25-45 fold lower than CQ and artemisinin, respectively, and non-cytotoxic. Others with promising activities were: AKLM 16 (IC_{50} 0.09±0.03 µg/ml, SI 933.3, 1.4 and 45 fold lower than CQ and artemisinin, respectively, and non-cytotoxic), AKLM 7 (IC_{50} 0.11±0.02 µg/ml, SI 818.2; 1.7 and 55 fold lower than CQ and artemisinin, respectively, and non-cytotoxic), and AKLM 6 (IC_{50} 0.45±0.15 µg/ml, SI 131.1, 7.1 and 225 fold lower than CQ and artemisinin, respectively, and non-cytotoxic). The HSCCC fraction AKLM 2 (IC_{50} 0.87±0.1 µg/ml, SI 22.9) contained 20% (2.999 g) of the recovered materials. Due to the high weight of the fraction, it was re-fractionated on silica gel 60 by column chromatography (CC) (EtOAc-*n*-C_6H_{14}; MeOH-EtOAc; MeOH-$CHCl_3$). A total of 408 x 50 ml CC sub-fractions were collected and combined into 11 portions based on the similarity of the retention factors (R_f) of the compounds in thin layer chromatography (TLC). Table 12 shows the anti-plasmodial activity and selectivity indices of the combined fractions from CC.

Table 12: Anti-plasmodial activity (IC_{50}) and cytotoxicity (CC_{50}) of combined sub-fractions of AKLM 2

CC Fraction	Wt (mg)	IC_{50} (µg/ml)	CC_{50} (µg/ml)	SI	IC_{50} fr. / IC_{50} CQ	IC_{50} fr. / IC_{50} Art	CC_{50} fr. / CC_{50} Pdx
AKLM 2	2,500	0.90±0.11	21.0±3.87	23.3	14	450	3,500
AKLM 2.1	15.3	5.0±1.31	>90	18.0	78	2,500	>15,000
AKLM 2.2	26.9	1.09±0.26	79.1±7.60	72.6	17	545	13,183
AKLM 2.3	57.6	4.11±0.29	53.1±9.20	12.9	64	2,055	8,850
AKLM 2.4	98.7	1.16±0.18	13.8±1.80	11.9	18	580	2,300
AKLM 2.5	126.1	3.63±0.04	24.6±3.30	6.8	57	1,815	4,100
AKLM 2.6	115.7	1.23±0.31	39.5±2.20	32.1	19	615	6,583
AKLM 2.7	239.0	3.41±0.48	85.4±4.60	25.0	53	1,705	14,233
AKLM 2.8	478.3	5.0±0.53	>90	18.0	78	2,500	>15,000
AKLM 2.9	351.8	2.40±0.57	56.7±8.00	23.6	38	1,200	9,450
AKLM 2.10	301.9	0.89±0.20	35.3±5.31	39.7	14	445	5,883
AKLM 2.11	672.8	0.64±0.34	44.7±4.45	69.8	10	320	7,450

AKLM-*Annickia kummeriae* leaves methanolic extract, *P. falciparum* K1 used for anti-plasmodial assays, fr – fraction, rat myoblast L-6 cells used for cytotoxicity assays, CQ - chloroquine (IC_{50} 0.063±0.034 µg/ml), Art - artemisinin (IC_{50} 0.002±0.00001 µg/ml), Pdx - podophyllotoxin (IC_{50} 0.009±0.003 µg/ml).

Of the eleven CC fractions, 2 showed high anti-plasmodial activity against *P. falciparum* K1 strain (IC_{50} 0.64±0.34-0.89±0.20 µg/ml and satisfactory selectivity (SI 39.7-69.8). The remaining 9 fractions exhibited moderate anti-plasmodial activity (IC_{50} 1.09±0.26-5.0±0.53 µg/ml) and poor to satisfactory selectivity (SI 11.9-72.6). The anti-plasmodial activity (IC_{50}) of the eleven fractions was compared with the standard drugs: CQ (IC_{50} 0.063±0.034 µg/ml), artemisinin (IC_{50} 0.002±0.0001 µg/ml) and podophyllotoxin (CC_{50} 0.009±0.00

µg/ml). The fractions of particular interest were: AKLM 2.10 (IC_{50} 0.89±0.20 µg/ml; SI 69.8; 13.9 and 445 fold lower than CQ and artemisinin, respectively, and non-cytotoxic) and AKLM 2.11 (IC_{50} 0.64±0.34 µg/ml, SI 69.8; 10 and 320 fold lower than CQ and artemisinin, respectively and non-cytotoxic). The fractions were further purified to single compounds or inseparable mixtures, identified and bioassayed for anti-protozoal activity and cytotoxicity.

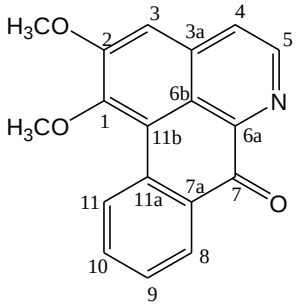
CHAPTER FOUR

IDENTIFICATION OF ANTI-PROTOZOAL CONSTITUENTS OF *ANNICKIA KUMMERIAE* (ENGL. & DIELS) SETTEN & MAAS

4.1 Isolation and identification

4.1.1 Lysicamine (127)

Repeated column chromatography (SiO_2, *n*-C_6H_{14}-EtOAc 1:1, EtOAc-MeOH 80:20) of AKLM 2.10 (scheme 1) from the methanolic extract of leaves *A. kummeriae* (IC_{50} 0.89±0.20 µg/ml, SI 39.7) gave 18 x 50 ml fractions which were combined into six based on retention factor (R_f)of the compounds on TLC. The 5th fraction was re-chromatographed (Sephadex LH-20, MeOH-$CHCl_3$ 1:1) and purified by re-crystallization (MeOH) to give lysicamine (**127**) (10.21 mg) as yellow needles (m.p. 209-211 °C, decomposed) which gave positive reaction for alkaloids with Dragendorff reagent.



127

The structure was established on the basis of 1D (^{1}H) and 2D-NMR experiments (HMQC, COSY, NOESY and HMBC), (Table 13-14, Appendix 1a-e) and MS data (Appendix 1f).

Table 13: 1D and 2D ^{1}H NMR (600 MHz, CD_3OD) spectral data of lysicamine (**127**)

Position	δ_{obs}	J_{obs}(Hz)	COSY	NOESY	δ_{lit}	J_{lit} (Hz)
3	7.57 (1H, *s*)			H-4	7.27 (1H, *s*)	
4	8.07 (1H, *d*)	5.2	H-5	H-3	7.88 (1H, *d*)	5.2
5	8.77 (1H, *d*)	5.2	H-4		8.98 (1H, *d*)	5.2
8	8.48 (1H, *dd*)	9.0, 1.4	H-9		8.60 (1H, *dd*)	8.0, 1.4
9	7.63 (1H, *t*)	9.0, 1.2	H-8, H-7		7.63 (1H, *t*)	8.0, 1.1
10	7.86 (1H, *t*)	9.0, 1.4	H-9, H-11		7.83 (1H, *t*)	8.0, 1.4
11	9.26 (1H, *dd*)	9.0, 1.2	H-10	1-OCH_3	9.19 (1H, *dd*)	8.0, 1.1
1-OCH_3	4.13 (3H, *s*)			H-11	4.09 (3H, *s*)	
2-OCH_3	4.06 (3H, *s*)				4.18 (3H, *s*)	

Literature values in $CDCl_3$ (δ_{lit}) obtained from Chang et al., 2000.

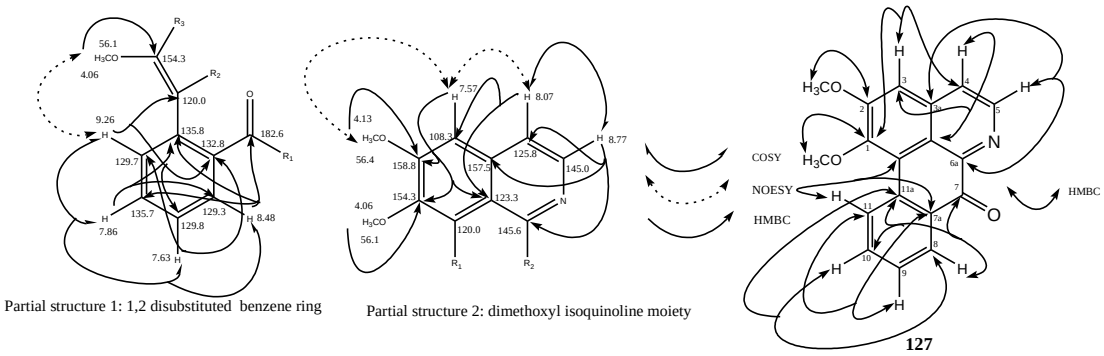
Table 14: 1D and 2D ^{13}C NMR (600 MHz, CD_3OD) data of lysicamine (**127**)

Position	δ_{obs}	HMQC	HMBC	δ_{lit}
1	145.3 (*s*)			145.3
2	152.8 (*s*)			152.0
3	108.3 (*d*)	7.57	C-1, C-6b, C-4,	106.4.4
3a	157.5 (*s*)			135.3
4	125.8 (*s*)	8.07	C-6b, C-3,	123.4
5	145.0 (*d*)	8.77	C-3a, C-6a	145.0
6a	155.6 (*s*)			156.7
6b	123.3 (*s*)			122.0
7	182.6 (*s*)			182.5
7a	132.8 (*s*)			132.0
8	129.3 (*d*)	8.48	C-7, C-10, C-11a	128.7
9	129.8 (*d*)	7.63	C-11, C-7a	128.7
10	135.7 (*d*)	7.86	C-8, C-11a	134.2
11	129.7 (*s*)	9.26	C-11b, C-7a, C-9	128.3
11a	135.8 (*s*)			134.7
11b	120.0 (*s*)			119.6
1-OCH_3	60.1 (*q*)	4.06	C-1	60.5
2-OCH_3	56.4 (*q*)	4.13	C-2	56.0

Literature values (δ_{lit} in $CDCl_3$,) obtained from Guinaudeau *et al*., 1983; δ_{obs} - ^{13}C NMR data and multiplicity deduced from HMQC and HMBC spectra

Analysis of the HMQC, HMBC, COSY and NOESY NMR data for **127** permitted the complete assignment of the ^1H and ^{13}C NMR spectra, including the two methoxy groups. The ^1H NMR spectrum of **127** exhibited resonances attributable to three aromatic systems: δ 9.26 (1H, *dd, J* 9.0, 1.2 Hz), 8.48 (1H, *dd, J* 9.0, 1.4 Hz), 7.86 (1H, *dd, J* 9.0, 1.4 Hz), 7.63 (1H, *dd, J* 9.0, 1.2 Hz), δ 8.77 (1H, *d, J* 5.2 Hz), 8.07 (1H, *d, J* 5.2 Hz) and 7.57 (1H, *s*) and two methoxyl groups: δ 4.13 (*s*,3H) and δ 4.06 (*s*,3H). A strongly deshielded signal at δ 9.26 (1H, *dd, J* 9.0, 1.2 Hz) formed part of a four-spin aromatic system with the other protons [δ 8.48 (1H, *d*, 1H, *J* 9.0, 1.4 Hz), 7.63 (1H, *d, J* 9.0, 1.2 Hz) and 7.86 (1H, *t, J* 9.0, 1.4 Hz)]. From the coupling constants (*J*) it was deduced that, the signal at δ 9.26 is *ortho* (*J* 9.0 Hz) to the one at δ 7.86 and *meta* (*J* 1.2 Hz) to the other at δ 7.63. The spectra further revealed the relationships of the proton signal at δ 8.48 to be *ortho* (*J* 9.0 Hz) to the one at δ 7.63 and *meta* (*J* 1.4 Hz) to the other at δ 7.86. The ^1H NMR and COSY spectrum further revealed the presence of an AB spin system [δ 8.77 (*d*, 1H, *J* 5.2 Hz) and 8.07 (*d*, 1H, *J* 5.2 Hz)] which is characteristic of H-4 and H-5 signals of oxo-aporphines (Tsai *et al*, 2008). COSY experiments confirmed the 3-bond interactions of H-4 and H-5; H-8 and H-9; H-9 and H-10 and H-10 and H-11 thus confirming the presence ortho disubstituted aromatic ring. The important 2D correlations for lysicamine (**127**) are summarized in Fig. 6.

Figure 6: Important 2D correlations for lysicamine (**127**)



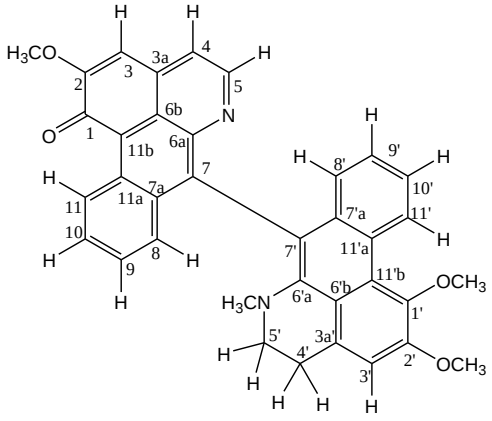
H-11 (δ 9.26) showed three-bond HMBCs to two aromatic quaternary carbon signals at δ 120.0 (C-11b) and 132.8 (C-7a) and a doublet at δ 129.8 (C-9). H-8 (δ 8.48) showed three-bond HMBCs to C-7 (δ 182.6), C-10 (δ 135.7) and C-11a (δ 135.8). H-10 (δ 7.86) showed three-bond HMBCs to C-8 (δ 129.3) and C-11a (δ 135.8). H-9 (δ 7.63) showed three-bond HMBCs to C-11 (δ 129.7) and C-7a (δ 132.8). NOESY spectrum revealed an interaction between H-11 (δ 9.26) and the 1-OCH_3 group (δ 4.06) which showed HMQC to the signal at δ 56.1 and a three-bond HMBC to C-1 (δ 154.3). These observations confirmed the presence of a 1, 2-disubstituted benzene ring. H-4 (δ 8.07) and H-5 (δ 8.77) exhibited HMQC correlations to the signals at δ 145.0 and 125.8, respectively. The HMBC spectrum of **127** showed three-bond $^{1}H \rightarrow ^{13}C$ intercations between H-4 (δ 8.07) and C-3 (δ 108.3) and C-6b (δ 123.3). H-5 (δ 8.77) showed three-bond HMBCs to C-3a (δ 135.7) and C-6a (δ 155.6) and a two-bond correlation to C-4 (δ 125.8). H-3 (δ 7.57) which exhibited HMQC to C-3 (δ 108.3) also showed HMBCs to C-2 (δ 152.8), C-1 (δ 145.3) and C-6b (δ 123.3) and a three-bond HMBCs to the quaternary methine carbon signal at δ 125.8 (C-4). 1-OCH_3 (δ 4.06) and 2-OCH_3 (δ 4.13) showed HMQC correlations with the quaternary carbon signals at δ 60.1 and 56.4, respectively. HMBCs were observed between 1-OCH_3 (δ 4.06) and C-1 (δ 145.3) while 2-OCH_3 (δ 4.13) had three-bond HMBC with C-2 (δ 152.8). The spectral data confirmed the presence of a dimethoxy-isoquinoline moiety and allowed unambiguous assignment of **127**.

The EI-MS showed the molecular ion peak at *m/z* 291 (100). Other characteristic peaks appeared at *m/z* 248, 233, 219, 188 and 177 corresponding to the formula $C_{18}H_{15}NO_3$. All the data for compound **127** were consistent with the reported values for lysicamine which was first isolated from *Lysichiton camtschatcense* (Araceae) (Katsui & Sato, 1966). Lysicamine (**127**) has been widely isolated from several plant species (Chang *et al*., 2000)

however; this is the first report on the presence of lysicamine (**127**) from *A. kummeriae* (Annonaceae).

4.1.2 Trivalvone (128)

Repeated column chromatography (SiO_2, *n*-C_6H_{14}-EtOAc 1:1, EtOAc-MeOH 75:25) of HSCCC AKLM 2.11 of the methanolic extract of *A. kummeriae* leaves (IC_{50} 0.64±0.34 µg/ml, SI 69.8) gave 23 x 50 ml fractions. Fractions 5-8 were combined and purified by PTLC (SiO_2, $CHCl_3$-MeOH-HCO_2H 98:1.8:0.2) to yield trivalvone (**128**) (8.10 mg) as brown crystals (m.p. 256-258°C) which gave positive reaction for alkaloids with Dragendorff's reagent.



128

The structure was established on the basis of 1D (^1H, ^{13}C, DEPT 135) and 2D-NMR experiments (HMQC, COSY and HMBC), Table 15-16, Appendix 2a-f) plus MS data (Appendix 2g). Unambiguous assignment of ^1H and ^{13}C NMR signals for **128** was done with the help of the HMQC and COSY whereas the connectivities of the molecular fragments were established by HMBC experiments.

Table 15: 1D and 2D ^1H NMR (500 MHz, $CDCl_3$) data of trivalvone (**128**)

Position	δ_{obs}	J_{obs}(Hz)	COSY	δ_{lit}	J_{lit} (Hz)
3	6.87 (1H, *s*)			6.87 (1H, *s*)	
4	7.54 (1H, *d*)	4.1	H-5	7.51 (1H, *d*)	4.0
5	8.90 (1H, *d*)	4.1	H-4	8.89 (1H, *d*)	4.0
8	7.76 (1H, *d*)	9.0, 2.1	H-9	7.75 (1H, *d*)	9.0, 2.0
9	7.35 (1H, *t*)	9.0, 2.1	H-8, H-10	7.35 (1H, *t*)	9.0, 2.0
10	7.85 (1H, *t*)	9.0, 2.1	H-9, H-11	7.83 (1H, *t*)	9.0, 2.0
11	10.20 (1H, *d*)	9.0, 2.1	H-10	10.20 (1H, *d*)	9.0, 2.0
3´	7.18 (1H, *s*)			7.17 (1H, *s*)	
4´	2.95 (2H, *m*)		H-5´	2.95 (2H, *m*)	
5´	3.26 (2H, *m*)		H-4´	3.26 (2H, *m*)	
8´	6.70 (1H, *d*)	9.0, 2.1	H-9´	6.89 (1H, *d*)	9.0, 2.0
9´	7.12 (1H, *t*)	9.0, 2.1	H-8´, H-10´	7.11 (1H, *t*)	9.0, 2.0
10´	7.43 (1H, *t*)	9.0, 2.1	H-9´, H-11´	7.42 (1H, *t*)	9.0, 2.0
11´	9.75 (1H, *d*)	9.0, 2.1	H-10´	9.75 (1H, *d*)	9.0, 2.0
2-OCH_3	4.07 (3H, *s*)			4.07 (3H, *s*)	
1´-OCH_3	4.01 (3H, *s*)			4.01 (3H, *s*)	

2′-OCH_3	4.07 (3H, *s*)	4.07 (3H, *s*)
N-CH_3	2.15 (3H, *s*)	2.15 (3H, *s*)

Literature values in $CDCl_3$ (δ_{lit}) obtained from Cortes *et al.*, 1990

The ^1H NMR (500 MHz, $CDCl_3$) spectrum revealed the presence of two 1, 2-disubstituted benzene ring residues as indicated by two parts of four-spin systems each. The presence of the first 1, 2-disubstituted benzene ring residue was deduced from ^1H NMR signal sets at δ 10.20 (1H, *dd*, *J* 9.0, 2.1 Hz), 7.76 (1H, *dd*, *J* 9.0, 2.1 Hz), 7.35 (1H, t, *J* 9.0, 2.1 Hz) and 7.85 (1H, t, *J* 9.0, 2.1 Hz); and δ 9.75 (1H, *dd*, *J* 9.0, 2.1 Hz), 6.70 (1H, *dd*, *J* 9.0, 2.1 Hz), 7.12 (1H, t, *J* 9.0, 2.1 Hz) and 7.43 (1H, t, *J* 9.0, 2.1 Hz). An AB spin system was observed for δ 8.89 (*d*, 1H, *J* 4.1 Hz) and δ 7.54 (*d*, 1H, *J* 4.1 Hz). Another aromatic signal at δ 6.87 (s, 1H) which is related in the molecular framework linking the first four spin system was observed in the ^1H NMR spectrum.

Table 16: 1D and 2D ^{13}C NMR (500 MHz, $CDCl_3$) data of trivalvone (**128**)

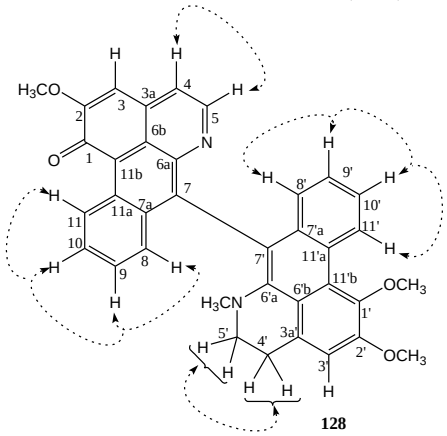
Position	δ	HMQC	HMBC	δ_{lit}
1	181.0 (*s*)			180.8
2	151.3 (*s*)			151.2
3	107.5 (*d*)	6.87	C-1, C-6b, C-4	107.3
3a	134.3 (*s*)			134.1
4	127.9 (*d*)	7.54	C-6b, C-3	127.8
5	151.0 (*d*)	8.90	C-3a, C-6a	150.8
6a	156.6 (*s*)			156.4
6b	122.6 (*s*)			122.5
7	134.0 (*s*)			133.8
7a	142.5 (*s*)			142.4
8	132.6 (*d*)	7.76	C-7, C-10, C-11a	132.4
9	128.7 (*d*)	7.35	C-11, C-7a	128.5
10	127.0 (*d*)	7.85	C-8, C-11a	126.8
11	121.9 (*d*)	10.20	C-11b, C-7a, C-9	121.7
11a	122.7 (*s*)			122.2
11b	136.2 (*s*)			136.0
1′	145.9 (*s*)			145.7
2′	150.6 (*s*)			150.5
3′	112.8 (*d*)	7.18	C-1′, C-6′b, C-4′	112.6
3′a	130.9 (*s*)			130.7
4′	25.6 (*t*)	2.95	C-6′b, C-3′	25.4
5′	49.7 (*t*)	3.26	C-3′a, C-6′a	49.5
6′a	143.8 (*s*)			143.6
6′b	121.1 (*s*)			120.9
7′	122.4 (*s*)			122.1
7′a	134.4 (*s*)			134.2
8′	127.9 (*d*)	6.70	C-7′, C-10′, C-11′a	127.2
9′	126.7 (*d*)	7.12	C-11′, C-7′a	126.5
10′	126.6 (*d*)	7.43	C-8, C-11′a	126.0
11′	124.7 (*d*)	9.75	C-6′b, C-7′a, C-9′	124.5
11′a	126.2 (*s*)			126.4
11′b	127.4 (*s*)			127.1
2-OCH_3	56.3 (*q*)	4.07	C-1	56.1
1′-OCH_3	60.0 (*q*)	4.01	C-1′	59.8
2′-OCH_3	56.6 (*q*)	4.07	C-2′	56.4

N-CH_3	41.6 (*q*)	2.15	C-5′	41.4

Multiplicity determined from DEPT 135 experiment, literature data (δ_{lit}) from Cortes *et al*., 1990.

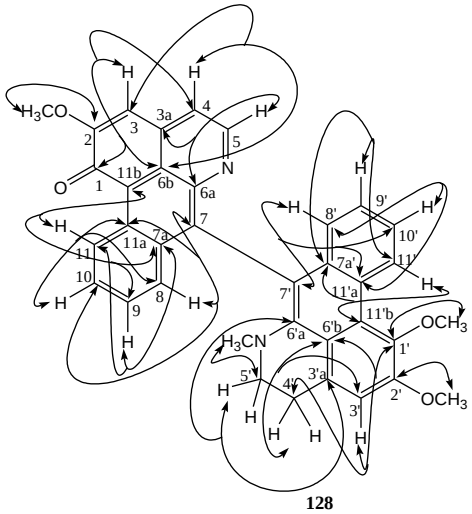
The COSY spectrum confirmed that the proton at δ 10.20 (*dd*, *J* 9.0, 2.1 Hz) was *ortho* to the one at δ 7.85 and *meta* to another at δ 7.35. The proton at δ 7.35 was *ortho* to the one at δ 7.76 and *meta* to the other at δ 7.85. The protons at δ 7.35 and 7.85 were *ortho* to each other. The observations indicated absence of substituent on ring D. COSY spectrum also confirmed that the proton at δ 9.75 was *ortho* to the one at δ 7.43 and *meta* to the other at δ 7.12. The proton at δ 7.12 was *ortho* to the one at δ 6.70 and *meta* to the other at δ 9.75. The protons at δ 7.12 and 7.43 were *ortho* to each other. These observations indicated absence of substituent on ring D′. The important COSY interactions are summarized in figure 7.

Figure 7: Important COSY interactions for trivalvone (**128**)



The assignments of the first and second unit containing the 1, 2-disubstituted benzene ring, the AB spin system and the methylene groups were unambiguously confirmed by HMBC experiment. Important HMBCs for trivalvone (**128**) are summarized in figure 8.

Figure 8: Important HMBCs for trivalvone (**128**)

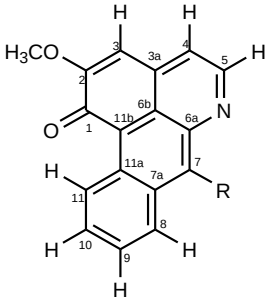


The first unit containing the 1, 2-disubstituted benzene ring was deduced from H-11 (δ 10.20) which exhibited HMQC to C-11 (δ 121.9) and three-bond HMBCs to C-11b (δ

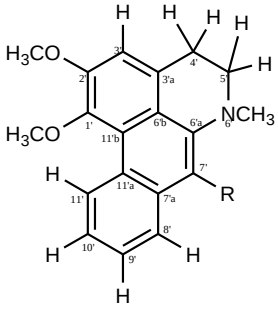
136.2), C-7a (142.5) and C-9 (δ 128.7). H-10 (δ 7.85) showed HMQC to C-10 (δ 127.0) and three-bond HMBCs to C-11a (δ 122.7) and C-8 (δ 132.6). H-9 (δ 7.35) showed three-bond HMBCs to C-7a (δ 142.5) and C-11 (δ 121.9). H-8 (δ 7.76) exhibited HMBCs to C-10 (δ 127.0), C-11a (δ 122.7) and C-7 (δ 134.0). H-5 (δ 8.89) showed 3-bond HMBCs with C-3a (δ 134.3) and C-6a (δ 156.6). H-4 (δ 7.54) displayed 3-bond HMBC with C-3 (δ 107.3) and C-1b (δ 122.6). H-3 (δ 6.87) showed HMBCs with C-1 (δ 181.0), C-6b (δ 122.6) and C-4 (δ 127.9). The methoxyl signal at δ 4.07 which showed HMQC to 2-OCH_3 (δ 56.3), also exhibited HMBC to C-2 (δ 151.3). These observations allowed assignment of the partial structure to oxo-aporphine alkaloid (Fig. 9).

The unit containing the other 1, 2-disubstituted benzene ring residue was also deduced from H-11´ (δ 9.75,) which exhibited HMQC to C-11´ (δ 124.7) and three-bond HMBC to C-7´a (δ 134.4), C-11´b (δ 127.4) and C-9´ (δ 126.7). H-10´ (δ 7.43) exhibited HMQC to C-10´ (δ 126.6) and HMBCs to C-11´a (δ 126.2) and C-8´ (δ 127.9). H-9´ (δ 7.12) showed three-bond HMBC to C-7´a (δ 134.4) and C-11´ (δ 124.7). H-8´ (δ 6.70) revealed HMBCs to C-10´ (δ 126.6), C-7´ (δ 122.4) and C-11´a (δ 126.2). H-3´ (δ 7.18, *s*, 1H) in the molecular framework linking the second four spin system, showed HMQC to C-3´ (δ 112.8) and HMBCs to C-4´ (δ 25.6), C-6´b (δ 121.1) and C-1´ (δ 145.9). A three-bond HMBC was also observed between 1´-OCH_3 (δ 4.01), which displayed HMQC to 1´-OCH_3 (δ 60.0), and C-1´ (δ 145.9) confirming the attachment of 1´-OCH_3 at C-1´. 2´-OCH_3 (δ 4.07), which exhibited HMQC to 2´-OCH_3 (δ 56.6), also showed HMBC to C-2´ (δ 150.6) confirming the attachment of 2´-OCH_3 at C-2´. H-4´ (δ 2.95, *m*, 2H), which exhibited HMQC to C-4´ (δ 25.6) showed 3-bond HMBC to C-6´b (δ 121.1) and C-3´ (δ 112.8). H-5´ (δ 3.26) showing HMQC with C-5´ (δ 49.7), displayed HMBCs to C-6´a (δ 143.8) and C-3´a (δ 130.9). N-CH_3 (δ 2.15), exhibiting HMQC to N-CH_3 (δ 41.6), revealed an HMBC to C-5´ (δ 49.7). These observations allowed assignment of a partial structure to the dihydroaporphine alkaloid (Fig. 10).

Figure 9 and 10: Partial structures of trivalvone (**128**)



Partial structure 1

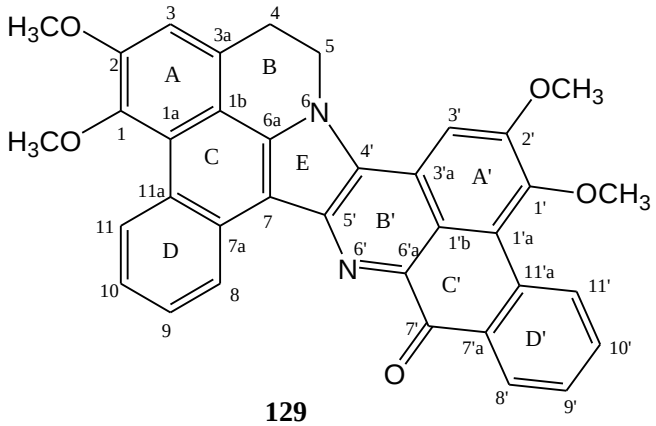


Partial structure 2

The MS showed the molecular ion peak at *m/z* 552 (M^+, 100%). Other important peaks were observed at *m/z* 554 ($[M+2]^+$, 90.4%), 553 ($[M+1]^+$, 41.3%), and 292 (M/2 + H, 8.4%) confirming the molecular mass of **128** to be *m/z* 552 amu which is consistent with the formula $C_{36}H_{28}N_2O_4$. The absence of any fragmentation in the region *m/z* 552-292 suggested a dimeric structure for **128**, resulting from a C-7→C-7′ oxidative coupling between the two aporphine units (Cortes & Davoust, 1990**)**. The NMR and MS data confirmed the structure of the bis-aporphine alkaloid, trivalvone (**128**)**,** a rare alkaloid first reported in 1990 from *Trivalvaria macrophylla* (Annonaceae) (Cortes *et al*, 1990) and subsequently from *Piptostigma fugax* (Annonaceae) (Achenbach & Schwinn, 1995). This is the first report on the presence of trivalvone (**128**) from *Annickia kummeriae* (Annonaceae).

4.1.3 Annickine (129)

Repeated column chromatography (SiO_2, *n*-C_6H_{14}-EtOAc 40:60, EtOAc-MeOH 75:25) of HSCCC fraction 2.11 (AKLM 2.11) of the methanolic extract of *A. kummeriae* leaves (IC_{50} 0.64±0.34 µg/ml, SI 69.8) gave 23 x 50 ml fractions. Fractions 13-19 were combined and purified by PTLC (SiO_2, $CHCl_3$-MeOH-HCO_2H 95:4.5:0.5) to yield **129** (3.2 mg) as brown amorphous solid (m.p. 263-265 °C) which gave positive reaction for alkaloids with Dragendorff's reagent.



129

The structure was established on the basis of 1D (^1H and ^{13}C) and 2D-NMR experiments (HMQC, NOESY, COSY and HMBC), (Table 17-18, Appendix 3a-e) plus MS data (Appendix 3f).

Table 17: 1D and 2D ^1H NMR (600 MHz, $CDCl_3$) data of annickine (**129**)

Position	δ_{obs}	J_{obs}(Hz)	COSY
3	7.28 (1H, *s*)		
4	3.61 (2H, *t*)	6.6	H-5
5	4.92 (2H, *t*)	6.6	H-4
8	9.01 (1H, *d*)	8.4	H-9
9	7.72 (1H, *d*)	8.4	H-8, H-10
10	7.61 (1H, *d*)	8.4	H-9, H-11
11	9.75 (1H, *d*)	8.4	H-10
3´	8.58 (1H, *s*)		
8´	8.61 (1H, *d*)	8.4	H-9´
9´	7.59 (1H, *d*)	8.4	H-8´, H-10´
10´	7.77 (1H, *d*)	8.4	H-9´, H-11´
11´	9.27 (1H, *d*)	8.4	H-10´
1-OCH_3	3.99 (3H, *s*)		
2-OCH_3	4.08 (3H, *s*)		

Table 18: 1D and 2D ^{13}C NMR (600 MHz, $CDCl_3$) data of annickine (**129**)

Position	δ	HMQC	HMBC
1	146.4 (*s*)		
1a	124.2 (*s*)		
1b	115.2 (*s*)		
2	153.4 (*s*)		
3	112.3 (*d*)	7.28	C-1, C-6b, C-4
3a	127.5 (*s*)		
4	28.4 (*t*)	3.61	C-6b, C-3
5	40.0 (*t*)	4.92	C-3a, C-6a
6a	137.4 (*s*)		
7	109.3 (*s*)		
7a	130.0 (*s*)		
8	124.5 (*d*)	9.01	C-7, C-10, C-11a
9	126.7 (*d*)	7.72	C-11, C-7a
10	124.7 (*d*)	7.61	C-8, C-11a
11	129.3 (*d*)	9.75	C-11b, C-7a, C-9
11a	127.7 (*s*)		
1´	149.5 (*s*)		
1´a	121.1 (*s*)		
1´b	118.9 (*s*)		
2´	154.9 (*s*)		
3´	106.2 (*d*)	8.58	C-1´, C-1´b, C-5´
3´a	115.3 (*s*)		
4´	142.2 (*s*)		
5´	137.5 (*s*)		
6´a	127.7 (*s*)		
7´	182.9 (*s*)		
7´a	132.4 (*s*)		
8´	128.4(*d*)	8.61	C-7´, C-10´, C-11´a
9´	128.5 (*d*)	7.59	C-7´a, C-11´
10´	133.7 (*d*)	7.77	C-8´, C-11´a
11´	128.7 (*d*)	9.27	C-1´a, C-7´a, C-9´
11´a	134.8 (*s*)		
1-OCH_3	60.3 (*q*)	3.99	C-1
2-OCH_3	56.7 (*q*)	4.08	C-2
1´-OCH_3	60.8 (*q*)	4.04	C-1´
2´-OCH_3	56.3 (*q*)	4.19	C-2´

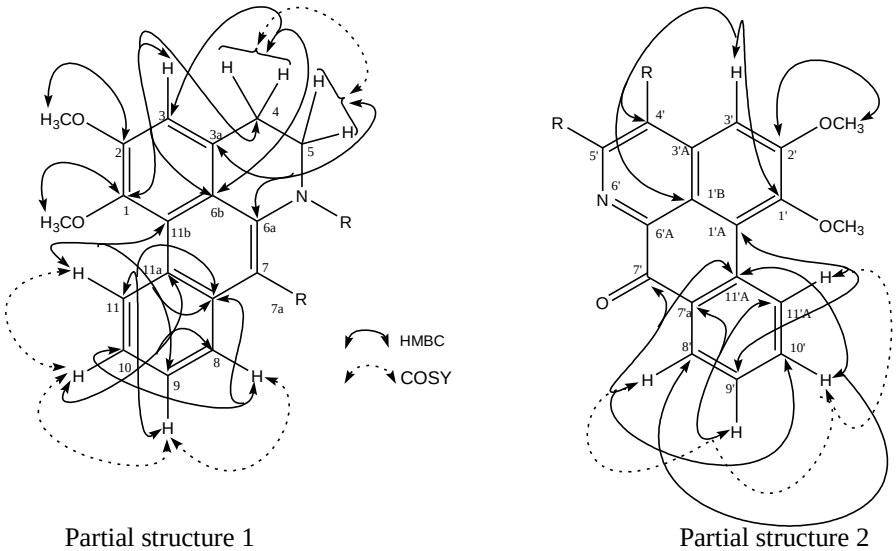
Multiplicity determined from HMQC and ^1H NMR experiment.

Unambiguous assignment of ^1H and ^{13}C NMR signals for the two partial structures of **129** was done with the help of HMQC and COSY while the connectivities of the molecular fragments were established by HMBC. The ^1H NMR revealed the presence of two 1, 2-disubstituted benzene ring residues as indicated by two parts of four-spin systems each. The partial structure 1 of compounds **129** contained a 1, 2-disubstituted benzene ring A residue which was confirmed from 2D NMR experiments. H-11 (δ 9.75) exhibited HMQC to C-11 (δ 121.9) and three-bond HMBC to C-1a (δ 124.2), C-7a (130.0) and C-9 (δ 126.7). Similarly, H-10 (δ 7.61) exhibited HMQC to C-10 (δ 124.7) and HMBCs to C-11a (δ 127.7) and C-8 (δ 124.5). H-9 (δ 7.72) showed three-bond HMBC to C-7a (δ 130.0) and C-11 (δ

121.9). Similarly, H-8 (δ 9.01) revealed three-bond HMBCs to C-10 (δ 124.7), C-7 (δ 109.2) and C-11a (127.7).

COSY interactions confirmed that H-11 (δ 9.75) is *ortho* to H-10 (δ 7.61) and *meta* to H-9 (δ 7.72) which is *ortho* to H-8 (δ 9.01). The observations indicated the absence of substituents on ring D. COSY also confirmed that H-4 (δ 3.61) is adjacent to H-5 (δ 4.92). H-3 (δ 7.28) showed HMQC to C-3 (δ 112.3) and HMBCs to C-4 (δ 28.4), C-6b (δ 115.1) and C-1 (δ 146.3). A three-bond HMBC was also observed between 1-OCH_3 (δ 3.99), which displayed HMQC to 1-OCH_3 (δ 60.3), and three-bond HMBC ($^1H \rightarrow ^{13}C$) to C-1 (δ 146.3). 2-OCH_3 (δ 4.08), which exhibited HMQC to 2-OCH_3 (δ 57.0), also showed HMBC C-2 (δ 153.5). Important COSY and HMBCs for partial structure 1 of an aporphine alkaloid **129** are shown in figure 11.

Figure 11: Important COSY and HMBCs for partial structures of annickine (**129**)



Partial structure 1 Partial structure 2

H-4 (δ 3.61) showed HMQC to C-4 (δ 28.4) and 3-bond HMBCs to C-1b (δ 115.1) and C-3 (δ 112.3). H-5 (δ 4.92) showed HMQC to C-5 (δ 40.1) and HMBCs to C-3a (δ 127.5) and C-6a (δ 137.4). These observations allowed assignment of the partial structure to the dihydroaporphine alkaloid which is closely related to of the structure of trivalvone (**128**) (Cortes & Davoust, 1990**)**. The only difference is N-methylation.

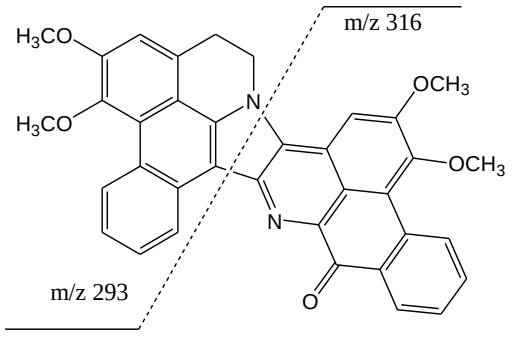
The presence of the second 1, 2-disubstituted benzene ring residue was deduced from ^1H NMR data: δ 9.26 (*d*), 7.77 (*t*), 7.59 (*t*) and 8.61 (*t*). COSY confirmed that H-11' (δ 9.26) is *ortho* to H-10' (δ 7.77) and *meta* to H-9' (δ 7.59) which is *ortho* to H-8' (δ 8.61). These observations showed the absence of substituent on ring D'. H-11' (δ 9.26) exhibited HMQC

to C-11' (δ 128.7) and three-bond HMBCs to C-1'A (δ 121.1), C-7'a (132.4) and C-9' (δ 128.5). Similarly, H-10' (δ 7.77) revealed HMQC to C-10' (δ 133.7) and three-bond HMBCs to C-11'a (δ 134.9) and C-8' (128.4). Likewise, H-9' (δ 7.59) showed HMQC to C-9' (δ 128.5) and three-bond HMBCs to C-7'a (δ 132.4) and C-11' (δ 128.7). Furthermore, H-8' (δ 8.61) showed HMQC to C-8' (δ 128.4) and three-bond HMBCs to C-11'a (δ 134.9) and C-7'a (δ 132.4). In addition, H-3' (δ 8.57) showed HMQC to C-3' (δ 106.2) and three-bond HMBC to C-1' (δ 149.5), C-2' (δ 153.4) and C-7' (δ 182.9) plus the rare two-bond HMBC to C-3'a (δ 115.3). 1'-OCH_3 (δ 4.04) showed HMQC to 1'-OCH_3 (δ 60.8) and HMBC to C-1' (δ 149.5) while 2'-OCH_3 (δ 4.18) showed HMQC to 2'-OCH_3 (δ 56.7) and HMBC to C-2' (δ 154.9). Important COSY and HMBCs for partial structure 2 of oxo-aporphine alkaloid **129** are shown in figure 12. These observations allowed assignment of the partial structure 2 to hydroxy-oxo-aporphine alkaloid.

From these data it was apparent that **129** is not a 7,7-bisaporphine alkaloid like trivalvone (**128**) and that in both of the aporphine moiety of the dimeric alkaloid, C-7s are quaternaries and that C-4/C-4´and C-5/C-5´ have participated in the dimerization process.

The EI-MS showed a molecular ion peak at *m/z* 566 (M^+, 100%). Other important peaks were observed at *m/z* 552 (68%), 316 (57%), 293 (22%) and 283 (20%) confirming the molecular mass of **129** to be *m/z* 566 amu which is consistent with the molecular formula $C_{36}H_{32}N_2O_6$ indicative of a dimeric aporphine (Wijeratne *et al*., 2001). The presence of two significant fragments at *m/z* 316 and 293 further confirmed this proposition (Figure 12) calculated for *m/z* 566.1842. The combined spectral data lead to unambiguous elucidation of annickine (**129**) which is hitherto unreported.

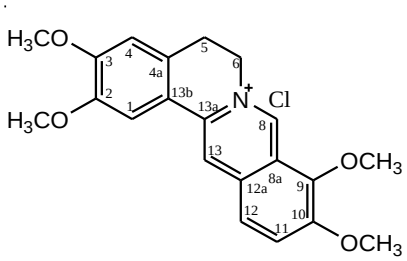
Figure 12: MS fragmentation of annickine (**129**)



129

4.1.4 Palmatine (82)

Repeated HSCCC fractionation ($CHCl_3$-MeOH-0.2 M HCl 7:3:4) of fractions 7-10 (AKLM 7-10) (IC_{50} 0.05±0.02-0.11±0.02 µg/ml, SI >818.2-1,800.0) of the methanolic extract of *A. kummeriae* leaves gave a yellow solid that was re-crystallized from methanol to yield palmatine (**82**) (1.52 g, mp. 203-205 ºC) which gave positive reaction for alkaloids with Dragendorff's reagent and for chlorides with silver nitrate reagent confirming presence of chloride counter ion.



82

The structure of palmatine (**82**) was established on the basis of 1D (^1H, ^{13}C, DEPT 135) and 2D-NMR experiments (HMQC, COSY and HMBC) (Table 19-20, Appendix 4a-f), IR (Appendix 4g) plus MS data (Appendix 4h).

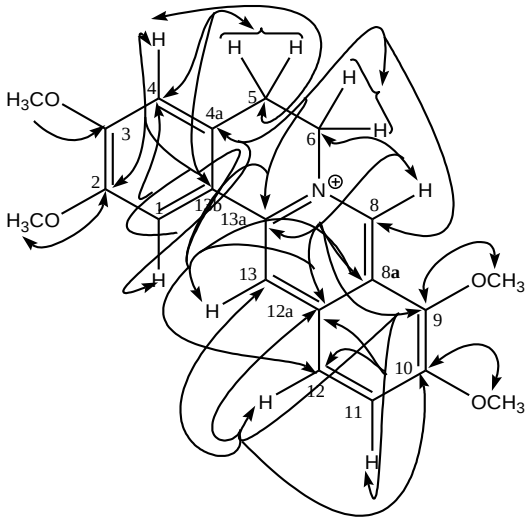
Table 19: 1D and 2D ^1H NMR (500 MHz, CD_3OD) spectral data of palmatine (**82**)

Position	δ_{obs}	J_{obs}(Hz)	COSY	δ_{lit}	J_{lit}(Hz)
1	7.63 (1H, *s*)			7.66 (1H, *s*)	
4	7.04 (1H, *s*)			7.04 (1H, *s*)	
5	3.30 (2H, *t*)	6.3	H-6	3.28 (2H, t)	6.3
6	4.95 (2H, *t*)	6.3	H-5	4.95 (2H, t)	6.3
8	9.75 (1H, *br, s*)		H-13	9.77 (1H, *br s*)	
11	8.09 (1H, *d*)	9.1	H-12	8.02 (1H, *d*)	9.0
12	8.01 (1H, *d*)	9.1	H-11	8.11 (1H, *d*)	9.0
13	8.79 (1H, *s*)		H-8	8.81 (1H, *s*)	
2-OCH_3	3.94 (3H, *s*)			3.94 (3H, *s*)	
3-OCH_3	4.00 (3H, *s*)			3.99 (3H, *s*)	
9-OCH_3	4.22 (3H, *s*)			4.20 (3H, *s*)	
10-OCH_3	4.10 (3H, *s*)			4.10 (3H, *s*)	

Literature data (δ_{lit}) are from Halbsguth *et al*., 2003

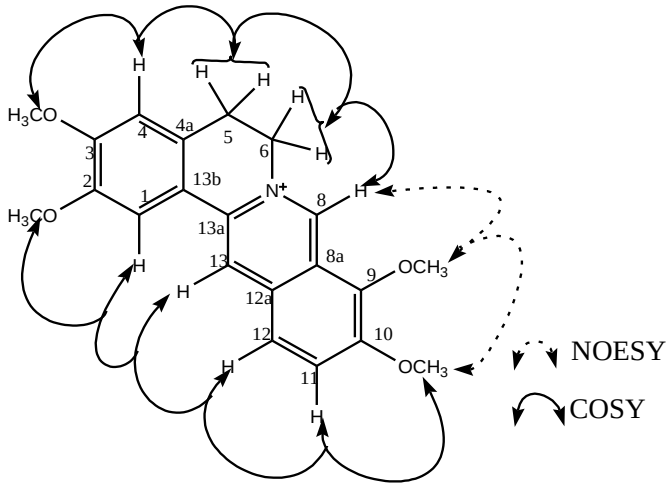
The ^{13}C NMR data were assigned with the help of HMQC and DEPT 135 experiments while, the connectivities of the molecular fragments were established by HMBC (Fig. 13), COSY and NOESY (Fig. 14). The analysis of the spectra and structure elucidation was also facilitated by comparison of observed and published ^1H and ^{13}C NMR data for palmatine (**82**) (Halbsguth *et al*., 2003; Li *et al*., 2006).

Figure 13: Important HMBCs for palmatine (**82**)



82

Figure 14: COSYs and NOESYs of palmatine (**82**)



82

The ^{1}H NMR spectrum revealed the signals at δ 8.01 (1H, *d*, *J* 9.1 Hz, H-12) and δ 8.07 (1H, *d*, *J* 9.1 Hz, H-11) that showed HMQCs to C-12 (δ 124.9) and C-11 (δ 128.4), respectively, were assigned to two *ortho* protons as confirmed by COSY (Fig. 14). H-12 (δ 8.01) showed HMBCs to the C-13 (δ 121.7), C-12a (δ 135.6) and C-9 (δ 146.1) while H-11 (δ 8.09) showed HMBCs to C-9 (δ 146.1), C-10 (152.3), C-12 (δ 124.9) and C-12a (δ 135.6) confirming the presence of the two *ortho* protons (H-11 and H-12) of a 1, 2, 3, 4 tetra-substituted benzene ring of a protoberberine skeleton. However in the reported literature the assignments have been interchanged [H-12 (δ 8.11) appeared downfield than H-11 (δ 8.02)] (Halbsguth *et al*., 2003).

The second aromatic residue, a 1, 2, 4, 5 tetra-substituted benzene ring was indicated by the presence of two signals at δ 7.63 (1H, *s*) and δ 7.04 (1H, *s*) assigned to H-1 and H-4, respectively. H-1 (δ 7.63) and H-4 (δ 7.04) showed HMQC to C-1 (δ 110.4) and C-4 (112.7), respectively. H-1 (δ 7.63) showed HMBCs to C-2 (δ 151.3), C-3 (δ 154.2), C-4a (δ 130.4), C-13b (δ 120.8) and C-13a (δ 140.1) while H-4 (δ 7.04) showed HMBCs to C-3 (δ 154.2), C-2 (δ 151.3), C-13b (δ 120.8), C-4a (δ 130.4) and C-5 (δ 28.2) confirming the presence of the two *para* protons (H-1 and H-4) of a 1, 2, 4, 5 tetra-substituted benzene ring of a protoberberine skeleton.

^{13}C, HMQC and HMBC NMR data for palmatine (**82**) are shown in table 20.

Table 20: 1D and 2D ^{13}C NMR (500 MHz, CD_3OD) data of palmatine (**82**)

Position	δ_{obs}	HMQC (δ)	HMBC	δ_{lit}
1	110.4 (d)	7.63	C-2, C-3, C-4a, C-13b, C-13a	109.9
2	151.3 (s)			150.8
3	154.2 (s)			153.1
4	112.7 (d)	7.04	C-3, C-2, C-13b, C-4a	112.0
4a	130.4 (s)			129.8
5	28.2 (t)	3.30	C-4, C-4a, C-13b	27.8
6	56.4 (t)	4.95	C-4a, C-13a, C-8	56.5
8	146.7 (d)	9.75	C-6, C-13a, C-12a, C-8a, C-9	146.2
8a	123.6 (s)			124.3
9	146.1 (s)			145.6
10	152.3 (s)			151.5
11	128.4 (d)	8.09	C-10, C-9, C-12, C-12a	128.0)
12	124.9 (d)	8.01	C-13, C-12a, C-9	*
12a	135.6 (s)			135.4
13	121.7 (d)	8.79	C-13b, C-13a, C-8, C-8a, C-12a, C-12, C-9	121.1
13a	140.1 (s)			139.9
13b	120.8 (s)			120.4
2-OCH_3	57.5 (q)	4.00	C-2	57.3
3-OCH_3	57.1 (q)	3.94	C-3	56.8)
9-OCH_3	63.0 (q)	4.22	C-9	62.4
10-OCH_3	57.8 (q)	4.10	C-10	57.4

Multiplicity determined from DEPT 135; literature data (δ_{lit}) are from Wafo *et al*., 1999; * Data not included in original report.

The third aromatic residue, a 1, 3, 4, 6 tetra-substituted pyridine ring, was indicated by the presence of two signals at δ 9.75 (1H, *s*) and 8.79 (1H, *s*) due to H-8 and H-13, respectively. H-8 (δ 9.75) and H-13 (δ 8.79) showed HMQCs to C-8 (δ 146.7) and C-13 (δ 121.7), respectively. The shifting downfield of H-8 (δ 9.75) indicated that the corresponding carbon (C-8) is directly attached to the quaternary nitrogen thus experiencing strong electron withdrawing effect due to the quaternary nitrogen atom next to it. In addition, H-8 showed HMBCs to C-6 (δ 56.3), C-8a (δ 123.6), C-12a (δ 135.6), C-13a (δ 140.1) and C-9 (δ

146.1) while H-13 showed HMBCs to C-13b (δ 120.8), C-8a (δ 123.6), C-12 (δ 124.9), C-12a (δ 135.6), C-13a (δ 140.1), C-9 (δ 146.1) and C-8 (δ 146.7) confirming the presence of the two *para* protons (H-8 and H-13) of a 1, 3, 4, 6 tetra-substituted pyridine ring of a protoberberine skeleton.

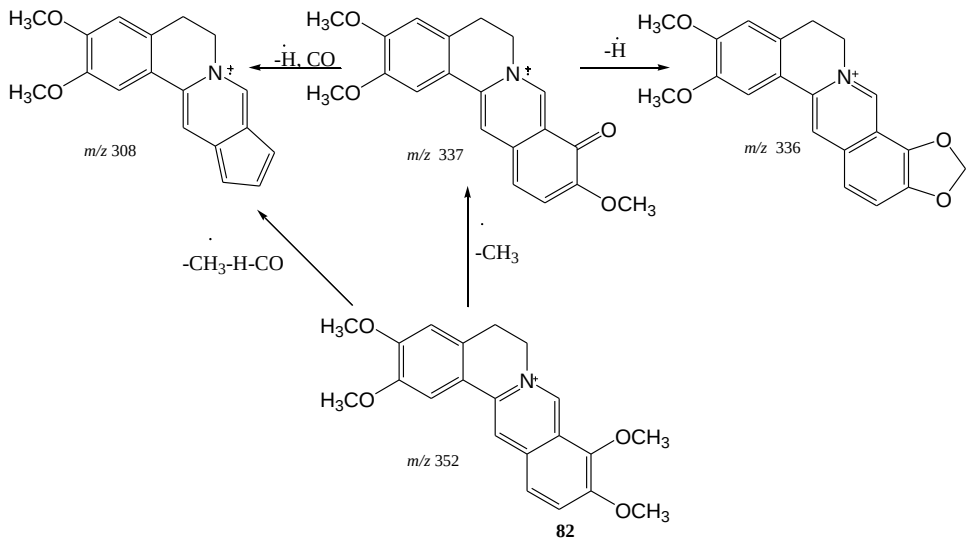
The non-aromatic region of the ^{1}H NMR spectrum exhibited two triplets at δ 3.30 (2H, *t, J* 6.2 Hz, H-5) and 4.95 (2H, *t, J* 6.2 Hz, H-6) which were confirmed by HMQC to be due to neighbouring methylene protons at C-5 and C-6 respectively. H-5 (δ 3.30) and H-6 (δ 4.95) showed HMQC to C-5 (δ 28.2) and C-6 (δ 56.3), respectively. COSY cross-peaks were observed between H-5 (δ 3.30) and H-6 (δ 4.95) confirming that H-5 and H-6 are vicinal to each other. H-5 (δ 3.30) showed HMBCs to C-4 (δ 112.7), C-13b (δ 120.8) and C-4a (δ 130.4) while H-6 showed HMBCs to C-4a (δ 130.4), C-13a (δ 140.1) and C-8 (δ 146.7) confirming the position of the two methylene protons. H-6 (δ 4.95) resonated at very low magnetic field indicating the presence of quaternary nitrogen attached to C-6. The spectral data also revealed that, the two methylene groups H-5 (C-5) and H-6 (C-6) are connected on one side to the aromatic ring containing the *para* protons (H-1 and H-4) with the four quaternary carbons making the 1, 2, 4, 5 tetra-substituted benzene ring residue and on the other side to the residue containing the *para* protons (H-8 and H-8) of the 1, 3, 4, 6 tetra-substituted pyridine ring in the protoberberine skeleton.

Furthermore, four methoxyl group were observed at δ 3.94 (3H, *s*), 4.00 (3H, *s*), 4.10 (3H, *s*) and 4.22 (3H, *s*) and the connectivities to the protoberberine skeleton established by HMBC as follows: 3-OCH_3 (δ 3.94) to C-3 (δ 154.2), 2-OCH_3 (δ 4.00) to C-2 (δ 151.3), 10-OCH_3 (δ 4.10) to C-10 (δ 152.3) and 9-OCH_3 (δ 4.22) to C-9 (δ 146.1). In addition, the methoxyl signals showed HMQCs to 3-OCH_3 (δ 57.1), 2-OCH_3 (δ 57.5), 10-OCH_3 (δ 57.8), 9-OCH_3 (δ 63.0). The unambiguous proton assignments of **82** were achieved by COSY and NOESY analysis. H-1 (δ 7.63) exhibited significant COSYs with 2-OCH_3 (δ 4.00) and H-13 (δ 8.79). H-12 (δ 8.01) showed COSYs with H-13 (δ 8.79) and H-11 (δ 8.07). H-11 (δ 8.09) showed COSYs to 10-OCH_3 (δ 4.10) and H-12 (δ 7.96). Further COSYs were observed between H-8 (δ 9.75) and 9-OCH_3 (δ 4.22) plus H-6 (δ 4.95). H-5 (δ 3.30) displayed COSYs to H-6 (δ 4.95) and H-4 (δ 7.04) which also showed further COSY to 3-OCH_3 (δ 3.94).

IR data showed the presence of characteristic bands due to conjugated double bond at 1603, 1515 and 1460 cm^{-1}.

The mass spectrum of **82** exhibited a molecular ion peak at *m/z* 352 which is consistent with the formula $C_{21}H_{22}NO_4^+$ (D.B.E 11.5). The non-integer value of the index of hydrogen deficiency suggested that **82** could be a quaternary ammonium salt consistent with palmatine (**82**). FAB-MS revealed the predominant ion at *m*/*z* 337 corresponding to the elimination of the methyl radical from the methoxyl group at C-9 or C-10, from the fragment ion at *m*/*z* 352(Appendix h and Fig. 15). The ion observed at *m*/*z* 308 corresponds to the loss of a neutral fragment with a molecular mass of 44 amu from palmatine (**82**), which may be explained by the loss of a methyl radical followed by hydrogen radical (CH_4) and CO. The ion at *m*/*z* 336 corresponds to the loss of hydrogen radical from the C-10 methoxyl radical and formation of 1, 2-dioxolan ring.

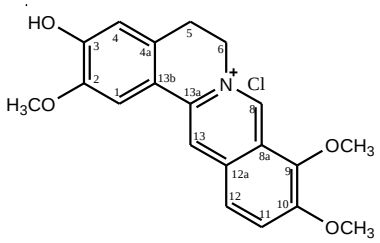
Figure 15: Diagnostic MS fragments of palmatine (**82**)



All the observed data for **82** were consistent with the reported values for palmatine except for the interchange of H-11 and H-12 in ^{1}H NMR (Halbsguth *et al*., 2003; Li *et al*., 2006). Palmatine (**82**) has been previously reported from many plant families: Papaveraceae, Berberidaceae, Fumariaceae, Menispermaceae, Ranunculaceae, Rutaceae, Annonaceae, Magnoliaceae and Convolvulaceae (Grycová *et al*., 2007).

4.1.5 Jatrorrhizine (83)

Repeated HSCCC ($CHCl_3$-MeOH-0.2 M HCl 7:3:4) of the combined fractions AKLM 7-10 (IC_{50} 0.05±0.02-0.11±0.02 µg/ml; SI >818.2-1,800.0) of the methanolic extract of *A. kummeriae* leaves was undertaken followed by purification on column chromatography (SiO_2 60; $CHCl_3$-MeOH-HCO_2H 9:0.75:0.25, 8:1.75:0.25, 6:3.75:0.5 and 5:4.5:0.5) and re-crystallization (MeOH) yielded jatrorrhizine (**83**) as orange crystals (40.82 mg, mp 204-206 ºC) that gave positive reaction for alkaloids with Dragendorff's reagent and for chlorides with silver nitrate reagent confirming presence of chloride counter ion.



83

The structure of jatrorrhizine (**83**) was established on the basis of 1D (^1H, ^{13}C) and 2D-NMR experiments (HMQC, COSY, HMBC and NOESY) (Table 21-22, Appendix 5a-f), IR (Appendix 5g) plus MS data (Appendix 5h).

Analysis of the 1D (^1H, ^{13}C) and 2D NMR (HMQC, ^1H-^1H COSY, HMBC and NOESY) data allowed complete assignment of all signals. The ^1H and ^{13}C NMR spectra exhibited resonances attributable to three aromatic and two characteristic non-aromatic systems similar to palmatine (**82**) (Halbsguth *et al*., 2003; Li *et al*., 2006). The pattern in the aromatic region of the ^1H NMR spectrum of **83** was exactly the same as that of palmatine (**82**).

Table 21:1D and 2D ^1H NMR (600 MHz, $CDCl_3$) data for jatrorrhizine (**83**)

Position	δ_{obs} J_{obs}(Hz)		COSY	NOESY	δ_{lit}	J_{lit}(Hz)
1	7.57 (1H, *s*)		2-OCH_3		7.33 (1H, *s*)	
4	6.76 (1H, *s*)		H-5		6.50 (1H, *s*)	
5	3.17 (2H, *t*)	6.1	H-6		3.07 (2H, *t*)	6.1
6	4.87 (2H, *t*)	6.1	H-5		4.79 (2H, *t*)	6.1
8	9.67 (1H,*br s*)		H-13		9.50 (1H, *br, s*)	
11	8.07 (1H, *d*)	9.1	H-12		7.96 (1H, *d*)	9.0
12	7.96 (1H, *d*)	9.1	H-11	9-OCH_3	7.85 (1H, *d*)	9.0
13	8.68 (1H, *s*)		H-8		8.44 (1H, *s*)	
2-OCH_3	3.99 (3H, *s*)		H-1		3.89 (3H, *s*)	
9-OCH_3	4.19 (3H, *s*)		H-8	10-OCH_3	4.16 (3H, *s*)	
10-OCH_3	4.10 (3H, *s*)		H-11	9-OCH_3	4.06 (3H, *s*)	

Literature data (δ_{lit}) are from Kim *et al*., 2000.

Table 22:1D and 2D ^{13}C NMR (600 MHz, $CDCl_3$) data for jatrorrhizine (**83**)

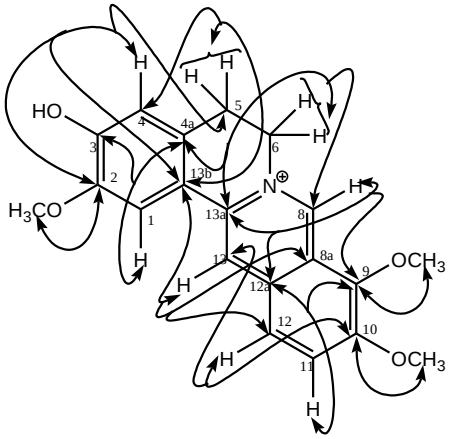
Position	δ_{obs}	HMQC (δ)	HMBC	δ_{lit}
1	109.6 (*d*)	7.57	C-3, C-4a, C-13a, C-13b	110.9
2	150.9 (*s*)			149.4
3	152.1 (*s*)			151.5
4	116.6 (*d*)	116.6	C-2, C-3, C-13b	116.3
4a	130.5 (*s*)			130.2
5	27.8 (*t*)	3.17	C-4, C-4a, C-13b	29.1
6	57.4 (*t*)	4.87	C-4a, C-8, C-13a	57.6
8	145.7 (*d*)	9.67	C-8a, C-9, C-12a, C-13a	145.2
8a	122.9 (*s*)			122.9
9	145.9 (*s*)			146.4
10	151.5 (*s*)			145.1
11	128.1 (*d*)	8.07	C-9, C-10, C-12, C-12a	127.9
12	124.2 (*d*)	7.96	C-8a, C-9, C-11, C-12a, C-13	125.7
12a	135.7 (*s*)			128.2
13	120.2 (*d*)	8.68	C-8, C-8a, C-9, C-12, C-12a, C-13a, C-13b	119.3
13a	141.1 (*s*)			139.9
13b	117.1 (*s*)			119.2
2-OCH_3	56.7 (*q*)	3.99	C-2	58.3
9-OCH_3	62.4 (*q*)	4.19	C-9	63.0
10-OCH_3	57.7 (*q*)	4.10	C-10	57.0

Literature data (δ_{lit}) are Kim *et al*., 2000.

The presence of six aromatic protons with a pattern representing the three tetra-substituted aromatic rings was evident in the 1, 2, 4, 5 tetra-substituted benzene ring: δ 7.57 (1H, *s*, H-1) and 6.76 (1H, *s*, H-4); a 1, 3, 4, 6 tetra-substituted pyridine ring: δ 9.67 (1H, *s*, H-8) and 8.68 (1H, *s*, H-13); and a 1, 2, 3, 4 tetra-substituted benzene ring: δ 8.07 (1H, *d*, *J* 9.1, H-11) and 7.96 (1H, *d*, *J* 9.1, H-12). Two methylene signals at δ 3.17 (2H, *t*, *J* 6.1 Hz, H-5) and 4.87 (2H, *t*, *J* 6.1 Hz, H-6) also resembled that of **82**. The only spectral difference in the ^1H NMR spectrum of **83** from palmatine (**82**) was three methoxyl groups at δ 3.99 (3H, *s*, 2-OCH_3), 4.19 (3H, *s*, 9-OCH_3) and 4.10 (3H, *s*, 10-OCH_3) instead of four in palmatine (**82**). The observations provided enough evidence that **83** had a skeleton similar to palmatine (**82**) with fewer methoxyl groups. HMQC, HMBC, COSY and NOESY NMR experiments revealed that the two doublets H-11 (δ 8.07) and H-12 (δ 7.96) which showed HMQCs to C-11 (δ 128.1) and C-12 (δ 124.2), respectively. COSY revealed strong cross peaks between δ 8.07 (H-11) and 7.96 (H-12). In addition, H-11 (δ 8.07) showed HMBCs to C-12a (δ 135.7) and C-9 (δ 145.7). H-12 (δ 7.96) showed HMBCs to C-13 (δ 120.2), C-8a (δ 122.9), C-11 (δ 128.1), C-12a (δ 135.7), C-9 (δ 145.7) and C-10 (δ 151.5), confirming the *ortho* arrangement for H-11and H-12 and the four quaternary carbons making the 1, 2, 3, 4 tetra-substituted benzene ring residue in a protoberberine skeleton.

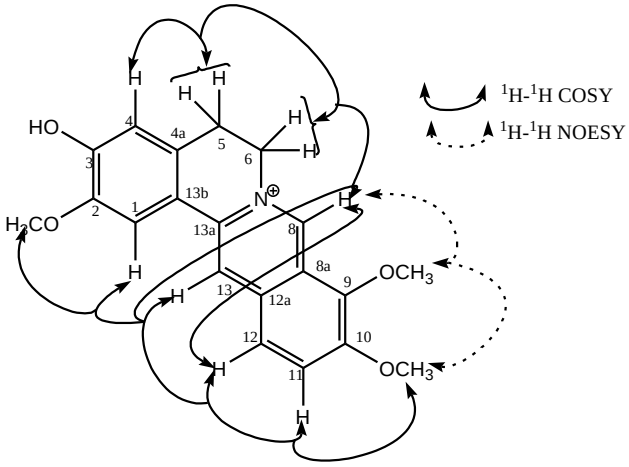
The HMBC, NOESY and COSY interactions are summarized in Figure 16 and 17.

Figure 16 and 17: Important HMBCs, COSYs and NOESYs for jatrorrhizine (**83**)



83

Figure 16:Important HMBCs



83

Figure 17:Important COSYs and NOESYs

The second aromatic system, a 1, 2, 4, 5-tetrasubstituted benzene ring, was revealed by the presence of two *para* aromatic signals at δ 7.57 (1H, *s*, H-1) and 6.76 (1H, *s*, H-4). H-1 (δ 7.57) and H-4 (δ 6.76) showed HMQCs to C-1 (δ 109.6) and C-4 (116.6), respectively. H-1 (δ 7.57) showed HMBCs to C-3 (δ 152.1), C-4a (δ 130.5), C-13a (δ 141.1), and C-13b (δ 117.1). H-4 (δ 6.76) showed HMBCs to C-2 (δ150.9), C-3 (δ152.1) and C-13b (δ117.1) confirming the assignment of the two characteristic *para* protons and the four quaternary carbons making the 1, 2, 4, 5 tetrasubstituted benzene ring residue in a protoberberine skeleton.

The third aromatic system, a 1, 3, 4, 6-tetrasubstituted pyridine ring, was characterized by the occurrence of two *para* aromatic proton signals at δ 9.67 (1H, *s*, H-8) and 8.76 (1H, *s*, H-13). H-8 (δ 9.67) and H-13 (δ 8.76) showed HMQCs to C-8 (δ 145.7) and C-13 (δ 120.2), respectively. The downfield shift of H-8 (δ 9.67) indicated that C-8 is directly attached to the quaternary nitrogen hence experiencing strong electron withdrawing effects. H-8 showed HMBCs to C-8a (δ 122.9), C-9 (δ 145.7), C-12a (δ 135.7) and C-13a (δ 141.1). H-13 showed HMBCs to C-8a (δ 122.9), C-12 (δ 124.2), C-13a (δ 141.1) and C-13b (δ 117.1) confirming the assignment of the two characteristic *para* protons (H-8 and H-13) and four quaternary carbons of the 1, 3, 4, 6-tetrasubstituted pyridine ring residue of a protoberberine skeleton.

Spectral similarities between **83** and **82** were also observed in the methylene region of the ^{1}H NMR spectrum which exhibited signals at δ 3.17 (2H, *t*, *J* 6.1 Hz, H-5) and δ 4.87 (2H, *t*, *J* 6.1 Hz, H-6) and confirmed in COSY, HMQC and HMBC spectra to be due to the

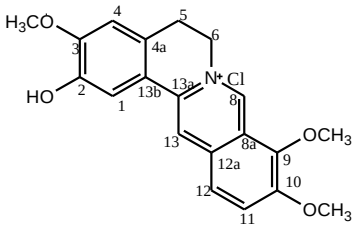
adjacent methylene protons at C-5 and C-6 respectively. H-5 (δ 3.17) and H-6 (δ 4.87) showed HMQCs to C-5 (δ 27.8) and C-6 (δ 57.4), respectively. COSY cross-peaks were observed between H-5 (δ 3.17) and H-6 (δ 4.87) confirming that H-5 and H-6 are neighbours. H-5 showed HMBCs to C-4 (δ 116.6), C-13b (δ 117.1) and C-4a (δ 130.5) while H-6 showed HMBCs to C-4a (δ 130.5), C-13a (δ 141.1) and C-8 (δ 145.7) confirming the assignment of the two methylene protons. H-6 appeared at low magnetic field due to the neighbouring quaternary nitrogen attached to C-6. The spectral data confirmed that the methylenes H-5 (C-5) and H-6 (C-6) in **83** are connected to one side of the aromatic system containing H-1 and H-4 with four quaternary carbons making the 1, 2, 4, 5-tetra-substituted benzene ring residue in one side of the protoberberine skeleton as in **82**. Connectivity on the other side of the ring containing H-4 and H-5 to the residue containing H-8 and H-13 and four quaternary carbons of the 1, 3, 4, 6-tetra-substituted pyridine ring residue in the protoberberine skeleton were also evident.

2-OCH_3 (δ 3.99), 9-OCH_3 (δ 4.19) and 10-OCH_3 (δ 4.10) revealed HMQCs to 2-OCH_3 (δ 56.6), 9-OCH_3 (δ 62.4) and 10-OCH_3 (δ 57.7), respectively. COSY spectrum revealed cross-peaks between 2-OCH_3 (δ 3.99) and H-1 (δ 7.57). The NOESY spectrum revealed interactions between H-8 (δ 9.67) and 9-OCH_3 (δ 4.19). In addition NOESY was observed between 9-OCH_3 (δ 4.19) and 10-OCH_3 (δ 4.10), indicating that they are close in space. The assignment of the methoxyl groups in the protoberberine skeleton were unambiguously achieved from the HMBC data. HMBCs were observed from 2-OCH_3 (δ 3.99) to C-2 (δ 150.9), 9-OCH_3 (δ 4.19) to C-9 (δ 145.7) and 10-OCH_3 (δ 4.10) to C-10 (δ 151.5) confirmed the assignments.

IR data showed the presence of the characteristic absorbance bands due to conjugated double bond at 1590, 1424 and 1362 cm^{-1}. MS exhibited a molecular ion peak at *m/z* 338 consistent with the formula $C_{20}H_{20}NO_4^+$ D.B.E of 11.5 indicating presence of a quaternary ammonium salt. All the data for compound **83** were consistent with the reported values for jatrorrhizine (Grycová *et al*., 2007). Jatrorrhizine (**83**) has been previously reported from several plant families: Papaveraceae, Berberidaceae, Fumariaceae, Menispermaceae, Ranunculaceae, Rutaceae, Annonaceae, Magnoliaceae and Convolvulaceae (Grycová *et al*., 2007).

4.1.6 Mixture of jatrorrhizine (83) and columbamine (130)

Repeated HSCCC ($CHCl_3$-MeOH-0.2 M HCl 7:3:4) of the combined fractions AKLM 4-6 of the methanolic extract of *A. kummeriae* leaves (IC_{50} 1.34±0.33-0.45±0.15 µg/ml, SI >25-131.0) followed by column chromatography (SiO_2 60, MeOH-CH_2Cl_2-HCO_2H 4:15:1) and PTLC (MeOH-CH_2Cl_2-HCO_2H 5:14:1) yielded an inseparable mixture (1.2:1.0) of jatrorrhizine (**83**) and columbamine (**130**) as amorphous orange solid which was re-crystallized (MeOH) to orange solid (34.2 mg, mp. 235-240 ºC). The mixture of jatrorrhizine (**83**) and columbamine (**130**) gave positive reaction for alkaloids with Dragendorff's reagent and for chlorides with silver nitrate reagent confirming presence of chloride counter ion.



130

The chemical structures of jatrorrhizine (**83**) and columbamine (**130**) were established on the basis of 1D (^1H) and 2D-NMR experiments (HMQC, COSY, NOESY and HMBC), (Table 23-24, Appendix 6a-e) plus MS data (Appendix 6f) and upon comparison with reported values (Rasoanaivo *et al*., 1991; Hsieh *et al*., 2004).

Table 23: 1D and 2D ^1H NMR (600 MHz, $CDCl_3$) data for columbamine (**130**)

Position	δ_{obs}	J_{obs} (Hz)	COSY	δ_{lit}	J_{lit} (Hz)
1	7.51 (1H, *s*)			7.52 (1H, *s*)	
4	7.00 (1H, *s*)			6.80 (1H, *s*)	
5	3.24 (2H, *t*)	6.0	H-6	3.30 (2H, *t*)	6.1
6	4.92 (2H, *t*)	6.0	H-5	4.97 (2H, *t*)	6.1
8	9.74 (1H, *br, s*)		H-13	9.45 (1H, *br, s*)	
11	8.10 (1H, *d*)	9.0	H-12	7.58 (1H, *d*)	9.2
12	7.99 (1H, *d*)	9.0	H-11	8.11 (1H, *d*)	9.2
13	8.63 (1H, *s*)		H-8	8.45(1H, *s*)	
2-OCH_3	3.95 (3H, *s*)			3.98 (3H, *s*)	
9-OCH_3	4.20 (3H, *s*)		H-8	4.08 (3H, *s*)	
10-OCH_3	4.10 (3H, *s*)		H-11	4.03 (3H, *s*)	

Literature data (δ_{lit}) are from Hsieh *et al*., 2004

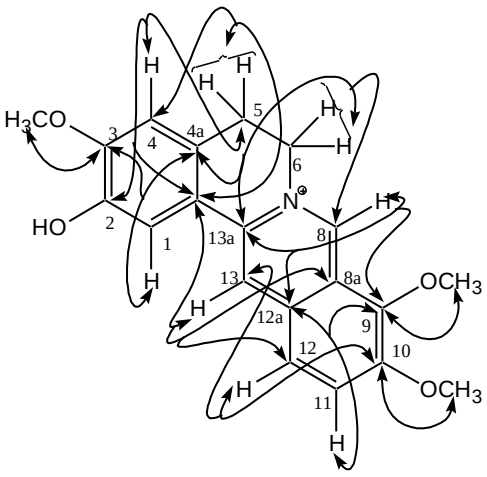
Table 24:1D and 2D ^{13}C NMR data (600 MHz, $CDCl_3$) for Columbamine (**130**)

Position	δ_{obs}	HMQC (δ)	HMBC	δ_{lit}
1	109.2 (*d*)	7.51	C-3, C-4a, C-13a, C-13b	114.9
2	149.2 (*s*)			147.3
3	152.8 (*s*)			150.4
4	111.7 (*d*)	7.00	C-2, C-3, C-13b	109.4
4a	127.8 (*s*)			133.6
5	27.7 (*t*)	3.24	C-4, C-4a, C-13b	26.3
6	57.4 (*t*)	4.92	C-4a, C-8, C-13a	55.6
8	146.1 (*d*)	9.74	C-8a, C-9, C-12a, C-13a	144.8
8a	123.2 (*s*)			117.4
9	145.5 (*s*)			148.0
10	151.7 (*s*)			149.9
11	127.8 (*d*)	8.10	C-9, C-10, C-12, C-12a	126.5
12	124.3 (*d*)	7.99	C-8, C-9, C-11, C-12a, C-13	123.3
12a	135.2 (*s*)			128.2
13	120.8 (*d*)	8.63	C-8, C-8a, C-9, C-12, C-12a, C-13a, C-13b	119.8
13a	140.0 (*s*)			138.3
13b	120.5 (*s*)			121.4
3-OCH_3	57.5 (*q*)	3.95	C-3	56.9
9-OCH_3	62.4 (*q*)	4.20	C-9	61.8
10-OCH_3	56.4 (*q*)	4.10	C-10	56.3

δ_{obs} -^{13}C data and multiplicity deduced from HMQC and HMBC:– literature data (δ_{lit}) are from Rasoanaivo *et al*., 1991

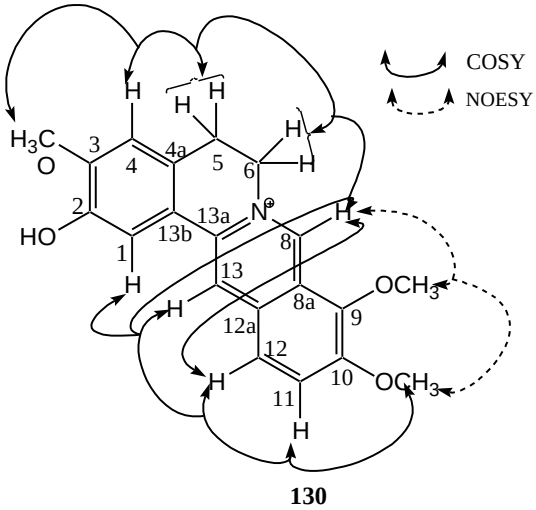
The aromatic region of the ^1H NMR spectrum consisted of eleven signals: 6 methine singlets and 4 doublets with two different integration intensities suggesting the presence a mixture of two different compounds in a ratio of 1.2:1.0. The non-aromatic region of the ^1H NMR spectrum revealed 6 methoxyl singlets and 4 methylene triplets. Jatrorrhizine (**83**) in the mixture was identified by comparison with the NMR data discussed elsewhere in this thesis. The ^1H and ^{13}C NMR data of columbmine (**130**) were unambiguously assigned with the help of COSY, NOESY, HMQC and HMBC experiments (Fig. 18-19).

Figure 18: Important HMBCs for columbamine (**130**)



130

Figure 19: Important COSYs and NOESYs for columbamine (**130**)



130

The starting point for the identification of and columbamine (**130**) in the mixture was the signal at δ 7.51 (1H, *s*, H-1) which exhibited HMQC to C-1 (δ 109.2) and long-range HMBCs to C-3 (δ 152.8), C-4a (δ 127.8), C-13a (δ 140.0), and C-13b (δ 120.5). H-4 (δ 7.0) exhibited long-range HMBCs to C-2 (δ 149.2), C-3 (δ 152.8) and C-13b (δ 120.5). Correlations were observed between H-4 (δ 7.00) and 3-OCH_3 (δ 3.95) in the COSY spectrum. 3-OCH_3 (δ 3.95) showed HMQC to 3-OCH_3 (δ 56.4). H-5 (δ 3.24) showed long-range HMBC to C-4 (δ 111.7). The observations confirmed presence of H-1 and H-4 in the 1, 2, 4, 5-tetra-substituted benzene ring residue of the protoberberine skeleton.

The COSY spectrum displayed correlations between H-5 (δ 3.24) and H-6 (δ 4.92) confirming that H-5 and H-6 are neighbours. H-6 (δ 4.92) displayed HMBCs to C-4a (δ 127.8), C-13a (δ 140.0) and C-8 (δ 146.1) confirming the assignment of the two methylene groups. H-6 signal shifted down-field due to electron withdrawing effect the quaternary nitrogen attached to C-6. Consequently, H-5 (C-5) and H-6 (C-6) are connected on one side to the aromatic system containing H-1 and H-4 and four quaternary carbons of the 1, 2, 4, 5-tetra-substituted benzene ring residue of the protoberberine skeleton. H-8 (δ 9.74) displayed HMQC to C-8 (δ 146.1) and HMBCs to C-13a (δ 140.0), C-8a (δ 123.2) and C-9 (δ 145.5). COSY spectrum showed long range correlation between H-8 (δ 9.74) and H-13 (δ 8.63). H-8 revealed a NOESY interaction with 9-OCH_3 (δ 4.20) which revealed HMBC to C-9 (δ 145.5) confirming attachment of the methoxyl group at C-9. The observations confirmed that H-5 (C-5) and H-6 (C-6) are connected to the aromatic system containing the two *para* protons (H-8 and H-13) and the four quaternary carbons of the 1, 3, 4, 6-tetra-substituted pyridine ring residue of the protoberberine skeleton.

HMBCs were observed between H-13 (δ 8.63) and C-13b (δ 120.5), C-13a (δ 140.0), C-8 (δ 146.1), C-8a (δ 123.2), C-9 (δ 145.5), C-12a (δ 135.2) and C-12 (δ 124.3). A typical ABX spin system at δ 8.10 (*d*, *J* 9.0 Hz, 1H, H-11), 7.99 (*d*, *J* 9.0 Hz, 1H, H-12) and 4.10 (*s*, 3H, 10-OCH_3) was observed in COSY spectrum indicating the presence of two *ortho* protons neighbouring a methoxyl group. Two-bond HMBCs were observed between H-11 (δ 8.10) and C-12 (δ 124.3) and C-10 (δ 151.7). Three-bond HMBCs were observed between H-11 (δ 8.10) and C-12a (δ 135.2) and C-9 (δ 145.5). Two-bond HMBC were also observed between H-12 (δ 7.99) and C-12a (δ 135.2) and C-11 (δ 127.8). A three-bond HMBC was observed between H-12 and C-8a (δ 123.2). A rare four-bond HMBC correlation was observed between H-12 and C-9 (δ 145.5). The observations confirmed the presence of *para* protons (H-8 and H-13) of the 1, 3, 4, 6-tetra-substituted pyridine ring residue of the protoberberine skeleton.

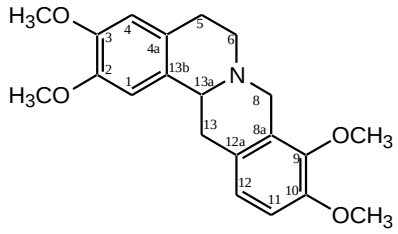
The ^{13}C NMR spectrum exhibited signals at δ 149.2 (C-2), 152.8 (C-3), 145.5 (C-9) and 151.7 (C-10) which were assigned to oxygenated aromatic carbons in *ortho* relationships on the aromatic rings (Agrawal, 1989). Since the molecule contains only three methoxyl groups, the fourth oxygenated functionality in the protoberberine molecule is unequivocally due to a hydroxyl group. The positions of the three methoxyl groups on the two aromatic rings were established by HMBC experiments.

The MS of mixture of jatrorrhizine (**83**) and columbamine (**130**) exhibited a molecular ion peak at *m/z* 338 consistent with the formula $C_{20}H_{20}NO_4^+$ (D.B.E 11.5) confirming the presence of quaternary nitrogen atom.

All the data for the second compound in the mixture were consistent with the reported values for columbamine (**130**) (Rasoanaivo *et al*., 1991; Hsieh *et al*., 2004). Columbamine (**130**) has been previously reported from several plant families: Papaveraceae, Berberidaceae, Fumariaceae, Menispermaceae, Ranunculaceae, Rutaceae, Annonaceae, Magnoliaceae and Convolvulaceae (Grycová *et al*., 2007).

4.1.7 Mixture of palmatine (82) and (–)-tetrahydropalmatine (131)

HSCCC ($CHCl_3$-MeOH-0.2 M HCl (7:3:4) of fraction 16 (AKLM 16) of the methanolic extract of *A. kummeriae* leaves (IC_{50} 0.09±0.03 µg/ml, SI 692) followed by column chromatography (SiO_2 60, MeOH-CH_2Cl_2-HCO_2H 5:14:1) and PTLC (SiO_2 60, MeOH:CH_2Cl_2:HCO_2H 4:15:1) gave an inseparable mixture (1.1:1.0) of palmatine (**82**) and (–)-tetrahydropalmatine (**131**) which was purified by re-crystallization (MeOH) to yield yellow amorphous solid (28.2 mg, m.p. 204-205 °C) that gave positive reaction for alkaloids with Dragendorff's reagent. The mixture posed separation difficulties as the two compounds have nearly the same molecular size and polarity.



131

The chemical structures of palmatine (**82**) and (–)-tetrahydropalmatine (**131**) were established on the basis of 1D (^1H) and 2D-NMR experiments (HMQC, COSY, NOESY and HMBC) (Table 25 – 26, Appendix 7a-e), plus MS data (Appendix 7f) and comparison with literature values (Rasoanaivo *et al*., 1991; Hsieh *et al*., 2004).

Table 25:1D and 2D ^1H NMR (600 MHz, CD_3OD) data for (–)-tetrahydropalmatine (**131**)

Position	δ_{obs}	J_{obs} (Hz)	COSY	δ_{lit}	J_{lit} (Hz)
1	6.89 (1H, *s*)		2-OCH_3	6.70 (1H, *s*)	
4	6.90 (1H, *s*)		3-OCH_3	6.58 (1H, *s*)	
5_{eq}	3.28 (1H, *m*)		H-6	2.65 (1H, *m*)	
5_{ax}	3.33 (1H, *m*)		H-6	3.10 (1H, *m*)	
6_{eq}	3.60 (1H, *m*)		H-5	3.16 (1H, *m*)	
6_{ax}	3.84 (1H, *m*)		H-5	2.59 (1H, *m*)	
8_{eq}	4.91 (1H, *d*)	15.7		4.20 (1H, *d*)	15.5
8_{ax}	4.78 (1H, *d*)	15.7		3.49 (1H, *d*)	15.5
11	7.07 (1H, *d*)	8.5	H-12,10-OCH_3	6.74 (1H, *d*)	8.4
12	6.98 (1H, *d*)	8.5	H-11	6.83 (1H, *d*)	8.4
13_{ax}	3.15 (1H, *dd*)	18.0, 10.3	H-13a	2.79 (1H, *dd*)	15.6, 11.4
13_{eq}	3.50 (1H, *dd*)	18.0, 5.7	H-13a	3.33 (1H, *dd*)	15.8, 3.8
13a	4.76 (1H, *dd*)	10.3, 5.7	H-13	3.49 (1H, *dd*)	11.4, 3.8
2-OCH_3	3.84 (3H, *s*)		H-1	3.84 (3H, *s*)	
3-OCH_3	3.85 (3H, *s*)		H-4	3.81 (3H, *s*)	
9-OCH_3	3.90 (3H, *s*)			3.82 (3H, *s*)	
10-OCH_3	3.87 (3H, *s*)		H-11	3.80 (3H, *s*)	

δ_{lit} – literature data are from Blanchfield *et al*., 2003

Table 26: 2D NMR (600 MHz, CD_3OD) data of (–)-tetrahydropalmatine (131)

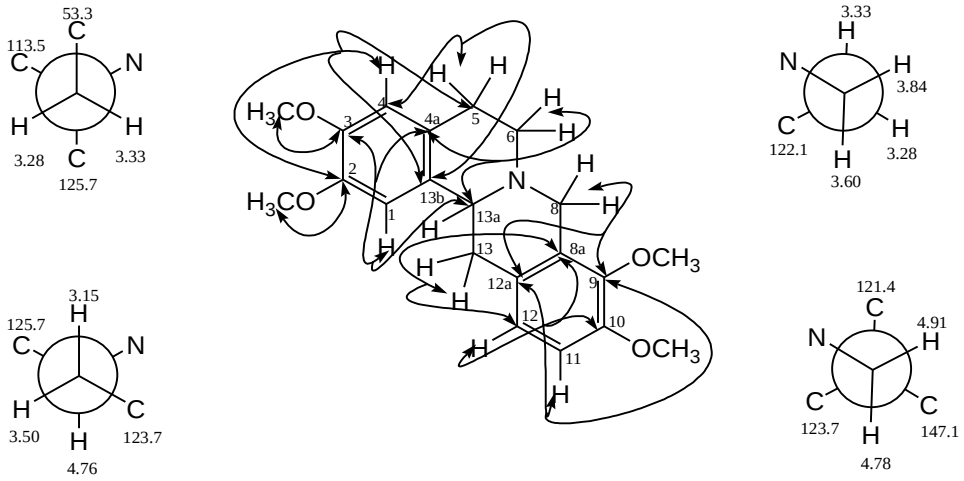
Position	δ_{obs}	HMQC (δ_H)	HMBC	δ_{lit}
1	111.3 (*d*)	6.89	C-3, C-4a, C-13a	108.5
2	151.6 (*s*)			147.5
3	150.4 (*s*)			147.3
4	113.5 (*d*)	6.90	C-2, C-5, C-13b	111.2
4a	125.7 (*s*)			126.7
5_{eq}	24.6 (*t*)	3.28	C-4, C-13b	29.1
5_{ax}	24.6 (*t*)	3.33	C-4, C-13b	29.1
6_{eq}	53.3 (*t*)	3.60	C-4a	51.5
6_{ax}	53.3 (*t*)	3.84	C-13a	51.5
8_{eq}	61.4 (*t*)	4.91	C-13a	59.8
8_{ax}	61.4 (*t*)	4.78	C-12a, C-9	59.8
8a	121.4 (*s*)			121.7
9	147.1 (*s*)			150.2
10	153.1 (*s*)			155.0
11	115.0 (*d*)	7.07	C-9, C-12a	114.8
12	125.0 (*d*)	6.98	C-10, C-8a, C-13	124.8
12a	123.7 (*s*)			122.6
13_{ax}	35.4 (*t*)	3.15 (ax)	C-13b	36.3
13_{eq}	35.4 (*t*)	3.50 (eq)	C-8a, C-12	36.3
13a	67.7 (*d*)		C-4a, C-12a	59.3
13b	125.7 (*s*)			126.6
2-OCH_3	53.5 (*q*)	3.84	C-2	55.8
3-OCH_3	56.4 (*q*)	3.85	C-3	55.8
9-OCH_3	63.1 (*q*)	3.90	C-9	60.1
10-OCH_3	56.1 (*q*)	3.87	C-10	56.0

Literature data (δ_{lit}) are from Hussain *et al.*, 1989; ^{13}C data and multiplicity deduced from HMQC and HMBC

The ^1H and ^{13}C NMR spectra of the mixture of palmatine (**82**) and (–)-tetrahydropalmatine (**131**) exhibited resonances attributable to the presence of aromatic and non-aromatic systems in the molecules. Palmatine (**82**) was identified from comparison with NMR data discussed earlier in this thesis.

^1H NMR and HMQC data were used as starting point for the identification of (–)-tetrahydropalmatine (**131**) in the mixture. The aromatic region of the ^1H NMR spectrum which displayed two singlet peaks and a pair of doublets with clear AB spin pattern consistent with two *para* arrangement in one ring and two *ortho* protons in the other. The aliphatic region of the ^1H NMR spectrum revealed four methylene groups appearing as a pair of AB doublets and four multiplets linked to the same molecular framework. Unambiguous assignment was done with the help of COSY, NOESY, HMQC and HMBC spectra (Fig. 20-21, Appendix 7b – 7e,).

Figure 20: Important HMBCs for (–)-tetrahydropalmatine (**131**)



131

Figure 21: Important COSYs and NOESYs for (–)-tetrahydropalmatine (**131**)

131

The first aromatic ring was characterized by the presence of two *para* protons at δ 6.89 (1H, *s*, H-1) and δ 6.90 (1H, *s*, H-4) which exhibited HMQCs C-1 (δ 111.3) and C-4 (δ 113.5), respectively. H-1 (δ 6.89) exhibited three-bond HMBC to C-3 (δ 150.4), C-4a (δ 122.1) and C-13a (δ 67.7) while H-4 (δ 6.90) displayed HMBC to C-2 (δ 151.6), C-13b (δ 125.7) and C-5 (δ 24.6). HMQCs were observed between 2-OCH_3 (δ 3.84) and 3-OCH_3 (δ 3.85) and carbons at 2-OCH_3 (δ 53.3) and 3-OCH_3 (δ 56.4), respectively. 2-OCH_3 (δ 3.84) and 3-OCH_3 (δ 3.85) displayed long-range HMBC to C-2 (δ 151.6) and C-3 (δ 150.4), respectively, confirming their assignment. The observations confirmed the existence of two *para* protons (H-1 and H-4), two methoxyl groups attached to the ring and the two quaternary carbons consistent with the 1, 2, 4, 6-tetra-substituted benzene ring in the protoberberine skeleton.

The second ring was deduced from the aromatic region of the ^{1}H and COSY NMR spectra. The aromatic region of the ^{1}H NMR spectrum revealed an AB spin system at δ 7.07 (1H, *d, J* 8.3 Hz, H-11) and δ 6.98 (1H, *d, J* 8.3 Hz, H-12) confirming the presence of two *ortho* protons on the ring. HMQC revealed the attachment of the H-11 (δ 7.07) and H-12 (δ 6.98) to C-11 (δ 115.0) and C-12 (δ 125.0), respectively. H-11 (δ 7.07) had three-bond HMBC to C-9 (δ 147.1) and C-12a (δ 123.7) while H-12 (δ 6.98) had HMBC to C-10 (δ 153.1) and C-13 (δ 35.4). COSY revealed long range interactions between the H-11 (δ 7.07) and the 10-OCH_3 (δ 3.87) which was also confirmed by NOESY. 10-OCH_3 (δ 3.87) showed HMQC to 10-OCH_3 (δ 56.1) and long-range HMBC to C-10 (δ 153.1). HMQC was observed from 9-OCH_3 (δ 3.90) to 9-OCH_3 (δ 63.1). Similarly, HMBC was also observed between 9-OCH_3 (δ 3.90) and C-9 (δ 147.1). The observations confirmed the assignment of 2 *ortho* protons (H-11 and H12), 2 methoxyls and the 2 quaternary carbons consistent with the 1, 2, 3, 4-tetra-substituted benzene ring in the protoberberine skeleton.

The aliphatic region of the ^{1}H NMR spectrum displayed 4 CH_2 groups consistent with (–)-tetrahydropalmatine (**131**) molecular framework. An AB system at δ 4.91 (1H, *d, J* 15.7, H-8_{eq}) and δ 4.78 (1H, *d, J* 15.7, H-8_{ax}) displayed *geminal* interaction as confirmed by the large coupling (*J* 15.7 Hz) between the signals as demonstrated by HMQC to C-8 (δ 61.4). The presence of such a deshielded, isolated CH_2 group is unique for the C-8 bridge in protoberberine alkaloids (Hussain, 1989; Blanchfield *et al*., 2003; Li *et al*., 2006). H-8_{ax} (δ 4.78) displayed three-bond HMBC to C-12a (δ 123.7) and C-9 (δ 147.1). Two-bond HMBCs were also observed between at H-8_{ax} (δ 4.78) and H-8_{eq} (δ 4.91) and C-8a (δ 121.4).

The ^{1}H NMR spectrum revealed the presence of an isolated CH–CH_2 moiety at δ 4.76 (1H, *dd, J* 5.7, 10.3 Hz, H-13a $_{ax}$), 3.50 (1H, *dd, J* 5.7, 18.0 Hz, H-13_{eq}) and 3.15 (1H, *dd, J* 10.3, 18.0 Hz, H-13_{ax}). H-$13a_{ax}$ (δ 4.76) had HMQC with C-13a (δ 67.7). The deshielding observed for H-13 and C-13 suggested that it is adjacent to the quaternary nitrogen atom. H-13_{ax} (δ 3.15) revealed *geminal* (*J* 18.0) and *vicinal* (*J* 10.3) couplings suggesting large dihedral angle (~180º) between H-13_{ax} and the H-13a $_{ax}$. Likewise, H-13_{eq} (δ 3.50) revealed much smaller *vicinal* coupling (*J* 5.7 Hz), suggesting smaller dihedral angle (~90º). The H-$13a_{ax}$ (δ 4.76) displayed three-bond HMBC to C-4a (δ 125.7).

The remaining aliphatic signals were due to the two sets of multiplets arising from the CH_2–CH_2 spin system. In the first set, the proton signals at δ 3.33 (1H, *m*, H-5_{ax}) and 3.28 (1H, *m*,

H-5$_{eq}$) had HMQC to C-5 (δ 24.6) confirming that both protons are attached to the same carbon. H-5$_{eq}$ and H-5$_{ax}$ displayed HMBC to C-4 (δ 113.5) and C-13b (δ 125.7). The second set appeared further downfield at δ 3.60 (1H, *m*, H-6$_{eq}$) and 3.84 (1H, *m*, H-6$_{ax}$) exhibiting HMQC to C-6 (δ 53.3) and confirming that both protons are attached to C-6. The deshielded C-6 (δ 53.3) confirmed that the CH_2 group is attached to nitrogen atom. H-6$_{ax}$ (δ 3.84) and H-6$_{eq}$ (δ 3.60) showed long-range HMBC to C-4a (δ 122.1). H-6$_{ax}$ and H-6$_{eq}$ displayed COSY interactions with H-5$_{eq}$ (δ 3.28) and H-5$_{ax}$ (δ 3.33). The observations revealed that the aliphatic part is linked to the two aromatic rings and confirmed the structure of the isolated alkaloid as (–)-tetrahydropalmatine (**131**).

The MS of the mixture of palmatine (**82**) and (–)-tetrahydropalmatine (**131**) exhibited molecular ion peaks at *m/z* 353 and *m/z* 356 consistent with the formulae $C_{21}H_{22}NO_4^+$ (D.B.E 11.5) and $C_{21}H_{27}NO_4$ (D.B.E 10). The non-integer DBE value confirmed the presence of quartenary nitrogen atom in palmatine (**82**) while the odd molecular mass confirmed the presence of a neutral alkaloid.

Comparison of the observed spectral data with literature values for palmatine (**82**) and (–)-tetrahydropalmatine (**131**) (Hussain *et al*., 1989; Halbsguth *et al*., 2003; Blanchfield *et al*., 2003; Li *et al*., 2006) confirmed the structures. (–)-Tetrahydropalmatine (**131**) has been previously reported from several plant families: Papaveraceae, Berberidaceae, Fumariaceae, Menispermaceae, Ranunculaceae, Rutaceae, Annonaceae, Magnoliaceae and Convolvulaceae (Hussain *et al*., 1989; Blanchfield *et al*., 2003; Grycová *et al*., 2007).

4.2. Anti-parasitic activity and cytotoxicity of compounds isolated from *Annickia kummeriae*

The anti-parasitic activity (*P. falciparum, T. b. rhodesiense* and *L. donovani*) and the cytotoxicity (rat myoblast L-6 cells) data for the isolated compounds are summarized in table 27.

Table 27: Anti-protozoal activity (IC_{50}), and cytotoxicity (CC_{50}) data of isolated compounds

	P. falciparum K1		*T.b. rhodesiense*		*L. donovani*		L-6 cells
Compound	IC_{50} ± S.E (µg/ml)	SI	IC_{50} ± S.E (µg/ml)	SI	IC_{50} ± S.E (µg/ml)	SI	CC_{50} ± S.E (µg/ml)
Lysicamine (**127**)	2.4±0.642	1.5	3.7±0.001	2.3	2.7±0.001	1.7	1.6±0.01
Trivalvone (**128**)	1.6±0.232	28.3	14.3±0.001	3.2	2.9±0.001	15.6	45.3±0.02
AKLM 2.1.4.4 (**129**)	2.3±0.440	17.9	2.8±0.001	14.7	9.1±0.005	4.5	41.1±0.06
Palmatine (**82**)	0.080±0.001	1,154	3.2±0.004	28.1	7.8±0.001	11.5	>90
Jatrorrhizine (**83**)	0.24±0.002	375.0	4.2±0.002	21.4	20.4±0.03	4.4	>90
Jatrorrhizine (**83**)/ columbamine (**130**)	0.14±0.017	358.6	4.0±0.001	12.6	13.1±0.02	3.8	50.2±0.08
Palmatine (**82**)/tetra-hydropalmatine (**131**)	0.098±0.002	629.6	4.3±0.005	14.4	7.0±0.06	8.81	61.7±0.01

P. falciparum – K1 strain, *T.b. rhodesiense* – STIB 900 strain, *L. donovani* - MHOM-ET-67/L82, L-6 - rat skeletal myoblast cells, IC_{50} – inhibitory concentration for 50% of tested parasites, CC_{50} – cytotoxic concentration for 50% of tested cells, chloroquine IC_{50} 0.063±0.03, artemisinin IC_{50} 0.002±0.0001, melarsoprol IC_{50} 0.002±0.0001, miltefosine IC_{50} 0.11±0.001, podophyllotoxin IC_{50} 0.009±0.0003 µg/ml

Four compounds showed strong activity against *P. falciparum* K1 strain *in vitro* (IC_{50} 0.08±0.001-0.24±0.002 µg/ml) and satisfactory selectivity (SI >375->1,154) while the remaining three exhibited moderate anti-plasmodial activity (IC_{50} 1.6±0.23-2.4±0.04 µg/ml) and poor to moderate selectivity (SI 1.6–28.8).

Palmatine (**82**) exhibited the strongest anti-plasmodial activity against *P. falciparum* K1 strain (IC_{50} 0.08±0.001 µg/ml) *in vitro* and a favourable selectivity (SI 1,153.8). Six compounds were only moderately active against *T. b. rhodesiense* STIB 900 strain *in vitro* (IC_{50} 2.8±0.001–4.3±0.0005 µg/ml) and moderate selectivity (SI 14.4-28.1) whereas the remaining one was inactive (IC_{50} 14.3±0.001 µg/ml) and had no selectivity (SI 3.2). Only two compounds were moderately active against *L. donovani* MHOM-ET-67/L82 axenic amastigotes (IC_{50} 2.7±0.0001-2.9±0.001 µg/ml) *in vitro* with poor to no selectivity (SI 1.7-15.6) while the remaining five were inactive (IC_{50} 7.0±0.001-20.4 ± 0.001 µg/ml) and poor to good selectivity indices (SI 3.8 - >11.5).

The anti-protozoal activities (IC_{50}) of isolated compounds were compared with the standard drugs (Table 28).

Table 28: Comparison of anti-protozoal activity (IC_{50}) and cytotoxicity (CC_{50}) of isolated compounds with standard drugs

Compound	IC_{50} cpd / IC_{50} CQ	IC_{50} cpd / IC_{50} Art	IC_{50} cpd / IC_{50} Mel	IC_{50} cpd / IC_{50} Milt	CC_{50} cpd / CC_{50} Pdx
Lysicamine (**127**)	38.1	1,200.0	1,850.0	23.6	177.8
Trivalvone (**128**)	25.4	800.0	7,150.0	26.4	5,033.3
AKLM 2.1.4.4 (**129**)	36.5	1,150.0	1,400.0	82.7	4,566.7
Palmatine (**82**)	1.3	40.0	1,600.0	70.9	>10,000
Jatrorrhizine (**83**)	3.8	120	2,100.0	185.5	>10,000
Jatrorrhizine (**83**) + columbamine (**130**) (1.2:1.0)	2.2	69.0	2,000.0	119.1	5,577.8
Palmatine (**82**) + **(–)-**tetrahydropalmatine (**131**) (1.1:1.0)	1.6	49.0	2,150.0	63.64	6,855.6

Cpd – isolated compound, CQ – chloroquine, Art – artemisinin, Mel – melarsoprol, Pdx - podophyllotoxin

Four compounds were of particular interest as they showed just slightly lower anti-plasmodial activity than chloroquine (1.3-3.8 folds) and artemisinin (40-120 folds). The remaining three had much weaker anti-plasmodial activity than chloroquine (25.4-38.1 folds) and artemisinin (800-1,150.0 folds). All the isolated compounds had very weak anti-trypanosomal activity (1,400.0-7,150.0 folds) compared to melarsoprol (IC_{50} 0.002±0.0001 µg/ml). Mild to moderate anti-leishmanial activity (23.6-185.5 folds) was noted for all the isolated compounds compared to miltefosine (IC_{50} 0.11±0.001 µg/ml). Lysicamine (**127**) revealed moderate cytotoxicity (177.8 folds) compared to podophyllotoxin (IC_{50} 0.009±0.0003 µg/ml). The remaining compounds were non-cytotoxic (4,566.7->10,000 folds).

Based on palmatine (**82**) molecular framework, the *in vitro* structure-activity relationship of the isolated compounds was examined for anti-protozoal activity and cytotoxicity. The methoxyl groups at C-2, C-3 (ring A) and C-9, C-10 (ring D) together with the quaternary nitrogen atom in position 7 were considered as the structural moeties required for strong anti-plasmodial activity. Structural comparison of palmatine (**82**) and jatrorrhizine (**83**) revealed the presence of a phenolic function at C-3 as the only difference. However, the presence of a free phenolic function at C-3 lowered the anti-protozoal activity of jatrorrhizine (**83**) significantly: anti-plasmodial (from IC_{50} 0.08±0.001 to 0.24±0.001 µg/ml), anti-trypanosomal (from IC_{50} 3.2±0.0004 to 4.2±0.001 µg/ml) and anti-leishmanial activity (from IC_{50} 7.8±0.001 to 20.4±0.001 µg/ml). The presence of the phenolic group at C-3 in jatrorrhizine (**83**) exhibited no change in cytotoxicity confirming the observed differences in bioactivity to be purely due the replacement of methoxyl with hydroxyl group at C-3 (Fig. 22).

Figure 22: Structure-activity-relationships of palmatine (**82**) and jatrorrhizine (**83**)



82

*P. falc*iparum IC_{50} 0.080, SI 1,154
T.b. rhodesiense IC_{50} 3.2, SI 28
L. donovani IC_{50} 7.8, SI 12
Cytotoxicity IC_{50} >90

83

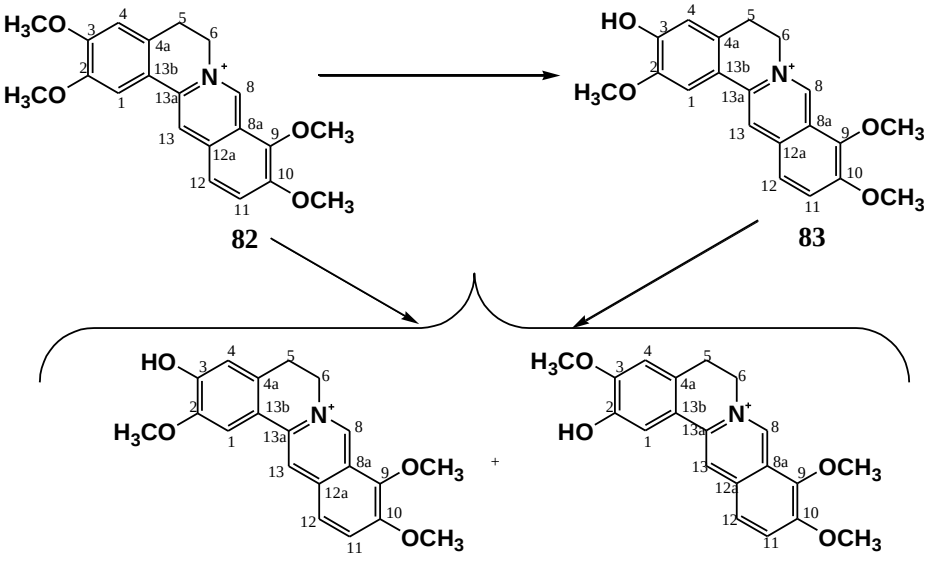
*P. falc*iparum IC_{50} 0.24, SI 375
T.b. rhodesiense IC_{50} 4.2, SI 21
L. donovani IC_{50} 20.4, SI 4.4
Cytotoxicity IC_{50} >90

The 1.2:1.0 mixture of jatrorrhizine (**83**) and columbamine (**130**) which contain phenolic group at the C-2 and C-3, respectively, resulted in a slight increase in anti-protozoal (0.6-1.0 fold) and cytotoxicity (1.8 folds) compared to jatrorrhizine (**83**) alone. However, the mixture further showed a general decline in anti-protozoal activity (1.3-1.7 folds) and increase in cytotoxicity (1.8 folds) compared to palmatine (**82**) (Fig. 23).

Figure 23: Comparison of anti-protozoal activity of palmatine (**82**), jatrorrhizine (**83**) and jatrorrhizine (**83**)- columbamine (**130**) mixture

*P. falc*iparum IC_{50} 0.080, SI 1,154
T.b. rhodesiense IC_{50} 3.2, SI 28
L. donovani IC_{50} 7.8, SI 12
Cytotoxicity IC_{50} >90

*P. falc*iparum IC_{50} 0.24, SI 375
T.b. rhodesiense IC_{50} 4.2, SI 21
L. donovani IC_{50} 20.4, SI 4.4
Cytotoxicity IC_{50} >90



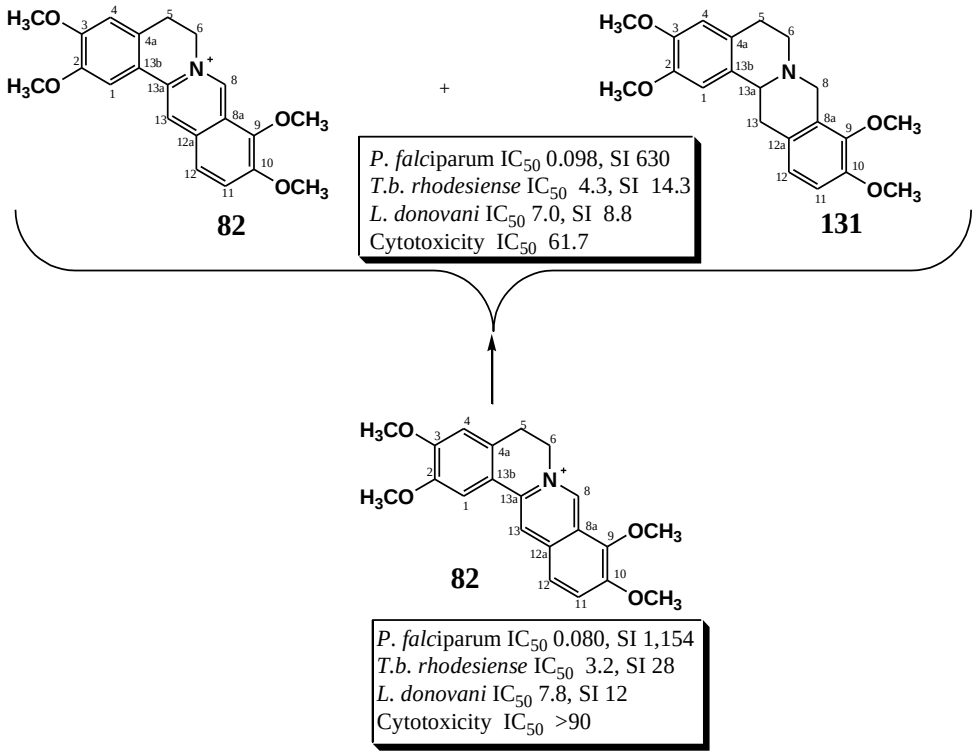
82 **83**

83 **130**

*P. falc*iparum IC_{50} 0.138, SI 364
T.b .rhodesiense IC_{50} 4.0, SI 13
L. donovani IC_{50} 13.1, SI 4
Cytotoxicity IC_{50} 50.2

Similarly, the mixture of palmatine (**82**) and (–)-tetrahydropalmatine (**131**) showed a remarkable decline in anti-plasmodial and anti-trypanosomal activity (1.2-1.3 fold), but a slight increase in anti-leishmanial activity (0.9 fold) and increase in cytotoxicity (1.5 folds) compared to palmatine (**82**) (Fig. 24).

Figure 24: Comparison of anti-protozoal activity of palmatine (**82**) and palmatine (**82**) -(–)-tetrahydropalmatine (**131**) mixture



The available literature indicated that plants that contain protoberberine and aporphine alkaloids are used in folkloric medicine as anti-hypertensive, anti-cancer, anti-septic, sedatives, analgesics, anti-inflammatory, anti-fungal, anti-bacterial and anti-protozoans (Guo *et al*., 1999; Hussain *et al*., 1989). Protoberberines isolated from *Enantia chlorantha* exhibited significant anti-plasmodial activity against CQ-sensitive and resistant strains of *P. falciparum*: palmatine (**82**) (IC_{50} 0.27 and 0.16 µg/ml, respectively) and jatrorrhizine (**83**) (IC_{50} 4.2 and 1.61 µg/ml, respectively) *in vitro* (Vennerstrom & Klayman, 1988). A mixture of protoberberine alkaloids from *Enantia chlorantha* containing; palmatine (**82**), jatrorrhizine (**83**) and columbamine (**130**) (Hepasor), prevented liver injury from chemically induced traumatization and also promoted the healing process after the injury (Virtanen *et al*., 1988). Palmatine (**82**) and jatrorrhizine (**83**) inhibited growth of *Babesia gibsoni* at a concentration ranging from 100 and 10 µg/ml (Guo *et al*., 1999).

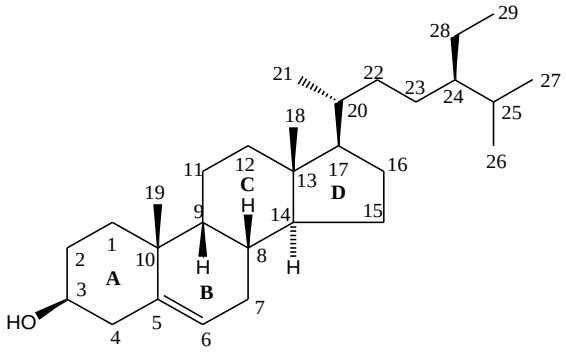
CHAPTER FIVE

IDENTIFICATION OF ANTI-PROTOZOAL CONSTITUENTS OF *ACRIDOCARPUS CHLOROPTERUS* OLIVER

5.1 Isolation and identification

5.1.1 β-Sitosterol (132)

Repeated column chromatography (SiO_2, pet ether-EtOAc) of the 4th MPLC fraction of the dichloromethane extract of *A. chloropterus* yielded **132** as a white amorphous solid (252.6 mg, m.p. 138-140 °C, decomposed), that gave positive colour tests for steroids with vanillin-sulfuric acid and *p*-anisaldehyde.



132

The structure was established on the basis of 1D (^1H, ^{13}C and DEPT 135) and 2D-NMR experiments (HMQC, COSY, NOESY and HMBC) (Table 29-30, Appendix 8a-f) plus MS data (Appendix 8g).

The steroidal nature of **132** was deduced from a combination of ^{13}C and DEPT-135 NMR, which revealed twenty nine carbons (6 x CH_3, 11 x CH_2, 9 x CH and 3 quaternary centers). ^1H NMR revealed 33 signals between δ 0.6 and 2.3 and only two protons with high chemical shifts: δ 5.34 (1H, br d, 4.8 Hz), characteristic of the H-6 of Δ^5–sterols, and 3.52 (1H, br d, 4.8 Hz, H-3_{ax}), suggesting a 3β-hydroxyl group (Goad, 1991; Morales *et a.l*, 2003; De-Eknamkul & Potduang, 2003). The signal at δ 71.9 (d) confirmed the presence of a secondary hydroxyl group (Morales *et al*., 2003, De-Eknamkul & Potduang, 2003).

Table 29:1D and 2D ^{1}H NMR (500 MHz, $CDCl_3$) data for β-sitosterol (**132**)

Position	δ_{obs}	J_{obs} (Hz)	COSY	δ_{lit}	J_{lit}(Hz)
1_{ax}	1.08 (1H, *m*)	14.5, 3.6, 3.6	H-2_{eq}		
1_{eq}	1.84 (1H, *m*)	14.9, 4.7			
2_{ax}	1.51 (1H, *m*)	15.4, 4.6	H-1_{eq}, H-3_{ax}		
2_{eq}	1.83 (1H, *m*)	11.2,			
3	3.52 (1H, *m*)	11.2, 4.8	H-4 $_{ax}$, H-4 $_{eq}$ H-2 $_{ax}$, H-2 $_{eq}$	3.52 (*m*)	
4_{ax}	2.23 (1H, *m*)	13.2, 2.1	H-3 $_{ax}$		
4_{eq}	2.30 (1H, *m*)	1.9, 2.6, 2.6			
6	5.34 (1H, *m*)	5.3, 1.9		5.36 (1H, *br*, *d*)	5.3
7_{ax}	1.50 (1H, *m*)	14.5, 2.1	H-7 $_{ax}$, H-7 $_{eq}$		
7_{eq}	1.97 (1H, *m*)	14.3,	H-4 $_{eq}$		
8_{eq}	1.46 (1H, *m*)	11.3, 11.2	H-6		
9_{ax}	0.94 (1H, *m*)	11.4, 4.9			
11_{ax}	1.50 (1H, *m*)	13.2, 3.4			
11_{eq}	1.60 (1H, *m*)	13.2, 3.4			
12_{ax}	1.18 (1H, *m*)	3.1			
12_{eq}	2.00 (1H, *m*)	13.2, 3.2			
14_{ax}	1.01 (1H, *m*)	10.6, 8.3	H-12 $_{eq}$		
15_{ax}	1.06 (1H, *m*)	11.1	H-11 $_{eq}$		
15_{eq}	1.56 (1H, *m*)				
16_{ax}	1.28 (1H, *m*)	10.8, 8.7			
16_{eq}	1.72 (1H, *m*)	10.7			
17_{ax}	1.15 (1H, *dd*)	9.9			
18_{eq}	0.70 (3H, *s*)			0.70 (3H, *s*)	
19_{eq}	1.01 (3H, *s*)			1.01 (3H, *s*)	
20	2.06 (1H, *m*)				
21	0.92 (3H, *d*)	6.6		0.92 (3H, *d*)	6.6
22_{ax}	1.34 (1H, *m*)				
22_{eq}	1.34 (1H, *m*)				
23_{ax}	1.31 (1H, *m*)				
23_{eq}	1.31 (1H, *m*)				
24	1.54 (1H, *m*)				
25	1.55 (1H, *m*)	6.4, 6.4			
26	0.84 (3H, *d*)	7.0		0.84 (3H, *d*)	7.0
27	0.80 (3H, *d*)	7.0		0.81 (3H, *d*)	7.0
28_{ax}	1.18 (1H, *m*)	13.4, 3.6			
28_{eq}	1.43 (1H, *m*)	7.3, 5.7			
29	0.85 (3H, *t*)	7.0		0.85 (3H, *t*)	7.0

Literature data (δ_{lit}) from Morales *et al.*, 2003

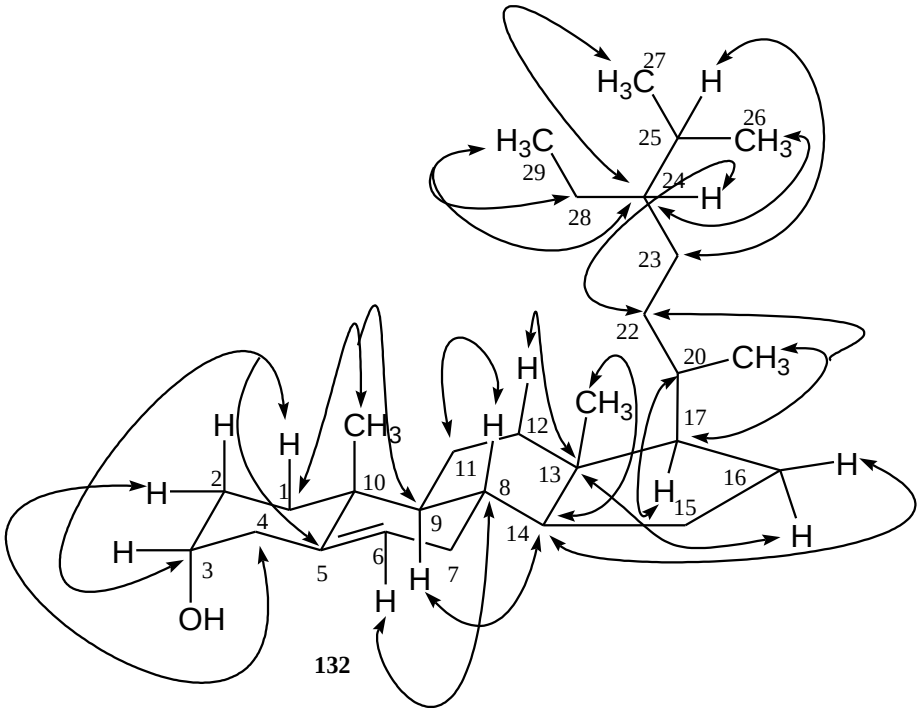
COSY cross peaks between H-3_{ax} (δ 3.52) and H-4_{eq} (δ 2.30, 1H, m, $J_{3ax,\ 4ax}$ 4.8 Hz), H-4_{ax} at δ (2.23, 1H, m, $J_{3ax,\ 4eq}$ 11.2 Hz), H-2_{ax} (δ 1.83, 1H, m, $J_{2ax,2eq}$ 15.4 Hz, $J_{2\ ax,3ax}$ 4.6 Hz) and H-2_{eq} (δ 1.51, 1H, m, $J_{2eq,\ 3ax}$ 11.2 Hz) confirmed 3*β*-hydroxyl orientation.

H-3 (δ 3.52) showed long range HMBC to C-5 (δ 140.8) and C-1 (δ 37.4) while H-19 (δ 1.01) showed HMBC to C-5 (δ 140.8) suggesting the olefinic bond at C-5/C-6 in ring B of the steroid. Three-bond HMBCs were also observed between H-19 and C-1 (δ 37.4) and C-9 (δ 50.3). The HMBCs observed between H-6 (δ 5.34) and C-4 (δ 42.4) as well as C-7 (δ 32.1) confirmed the position of the double bond at C-5/C-6. The downfield chemical shift of

the 3α-methine proton (δ 3.52) is consistent with the deshielding of the axial proton by the C-5/C-6 double bond (Forgo & Köver, 2004).

COSY spectrum of sitosterol (**132**) confirmed the presence of four almost isolated ^{1}H spin systems, one spin system for each of the four rings A – D of the triterpene skeleton, ring A: H-1_{ax} (δ 1.08), H-1_{eq} (δ 1.84), H-2_{ax} (δ 1.51), H-2_{eq} (δ 1.83), H-3_{ax} (δ 3.52), H-4_{ax} (δ 2.23) and H-4_{eq} (δ 2.30); ring B: H-6 (δ 5.34), H-7_{ax} (δ 1.50) and H-7_{eq} (δ 1.97); ring C: H-8 (δ 1.46), H-9 (δ 0.94), H-11_{ax} (δ 1.50), H-11_{eq} (δ 1.60), H-12_{ax} (δ 1.18) and H-12_{eq} (δ 2.00); and ring D: H-14 (δ 1.01), H-15_{ax} δ 1.06), H-15_{eq} (δ 1.56), H-16_{ax} (δ 1.28) , H-16_{eq} (δ 1.72) and H-17 (δ 1.15). The orientation of H-7β (δ 1.97) was deduced from the COSY cross peaks with H-6 (δ 5.34), which in turn showed COSY interaction with H-8_{eq} (δ 1.46). The data confirmed that H-6, H-7_{eq} and H-8_{eq} are on the same β face of the steroid ring. Other important HMBC and COSY data are summarized in table 30. All important HMBCs are summarized in figure 25.

Figure 25: Important HMBCs for β-sitosterol (**132**)



132

Table 30:1D and 2D ^{13}C NMR (500 MHz, $CDCl_3$) data for β-sitosterol (**132**)

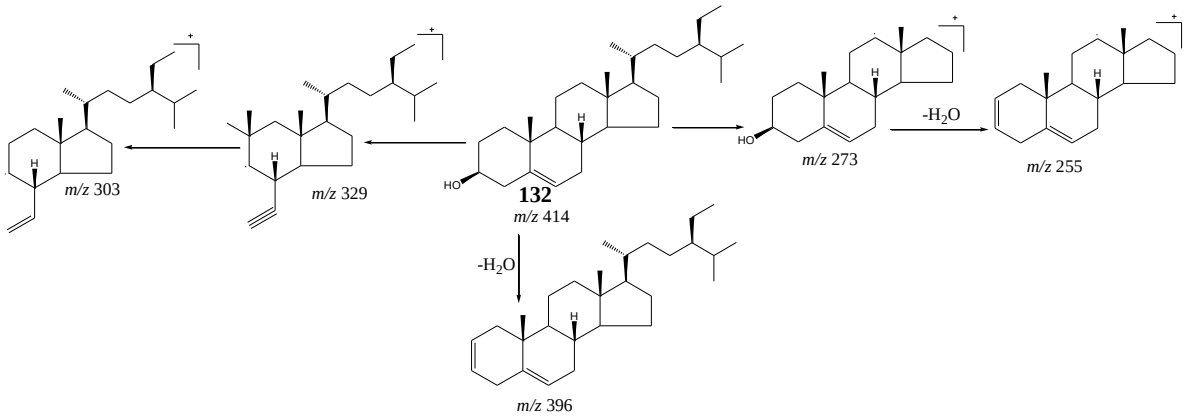
Position	δ_{obs}	HMQC (δ)	HMBC	δ_{lit}
1	37.4 (*t*)	1.08, 1.84	C-19, C-10, C-5, C-3	37.3
2	31.8 (*t*)	1.83, 1.51	C-5, C-4, C-3, C-1	31.6
3	71.9 (*d*)	3.52	C-5, C-1	71.7
4	42.4 (*t*)	2.30, 2.23	C-6, C-5	42.2
5	140.8 (*s*)			140.8
6	121.8 (*d*)	5.34	C-10, C-8, C-7	121.6
7	32.0 (*t*)	1.50, 1.97	C-6	31.9
8	32.0 (*d*)	1.46	C-14, C-11, C-9, C-6	31.9
9	50.3 (*d*)	0.94	C-14, C-11	50.2
10	36.7 (*s*)			36.5
11	21.2 (*t*)	1.60, 1.50	C-13, C-12, C-9, C-8	21.1
12	39.8 (*t*)	1.18, 2.0	C-18, C-11	39.8
13	42.4 (*s*)			42.3
14	57.0 (*d*)	1.01	C-13, C-11, C-9, C-8	56.8
15	24.5 (*t*)	1.56, 1.06	C-16, C-13	24.3
16	29.1 (*t*)	1.72, 1.28	C-15, C-14, C-13	28.3
17	56.1 (*d*)	1.15	C-23, C-22, C-18	56.1
18	12.2 (*q*)	0.70	C-17, C-14, C-12	11.9
19	19.5 (*q*)	1.01	C-9, C-5, C-1	19.4
20	40.7 (*d*)	2.06	C-23, C-22	36.2
21	21.4 (*q*)	0.92	C-23, C-22, C-17	18.8
22	33.91 (*t*)	1.34, 1.34	C-29, C-28, C-24, C-21, C-17	33.9
23	26.02 (*t*)	1.31, 1.31	C-26, C-25, C-24, C-17, C-20	26.1
24	51.4 (*d*)	1.54	C-29, C-28, C-22,	45.9
25	32.0 (*d*)	1.55	C-29, C-23	29.2
26	21.2 (*q*)	0.84	C-24, C-23	19.8
27	19.1 (*q*)	0.80	C-28, C-24	19.1
28	25.6 (*t*)	1.43, 1.18	C-27, C-24	23.1
29	12.4 (*q*)	0.85	C-28, C-25, C-24	12.3

Multiplicity determined from DEPT 135 experiments; Literature data (δ_{lit}) from Goad, 1991.

LREIMS gave the molecular ion at *m/z* 414 M^+ corresponding to the formula $C_{29}H_{50}O$. Other prominent peaks were seen at *m/z* 396 $[M\text{-}H_2O]^+$, 329 $[M\text{-}C_5H_9O]^+$, 303 $[M\text{-}C_7H_{11}0]^+$, 273 $[M\text{-}C_{10}H_{21}]^+$ and 255 $[M\text{-}C_{10}H_{22}0]^+$ consistent with the suggested β-sitosterol (**132**) (Fig. 26).

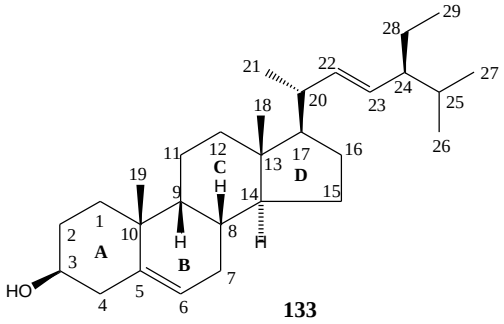
All the data confirmed the structure of **132** as β-sitosterol and was consistent with literature values (Goad, 1991; Morales *et al*., 2003, De-Eknamkul & Potduang, 2003). β-Sitosterol (**132**) has been reported to occur in several plant species (Connolly & Hill, 1989). However, this is the first report on its isolation from *A. chloropterus.*

Figure 26: Important MS fragmentation observed in β-sitosterol (**132**)



5.1.2 Stigmasterol (133)

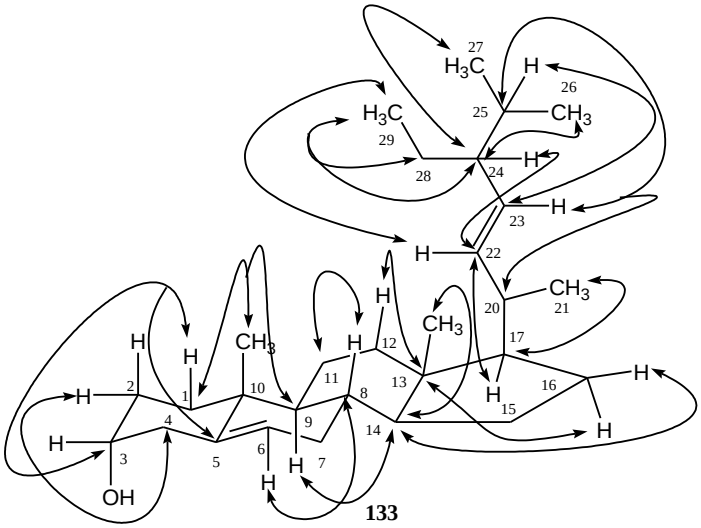
Repeated column chromatography (SiO_2, pet ether-EtOAc) of the combined 4th MPLC fraction of the dichloromethane extract of *A. chloropterus* yielded **133** as white needles (320.3 mg, m.p. 166-169 °C, decomposed), that gave positive colour test for steroids with vanillin-sulfuric acid and *p*-anisaldehyde.



The structure was established on the basis of 1D (^{1}H, ^{13}C and DEPT 135) and 2D-NMR experiments (HMQC, COSY and HMBC), (Table 31-32, Appendix 9a-f) plus MS data (Appendix 9g). The steroidal nature of **133** was deduced from a combination of ^{13}C, HMQC and DEPT-135 NMR data, which revealed 29 nine carbons (6 x CH_3, 9 x CH_2, 11 x CH, and 3 quaternary centers). The signal at δ 71.9 (d) indicated the presence of a secondary hydroxyl group. The ^{1}H NMR data revealed the presence of two methyl groups attached to tertiary centres: δ 0.69 (3H, *s*) and 1.01 (3H, *s*); three methyl groups attached to secondary centres: δ 0.79 (3H, *d*, *J* 6.5 Hz), 0.84 (3H, *d*, *J* 6.5 Hz), 1.04 (3H, *d*, *J* 6.5 Hz); and one methyl group attached to a primary centre: δ 0.81 (3H, *t*, *J* 7.5 Hz), suggesting the presence of a steroidal skeleton. The signal at δ 5.35 (1H, *m*) was characteristic of Δ^5-sterols.The peaks at δ 5.18 (1H, *dd*, *J* 8.8 Hz, 15.3 Hz) and 5.03 (1H, *dd*, *J* 8.3, 11.8 Hz) was typical for the H-22/H-23 olefinic protons in the side chain of stigmasterol (Forgo & Köver, 2004).

The signal due to H-3_{ax} proton resonated at the expected chemical shift δ 3.52 (1H, *m*, H-3_{ax}) for the Δ^5-sterols confirming C-5/C-6 unsaturated sterol (Forgo & Köver, 2004). The downfield chemical shift of the 3α- methine proton at δ 3.52 is in agreement with the deshielding of the axial protons by the C-5/C-6 double bond. H-3 (δ 3.52) revealed HMBCs with C-5 (δ 140.9) and C-1 (δ 37.4). Axial-equatorial coupling was observed between H-3_{ax} and H-2_{eq} (δ 1.51, 1H, *m*, $J_{2eq,3ax}$ 11.2 Hz) while an axial-axial coupling was observed for H-2_{ax} (δ 1.84, 1H, *m*, $J_{2ax,3ax}$ 4.6 Hz). Similarly, COSY interaction between H-3_{ax} and H-4_{ax} (δ 2.27, 1H, *m*, $J_{3ax,4ax}$ 4.8 Hz) as well as H-4_{eq} (δ 2.23,1H, *m*, $J_{3ax,4eq}$ 11.2 Hz) was noted. COSY interactions were observed between H-2_{ax} (δ 1.84) and H-1_{eq} (δ 1.86, 1H, *m*, $J_{2ax,1eq}$ 3.6 Hz). H-6 showed interactions with H-7_{eq} (δ 1.96, 1H, *m*, $J_{6,7eq}$ 5.3 Hz), H-4_{eq} (δ 2.27, 1H, *m*, $J_{4eq,6}$ 1.9 Hz) and H-7_{ax} (δ 1.49, 1H, *m*, $J_{6,7ax}$ 1.9 Hz) in the COSY spectrum. H-22 (δ 5.18, 1H, *d*, 8.8, 15.3 Hz) showed HMQC to C-22 (δ 138.5) and strong COSY interaction to H-23 (δ 5.03, 1H, *d*, *J* 8.3, 11.8 Hz). The two olefinic carbon signals at δ 121.9 (d) and 140.9 (s) were indicative of the double bond at C-5/C-6 of the steroidal skeleton (Forgo & Köver, 2004). The signal at δ 5.35 (m) was assigned to H-6 due to the HMBCs to C-8 (δ 32.0), C-10 (δ 36.7) and C-7 (δ 32.0). The HMBCs observed between H-6 (δ 5.35) and C-4 (δ 42.4) as well as C-7 (δ 32.0) confirmed the position of the double bond at C-5/C-6. All important HMBCs are shown in figure 27.

Figure 27: Important HMBCs of stigmasterol (**133**)



133

Table 31: ^{1}H NMR and COSY (500 MHz, $CDCl_3$) data for stigmasterol (**133**)

Position	δ_{obs}	J_{obs} (Hz)	COSY	δ_{lit} (Hz)	J_{lit}
1_{ax}	1.05 (1H, *m*)	14.5, 3.6, 3.6	H-2_{eq}		
1_{eq}	1.86 (1H, *m*)	14.9, 4.7			
2_{ax}	1.51 (1H, *m*)	15.4, 4.6	H-1_{eq}, H-3_{ax}		
2_{eq}	1.84 (1H, *m*)	11.2,			
3	3.52 (1H, *m*)	11.2, 4.8	H-4_{ax}, H-4_{eq}, H-2_{ax}, H-2_{eq}	3.52 (1H, *m*)	
4_{ax}	2.24 (1H, *m*)	13.2, 2.1	H-3_{ax}		
4_{eq}	2.27 (1H, *m*)	1.9, 2.6, 2.6			
6	5.35 (1H, *m*)	5.3, 1.9		5.36 (1H, *br, d*)	5.3
7_{ax}	1.49 (1H, *m*)	14.5, 2.1	H-6, H-8_{eq}		
7_{eq}	1.96 (1H, *m*)	14.3,			
8_{eq}	1.45 (1H, *m*)	11.3, 11.2	H-6		
9_{ax}	0.95 (1H, *m*)	11.4, 4.9	H-8_{eq}		
11_{ax}	1.50 (1H, *m*)	13.2, 3.4	H-12_{ax}, H-12_{eq}		
11_{eq}	1.60 (1H, *m*)	13.2, 3.4			
12_{ax}	1.20 (1H, *m*)	3.1	H-11_{ax}, H-11_{eq}		
12_{eq}	2.00 (1H, *m*)	13.2, 3.2			
14_{ax}	1.01 (1H, *m*)	10.6, 8.3	H-8_{eq}		
15_{ax}	1.04 (1H, *m*)	11.1	H-16_{eq}		
15_{eq}	1.55 (1H, *m*)				
16_{ax}	1.27 (1H, *m*)	10.8, 8.7			
16_{eq}	1.71 (1H, *m*)	10.7			
17_{ax}	1.15 (1H, *dd*)	9.9			
18_{eq}	0.69 (3H, *s*)			0.70 (*3H, s*)	
19_{eq}	1.01 (3H, *s*)			1.01 (*3H, s*)	
20	2.04 (1H, *m*)				
21	1.04 (3H, *d*)	6.6		0.92 (*3H, d*)	6.6
22	5.18 (1H, *dd*)	8.8, 15.3			
23	5.03 (1H, *dd*)	8.3, 11.8			
24	1.51 (1H, *m*)				
25	1.56 (1H, *m*)	6.4, 6.4	H-23		
26	0.87 (3H, *d*)	6.5	H-22	0.84 (3H, *d*)	7.0
27	0.79 (3H, *d*)	6.5		0.81 (3H, *d*)	7.0
28_{ax}	1.43 (1H, *m*)	13.4, 3.6			
28_{eq}	1.15 (1H, *m*)	7.3, 5.7			
29	0.81 (3H, *t*)	7.5		0.85 (3H, *t*)	7.0

Literature data (δ_{lit}) from Morales *et al.*, 2003

The β orientation of H-6 was confirmed from COSY interaction with H-7_{eq} (δ 1.96), which in turn showed COSY cross peak with H-8_{eq} (δ 1.45) confirming them to be on the same β face. HMBCs were also observed between H-19 (δ 1.01, 3H) and C-1 (δ 37.4), C-5 (δ 140.9), as well as C-9 (δ 50.8) suggesting that H-6, H-7_{eq} and H-8_{eq} were on the β face of the steroid ring. H-22 (δ 5.18) exhibited HMBCs to C-20 (δ 40.7), C-17 (δ 56.1), C-23 (δ 129.4) and C-24 (δ 51.4). Similarly, H-23 (δ 5.03) showed HMBCs to C-20 (δ 40.7), C-22 (δ 138.5), C-24 (δ 51.4), C-25 (δ 32.0) and C-28 (δ 25.6) confirming the position of the double bond atC-22/C-23.

COSY spectrum of stigmasterol (**133**) confirmed the presence of four almost isolated ^{1}H spin systems, one spin system for each of the four rings A – D of the triterpene skeleton, ring A: H-1_{ax} (δ 1.05), H-1_{eq} (δ 1.86), H-2_{ax} (δ 1.51), H-2_{eq} (δ 1.84), H-3_{ax} (δ 3.52), H-4_{ax} (δ 2.24) and H-4_{eq} (δ 2.27); ring B: H-6 (δ 5.35), H-7_{ax} (δ 1.49) and H-7_{eq} (δ 1.96); ring C: H-8 (δ 1.45), H-9 (δ 0.95), H-11_{ax} (δ 1.50), H-11_{eq} (δ 1.60), H-12_{ax} (δ 1.20) and H-12_{eq} (δ 2.00); and ring D: H-14 (δ 1.01), H-15_{ax} δ 1.04), H-15_{eq} (δ 1.55), H-16_{ax} (δ 1.27), H-16_{eq} (δ 1.71) and H-17 (δ 1.15). Other important HMBC and COSY are summarized in table 32.

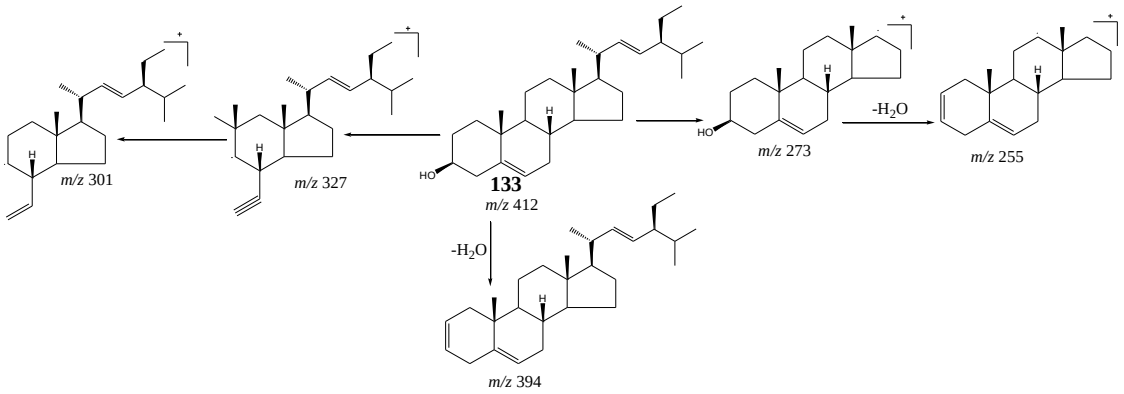
Table 32: 1D and 2D NMR (500 MHz, $CDCl_3$) data for stigmasterol (**133**)

Position	δ_{obs}	HMQC (δ)	HMBC	δ_{lit}
1	37.4 (t)	1.05, 1.86	C-19, C-10, C-5, C-3	37.3
2	31.8 (t)	1.84, 1.51	C-5, C-4, C-3, C-1	31.7
3	71.9 (d)	3.52	C-5, C-1	71.8
4	42.4 (t)	2.27, 2.24	C-6, C-5	42.4
5	140.9 (s)			140.8
6	121.9 (d)	5.35	C-10, C-8, C-7	121.7
7	32.0 (t)	1.49, 1.96	C-6	31.9
8	32.0 (d)	1.45	C-14, C-11, C-9, C-6	31.9
9	50.3 (d)	0.95	C-14, C-11	50.2
10	36.7 (s)			36.6
11	21.2 (t)	1.60, 1.50	C-13, C-12, C-9, C-8	21.1
12	39.8 (t)	1.20, 2.0	C-18, C-11	39.7
13	42.4 (s)			42.4
14	57.0 (d)	1.01	C-13, C-11, C-9, C-8	56.9
15	24.5 (t)	1.55, 1.04	C-16, C-13	24.4
16	29.1 (t)	1.71, 1.27	C-15, C-14, C-13	29.0
17	56.1 (d)	1.15	C-23, C-22, C-18	56.1
18	12.2 (q)	0.69	C-17, C-14, C-12	12.1
19	19.5 (q)	1.01	C-9, C-5, C-1	19.4
20	40.7 (d)	2.04	C-23, C-22	40.5
21	21.4 (q)	1.04	C-23, C-22, C-17	21.1
22	138.5 (d)	5.18	C-29, C-28, C-24, C-21, C-17	138.4
23	129.4 (d)	5.03	C-26, C-25, C-24, C-17, C-20	129.3
24	51.4 (d)	1.51	C-29, C-28, C-22,	51.3
25	32.0 (d)	1.56	C-29, C-23	31.9
26	21.2 (q)	0.87	C-24, C-23	21.3
27	19.1 (q)	0.79	C-28, C-24	19.0
28	25.6 (t)	1.43, 1.15	C-27, C-24	25.4
29	12.4 (q)	0.81	C-28, C-25, C-24	12.3

δ_{lit} -Literature data from Goad, 1991; Multiplicity determined from DEPT 135 experiments

LREIMS gave the molecular ion at *m/z* 412 M^+ corresponding to the formula $C_{29}H_{48}O$. Other prominent peaks were seen at *m/z* 394 $[M\text{-}H_2O]^+$, 327 $[M\text{-}C_5H_9O]^+$, 301 $[M\text{-}C_7H_{11}0]^+$, 273 $[M\text{-}C_{10}H_{19}]^+$ and 255 $[M\text{-}C_{10}H_{22}0]^+$ consistent with stigmasterol (**133**) (Fig. 28).

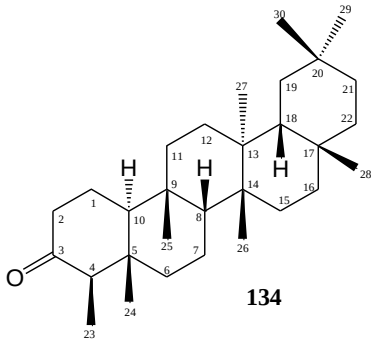
Figure 28: Important MS fragmentation for stigmasterol (**133**)



All the data confirmed the structure of **133** as stigmasterol and was consistent with literature values (Connolly & Hill, 1989; Morales *et al*., 2003; Forgo & Köver, 2004). Stigmasterol (**133**) has been reported widely from various plant species (Connolly & Hill, 1989; Morales *et al*., 2003; Forgo & Köver, 2004). However, this is the first report on its isolation from *A. chloropterus*.

5.1.3 Friedelin (134)

The 2nd MPLC fraction of the dichloromethane extract of *A. chloropterus* was re-chromatographed on MPLC (SiO_2, *n*-C_6H_{14}-EtOAc 98:2) to yield a pure compound in sub-fractions 18-26 which were combined to afford a white amorphous residue on evaporation. Re-crystallization from dichloromethane yielded **134** as white needles (365.1 mg, m.p. 257-259 °C, decomposed), that gave positive colour test for steroids with vanillin-sulfuric acid and *p*-anisaldehyde.

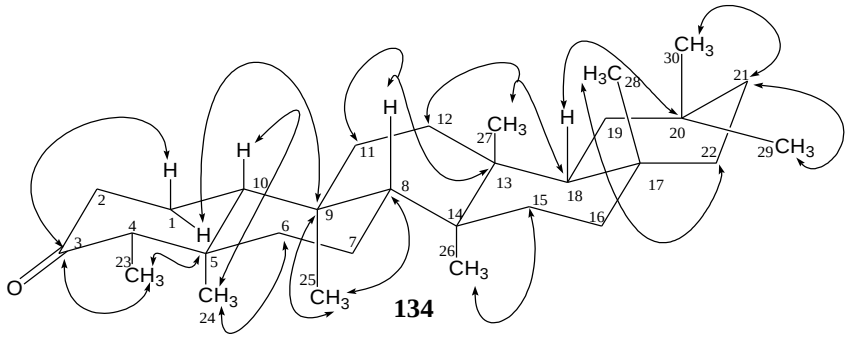


134

The structure was established on the basis of 1D (^1H, ^{13}C and DEPT 135) and 2D-NMR experiments (HMQC, HMBC, COSY, TOCSY and NOESY) (Table 33 – 34, Appendix 10a-g), IR (Appendix 10h) plus MS (appendix 10i). IR spectrum displayed the carbonyl absorption at 1712 cm^{-1}. ^1H NMR exhibited 33 signals in the upfield region (δ 0.71-2.39)

revealing 8 x CH_3: 1 secondary (δ 0.87, d, H-23) and 7 tertiary (δ 0.71, H-24; 0.86, H-25; 1.00, H-26; 1.05, H-27; 1.18, H-28; 1.00, H-29 and 0.95, H-30). ^{13}C NMR revealed the presence of 30 carbons including 8 x CH_3 (δ 35.0, 32.1, 31.8, 20.3, 18.7, 18.0, 14.7 and 6.8), 11 x CH_2 (δ 41.5, 41.3, 39.3, 36.0, 35.6, 35.3, 32.8, 32.4, 30.5, 22.3 and 18.2), 4 x CH (δ 59.5, 58.2, 53.1 and 42.8), and seven quaternary centres (δ 213.3, 42.2, 39.7, 38.3, 37.4, 30.0 and 28.2), one of which is a ketone (δ 213.25). COSY, ^{13}C, DEPT-135, HMQC and HMBC NMR data suggested a pentacyclic triterpenoid. All the important HMBCs are summarized in figure 29.

Figure 29: Important HMBCs for friedelin (**134**)



134

The diastereotopic hydrogens (δ 2.39, H-2_{eq}; 2.30, H-2_{ax}) attached to C-2 (δ 41.5) in ring A were identified. H-2_{eq} (δ 2.39) showed HMBCs to C-1 (δ 22.3), C-10 (δ 59.5) and C-4 (δ 58.2) while H-2_{ax} (δ 2.30) showed interactions with C-1 (δ 22.3) and C-10 (δ 59.5). COSY interactions between H-2_{eq} and H-1_{eq} (δ 1.96, 1H, m, $J_{2eq,1eq}$ 13.9 Hz) were observed. H-4_{eq} (δ 2.24) showed HMBC with C-5 (δ 42.2) while H-24 (δ 0.71) showed HMBCs with C-10 (δ 59.5), C-5 (δ 42.2) and C-6 (δ 41.3). H-23 (δ 0.87) exhibited HMQC to C-23 (δ 6.8) and HMBCs to C-4 (δ 58.2), C-5 (δ 42.2) and C-3 (δ 213.3), indicating a ketone group at C-3.

H-25 (δ 0.86, *s*, 3H) showed HMBCs C-8 (δ 53.1), C-9 (δ 37.4) and C-11 (δ 35.6). Similarly, H-27 (δ 1.05, *s*, 3H) exhibited HMBCs to C-12 (δ 30.5), C-13 (δ 39.7), C-14 (δ 38.3) and C-18 (δ 42.8) in ring D. Likewise, H-26 (δ 1.00, *s*, 3H) showed HMBCs to C-8 (δ 53.10), C-14 (δ 38.3) and C-15 (δ 32.8). H-28 (δ 1.18, *s*, 3H) revealed HMBCs to C-16 (δ 36.0), C-17 (δ 30.0), C-22 (δ 39.3) while H-18 (δ 1.54, *m*, 1H) interacted with C-16 (δ 36.0), C-17 (δ 30.0), C-22 (δ 39.3) and C-28 (δ 32.1). H-29 (δ 1.00, *s*, 3H) signal was superimposed on H-26 (δ 1.00, *s*, 3H) and were confirmed by HMQC and HMBC. H-29 (δ1.00 (3H, *s*) showed HMQC to C-29 δ 31.8 and revealed HMBCs to C-19 (δ 35.3), C-20

(δ 28.2) and C-21 (δ 32.4) while H-19 (δ 1.38, *m*, 1H) interacted with C-18 (δ 42.8). Long-range COSY interactions were observed between H-24 and H-10 (δ 1.54) as well as H-7 (δ 1.75) in ring B.

Table 33:1D and 2D ^{1}H NMR (500 MHz, $CDCl_3$) data for friedelin (**134**)

Position	δ_{obs}	J_{obs} (Hz)	COSY	δ_{lit}
1_{ax}	1.68 (1H, *m*)	14.0	H-2, H-23,H-24, H-25	1.68 (1H, *m*)
1_{eq}	1.96 (1H, *m*)	13.9		1.96 (1H, *m*)
2_{ax}	2.30 (1H, *m*)	14.0		2.30 (1H, *m*)
2_{eq}	2.39 (1H, *m*)			2.39 (1H, *m*)
4_{eq}	2.24 (1H, *m*)	14.0		2.24 (1H, *m*)
6_{ax}	1.28 (1H, *m*)		H-25	1.28 (1H, *m*)
6_{eq}	1.75 (1H, *m*)			1.75 (1H, *m*)
7_{ax}	1.38 (1H, *m*)		H-23	1.38 (1H, *m*)
7_{eq}	1.48 (1H, *m*)			1.48 (1H, *m*)
8	1.39 (1H, *m*)			1.39 (1H, *m*)
10	1.54 (1H, *m*)		H-24	1.54 (1H, *m*)
11_{ax}	1.26 (1H, *m*)			1.26 (1H, *m*)
11_{eq}	1.46 (1H, *m*)			1.46 (1H, *m*)
12_{ax}	1.35 (1H, *m*)			1.35 (1H, *m*)
12_{eq}	1.35 (1H, *m*)			1.35 (1H, *m*)
15_{ax}	1.27 (1H, *m*)			1.27 (1H, *m*)
15_{eq}	1.46 (1H, *m*)			1.46 (1H, *m*)
16_{ax}	1.36 (1H, *m*)		H-12_{eq}	1.36 (1H, *m*)
16_{eq}	1.57 (1H, *m*)			1.57 (1H, *m*)
18_{ax}	1.54 (1H, *m*)		H-11_{eq}	1.54 (1H, *m*)
19_{ax}	1.20 (1H, *m*)			1.20 (1H, *m*)
19_{eq}	1.38 (1H, *m*)			1.38 (1H, *m*)
21_{ax}	1.30 (1H, *m*)			1.30 (1H, *m*)
21_{eq}	1.51 (1H, *m*)			1.51 (1H, *m*)
22_{ax}	0.94 (1H, *m*)			0.94 (1H, *m*)
22_{eq}	1.50 (1H, *m*)			1.50 (1H, *m*)
23	0.87 (3H, *m*)		H-1_{ax}	0.87 (3H, *m*)
24	0.71 (3H, *s*)		H-1_{ax}, H-10	0.71 (3H, *s*)
25	0.86 (3H, *s*)		H-1ax	0.86 (3H, *s*)
26	1.00 (3H, *s*)			1.00 (3H, *s*)
27	1.05 (3H, *s*)			1.05 (3H, *s*)
28	1.18 (3H, *s*)			1.18 (3H, *s*)
29	1.00 (3H, *s*)		H-23	1.00 (3H, *s*)
30	0.95 (3H, *s*)		H-22	0.95 (3H, *s*)

Literature data (δ_{lit})from Klass *et al.*, 1992

Analysis of the COSY, TOCSY and NOESY spectra for friedelin (**134**) confirmed the presence of five almost isolated ^{1}H spin systems, one spin system for each of the five rings A – E of the triterpenes skeleton, ring A: H-1_{ax} (δ 1.68), H-1_{eq} (δ 1.96), H-2_{ax} (δ 2.30), H-2_{eq} (δ 2.39) and H-4 (δ 2.24); ring B: H-6_{ax} (δ 1.28), H-6_{eq} (δ 1.75), H-7_{ax} (δ 1.38) and H-7_{eq} (δ 1.48); ring C: H-8 (δ 1.39), H-10 (δ 1.54), H-11_{ax} (δ 1.26), H-11_{eq} (δ 1.46), H-12_{ax} (δ 1.35)

and H-12$_{eq}$ (δ 1.35); ring D: H-15$_{ax}$ (δ 1.27), H-15$_{eq}$ (δ 1.46), H-16$_{ax}$ (δ 1.36) and H-16$_{eq}$ (δ 1.57) and ring E: H-18 (δ 1.54), H-19$_{eq}$ (δ 1.20) H-29 (δ 1.00), H-30 (δ 0.95), H-21$_{ax}$ (δ 1.30), H-21$_{eq}$ (δ 1.51), H-22$_{ax}$ (δ 0.94) and H-22$_{eq}$ (δ 1.50). Consequently, COSY, TOCSY, HMQC and HMBC data confirmed the presence of a 3-*keto*-friedelane-triterpenoid.

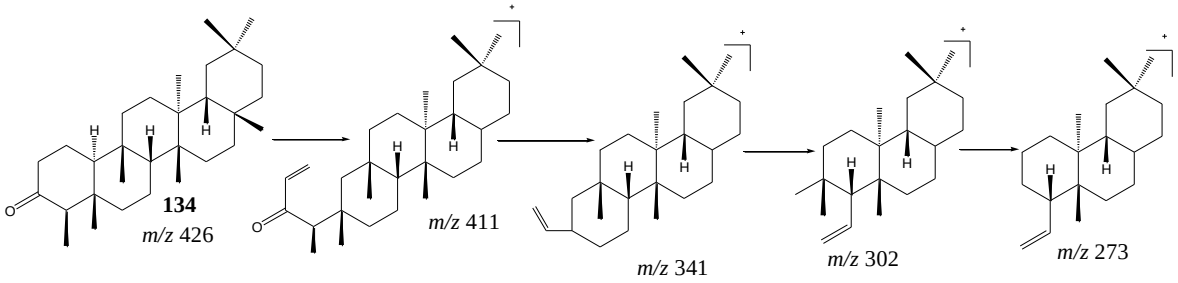
Table 34: 1D and 2D ^{13}C NMR (500 MHz, $CDCl_3$) data for friedelin (**134**)

Position	δ_{obs}	HMQC (δ)	HMBC	δ_{lit}
1	22.3 (*t*)	1.96, 1.68	C-2, C-3, C-10, C-9	22.2
2	41.5 (*t*)	2.39, 2.30	C-1, C-10, C-4	41.4
3	213.3 (*s*)			212.8
4	58.2 (*d*)	2.24	C-5, C-10	58.1
5	42.2 (*s*)			42.0
6	41.3 (*t*)	1.75, 1.28		41.2
7	18.2 (*t*)	1.48, 1.38		18.1
8	53.1 (*d*)	1.39		53.0
9	37.4 (*s*)			37.4
10	59.5 (*d*)	1.54		59.4
11	35.6 (*t*)	1.46, 1.26	C-12	35.5
12	30.5 (*t*)	1.35, 1.35	C-13	30.4
13	39.7 (*s*)			39.6
14	38.3 (*s*)			38.2
15	32.8 (*t*)	1.46, 1.27		32.3
16	36.0 (*t*)	1.57, 1.36		35.9
17	30.0 (*s*)			29.9
18	42.8 (*d*)	1.54	C-16, C-17, C-22, C-28	42.8
19	35.3 (*t*)	1.38, 1.20	C-18	35.7
20	28.2 (*s*)			28.0
21	32.4 (*t*)	1.51, 1.30		32.7
22	39.3 (*t*)	1.50, 0.94		39.2
23	6.8 (*q*)	0.87	C-4, C-5, C-3	6.7
24	14.7 (*q*)	0.71	C-10, C-5, C-6	14.5
25	18.0 (*q*)	0.86	C-8, C-9, C-11	17.8
26	20.3 (*q*)	1.00	C-8, C-14, C-15	20.1
27	18.7 (*q*)	1.05	C-12, C-13, C-14, C-18	18.5
28	32.1 (*q*)	1.18	C-16, C-17, C-22	32.0
29	31.8 (*q*)	1.00	C-20, C-19, C-21	31.7
30	35.0 (*q*)	0.95	C-20, C-18, C-21	34.9

Literature data (δ_{lit}) from Connolly & Hill, 1991**;** Multiplicity determined from DEPT 135 experiments

Molecular ion peak was observed at *m/z* 426 (M^+) in LREIMS corresponding to the formula $C_{30}H_{50}O$. The fragment ion peaks at *m/z* 273 together with those at 341 and 302 were suggestive of a friedelane derivative with a 3-*keto*-friedelane derivative (Budzikiewicz *et al*, 1963). The spectral patterns are characteristic of 3-*keto*-friedelane moiety (Budzikiewicz et al., 1963; Klass *et al.*, 1992). Important MS fragmentations for friedelin (**134**) are shown in figure 30.

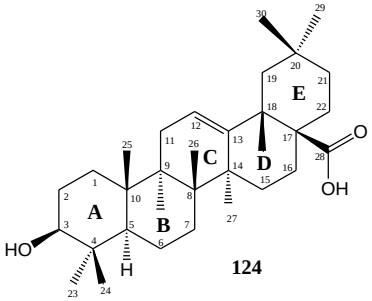
Figure 30: Important MS fragmentation for friedelin (**134**)



All the data confirmed the structure of **134** as friedelin and was consistent with literature values (Budzikiewicz et al., 1963; Connolly & Hill, 1989; Klass *et al*, 1992). Friedelin (**134**) has been previously obtained from several plant species (Budzikiewicz et al., 1963; Connolly & Hill, 1989; Klass *et al*, 1992). However, this is the first report on the isolation of friedelin (**134**) from *A. chloropterus*.

5.1.4 Oleanolic acid (124)

Repeated column chromatography (SiO_2, *n*-C_6H_{14} with increasing % EtOAc) of dichloromethane extract of *A. chloropterus* resulted in pure compound in fractions 22-24 which were combined and evaporated to give a white amorphous residue. Re-crystallization in $CHCl_3$-C_6H_{14} (1:4) yielded **124** as white needles (28.0 mg, m.p. 301-303 °C, decomposed) that gave positive colour test for steroids with vanillin-sulfuric acid and *p*-anisaldehyde.



The structure was established on the basis of 1D (^{1}H, ^{13}C and DEPT 135) and 2D-NMR experiments (HMQC, HMBC and COSY) (Table 35-36, Appendix 11a-f) plus MS (Appendix 11g).

The ^{1}H NMR data for **124** revealed 7 tertiary methyl groups in the region δ 0.75-1.13 (δ 0.75, 0.77, 0.91, 0.92, 0.93, 0.99 and 1.14), one peak at δ 3.22 (1H, dd, *J* 13.5, 3.8 Hz) due to axial H-3 and an olefinic signal at δ 5.28 (1H, *br s*) characteristic of a Δ^{12}-oleanane

skeleton (Ikuta & Itokawa, 1988; Conrad *et al*., 1998; Klass *et al*, 1992; Mahato & Kundu, 1994; Thanakijcharoenpath & Theanphong, 2005).

^{13}C NMR data confirmed the presence of seven methyls in the region δ 15-34 (δ 15.5, 15.7, 17.3, 26.1, 23.7, 28.2 and 33.2), a hydroxylated carbon at δ 79.2 and a trisubstituted double bond at δ 122.8 and 143.8. HMQCs were observed between methyls: H-23 (δ 0.99) and δ C-23 (28.2), H-24 (δ 0.77) and C-24 (δ 15.7), H-25 (δ 0.92) and C-25 (δ 15.5), H-26 (δ 0.75) and C-26 (δ 17.3), H-27 (δ 1.14) and C-27 (δ 26.1), H-29 (δ 0.91) and C-29 (δ 33.2), and H-30 (δ 0.93) and C-30 (δ 23.72). Similarly, HMQCs facilitated the assignment of 10 methylene groups: H-1$_{eq}$ (δ 1.64) and H-1$_{ax}$, (δ 0.98) to C-1 (δ 38.9); H-2$_{eq}$ (δ 1.63) and H-2$_{ax}$ (δ 1.61) to C-2 (δ 27.3); H-6$_{eq}$ (δ 1.38) and H-6$_{ax}$ (δ 1.56) to C-6 (δ 18.5); H-7$_{eq}$ (δ 1.55) and H-7$_{ax}$ (δ 1.30) to C-7 (δ 32.6); H-11$_{eq}$ (δ 1.64) and H-11$_{ax}$ (δ 1.61) to C-11 (δ 23.1); H-15$_{eq}$ (δ 1.11) and H-15$_{ax}$ (δ 1.08) to C-15 (δ 27.8); H-16$_{eq}$ (δ 1.88) and H-16$_{ax}$ (δ 1.88) to C-16 (δ 23.5); H-19$_{eq}$ (δ 1.18) and H-19$_{ax}$ (δ 1.15) to C-19 (δ 46.0); H-21$_{eq}$ (δ 1.35) and H-21$_{ax}$ (δ 1.22) to C-21 (δ 33.9); and H-22$_{eq}$ (δ 1.8) and H-22$_{ax}$ (δ 1.43) to C-22 (δ 32.7). Likewise, HMQC data enabled the assignment of the 5 methine protons at H-3 (δ 3.22) to C-3 (δ 79.2), H-5 (δ 0.75) to C-5 (δ 55.3), H-9 (δ 1.56) to C-9 (δ 47.7), H-12 (δ 5.28) to C-12 (δ 122.8), and H-18 (δ 2.63) to C-18 (δ 41.1).

HMBCs were observed between H-23 (δ 0.99, *s*, 3H)/H-24 (δ 0.77, *s*, 3H) and C-4 (δ 38.9), C-5 (δ 55.3), C-6 (δ 18.5) and C-10 (δ 37.2); H-25 (δ 0.92, *s*, 3H) and C-10 (δ 37.2), C-9 (δ 47.8), C-8 (δ 39.4) and C-11 (δ 23.1); H-26 (δ 0.75, *s*, 3H) and C-8 (δ 39.4), C-14 (δ 41.7), C-13 (δ 143.8) and C-15 (δ 27.8); H-27 (δ 1.14, *s*, 3H) and C-8 (δ 39.4), C-14 (δ 41.7) and C-15 (δ 27.8); H-29 (δ 0.91, *s*, 3H)/H-30 (δ 0.93, *s*, 3H) and C-19 (δ 46.0) and C-20 (δ 28.3). The HMBCs between H-23 (δ 0.99)/H-24 (δ 0.77) and C-3 (δ 79.2), C-4 (δ 38.9) and C-5 (δ 55.3) allowed the location of the hydroxyl group at C-3. H-3 (δ 3.22) showed HMBCs with C-1 (δ 38.9), C-2 (δ 27.3), C-4 (δ 38.5) and C-5 (δ 55.3) confirming the presence of a hydroxyl group at C-3. Similarly, the HMBCs between H-12 (δ 5.28) and C-9 (δ 37.4), C-13 (δ 143.8) and C-18 (δ 41.1) confirmed the position of the olefinic bond at C-12/C-13. Other important HMBCs are summarized in table 36 and Figure 31.

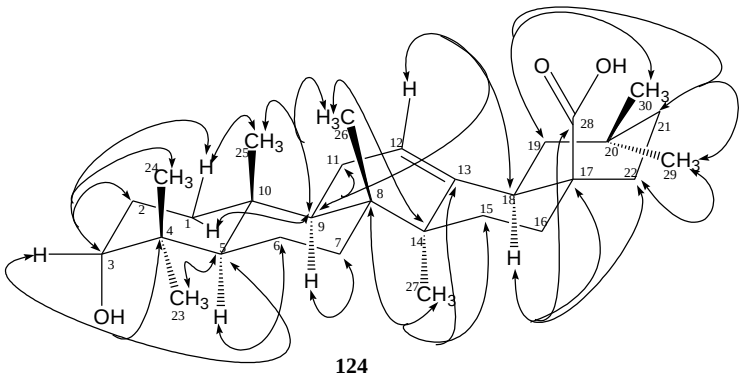
Table 35:1D and 2D ^{1}H NMR (500 MHz, $CDCl_3$) data for oleanolic acid (**124**)

Position	δ_{obs}	J_{obs} (Hz)	COSY	δ_{lit}	J_{lit}(Hz)

1_{ax}	0.98 (1H, *m*)				
1_{eq}	1.64 (1H, *m*)				
2_{ax}	1.61 (1H, *m*)		H-1, H-3		
2_{eq}	1.63 (1H, *m*)				
3_{eq}	3.22 (1H, *dd*)	10.0, 4.8	H-2	3.20 (1H, *dd*)	10.1
5	0.75 (1H, *dd*)	12.0, 2.0			
6_{ax}	1.38 (1H, *m*)	12.0, 10.0			
6_{eq}	1.56 (1H, *m*)	2.0, 3.0, 9.0			
7_{ax}	1.30 (1H, *m*)	2.0, 3.0, 9.0			
7_{eq}	1.55 (1H, *m*)	9.0			
9	1.56 (1H, *dd*)	6.0, 12.0			
11_{ax}	1.61 (1H, *m*)	4.0, 11.0, 12.0	H-9, H-12,		
11_{eq}	1.64 (1H, *m*)	4.0, 6.0, 11.0			
12	5.28 (1H, *m*)	4.0	H-11	5.26 (1H, *br*, s)	
15_{ax}	1.08 (1H, *m*)	4.0, 13.6, 14.0	H-16		
15_{eq}	1.11 (1H, *m*)	4.0, 3.0, 14.0			
16_{ax}	1.88 (1H, *m*)	4.0, 13.0, 13.6	H-15, H-18		
16_{eq}	1.88 (1H, *m*)	4.0, 13.0, 3.0			
18_{ax}	2.82 (1H, *dd*)	11.0	H-12, H-16, H-19	2.80 (1H, *dd*)	10.2
19_{ax}	1.15 (1H, *m*)	11.0	H-18		
19_{eq}	1.18 (1H, *m*)	2.0			
21_{ax}	1.22 (1H, *m*)	2.2,14.0,13.0	H-22		
21_{eq}	1.35 (1H, *m*)	1.3, 2.9, 13.0			
22_{ax}	1.43 (1H, *m*)	1.3, 14.0, 13.0	H-21		
22_{eq}	1.78 (1H, *m*)	2.1, 3.0, 13.0			
23	0.99 (3H, *s*)			0.96 (3H, *s*)	
24	0.77 (3H, *s*)			0.75 (3H, *s*)	
25	0.92 (3H, *s*)			0.89 (3H, *s*)	
26	0.75 (3H, *s*)			0.73 (3H, *s*)	
27	1.14 (3H, *s*)			1.11 (3H, *s*)	
29	0.91 (3H, *s*)			0.88 (3H, *s*)	
30	0.93 (3H, *s*)			0.91 (3H, *s*)	

Literature data (δ_{lit}) from Thanakijcharoenpath & Theanphong, 2005

Fig. 31: Selected HMBCs of oleanolic acid (**124**)



124

Analysis of the COSY spectra for oleanolic acid (**124**) confirmed the presence of five almost isolated ^{1}H spin systems, one spin system for each of the five rings A – E of the triterpenes skeleton, ring A: H-1_{ax} (δ 0.98), H-1_{eq} (δ 1.64), H-2_{ax} (δ 1.61), H-2_{eq} (δ 1.63) and

H-3 (δ 3.22); ring B: H-5 (δ 0.75), H-6_{ax} (δ 1.38), H-6_{eq} (δ 1.56), H-7_{ax} (δ 1.30) and H-7_{eq} (δ 1.55); ring C: H-9 (δ 1.56), H-11_{ax} (δ 1.61), H-11_{eq} (δ 1.64) and H-12 (δ 5.28); ring D: H-15_{ax} (δ 1.08), H-15_{eq} (δ 1.11), H-16_{ax} (δ 1.88) and H-16_{eq} (δ 1.88) and ring E: H-18 (δ 2.82), H-19_{eq} (δ 1.15) H-29 (δ 0.91), H-30 (δ 0.93), H-21_{ax} (δ 1.22), H-21_{eq} (δ 1.35), H-22_{ax} (δ 1.43) and H-22_{eq} (δ 1.78).

Table 36: 1D and 2D ^{13}C NMR (500 MHz, $CDCl_3$) data for oleanolic acid (**124**)

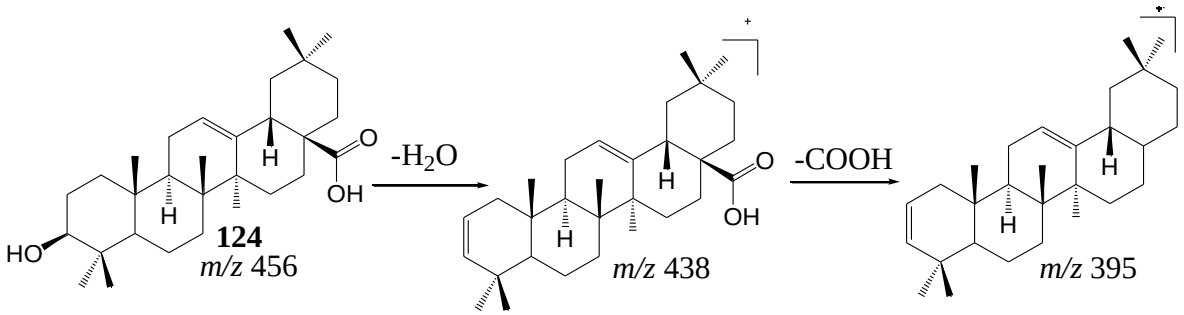
Position	δ_{obs}	HMQC (δ)	HMBC	δ_{lit}
1	38.9 (*t*)	1.64, 0.98	C-3, C-9, C-10	38.5
2	27.3 (*t*)	1.63, 1.61	C-3	27.1
3	79.2 (*d*)	3.22	C-1, C-2, C-4, C-5	78.7
4	38.5 (*s*)			38.7
5	55.3 (*d*)	0.75	C-6, C-23, C-25	55.2
6	18.5 (*t*)	1.56, 1.38		18.3
7	32.6 (*t*)	1.55, 1.30		32.6
8	39.4 (*s*)			39.3
9	47.8 (*d*)	1.56		47.6
10	37.2 (*s*)			37.0
11	23.1 (*t*)	1.64, 1.61	C-9, C-12, C-13	23.1
12	122.8 (*d*)	5.28	C-11, C-13, C-18	122.1
13	143.8 (*s*)			143.4
14	41.7 (*s*)			41.6
15	27.8 (*t*)	1.11, 1.08		27.7
16	23.5 (*t*)	1.88, 1.88		23.4
17	46.7 (*s*)			46.6
18	41.1 (*d*)	2.82	C-17, C-19, C-22, C-28	41.3
19	46.0 (*t*)	1.18, 1.15	C-17, C-18, C-20, C-21, C-29, C-30	45.8
20	30.8 (*s*)			30.6
21	33.9 (*t*)	1.35, 1.22		33.8
22	32.7 (*t*)	1.78, 1.43		32.3
23	28.2 (*q*)	0.99	C-3, C-4, C-5, C-6, C-10, C-23	28.1
24	15.7 (*q*)	0.77	C-3, C-4, C-5, C-6, C-10, C-24	15.6
25	15.5 (*q*)	0.92	C-1, C-5, C-8, C-9, C-10, C-11	15.3
26	17.3 (*q*)	0.75	C-7, C-8, C-9, C-13, C-14, C-15	16.8
27	26.1 (*q*)	1.14	C-5, C-8, C-13, C-14, C-15	26.0
28	183.3 (*s*)			177.9
29	33.2 (*q*)	0.91	C-19, C-20, C-22, C-30	33.1
30	23.7 (*q*)	0.93	C-19, C-20, C-21, C-29	23.6

Literature data (δ_{lit}) from Connolly & Hill, 1991**;** Multiplicity determined from DEPT 135 experiments

^1H, ^{13}C, DEPT, COSY, HMQC and HMBC NMR data confirmed the presence of an oleanane-type triterpenoid with a 3*β*-hydroxyl group and established the structure as oleanolic acid (**124**) (Ikuta & Itokawa, 1988; Conrad *et al*., 1998; Klass *et al*, 1992; Mahato & Kundu, 1994; Takahashi *et al.*, 1999; Thanakijcharoenpath & Theanphong, 2005).

Molecular ion peak at *m/z* 456 [M^+] in LREIMS corresponded to the formula $C_{30}H_{48}O_3$. The fragment ion peaks at *m/z* 395 together with those at 438 were suggestive of a carboxylic acid derivative (Budzikiewicz *et al*., 1963; Klass *et al.*, 1992). Important MS fragmentations observed in oleanolic acid (**124**) are shown in figure 32.

Figure 32: Important MS fragmentations for oleanolic acid (**124**)



124
m/z 456

m/z 438

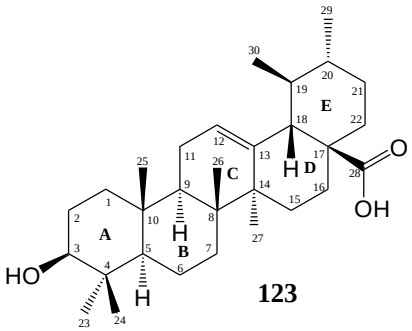
m/z 395

All the data confirmed the structure of **124** as oleanolic acid and was consistent with literature values (Ikuta & Itokawa, 1988; Conrad *et al*., 1998; Klass *et al*, 1992; Mahato & Kundu, 1994; Takahashi *et al.*, 1999; Thanakijcharoenpath & Theanphong, 2005).

Oleanolic acid (**124**) has been previously isolated from *Acridocarpus vivy* collected from Madagascar rain forest (Cao *et al*., 2004) and from other several plant species (Connolly & Hill, 1989; Ikuta & Itokawa, 1988; Conrad *et al*., 1998; Klass *et al*, 1992; Takahashi *et al.*, 1999; Thanakijcharoenpath & Theanphong, 2005). However, this is the first report on its isolation from *A. chloropterus*.

5.1.5 Ursolic acid (123)

Repeated column chromatography (SiO_2, *n*-C_6H_{14} with increasing EtOAc) of dichloromethane extract of *A. chloropterus* resulted in a pure compound in fractions 18-19 which were combined and evaporated to yield a white amorphous residue. Re-crystallization yielded white powder of **123** (12.0 mg, m.p. 268-270 °C, decomposed), that gave positive colour test for steroids with vanillin-sulfuric acid and *p*-anisaldehyde.



123

The structure was established on the basis of 1D (^{1}H and ^{13}C) and 2D-NMR experiments (HMQC, HMBC, COSY and NOESY) (Table 37-38, Appendix 12a-f) plus MS data (Appendix 12g).

The ^{1}H NMR data for **123** revealed 2 secondary and 5 tertiary methyl groups at δ 0.67, 0.74, 0.86, 0.89, 0.91, 1.04 and 1.31 suggesting presence of ursane skeleton. The signal at δ 3.14 (1H, *dd*, *J* 13.4, 3.8 Hz) was assigned to H-3$_{ax}$ while the peak at δ 5.21 (1H, *dd*, *J* 3.2 Hz) was characteristic of a Δ^{12}-ursane skeleton (Ikuta & Itokawa, 1988; Conrad *et al*., 1998; Klass *et al*, 1992; Mahato & Kundu, 1994; Thanakijcharoenpath & Theanphong, 2005).

^{13}C NMR data confirmed presence of 7 methyls at δ 15.2, 16.1, 16.8, 18.0, 21.1, 23.4 and 28.2. DEPT 135 and HMQC data for the methyls: H-23 (δ 0.89) to C-23 (δ 28.2), H-24 (δ 0.67) to C-24 (δ 16.1), H-25 (δ 0.86) to C-25 (δ 15.2), H-26 (δ 0.74) to C-26 (δ 16.8), H-27 (δ 1.04) to C-27 (δ 23.4), H-29 (δ 0.9) to C-29 (δ 18.0) and H-30 (δ 1.31) to C-30 (δ 21.1); methylenes: H-1$_{ax}$ (δ 1.00)/H-1$_{eq}$ (δ 1.53) to C-1 (δ 38.0), H-2$_{ax}$ (δ 1.80)/H-2$_{eq}$ (δ 1.80) to C-2 (δ 27.0), H-6$_{ax}$ (δ 1.48)/H-6$_{eq}$ (δ 1.28) to C-6 (δ 18.0); H-7$_{ax}$ (δ 1.45)/H-7$_{eq}$ (δ 1.26) to C-7 (δ 32.7), H-11$_{ax}$ (δ 1.86)/H-11$_{eq}$ (δ 1.83) to C-11 (δ 22.8), H-15$_{ax}$ (δ 1.00)/ H-15$_{eq}$ (δ 1.80) to C-15 (δ 27.5), H-11$_{ax}$ (δ 1.92)/H-11$_{eq}$ (δ 1.53) to C-16 (δ 23.8); H-21$_{ax}$ (δ 1.27)/ H-21$_{eq}$ (1.43) to C-21 (δ 30.2) and H-22$_{ax}$ (δ 1.51)/H-22$_{eq}$ (1.58) to C-22 (δ 36.3); methines: H-3$_{ax}$ (δ 3.14) to C-3 (δ 76.8), H-5 (δ 0.68) to C-5 (δ 54.8), H-9 (δ 1.40) to C-9 (δ 47.0), H-12 (δ

5.21) to C-12 (δ 124.6), H-18 (δ 2.10) to C-18 (δ 52.4), H-19 (δ 1.31) to C-19 (δ 38.4), and H-20 (δ 1.31) to C-20 (δ 38.4) confirmed the ^{1}H and ^{13}C NMR assignments.

Table 37:1D and 2D ^{1}H NMR (600 MHz, DMSO) data for ursolic acid (**123**)

Position	δ_{obs}	J_{obs} (Hz)	COSY	NOESY	δ_{lit}	J_{lit} (Hz)
1_{ax}	1.00 (1H, *m*)	2.8, 13.0		H-5, H-9		
1_{eq}	1.53 (1H, *m*)	2.8, 3.4, 13.0				
2_{ax}	1.80 (1H, *m*)	9.0, 2.8, 13	H-1, H-3	H-24, H-25		
2_{eq}	1.80 (1H, *m*)	6.0, 3.4, 13.0				
3_{eq}	3.14 (1H,*dd*)	10.0, 4.8	H-2	H-23, H-24, H-25	2.99(1H, *dd*)	10.1, 5.2
5	0.68 (1H,*dd*)	12.0, 2.0		H-1		
6_{ax}	1.28 (1H, *m*)	12.0, 10.0				
6_{eq}	1.48 (1H, *m*)	2.0, 3.0, 9.0				
7_{ax}	1.26 (1H, *m*)	2.0, 3.0, 9.0				
7_{eq}	1.45 (1H, *m*)	9.0				
9	1.46 (1H, *m*)	6.0, 12.0				
11_{ax}	1.83 (1H, *m*)	4.0,11.0,12.0	H-9, H-12	H-25		
11_{eq}	1.86 (1H, *m*)	4.0, 6.0, 11.0				
12	5.21 (1H, *t*)	4.0	H-11	H-18, H-29	5.12 (1H, *br*, *t*)	3.4
15_{ax}	1.00 (1H, *m*)	4.0,13.6, 14.0	H-16			
15_{eq}	1.80 (1H, *m*)	4.0, 3.0, 14.0				
16_{ax}	1.53 (1H, *m*)	4.0,13.0, 13.6	H-15			
16_{eq}	1.92 (1H, *m*)	4.0, 13.0, 3.0	H-18			
18_{ax}	2.10 (1H,*dd*)	2.0, 11.0	H-12, H-16, H-19	H-12, H-27, H-29, H-30	2.10 (1H, *d*)	11.6
19_{eq}	1.31 (1H,*dd*)	6.6, 11.3	H-18			
20	1.31 (1H, *m*)	2.0, 6.3	H-22			
21_{ax}	1.27 (1H, *m*)	2.2, 14.0,	H-21			
21_{eq}	1.43 (1H, *m*)	13.0				
		1.4, 3.0, 13.0				
22_{ax}	1.51 (1H, *m*)	1.4, 14.0,				
22_{eq}	1.58 (1H, *m*)	13.0				
		2.2, 3.0, 13.0				
23	0.89 (3H, *s*)				0.88 (3H, *s*)	
24	0.67 (3H, *s*)				0.67 (3H, *s*)	
25	0.86 (3H, *s*)			H-2, H-11	0.86 (3H, *s*)	
26	0.74 (3H, *s*)				0.74 (3H, *s*)	
27	1.04 (3H, *s*)			H-18	1.03 (3H, *s*)	
29	0.81 (3H, *d*)	6.6		H-12, H-18	0.80 (3H, *s*)	
30	0.91 (3H, *d*)	6.3		H-18	0.89 (3H, *s*)	

Literature data (δ_{lit}) from Thanakijcharoenpath & Theanphong, 2005

The HMBCs between H-12 (δ 5.21) and C-9 (δ 47.0), C-13 (δ 138.2) and C-18 (δ 52.4) confirmed the location of the double bond at C-12/C-13 ring junction. The HMBCs observed between the methyl protons: H-23/H-24 and C-4 (δ 38.2), C-5 (δ 54.8), C-6 (δ 18.0) and C-10 (δ 36.5); H-25 and C-10 (δ 36.5), C-9 (δ 47.0), C-8 (δ 38.5) and C-11 (δ 22.8); H-26 and C-8 (δ 38.5), C-14 (δ 41.6), C-13 (δ 138.2) and C-15 (δ 27.5); H-27 and C-

8 (δ 38.5), C-14 (δ 41.6) and C-15 (δ 27.5); and H-29/H-30 and C-19 (δ 38.4) and C-20 (δ 38.4) confirmed further ^{1}H, ^{13}C NMR assignments.

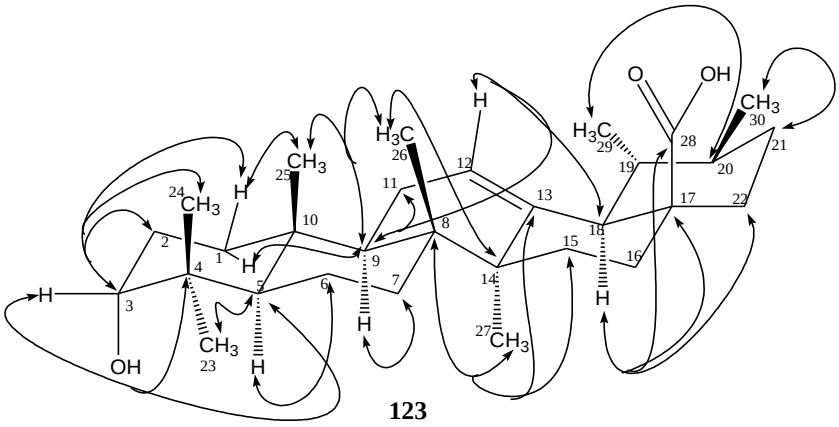
The carboxyl group was assigned following HMBCs from H-16$_{ax}$ (δ 1.53), H-16$_{eq}$ (δ 1.92) H-22$_{ax}$ (δ 1.51) and H-22$_{eq}$ (δ 1.58) to C-28 (δ 178.3). The HMBCs for ursolic acid (**123**) are summarized in table 38 whereas the key HMBCs are illustrated in figure 33.

Table 38: 1D and 2D ^{13}C NMR (500 MHz, $CDCl_3$) data for ursolic acid (**123**)

Position	δ_{obs}	HMQC (δ)	HMBC	δ_{lit}
1	38.0 (*t*)	1.53, 1.00		38.8
2	27.0 (*t*)	1.80, 1.80		27.3
3	76.8 (*d*)	3.14	C-1, C-2, C-4, C-5	78.8
4	38.2 (*s*)			38.8
5	54.8 (*d*)	0.68	C-6, C-23, C-25	55.4
6	18.0 (*t*)	1.48, 1.28		18.4
7	32.7 (*t*)	1.45, 1.26		33.0
8	38.5 (*s*)			39.6
9	47.0 (*d*)	1.46		47.5
10	36.5 (*s*)			37.0
11	22.8 (*t*)	1.86, 1.83	C-12, C-13	16.9
12	124.6 (*d*)	5.21	C-11, C-13	125.5
13	138.2 (*s*)			138.0
14	41.6 (*s*)			42.0
15	27.5 (*t*)	1.80, 1.00		28.2
16	23.8 (*t*)	1.92, 1.53		24.3
17	46.8 (*s*)			48.1
18	52.4 (*d*)	2.10		52.8
19	38.4 (*d*)	1.31	C-17, C-18, C-20, C-21, C-29, C-30	39.1
20	38.4 (*d*)	1.31		38.8
21	30.2 (*t*)	1.43, 1.27		30.7
22	36.3 (*t*)	1.58, 1.51		36.7
23	28.2 (*q*)	0.89	C-3, C-4, C-5, C-23	28.2
24	16.1 (*q*)	0.67	C-3, C-4, C-5, C-24	15.5
25	15.2 (*q*)	0.86	C-1, C-5, C-9, C-10	15.7
26	16.8 (*q*)	0.74	C-7, C-8, C-9, C-14	16.9
27	23.4 (*q*)	1.04	C-5, C-8, C-13, C-14, C-15	23.3
28	178.3 (*s*)			177.7
29	18.0 (*q*)	0.81	C-19, C-20, C-21, C-30	23.6
30	21.1 (*q*)	0.91	C-19, C-20, C-21, C-29	21.2

Literature data (δ_{lit}) from Connolly & Hill, 1991**;** Multiplicity determined from DEPT 135 experiments

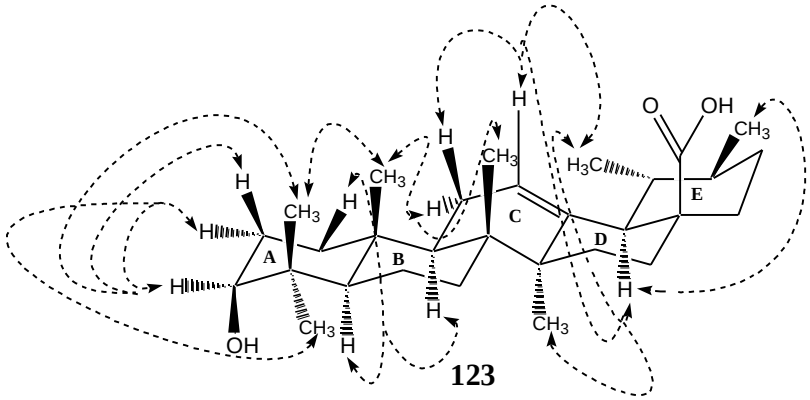
Figure 33: Important HMBCs for ursolic acid (**123**)



123

Analysis of the COSY and NOESY spectra for ursolic acid (**123**) confirmed the presence of five almost isolated ^{1}H spin systems, one spin system for each of the five rings A – E of the triterpenes skeleton, ring A: H-1$_{ax}$ (δ 1.00), H-1$_{eq}$ (δ 1.53), H-2$_{ax}$ (δ 1.80), H-2$_{eq}$ (δ 1.80) and H-3 (δ 3.14)]; ring B: H-5 (δ 0.68), H-6$_{ax}$ (δ 1.28), H-6$_{eq}$ (δ 1.48), H-7$_{ax}$ (δ 1.26) and H-7$_{eq}$ (δ 1.45)]; ring C: H-9 (δ 1.46), H-11$_{ax}$ (δ 1.83), H-11$_{eq}$ (δ 1.86) and H-12 (δ 5.21)]; ring D: H-15$_{ax}$ (δ 1.00), H-15$_{eq}$ (δ 1.80), H-16$_{ax}$ (δ 1.53) and H-16$_{eq}$ (δ 1.92)] and ring E: H-18 (δ 2.10), H-19$_{eq}$ (δ 1.31), H$_3$-29 (δ 0.81), H$_3$-30 (δ 0.91), H-20 (δ 1.31), H-21$_{ax}$ (δ 1.27), H-21$_{eq}$ (δ 1.43), H-22$_{ax}$ (δ 1.51) and H-22$_{eq}$ (δ 1.58)]. The diagnostic NOESY interactions for ursolic acid (**123**) are shown in figure 34

Figure 34: Important NOESYs for ursolic acid (**123**)



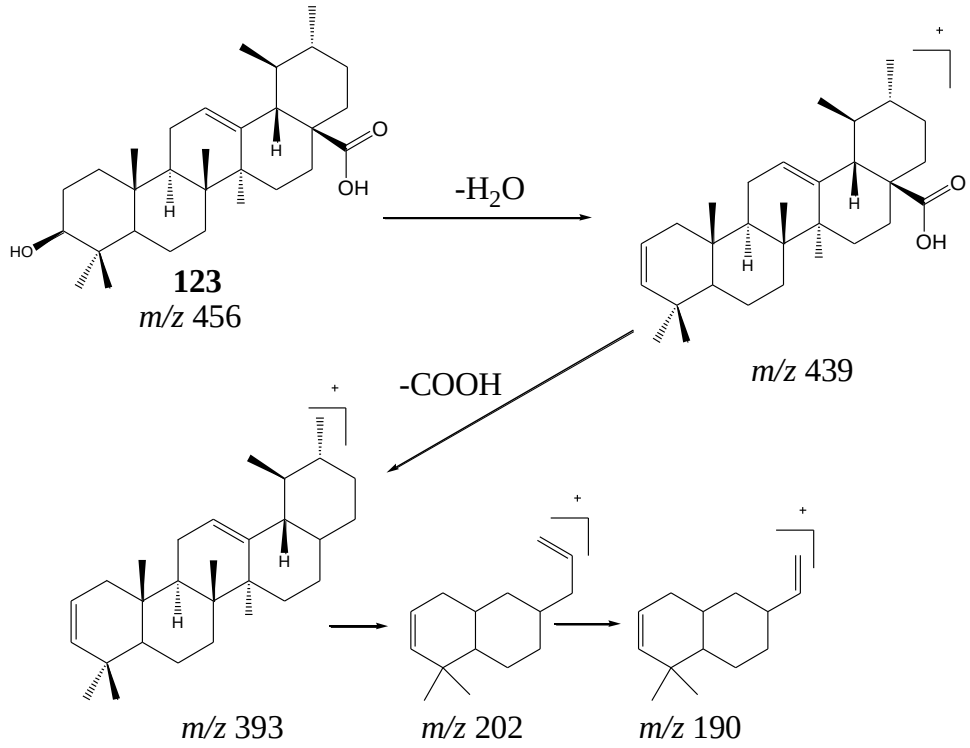
123

NOESY interactions observed between H-1 and H-5, H-1 and H-9, H-2 and H-24, H-2 and H-25, H-3 and H-24, H-3 and H-23, H-11 and H-25, H-12 and H-29, H-18 and H-27, H-18 and H-29, H-18 and H-12, and H-25 and H-26 confirmed the structure of **123** as 3β-hydroxy-12-en-28-oic acid (ursolic acid) (**123**).

^{1}H, ^{13}C, DEPT COSY, NOESY, HMQC and HMBC spectral data established the structure as ursolic acid **123** (Ikuta & Itokawa, 1988; Conrad *et al*., 1998; Klass *et al.*, 1992; Mahato & Kundu, 1994; Thanakijcharoenpath and Theanphong, 2005).

Molecular ion peak was observed at *m/z* 456 in LREIMS corresponding to the formula $C_{30}H_{48}O_3$. The fragment ion peaks at *m/z* 393 together with those at 439, 202 and 190 were suggestive of a carboxylic acid derivative (Budzikiewicz *et al*., 1963; Klass *et al*, 1992). Important MS fragmentations for ursolic acid (**123**) are shown in figure 35.

Figure 35: Important MS fragmentations for ursolic acid (**123**)



123
m/z 456

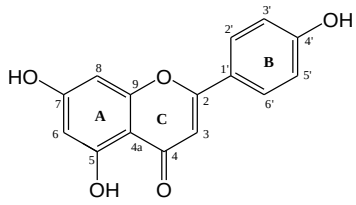
m/z 439

m/z 393 *m/z* 202 *m/z* 190

All the data confirmed the structure of **123** as ursolic acid and was consistent with literature values (Connolly & Hill, 1989; Ikuta & Itokawa, 1988; Conrad *et al*., 1998; Klass *et al*, 1992; Mahato & Kundu, 1994; Takahashi *et al.*, 1999; Thanakijcharoenpath & Theanphong, 2005). Ursolic acid (**123**) has been previously isolated from *Acridocarpus vivy* collected from the Madagascar rain forest (Cao *et al*., 2004) and from several plant species (Connolly & Hill, 1989; Ikuta & Itokawa, 1988; Conrad *et al*., 1998; Klass *et al*, 1992; Takahashi *et al.*, 1999; Thanakijcharoenpath & Theanphong, 2005). However, this is the first report on its isolation from *A. chloropterus*.

5.1.6 4′, 5, 7-trihydroxyflavone (apigenin) (135)

PTLC of ACSD 8 (SiO_2, $C_6H_5CH_3$-MeOH 3:7) gave an amorphous solid which was re-crystallized from chloroform-methanol (1:1) to yield yellow powder (8.21 mg) of **135**, m.p. 350-352 °C (decomposed), that gave positive colour test for flavonoids with vanillin-sulfuric acid and *p*-anisaldehyde.



135

The structure was established on the basis of 1D (^{1}H, ^{13}C and DEPT 135) and 2D-NMR experiments (HMQC, HMBC, COSY), Table 39 – 40, Appendix 13a-f, plus MS (Appendix 13g).

Table 39: ^{1}H NMR and COSY (500 MHz, DMSO) data for apigenin (**135**)

Position	δ_{obs}	J_{obs} (Hz)	COSY	δ_{lit}	J_{lit} (Hz)
3	6.75 (1H, s)			6.72 (1H, s)	
6	6.15 (1H, d)	2.08	H-8	6.18 (1H, d)	2.1
8	6.44 (1H, d)	2.08	H-6	6.46 (1H, d)	2.1
2′	7.91 (1H, d)	8.90	H-3′	7.88 (1H, d)	8.8
3′	6.92 (1H, d)	8.90	H-2′	6.91 (1H, d)	8.8
5′	6.92 (1H, d)	8.90	H-6′	6.91 (1H, d)	8.8
6′	7.91 (1H, d)	8.90	H-5′	7.88 (1H, d)	8.8
5-OH	12.96 (1H, s)			12.92 (1H, s)	

J_{lit} - Literature data from Shen *et al.*, 1993

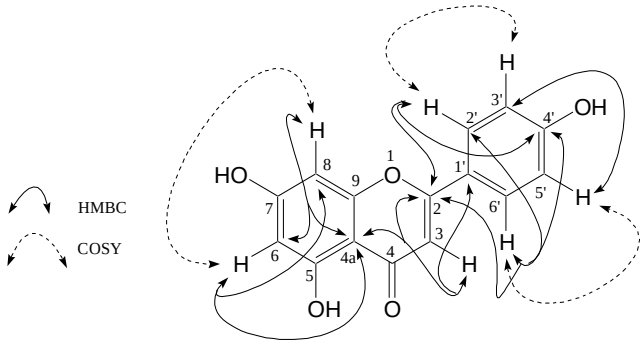
Table 40: 1D and 2D NMR (500 MHz, $CDCl_3$) data for apigenin (**135**)

Position	δ_{obs}	HMQC (δ)	HMBC	δ_{lit}
2	165.2 (s)			163.6
3	102.7 (d)	6.72	C-2, C-7, C-1′, C-10	102.6
4	181.6 (s)			181.6
4a	103.3 (s)			103.5
5	161.4 (s)			161.2
6	99.1 (d)	6.18	C-5, C-10, C-8	98.7
7	163.6 (s)			163.9
8	94.1 (d)	6.46	C-2, C-9, C-10, C-6	93.8
9	157.4 (s)			157.1
1′	121.1 (s)			121.0
2′	128.5 (d)	7.88	C-4,	128.3
3′	116.0 (d)	6.91	C-4, C-1′	115.8
4′	161.3 (s)			161.0
5′	116.0 (d)	6.91	C-4, C-1′	115.8
6′	128.5 (d)	7.88	C-4	128.3

δ_{lit} - Literature data from Burns *et al.*, 2007; Multiplicity determined from DEPT 135 experiments

The ^{1}H and ^{13}C NMR data revealed resonances due to aromatic rings. The signals at δ 6.15 (1H, d, *J* 2.08 Hz) and δ 6.44 (1H, d, *J* 2.08 Hz) in the ^{1}H NMR and δ 99.1 and δ 94.1 in ^{13}C NMR were characteristic of the two *meta*-coupled protons (H-6 and H-8) in a 5, 7-disubstituted A-ring of a flavonoid (Agrawal, 1989; Shen *et al*., 1993). The broad singlet at δ 12.96 assigned 5-OH was attributed to the hydrogen bonding of the hydroxyl moiety at C-5 (δ 161.4) to the carbonyl group at C-4 (δ 181.6). The diagnostic COSY and HMBCs interactions are shown in figure 36.

Figure 36: Selected HMBCs and COSYs of apigenin (**135**)



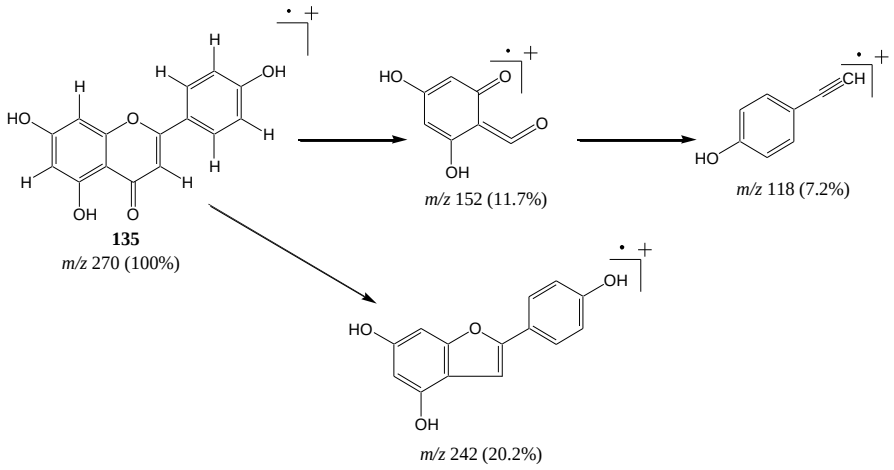
135

COSY revealed interactions between H-6 (δ 6.15) and H-8 (δ 6.44) and also between H-3′/H-5′ (δ 6.92) and H-2′/H-6′ (δ 7.91). HMBCs observed between H-6 (δ 6.15) and C-8 (δ 94.1), C-10 (δ 103.3) and C-5 (δ 161.4) confirmed the assignments. Similarly, HMBCs between H-8 (δ 6.44) and C-6 (δ 99.1), C-10 (δ 103.3), C-7 (δ 163.6) and C-9 (δ 157.4) confirmed the assignments. C-7 (δ 163.6) was assigned from HMBCs with H-6 (δ 6.15) and H-8 (δ 6.44). These observations confirmed the presence of a 5, 7-dihydroxy pattern of ring A. The signal at δ 6.75 (s) was assigned to H-3 on the basis of the HMBCs with C-2 (δ 165.2), C-5 (δ 161.4), C-1′ (δ 121.1) and C-4a (δ 103.3) suggesting that ring C has only one unsubstituted carbon. The two vicinal protons at δ 6.92 (2H, d, *J* 8.90 Hz) and δ 7.91 (2H, d, *J* 8.90 Hz) showed HMBCs with C-4′ (δ 161.3) and were assigned to H-3′/H-5′ and H-2′/H-6′, respectively, in ring B. The structure was proposed to be 4′, 5, 7-trihydroxyflavone (apigenin) (**135**) on the strength of NMR data (Agrawal, 1989; Shen *et al*., 1993; Burns *et al*., 2007).

LREIMS gave the molecular ion M^{+} at *m/z* 270, corresponding to $C_{15}H_{10}O_5$ as the formula consistent with the structure 4′, 5, 7-trihydroxyflavone (apigenin) (**135**) (Fig. 37). Other

prominent peaks were seen at *m/z* 242 $[M\text{-}CO]^+$, *m/z* 152 $[M\text{-}C_8H_60]^+$ and *m/z* 118 $[M\text{-}C_7H_4O_4]^+$.

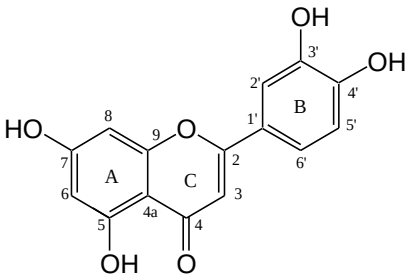
Figure 37: Key MS fragments of apigenin (**135**)



Comparison of the observed and reported data confirmed the structure of **135** as 4′, 5, 7-trihydroxyflavone (apigenin) (Agrawal, 1989; Shen *et al*., 1993). Apigenin (**135**) has also been isolated from many other plant species including *Acacia* spp., *Alnus* spp., *Barleria christata*, *Betula* spp. and *Combretum* spp (Wollenweber & Jay, 1988). However, this is the first report on its presence in *A. chloropterus*.

5.1.7 3′, 4′, 5, 7-tetrahydroxyflavone (luteolin) (136)

PTLC (SiO_2, $C_6H_5CH_3$-MeOH 2:8) of the 8th sub-fraction from the combined fractions 81-90 of ACSD 8 gave a yellow powder which was purified by re-crystallization ($CHCl_3$-MeOH 1:1) to give **136** as yellow crystals (6.0 mg), m.p. 323-325 °C (decomposed), that gave positive colour test for flavonoid with vanillin-sulfuric acid and *p*-anisaldehyde.



136

The structure was established on the basis of 1D (^{1}H, ^{13}C and DEPT 135) and 2D-NMR experiments (HMQC, HMBC, COSY), Table 41 – 42, Appendix 14a-f, plus MS (Appendix 14g).

Table 41: ^{1}H NMR and COSY (500 MHz, DMSO) data for luteolin (**136**)

Position	δ_{obs}	J_{obs} (Hz)	COSY	δ_{lit}	J_{lit} (Hz)
3	6.67 (1H, s)			6.67 (1H, s)	
6	6.18 (1H, d)	2.1	H-8	6.18 (1H, d)	2.2
8	6.44 (1H, d)	2.1	H-6	6.44 (1H, d)	2.2
2′	7.39 (1H, d)	8.3		7.53 (1H, d)	8.4
5′	6.88 (1H, d)	8.3	H-6′	6.93 (1H, d)	8.4
6′	7.41 (1H, d)	8.3, 2.3	H-5′	7.41 (1H, s)	8.4, 2.0
5-OH	12.98 (s)				

δ_{lit} - Literature data from Meselhy *et al.*, 2003

Table 42: 1D and 2D ^{13}C NMR (500 MHz, $CDCl_3$) data for luteolin (**136**)

Position	δ_{obs}	HMQC (δ)	HMBC	δ_{lit}
2	164.3			163.8
3	102.8	6.67	C-2, C-1′, C-10	102.8
4	181.7			181.6
4a	103.6			103.6
5	161.5			161.4
6	98.9	6.18	C-10, C-8	98.7
7	163.9			164.1
8	93.9	6.44	C-7, C-9, C-10, C-6	93.6
9	157.3			157.2
1′	121.4			121.4
2′	113.3	7.53	C-4, C-4′, C-3′, C-6′	113.1
3′	145.8			145.6
4′	149.8			149.6
5′	116.0	6.93	C-4′, C-1′	115.8
6′	119.0	7.41	C-2, C-4′, C-3′, C-2′	118.8

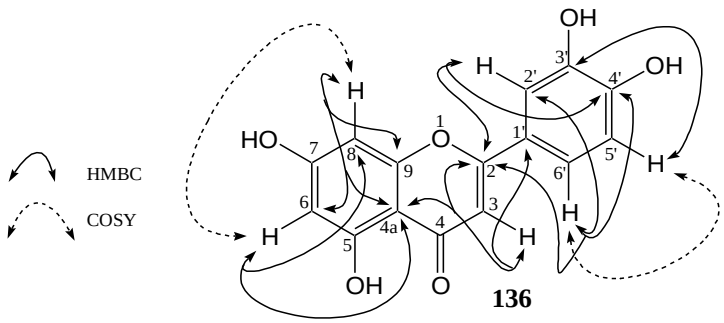
δ_{lit} - Literature data from Burns *et al.*, 2007; Multiplicity determined from DEPT 135 experiments

The signals at δ 6.18 (1H, d, *J* 2.1 Hz) and δ 6.44 (1H, d, *J* 2.1 Hz) in ^{1}H NMR and δ 98.9 and δ 93.9 in ^{13}C NMR, respectively, were characteristic of the two *meta*-protons (H-6 and H-8) in a 5, 7-disubstituted ring A of a flavonoid (Agrawal, 1989; Shen *et al.*, 1993; Meselhy, 2003; Burns *et al.*, 2007). The ^{1}H NMR spectrum of **136** exhibited an ABX spin-system at δ 6.88 (1H, d, *J* 8.3 Hz), 7.39 (1H, d, *J* 2.3 Hz) and δ 7.41 (1H, dd, ^1J 8.3, ^2J 2.3 Hz) due to a 3′, 4′-disubstitution pattern of ring B. The signals at δ 7.39 (1H, d, *J* 2.3 Hz) and δ 7.41 (1H, dd, ^1J 8.3, ^2J 2.3 Hz) interacted to δ 113.3 and δ 119.0, respectively, in

HMQC experiment, and are characteristic of the *meta* protons in ring B. Similarly, the peak δ 6.88 (d, 1H, *J* 8.3 Hz) interacted with carbon at δ 116.0 in the HMQC experiment.

The ^{1}H NMR spectrum of **136** also exhibited resonances due to two vicinal protons at δ 6.88 (1H, d, *J* 8.3 Hz) and δ 7.41 (1H, dd, ^{1}J 8.3 Hz, ^{2}J 2.3 Hz) as confirmed by COSY interaction observed between the signal at δ 7.41 (1H, dd, ^{1}J 8.3 Hz, ^{2}J 2.3 Hz) and δ 6.88 (1H, d, 8.3 Hz). The broad singlet at δ 12.98 was assigned to 5-OH due to the intra-molecular hydrogen bonding between the carbonyl at C-4 (δ 181.6) and the hydroxyl at C-5 (δ 161.4). The diagnostic COSY and HMBC interactions are shown in figure 38.

Figure 38: Selected HMBCs and COSYs of luteolin (**136**)



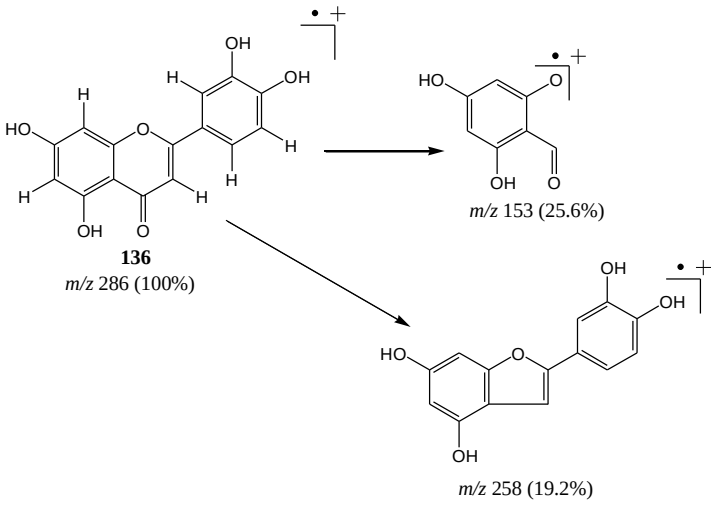
The presence of the two *meta* protons in ring A was confirmed by the long-range COSY interactions between the peaks at δ 6.18 (H-6) and δ 6.44 (H-8). C-7 (δ 163.9) showed HMBCs with H-6 (δ 6.18) and H-8 (δ 6.44). The observations confirmed the presence of 5, 7-dihydroxy pattern in ring A. HMBCs between H-6 (δ 6.18) and C-8 (δ 93.9), C-4a (δ 103.6) and C-5 (δ 161.5) confirmed that assignment of ring A. Similarly, HMBCs between H-8 (δ 6.44) and C-6 (δ 98.9), C-4a (δ 103.6), C-7 (δ 163.9) and C-9 (δ 157.3) confirmed that assignment of ring A.The signal at δ 6.67 (s) was assigned to H-3 on the basis of the HMBCs with C-2 (δ 164.3), C-5 (δ 161.5), C-1′ (δ 121.4) and C-10 (δ 103.6), suggesting that ring C has only one unsubstituted carbon.

HMBCs were observed between H-2′ (δ 7.39, 1H, d, *J* 2.3 Hz) and C-2 (δ 164.3), C-4′ (δ 149.8), C-3′ (δ 145.8) and C-6′ (δ 119.0) thus confirming the assignment in ring B. The doublet signal at δ 6.88 (1H, d, 2.3 Hz) showed HMBCs to C-4′ (δ 149.8) and C-1′ (δ 121.4) and was assigned to H-5′ in ring B. The peak at δ 7.41 (1H, dd, ^{1}J 8.3, ^{2}J 2.3 Hz, H-6′)

showed HMBCs to C-2 (164.3), C-4′ (δ 149.8), C-3 (δ 145.8) and C-2′ (δ 113.3) and was assigned to H-6′ in ring B. The NMR data suggested the presence of 3′,4′,5,7-tetrahydroxyflavone (luteolin) (**136**). Comparison of the observed and reported data confirmed the structure as 3′, 4′, 5, 7-tetrahydroxyflavone (luteolin) (**136**) (Agrawal, 1989 and Shen *et al*., 1993; Meselhy, 2003).

LREIMS gave the molecular ion M^+ at *m/z* 286, which corresponds to the formula $C_{15}H_{10}O_6$. Other prominent peaks were seen at *m/z* 258 $[M\text{-}CO]^+$ and *m/z* 153 $[M\text{-}C_8H_60]^+$ consistent with the structure 3′,4′,5,7-tetrahydroxyflavone (luteolin) (**136**) (Fig. 39).

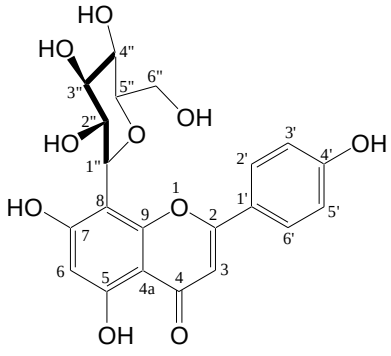
Figure 39: Key MS fragments of luteolin (**136**)



Luteolin (**136**) is one of several flavonoids widely distributed in the plant kingdom and it has aready been isolated from many other plant species including *Acacia* spp., *Alnus* spp., *Barleria christata, Betula* spp. and *Combretum* spp (Wollenweber & Jay, 1988). However, this is the first report on its presence in *A. chloropterus*.

5.1.8 8-glucopyranosyl-4′, 5, 7-trihydroxyflavone (vitexin) (137)

PTLC (SiO_2, $C_6H_5CH_3$-MeOH 7.5:2.5) gave a solid which was purified by re-crystallization ($CHCl_3$-MeOH 1:1) to give **137** as pale yellow crystals (4.2 mg), m.p. 269-270 °C (decomposed), that gave positive colour test for flavonoids with vanillin-sulfuric acid and *p*-anisaldehyde.



137

The structure was established on the basis of 1D (^1H, ^{13}C and DEPT 135) and 2D-NMR experiments (HMQC, HMBC, COSY), Table 43 – 44, Appendix 15a-f, plus MS (Appendix 15g).

Table 43: ^1H NMR and COSY (500 MHz, DMSO) data for vitexin (**137**)

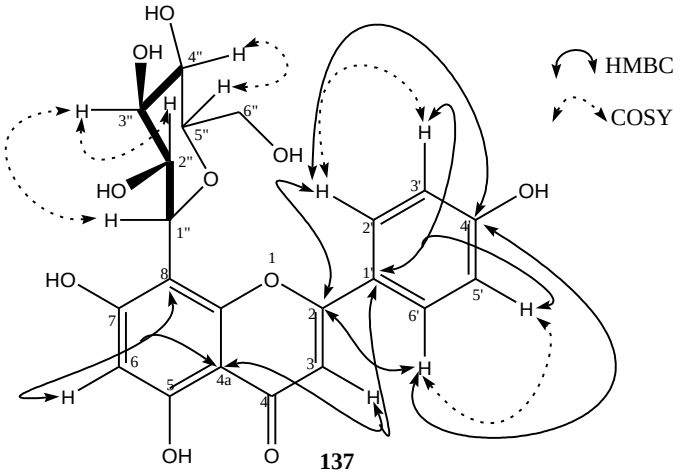
Position	δ_{obs}	J_{obs} (Hz)	COSY	δ_{lit}	J_{lit} (Hz)
3	6.78 (1H, s)			6.78 (1H, s)	
6	6.25 (1H, s)			6.27 (1H, s)	
2′	8.02 (1H, d)	8.40	H-6′	8.01 (1H, d)	9.0
3′	6.89 (1H, d)	8.40	H-5′	6.88 (1H, d)	9.0
5′	6.89 (1H, d)	8.40	H-3′, H-6′	8.88 (1H, d)	9.0
6′	8.02 (1H, d)	8.40	H-5′, H-2′	8.01 (1H, d)	9.0
1″	4.69 (1H, d)	10.23	H-2″	4.68 (1H, d)	10.0
2″	3.85 (1H, dd)	10.2, 10.2	H-1″, H-3″	3.83 (1H, dd)	10.0, 10.0
3″	3.28 (1H, d)	10.23	H-2″, H-4″	3.30 (1H, d)	10.0
4″	3.36 (1H, d)	10.23	H-3″, H-5″	3.36 (1H, d)	10.0
5″	3.24 (1H, m)		H-4″	3.24 (1H, m)	
6_{ax}″	3.76 (1H, dd)	12.1, 6.8	H-6″$_{eq}$	3.75 (1H, dd)	12.0, 6.5
6_{eq}″	3.52 (1H, dd)	12.1, 6.2	H-6″$_{ax}$	3.51 (1H, dd)	12.0, 6.0
OH	4.58 (1H, br s)			4.58 (1H, br s)	
OH	4.95 (1H, br s)			4.95 (1H, d)	3.6
OH	4.95 (1H, br s)			4.98 (1H, d)	5.5
5-OH	13.17 (1H, br s)			13.16 (1H, br s)	

Literature data from Vázquez *et al.*, 2001

The ^1H and ^{13}C NMR spectra suggested that **137** was a flavone glycoside showing a 5, 7-dihydroxy-8-C-substituted ring A. The anomeric sugar proton at δ 4.69 (1H, d, *J* 10.2 Hz, H-1″) revealed that, compound **137** had one glucose unit at C-8. The most downfield signal was due to the quaternary carbon C-4 (δ 182.05) due to hydrogen bonding with hydroxyl

group at C-5. The 21 ^{13}C peaks: 1 x CH_2, 11 x CH and nine quaternaries were confirmed by DEPT 135 experiment. HMQCs were observed between H-1″ (δ 4.69) and C-1″ (δ 73.4), H-2″ (δ 3.85) and C-2″ (δ 70.9), H-3″ (δ 3.28) and C-3″ (δ 78.7), H-4″ (δ 3.36) and C-4″ (δ 70.5), and H-6″$_{ax}$ (δ 3.52) /H-6″$_{eq}$ (δ 3.76) to C-6″ (δ 61.3) confirming the presence of C-β-D-glucopyranoside moiety. The COSY interactions and HMBCs are shown in figure 40.

Figure 40: Selected HMBCs and COSYs of vitexin (**137**)



137

Table 44: 1D and 2D NMR (500 MHz, $CDCl_3$) data for vitexin (**137**)

Position	δ	HMQC (δ)	HMBC	δ_{lit}
2	163.9 (s)			163.5
3	102.4 (d)	6.78	C-2, C-1′, C-10	102.3
4	182.1 (s)			181.8
4a	103.9 (s)			103.8
5	160.4 (s)			160.2
6	98.2 (d)	6.27	C-5, C-8, C-10	97.9
7	156.0 (s)			162.2
8	104.6 (s)			104.3
9	161.2 (s)			155.7
1′	121.6 (s)			121.3
2′	129.0 (d)	8.01		128.7
3′	115.8 (d)	6.88	C-1′, C-2, C-3′, C-3	115.5
4′	160.4 (s)			160.8
5′	115.8 (d)	8.88	C-1′, C-2, C-3′, C-3	115.5
6′	129.0 (d)	8.01		128.7
1″	73.4 (d)	4.68		73.2
2″	70.9 (d)	3.83		70.6
3″	78.7 (d)	3.30		78.4
4″	70.5 (d)	3.36		70.3
5″	81.9 (d)	3.24		81.5
6″	61.3 (t)	3.76_{ax}, 3.52_{eq}		61.0

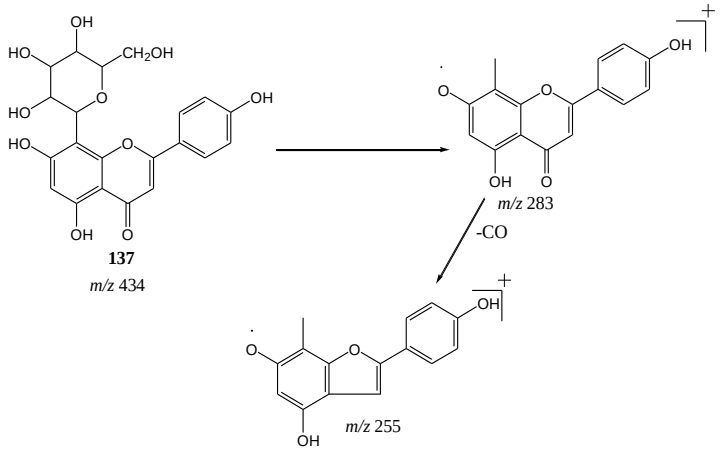
Multiplicity determined from DEPT 135 experiments

The COSY interaction between H-1″ (δ 4.69) and H-2″ (δ 3.85), H-2″ (δ 3.85) and H-3″ (δ 3.28), H-3″ (δ 3.28) and H-4″ (δ 3.36), H-4″ (δ 3.36) and H-5″ (δ 3.24), and H-6″$_{ax}$ (δ 3.52) and H-6″$_{eq}$ (δ 3.76) confirmed the presence of C-β-D-glucopyranoside moiety.

H-6 (δ 6.25) showed HMBCs to C-5 (δ 160.4), C-8 (δ 104.6) and C-9 (δ 103.9). Similarly, H-3 (δ 6.78) showed HMBCs to C-2 (δ 163.9), C-1′ (δ 121.6) and C-4a (δ 103.9). H-3′/H-5′ (δ 8.02, 2H, d, *J* 8.4 Hz) and H-2′/H-6′ (δ 6.89, 2H, d, *J* 8.4 Hz) showed HMBCs to C-1′ (δ 121.6), C-2 (δ 163.9), and C-3′/C-5′ (δ 115.8). NMR data suggested the presence of 8-glucopyranosyl-4′, 5, 7-trihydroxyflavone (vitexin) (**137**). The COSYs and HMBC interactions confirmed the assignments. Comparison of the observed and reported data confirmed the structure as 8-glucopyranosyl-4′, 5, 7-trihydroxyflavone (vitexin) (**137**) (Marbry *et al*., 1970; Markham, 1982; Agrawal, 1989; Vázquez *et al*., 2001).

LREIMS gave a peak $[M+2]^+$ at *m/z* 434 corresponding to the formula $C_{21}H_{20}O_{10}$. Other prominent peaks were seen at *m/z* 283 $[M\text{-}C_5H_{11}O_5]^+$ and *m/z* 255 $[M\text{-}C_5H_{11}O_5\text{-}CO]^+$ consistent with the structure 8-glucopyranosyl-4′, 5, 7-trihydroxyflavone (vitexin) (**137**) (Fig. 41).

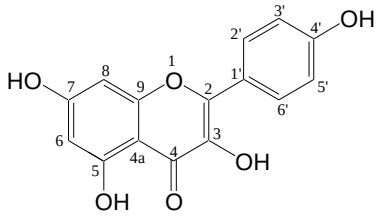
Figure 41: Key MS fragments of vitexin (**137**)



Vitexin (**137**) is one of several flavonoids widely distributed in the plant kingdom and it has aready been isolated from many other plant species including *Acacia* spp., *Alnus* spp., *Barleria christata, Betula* spp. and *Combretum* spp (Wollenweber & Jay, 1988). However, this is the first report on its presence in *A. chloropterus*.

5.1.9 3, 4′, 5, 7-tetrahydroxyflavone (kaempferol) (138)

PTLC (SiO_2, $C_6H_5CH_3$-MeOH 7.0: 3.0) gave a solid which was purified by re-crystallization ($CHCl_3$-MeOH 1:1) to pale yellow needles (3.8 mg), m.p. 276-278 °C (decomposed), that gave positive colour test for flavonoids with vanillin-sulfuric acid and *p*-anisaldehyde.



138

The structure was established on the basis of 1D (^1H, ^{13}C and DEPT 135) and 2D-NMR experiments (HMQC, HMBC, COSY), Table 45-46, Appendix 16a-f, plus MS (Appendix 16g).

Table 45: ^1H NMR and COSY (500 MHz, DMSO) data for kaempferol (**138**)

Position	δ_{obs}	J_{obs} (Hz)	COSY	δ_{lit}	J_{lit} (Hz)
6	6.19 (1H, d)	1.9	H-8	6.23 (1H, d)	1.9
8	6.45 (1H, d)	1.9	H-6	6.35 (1H, d)	1.9
2′	8.04 (1H, d)	8.9	H-3′	7.95 (1H, d)	8.9
3′	6.93 (1H, d)	8.9	H-2′	6.88 (1H, d)	8.9
5′	6.93 (1H, d)	8.9	H-6′	6.88 (1H, d)	8.9
6′	8.04 (1H, d)	8.9	H-5′	7.95 (1H, d)	8.9
3-OH	9.35 (1H, *br* s)			10.05 (1H, s)	
4-OH	10.10 (1H, *br* s)			10.44 (1H, s)	
5-OH	12.48 (1H, *br* s)			12.96 (1H, s)	
7-OH	10.85 (1H, s)			12.79 (1H, s)	

Literature data from Lin *et al.*, 2001

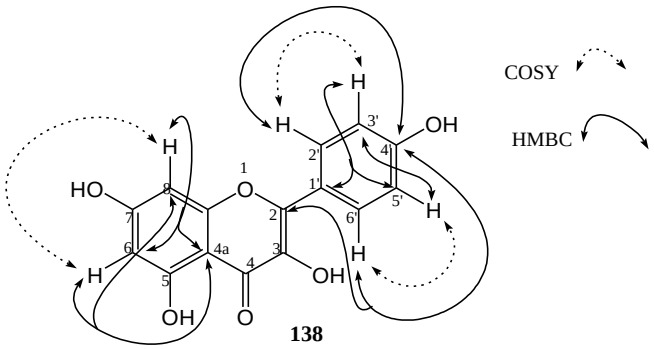
Table 46: 1D and 2D NMR (500 MHz, $CDCl_3$) data for kaempefrol (**138**)

Position	δ_{obs}	HMQC (δ)	HMBC	δ_{lit}
2	146.8 (s)			148.1
3	135.6 (s)			137.1
4	175.9 (s)			178.0
4a	103.1 (s)			104.5
5	160.7 (s)			160.6
6	98.2 (d)	6.19	C-5, C-7, C-8, C-10	99.3
7	163.8 (s)			165.7
8	93.5 (d)	6.45	C-5, C-6, C-9, C-10	94.5
9	156.2 (s)			158.3
1′	121.7 (s)			123.8
2′	129.5 (d)	8.04	C-4′, C-2, C-6′, C-3′	130.7
3′	115.4 (d)	6.93	C-4′, C-1′,C-2′, C-5′	116.3
4′	159.1 (s)			162.5
5′	115.4 (d)	6.93	C-4′, C-1′,C-2′, C-3′	116.3
6′	129.5 (d)	8.04	C-4′, C-2, C-2′, C-3′	130.7

δ_{lit} – Literature data from Vega *et al.*, 2007; Multiplicity determined from DEPT 135 experiments

The ^{1}H NMR revealed two characteristic *meta*-protons (H-6 and H-8), unique for a 5, 7-disubstituted ring A of a flavonoid at δ 6.19 (1H, d, *J* 1.9 Hz) and δ 6.45 (1H, d, *J* 1.9 Hz) with HMQCs to carbons at C-6 (δ 98.2) and C-8 (δ 93.5), respectively. The signal at δ 12.48 (s) was assigned to 5-OH due to the hydrogen bonding interaction of the hydroxyl group at C-5 (δ 160.7) with the carbonyl group at C-4 (δ 175.9). The absence of signals at δ 6.60-6.99 in ^{1}H NMR and δ 157.4-165.8 in ^{13}C NMR suggested substitution at C-3 (δ 135.6). The COSY interactions and HMBCs are shown in figure 42.

Figure 42: Selected HMBCs and COSYs of kaempefrol (**138**)



138

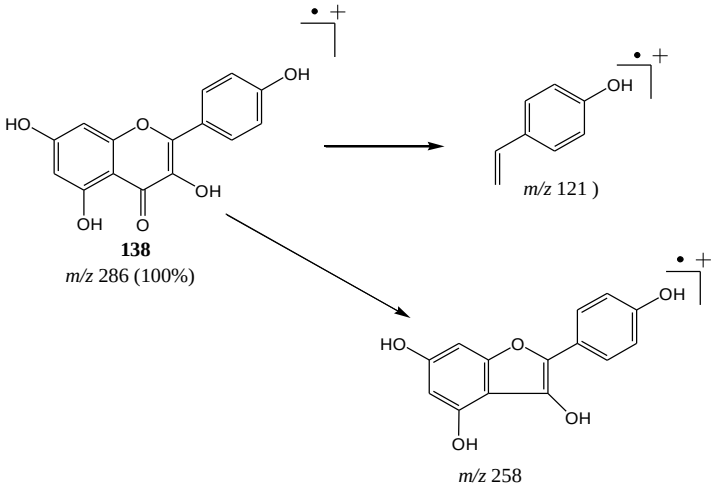
Long range COSY interaction between the H-6 (δ 6.19) and H-8 (δ 6.45) was noted. The two vicinal protons H-2′/H-6′ (δ 8.04, 2H, d, *J*, 8.9 Hz) and H-3′/H-5′ (δ 6.93, 2H, d, *J*, 8.9 Hz) were confirmed in COSY experiment. H-6 (δ 6.19) showed HMBCs to C-8 (δ 93.5), C-4a (δ 103.1), C-5 (δ 160.7) and C-7 (δ 163.8). H-8 (δ 6.45) showed HMBCs with C-6 (δ 98.2), C-4a (δ 103.1), C-7 (δ 163.8) and C-9 (δ 156.2). C-7 (δ 163.8) showed HMBCs to H-6 (δ 6.19) and H-8 (δ 6.45). These observations confirmed the presence of a 5, 7-dihydroxy pattern in ring A (Marbry *et al*., 1970; Markham, 1982; Agrawal, 1989; Lin *et al*., 2001; Vega *et al*., 2007).

H-2′/H-6′ (δ 8.04, 2H, d, *J*, 8.9 Hz) had HMBCs with C-4′ (δ 159.1), C-2 (δ 146.8), C-2′/C-6′ (δ 129.5) and C-3′/C-5′ (δ 115.4) and HMQC with C-2′/C-6′ (δ 129.5). Similarly, H-3′/H-5′ (δ 6.93, 2H, d, *J*, 8.9 Hz) had HMBCs with C-4′ (δ 159.1), C-2′/C-6′ (δ 129.5), C-1′ (δ 121.7). These observations suggested **138** to be a 3, 4′, 5, 7-tetrahydroxyflavone.

Comparison of the observed and reported data confirmed the structure **138** as 3,4′,5,7-tetrahydroxyflavone (kaempferol) (Marbry *et al*., 1970; Markham, 1982; Agrawal, 1989;

Lin *et al*., 2001; Vega *et al*., 2007). LREIMS gave the molecular ion M^+ at *m/z* 286, which corresponds to the formula $C_{15}H_{10}O_6$. Other prominent peaks were seen at *m/z* 258 $[M\text{-}CO]^+$ and *m/z* 153 $[M\text{-}C_8H_60]^+$ consistent with the suggested 3, 4′,5,7-tetrahydroxyflavone (**138**) (Fig. 43).

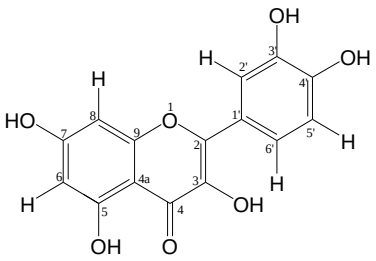
Figure 43: Key MS fragments of kaempferol (**138**)



Kaempferol (**138**) is one of several flavonoids widely distributed in the plant kingdom and it has aready been isolated from many other plant species including *Acacia* spp., *Alnus* spp., *Barleria christata, Betula* spp. and *Combretum* spp (Wollenweber & Jay, 1988; Marbry *et al*., 1970; Markham, 1982; Lin *et al*., 2001; Vega *et al*., 2007). However, this is the first report on its presence in *A. chloropterus*.

5.1.10 3, 3′, 4′, 5, 7-pentahydroxyflavone (quercetin) (139)

Gel filtration of sub-fraction 9 (sephadex LH-20, $CHCl_3$-MeOH 1:1) of fraction 81-90 of column chromatography of fraction ACSD 7 resulted to eight fractions. Fraction 7 contained a single spot on TLC which gave a yellow solid on evaporation. Re-crystallization ($CHCl_3$-MeOH 1:1) yielded **139** as dark yellow powder (5.8 mg), m.p. 313-315 °C (decomposed), that gave positive colour test for flavonoids in the vanillin-sulfuric acid and *p*-anisaldehyde.



139

The structure was established on the basis of 1D (^{1}H, ^{13}C and DEPT 135) and 2D-NMR experiments (HMQC, HMBC, COSY), Table 47 – 48, Appendix 17a-f, plus MS (Appendix 17g).

Table 47: ^{1}H NMR and COSY (500 MHz, DMSO) data for quercetin (**139**)

Position	δ_{obs}	J_{obs} (Hz)	COSY	δ_{lit}	J_{lit} (Hz)
6	6.19 (1H, d)	2.0	H-8	6.18 (1H, d)	2.0
8	6.41 (1H, d)	2.0	H-6	6.39 (1H, d)	2.0
2′	7.69 (1H, d)	2.2	H-6′	7.73 (1H, d)	2.0
5′	6.89 (1H, d)	8.5	H-6′	6.88 (1H, d)	8.4
6′	7.55 (1H, d)	8.5, 2.2	H-2′,5′	7.63 (1H, d)	8.4, 2.0
5-OH	12.98 (1H, s)				

Literature data from Hsieh *et al.*, 2004

Table 48: 1D and 2D ^{13}C NMR (500 MHz, $CDCl_3$) data for quercetin (**139**)

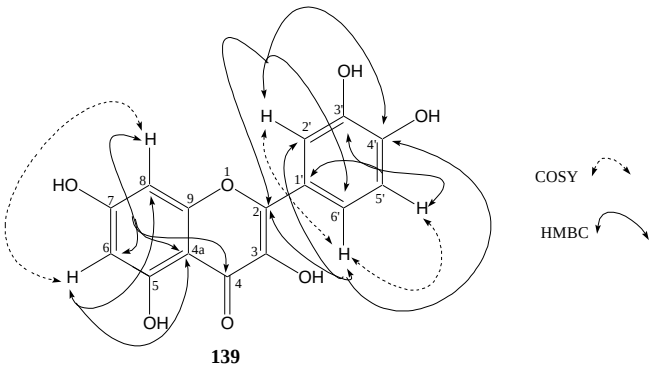
Position	δ_{obs}	HMQC (δ)	HMBC	δ_{lit}
2	145.1			147.2
3	135.8	H-3	C-2, C-1′, C-10	136.6
4	175.9			176.7
4a	103.1			103.9
5	160.8			157.0
6	98.3	H-6	C-10, C-8	99.0
7	164.0			164.7
8	93.4	H-8	C-7, C-9, C-10, C-6	94.2
9	156.2			161.6
1′	122.0			122.8
2′	115.1	H-2′	C-4, C-4′, C-3′, C-6′	116.5
3′	146.9			145.9
4′	147.8			148.6
5′	115.7	H-5′	C-4′, C-1′	115.9
6′	120.1	H-6′	C-2, C-4′, C-3′, C-2′	120.8

δ_{lit} – Literature data from Fathiazad *et al.*, 2006: Multiplicity determined from DEPT 135 experiments

The ^{1}H and ^{13}C NMR spectra of **138** were similar to those of luteolin (**136**) except for the absence of the isolated proton at δ 6.18. The signal at δ 12.50 (s) was assigned to 5-OH, the downfield shift being due to the intra-molecular hydrogen bonding with the carbonyl at C-4 (δ 175.9).

The two *meta*-protons (H-6 and H-8) typical of the 5, 7-disubstituted ring A of flavonoids were observed at δ 6.19 (1H, d, *J* 2.0 Hz) and δ 6.41 (1H, d, *J* 2.0 Hz). The signals at δ 6.19 and 6.41 showed HMQC to C-6 (δ 98.3) and C-8 (δ 93.4) respectively. The ^{1}H NMR spectrum of **139** also showed an ABX spin-system at δ 6.89 (1H, d, *J* 8.5 Hz), δ 7.55 (1H, dd, ^{1}J 8.5 Hz, ^{2}J 2.2 Hz) and δ 7.69 (1H, d, *J* 2.2 Hz) owing to a 1′, 3′, 4′-trisubstitution pattern in ring B. The signals at δ 7.69 (1H, d, *J* 2.2 Hz) and δ 7.55 (1H, dd, ^{1}J 8.5, ^{2}J 2.2 Hz) showed HMQC to C-2′ (δ 115.1) and C-6′ (δ 120.1), and are characteristic of the two *meta*-protons (Marbry *et al*., 1970; Markham, 1982; Agrawal, 1989; Vázquez *et al*., 2001; Hsieh *et al*., 2004). Important HMBCs and COSY interactions are shown in figure 44.

Figure 44: Selected HMBCs and COSYs of quercetin (**139**)



139

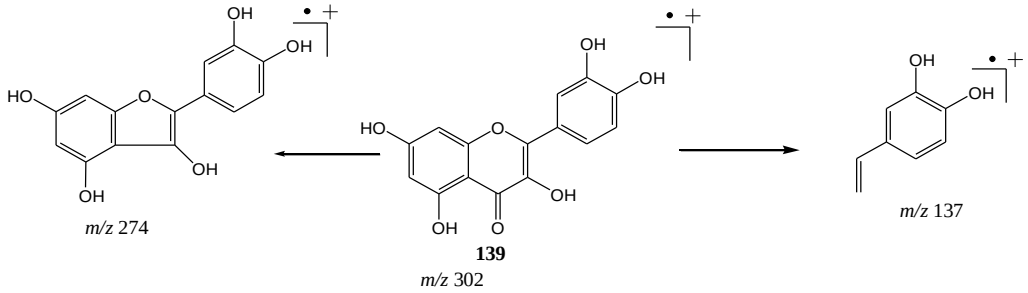
COSY interaction between H-6′ (δ 7.55, 1H, dd, ^{1}J 8.5 Hz, ^{2}J 2.2 Hz) and H-5′ (δ 6.89, 1H, d, 8.5 Hz) was observed. Long range interaction of the two *meta*-protons H-6 (δ 6.19) and H-8 (δ 6.41) was confirmed by COSY. Another long range COSY interactions between H-2′ (δ 7.69) and H-6′ (δ 7.55) was noted and confirmed the assignment of the ABX spin system.

H-6 (δ 6.19) was confirmed from HMBCs with δ C-7 (164.0), C-5 (δ 160.8), C-4a (δ 103.1) and C-8 (δ 93.4). Similarly, H-8 (δ 6.41) was confirmed from the HMBCs with C-4 (δ 175.9), C-7 (δ 164.0), C-9 (δ 156.2), C-4a (δ 103.1) and C-6 (δ 98.3). H-5′ (δ 6.89) showed HMQC with C-5′ (δ 115.7), H-2′ (δ 7.69) showed HMBCs with C-4′ (δ 147.8), C-3′ (δ 146.9), C-2 (δ 145.1) and C-6′ (δ 120.1). H-5′ (δ 6.89) showed HMBCs with C-4′ (δ 147.8), C-2 (δ 145.1) and C-1′ (δ 122.0). H-6′ (δ 7.55) showed HMBCs with C-4′ (δ 147.8), C-5′ (δ 115.7) and C-2′ (δ 115.1). The observed NMR data suggested the presence of 3, 3′, 4′, 5, 7-pentahydroxyflavone (quercetin) (**139**). Comparison of the observed and reported data confirmed the structure as 3, 3′, 4′, 5, 7-pentahydroxyflavone (quercetin) (**139**) (Marbry *et*

al., 1970; Markham, 1982; Agrawal, 1989; Vázquez *et al*., 2001; Hsieh *et al*., 2004; Fathiazad *et al*., 2006).

LREIMS gave the molecular ion M^+ at *m/z* 302, which corresponds to the formula $C_{15}H_{10}O_7$. Other prominent peaks were seen at *m/z* 274 and *m/z* 137 consistent with the suggested quercetin (**139**) (Fig. 45).

Figure 45: Key MS fragments of quercetin (**139**)



Quercetin (**139**) is one of several flavonoids widely distributed in the plant kingdom and it has aready been isolated from many other plant species including *Acacia* spp., *Alnus* spp., *Barleria christata, Betula* spp. and *Combretum* spp (Wollenweber & Jay, 1988; Marbry *et al*., 1970; Markham, 1982; Lin *et al*., 2001). However, this is the first report on its presence in *A. chloropterus*.

5.2 Antiparasitic and cytotoxicity activity of compounds from *Acridocarpus chloropterus*

The anti-parasitic activity and cytotoxicity of the isolated compounds to *P. falciparum, T. b. rhodesiense, L. donovani* and rat myoblast L-6 cells, respectively, are summarized in table 49.

Table 49: Anti-protozoal activity (IC_{50}) and cytotoxicity (CC_{50}) data of isolated compounds from *Acridocarpus chloropterus*

	P. falciparum K1		*T. b. rhodesiense*		*L. donovani*		L-6 cells
Compound	IC_{50} ± S.E (µg/ml)	SI	IC_{50} ± S.E (µg/ml)	SI	IC_{50} ± S.E (µg/ml)	SI	CC_{50} ± S.E (µg/ml)
β-Sitosterol (**132**)	>5.0	>6.6	33.5±0.01	1.0	>30.0	>1.1	32.8±0.00
Stigmasterol (**133**)	>5.0	>18.0	6.4±0.00	>14.1	>30.0	>3.0	>90
Friedelin (**134**)	>5.0	>18.0	56.6±0.00	>1.6	>30.0	>1.1	>90
Oleanolic acid (**124**)	>5.0	>8.5	16.3±0.01	2.6	3.5±0.00	12.1	42.3±0.00
Ursolic acid (**123**)	>5.0	>1.4	7.8±0.00	0.9	0.8±0.00	8.9	7.1±0.00
Apigenin (**135**)	>5.0	>7.9	9.0±0.00	4.4	5.9±0.00	6.7	39.4±0.00
Luteolin (**136**)	>5.0	>18	35.4±0.00	2.5	11.8±0.00	7.6	>90
Vitexin (**137**)	>5.0	>18	14.9±0.01	6.0	>30.0	>3.0	>90
Kaempferol (**138**)	>5.0	>5.2	16.4±0.00	1.6	2.2±0.00	11.9	26.1±0.00
Quercetin (**139**)	2.6±0.05	>8.0	3.6±0.00	5.9	2.1±0.00	11.9	21.2±0.01

P. falciparum – K1 strain, *T.b. rhodesiense* – STIB 900 strain, *L. donovani* - MHOM-ET-67/L82, L-6 - rat skeletal myoblast cells, IC_{50} – inhibitory concentration for 50% of tested parasites, CC_{50} – cytotoxic concentration for 50% of tested cells, chloroquine IC_{50} 0.063±0.03, artemisinin IC_{50} 0.002±0.000, melarsoprol IC_{50} 0.002±0.000, militefosine IC_{50} 0.11±0.001, Pdx - podophyllotoxin IC_{50} 0.009±0.000

Quercetin (**139**) exhibited moderate anti-plasmodial activity (IC_{50} 2.6±0.05 µg/ml) and moderate selectivity index (SI >8). The remaining 9 compounds showed mild activity (IC_{50} >5.0 µg/ml). Similarly, quercetin (**139**) was moderately active against *T. b. rhodesiense* STIB 900 strain (IC_{50} 3.6 ± 0.00 µg/ml) *in vitro* and satisfactory selectivity (SI 5.9). Ursolic acid (**123**), β-sitosterol (**132**) and apigenin (**135**) had mild anti-trypanosomal activity (IC_{50} 6.4±0.05-9.0±0.00 µg/ml) whereas the remaining six compounds were inactive (IC_{50} 16.3±0.01-56.6±0.01 µg/ml) and poor selectivity (SI 1.6 – 6.0).

Ursolic acid (**123**) exhibited strong anti-leishmanial activity (IC_{50} 0.8±0.000 µg/ml) *in vitro* and moderate selectivity (SI 8.9). Oleanolic acid (**124**), kaempferol (**138**) and quercetin (**139**) compounds exhibited moderate activity (IC_{50} 2.1 ± 0.00 – 3.5 ± 0.00 µg/ml) and moderate selectivity (SI 11.1). Apigenin (**135**) (IC_{50} 5.9±0.00 µg/ml) and the remaining four compounds were inactive (IC_{50} 11.8±0.01->30.0 µg/ml) and had narrorw or no selectivity (SI >1.1 - >3.0).

Based on the molecular framework of isolated triterpenes and flavonoids, the relationship between *in vitro* anti-protozoal and cytotoxicity activity and chemical structures were examined with respect to positions of different functional groups. Structural comparison between β-sitosterol (**132**) and stigmasterol (**133**) revealed the presence of an olefinic bond at C-22/C-23 in the Δ^5-sterol molecular framework to be the only difference (Fig. 46).

Figure 46: Structure-activity-relationship between β-sitosterol (**132**) and stigmasterol (**133**)



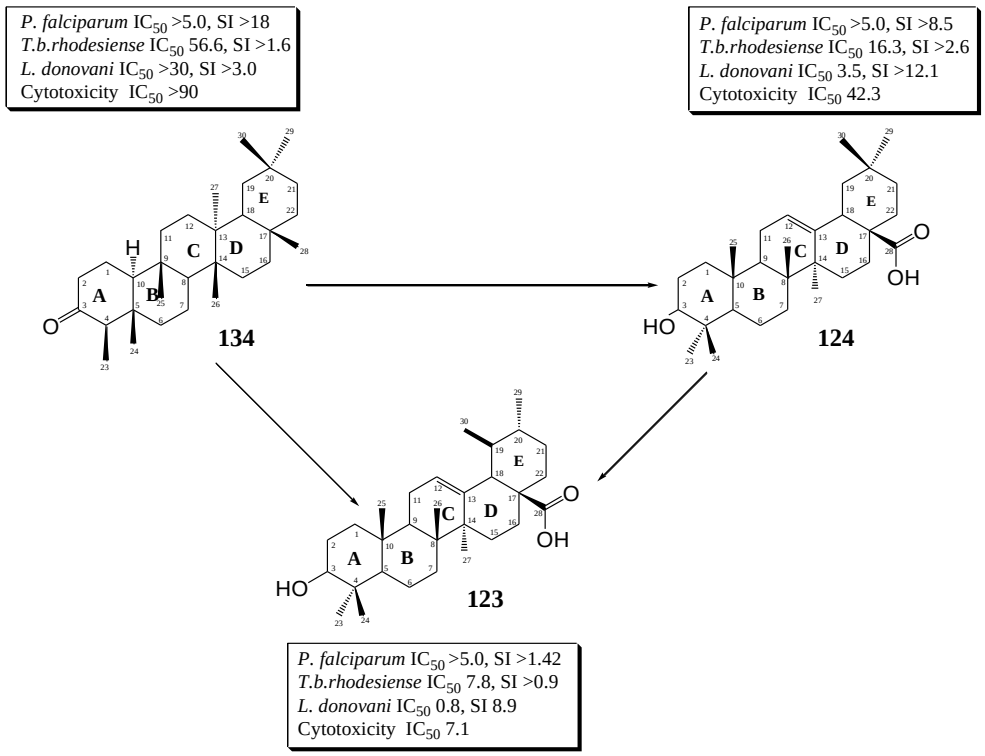
P. falciparum IC_{50} >5.0, SI >6.6
T.b.rhodesiense. IC_{50} 33.5, SI 1.0
L. donovani IC_{50} >30, SI 1.1
Cytotoxity IC_{50} 32.8

P. falciparum IC_{50} >5.0, SI>18.0
T.b.rhodesiense. IC_{50} 6.4, SI >14.1
L. donovani. IC_{50} >30, SI> 3.0)
Cytotoxity IC_{50} >90

However, the presence of an olefinic bond at C-22/C-23 position in stigmasterol (**133**) had no effect on anti-plasmodial and anti-leishmanial activity, but significantly increased the anti-trypanosomal activity (from IC_{50} 33.5±0.01 to 6.4±0.00 µg/ml) 5.2 fold compared to β-sitosterol (**132**). The presence of the olefinic bond at C-22/C-23 in stigmasterol (**133**) resulted in decrease in cytotoxicity (from IC_{50} 32.8±0.00 µg/ml to >90 µg/ml), 2.7 fold confirming the observed differences in bioactivities to be purely due the replacement of a single-bond with double-bond at C-22/C-23.

The relationship between the *in vitro* anti-protozoal activity and cytotoxicity and chemical structure of friedelin (**134**) in comparisons to oleanolic acid (**124**) and ursolic acid (**123**) chemical structures were investigated (Fig. 42). Structural comparison of friedelin (**134**) and oleanolic acid (**124**) revealed the replacement of several functional groups: carbonyl at C-3 with OH, H-4 with 23-CH_3, H-10 with 25-CH_3, H-8 with 26-CH_3, single bond at C-12/C-13 with double bond and 28-CH_3 with CO_2H. Although the replacements had no effect on anti-plasmodial activity, they significantly increased anti-trypanosomal (IC_{50} 56.6±0.001 to 16.3±0.001 µg/ml) and anti-leishmanial activity (IC_{50} >30.0 to 3.5±0.00 µg/ml). The replacements resulted in increase in cytotoxicity (IC_{50} >90.0 to 42.3±0.00 µg/ml), 2.1 fold suggesting the observed differences in bioactivities to be partly due to cytotoxicity.

Figure 47: Structure-activity-relationship of friedelin (**134**), oleanolic acid (**124**) and ursolic acid (**123**)

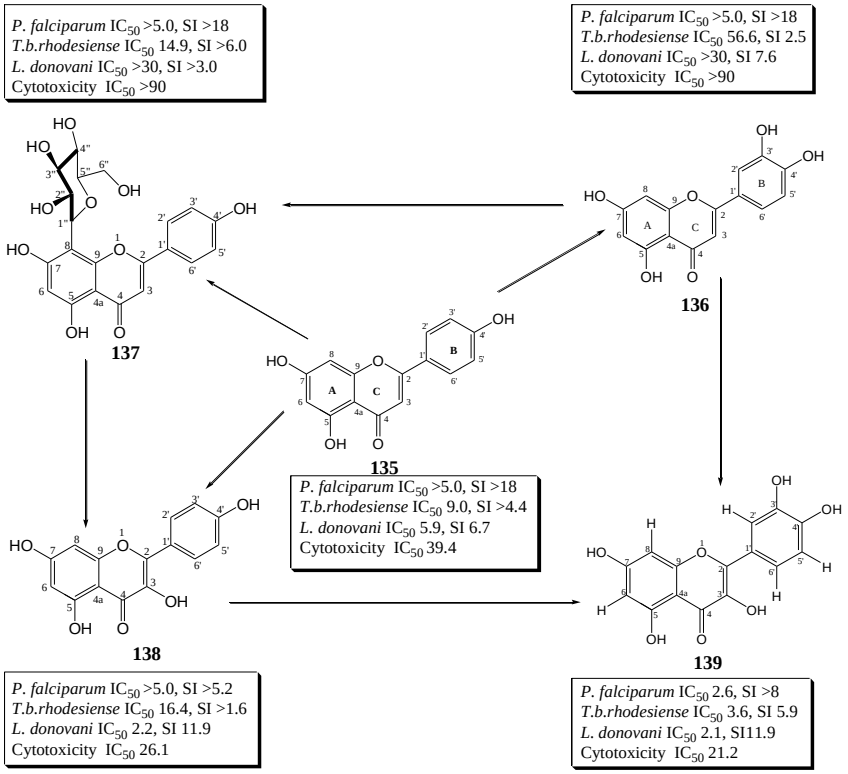


Similarly, the structural comparison of friedelin (**134**) and ursolic acid (**124**) revealed the replacement of several functional groups: carbonyl at C-3 with OH, H-4 with 23-CH_3, H-10 with 25-CH_3, H-8 with 26-CH_3, single bond at C-12/C-13 with double bond, 28-CH_3 with CO_2H, H-19 with 30-CH_3 and 30-$CH_3$with H-20. Although the replacements had no effect on anti-plasmodial activity, they significantly increased the anti-trypanosomal (IC_{50} 56.6±0.001 to 7.8±0.00 µg/ml) and anti-leishmanial activity (IC_{50} >30.0 to 0.8±0.00 µg/ml). The replacements resulted in increase in cytotoxicity (IC_{50} >90.0 to 7.1±0.00 µg/ml), 12.7 fold suggesting the observed differences in bioactivities may be partly contributed by cytotoxicity.

Further structural comparison of oleanolic acid (**123**) and ursolic acid (**124**) revealed the replacement of two functional groups: H-19 with 30-CH_3 and 30-$CH_3$with H-20. The replacements had no effect on anti-plasmodial activity of ursolic acid (**124**) but, significantly increased the anti-trypanosomal (IC_{50} 16.3±0.01 to 7.8±0.00 µg/ml) and anti-leishmanial (IC_{50} 3.5 ± 0.00 µg/ml to 0.8 ± 0.00 µg/ml). The replacements resulted to increased cytotoxicity (IC_{50} 42.3 ± 0.00 to 7.1 ± 0.00 µg/ml), 6.0 fold suggesting the observed differences in bioactivities to be partly due to cytotoxicity. The molecular framework of apigenin (**135**) was used as a template to examine the relationships between

in vitro anti-protozoal activity and cytotoxicity and chemical structures of the isolated compounds (Fig. 48).

Figure 48: Structure-activity-relationship between apigenin (**135**) and other isolated flavonoids



The structural comparison of apigenin (**135**) and luteolin (**136**) revealed the replacement of H-3′ with OH. The replacement had no effect on anti-plasmodial activity but, significantly decreased the anti-trypanosomal (IC_{50} 9.0±0.00 to 35.4±0.00 µg/ml) and anti-leishmanial activity (IC_{50} 5.9±0.00 to 11.8±0.00 µg/ml). The replacements resulted to decrease in cytotoxicity (IC_{50} 39.4 ± 0.00 to >90.0 µg/ml), 2.3 fold suggesting the observed differences in bioactivities to be only due to the replacement of H-3′ with OH.

Similarly, the structural comparison of apigenin (**135**) and vitexin (**137**) revealed the replacement of H-8 with glycoside unit. The replacement did not change anti-plasmodial activity but remarkably decreased the anti-trypanosomal (IC_{50} 9.0±0.00 to 14.9±0.01 µg/ml) and anti-leishmanial activity (IC_{50} 5.9±0.00 to >30.0 µg/ml) plus cytotoxicity (IC_{50} 39.4±0.00 to >90.0 µg/ml). The replacement of H-3 in apigenin (**135**) with OH gave kaempferol (**138**) could not change and had no effect on the anti-plasmodial activity but remarkably decreased the anti-trypanosomal (IC_{50} 9.0±0.00 to 16.4±0.01 µg/ml). Increase in anti-leishmanial activity (IC_{50} 5.9 ± 0.00 µg/ml to 2.2 ± 0.00 µg/ml) plus cytotoxicity (IC_{50}

39.4±0.00 to 26.1±0.00 µg/ml). Replacement of H-3′ and H-3 in apigenin (**135**) with OH gave quercetin (**139**) with improved anti-protozoal activity: anti-plasmodial (IC_{50} >5.0 to 2.6±0.05 µg/ml), anti-trypanosomal (IC_{50} 9.0±0.00 to 3.6±0.00 µg/ml). Cytotoxicity also increased significantly (IC_{50} 39.4±0.00 to 21.2±0.01 µg/ml) indicating that the observed improvements in anti-protozoal activity could be partly contributed by cytotoxicity.

The strongest anti-protozoal activity among the isolated flavonoids was showed by quercetin (**139**) indicating that, the 3-OH and 3′-OH in the apigenin (**135**) molecular framework are the structural moeties responsible for the observed strong anti-protozoal activity. The presence of the phenolic group at the C-3 in apigenin (**135**) molecular framework as in kaempferol (**138**) increased cytotoxicity activity whereas, further addition of phenolic group at the C-3′ as in quercetin (**139**) resulted in further increase in cytotoxicty.

The available literature indicated that the isolated compounds exhibit wide spectrum of pharmacological activities. Thus, β-Sitosterol (**132**) and stigmasterol (**133**) are among of several phytosterols with chemical structures similar to cholesterol, that are widely distributed in the plant kingdom. They reduce levels of cholesterol in blood, and sometimes are used for the treatment of hypercholesterolemia (Chung & Choi, 2007; 4S, 1994; Batta *et al*., 2006). Anti-inflammatory, analgesic and anti-pyretic activity of β-sitosterol (**132**) have been reported previously (Gupta *et al*., 1980). A hexane fraction of aerial parts of *Tillandsia streptocarpa* containing: β-sitosterol (**132**) and stigmasterol (**133**), showed anti-edematogenic activity (Delaporte *et al*., 2004). β-Sitosterol (**132**) modulated anti-oxidant enzymes *in vitro* (Vivancos & Moreno, 2005), improves urinary symptoms and is a major ingredient of herbal therapy for benign prostatic hypertrophy (BPH). It also decreases post-void residual urinary volume and increases urinary flow rate in BPH patients (Wilt *et al*., 1999; Berges *et al*., 1995; Klipppel *et al*., 1997).

β-Sitosterol (**132**) demonstrated 70% protection against the lethal action of the venom of jararaca snakes (*Bothrops jararaca*) on mice (Mors *et al*., 2000). The mixture of β-sitosterol (**132**) and stigmasterol (**133**) in the ratio 3:1 neutralized viper venom induced lethality, hemorrhagic, defibrinogenating, and oedema-producing action and phospholipase activity in laboratory animals (Mors *et al*., 1989). Cobra venom-induced lethality, neurotoxicity and cardiotoxicity effectively antagonized. The mixture of β-sitosterol (**132**) and stigmasterol (**133**) effectively neutralize lethal action of *Crotalus durissus terrificus* snake venom (Mors *et al*., 1989). The mixture of β-sitosterol (**132**) and stigmasterol (**133**) neutralize snake

venom, as well as potentiate the action of equine polyvalent snake venom anti-serum in experimental animals (Alam & Gomes 1998; Chatterjee *et al*., 2006).

Friedelin (**134**) demonstrated 40% protection against the lethal action of the venom of jararaca snakes (*Bothrops jararaca*) on mice (Mors *et al.*, 2000). Oleanolic acid (**124**) is recognized to exhibit hepato-protective, anti-inflammatory and anti-hyperlipidemic properties (Liu, 1995). It is still used alone or in combination with other hepato-protective ingredients as oral medications (Liu, 1995). The beneficial effects of oleanolic acid (**124**) on the liver are due to its anti-oxidant and anti-inflammatory actions, and its effects on drug-metabolizing enzymes (Liu, 1995). Oleanolic acid (**124**) exhibits potent suppressive effect on HIV replication at concentrations of 10 and 20 nM with inhibition of 85 and 97%, respectively compared to the AZT (70%) (Lichtner *et al*., 1999). It has further been shown that oleanolic acid (**124**) exhibits anti-HIV activity (EC_{50} of 1.7 µg/ml, TI 12.8 (Zhu et al, 2001).

Ursolic acid (**123**), a well known compound for hepatoprotective effects for both acute chemically induced liver injury and chronic liver fibrosis plus cirrhosis (Liu, 1995), is used alone or in combination with other hepatoprotective ingredients as oral medication (Liu, 1995). The beneficial effects of ursolic acid (**123**) on the liver may be due to its anti-oxidant effect, anti-inflammatory actions, and its effects on drug-metabolizing enzymes (Liu, 1995). It has shown potent anti-HIV activity (EC_{50} 2.0 µg/ml).

Apigenin (**135**), a widely distributed flavonoid in the plants exhibits good anti-oxidant activity through inhibition of xanthine oxidase activity (uric acid production) IC_{50} 86 mM with similar activity level as the standard drug, allopurinol (IC_{50} 74 mM) (Halliwell & Gutteridge, 1993). Apigenin (**135**) also exhibits cardiotonic action on the heart through different mechanisms by inhibition of the calcium release from sarcoplasmic reticulum enzymatic systems such as protein kinase-C and the calcium influx (Sanchez *et al*., 1996). Luteolin (**136**) is also widely distributed in the plant kingdom which for along time has been recognized to play an important role in the human body as an anti-oxidant, a free radical scavenger, an agent in the prevention of inflammation, a promoter of carbohydrate metabolism, and an immune system modulator (Grimberg & Cohen, 2000; Bagli *et al*., 2004; Fang *et al*., 2007). Luteolin (**136**) exhibit strong anti-oxidant activity through inhibition of xanthine oxidase activity (uric acid production) IC_{50} 77 mM which is comparable with allopurinol (IC_{50} 74 mM) (Halliwell & Gutteridge, 1993).

Luteolin (**136**) inhibits insulin-like growth factor 1 (IGF-1) in prostate cancer cells (PC-3 and DU145) (Fang *et al*., 2007). Elevated levels of IGF-1 increases risk of the three types of cancer: prostate, colorectal and lung (Grimberg & Cohen, 2000). IGF-1 activation is required for prostate cell proliferation. The observations suggest that IGF-1 inhibitory agents may be of preventive and/or therapeutic value.

Vitexin (**137**) exhibits anti-thyroid activity both *in vitro* and *in vivo* by inhibition of thyroid peroxidase (TPO) (Gaitan *et al*., 1995). Kaempferol (**138**), a natural flavonoid isolated from tea and other plant sources, is known to suppress growth of a number of human malignancies (Wang *et al*., 1999; Sharma *et al*., 2007). It exhibits anticancer activity by elevating reactive oxygen species (ROS) generation and by inhibiting thioredoxin reductase 1 (TRX-1), which is critical for maintaining the cellular redox environment (Wang *et al*., 1999; Sharma *et al*., 2007). Kaempferol (**138**) inhibits migration and invasiveness of glioma cells by inducing apoptosis (Shen *et al*., 2006). It also inhibits viral replication including HIV and herpes simplex virus type 1 (HSV-1) (Narayana *et al*., 2001). Recent reports indicate that kaempferol (**138**) possess anti-ulcerogenic activity and inhibited dose-dependent gastric damage produced by acidified ethanol when administered intraperitoneally (25-100 mg/kg) in rats (Parmar & Parmar, 1998). It also exhibits anti-diarrhoeal and anti-spasmodic inhibitory activity on intestinal functions through 2-adrenergic and calcium systems (Izzo *et al*., 1994).

Quercetin (**139**), a natural poly-phenolic flavonoid commonly found in fruits, vegetables, herbs, grains and beverages such as tea and red wine, has anti-oxidant property (free radical scavenging and metal chelating) with beneficial implications on human health, such as in the treatment and prevention of cancer, cardiovascular diseases, and other pathologies (Bravo, 1998). Previous epidemiological studies revealed that the Mediterranean diet, based primarily on flavonoid-rich foods, correlates with increased longevity (Orgogozo *et al*., 1997) and decreased incidence of cardiovascular diseases (Hertog *et al*., 1993; 1995; Renaud *et al*., 1998; 1999).

CHAPTER SIX

EXPERIMENTAL

6.1 Reagents, equipment and Materials

6.1.1 Reagents

Formic acid, hydrochloric acid, sulphuric acid, acetic acid, citric acid, *p*-anisaldehyde, vanillin, dragendorf reagent, sodium chloride and sodium hydrogen carbonate were bought from Kobian Chemicals, Nairobi, Kenya and Fluka AG in Switzerland. Solvents: acetone, *n*-hexane, petroleum ether, dichloromethane, chloroform, ethyl acetate, toluene, ethanol and methanol were also bought from Kobian Chemicals, Nairobi, Kenya and Fluka AG in Switzerland. Analytical grade or double-distilled solvents were used for the extraction and chromatographic isolation and purification of compounds. [^{3}H]-Hypoxanthine and Rosewell Park Memorial Institute 1640 (RPMI 1640) powdered medium were bought from Gibco Laboratories, California, U.S.A whereas, dextrose, Giemsa stain, resazurin dye, glycerol and *N*-2-hydroxyethylpiperazine *N*-2-ethanesulfonic acid (HEPES) were bought from Sigma-Aldrich, Germany. Deuterated solvents: chloroform, methanol, water and dimethyl sulphoxide (DMSO) used for spectroscopic analysis, were bought from Fluka AG, Switzerland.

6.1.2 Equipment

6.1.2.1 Solvent evaporation

Solvent evaporation was performed on a Büchi Rotavapor RE 111 with a water bath at 30 °C and 14 mbar. The high vacuum drying was performed in Edwards's vacuum pump at 4 x 10^{-2}mbar.

6.1.2.2 Chromatography

6.1.2.2.1 Thin layer chromatography (TLC)

Analytical thin layer chromatography was performed on both aluminium and plastic sheets precoated with silica gel 60 F_{254} (Merck) with a 0.2 mm layer thickness. Visualisation of TLC spots was carried out under UV light at 254 or 366 nm and by spraying with dragendorff reagent or *p*-anisaldehyde reagent. Preparative thin layer chromatography (PTLC) was done using normal phase silica gel 60 F_{254} (Merck) precoated on glass plates (20 x 20 cm), with varying thickness (0.25, 0.5, 1.0 or 2.0 mm). Detection was done under UV light at 254 or 366 nm.

6.1.2.2.2 Column chromatography (CC)

Glass columns (20-25 mm diameter) wet packed with silica gel (400 or 230-400 Mesh ASTM, Merck) were used for column chromatography. Size-exclusion chromatography was carried out using Sephadex® LH-20 (Pharmacia), eluting with either MeOH or MeOH-$CHCl_3$ 3:1.

6.1.2.2.3 Medium pressure liquid chromatography (MPLC)

Medium pressure liquid chromatography (MPLC) was performed with a Büchi B-680 system (plate 3), consisting of a Büchi B-688 chromatography pump, a Büchi B-687 gradient former, a Knauer variable wavelength monitor, a Knauer strip chart recorder and a Büchi B-684 fraction collector (Plate 3).

Plate 3: Photgraph of medium pressure liquid chromatography Büchi B-680 system



6.1.2.2.4 High speed counter-current chromatograph (HSCCC)

Potomac (P.C. Inc., Buffalo, NY-USA) preparative high speed counter-current chromatograph (HSCCC) equipped with three preparative multilayer coils (wound with 1.7 mm internal diameter, polytetrafluoroethylene PTFE tubing tubing of 80 ml and 240 ml connected in series with a total capacity of 320 ml) was used (Plate 4). The revolution speed

was 611 rpm and the solvent was pumped into the column with a Büchi B-688 chromatography pump. Continuous monitoring of the effluent was achieved with a Model UV-II detector Monitor at 254 nm. A manual sample injection valve with a 20 mL loop was used to introduce the sample into the column and the eluate collected in a Büchi B-684 fraction collector.

Plate 4: Photograph of preparative high speed counter-current chromatograph



6.1.2.3 Spectroscopy

6.1.2.3.1 Infra-red (IR) spectroscopy

IR spectra were measured at the Department of Chemistry of the University of Basel on a Perkin Elmer model 1600 FT-IR spectrophotometer using potassium bromide pellets. Resonance frequencies were given in cm^{-1} and intensities reported as *s* - strong, *m* - medium and *w* - weak.

6.1.2.3.2 Mass spectroscopy (MS)

Mass spectra were measured at the Department of Chemistry of the University of Basel on mass spectrometer VG 70S (EIMS) and a Finnigan MAT 312 FABMS. The m/z are reported in amu with the corresponding relative intensities in parentheses.

6.1.2.3.3 Nuclear magnetic resonance (NMR) spectroscopy

NMR spectra were measured on Bruker Avance 400 (^{1}H NMR 400 MHz; ^{13}C NMR 101 MHz), Bruker VRX 500 (^{1}H NMR 500 MHz; ^{13}C NMR 125 MHz) and Bruker DRX 600 (^{1}H NMR 600 MHz; ^{13}C NMR 150.9 MHz) based at the Department of Chemistry of the University of Basel. Bruker Avance 400 (^{1}H NMR 400 MHz; ^{13}C NMR 101 MHz) of the University of Botswana through NABSA was also used. Deuterated $CDCl_3$, H_2O, $(CH_3)_2CO$, DMSO and MeOH were used as solvents. Chemical shifts were given in δ (ppm) values with TMS (δ 0) as an internal standard. Resonances were designated as *s* - singlet, *d* - doublet, *t* - triplet, *q* – quartet and m - multiplet. Coupling constants (J) were reported in Hz. The ^{13}C NMR spectra were measured using broad band decoupling with $CDCl_3$ as the reference (δ 77.0 ppm). The multiplicities were determined by DEPT 135 experiments and are indicated as follow: *s* - singlet, *d* - doublet, *t* - triplet and *q* - quadruplet; *br* - broad. HMQC and HMBC experiments are reported as $^{13}C \rightarrow {}^1H$, COSY and NOESY experiments $^1H \rightarrow {}^1H$ (intensity. HMBC experiments were carried out using delays optimized for $^nJ_{CH}$ = 7 Hz (*n* = 2 or 3).

6.1.2.4 Melting points

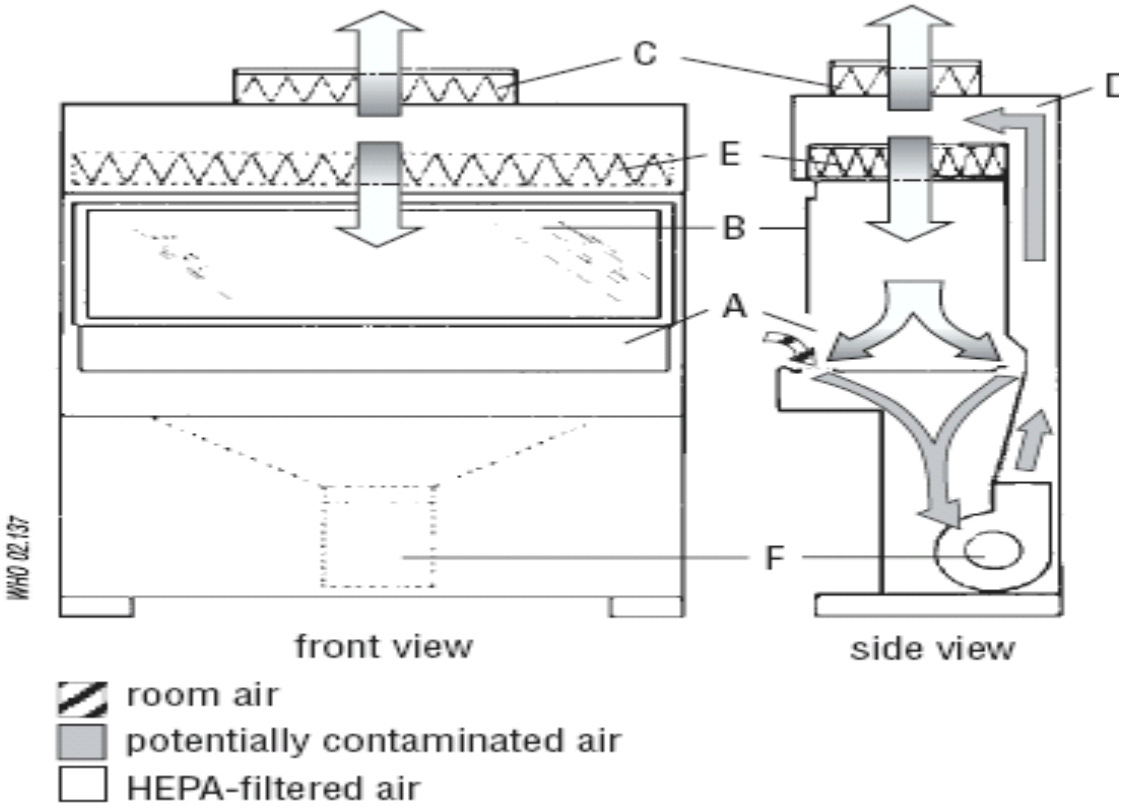
Melting points of recrystallized solids were measured on a Büchi B-540 apparatus and are uncorrected.

6.1.2.5 Bioassay equipment

6.1.2.5.1 Biosafety cabinet (BSC)

The biosafety cabinet used for bioassays was enclosed on three sides, top, and bottom, and was designed to draw air inward by means of mechanical ventilation (Plate 5-6). An internal fan draws room air (supply air) into the cabinet through the front opening and into the front intake grill. The supply air then passes through a high-efficiency particulate air (HEPA) filter before flowing downwards over the work surface. Any aerosol particles generated at the work surface are immediately captured in this downward airflow and passed through the front or rear exhaust grills, thereby providing the highest level of protection against pathogenic culture aerosols.

Plate 5: Diagram of a biological safety cabinet (WHO, 2004).



A - front opening; B, - sash; C - exhaust HEPA filter; D - rear plenum; E - supply HEPA filter; F - blower.

Bioassays were done with insertion of only the hands and arms as shown in the plate 6.

Plate 6: Photograph of biological safety cabinet





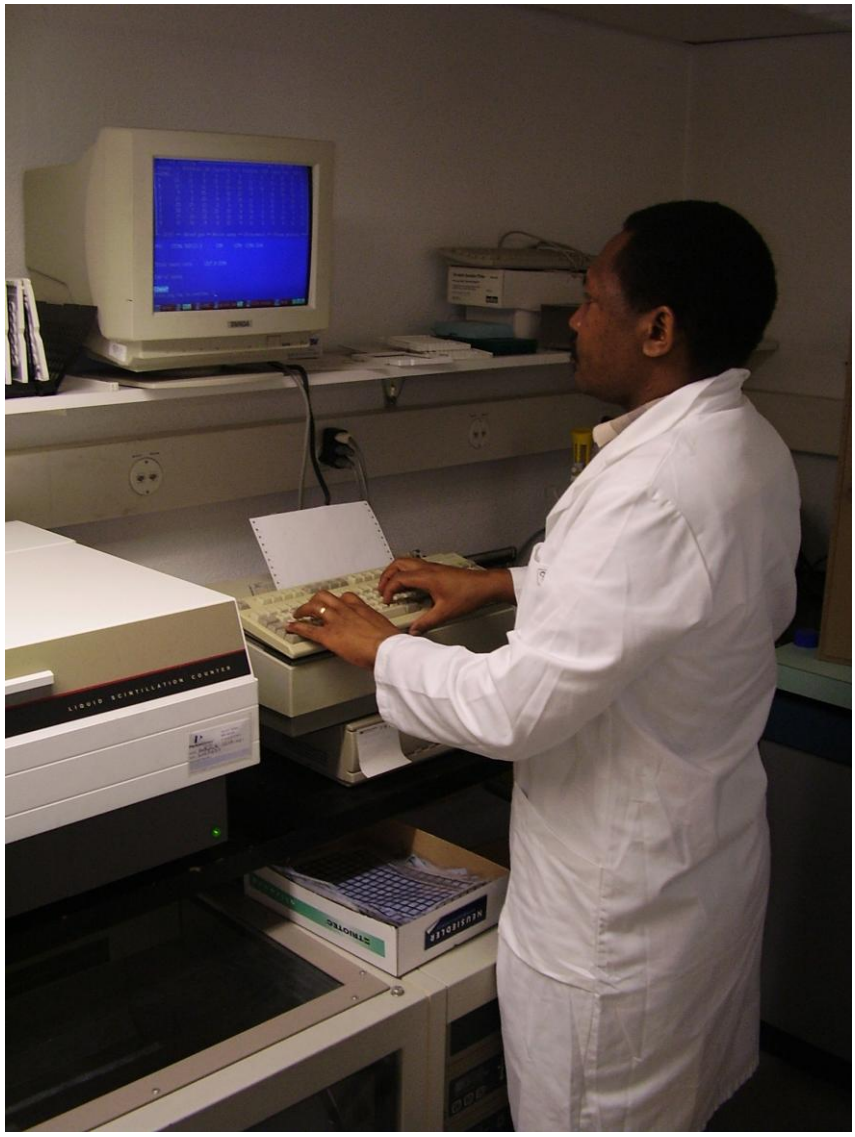
6.1.2.5.2 Betaplate cell harvester

The Betaplate cell harvester (Wallac**,** Zurich, Switzerland) was used to transfer cultured red blood cells from each well of a Costar™ 96-well micro-titre plate onto a glass fiber filter.

6.1.2.5.3 Betaplate liquid scintillation counter

The Betaplate liquid scintillation counter (Wallac) (Plate 7) was used to count the uptake of [^{3}H]-hypoxanthine by *Plasmodium falciparum* in cultured cells.

Plate 7: Photograph of Betaplate liquid scintillation counter



6.1.2.5.4 Micro-plate fluorometer

The micro-plate fluorometer system (Spectramax Gemini, Molecular Devices) (Plate 8) using an excitation and emission wavelengths of 536 and 588 nm was used to read the viability of cultured cells from each well of a Costar^{TM} 96-well micro-titre plate for the determination of cytotoxicity, anti-trypanosomal and anti-leishmanial activity.

Plate 8: Photograph of Spectramax micro-plate fluorometer



6.2 Plant material

6.2.1 Collection and identification

Annickia kummeriae was collected from Shambangeda Village, Amani Nature Reserve, Muheza District, Tanga Region, Tanzania in August 2003. *Acridocarpus chloropterus* was collected from Pugu Forest Reserve in Coast Region, Tanzania in August 2004. *Drypetes natalensis* and *Pseudospondias microcarpa* were collected from Buyango Village, in Bukoba Rural District, Kagera Region, Tanzania in August 2004. The plants were taxonomically identified by Mr. Simon Mathenge of the Department of Botany, University of Nairobi, Nairobi, Kenya. The voucher specimens were deposited at the Department of Botany Herbarium, University of Nairobi, Kenya. The collected plant species and parts are shown in table 50.

Table 50: Plant species collected from Tanga, Coast and Kagera regions in Tanzania

Plant species	Family	Plant part	Specimen No.
Acridocarpus chloropterus	Malpighiaceae	Rootbark, stembark, leaves	HM 2004/01
Pseudospondias microcarpa	Anacardiaceae	Rootbark, stembark, leaves	HM 2004/02
Drypetes natalensis	Euphorbiaceae	Rootbark, stembark	HM 2004/03
Annickia kummeriae	Annonaceae	Rootbark, stembark, leaves	HM 2004/04

6.2.2 Extraction

The plants were air-dried under shade for 14 days under normal temperature and humidity. The air dried plant materials were pulverised and a known amount of sample was extracted sequentially with solvents of increasing polarity: hexane or petroleum ether (PE), dichloromethane (CH_2Cl_2) or chloroform ($CHCl_3$) and ethanol (EtOH) or methanol

(MeOH). The extraction was done at room temperature for 48 h with intermittent shaking, the solvent extract decanted and filtered off. After filtration, the solvent was removed under reduced pressure and the extracts dried further under a stream of nitrogen for 24 h before being weighed and used for biological assays.

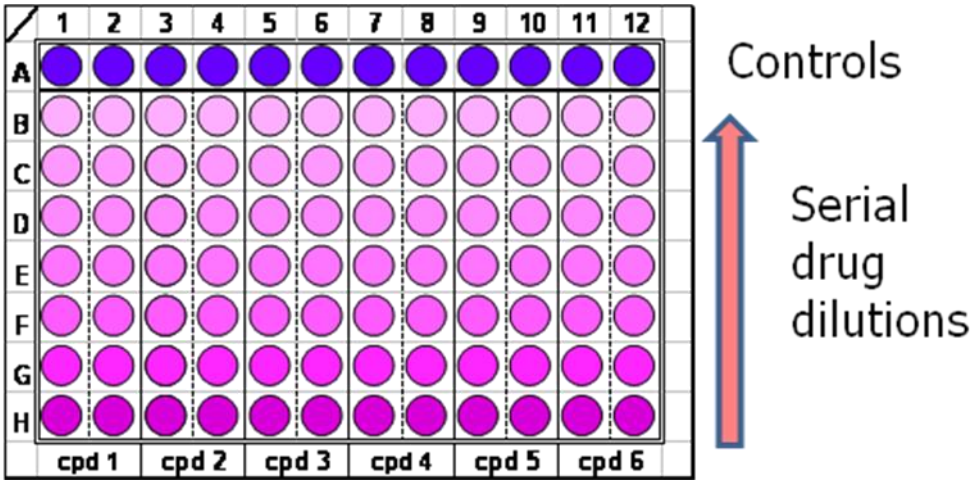
6.3 Biological assays

6.3.1 Anti-plasmodial screening: *in vitro Plasmodium falciparum* assay

The anti-plasmodial assay to evaluate the ability of the pure compounds to inhibit growth of *Plasmodium falciparum* by preventing the uptake of [^{3}H]-hypoxanthine *in vitro* was carried out at the Swiss Tropical Institute, Basel, Switzerland following a standard method with some modifications (Matile & Pink, 1990). The uptake of the radio-labelled nucleic acid precursor [^{3}H]-hypoxanthine by *P. falciparum* maintained *in vitro* on human red blood cells was used as an indicator of growth of the *P. falciparum* K1 strain (CQ and pyrimethamine resistant).

Crude extracts, fractions and pure compounds were dissolved in dimethyl sulfoxide (DMSO) at 1.0 mg/100 µl and if necessary were heated and/or sonicated. The stocks were kept at 4 °C for a maximum of 2 weeks, and thereafter at -20 °C. For the assays fresh dilutions in medium were prepared each time. Parasite culture preparations were carried out asceptically in a biological safety cabinet. The Rosewell Park Memorial Institute (RPMI) 1640 medium was prepared without hypoxanthine, supplemented with N-[2-Hydroxyethyl] piperazine-N`-[2-ethane-sulphonic acid] ($C_8H_{18}N_20_4S$) HEPES (5.94 g/l), $NaHCO_3$ (2.1 g/l), Neomycin (100 U/ml), Albumax® (5 g/l) and washed human red cells from blood group A^+. Each compound was evaluated in duplicate at seven concentrations (two-fold dilution steps). Aliquots of 100 µl of medium were dispensed into each well of a Costar™ 96-well micro-titre plate. Further aliquots of 100 µl of medium, containing 4 x the highest concentration of extract or compound were added to wells in row H and serially diluted. Six drugs were tested in this way on each plate (Plate 9).

Plate 9: Diagramatic representation of a Costar™ 96-well micro-titre plate and drug dilution



For each assay chloroquine (Sigma C6628) and artemisinin (Arteannuin, Qinghaosu; Sigma 36,159-3) were used as the standard drugs with the highest concentration at 200 ng/ml as positive control. Serial drug dilutions were prepared with a multi-pipette and 100 µl taken from wells in row B and transfered, after gentle mixing, to wells in row C. A serial dilution factor of 1:2 was used. After mixing, 100 µl was further transfered from wells in row C to wells in row D. The process was repeated up to row H. The 100 µl removed from wells of row H was discarded. Drug concentrations ranging from 5 µg/ml-78 ng/ml were tested. For active compounds the highest concentration was appropriately lowered. Wells of rows A served as controls without test drug. *Plasmodium falciparum* infected red blood cell solution 100 µl with 2.5% haematocrit at 0.3% parasitaemia was added to each well of the plate except A9 – A12 which only received non-infected red cells. All other wells had a final haematocrit of 1.25% and a parasitaemia of 0.15% at the beginning of the incubation. The plates were kept in an incubation chamber at 37 °C in a humidified atmosphere containing the special gas mixture (4% CO_2, 3% O_2, 93% N_2). After 48 hours, 50 µl of ^{3}H-hypoxanthine (0.5 µCi) was added to each well of the micro-titre plate. The plates were then incubated for another 24 hours under the same conditions as before. The plates were harvested with a Betaplate™ cell harvester (Wallac, Zurich, Switzerland), which transfered the red blood cells onto a glass fiber filter and washed with distilled water. The dried filters were inserted into a plastic foil with 10 ml of scintillation fluid, and counting was done in a Betaplate™ liquid scintillation counter (Wallac, Zurich, Switzerland). Data was transfered into a graphic programme (EXCEL) to generate sigmoidal inhibition curves from which IC_{50} values were calculated. The results are summarized in tables 3 & 10-12.

6.3.2 *In vitro* assay for African trypanosomes (Alamar blue assay)

The *in vitro* anti-trypanosomal assay to evaluate the ability of the pure compounds to inhibit growth of *T. b. rhodesiense* (STIB 900) was carried out at the Swiss Tropical Institute, Basel, Switzerland according to a standard operating procedure (Räz *et al.*, 1997). Crude extracts, fractions and pure compounds were dissolved in dimethyl sulfoxide (DMSO) at 1.0 mg/100µl and if necessary were heated and/or sonicated. The stocks were kept at 4 °C for a maximum of 2 weeks, and thereafter at -20 °C. For the assays fresh dilutions in medium were prepared each time. Parasite culture preparations were carried out asceptically in a biological safety cabinet. Minimum essential medium (MEM) with Earle's salts was supplemented with 25 mM HEPES, 1 g/l additional glucose and 10 ml/l MEM non-essential amino acids (100x). The medium was further supplemented with 0.2 mM 2-mercaptoethanol, 2 mM sodium-pyruvate, 0.1 mM hypoxanthine and 15 % heat inactivated horse serum. Aliquots (50 µl) of medium warmed to room temperature were added to each well of a Costar™ 96-well microtitre plate in rows A to G. Row H was left empty. Further aliquots (75 µl) of medium, containing twice the highest concentration of extract or compound were added to wells of row H. Four drugs were tested in this way on each plate (drug 1 columns 1-3, drug 2 columns 4-6, drug 3 columns 7-9 and drug 4 columns 10-12). For each assay melarsoprol (Arsobal®, Aventis, France) was tested as the standard drug with the highest concentration at 100 ng/ml for positive control.

Serial drug dilutions were prepared with a multi-pipette and 25 µl taken from wells of row H and transfered into wells of row G. After mixing, 25 µl were transfered from wells of row G to wells of row F and the process repeated until row B. The 25 µl which were removed from wells of row B were discarded. A serial dilution factor of 1:3 was used. The drug concentrations ranging from 90-0.13 µg/ml were tested. Each compound was evaluated in triplicate at seven concentrations in threefold dilution steps. For active compounds the highest concentration was appropriately lowered. Wells of row A served as controls without drug. Subsequently, 50 µl of medium without trypanosomes were added to columns 3, 6, 9 and 12 wells B to H, which served as controls to provide the background signal in the fluorescence scanner. However, 50 µl of a suspension containing 3×10^2 bloodstream forms of the parasite were added to all remaining wells leading to an initial trypanosome density of 3×10^3/ml. The trypanosome density were adjusted with a cell counter (CASY, Schärfe System, Germany). The plates were incubated at 37 °C in a humified atmosphere containing 5% CO_2. After 70 hours the plates were inspected under an inverted microscope to assure growth of the controls and sterility of the plate. Then 10 µl of Alamar blue (Trek Diagnostic

Systems, UK) were added to each well and the plates incubated for another 2 hours at 37 °C in 5% CO_2 in air. The plates were read in a micro-plate fluorometer system (Spectramax Gemini, Molecular Devices) using an excitation and emission wavelengths of 536 and 588 nm, respectively. Data were transferred into a graphic programme (Softmax Pro) to generate sigmoidal inhibition curves from which IC_{50} values were calculated. The results are summarized in tables 4 & 10.

6.3.3 *In vitro* leishmanicidal assay

The axenic *in vitro* leishmanicidal screeining was carried out at the Swiss Tropical Institute in Basel, Switzerland according to a standard method (Räz *et al*., 1997). The strain was maintained in the Syrian golden hamster. Amastigotes were collected from the spleen of an infected hamster. Amastigotes were grown in axenic culture at 37 °C in SM medium at pH 5.4 supplemented with 10% heat-inactivated foetal bovine serum under an atmosphere of 5% CO_2 in air (Cunningham, 1977). Crude extracts, fractions and pure compounds were dissolved in dimethyl sulfoxide (DMSO) at 1.0 mg/100µl and if necessary were heated and/or sonicated. The stocks were kept at 4 °C for a maximum of 2 weeks, and thereafter at -20 °C. For the assays fresh dilutions in medium were prepared each time. For the assays, the crude extracts, purified fractions and compounds were further diluted in serum-free culture medium and finally to the appropriate concentration in complete medium.

Parasite culture preparations were carried out asceptically in a biological safety cabinet. Assays were performed in 96-well flat-bottom microtiter plates, (Costar, Corning Inc.) each well contained 100 µl of culture medium with 10^5 amastigotes from axenic culture. Concentration of amastigotes was determined in a CASY cell analysing system (Schärfe System, Reutlingen, Germany). Before counting the amastigotes, the parasite culture was passed twice through a 22-gauge needle to break up clusters of amastigotes. The highest concentration for the test crude extracts, purified fractions and compounds was 90 µg/ml. Seven 3-fold dilutions were used covering a range from 30-0.041 µg/ml. Each drug was tested in duplicate and each assay was repeated at least once. Miltefosine was used as the reference drug. After 72 hours of incubation the plates were inspected under an inverted microscope to assure growth of the controls and sterile conditions. 10 µl of Alamar blue (12.5 mg resazurin dissolved in 100 ml distilled water) was added to each well and the plates incubated for another 2 hours. The plates were read with a Spectramax Gemini XS microplate fluorometer (Molecular Devices Cooperation, Sunnyvale, CA, USA) using an excitation wavelength of 536 nm and an emission wave length of 588 nm. Data were

analysed using the microplate reader software Softmax Pro (Molecular Devices Cooperation, Sunnyvale, CA, USA). Decrease of fluorescence (inhibition) were expressed as percentage of the fluorescence of control cultures and plotted against the drug concentrations. From the sigmoidal inhibition curve the IC_{50} value were calculated. The results are summarized in tables 6 & 10.

6.3.4 Cytotoxicity assay

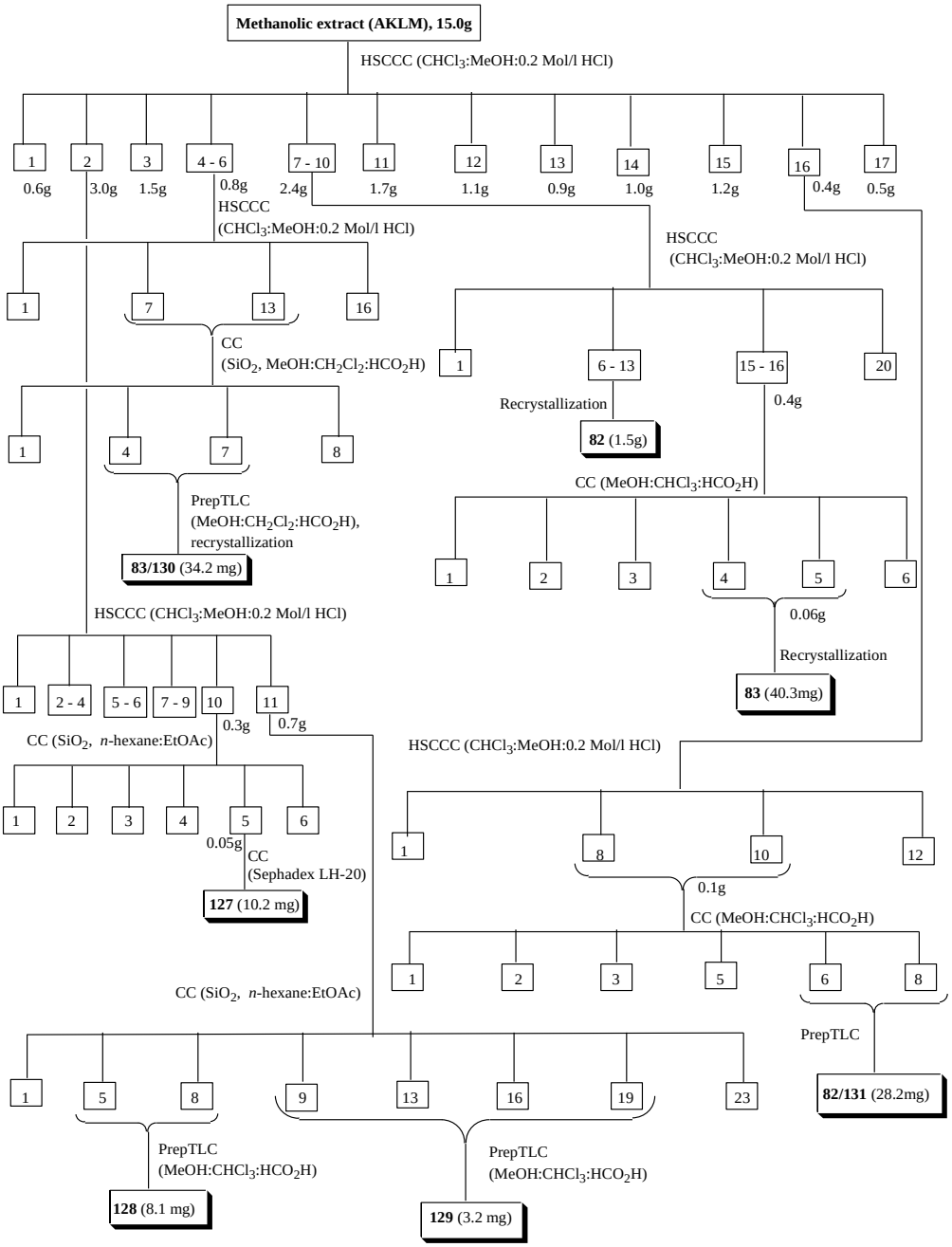
The *in vitro* cytotoxicity assay was carried out at the Swiss Tropical Institute, Basel, Switzerland according to a standard method (Räz *et al*., 1997). Rat skeletal myoblast cells (L-6 cells) were maintained as stock culture in RPMI 1640 medium + 10% FBS + 1% *L*-glutamine (200 mM). Pure compounds were dissolved in dimethylsulfoxide (DMSO) at 2 mg/100 µl and if necessary heated and/or sonicated. The stock solution was stored at -20 °C. Since DMSO is toxic, care were taken not to exceed a final concentration of 1% DMSO. For each assay podophyllotoxin was tested as a standard cytotoxin with the highest concentration at 30 µg/ml. Aliquots of 100 µl of a cell suspension of 4 x 10^4 cells/ml were added into columns 1 and 2, 4 and 5, 7 and 8, and 10 and 11 of each well of a Costar™ 96-well microtitre plates. Cells were allowed to attach overnight. After 24 hours of incubation, the medium was removed completely, and 100 µl of fresh medium added to all wells of the plate, except row H, using a multi-channel pipette. Medium (150 µl) containing the highest drug concentration was added to the wells of row H. Four drugs were tested on one plate (drug 1 columns 1-3, drug 2 columns 4-6, drug 3 columns 7-9 and drug 4 columns 10-12). Serial drug dilutions were prepared by using a 12-channel multi-pipette. First, 50 µl were taken from wells of row H and put into row G, mixed well, then 50 µl taken out of row G and put into row F and the process was repeated till row B. The last 50 µl of row B was discarded. A serial dilution factor of 1:3 was used in the range 270-0.37 µg/ml. Wells in row A served as controls without drugs. The plates were incubated for 72 hours at 37 °C, 5% CO_2 in air. To determine the IC_{50}, 10 µl of the fluorescent dye Alamar blue (Trek Diagnostic Systems, East Grinstead, UK) were added to each well and the plates incubated for another 2 hours. The plate was read using a fluorescence plate reader, at excitation and emission wavelengths of 536 and 588 nm, respectively. Data were analysed using the plate reader software (SoftMax). The results are summarized in tables 8 & 10.

6.4 Isolation of compounds

6.4.1 Extraction and bioassay-guided isolation of compounds from *Annickia kummeriae*

The air-dried and ground leaves of *Annickia kummeriae* (1.1 kg) was soaked in sequentially at room temperature in petroleum ether, dichloromethane and then methanol, each soaking lasted for 48 hours. The resulting methanolic leaves extract (82.5 g) was obtained by filtration and concentration *in vacuo* at 30 ˚C. The isolation process of compounds **82-83**, **127-129**, **130-131** from the leaves of *Annickia kummeriae* is summarized in scheme 1.

Scheme 1: Isolation of compounds **82-83**, **127-129**, **130-131** from the leaves of *Annickia kummeriae*



The high speed countercurrent chromatography (HSCCC) was used for fractionation. The two-phase solvent system: chloroform-methanol-0.2 M HCl (7:3:4, 1.4 l), was thoroughly equilibrated and separated shortly before use. The multi-layer coiled column of HSCCC was first entirely filled with the upper phase as a stationary phase. The lower organic mobile phase was then pumped into the head end of the column inlet at a flow-rate of 5.0 ml/min, while the apparatus was rotated forward at a revolution speed of 611 rpm. After the hydrodynamic equilibrium was reached (120 minutes), 20 ml of 3.0 g of sample solution was injected and fractionated at a time through the sample loop at a flow rate 5.0 ml min^{-1}. A total of 15.0 g crude methanolic extract was fractionated resulting to seventeen HSCCC fractions. Repeated high speed counter-current chromatographic fractionation of HSCCC fraction AKLM 2 (IC_{50} 0.87±0.1 µg/ml, SI 22.9) using stepwise elution with a biphasic solvent system ($CHCl_3$-MeOH-0.2 M HCl 7:3:4) gave 11 x 50 ml sub-fractions (AKLM 2.1-2.11). Biological screening indicated substantial anti-plasmodial activity in AKLM 2.10 (IC_{50} 0.89±0.20 µg/ml; SI 39.7) and AKLM 2.11 (IC_{50} 0.64±0.34 µg/ml; SI 69.8).

Repeated column chromatography of AKLM 2.10 (SiO_2; C_6H_{14}-EtOAc 1:1, and EtOAc-MeOH 80:20) gave 18 x 50 ml fractions which were combined into six (AKLM 2.10.1-2.10.6) based on the R_f of the eluted compounds in thin layer chromatography. AKLM 2.10.5 was re-chromatographed on Sephadex LH-20 (MeOH-$CHCl_3$ 1:1) and purified through re-crystallization (MeOH) to give lysicamine (**127**) (10.21 mg) as yellow needles: m.p. 209-211 ºC; EIMS: *m/z* 291 (100), 275 (14), 248 (82), 233 (7) and 177 (8). ^{1}H NMR, NOESY and COSY (CD_3OD) data are shown in table 13; ^{13}C NMR, HMQC and HMBC data are shown in table 14.

Repeated column chromatography (SiO_2; C_6H_{14}-EtOAc 40:60 and EtOAc-MeOH 75:25) of AKLM 2.11 gave 23 x 50 ml fractions. AKLM 2.11.5-2.11.8 were combined and purified PTLC (SiO_2; $CHCl_3$-MeOH-HCO_2H 98:1.8:0.2) to yield trivalvone (**128**) (8.10 mg) as brown crystals, m.p. 256-258 ºC; EIMS: *m/z*: 554 (90), 552 (100), 275 (56), 246 (21) and 232 (14); ^{1}H NMR and COSY (CD_3OD) data are shown in table 15, ^{13}C NMR, HMQC and HMBC data are shown in table 16.

AKLM 2.11.13-2.11.19 fractions were combined and purified by PTLC (SiO_2; $CHCl_3$-MeOH-HCO_2H 95:4.5:0.5) to yield **129 (**3.2 mg) as brown amorphous solid: m.p. 263-265 ºC; EIMS: *m/z* 663 (9), 419 (13), 307 (22), 154 (100) and 57 (88); ^{1}H NMR and COSY ($CDCl_3$) data are shown in table 17; ^{13}C NMR, HMQC and HMBC data are shown in table 18. Repeated high speed counter-current chromatographic fractionation ($CHCl_3$-MeOH-0.2

M HCl 7:3:4) of combined fractions AKLM 7-10 (IC_{50} 0.05±0.02-0.11±0.02 µg/ml; SI >818.2-1,800.0) of the methanolic extract of *A. kummeriae* leaves gave 20 x 50 ml sub-fractions (AKLM 7/10.1-AKLM 7/10.20). TLC analysis indicated similar pure compound in AKLM 7/10.6-AKLM 7/10.13 and AKLM 7/10.15-AKLM 7/10.16. Re-crystallization of AKLM 7/10.6-AKLM 7/10.13 (MeOH) yielded palmatine (**82**) (1.52 g) as yellow crystalline material: m.p. 203-205 ºC; IR, ν_{max} (KBr): 3356, 1603, 1515, 1460, 1366, 1274, 1241, 1142, 1109, 1065, and 1016 cm^{-1}; FABMS: *m/z* 352 (76), 351 (4), 337 (8), 336 (5), 334 (1), 321 (2), 320 (3), 319 (1), 318 (1), 308 (6), 307 (20) and 294 (2); ^{1}H NMR and COSY ($CDCl_3$) data are shown in table 19; ^{13}C NMR, HMQC and HMBC data are shown in table 20.

The purification of AKLM 7-10.15-16 on column chromatography (SiO_2 60; $CHCl_3$-MeOH-HCO_2H 9:0.75:0.25, 8:1.75:0.25, 6:3.75:0.5 and 5:4.5:0.5) gave 6 x 50 ml fractions (AKLM 7-10.15-16.1-6). The AKLM 7-10.15-16.4-5 contained an orange amorphous solid after evaporation and re-crystallization (MeOH) yielded jatrorrhizine (**83**) (40.82 mg) as orange crystals: m.p. 204-206 ºC, IR, ν_{max} (KBr): 3424, 2927, 2852, 2371, 2342, 1589, 1424, 1362, 1281, 1233, 1184, 1143, 1108, 1059 and 1022 cm^{-1}; FABMS: *m/z* 338 (100), 233 (5), 176 (58), 154 (100), 117 (36), 77 (3) and 41 (68). ^{1}H NMR, NOESY and COSY ($CDCl_3$) data are shown in table 21; ^{13}C NMR, HMQC and HMBC data are shown in table 22.

Repeated HSCCC ($CHCl_3$-MeOH-0.2 M HCl 7:3:4) of AKLM 4-6 (IC_{50} 1.34±0.33-0.45±0.15 µg/ml, SI >25-131.0) gave 16 x 50 ml fractions (AKLM 4-6.1-16). Isocratic column chromatography (SiO_2, MeOH-CH_2Cl_2-HCO_2H 4:15:1) of (AKLM 4-6.7-13) gave 8 x 50 ml (AKLM 4-6.7-13.1-8) and PTLC (MeOH-CH_2Cl_2-HCO_2H 5:14:1) of the combined CC fractions (AKLM 4-6.7-13.4-7) yielded an orange amorphous solid which was purified through re-crystallization (MeOH) to give an inseparable 1.2:1.0 mixture of jatrorrhizine (**83**) and columbamine (**130**) (34.2 mg) as an orange solid: m.p. 235-240 ºC, EIMS: *m/z* 338 (100), 233 (5), 176 (58), 154 (100), 117 (36), 77 (3) and 41 (68); ^{1}H NMR and COSY ($CDCl_3$) data are shown in table 23; ^{13}C NMR, HMQC and HMBC data are shown in table 24.

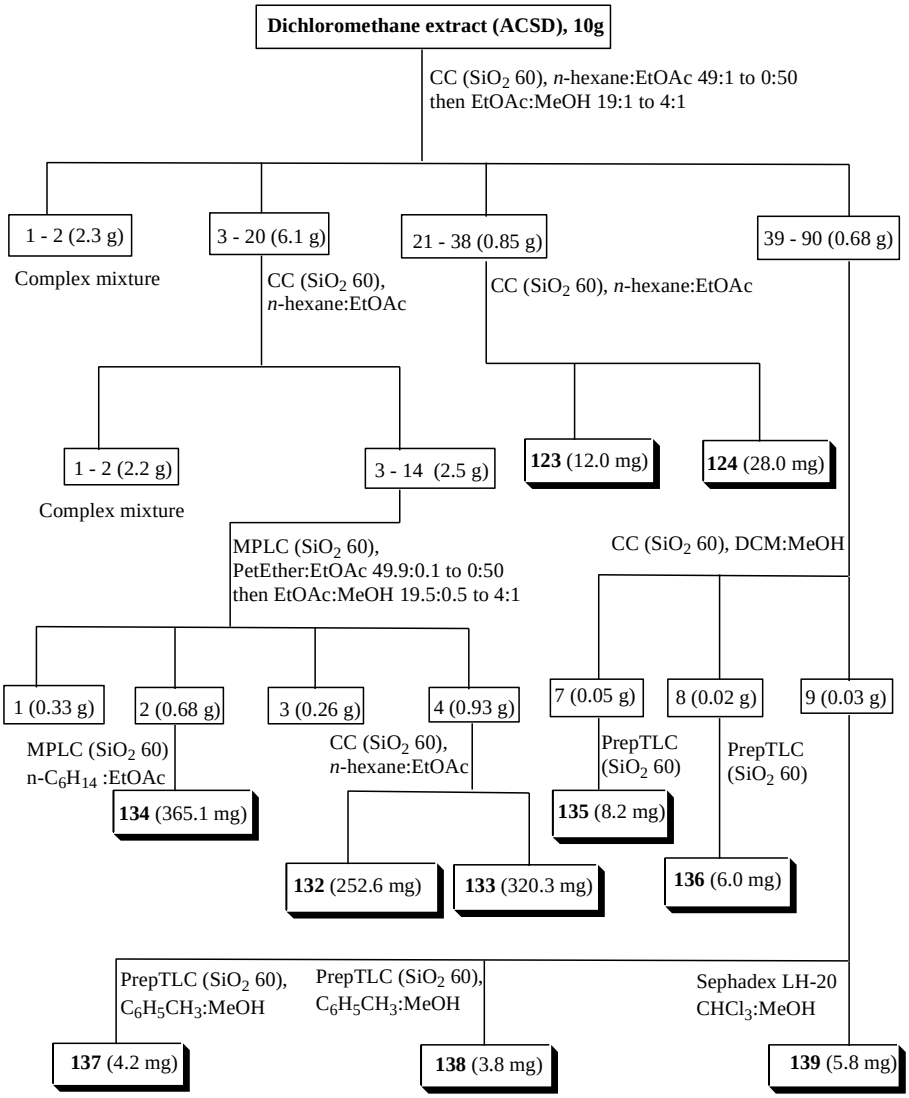
HSCCC ($CHCl_3$-MeOH-0.2 M HCl 7:3:4), of AKLM 16 (IC_{50} 0.09±0.03 µg/ml, SI 692) gave 12 x 50 ml fractions (AKLM 16.1-12). AKLM 16.8-10 were combined and subjected to column chromatography (SiO_2, MeOH-CH_2Cl_2-HCO_2H 5:14:1) resulting in 8 x 50 ml fractions (AKLM 16.8-10.1-8). PTLC (SiO_2, MeOH-CH_2Cl_2-HCO_2H 4:15:1) of the

combined CC fractions (AKLM 16.8-10.6-8) yielded an inseparable 1.1:1.0 mixture of palmatine (**82**) and (–)-tetrahydropalmatine (**131**) (28.2) mg as a yellow amorphous solid: m.p. 204-205 ºC, FABMS: *m/z* 354 (36), 353 (100), 338 (46), 323 (14), 294 (11) and 164 (10). ^{1}H NMR and COSY (CD_3OD) data are shown in table 25; ^{13}C NMR, HMQC and HMBC data are shown in table 26.

6.4.2 Extraction and isolation of compounds from *Acridocarpus chloropterus*

The air-dried and ground stem bark of *Acridocarpus chloropterus* (1.3 kg) was soaked in dichloromethane for 48 hours at room temperature. The resulting dichloromethane stem bark extract (49.3 g) was obtained by filtration and concentration *in vacuo* at 30 ˚C. An overview of the chromatographic separation of the dichloromethane extract of *Acridocarpus chloropterus* (ACSD) is given in scheme 2.

Scheme 2: Isolation of anti-protozoal compounds from *Acridocarpus chloropterus* stem bark



The crude dichloromethane extract (10.0 g) of *A. chloropterus* stem bark (ACSD) was fractionated by column chromatography (SiO2, *n*-C_6H_{14}-EtOAc, EtOAc–MeOH), gave 90 x 50 ml fractions. TLC analysis led to the combination of these fractions into four series as follows: fractions 1-2 (ACSD 1), 3-20 (ACSD 2), 21-38 (ACSD 3) and 39-90 (ACSD 4). ACSD 1 consisted of a complex mixture of non-polar compounds and was not analyzed further.

Repeated column chromatography (SiO_2, pet ether–EtOAc, EtOAc–MeOH) of the ACSD 2 (2.5 g) yielded 14 x 50 ml fractions (ACSD 2.1-ACSD 2.14). MPLC (SiO_2, pet ether-EtOAc, EtOAc–MeOH) of the combined fractions (ACSD 2.6-ACSD 2.10) yielded 34 x 50 ml fractions. TLC analysis led to the combination of these fractions into four groups: ACSD 2.6/2.10.1-ACSD 2.6/2.10.4. ACSD 2.6/2.10.1 consisted of a complex mixture of non-polar compounds and was not analyzed further. ACSD 2.6/2.10.2 was re-chromatographed by MPLC (SiO_2, *n*-C_6H_{14}–EtOAc 98:2) to yield a pure compound in fractions 18-26 (ACSD 2.6/2.10.2.18-ACSD 2.6/2.10.2.26) which were combined to afford a white amorphous residue on evaporation. Re-crystallization (CH_2Cl_2) yielded friedelin (**134**) (365.1 mg) as white needles: m.p. 257-259 ºC; IR, ν_{max} (KBr): 2925, 1712, 1458, 1385, 1305, 1186, 1072, 1049, 1002, 919, 790, 756 and 567 cm^{-1}; EIMS: *m/z* 426 (55), 411 (26), 341 (18), 302 (45), 273 (74), 246 (39), 218 (52), 205 (68), 163 (53), 125 (93), 95 (100), 69 (95) and 55 (49); ^1H NMR and COSY ($CDCl_3$) data are shown in table 33; ^{13}C NMR, HMQC and HMBC data are shown in table 34.

Repeated column chromatography (SiO_2, pet ether–EtOAc) of ACSD 2.6/2.10.4 resulted to 24 x 50 ml fractions (ACSD 2.6/2.10.4.1-ACSD 2.6/2.10.4.24). Sub-fractions ACSD 2.6/2.10.4.10-ACSD 2.6/2.10.4.24 formed crystals upon standing. TLC analysis led to the combinations of fractions ACSD 2.6/2.10.4.10-ACSD 2.6/2.10.4.18 and ACSD 2.6/2.10.4.19-ACSD 2.6/2.10.4.24. Re-crystallization (CH_2Cl_2) of ACSD 2.6/2.10.4.10-ACSD 2.6/2.10.4.18 yielded β-sitosterol (**132**) as white needles (252.6 mg): m.p. 138-140 ºC; EIMS: *m/z* 414 (100), 396 (48), 381 (34), 329 (39), 303 (49), 273 (25), 255 (28), 213 (36), 145 (38), 107 (47), 95 (44), 81 (39) and 43 (53); ^1H NMR and COSY ($CDCl_3$) data are shown in table 29; ^{13}C NMR, HMQC and HMBC data are shown in table 30.

Recrystallization of ACSD 2.6/2.10.4.19-ACSD 2.6/2.10.4.24 gave stigmasterol (**133**) as white needles (320.3 mg): m.p. 166-169 ºC; EIMS: *m/z* 412 (86), 351 (37), 255 (72), 213 (27), 159 (48), 83 (71) and 55 (100); ^{1}H NMR and COSY ($CDCl_3$) data are shown in table 31; ^{13}C NMR, HMQC and HMBC data are shown in table 32.

Repeated column chromatography (SiO_2, *n*-C_6H_{14}-EtOAc) of ACSD 3 (0.85 g) yielded 32 x 50 ml fractions (ACSD 3.1-ACSD 3.32). TLC analysis showed two distinct pure compounds in fractions ACSD 3.18-ACSD 3.19 and ACSD 3.22-ACSD 3.24 which were combined and evaporated to yield white amorphous residues, respectively. Re-crystallization ($CHCl_3$: *n*-C_6H_{14} 1:4) of ACSD 3.18-ACSD 3.19 yielded ursolic acid (**123**) as white powder (12.0 mg): m.p. 268-270 ºC; EIMS: *m/z* 456 (18), 423 (8), 395 (6), 300 (22) and 250 (20); ^{1}H NMR and COSY ($CDCl_3$) data are shown in table 37; ^{13}C NMR, HMQC and HMBC data are shown in table 38.

Re-crystallization ($CHCl_3$: *n*-C_6H_{14} 1:4) of ACSD 3.22-ACSD 3.24 gave oleanolic acid (**124**) as white powder (28.0 mg): m.p. 301-303 ºC; EIMS: *m/z* 456 (14), 438 (9), 423 (8), 395 (6) and 300 (13); ^{1}H NMR and COSY ($CDCl_3$) data are shown in table 35; ^{13}C NMR, HMQC and HMBC data are shown in table 36.

Repeated column chromatography (SiO_2, CH_2Cl_2-MeOH) of ACSD 4 (0.68 g) yielded 82 x 50 ml fractions which were pooled to nine fractions (ACSD 4.1-ACSD 4.9) based on TLC analysis. ACSD 4.1-ACSD 4.6 contained complex natural products mixtures. ACSD 4.7-ACSD 4.9 contained UV fluorescent (dark violet at 366 nm). PTLC of ACSD 4.7 (SiO_2, $C_6H_5CH_3$-MeOH 8:2) gave an amorphous solid which was re-crystallized ($CHCl_3$-MeOH 1:1) to yield apigenin (**135**) as yellow powder (8.2 mg): m.p. 350-352 ºC; EIMS: *m/z* 270 (100), 242 (19), 153 (18), 121 (13) and 44 (12); ^{1}H NMR and COSY ($CDCl_3$) data are shown in table 39; ^{13}C NMR, HMQC and HMBC data are shown in table 40.

PTLC (SiO_2, $C_6H_5CH_3$-MeOH 7.5:2.5) of ACSD 4.8 gave a yellow powder which was re-crystallized ($CHCl_3$-MeOH 1:1) to yield luteolin (**136**) as yellow crystals (6.0 mg): m.p. 323-325 ºC; EIMS: *m/z* 286 (100), 258 (22), 153 (27), 69 (9) and 57 (11); ^{1}H NMR and COSY ($CDCl_3$) data are shown in table 41; ^{13}C NMR, HMQC and HMBC data are shown in table 42.

PTLC (SiO_2, $C_6H_5CH_3$-MeOH 7.5:2.5) of ACSD 4.9 gave a yellow solid which was by re-crystallized ($CHCl_3$-MeOH 1:1) to yield vitexin (**137**) (4.2 mg): m.p. 269-270 ºC; EIMS: *m/z* 434 (8), 414 (11), 396 (14), 378 (27), 342 (42), 324 (88), 312 (100), 283 (100), 254 (53), 165 (100), 121 (38) and 43 (54); ^{1}H NMR and COSY ($CDCl_3$) data are shown in table 43; ^{13}C NMR, HMQC and HMBC data are shown in table 44.

PTLC (SiO_2, $C_6H_5CH_3$-MeOH 7.0: 3.0) of ACSD 4.9 gave a solid which was re-crystallized ($CHCl_3$-MeOH 1:1) to yield kaempferol (**138**) as pale yellow needles (3.8 mg): m.p. 276-278 ºC; EIMS: *m/z* 286 (100), 229 (8) and 121 (13); ^{1}H NMR and COSY ($CDCl_3$) data are shown in table 45; ^{13}C NMR, HMQC and HMBC data are shown in table 46.

Gel filtration of ACSD 4.9 (Sephadex LH-20, $CHCl_3$-MeOH 1:1) yielded dirty yellow powder which on re-crystallization ($CHCl_3$-MeOH 1:1) yielded quercetin (**139**) as dark yellow powder (5.8 mg): m.p. 313-315 ºC; EIMS: *m/z* 302 (100), 137 (8) and 69 (4); ^{1}H NMR and COSY ($CDCl_3$) data are shown in table 47; ^{13}C NMR, HMQC and HMBC data are shown in table 48.

CHAPTER SEVEN

CONCLUSION AND RECOMMENDATIONS

6.1 Conclusions

Pharmacochemical investigations reported in this thesis comprised of screening of crude extracts from four Tanzanian medicinal plant species, namely *Annickia kummeriae*, *Acridocarpus chloropterus*, *Drypetes natalensis* and *Pseudospondias microcarpa* for their anti-plasmodial, anti-trypanosomal, anti-leishmanial and cytotoxicity activity.

It was observed that, the extracts which had the strongest anti-plasmodial activities were those of *A. kummeriae* (Annonaceae): methanolic leaves extract (IC_{50} 0.12±0.01 µg/ml, SI 250.0), dichloromethane stem bark extract (IC_{50} 0.31±0.05 µg/ml and SI 187.7), methanolic stem bark extract (IC_{50} 0.31±0.04 µg/ml and SI 173.6), dichloromethane root bark extract (IC_{50} 0.36±0.06 µg/ml and SI 29.20) and the methanolic root bark extract (IC_{50} 0.35±0.04 µg/ml and SI 170.60). The *A. kummeriae* methanolic leaf extract (9.25±0.54 µg/ml and SI 3.2), pet ether stem bark extract (9.74±1.82 µg/ml and SI 2.3) and dichloromethane root bark extract (9.79±2.5 µg/ml and SI 1.1) were considered mildly active against axenic *Leishmania donovani* amastigotes but with very narrow selectivity. Bioassay-guided chromatographic fractionation of *A. kummeriae* (Annonaceae) methanolic leaf extract led to the isolation and identification of fractions with higher anti-plasmodial activity and more favorable selectivity indices than solvent extracts. Six antiprotozoal alkaloids: palmatine (**82**), jatrorrhizine (**83**), lysicamine (**127**), trivalvone (**128**), annickine (**129**), columbamine (**130**), and (–)-tetrahydropalmatine (**131**) were isolated from the above extracts. From the chemical structure-biological activity relationship comparisons, it was evident that, the methoxyl groups at C-2, C-3 (ring A) and C-9, C-10 (ring D) together with the quaternary nitrogen atom in position 7 are the structural moeties required for strong anti-plasmodial activity in protoberberine alkaloids. The results of the *in vitro* anti-plasmodial activity and cytotoxicity revealed that protoberberine and aporphine alkaloids from *A. kummeriae* exhibit good anti-plasmodial activity and favourable selectivity. These findings confirm direct correlation between the observed *in vitro* strong anti-plasmodial activity of compounds isolated from *A. kummeriae* and the positive effects when used *in vivo* for the treatment of malaria by the Sambaa and Bondei tribes of Tanzania. The strongest anti-

plasmodial activity observed *in vitro* renders this plant a candidate for further scientific attention for antimalarial drug discovery and development.

The methanolic extracts of *Drypetes natalensis* stem bark (IC_{50} 1.42±0.54 µg/ml and SI 63.3) and root bark (IC_{50} 1.06±0.20 µg/ml and SI 17.9) and the methanolic stem bark extract of *Pseudospondias microcarpa* (IC_{50} 1.13±0.16 µg/ml and SI 79.6) showed good *in vitro* anti-plasmodial activity against *P. falciparum* which rendered them good candidates for further scientific attention for the isolation of bioactive compounds. The dichloromethane extracts of *Acridocarpus chloropterus* stem bark (IC_{50} 5.50±1.27 µg/ml and SI 14.1) and root bark (IC_{50} 5.06±0.92 µg/ml and SI 12.8) had mild *in vitro* anti-plasmodial activity against *P. falciparum*.

Phytochemical investigation of *A. chloropterus* led to the isolation and identification of five triterpenes as β-sitosterol (**132**), stigmasterol (**133**), friedelin (**134**), oleanolic acid (**124**), ursolic acid (**123**) and five flavonoids: apigenin (**135**), luteolin (**136**), vitexin (**137**), kaempferol (**138**) and quercetin (**139**). Quercetin (**139**) showed moderate *in vitro* anti-plasmodial activity (IC_{50} 2.64 µg/ml) whereas the rest of compounds were inactive. Mild to weak *in vitro* antitrypanosomal activity was observed in quercetin (**139**) (IC_{50} 3.60 µg/ml), ursolic acid (**123**) (IC_{50} 7.80 µg/ml) and apigenin (**135**) (IC_{50} 9.0 µg/ml). Promising *in vitro* anti-leishmanial activity and favorable selectivity were found in ursolic acid (**123**), quercetin (**139**), kaempferol (**138**), apigenin (**135**) and oleanolic acid (**124**) (IC_{50} of 0.80, 2.10, 2.20, 5.90 and 3.5 µg/ml, respectively).

The strongest anti-leishmanial activity among the isolated triterpenes was exhibited by ursolic acid (**124**) confirming that, the hydroxyl at C-3 with methyls at C-23, C-25, C-26 and C-30, C-12/C-13 double bond, the carboxylic acid group at C-28 and H-20 are the structural moeties responsible for the strong anti-leishmanial activity observed. The strongest anti-protozoal activity among the isolated flavonoids was exhibited by quercetin (**139**) confirming that, the 3-OH and 3′-OH in the apigenin (**135**) molecular framework are the structural moeties responsible for the observed strong anti-protozoal activity. Strong to moderate anti-leishmanial activity of the triterpenes and flavonoids render them to be lead compounds for structure-activity-efficacy/toxicity relationship studies in the development of new antiprotozoal drugs.

6.2 Recommendations

From the *in vitro* anti-protozoal activity and cytotoxicity of *A. kummeriae, P. microcarpa* and *D. natalensis,* it is evident that these plants exhibit reasonable anti-protozoal activity and acceptable selectivity for drug activity. Therefore, it is important that the medicinal plants should also be investigated to evaluate the *in vivo* activity of these extracts in animals in the form they are prescribed by traditional healers, for their efficacy and safety.

The alkaloids with good anti-plasmodial and moderate anti-trypanosomal activity may provide lead compounds which could be chemically modified by structure-activity-efficacy/toxicity relationship studies for anti-protozoal drug development.

The high to moderate anti-leishmanial activity of the triterpenes and flavonoids from *A. chloropterus* render them to be lead compounds for structure-activity-efficacy/toxicity relationship studies for the development of new anti-protozoal drugs.

Conservation and propagation of medicinal genetic resources need to be initiated through the establishment of botanical gardens and community involvement in farming for commercialization of medicinal resources.

REFERENCES

Achenbach, H. & Schwinn, A. (1995). Aporphinoid alkaloids and terpenoids from *Piptostigma fugax. Phytochemistry* **38**, 1037-1048.

Agbaje, E.O. & Onabanjo, A.O. (1991). The effects of extracts of *Enantia chlorantha* in malaria. *Annals of Tropical Medicine and Parasitology* **85**, 585–590.

Agrawal, P.K. (1989). *Carbon-13 NMR of Flavonoids*. Elsevier, Amsterdam.

Aguiar, R.M., David J.P. & David J.M. (2005). Unusual naphthoquinones, catechin and triterpene from *Byrsonima microphylla*. *Phytochemistry* 2388-2392.

Alam, M.I. & Gomes, A. (1998). Adjuvant effects of anti-serum action potentiation by a (herbal) compound 2-hydroxy-4-methoxybenzoic acid isolated from root extract of the Indian medicinal plant ″Sarsaparilla″ (*Hemidesmus inducus*). *Toxicon* **36**, 1423-1431.

Allen, J.R.F. & Holmstedt, B.R. (1980). The simple ß-carboline alkaloids. *Phytochemistry* **19**, 1573-1582.

Alten, B., Caglar, S., Kaynas, S. & Simsek, F.M. (2003). Evaluation of protective efficacy of K-OTAB impregnated bednets for cutaneous leishmaniasis control in Southeast Anatolia, Turkey, *Journal of Vector Ecology* 28,153-164.

Alvar, J., Cañavate, C., Gutiérrez-Solar, B., Jiménez, M., Laguna, F., López-Vélez, R., Molina, R. & Moreno, J. (1997). *Leishmania* and human immunodeficiency virus coinfection: the first 10 years. *Clinical Microbiology Rev*iew **10**, 298-319.

Amusan, O.O.G., Adesogan, E.K. & Makinde, J.M. (1996). Antimalarial active principles of *Spathodea companulata* stem bark. *Phytotherapy Research* **10**, 692-693.

Andrade-Neto, V.F., Pohlit, A.M., Pinto, A.C.S., Silva, E.C.C., Nogueira, K.L., Melo, M.R.S., Henrique, M.C., Amorim, R.C.N., Silva, L.F.R., Costa, M.R.F., Nunomura, R.C.S., Nunomura, S.M., Alecrim, W.D., Alecrim, G.C., Chaves, F.C.M. & Vieira, P.P.R. (2007). *In vitro* inhibition of *Plasmodium falciparum* by substances isolated from Amazonian antimalarial plants. *Memórias do Instituto Oswaldo Cruz Rio de Janeiro*, **102,** 359-365.

Appendino, G. (1993). Taxol (paclitaxel): historical and ecological aspects. *Fitoterapia* **64**, 5-25.

Atindehou, K.K., Schmid, C, Brun, R., Koné, M.W. & Traore, D. (2004). Antitrypanosomal and antiplasmodial activity of medicinal plants from C̆ote d'Ivoire. *Journal of Ethnopharmacology* **90**, 221–227.

Bagli, E., Stefaniotou, M., Morbidelli, L., Ziche, M., Psillas, K., Murphy, C. & Fotsis, T. (2004). Luteolin inhibits vascular endothelial growth factor-induced angiogenesis; inhibition of endothelial cell survival and proliferation by targeting phosphatidylinositol 3′-kinase activity. *Cancer Research* **64**, 7936-7946.

Balunas, M.J. & Kinghorn, A.D. (2005). Drug discovery from medicinal plants. *Life Sciences* **78**, 431-441.

Batta, A.K., Guorong, X.U., Honda, A., Miyazaki, T. & Salen, G. (2006). Stigmasterol reduces plasma cholesterol levels and inhibits hepatic synthesis and intestinal absorption in the rat. *Clinical and Experimental Pharmacology and Physiology* **55**, 292-299.

Bennett, B.C. & Alarcon, R. (1994). *Osteophloeum platyspermum* and *Virola duckei* (Myristicaceae): Newly reported as hallucinogens from Amazonian Ecuador. *Economic Botany* **48**, 152-158.

Benyhe, S. (1994). Morphine: new aspects in the study of an ancient compound. *Life Sciences* **55**, 969-979.

Berger, I., Barrientos, A.C., Cáceres, A., Hernández, M., Rastrelli, L., Passreiter, C.M. & Kubelka, W. (1998). Plants used in Guatemala for the treatment of protozoal infections, II. Activity of extracts and fractions of five Guatemalan plants against *Trypanosoma cruzi*. *Journal of Ethnopharmacology* **62**, 107-115.

Berges R.R., Windeler J., Trampisch H.J. & Senge T.H (1995). Randomized, placebo-controlled, double-blind clinical trial of β-sitosterol in patients with benign prostatic hyperplasia. *Lancet* **345**, 1529-1532.

Breman, J.D. (1997). Human leishmaniasis: clinical, diagnostic, and chemotherapeutic developments in the last 10 years. *Clinical Infectious Diseases* **24**, 684-703.

Blanchfield, J.T., Sands, D.P.A., Kennard, C.H.L., Karl, A., Byriel, K.A. & Kitching W. (2003). Characterisation of alkaloids from some Australian *Stephania* (Menispermaceae) species. *Phytochemistry* **63**, 711-720.

Bodley, A.L. & Shapiro, T. (1995). Molecular and cytotoxic effects of camptothecin, a topoisomerase I inhibitor, on trypanosomes and Leishmania. *Proceedings of the National Academy of Sciences, U. S. A.* **92**, 3726-3730.

Bodley, A.L., Wani, M.C., Wall, M.E. & Shapiro, T. (1995). Antitrypanosomal activity of camptothecin analogs: structure-activity correlations. *Biochemical Pharmacology* **50**, 937-942.

Bodley, A.L., McGarry, M.W. & Shapiro, T.A. (1995). Drug Cytotoxicity assay for African *Trypanosomes* and *Leishmania*. *Journal of Infectious Diseases* **172**, 1157–1159.

Bravo, L. (1998). Polyphenols: chemistry, dietary sources, metabolism, and nutritional significance. *Nutrition Reviews* **56**, 317-333.

Bringmann G. (1996). *A*frican plants as sources of pharmacologically exciting biaryl and quarteraryl Alkaloids. *Proc. 1st Int. IOCD Symp.* Victoria falls, Zimbabwe, p1.

Bringmann, G., Saeb, W., Assi, L.A., Francois, G., Narayanan, A.S.S., Peters, K. & Peters, E-M. (1997). Betulinic acid: isolation from *Triphyophyllum peltatum* and *Ancistrocladus heyneanus*, antimalarial activity, and crystal structure of the benzyl ester. *Planta Medica* **63**, 255-257.

Brogger-Christensen, S. & Kharazmi, A. (2001). Antimalarial natural products. In *Compounds from Natural Sources: Isolation, Characterization, and Biological Properties*; Tringali, C., (ed.) Taylor & Francis, New York.

Bruneton, J. (1999). *Pharmacognosie: Phytochimie, Plantes Médicinales*. 3è Edition, Editions TEC & DOC, Paris Cedex 08, 409-973.

Bryceson, A.D.M. (1996) Leishmaniasis. In: *Manson's Tropical Diseases*, 20th Edition, G. Cook (eds), W. B. Suanders & Co., New Delhi, **65**, 1213−1245.

Cortes, D., Davoust, D., Hadi, A.H.A., Myint, SH., Hoquemiller, R. & Cave, A. (1990). Trivalvone, une nouvelle bis-aporphine des ecorces de *Trivalvaria macrophylla*. *Journal of Natural Products* **53**, 862.

Budzikiewicz, H., Wilson, J.M. & Djerassi, C. (1963). Mass spectrometry in structural and stereochemical problems. XXXII. Pentacyclic triterpenes. *Journal of American Chemical Society* **85**, 3688-3699.

Burns, D.C., Ellis, D.A. & March, R.E. (2007). A predictive tool for assessing ^{13}C NMR chemical shifts of flavonoids. *Magnetic Resonance in Chemistry* **45**, 835-845.

Butler, M.S. (2004). The role of natural product chemistry in drug discovery. *Journal of Natural Products* **67**, 2141-2153.

Buzas, A., Osowiecki, M. & Regnier, C. (1959). Sur la présence de quinidine (et l'hydroquinidine) dans l'écorce de l'*Enantia polycarpa*. *Comptes Rendus de l'Académie des sciences* **248**, 2791-2793.

Buzas, A., Egnell, C. & Orsay, F. (1965). Sur la présence de quinidine à cˆoté d'alcaloïdes berberiniques dans les écorces d'*Enantia pilosa* et *E. polycarpa*. *Annales Pharmaceutiques Françaises* **23**, 351-354.

Calzada, F., Meckes, M. and Cedillo-Rivera, R. (1999). Antiamoebic and antigiardial activity of plant flavonoids. *Planta Medica* **65**, 78-80.

Cao, S., Guza, R.C., Miller, J.S., Andriantsiferana, R., Rasamison, V.E. & Kingston, D.G.I. (2004). Cytotoxic triterpenoids from *Acridocapus vivy* from the Madagascar rain forest. *Journal of Natural Products* **67**, 986-989.

Chan-Bacab, M.J. & Peña-Rodríguez, L.M. (2001). Plant natural products with leishmanicidal activity. *Natural Product Reports* **18**, 674-688.

Chang, Y-C., Chang, F.R. & Wu, Y-C. (2000). The constituents of *Lindera glauca. Journal Chinese Chemical Society* **47**, 373-380.

Chatterjee, I., Chakravarty, A.K. & Gomes, A. (2006). *Daboia russellii* and *Naja Kaouthia* venom neutralization by lupeol acetate isolated from the root extract of Indian sarsaparilla, *Hemidesmus indicus*. *Journal of Ethnopharmacology* **106**, 38-43.

Cavin, J.C.; Krasmer, S.M. & Rodriguez, E. (**1987**). Plant-derived alkaloids active against *Trypanosoma cruzi*. *Journal of Ethnopharmacology* **19**: 89-94.

Chiang, L.C., Chiang, W., Liu, M.C. & Lin, C.C. (2003). *In vitro* anti-viral activities of *Caesalpinia pulcherrima* and its related flavonoids. *Journal of Antimicrobial Chemotherapy* **52**, 194-198.

Chung, D-W & Choi, Y.T. (2007). Synthesis and solubility of hydrophilic derivatives of β-sitosterol. *Journal of Industrial and Engineering Chemistry* **13**, 367-372.

Conrad, J., Vogler, B., Klaiber, I., Roos, G., Walter, U. & Kraus, W. (1998). Two triterpenes esters from *Terminalia macroptera* bark. *Phytochemistry* **48**, 647-650.

Collins, F.H. & Paskewitz, S.M. (1995). Malaria: Current and future prospects for control. *Annual Review of Entomology* **40**, 195-219.

Connolly, J.D. & Hill, R.A. (1991). Triterpenoids. In: *Methods in Plant Biochemistry vol 7*, Dey P.M., Harbone J.B., Charlwood. & Banthrope D.V.(eds). Academic press, New York, p331-359.

Cortes, D., Davoust, D., Hadi, A.H.A., Myint, S.H., Hoquemiller, R. & Cave, A. (1990). Trivalvone, une nouvelle bis-aporphine des ecorces de *Trivalvaria macrophylla*. *Journal of Natural Products* **53**, 862-866.

Cragg, G.M.; Newman, D.J. & Snader, K.M. (1997). Natural products in drug discovery and development. *Journal of Natural Products* **60**, 52-60.

Croft, S.L. & Coombs, G.H. (2003). *Leishmaniasis* - current chemotherapy and recent advances in the search for novel drugs. *Trends in Parasitology* **19**, 502-508.

Croft, S.L., Neal, R.A., Pendergast, W. & Chan, J.H. (1987). The activity of alkyl phosphorylcholines and related derivatives against *Leishmania donovani*. *Biochemical Pharmacology* **36**, 2633-2636.

Cunningham, I. (1977). New culture medium for maintenance of tsetse tissues and growth of trypa-nosomatids. *Journal of Protozoology* **24**, 325-329.

Curtis, C.F. (1990). Pyrethroid impregnation of bed nets and curtains against malaria mosquitoes. *Pesticide Outlook* **1**, 8-11.

Cutkomp, L.K. (1967). Progress in insect control by irradiation induced sterility. *Proceedings of the National Academy of Sciences, U.S.A.* **13**, 61-70.

Dalziel, J.M. (1937). *The Useful Plants of West Tropical Africa*. The Crown Agents for the Colonies, London.

De Almeida-Alves, T.M., Nagem, T.J., De Carvalho, L.H., Krettli, A.U. & Zani, C.L. (1997). Antiplasmodial triterpene from *Vernonia brasiliana*. *Planta Medica* **63**, 554-555.

De-Eknamkul, W. & Potduang, B. (2003). Biosynthesis of β-sitosterol and stigmasterol in *Croton sublyratus* proceeds via a mixed origin of isoprene units. *Phytochemistry* **62**, 389-398.

Delaporte, R.H., Sarragiotto, M.H., Takemura, O.S., Sanchez, G.M., Filho, B.P. & Nakamura, C.V. (2004). Evaluation of the antioedematogenic, free radical

scavenging and antimicrobial activities of aerial parts of *Tillandsia streptocarpa* Baker-Bromeliaceae. *Journal Ethnopharmacology* **95**, 229-233.

Desjeux, P. (1996). Leishmaniasis: public health aspects and control. *Clinical Dermatology* **14**, 417 -423.

Drahl, C., Cravatt, B.F. & Sorensen, E.J. (2005). Protein-reactive natural products. *Angewandte Chemie International Edition* **44**, 5788-5809.

Dumas, M. & Bisser, S. (1999) Clinical aspects of human African trypanosomiasis. In: *Progress in Human African Trypanosomiasis, Sleeping Sickness, Ch. 13*. Springer-Verlag, Paris, 215-233.

Ercil, D., Kaloga, M., Radtke, O., Sakar, M., Kiderlen, A., & Kolodziej, H. (2005). *O*-galloyl flavonoids from *Geranium pyrenaicum* and their in vitro antileishmanial activity. *Turkish Journal of Chemistry*, 29, 437–443.

Fabricant, D.S. & Farnsworth, N.R. (2001). The value of plants used in traditional medicine for drug discovery. *Environmental Health Perspectives* **109**, 69-75.

Fang, J., Zhou, Q., Shi, X. & Jiang, B. (2007). Luteolin inhibits insulin-like growth factor 1 receptor signaling in prostate cancer cells. *Carcinogenesis* **28**, 713-723.

Farnsworth, N.R., Akerele, O., Bingel, A.S., Soejarto, D.D. and Guo, Z. (1985). Medicinal plants in therapy. *Bulletin of the World Health Organization* **63**, 965-981.

Fathiazad, F., Delazar, A., Amiri, R. & Sarker, S.D. (2006). Extraction of flavonoids and quantification of rutin from waste tobacco leaves. *Iranian Journal of Pharmaceutical Research* **3**, 222-227.

Forgo P,. & Köver, K.E. (2004). Gradient enhanced selective experiments in the ^{1}H NMR chemical shift assignment of the skeleton and side-chain resonances of stigmasterol, a phytosterol derivative. *Steroids* **69**, 43-50.

Foye, W.O., Lemke, T.L. & Williams, D.A. (1995). *Principles of Medicinal Chemistry*, 4th Edn., 995. Williams & Wilkins, Baltimore, MD.

Freiburghaus, S.F., Jonker, S.A., Nkunya, M.H.H., Mwasumbi, L.B. & Brun, R. (1997a). *In Vitro* trypanocidal activity of some rare Tanzanian medicinal plants. *Acta Tropica* **66**, 79-81.

Freiburghaus, F., Jonker, SA., Nkunya, M.H.H., Mwasumbi, L.B. & Brun, R. (1997b). *In vitro* trypanocidal activity of some rare Tanzanian medicinal plants. *Acta Tropica* **67**, 181-185.

Frölich, S., Schubert, C., Bienzle, U. & Jenett-Siems, K. (2005). *In vitro* antiplasmodial actvity of prenylated chalcone derivatives of hops (*Humulus lupulus*) and their interaction with haemin. *Antimicrobial Agents Chemotherapy* **55**, 883-887.

Gaitan, E., Cooksey, R.C., Legan, J. & Lindsay, R. (1995). Antithyroid effects *in vivo* and *in vitro* of vitexin: AC-glucosylflavone in millet. *Journal of Clinical Endocrinology and Metabolism* **80**: 1144-1147.

Geiss, F., Heinrich, M., Hunkler, D. & Rimpler, H. (1995). Proanthocyanidins with (+)-epicatechin units from *Byrsonima crassifolia* bark. *Phytochemistry* **39**, 635-643.

Gessler, M. (1995). The Antimalarial Potential of Medicinal Plants Traditionally Used in Tanzania, and their Use in the Treatment of Malaria by Traditional Healers, Ph.D. Thesis, University of Basel.

Gessler, M.C., Msuya, D.E., Nkunya, M.H.H., Mwasumbi, L.B., Schar, A., Heinrich, M. & Tanner, M. (1995). Traditional healers in Tanzania: the treatment of malaria with plant remedies. *Journal of Ethnopharmacology* **48**, 131-144.

Ghazanfar, S.A. & Al-Sabahi, M.A. (1993). Medicinal plants of northern and central Oman (Arabia). *Economic Botany* **47**, 89-98.

Githeko, A.K., Lindsay, S.W. & Confalonieri, U.E. (2000). Climate change and vector-borne diseases: a regional analysis. *Bulletin of the World Health Organization* **78**, 1136-1147.

Goad, J.L. (1991). Phytosterols. In: *Methods in Plant Biochemistry vol 7*, Dey, P.M., Harbone, J.B., Charlwood. & Banthrope D.V. (Eds). Academic Press, New York, 369-434.

Grabley, S. & Thiericke, R. (1999). The impact of natural products on drug discovery. In *Drug Discovery from Nature*, Grabley, S.; Thiericke, R. (Eds.), Springer, Berlin/Heidelberg.

Graul, A.I. (2001). The year's new drugs. *Drug News Perspective* **14**, 12-31.

Grimberg, A. & Cohen, P. (2000). Role of insulin-like growth factors and their binding proteins in growth control and carcinogenesis. *Journal of Cellular Physiology* **183**, 1-9.

Grycová, L., Dostál, J. & Marek, R. (2007). Review: Quaternary protoberberine alkaloids. *Phytochemistry* **68**, 150-175.

Guinaudeau, H., Leboeuf, M. & Cave, A. (1983). Aporphinoid alkaloids, III. *Journal of Natural Products* **46**, 761-835.

Gupta, M.B., Nath, R., Srivastava, N., Shanker, K., Kishor, K., Bhargava, K.P., 1980. Anti-inflammatory and antipyretic activities of beta-sitosterol. *Planta Medica* **39**, 157-163.

Guo, Y., Kojima, K., Lin, L., Fu, X., Zhao, C., Hatano, K., Chen, Y-J. & Ogihara, Y. (1999). A new *N*-methyltetrahydroprotoberberine alkaloids from *Tinospora hainanensis. Chemical and Pharmaceutical Bulletin* **47**, 287-289.

Halbsguth, C., Meiβner, O. & Häberlein, H. (2003). Positive cooperation of protoberberine type 2 alkaloids from *Corydalis cava* on the $GABA_A$ binding site. *Planta Medica* **69**, 305-309.

Hallock, Y.F., Manfredi, K.P., Blunt, J.W., Cadellina, J.H.I, Schaffer, M., Gulden, K-P., Bringmann, G., Lee, A.Y., Clardy, J., Francois, G. & Boyd, M.R. (1994).

Korupensamines A-D, Novel Antimalarial Alkaloids from *Ancistrocladus korupensis*. *Journal of Organic Chemistry* **59**, 6349-6355.

Halliwell, B., Gutteridge, J.M.C. (1993). *Free Radicals in Biology and Medicine*. Clarendon Press, Oxford, UK.

Hammond, P.M. (1995). The record to date: described species. In: *Global Biodiversity Assessment*. Heywood, V.H., Watson, R.T. (Eds.), Cambridge University Press, Cambridge, p. 113-138.

Herwaldt, B.L. (1999). *Leishmaniasis*. *Lancet* **354**, 1191-1199.

Hertog, M.G., Feskens, E.J., Hollman, P.C., Katan, M.B. & Kromhout, D. (1993). Dietary antioxidant flavonoids and risk of coronary heart disease: the Zutphen Elderly Study. *Lancet* **342**, 1007-1011.

Hertog, M.G., Kromhout, D., Aravanis, C., Blackburn, H., Buzina, R., Fidanza, F., Giampaoli, S., Jansen, A., Menotti, A., Nedeljkovic, S., Pekkarinen, M., Simic, B.S., Toshima, H., Feskens, E.J.M., Hollman, P.C.H. & Katan, M.B. (1995). Flavonoid intake and long-term risk of coronary heart disease and cancer in the seven countries study. *Archives of Internal Medicine* **155**, 381-386.

Ho, J., Badaro, R., Hatzigeorgiu, D., Reed, S. & Johnson, Jr. W., (1994). Cytokines in the treatment of leishmaniasis: from studies of immunopathology to patient therapy. *Biotherapy* **7**, 223-235.

Hoet, S., Opperdoes, F., Brun, R. & Quetin-Leclercq, J. (2004). Natural products active against African trypanosomes: a step towards new drugs. *Natural Product Reports* **21**, 353-364.

Howard, R. J. (1987). Vaccination against malaria: recent advances and the problems of antigenic diversity and other parasite evasion mechanisms. *International Journal of Parasitology* **17**, 17-29.

Hsieh, T.J., Chia, Y.Ch., Wu, Y.C. & Chen, C.Y. (2004). Chemical constituents from the stems of *Mahonia japonica. Journal of Chinese Chemical Society* **51**, 443-446.

Huang, P.L., Huang, P.L., Huang, P., Huang, I.H. and Huang, L.S. (1992). *Chemistry and Industry*, **8**, 290-292.

Hussain, R.A., Kim, J., Beecher, C.W.W. & Kinghorn, D. (1989). Unambiguous carbon-13 NMR assignments of some biologically active protoberberine alkaloids. *Heterocycles* 29, 2257-2260.

Ikuta, A. and Itokawa, H. (1988). Triterpenoids of *Paeonia japonica* callus tissue. *Phytochemistry* 27, 2813-2815.

Itoigawa, M., Takeya, K., Ito, C. and Furu-Kawa, H. (1999). Structure activity relationship of cardiotonic flavonoids in guinea pig papillary muscle. *Journal of Ethnopharmacology* **65**, 267-72.

Izzo, A.A., Carlo, G.D, Mascolo, N., Capasso, F. & Autore, G. (1994). Effects of quercetin on gastrointestinal tract: further studies. *Phytotherapy Research* **8**:179-85.

Jones, D.J.L., Lamb, J.H., Verschoyle, R.D., Howells, L.M., Butterworth, M., Lim, C.K., Ferry, D., Farmer, P.B. & Gescher, A.J. (2004). Characterisation of metabolites of the putative cancer chemopreventive agent quercetin and their effect on cyclo-oxygenase activity, *British Journal of Cancer* **91**, 1213-1219.

Jössang, A., Leboeuf, M. & Cave, A. (1977a). Alcalöides des Annonacées. XVII. Alcalöides de l'*Enantia polycarpa* Engl. et Diels. *Planta Medica* **32**, 249–257.

Jössang, A., Leboeuf, M. & Cave, A., (1977b). La polycarpine, nouvelle Alcalöide isoquinolique de l'*Enantia polycarpa* Engler et Diels. *Comptes rendus de l'Académie des Sciences* **284**, 567–569.

Kain, K.C. (1995). Chemotherapy and prevention of drug-resistant malaria. *Wilderness Environmental Medicine* **6**, 307-324.

Katinka, P. (1999). *Ecology and Control of Anopheles Mosquitoes and Human Malaria in Guinea Bissau, West Africa.* Ph.D Thesis, Uppsala University.

Katsui, N. & Sato, K. (1966). Alkaloids of *Lysichton camtschatcense* Schott var. Japonicum Makino. *Tetrahedron Letters* **50**, 6257-6261.

Kayser, O., Kiderlen, A.F. & Croft, S.L. (2003). Natural products as antiparasitic drugs. *Parasitology Research* **90**, S55-S62.

Kim, J.P., Jung, M.Y., Kim, J.P. & Kim, S.Y. (2000). Antiphotooxidative activity of protoberberines derived from *Coptis japonica* makino in the chlorophyll-sensitized photooxidation of oil. *Journal of Agriculture and Food Chemistry* **48**, 1058-1063.

Kimbi, H.K., Fagbenro-Beyioku, A.F. & Oyibo, W.A. (1988). *Indian Journal of Malariol*ogy **35**, 35–38.

Kinghorn, A.D. (1994). The discovery of drugs from higher plants. In: *The Discovery of Natural Products with Therapeutic Potential*. Gullo V.P., (ed.). Butterworth-Heinemann; Boston, MA: p81-108.

Kirira, P.G., Rukunga, G.M., Wanyonyi, A.W., Muregi, F.M., Gathirwa, J.W., Muthaura, C.N., Omar, S.A., Tolo, F., Mungai, G.M & Ndiege, I.O. (2006). Antiplasmodial activity and toxicity of extracts of plants used in traditional malaria therapy in Meru and Kilifi districts of Kenya. *Journal of Ethnopharmacology* **106**, 403-407.

Kitua, A.Y. & Malebo, H.M. (2004). Malaria Control in Africa and the Role of Traditional Medicine. In: Traditional Herbal Medicines for Modern Times: Traditional Medicinal Plants and Malaria. Willcox M., Bodeker G. & Rasoanaivo P. (Eds.), CRC Press LLC, Washington, D.C. p3-18.

Klass, J., Tinto, W.F., McLean, S. & Reynolds, W.F. (1992). Friedelane triterpenoids from *Peritassa compta*: complete ^{1}H and ^{13}C assignments by 2D NMR spectroscopy. *Journal of Natural Products* **55**, 1626-1630.

Klayman, D.L. (1985). Qinghaosu (Artemisinin): an antimalarial drug from China. *Science* **228**, 1049-1055.

Klipppel, KF., Hiltl, DM. & Schipp, B. (1997). A multicentric, placebo-controlled, double-blind clinical trial of β-sitosterol (phytosterol) for the treatment of benign prostatic hyperplasia. *British Journal of Urology* **80**, 427-432.

Koehn, F.E. & Carter, G.T. (2005). The evolving role of natural products in drug discovery. *Nature Reviews: Drug Discov*ery **4**, 206-220.

Kuhlencord, A., Maniera, T., Eibl, H. & Unger, C. (1992). Hexadecylphosphocholine: oral treatment of visceral leishmaniasis in mice. *Antimicrobial Agents Chemotherapy* **36**, 1630-1634.

Kuria, K.A.M., Chepkwony, H., Govaerts, C., Roets, E., Busson, R., De Witte, P., Zupko, I., Hoornaert, G., Quirynen, L., Maes, L., Janssens, L., Hoogmartens, J. & Laekeman, G. (2002). The antimalarial activity of isolates from *Ajuga remota*. *Journal of Natural Products* **65**, 789-793.

Kuzoe, F.A.S. (1993). Current situation of African Trypanosomiasis. *Acta Tropica* **54**, 153-162.

Kuzoe, F.A.S. & Schofield, C.J. (2004) *Strategic review of traps and targets for tsetse and African trypanosomiasis control, UNICEF / UNDP / WorldBank / WHO Special Programme for Research and Training in Tropical Disease Research, TDR / IDE / TRY / 05.1*, Geneva: World Health Organization.

Launert, E. (1963). *Flora of Tropical East Africa*: *Acridocarpus chloropterus* Oliv. Royal Botanic Gardens, Kew, London, England, UK, **2** (1), 109.

Leboeuf, M. & Cave, A. (1972). Alcalöides des Annonacées. *Plantes Médicinales et Phytothérapie* **6**, 87-90.

Leboeuf, M., Cave, A., Bhaumik, P.K., Mukherjee, B. & Mukherjee, R. (1982). The phytochemistry of the Annonaceae. *Phytochemistry* **21**, 2783-2813.

Li, C-Y., Lu, H-J., Lin, C-H., & Wu, T-S. (2006). A rapid and simple determination of protoberberine alkaloids in cortex phellodendri by ^{1}H NMR and its application for quality control of commercial traditional Chinese medicine prescriptions. *Journal of Pharmiaceutical and Biomedical Analysis* **40**, 173-178.

Lichtner, M., Mengoni, F., Battinelli, L., Mazzanti, G., Braca, A., Mastroianni, C.M. & Vullo, V. (1999). Anti-HIV activity of oleanolic acid on infected human mononuclear cells. *Antimicrobial Agents Chemotherapy* 39, 318.

Lin, J.H., Lin, Y.T., Huang, Y.J., Wen, K.C., Chen, R.M., Ueng, T.H. & Liao, C.H. (2001). Isolation and cytotoxicity of flavonoids from *Daphnis genkwae* Flos, *Journal of Food and Drug Analysis* **9**, 6-11.

Liu, J. (1995). Pharmacology of oleanolic acid and ursolic acid. *Journal of Ethnopharmacology* **49**, 57-68.

Lu, B.L. (1996). Recent advances in mosquito control. *Acta Entomologica* **29**, 110-111.

Lutomski, V.J., Malek, B. & Raybacka, L. (1975). Pharmacochemical Investigation of the Raw Materials from *Passiflora* Genus. *Planta Medica* **27**, 112-121.

Lux, H., Heise, N., Klenner, T., Hart, D. & Opperdoes, F.D. (2000). Ether-lipid (alkylphospholipid) metabolism and the mechanism of action of ether-lipid analogues in *Leishmania*. *Molecular and Biochemical Parasitology* **111**, 1-14.

MacKinnon, S., Durst, T., Arnason, J.T., Angerhofer, C.J., Pezzuto, J.M., Sanchez-Vindas, P.E., Poveda, L.J. & Gbeassor, M. (1997). Antimalarial activity of tropical meliaceae extracts and gedunin derivatives. *Journal of Natural Products* **60**, 336-341.

Mahato, S.B. & Kundu, A.P., 1994. ^{13}C NMR Spectra of pentacyclic triterpenoids−a complication and some salient features. *Phytochemistry*, **37**, 1517-1573.

Mahiou, V., Roblot, F., Hocquiemiller, R., Cave, A., Dearias, A. R., Inchaust, A., Yalluf, G., Fournet, A. & Angelo, A. (1994). New aporphine alkaloids from *Guatteria foliosa. Journal of Natural Products* **57**, 890-895.

Malebo, H.M. (2000). Antimalarial Flavonoids, Antifungal Pyrones and Hexalobines from Three Annonaceae Species. M.Sc. Thesis, University of Dar-Es-Salaam, Tanzania.

Marbiah, N.T., Petersen, E., David, K., Magbity, E., Lines, J. & Bradley, D.J. (1998). A controlled trial of lambda-cyhalothrin-impregnated bed nets and/or dapsone/pyrimethamine for malaria control in Sierra Leone. *American Journal of Tropical Medicine and Hygiene* **58**, 1-6.

Marbry, T.J., Markham, K.R. & Thomas, M.B. (1970). *The Systematic Identification of Flavonoids*, Springer-Verlag, Berlin.

Markham, K.R. (1982). *Techniques of Flavonoid Identification*, Academic Press, London.

Marsden, P.D. (1996). American Trypanosomiasis. In: *Manson's Tropical Diseases, 20th Edition*, Vol 64, G. Cook (ed), W. B. Suanders & Co. New Delhi **64**, 1197-1212.

Martens, W.J., Slooff, R. & Jackson, E.K. (1997). Climate change, human health and sustainable development. *Bulletin of the World Health Organization* **75**, 583-588.

Matile, H. & Pink, J.R.L. (1990). *Plasmodium falciparum* malaria parasite cultures and their use in immunology. In: Immunological Methods. Lefkovits I. & Pernis B. (eds.). Academic Press, San Diego, 221-229.

Maudlin, I., Holmes, P.H. & Miles, M.A. (2004). *The Trypanosomiases*. CABI Publishing Wallingford, U.K.

Mazloumi, A.S., Hodjati, M.H., Mohite, H. & Davies, C.R. (2002). Effect of insecticide-impregnated dog collars on incidence of zoonotic visceral leishmaniasis in Iranian children: a matched-cluster randomized trial. *Lancet* **360**, 374-79.

Meselhy, R.M. (2003). Constituents from Moghat, the roots of *Glossostemon bruguieri* (Desf.). *Molecules* **8**, 614-621.

Miller, J.S. & Gereau, R.E. (2000). In: *Biologically Active Natural Products: Pharmaceuticals*, Cutler, S.J.; Cutler, H.G. (eds). CRC Press: New York, p25-37.

Milne-Redhead, E. & Polhill, R.M. (1968). *Malpighiaceae: Flora of Tropical Africa*, Whitefriars Press, London.

Molyneux, D.H. & Ashford, R.W. (1983). *The Biology of Trypanosoma and Leishmania, Parasite of Man and Domestic Animals.* Taylor & Francis, London.

Molyneux, D.H., Pentreath, V. & Doua, F. (1996). African trypanosomiasis in man. In: *Manson's Tropical Diseases, 20th Edn*, vol. 63, G. Cook (eds), New Delhi, 1171.

Moody, J.O., Hylands, P.J. & Bray, D.H. (1995). *In vitro* evaluation of *Enantia chlorantha* constituents and derivatives for antiplasmodial and anticandidal activity. *Pharmaceutical and Pharmacology Letters* **2**, 80.

Morales, G., Sierra, P., Mancilla, A., Paredes, A.N., Loyola, LA., Gallado, O. & Borquez, J., (2003). Secondary metabolites from four medicinal plants from northern Chile: antimicrobial activity and biotoxicity against Artemia salina. *Journal of Chilean Chemical Society* **48**, 1-11.

Mors, W.B., Nascimento, M.C.D., Pereira, B.M.R. & Pereira, N.A. (2000). Plant natural products active against snake bite- the molecular approach. *Phytochemistry* **55**, 627-642.

Mors, W.B., Nascimento, M.C.D., Parente, J.P., Da Silva, M.H., Melo, P.A., Suarezkurtz, G., 1989. Neutralization of lethal and myotoxic activities of south American Rattle snake venom by extracts of *Eclipta prostrate* (Asteraceae). *Toxicon* **27**, 1003-1009.

Mshinda, H., Killeen, G.F., Mukabana, W.R., Mathenge, E.M., Mboera, L.E.G. & Knols, B.G.J. (2004). Development of genetically modified mosquitoes in Africa. *Lancet Infectious Diseases* **4**, 264-265.

Muhie, S. (1996). Chemical Investigations for Anti-malarial and Anti-trypanosomal and other Chemical Constituents of *Uvaria lucida Lucida* and *Enantia kummeriae*. M.Sc. Thesis, University of Dar-es-Salaam, Tanzania.

Muregi, F.W., Chhabra, S.C., Njagi, E.N.M., Lang'at-Thoruwa, C.C., Njue, W.M., Orago, A.S.S., Omar, S.A. & Ndiege, I.O. (2003). *In vitro* antiplasmodial activity of some plants used in Kisii, Kenya against malaria and their chloroquine potentiation effects. *Journal of Ethnopharmacology* **84**, 235-239.

Muregi, FW., Chhabra, S.C., Njagi, E.N.M., Lang'at-Thoruwa, C.C., Njue, W.M., Orago, A.S.S., Omar, S.A., Ndiege, I.O. (2004). Antiplasmodial activity of some Kenyan medicinal plant extracts singly and in combination with chloroquine. *Phytotherapy Research* **18**, 379-384.

Narayana, K.R., Reddy, M.S.,. Chaluvadi, M.R. & Krishna, D.R. (2001). Bioflavonoids classification, pharmacological, biochemical effects and therapeutic potential, *Indian Journal of Pharmacology* **33**, 2-16.

Neri-Barbosa, J.F., Quiroz-Martinez, H., Rodriguez-Tovar, M.L., Tejada, L.O. & Badii, M.H. (1997). Use of bactimos briquets (B.t.i. formulation) combined with the backswimmer, *Notonecta irrorata* (Hemiptera: Notonectidae), for control of mosquito larvae. *Journal of American Mosquito Control Association* **10**, 487-491.

Newman, D.J., Cragg, G.M. & Snader, K.M. (2000). The influence of natural products upon drug discovery. *Natural Product Reports* **17**, 215-234.

Newman, D.J., Cragg, G.M. & Snader, KM. (2003). Natural products as sources of new drugs over the period 1981-2002. *Journal of Natural Product* **66**, 1022-1037.

Nkunya, M.H.H. (1992). Progress in the search for antimalarials. *NAPRECA Monograph Series No. 4*, Addis Ababa, p1.

Nkunya, M.H.H. (2005). Unusual metabolites from some Tanzanian indigenous plant species. *Pure and Applied Chemistry* **77**, 1943-1955.

Obua, C., Odyek, O., Anokbonggo, W.W., Apio, S.K., Waako, P. & Ogwal-Okeng, J.W. **(**2002). Antimalarial activity of some plants used in traditional medicine in Uganda. *Eastern and Central Africa Journal of Pharmaceutical Sciences* **5**, 33-37.

Olliaro, P. & Cattani, J. (1996). Malaria, the submerged disease. *Journal of American Medical Association* **275**, 230.

Orgogozo, J.M., Dartigues, J.F., Lafont, S., Letenneur, L., Commenges, D., Salamon, R., Renaud S. & Breteler M.B. (1997). Wine consumption and dementia in the elderly: a prospective community study in the Bordeaux area. *Revista de Neurología* **153**, 185-192.

Paliwal, S. (2005). Induction of cancer-specific cytotoxicity towards human prostate and skin cells using quercetin and ultrasound (abstract). *British Journal of Cancer* **92**, 499-502.

Panichpol, K. & Waterman, P.G. (1978). Novel flavonoids from the stem of *Popowia cauliflora*. *Phytochemistry* **17**, 1363.

Parmar, N.S. & Parmar, S. (1998). Anti-ulcer potential of flavonoids. *Indian Journal of Physiology and Pharmacology* **42**, 343-51.

Pavanand, K., Yongvanitchit, K., Webster. H.K., Dechatiwongse, T., Nutakul, W., Jewvachdamrongkul, Y. & Basindhi, J. (1988). *In vitro* antimalarial activity of a Thai medicinal Plant *Picrasma javanica. Phytotherapy Research* **2**, 33.

Penso, G. (1976). Inventory of Medicinal Plants and Compilation of a List of the Most Widely Used Plants. WHO Document DPM/WP/78.2. Geneva,

Phillipson, J.D. & Wright C.W. (1991). Antiprotozoal agents from plant sources. *Planta Medica* **57,** 53–59.

Rasoanaivo, P., Ratsimamanga-Urverg S., Rakoto-Ratsimamanga, A., Raharisololalao, A. (1991). Constituants chimiques de trois especes de Burasaia (Menispermacees) endemiques de Madagascar. *Biochemical and Systematic Ecology* **19**, 433-437.

Räz, B., Iten, M., Grether-Bühler, Y., Kaminsky, R. & Brun, R. (1997). The Alamar blue assay to determine drug sensitivity of African trypanosomes (*T.b.rhodesiense* and *T.b.gambiense*). *Acta Tropica* **68**, 139-147.

Renaud, S.C., Gueguen, R., Schenker, J. & D'houtaud, A. (1998). Alcohol and mortality in middle-aged men from eastern France. *Epidemiology* **9**, 184-188.

Renaud, S.C., Gueguen, R., Siest, G. & Salamon, R. (1999). Wine, beer, and mortality in middle-aged men from eastern France. *Archives of Internal Medicine* **159**, 1865-1870.

Sahpaz, S., Bories, C.H., Loiseau, P.M., Cortes, D., Hocquiemiller, R., Laurens, A. & Cave, A. (1994). Cytotoxic and antiparasitic activity from *Annona senegalensis* seeds. *Planta Medica* **60**, 538.

Salem, M.M. & Werbovetz, K.A. (2005). Antiprotozoal compounds from *Psorothamnus polydenius*. *Journal of Natural Products* **68**, 108-111.

Sannomiya, M., Fonseca, V., Da Silva, M.A., Rocha, L.R.M., Dos Santos, L.C., Hiruma-Lima, C.A., Souza-Brito, A.R.M. & Vilegas, W. (2005). Flavonoids and antiulcerogenic activity from *Byrsonima crassa* leaves extracts. *Journal of Ethnopharmacology* **95**, 1-6.

Scandinavian Simvastatin Survival Study (SSSS) Group (1994). Randomised trial of cholesterol lowering in 4,444 patients with coronary heart disease. *Lancet* **344**, 1383-1389.

Sanchez, De RVR., Somoza, B., Ortega, T. & Villar, A. (1996). Flavonoids action on heart. *Planta Medica* **62**, 554-62.

Senn, M.W. (2006). Structures and Evaluation of Biologically Active Constituents of C*ussonia zimmermannii* Harms. Ph.D. Thesis, University of Basel.

Schippmann, U., Leaman, D.J. & Cunningham, A.B. (2002). Impact of cultivation and gathering of medicinal plants on biodiversity: global trends and issues. In: FAO, *Biodiversity and the Ecosystem Approach in Agriculture, Forestry and Fsheries*. Inter-departmental Working Group on Biological Diversity for Food and Agriculture. Satellite Event on the Occasion of the Ninth Regular Session of the Commission on Genetic Resources for Food and Agriculture. 12-13 October, Rome.

Schwikkard, S. & Van Heerden, F.R. (2002). Antimalarial activity of plant metabolites. *Natural Products Report* **19**, 675-692.

Sharma, V., Joseph, C., Ghosh, S., Agarwal, A., Mishra M.K, & Sen, E. (2007). Kaempferol induces apoptosis in glioblastoma cells through oxidative stress *Molecular Cancer Ther*apy **6**, 2544-2553.

Shen, S.C., Lin, C.W., Lee, H.M., Chien, L.L. & Chen, Y.C. (2006). Lipopolysaccharide plus 12-O-tetradecanoylphorbol 13-acetate induction of migration and invasion of glioma cells in vitro and in vivo: differential inhibitory effects of flavonoids. *Neuroscience* **140**, 477-489.

Shen, C, C., Chang, Y.S. & Ho, L.K. (1993). Nuclear magnetic resonance studies of 5,7-dihydroxyflavonoids. *Phytochemistry* **34**, 843-845.

Sneader, W. (1985). *Drug Discovery: The Evolution of Modern Medicines*, Wiley, Chichester.

Sundar, S., Jha, T.K., Thakur, C.P., Engel, J., Sindermann, H., Fischer, C., Junge, K., Bryceson, A. & Berman, J. (2002). Oral miltefosine for Indian visceral leishmaniasis. *New England Journal of Medicinal* **347**, 1739-1746.

Sung'hwa, F. (1996). Kawain Derivatives and Other Natural Products from *Ophrypetalum odoratum* and *Lettowianthus stellatus*. M.Sc. Thesis, University of Dar es Salaam, Tanzania.

Takahashi, H., Iuchi, M., Fujita, Y., Minami, H. & Fukuyama Y. (1999). Coumaroyl triterpenes from *Casuarina equisetifolia*. *Phytochemistry* **51**, 543-550.

Tasdemir, D., Lack, G., Brun, R., Rüedi, P., Scapozza, L. & Perozzo, R. (2006). Inhibition of *Plasmodium falciparum* fatty acid biosynthesis: evaluation of FabG, FabZ, and FabI as drug targets for flavonoids. *Journal of Medicinal Chemistry* **49**, 3345-3353.

Thanakijcharoenpath, W. & Theanphong, O. (2005). Triterpenoids from the stem of *Diospyros glandulosa. Thai Journal of Pharmaceutical Sciences* **31**, 1-8.

Trigg, J.K. (1996). Evaluation of eucalyptus-based repellent against *Anopheles* spp. in Tanzania. *Journal of American Mosquito Control Association* **12**, 243 – 244.

Tsai, T.H., Wang, G.J. & Lin, L.C. (2008). Vasorelaxing alkaloids and flavonoids from *Cassytha filiformis*. *Journal of Natural Products* **71**, 289–291.

Van Agtmael, M.A., Eggelte, T.A. & Van Boxtel, C.J. (1999). Artemisinin drugs in the treatment of malaria: from medicinal herb to registered medication. *Trends Pharmacological Sciences* **20**, 199-205.

Vázquez, E., Martínez, E.M., Cogordán, J.A. & Delgado, G. (2001). Triterpene, phenols, and other constituents from the leaves of *Ochroma pyramidale* (Balsa wood, Bombacaceae). Preferred conformations of 8-C-b-D-glucopyranosyl-apigenin (vitexin). *Journal of Mexican Chemical Society* **45**, 254-258.

Vega, M.R.G., Esteves-Souza, A., Vieira, I.J.C., Mathias Braz-Filhob, R. & Echevarria, A. (2007). Flavonoids from *Annona dioica* leaves and their effects in ehrlich carcinoma cells, DNA-topoisomerase I and II. *Journal of Brazilian Chemical Society* **18**, 1554-1559.

Verdcourt, B. (1971). *Enantia kummeriae* Engl. & Diels, family Annonaceae. In: Flora of Tropical East Africa. p1.

Vennerstrom, J.L. & Klayman, D.L. (1988). Protoberberine alkaloids as antimalarials. *Journal of Medicinal Chemistry* **31**, 1087-1093.

Vreysen, M.J.B., Saleh, K.M., Ali, M.Y., Abdullah M.A., Zhu, Z.R. Juma K.G., Dyck V.A., Msangi A.R., Mkonyi P.A. & Feldmann H.U. (2000). *Glossina austeni* (Diptera: Glossinidae) eradicated on the island of Unguja, zanzibar, using the sterile insect technique, *Journal of Economic Entomolology* **93**, 123-135.

Vrijsen, R., Everaert, L. & Boeye, A. (1988). Antiviral activity of flavones and potentiation by ascorbate. *Journal of General Virology* **69**, 1749-51.

Virtanen, P., Lassila, V., Njimi, T. & Mengata, D.E. (1988). Natural protoberberine alkaloids from *Enantia chlorantha*, palmatine, columbamine and jatrorrhizine for thioacetamide-traumatized rat liver. *Acta Anatomica* (Basel) **131**, 166-170.

Vivancos, M. & Moreno, J.J. (2005). β-Sitosterol modulates antioxidant enzyme response in RAW 264.7 macrophages. *Free Radical Biology and Medicine* **39**, 91-97.

Wafo, P., Nyasse, B., Fontaine, C. & Sondengam, B.L. (1999). Aporphine alkaloids from *Enantia chlorantha*. *Fitoterapia* **70**, 157-160.

Wang, I.K., Lin-Shiau, S.Y. & Lin, J.K. (1999). Induction of apoptosis by apigenin and related flavonoids through cytochrome c release and activation of caspase-9 and caspase-3 in leukaemia HL-60 cells. *European Journal of Cancer* **35**, 1517-1525.

Wani, M.C., Taylor, H.L., Wall, M.E., Coggon, P., McPhail, A.T. (1971). Plant antitumor agents. VI. The isolation and structure of taxol, a novel antileukemic and antitumor agent from *Taxus brevifolia*. *Journal of American Chemical Society* **93**, 2325-2327.

Wall, M.E., Wani, M.C., Cook, C.E., Palmer, K.H., McPhail, A.T. & Sim, G.A. (1966). Plant antitumor agents. I. The isolation and structure of camptothecin, a novel alkaloidal leukemia and tumor inhibitor from *Camptotheca acuminata*. *Journal of American Chemical Society* **88**, 3888-3890.

Waterman, P.G. and Pootakaham, K. (1979). *Planta Medica* **35**, 366.

Watt, J.M. & Breyer-Brandwijk, M.G. (1962). The Medicinal and Poisonous Plants of Southern and Eastern Africa. E&S. Livingstone Ltd, Edinburgh & London.

Wedge, D.E. & Camper, N.D. (2000). In: *Biologically Active Natural Products: Pharmaceuticals.* Cutler S.J.; Cutler H.G. (Eds). CRC Press: New York, p1-15.

WHO (1984). *Chemical Methods for Control of Arthropod Vectors and Pests of Public Health*. WHO, Geneva, **49**, p

WHO (1986). *Chemotherapy of Malaria*, Revised Edition, WHO, Geneva.

WHO (1995). *Planning Overview of Tropical Diseases Control.* Division of Tropical Diseases. WHO, Geneva.

WHO (1996). *Report of the WHO Informal Consultation on the Evaluation and Testing of Insecticides.* WHO, Geneva.

WHO (1997). *Chagas Disease*. Thirteenth Programme Report UNDP/TDR, WHO, Geneva.

WHO (2001) *Leishmaniasis: The Disease and its Impact.* [Online] http://www.who.int/emc/diseases/leish/leisdis1.html, acessed on 14 April 2005.

WHO (2002). *The World Health Report 2002: Reducing Risks, Promoting Healthy Life*. WHO, Geneva.

WHO (2004). *Laboratory Biosafety Manual* 3rd Edn. WHO/CDS/CSR/LYO/2004.11

WHO (2005). *World Malaria Report 2005*. WHO, Geneva.

Wijeratne, E.M.K., Lankananda, B.D., Tezuka, Y., Nagaoka, T. & Gunatilaka, A.A.L (2001). Dimeric aporphine alkaloids of *Phoenicanthus oblique* from Sri Lanka. *Journal of Natural Products* **64**, 1465-1467.

Wilt, T.J., MacDonald, R. & Ishani, A. (1999). β-Sitosterol for the treatment of benign prostatic hyperplasia: a systematic review. *British Journal of Urology International* **83**, 976-983.

Wollenweber, E. & Jay, M. (1988). Flavones and flavonoids. In: The flavonoids. Harbone J.B. [Ed.]. Chapman & Hall Ltd, London, England, 233-302.

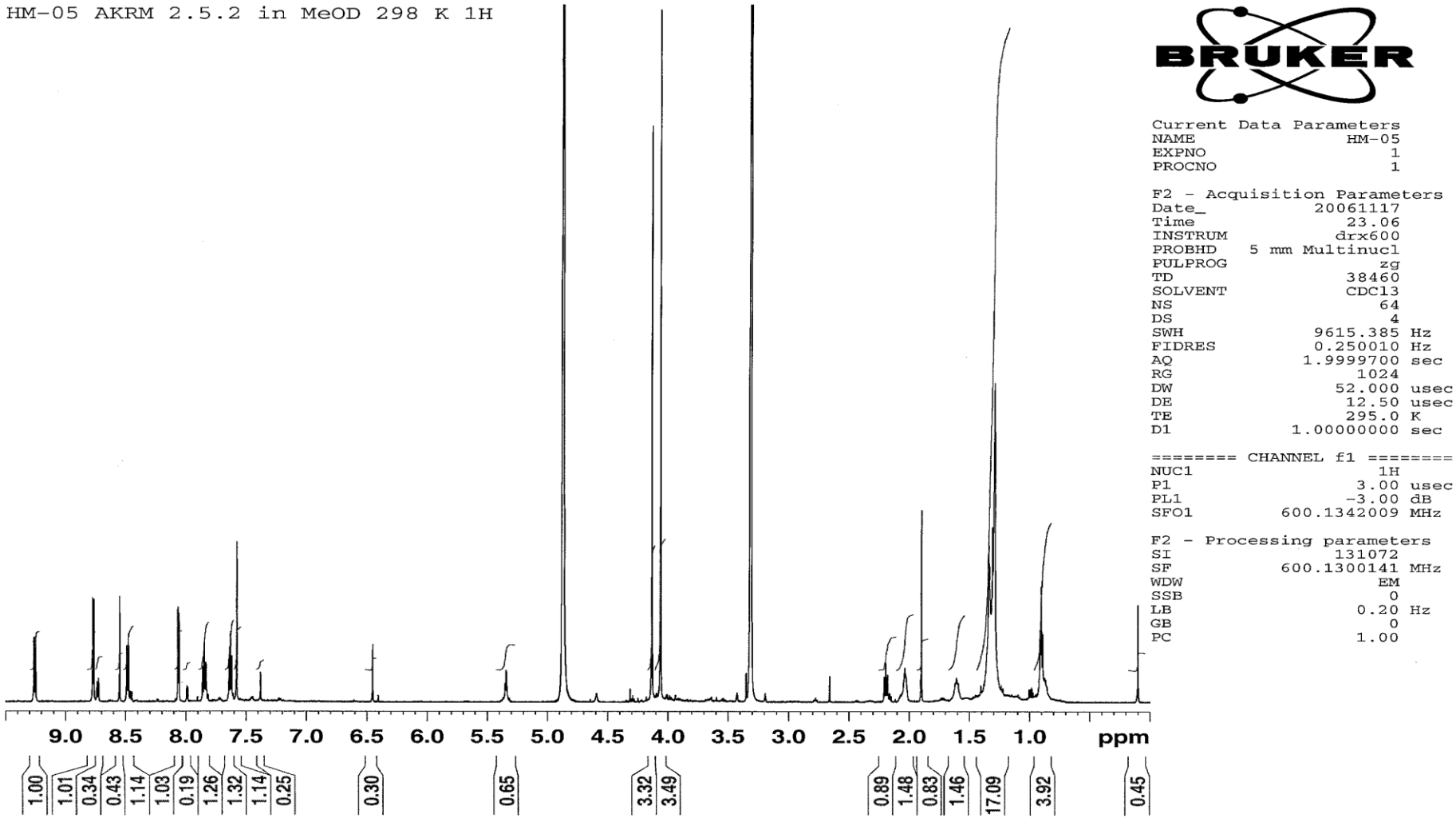
Wright, C.W. & Phillipson, J.D (1990). Natural products and the development of selective antiprotozoal drugs. *Phytotherapy Research* **4**, 4.

Zafra-Polo, M.C., Gonzalez, M.C., Estornell, E., Sahpaz, S. & Cortes, D. (1996). Acetogenins from Annonaceae: Inhbitors of mitochondrial complex I. *Phytochemistry* **42**, 253.

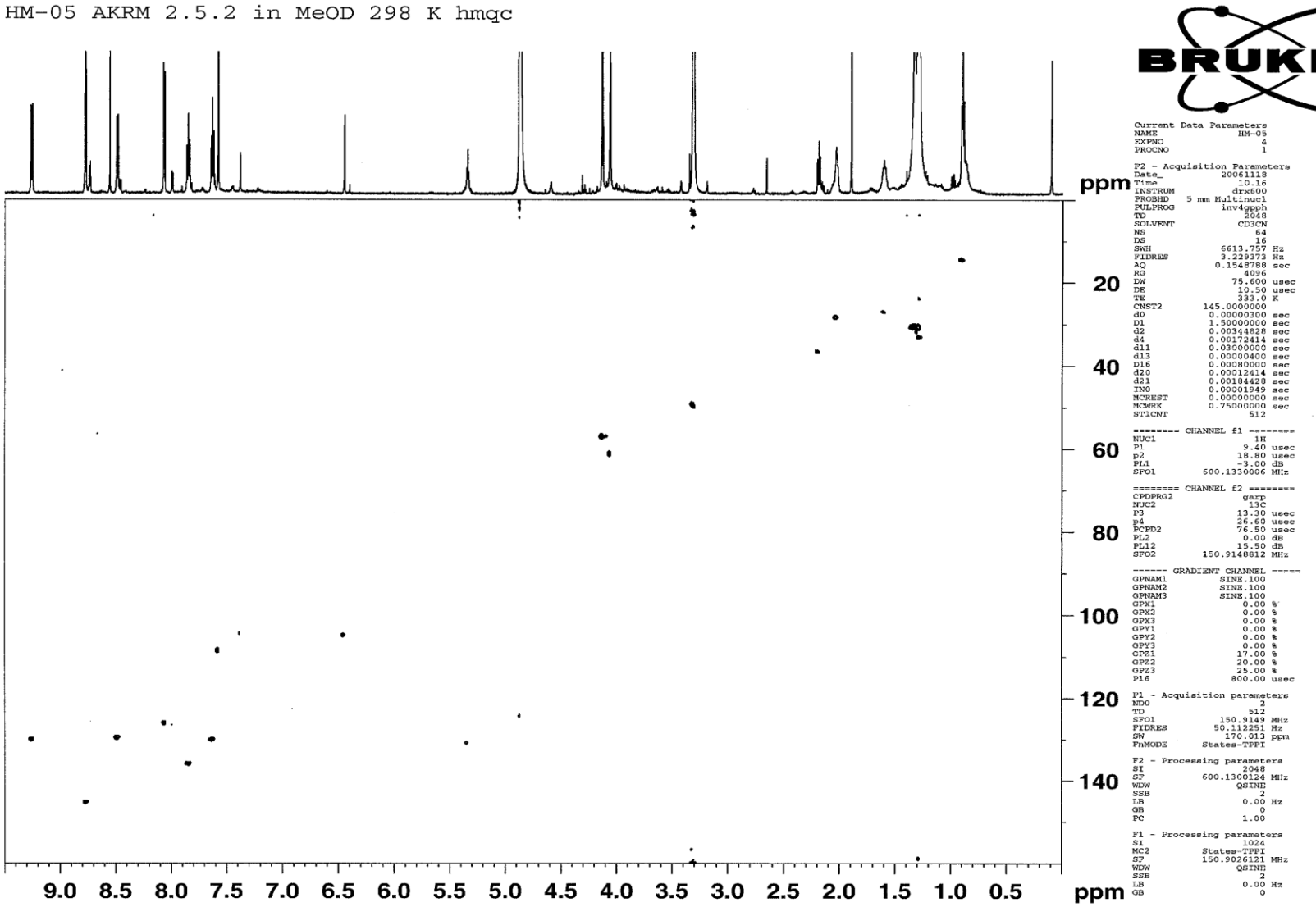
Zhai, L., Chen, M., Blom, J., Theander, T.G., Christensen, S.B. & Kharazmi, A. (1999). The antileishmanial activity of novel oxygenated chalcones and their mechanism of action. *Antimicrobial Agents Chemotherapy* **43**, 793-803.

Zhu, Y-M., Shen, J-K., Wang H-K., Cosentinoc, LM. & Leeb, K-H. (2001). Synthesis and anti-HIV activity of oleanolic acid derivatives. *Bioorganic and Medicinal Chemistry Letters* **11**, 3115–3118.

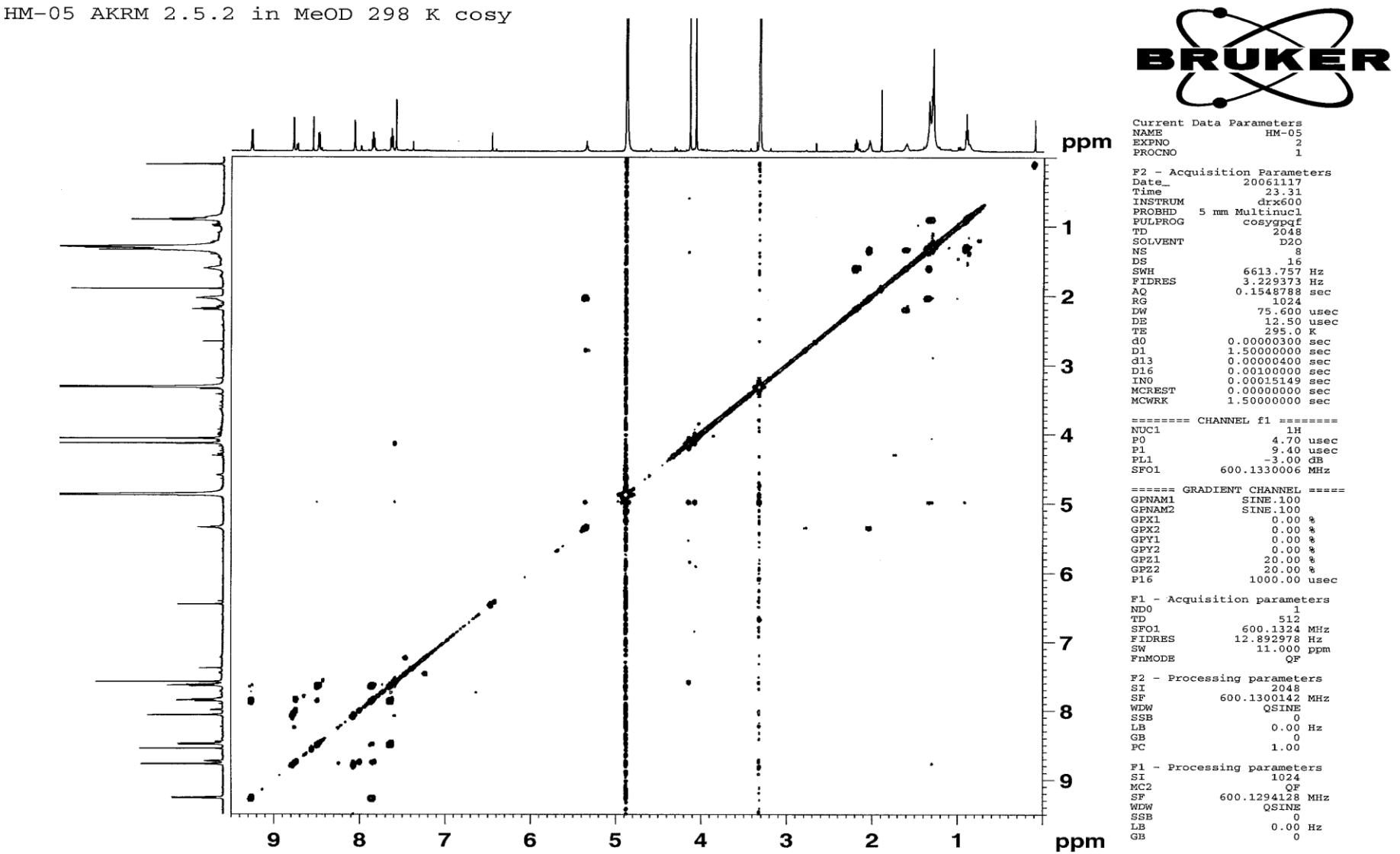
Appendix 1a: ^{1}H NMR spectrum of lysicamine (**127**)



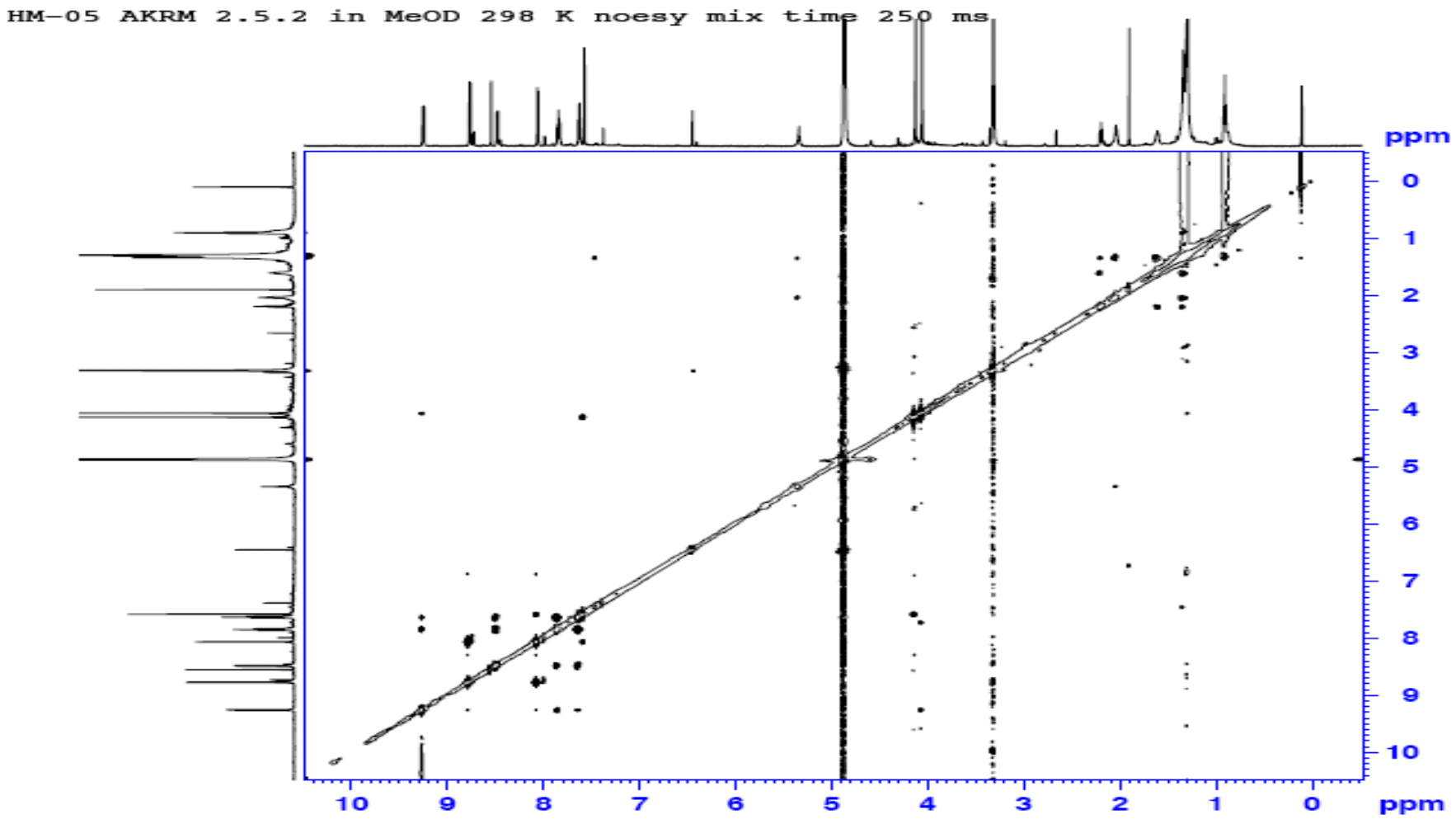
Appendix 1b: HMQC spectrum of lysicamine (**127**)



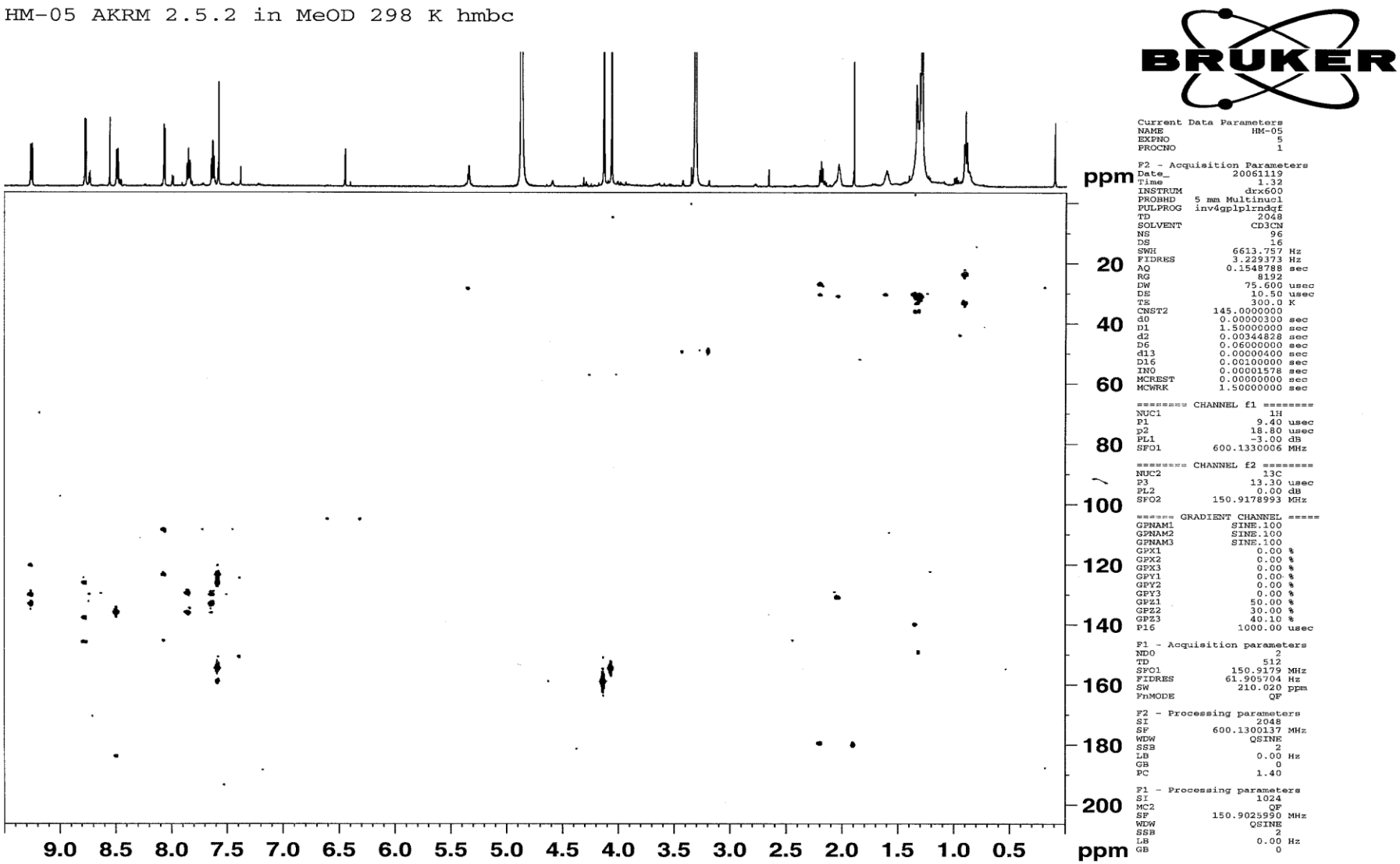
Appendix 1c: COSY spectrum of lysicamine (**127**)



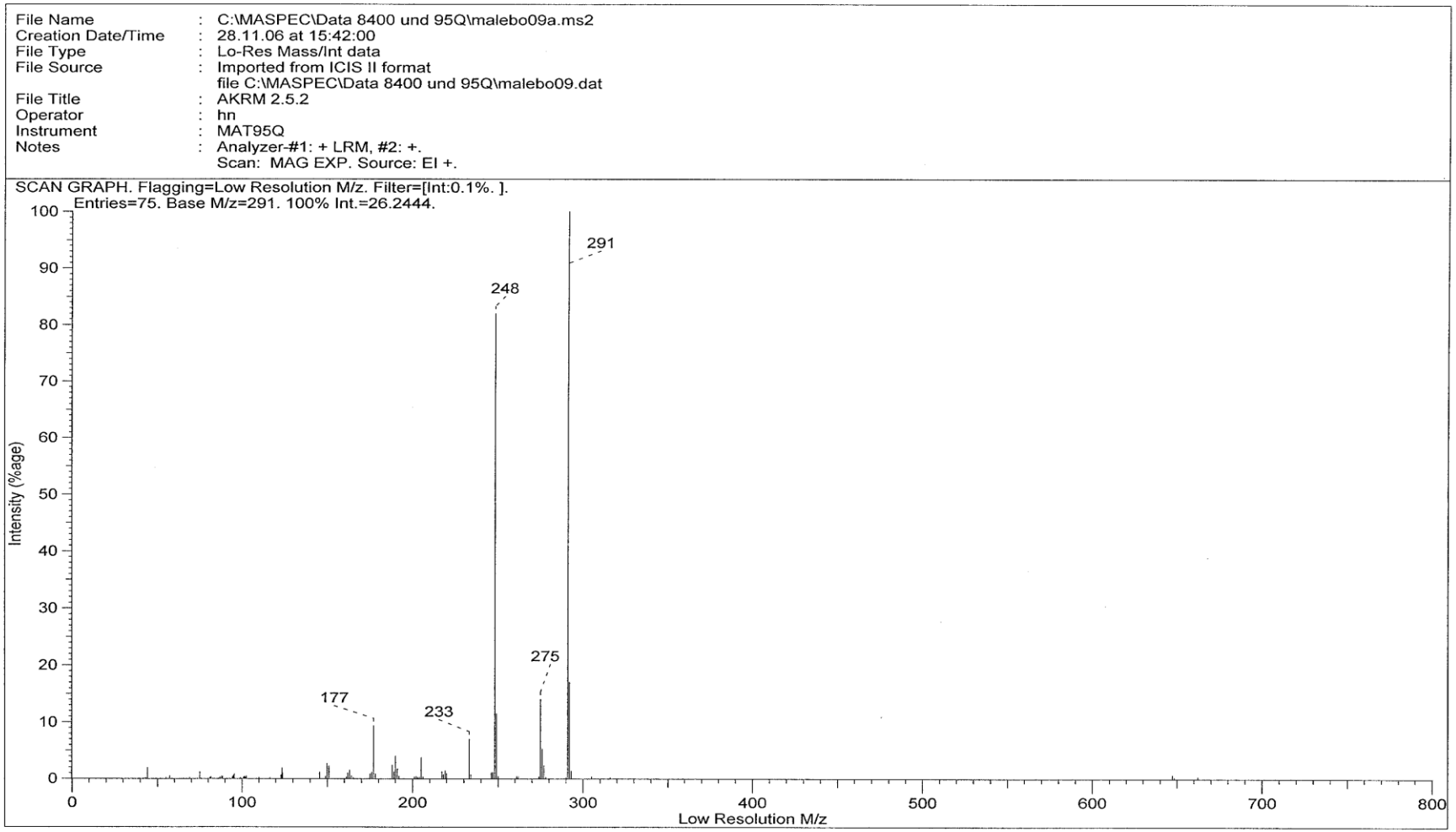
Appendix 1d: NOESY spectrum of lysicamine (**127**)



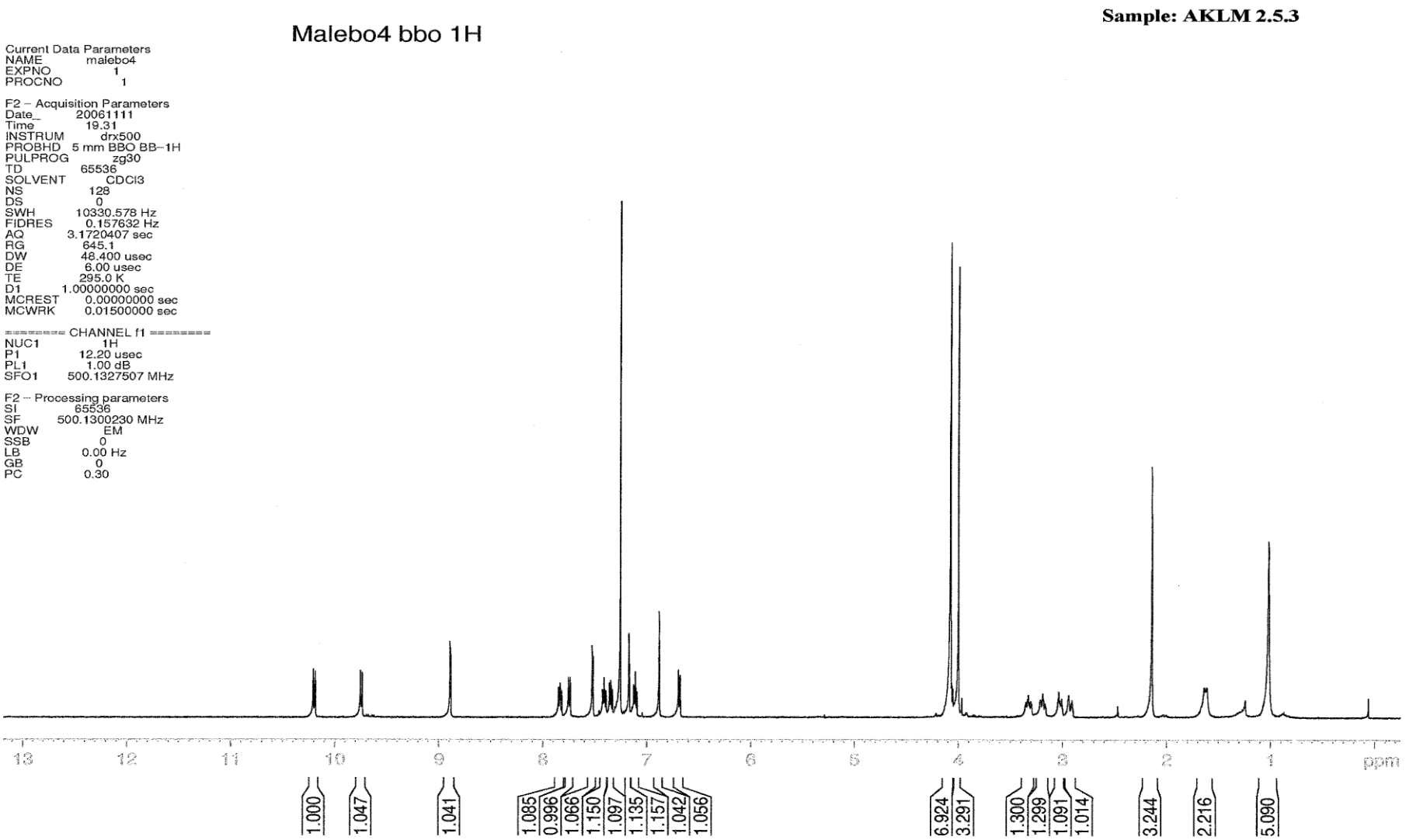
Appendix 1e: HMBC spectrum of lysicamine (**127**)



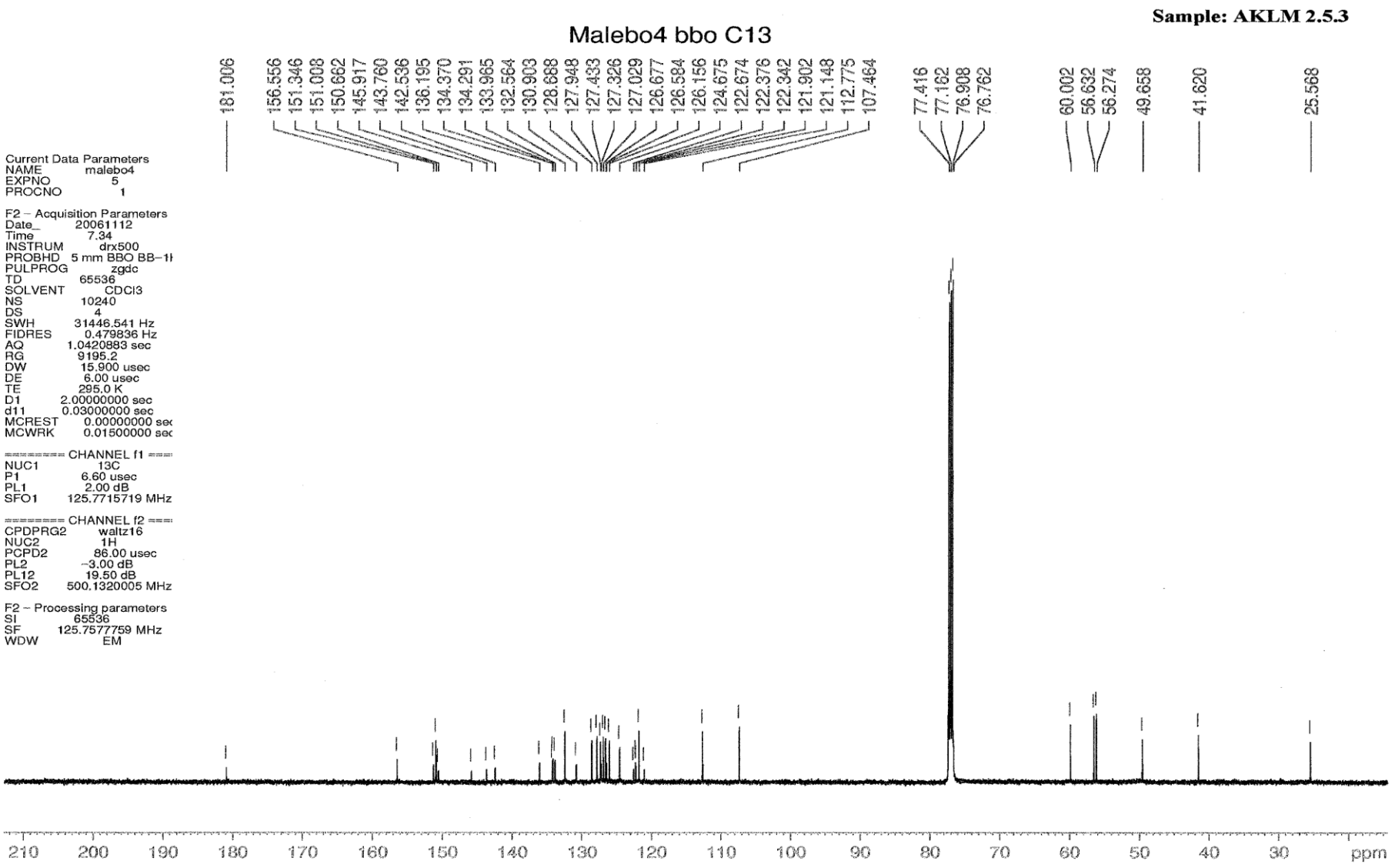
Appendix 1f: MS spectrum of lysicamine (**127**)



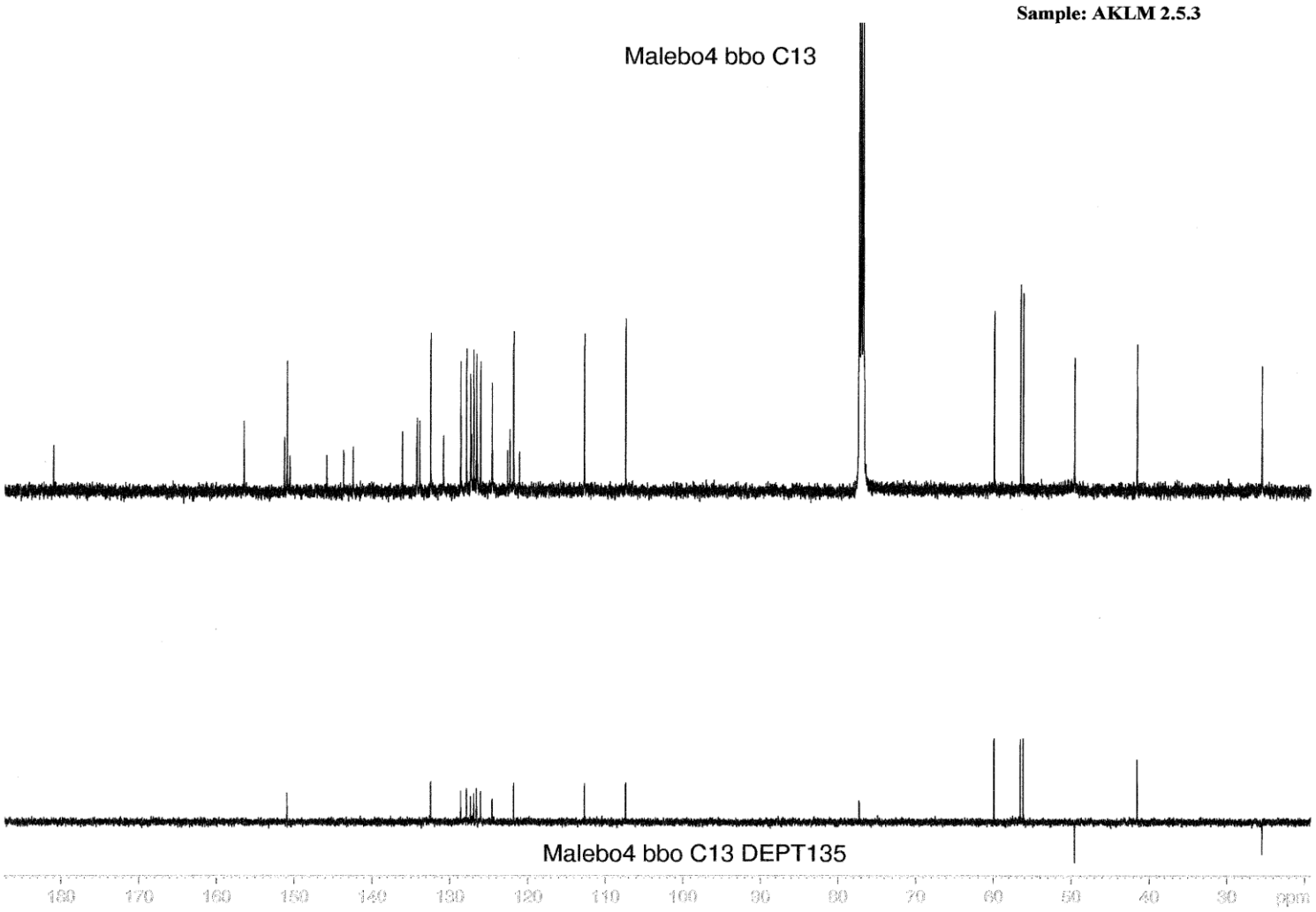
Appendix 2a: ^{1}H NMR spectrum of trivalvone (**128**)



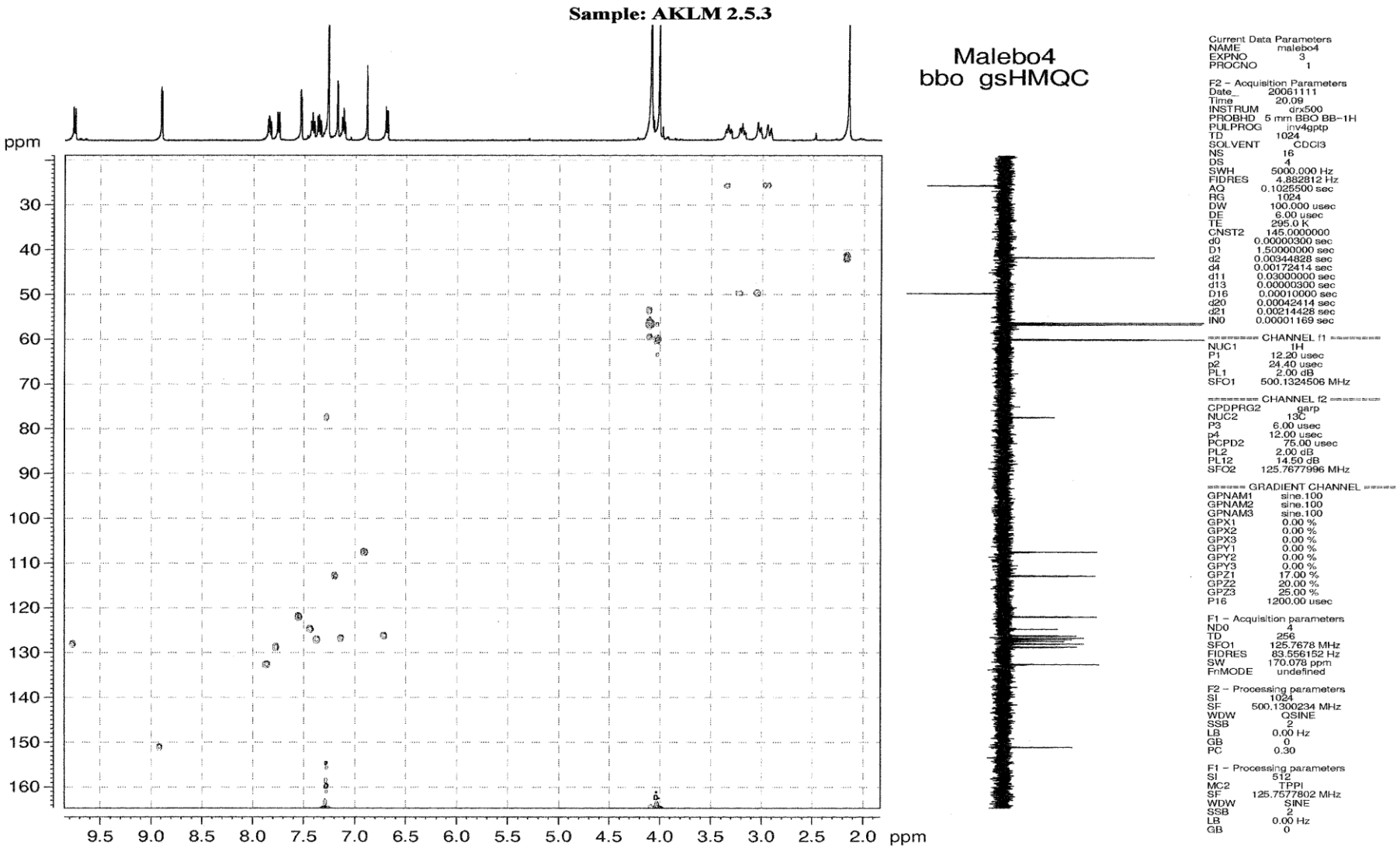
Appendix 2b: ^{13}C NMR spectrum of trivalvone (**128**)



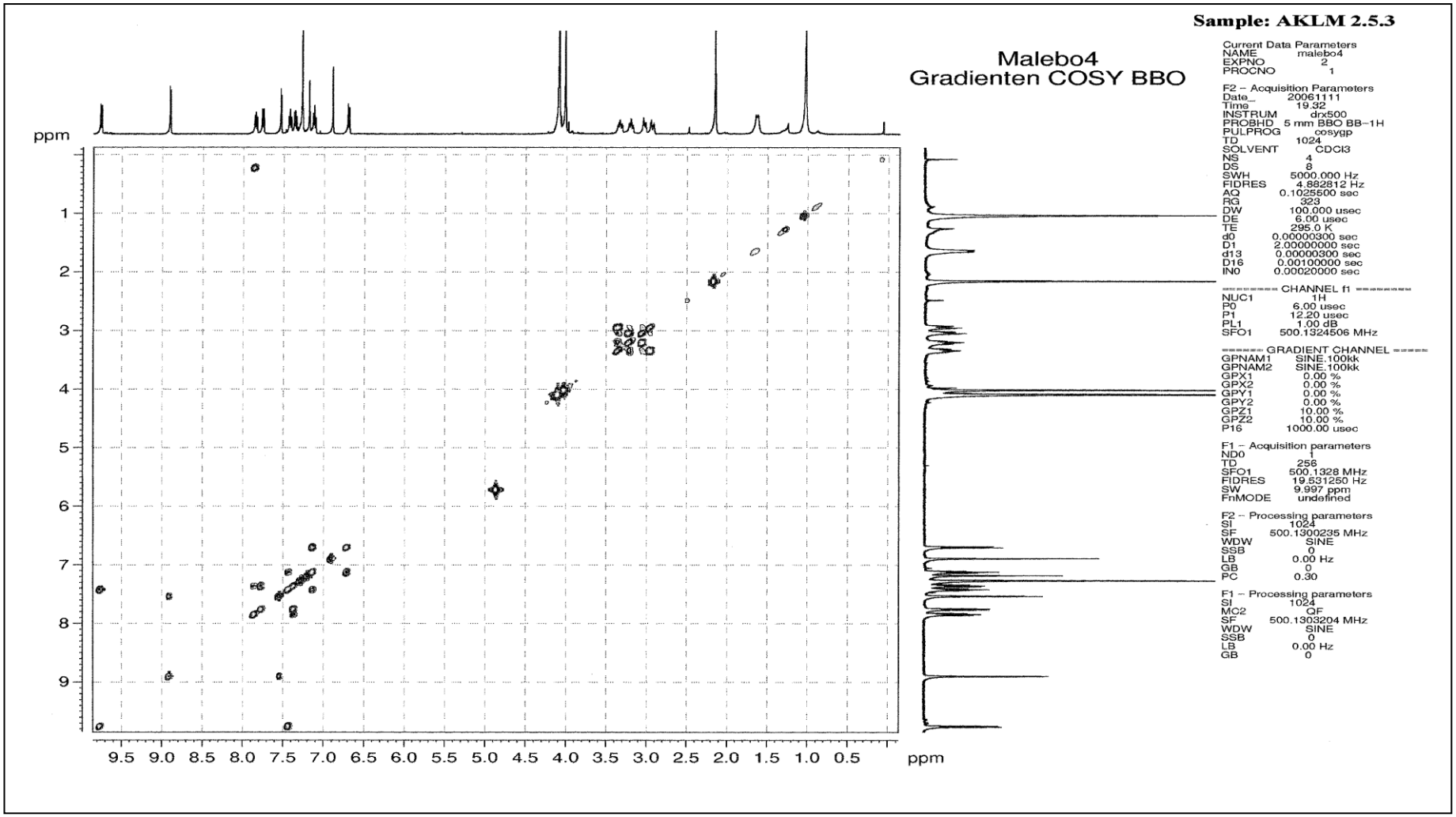
Appendix 2c: DEPT 135 spectrum of trivalvone (**128**)



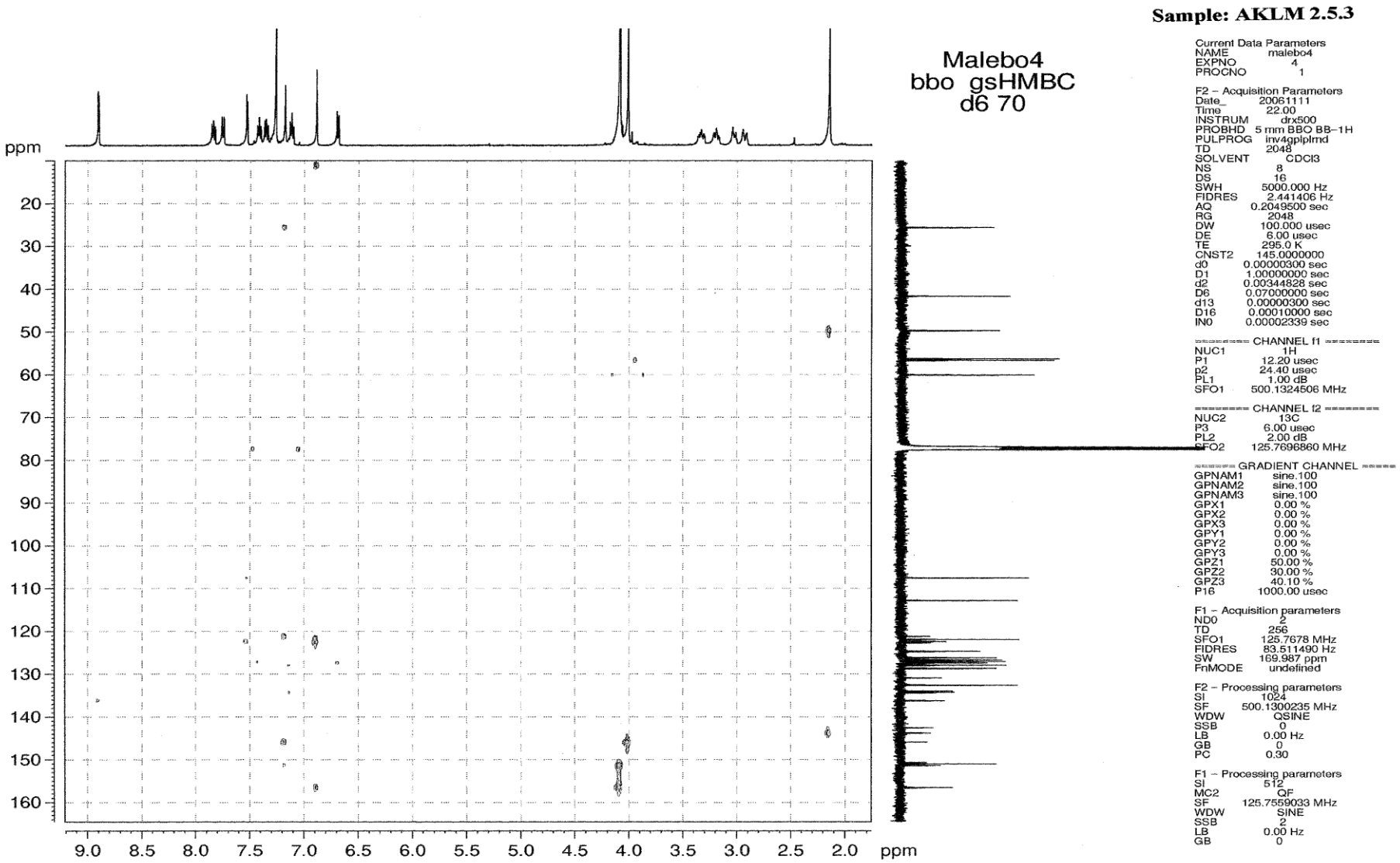
Appendix 2d: HMQC spectrum of trivalvone (**128**)



Appendix 2e: COSY spectrum of trivalvone (**128**)



Appendix 2f: HMBC spectrum of trivalvone (**128**)



Sample: AKLM 2.5.3

Current Data Parameters
NAME malebo4
EXPNO 4
PROCNO 1

F2 – Acquisition Parameters
Date_ 20061111
Time 22.00
INSTRUM drx500
PROBHD 5 mm BBO BB–1H
PULPROG inv4gplplrnd
TD 2048
SOLVENT CDCl3
NS 8
DS 16
SWH 5000.000 Hz
FIDRES 2.441406 Hz
AQ 0.2049500 sec
RG 2048
DW 100.000 usec
DE 6.00 usec
TE 295.0 K
CNST2 145.0000000
d0 0.00000300 sec
D1 1.00000000 sec
d2 0.00344828 sec
D6 0.07000000 sec
d13 0.0000300 sec
D16 0.00010000 sec
IN0 0.00002339 sec

======== CHANNEL f1 ========
NUC1 1H
P1 12.20 usec
p2 24.40 usec
PL1 1.00 dB
SFO1 500.1324506 MHz

======== CHANNEL f2 ========
NUC2 13C
P3 6.00 usec
PL2 2.00 dB
SFO2 125.7696860 MHz

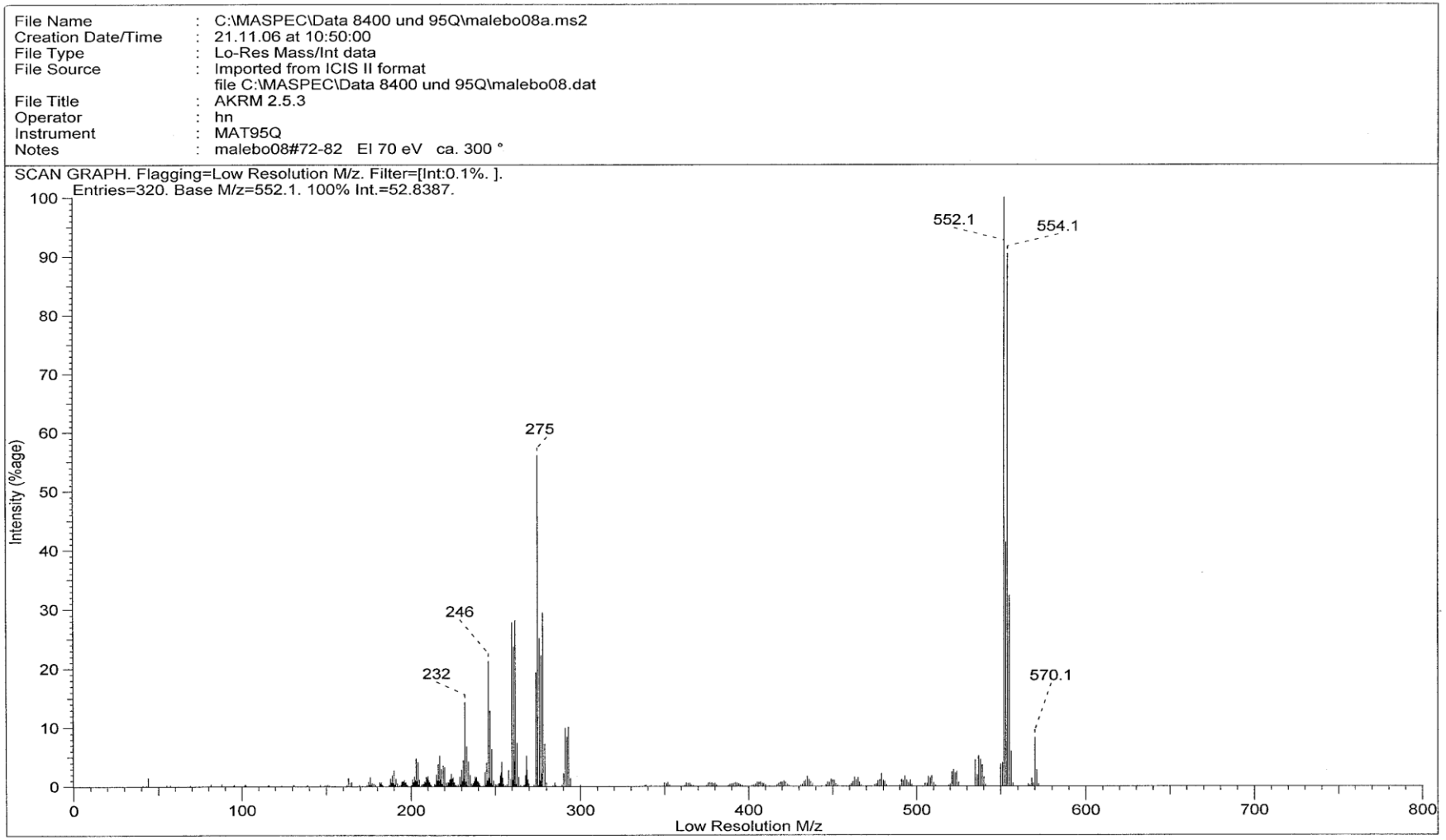
======== GRADIENT CHANNEL ====
GPNAM1 sine.100
GPNAM2 sine.100
GPNAM3 sine.100
GPX1 0.00 %
GPX2 0.00 %
GPX3 0.00 %
GPY1 0.00 %
GPY2 0.00 %
GPY3 0.00 %
GPZ1 50.00 %
GPZ2 30.00 %
GPZ3 40.10 %
P16 1000.00 usec

F1 – Acquisition parameters
ND0 2
TD 256
SFO1 125.7678 MHz
FIDRES 83.511490 Hz
SW 169.987 ppm
FnMODE undefined

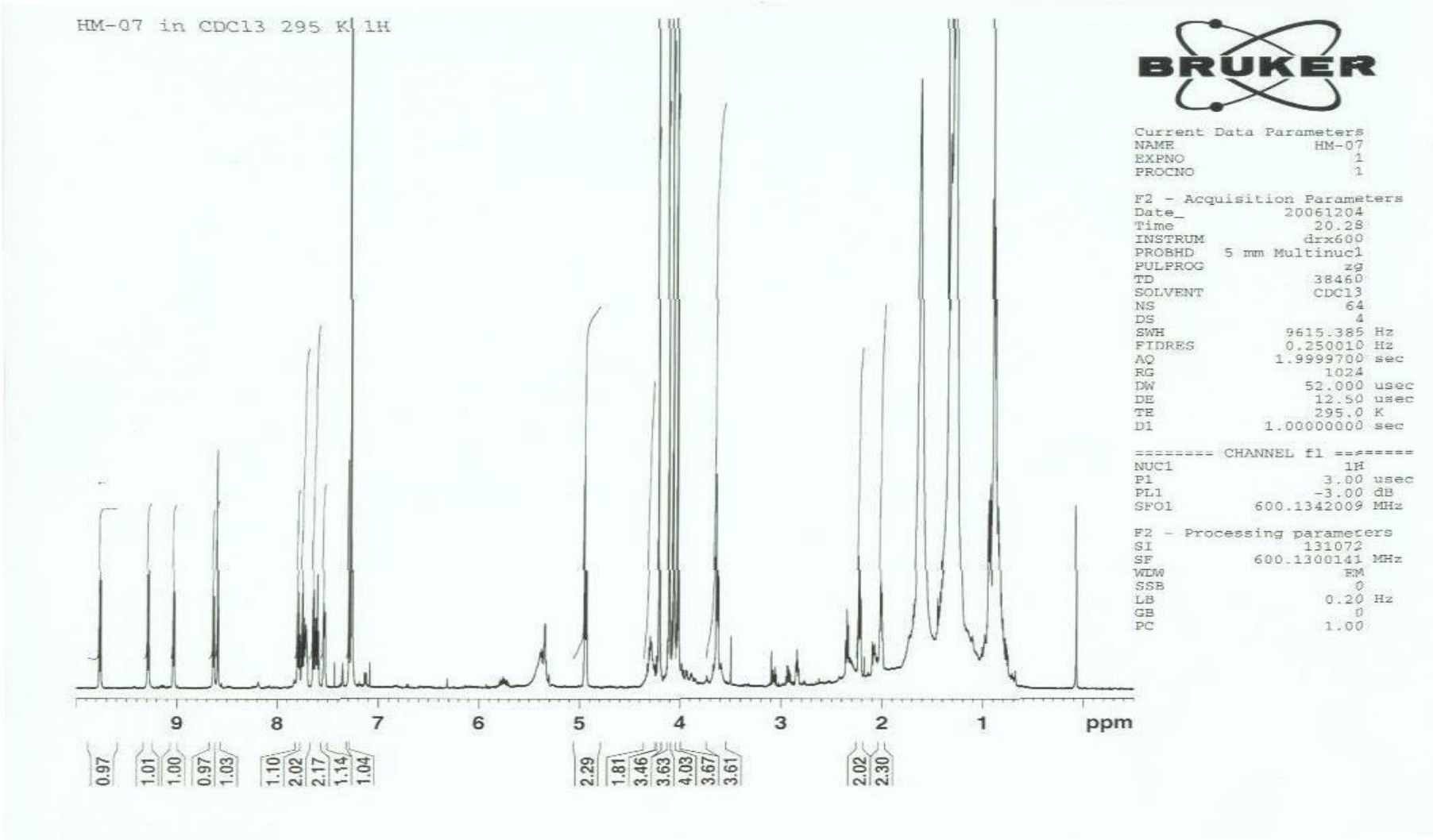
F2 – Processing parameters
SI 1024
SF 500.1300235 MHz
WDW QSINE
SSB 0
LB 0.00 Hz
GB 0
PC 0.30

F1 – Processing parameters
SI 512
MC2 QF
SF 125.7559033 MHz
WDW SINE
SSB 2
LB 0.00 Hz
GB 0

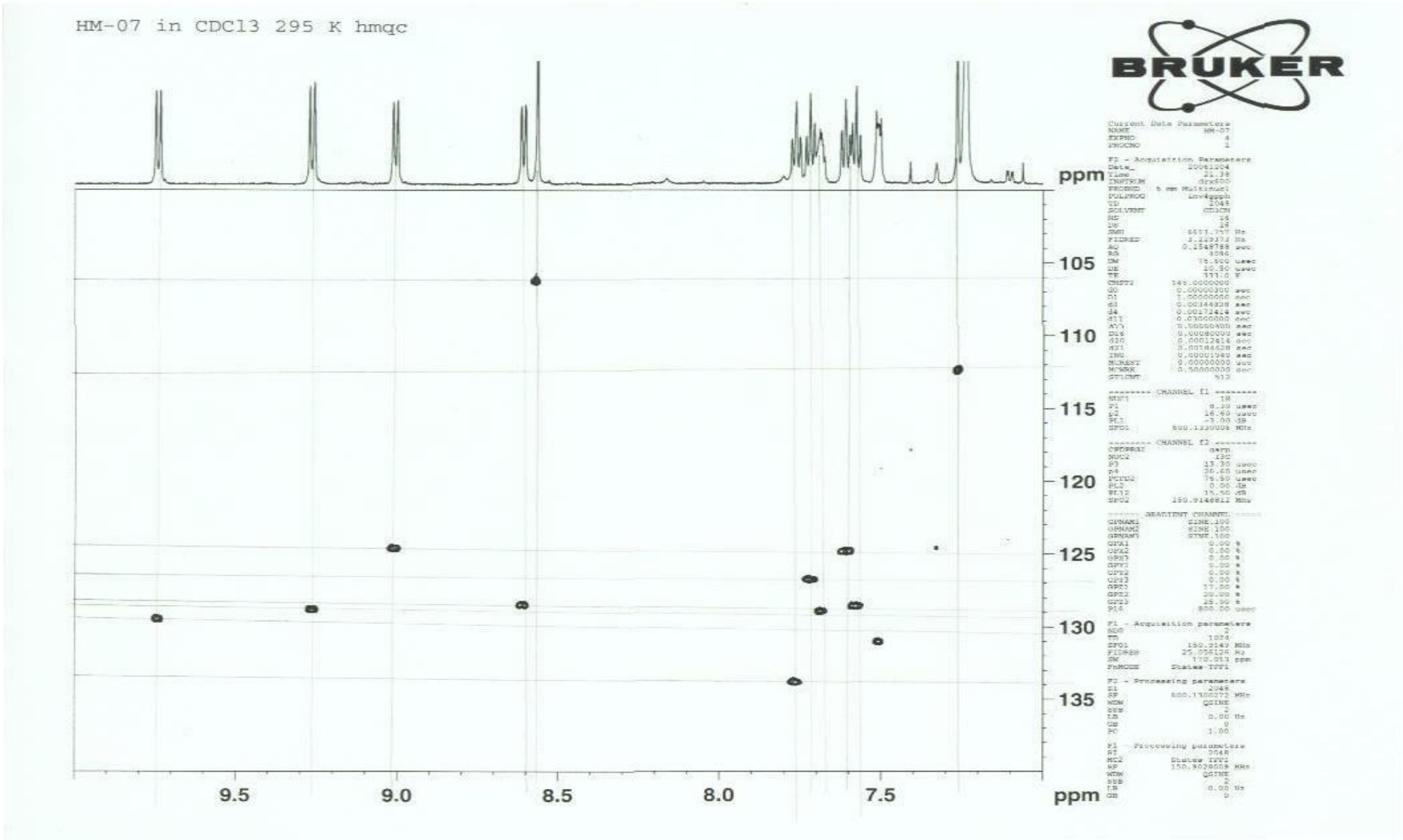
Appendix 2g: MS spectrum of trivalvone (**128**)



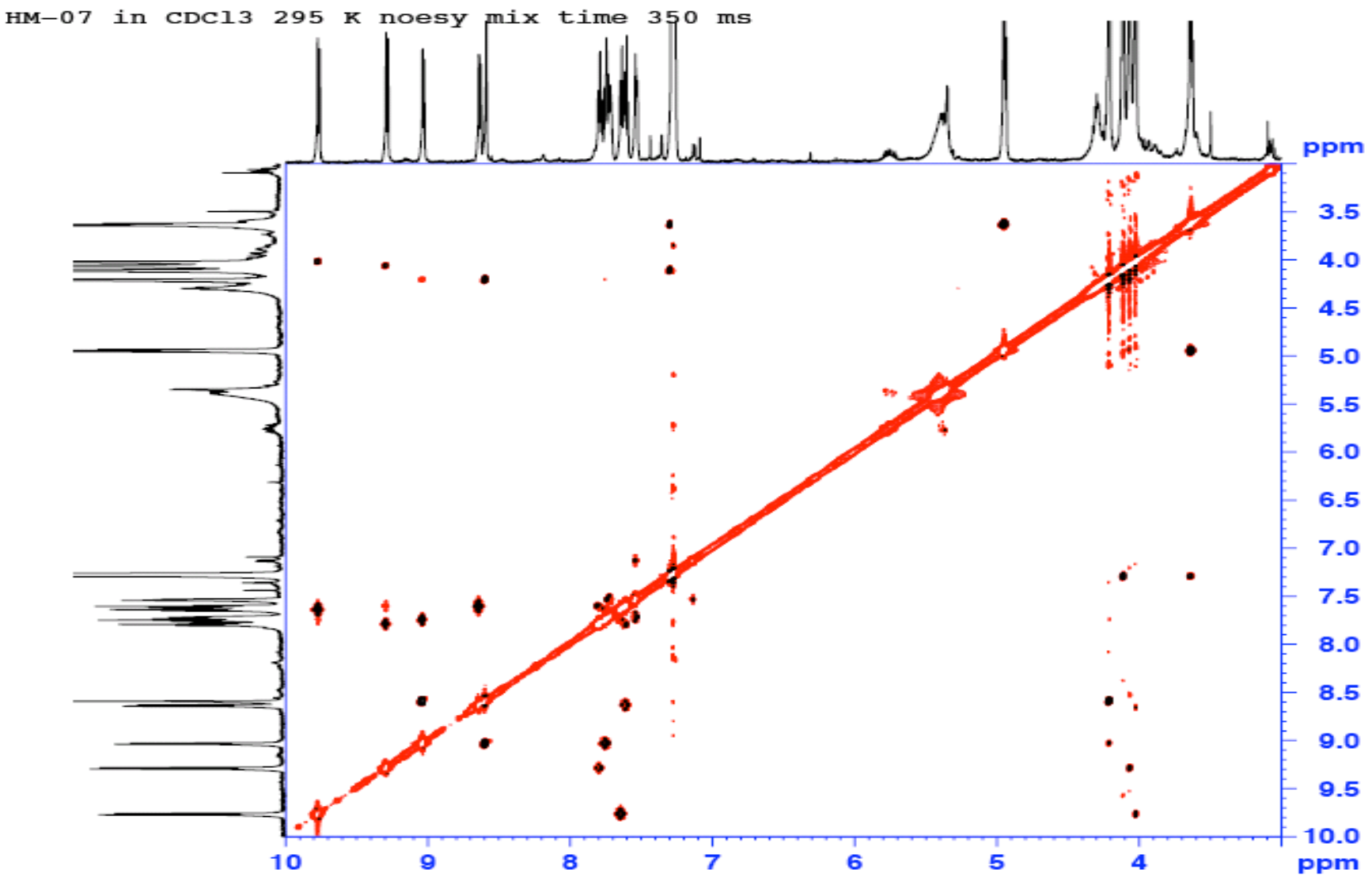
Appendix 3a: ^{1}H NMR spectrum of Annickine (**129**)



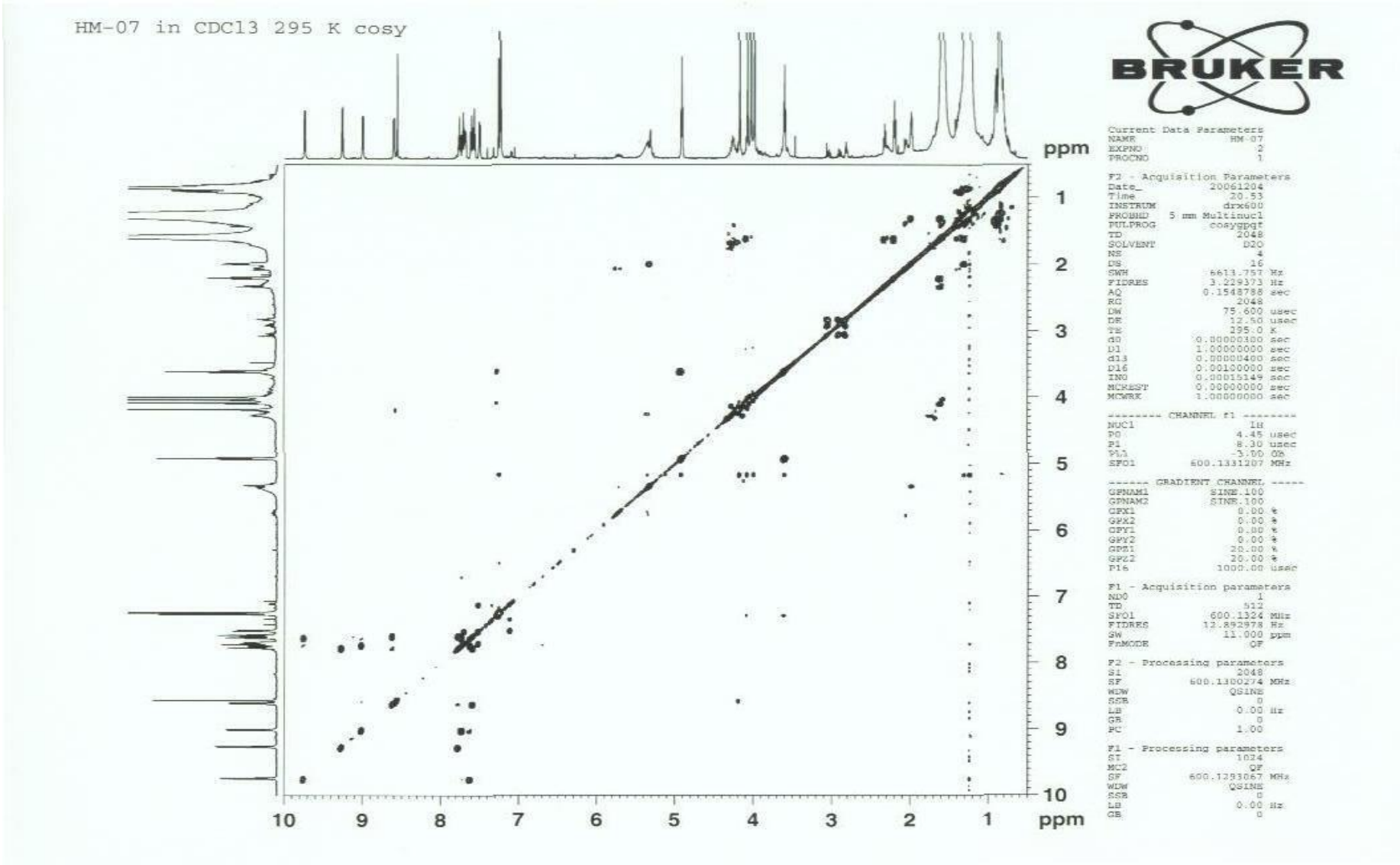
Appendix 3b: HMQC spectrum of Annickine (**129**)



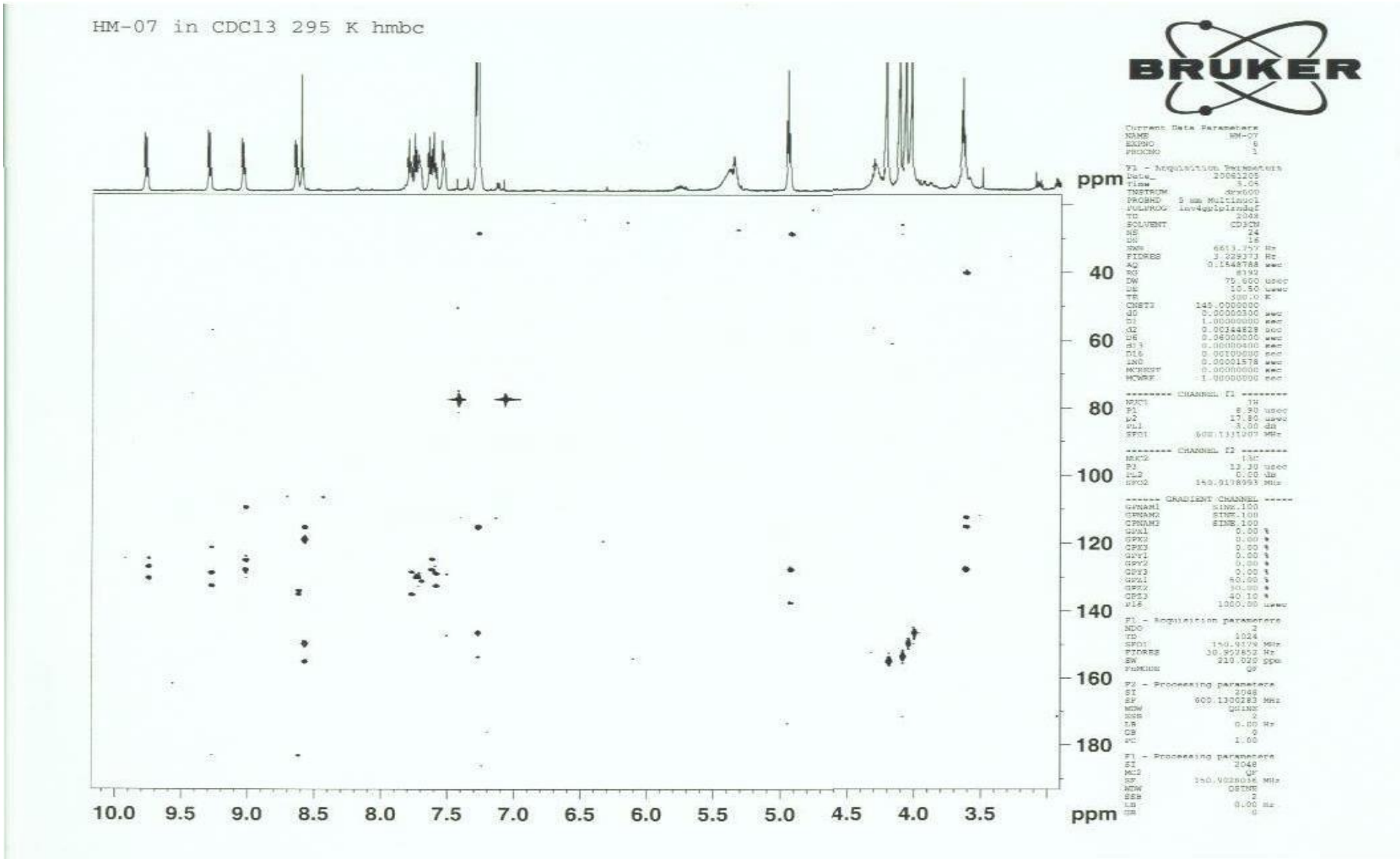
Appendix 3c: NOESY spectrum of Annickine (**129**)



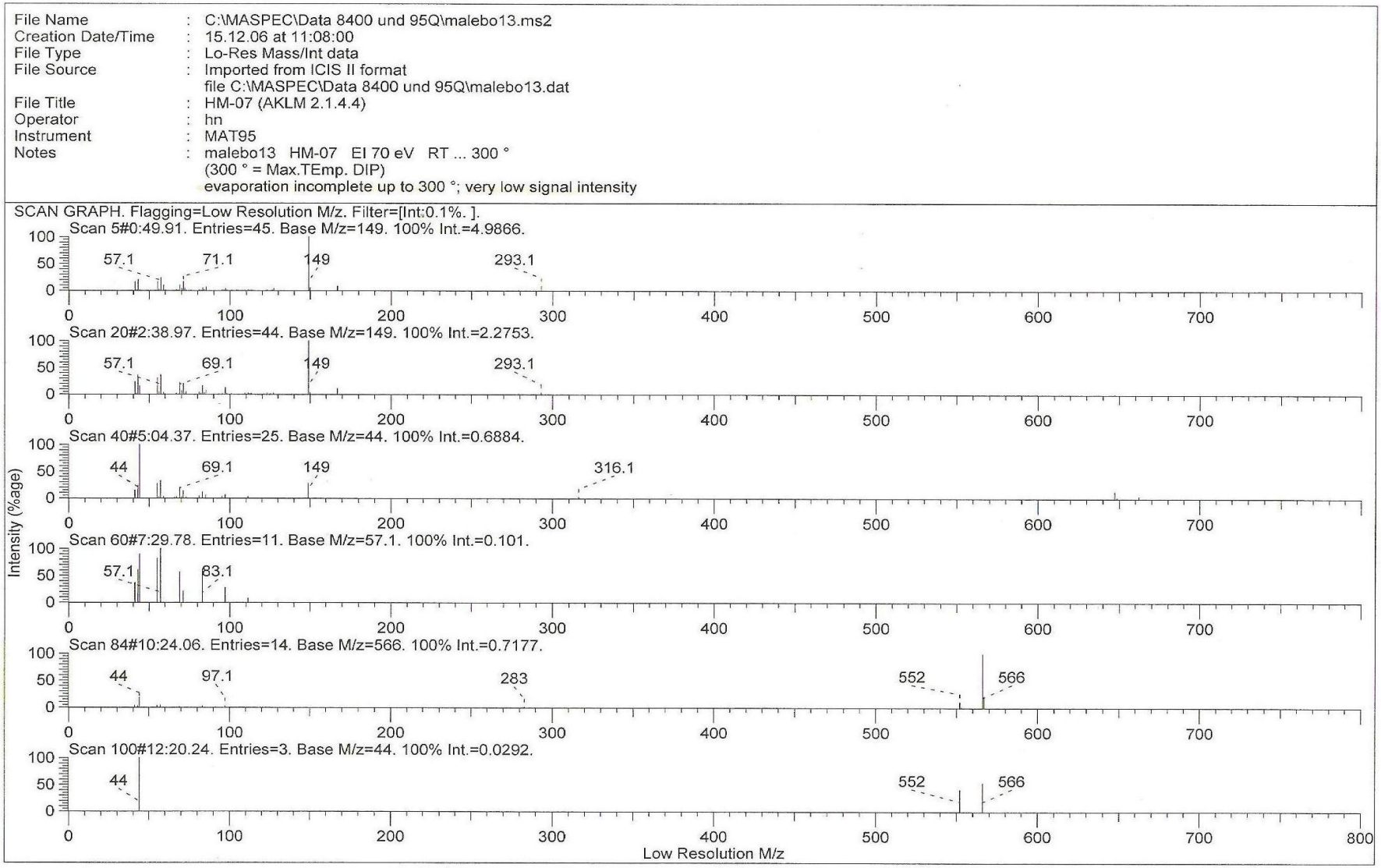
Appendix 3d: Cosy spectrum of Annickine (**129**)



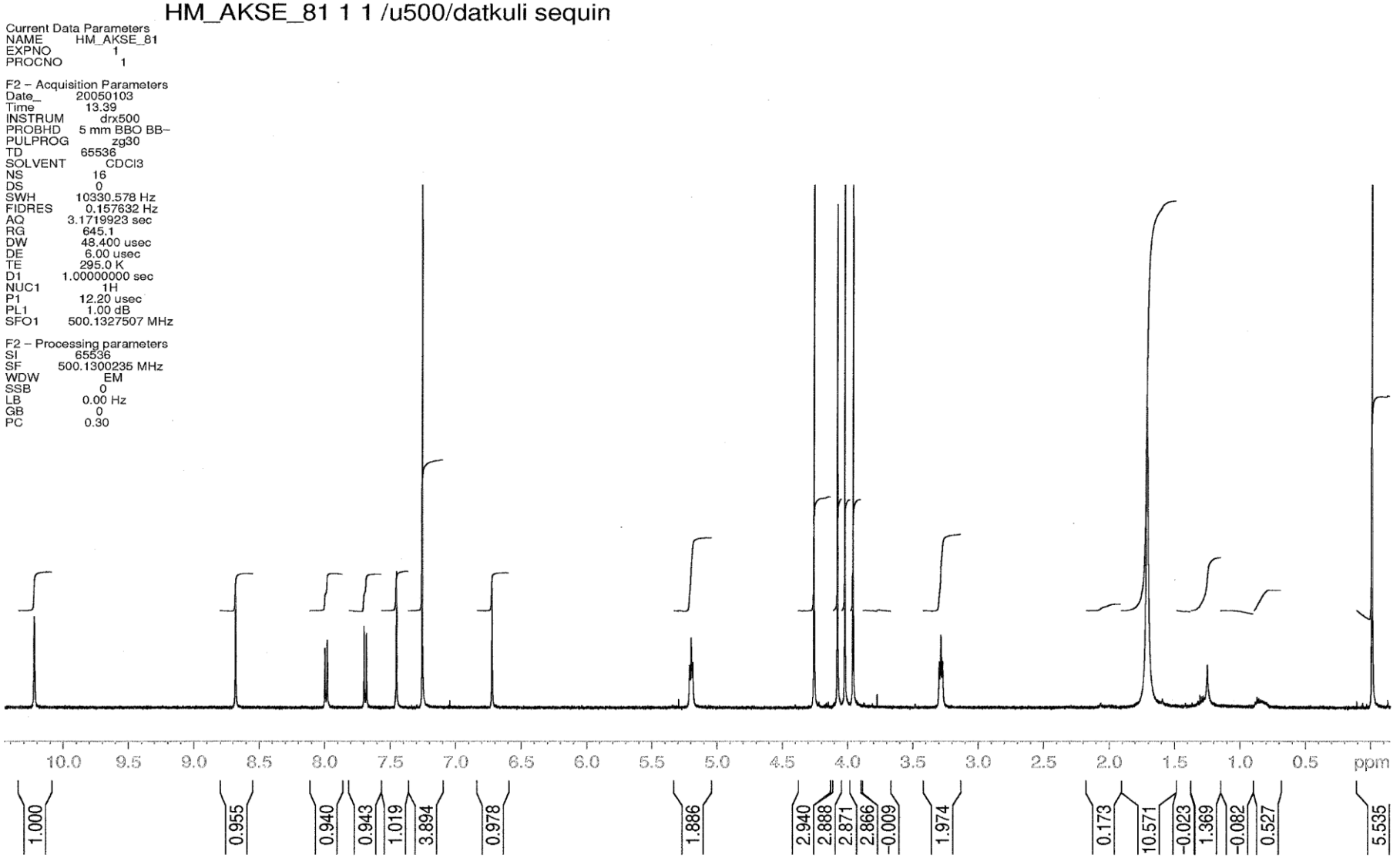
Appendix 3e: HMBC spectrum of Annickine (**129**)



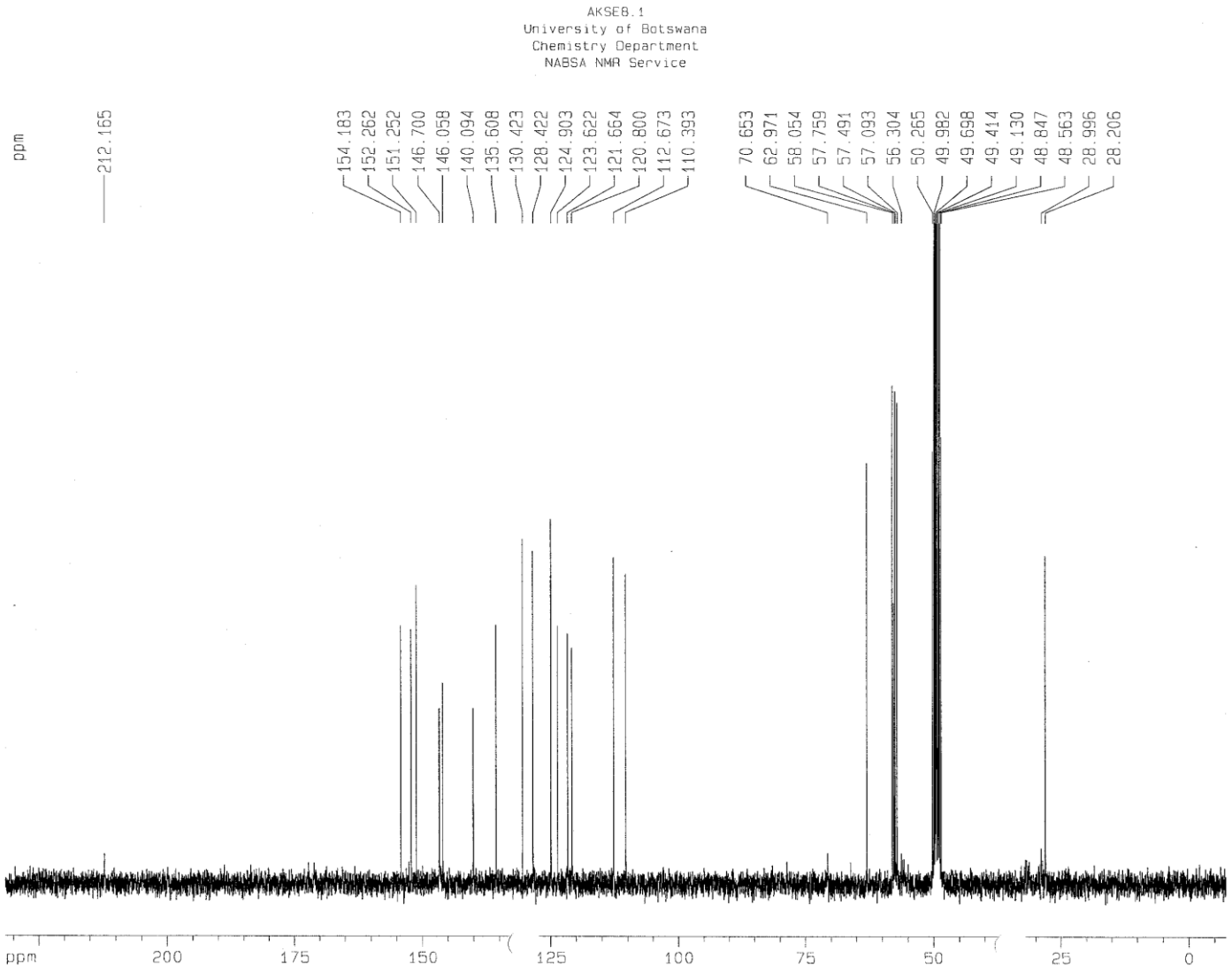
Appendix 3f: MS spectrum of Annickine (**129**)



Appendix 4a: ^{1}H NMR spectrum of palmatine (**82**)



Appendix 4b: ^{13}C NMR spectrum of palmatine (**82**)




```
Current Data Parameters
NAME                 akse81
EXPNO                    11
PROCNO                    1

F2 - Acquisition Parameters
Date_              20041007
Time                   8.47
INSTRUM               spect
PROBHD     5 mm QNP  1H
PULPROG              zgpg30
TD                    65536
SOLVENT                MeOH
NS                     7168
DS                        4
SWH               18832.393 Hz
FIDRES            0.287360 Hz
AQ                1.7400308 sec
RG                     8192
DW                  26.550 usec
DE                   6.00 usec
TE                  300.0 K
D1              2.00000000 sec
d11             0.03000000 sec
d12             0.00002000 sec

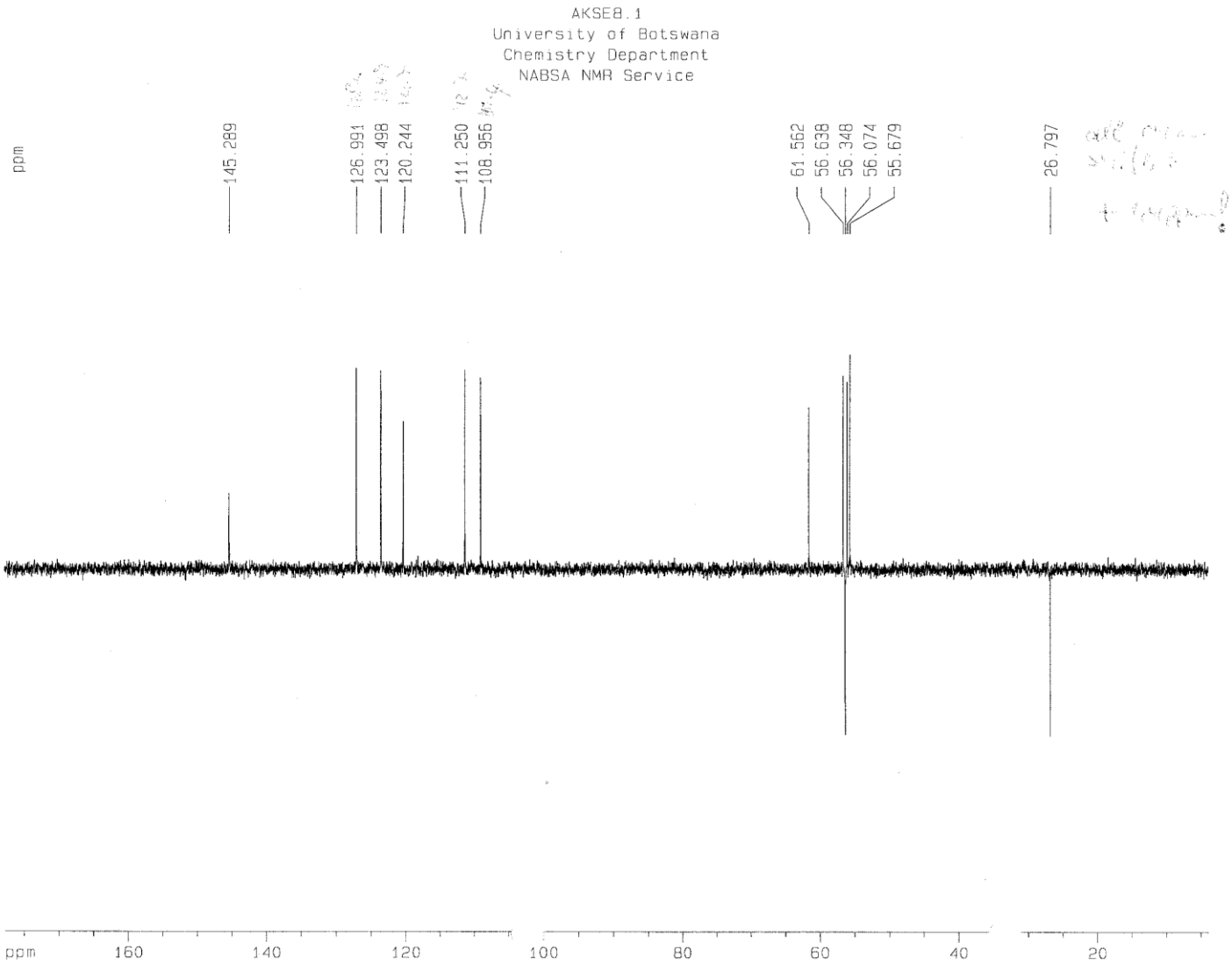
============ CHANNEL f1 =============
NUC1                   13C
P1                  10.75 usec
PL1                  1.00 dB
SFO1            75.4760200 MHz

============ CHANNEL f2 =============
CPDPRG2            waltz16
NUC2                   1H
PCPD2               80.00 usec
PL2                  0.00 dB
PL12                19.00 dB
PL13                22.00 dB
SFO2           300.1312005 MHz

F2 - Processing parameters
SI                    32768
SF              75.4676118 MHz
WDW                      EM
SSB                       0
LB                   1.00 Hz
GB                        0
PC                     1.40

1D NMR plot parameters
CX                   20.00 cm
F1P                231.571 ppm
F1                17476.14 Hz
F2P                 -7.238 ppm
F2                -546.26 Hz
PPMCM             11.94049 ppm/cm
HZCM             901.11993 Hz/cm
```

Appendix 4c: DEPT 135 spectrum of palmatine (**82**)



Current Data Parameters

NAME	akse81
EXPNO	12
PROCNO	1

F2 - Acquisition Parameters

Date_	20041007
Time	11.56
INSTRUM	spect
PROBHD	5 mm QNP 1H
PULPROG	dept135
TD	65536
SOLVENT	MeOH
NS	720
DS	4
SWH	17985.611 Hz
FIDRES	0.274439 Hz
AQ	1.8219508 sec
RG	8192
DW	27.800 usec
DE	6.00 usec
TE	300.0 K
CNST2	145.0000000
D1	2.00000000 sec
d2	0.00344828 sec
d12	0.00002000 sec
DELTA	0.00001369 sec

========== CHANNEL f1 ==========

NUC1	13C
P1	10.75 usec
p2	21.50 usec
PL1	1.00 dB
SFO1	75.4752653 MHz

========== CHANNEL f2 ==========

CPDPRG2	waltz16
NUC2	1H
P3	9.50 usec
p4	19.00 usec
PCPD2	80.00 usec
PL2	0.00 dB
PL12	19.00 dB
SFO2	300.1312005 MHz

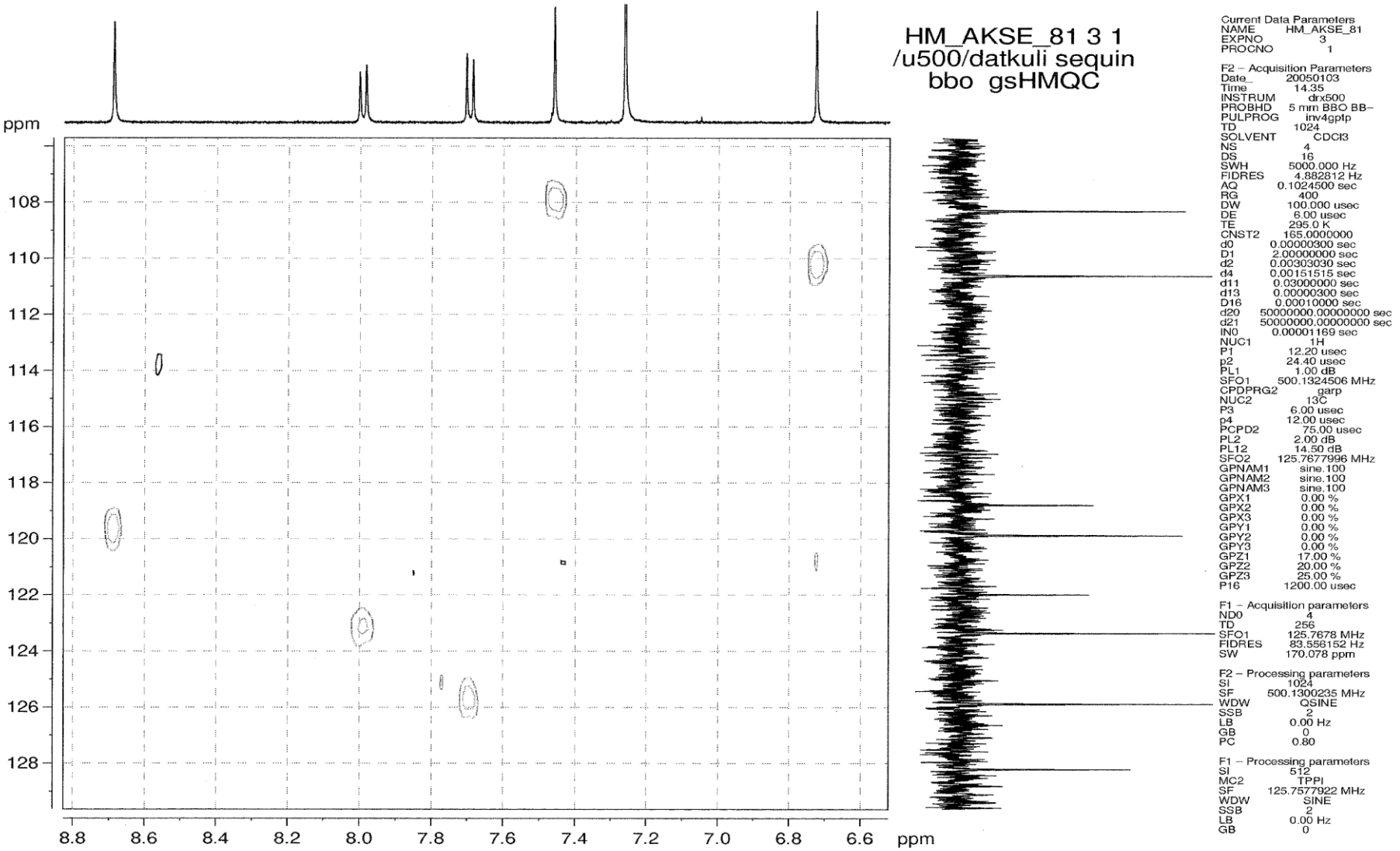
F2 - Processing parameters

SI	32768
SF	75.4677190 MHz
WDW	EM
SSB	0
LB	1.00 Hz
GB	0
PC	1.40

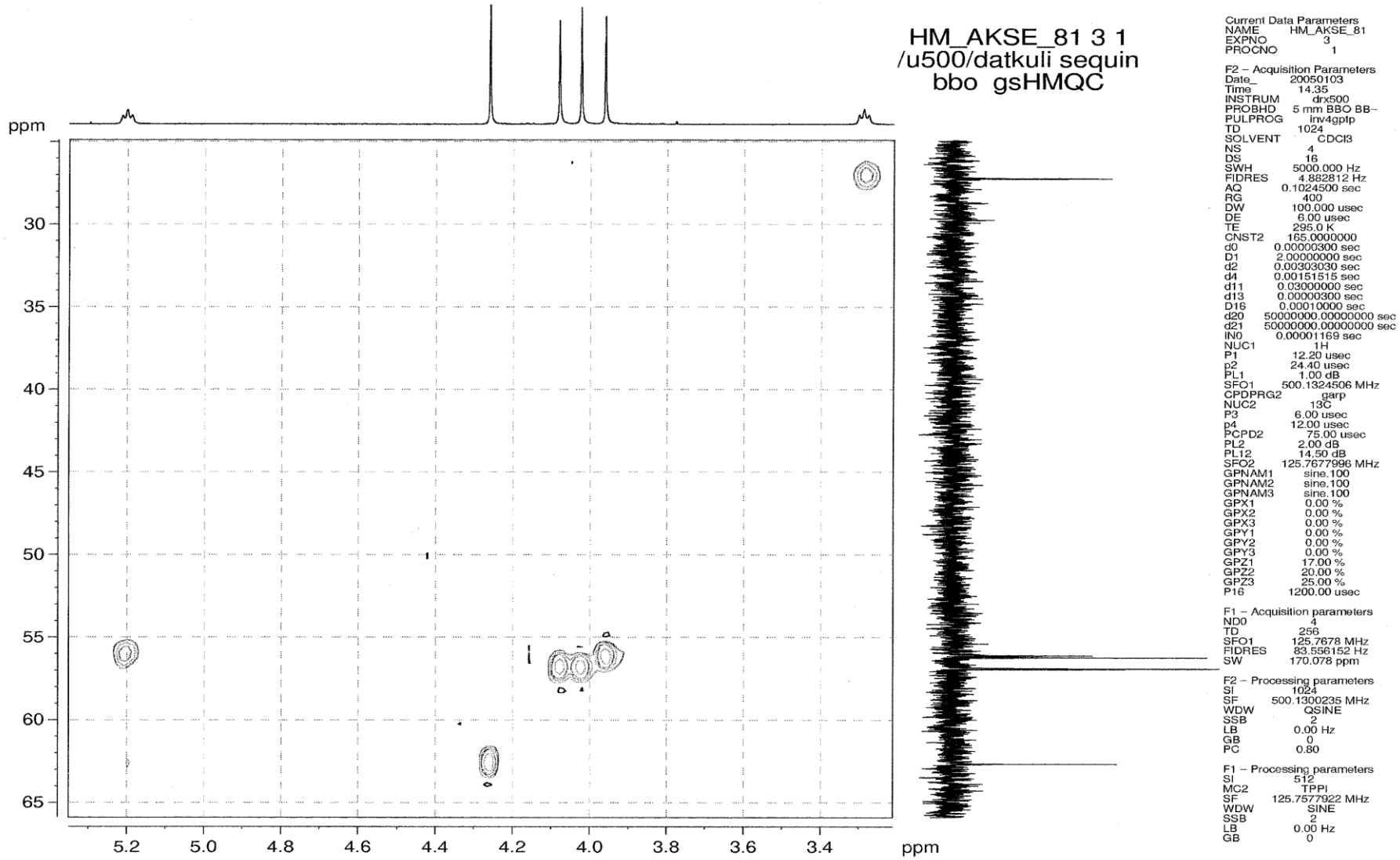
1D NMR plot parameters

CX	20.00 cm
F1P	177.787 ppm
F1	13417.16 Hz
F2P	3.896 ppm
F2	294.02 Hz
PPMCM	8.69454 ppm/cm
HZCM	656.15717 Hz/cm

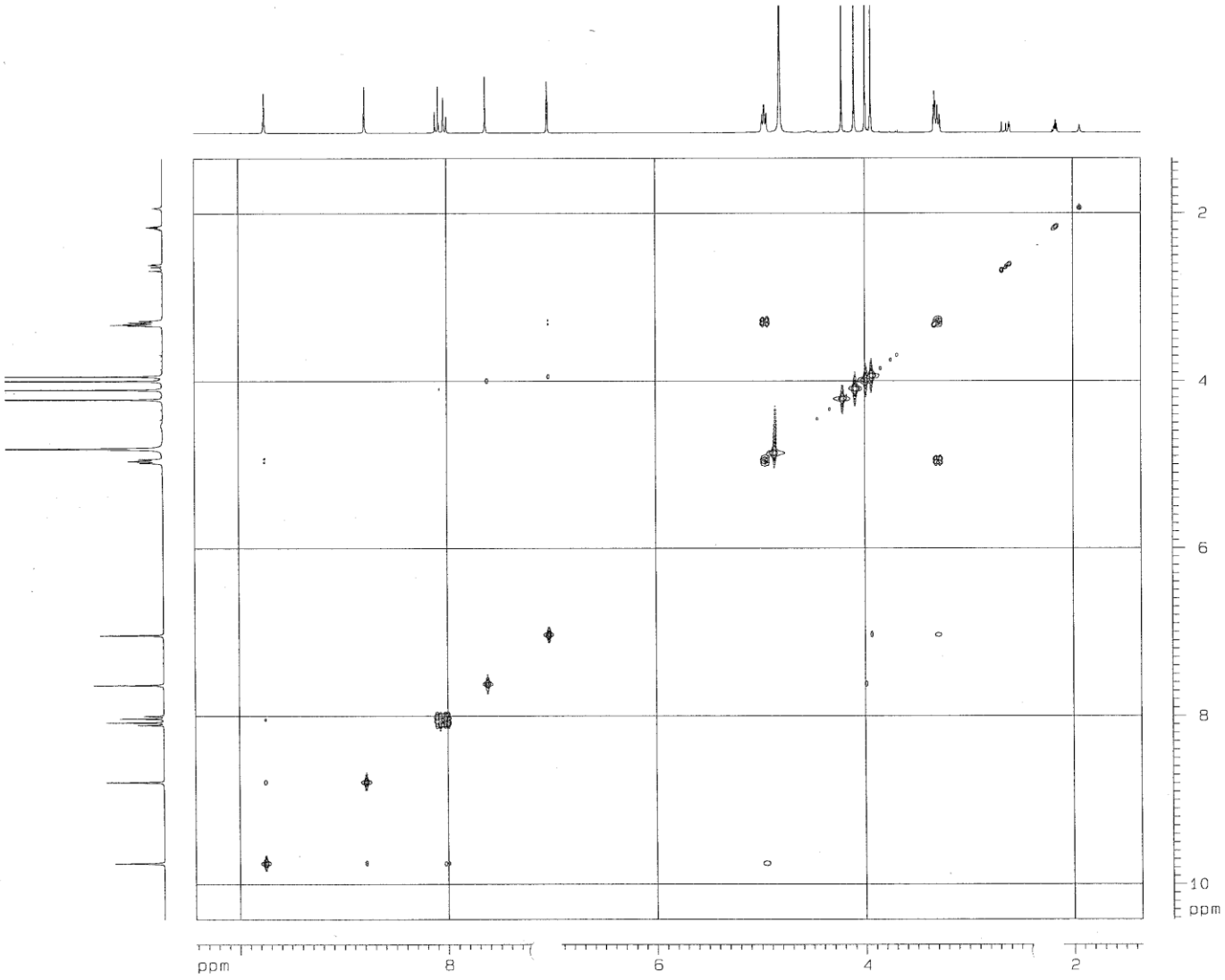
Appendix 4d (i): HMQC spectrum of palmatine (**82**)



Appendix 4d (ii): HMQC spectrum of palmatine (**82**)



Appendix 4e: COSY spectrum of palmatine (**82**)



AKSE8.1
University of Botswana
Chemistry Department
NABSA NMR Service

Current Data Parameters

NAME	akse81
EXPNO	13
PROCNO	1

F2 - Acquisition Parameters

Date_	20041007
Time	11.57
INSTRUM	spect
PROBHD	5 mm QNP 1H
PULPROG	cosygs
TD	2048
SOLVENT	MeOH
NS	16
DS	8
SWH	2723.312 Hz
FIDRES	1.329742 Hz
AQ	0.3760628 sec
RG	161.3
DW	183.600 usec
DE	6.00 usec
TE	300.0 K
d0	0.00000300 sec
D1	1.36769795 sec
d13	0.00000300 sec
D16	0.00010000 sec
IN0	0.00036720 sec

======== CHANNEL f1 ========

NUC1	1H
P0	10.25 usec
P1	10.25 usec
PL1	0.00 dB
SFO1	300.1317656 MHz

======== GRADIENT CHANNEL ========

P16	1000.00 usec

F1 - Acquisition parameters

ND0	1
TD	206
SFO1	300.1318 MHz
FIDRES	13.219959 Hz
SW	9.074 ppm

F2 - Processing parameters

SI	1024
SF	300.1300000 MHz
WDW	SINE
SSB	0
LB	0.00 Hz
GB	0
PC	1.40

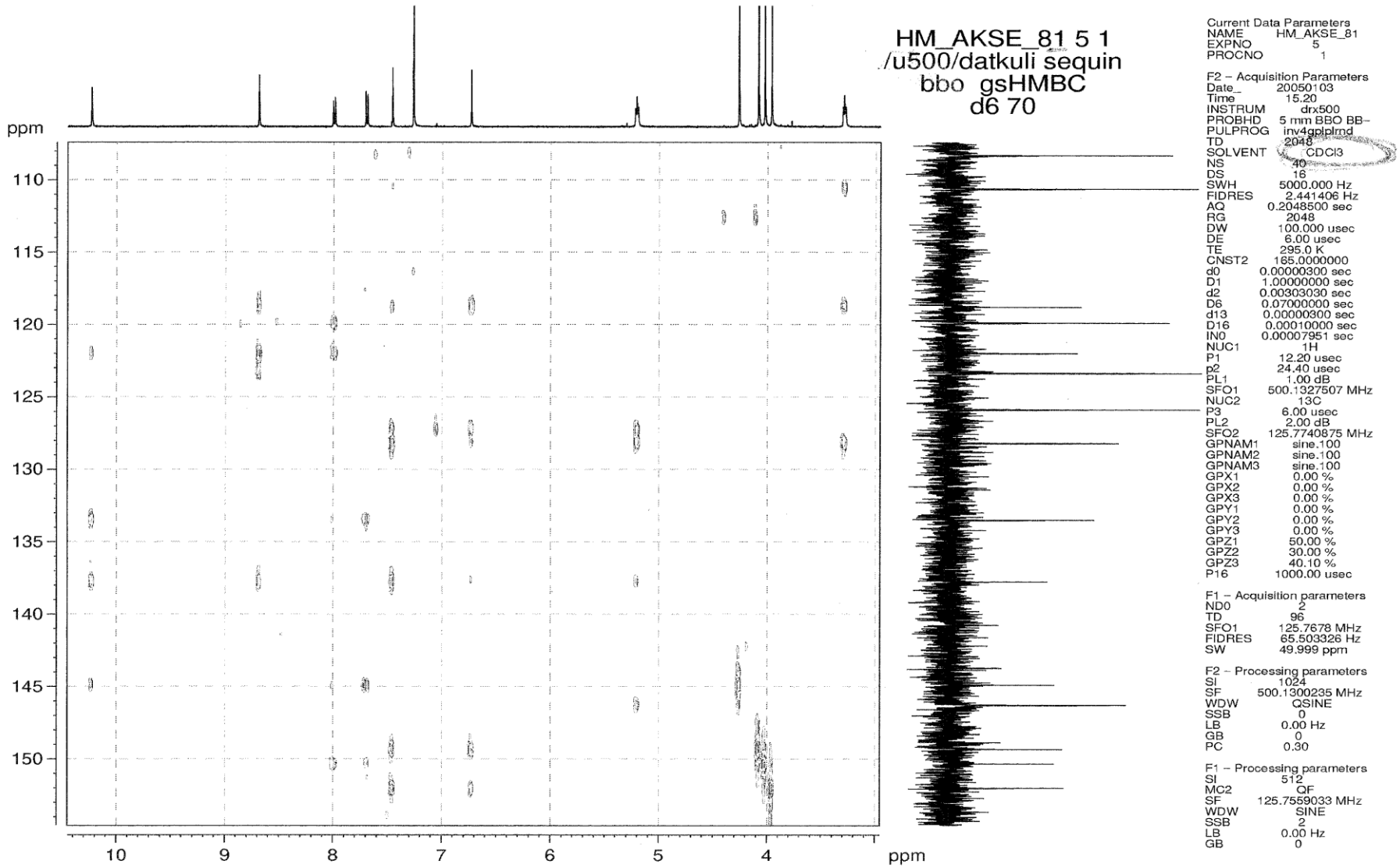
F1 - Processing parameters

SI	1024
MC2	QF
SF	300.1300000 MHz
WDW	SINE
SSB	0
LB	0.00 Hz
GB	0

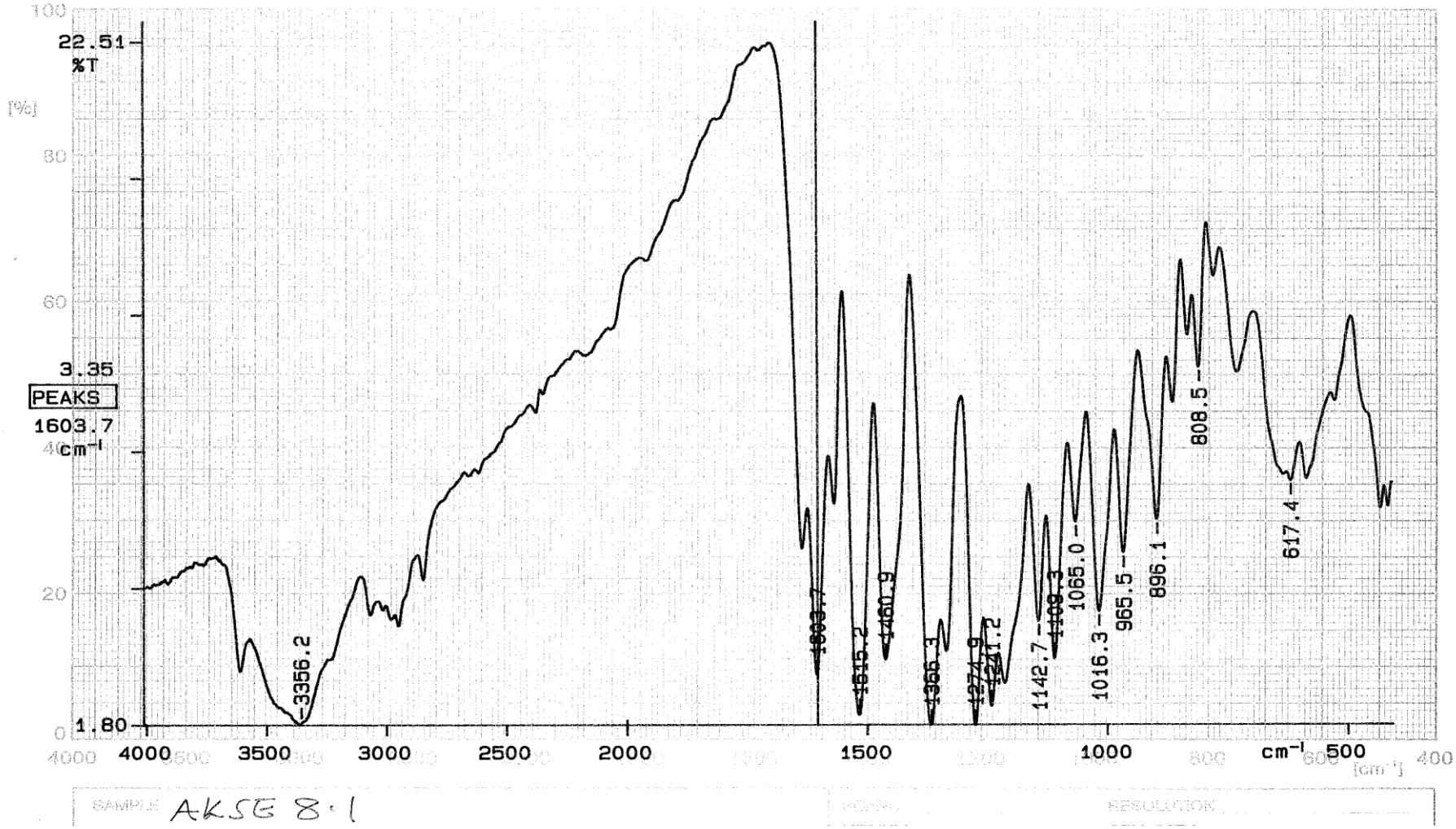
2D NMR plot parameters

CX2	15.00 cm
CX1	15.00 cm
F2PLO	10.420 ppm
F2LO	3127.26 Hz
F2PHI	1.346 ppm
F2HI	403.95 Hz
F1PLO	10.420 ppm
F1LO	3127.26 Hz
F1PHI	1.346 ppm
F1HI	403.95 Hz
F2PPMCM	0.60492 ppm/cm
F2HZCM	181.55411 Hz/cm
F1PPMCM	0.60492 ppm/cm
F1HZCM	181.55411 Hz/cm

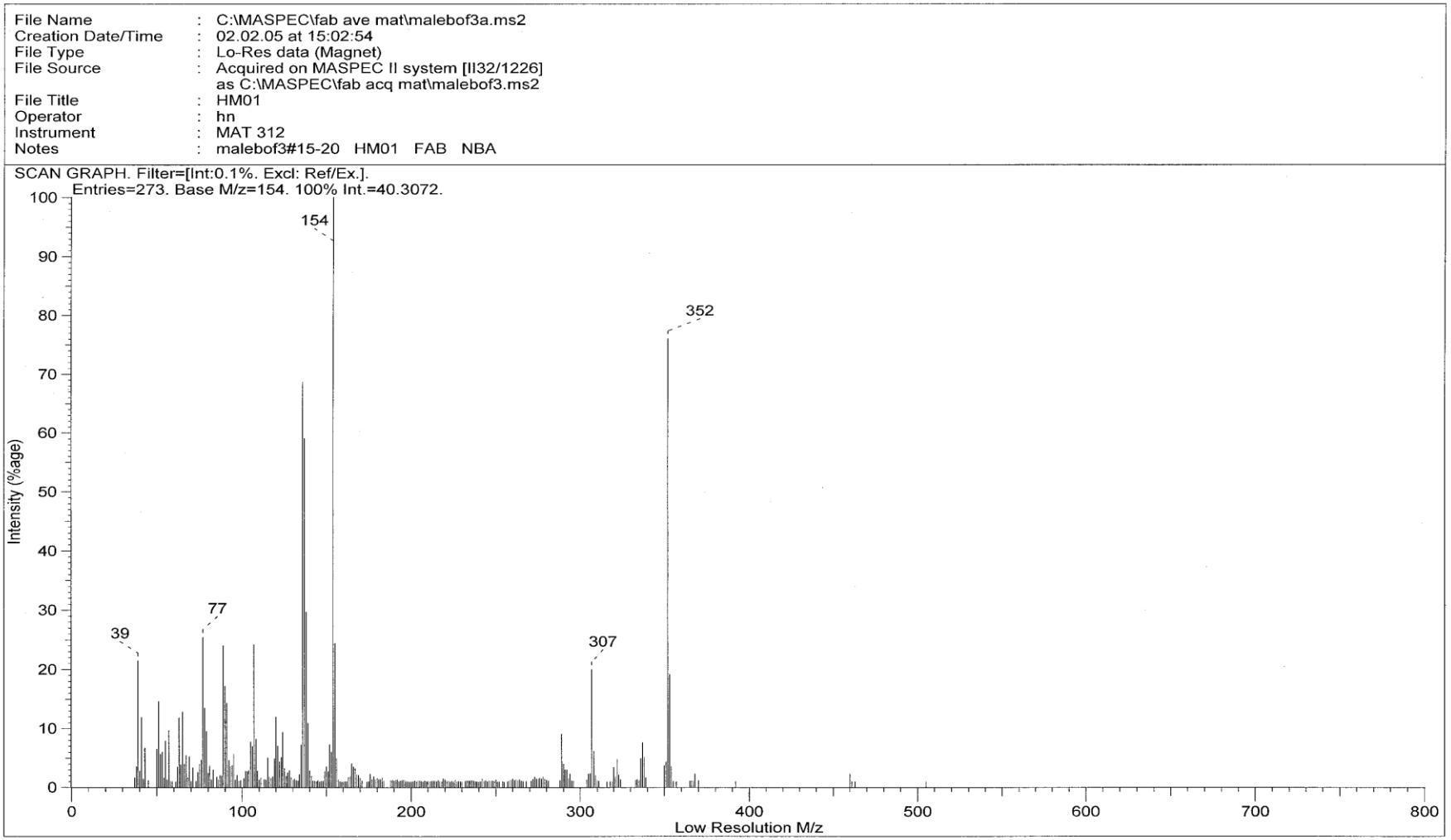
Appendix 4f: HMBC spectrum of palmatine (**82**)



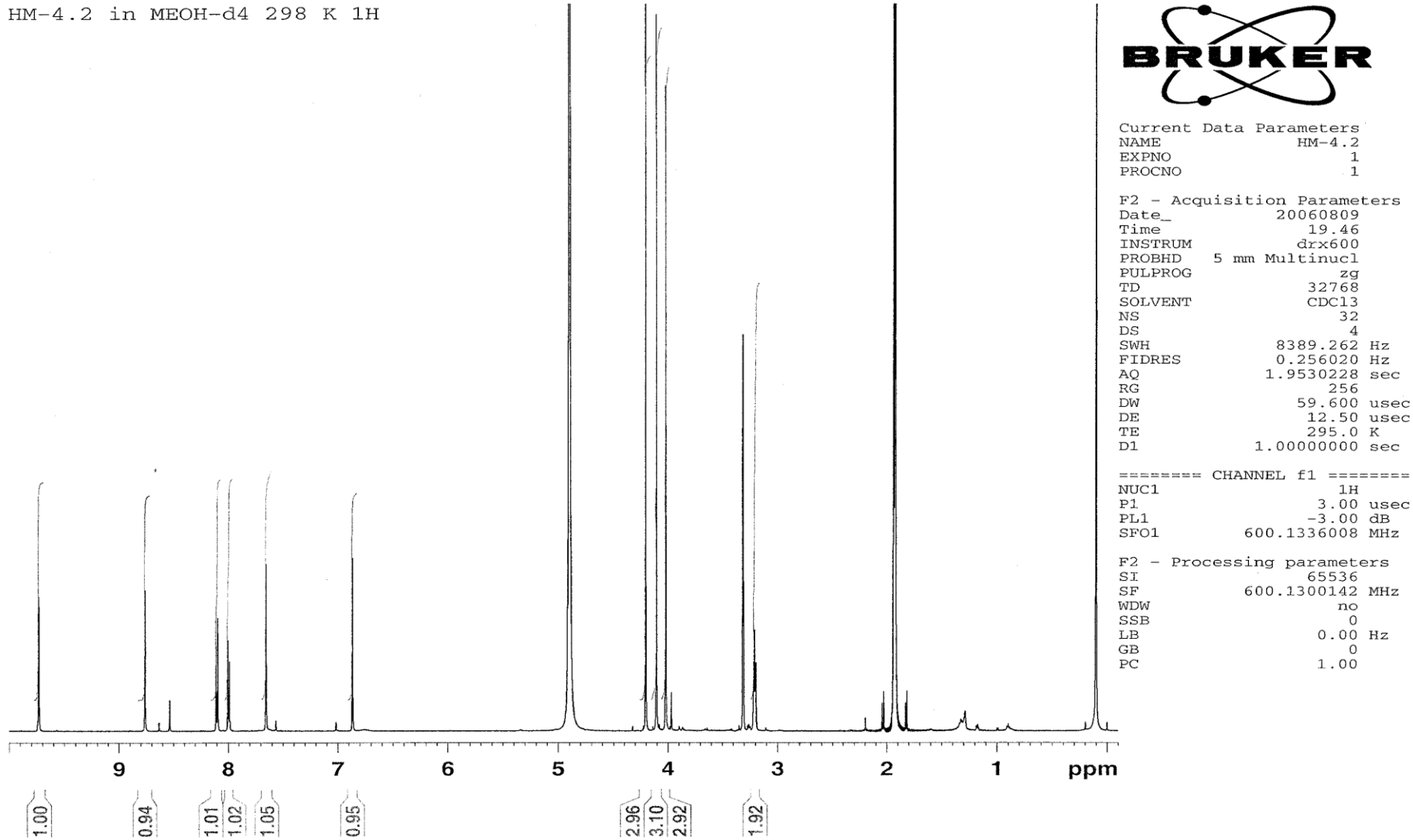
Appendix 4g: IR spectrum of palmatine (**82**)



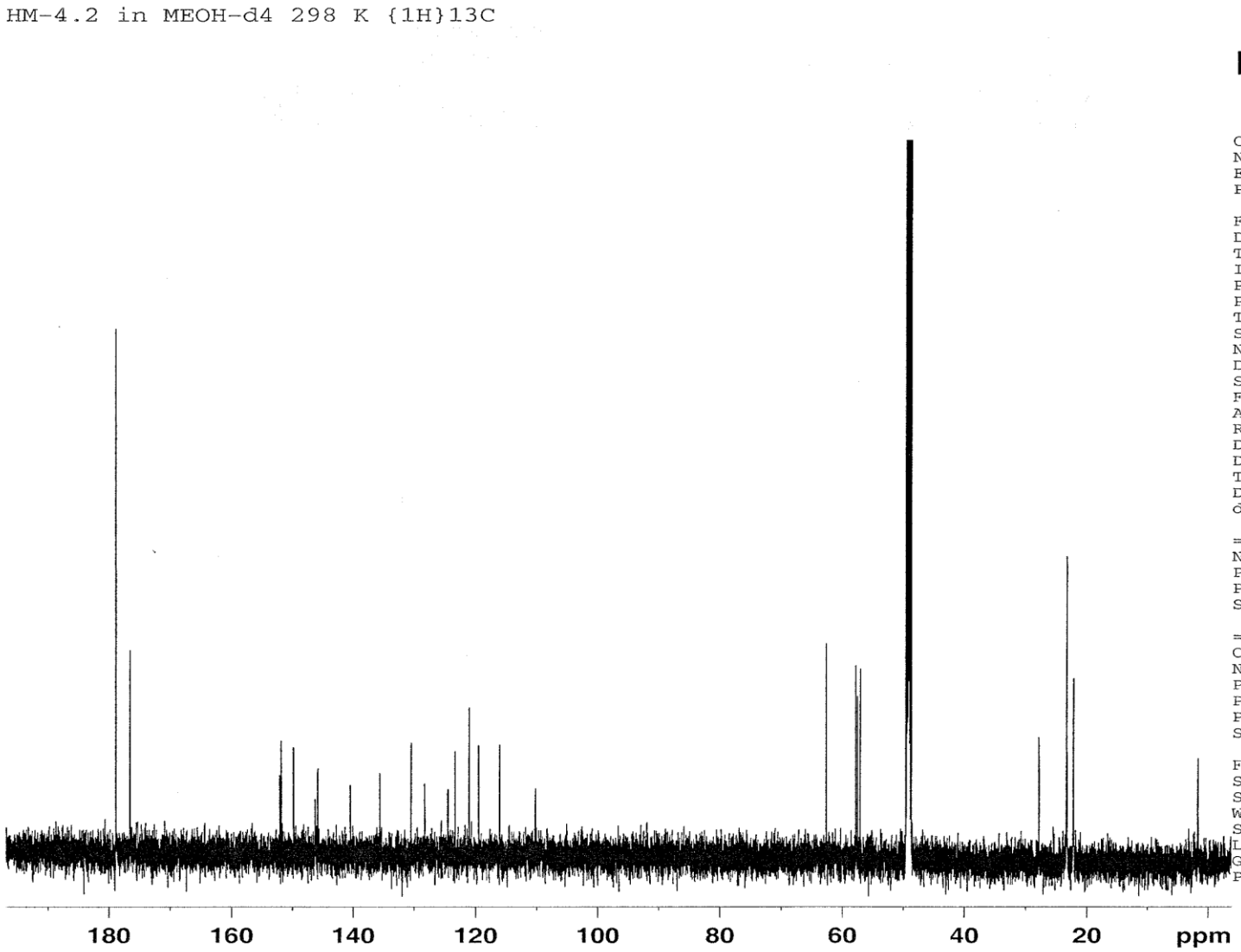
Appendix 4h: MS spectrum of palmatine (**82**)



Appendix 5a: ^{1}H NMR spectrum of jatrorrhizine (**83**)



Appendix 5b: ^{13}C NMR spectrum of jatrorrhizine (**83**)



BRUKER

```
Current Data Parameters
NAME                  HM-4.2
EXPNO                      6
PROCNO                     1

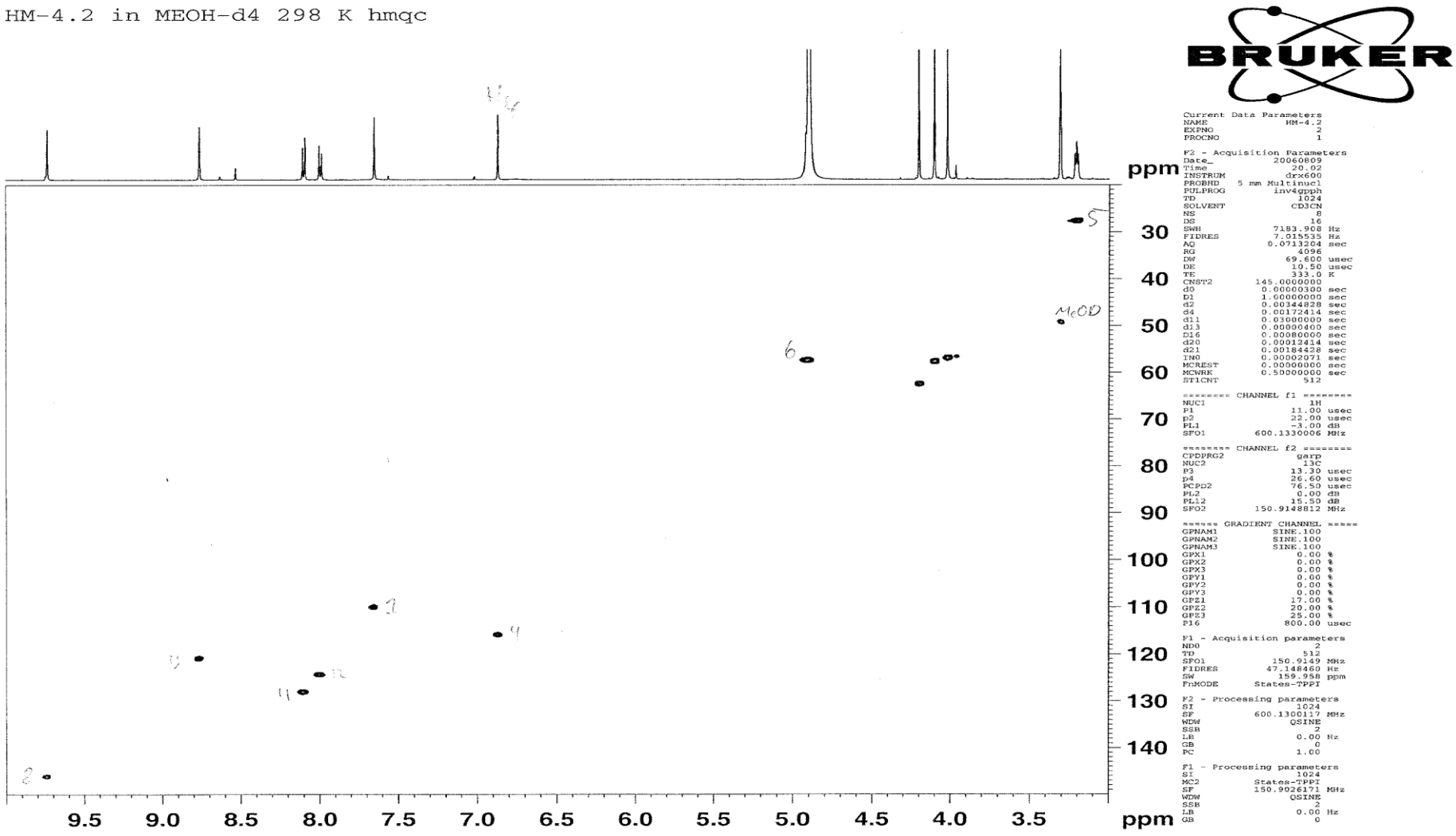
F2 - Acquisition Parameters
Date_              20060810
Time                  16.15
INSTRUM              drx600
PROBHD    5 mm Multinucl
PULPROG              zgdc30
TD                    65536
SOLVENT               CD3CN
NS                     2048
DS                        1
SWH               30303.031 Hz
FIDRES             0.462388 Hz
AQ                1.0813940 sec
RG                     4096
DW                  16.500 usec
DE                  12.50 usec
TE                   295.0 K
D1              1.50000000 sec
d11             0.03000000 sec

======== CHANNEL f1 ========
NUC1                    13C
P1                   13.50 usec
PL1                  -3.00 dB
SFO1          150.9171448 MHz

======== CHANNEL f2 ========
CPDPRG2              mlev16
NUC2                    1H
PCPD2                75.00 usec
PL2                   0.00 dB
PL12                 15.00 dB
SFO2          600.1330006 MHz

F2 - Processing parameters
SI                    65536
SF            150.9025752 MHz
WDW                      EM
SSB                       0
LB                     1.00 Hz
GB                        0
PC                     1.00
```

Appendix 5c: HMQC spectrum of jatrorrhizine (**83**)




```
Current Data Parameters
NAME                  HM-4.2
EXPNO                      2
PROCNO                     1

F2 - Acquisition Parameters
Date_              20060809
Time                  20.02
INSTRUM             drx600
PROBHD    5 mm Multinucl
PULPROG           inv4gpph
TD                    1024
SOLVENT               CD3CN
NS                        8
DS                       16
SWH                7183.908 Hz
FIDRES             7.015535 Hz
AQ                 0.0713204 sec
RG                      4096
DW                   69.600 usec
DE                   10.50 usec
TE                   333.0 K
CNST2            145.0000000
d0                0.00000300 sec
D1                1.00000000 sec
d2                0.00344828 sec
d4                0.00172414 sec
d11               0.03000000 sec
d13               0.00000400 sec
D16               0.00080000 sec
d20               0.00012414 sec
d21               0.00184428 sec
IN0               0.00002071 sec
MCREST            0.00000000 sec
MCWRK             0.50000000 sec
ST1CNT                   512

======== CHANNEL f1 ========
NUC1                     1H
P1                    11.00 usec
p2                    22.00 usec
PL1                   -3.00 dB
SFO1             600.1330006 MHz

======== CHANNEL f2 ========
CPDPRG2                garp
NUC2                    13C
P3                    13.30 usec
p4                    26.60 usec
PCPD2                 76.50 usec
PL2                    0.00 dB
PL12                  15.50 dB
SFO2             150.9148812 MHz

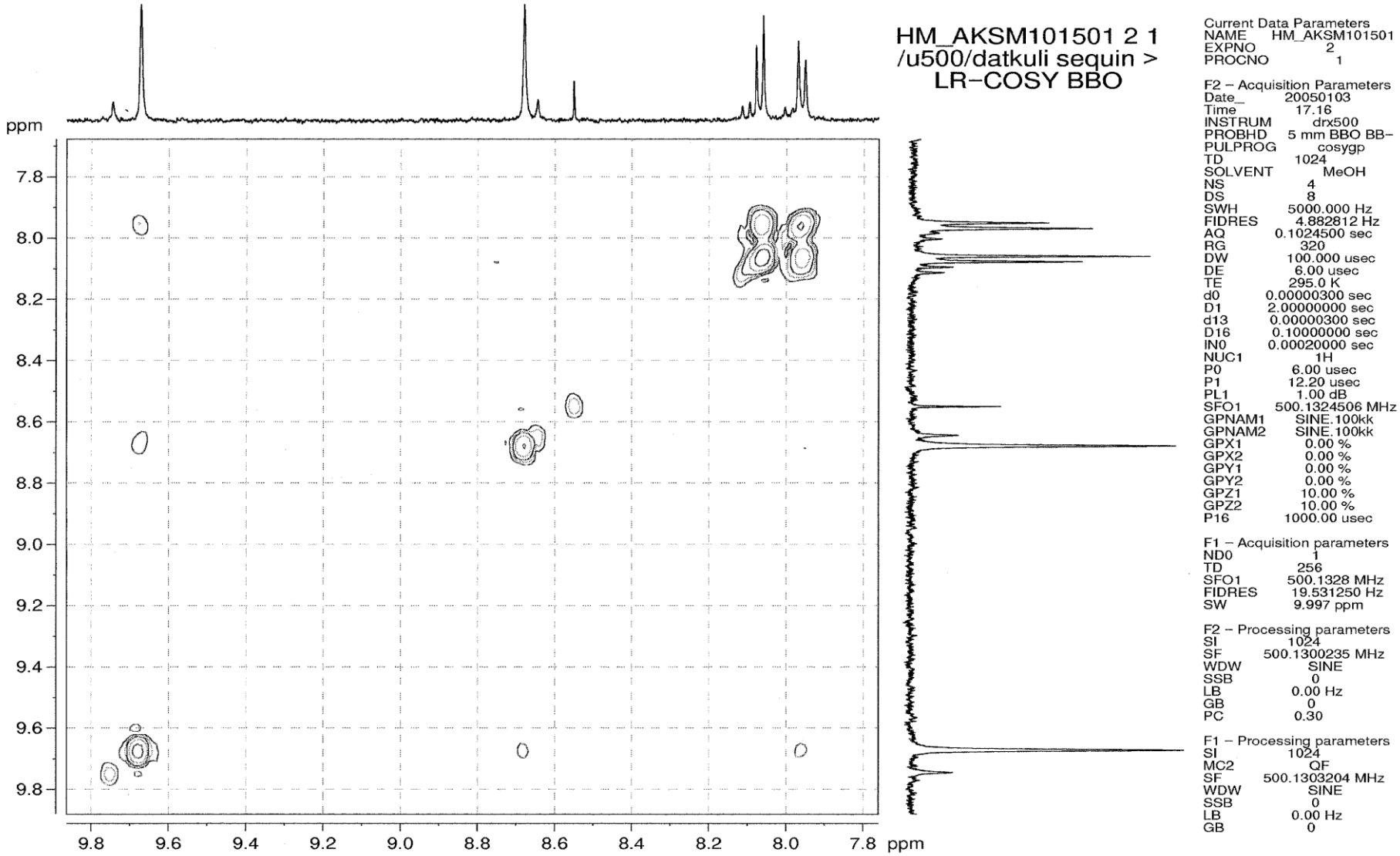
====== GRADIENT CHANNEL =====
GPNAM1             SINE.100
GPNAM2             SINE.100
GPNAM3             SINE.100
GPX1                   0.00 %
GPX2                   0.00 %
GPX3                   0.00 %
GPY1                   0.00 %
GPY2                   0.00 %
GPY3                   0.00 %
GPZ1                  17.00 %
GPZ2                  20.00 %
GPZ3                  25.00 %
P16                  800.00 usec

F1 - Acquisition parameters
ND0                       2
TD                      512
SFO1             150.9149 MHz
FIDRES           47.148460 Hz
SW               159.958 ppm
FnMODE        States-TPPI

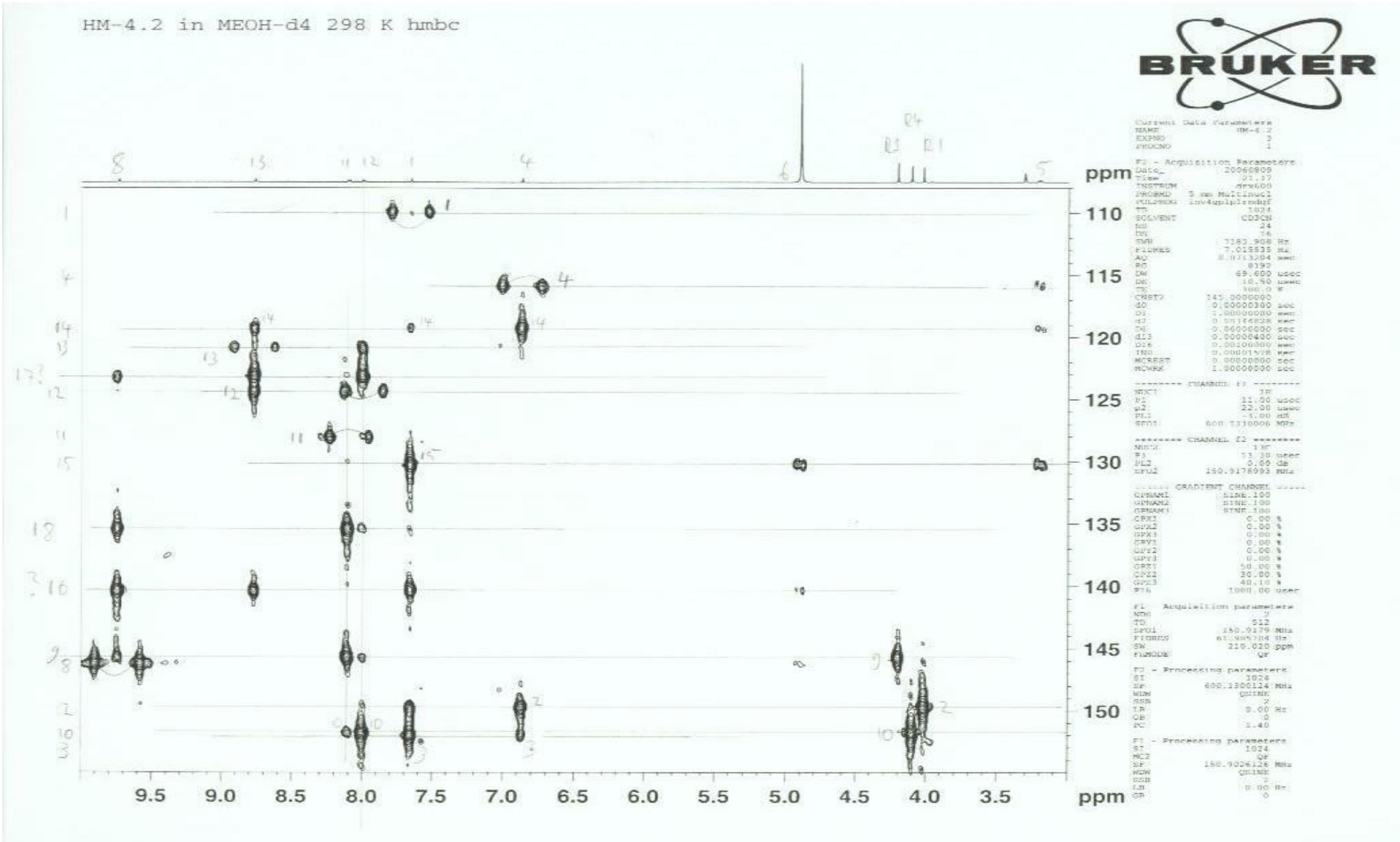
F2 - Processing parameters
SI                      1024
SF               600.1300117 MHz
WDW                    QSINE
SSB                        2
LB                    0.00 Hz
GB                         0
PC                     1.00

F1 - Processing parameters
SI                      1024
MC2           States-TPPI
SF               150.9026171 MHz
WDW                    QSINE
SSB                        2
LB                    0.00 Hz
GB                         0
```

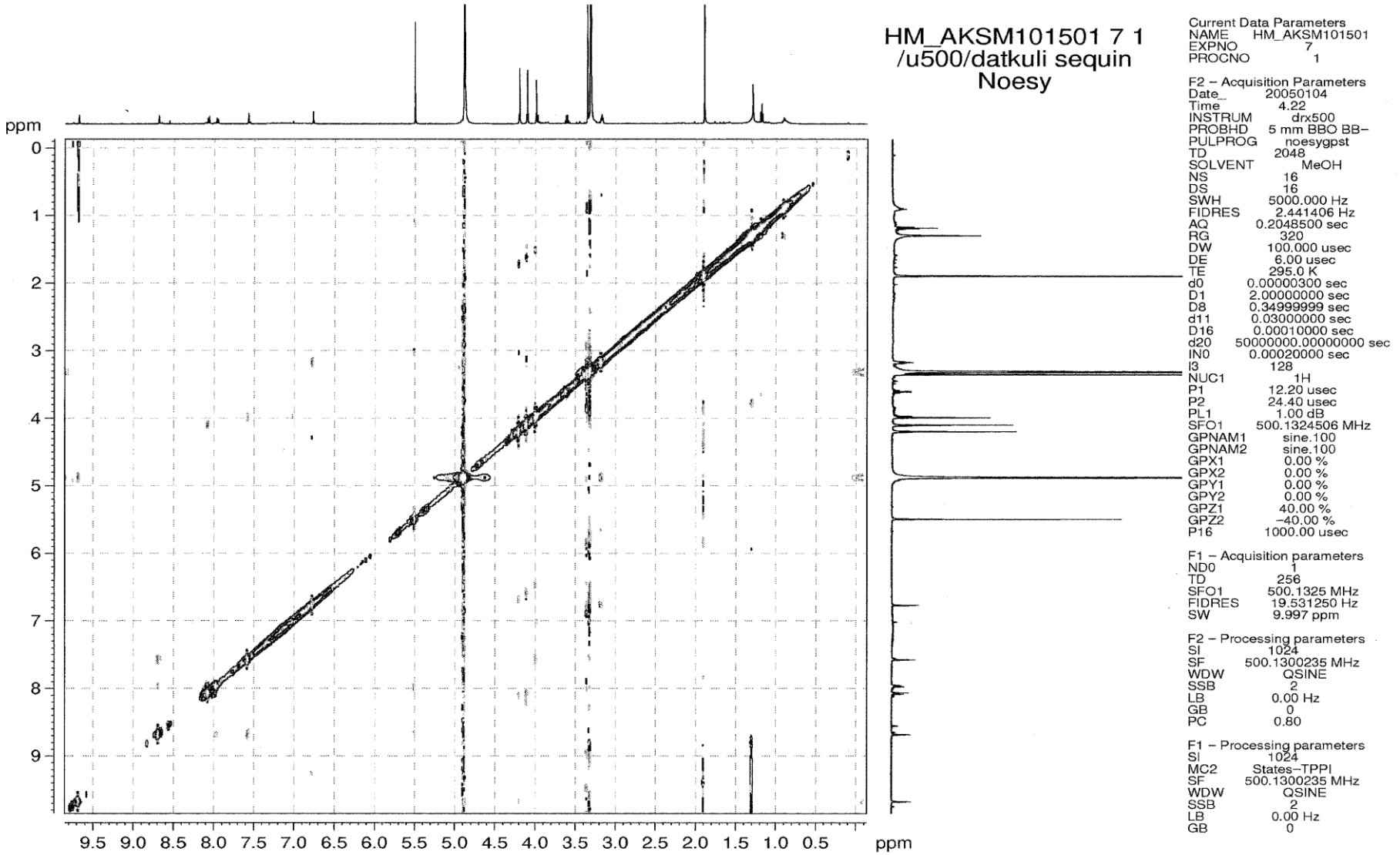
Appendix 5d: COSY spectrum of jatrorrhizine (**83**)



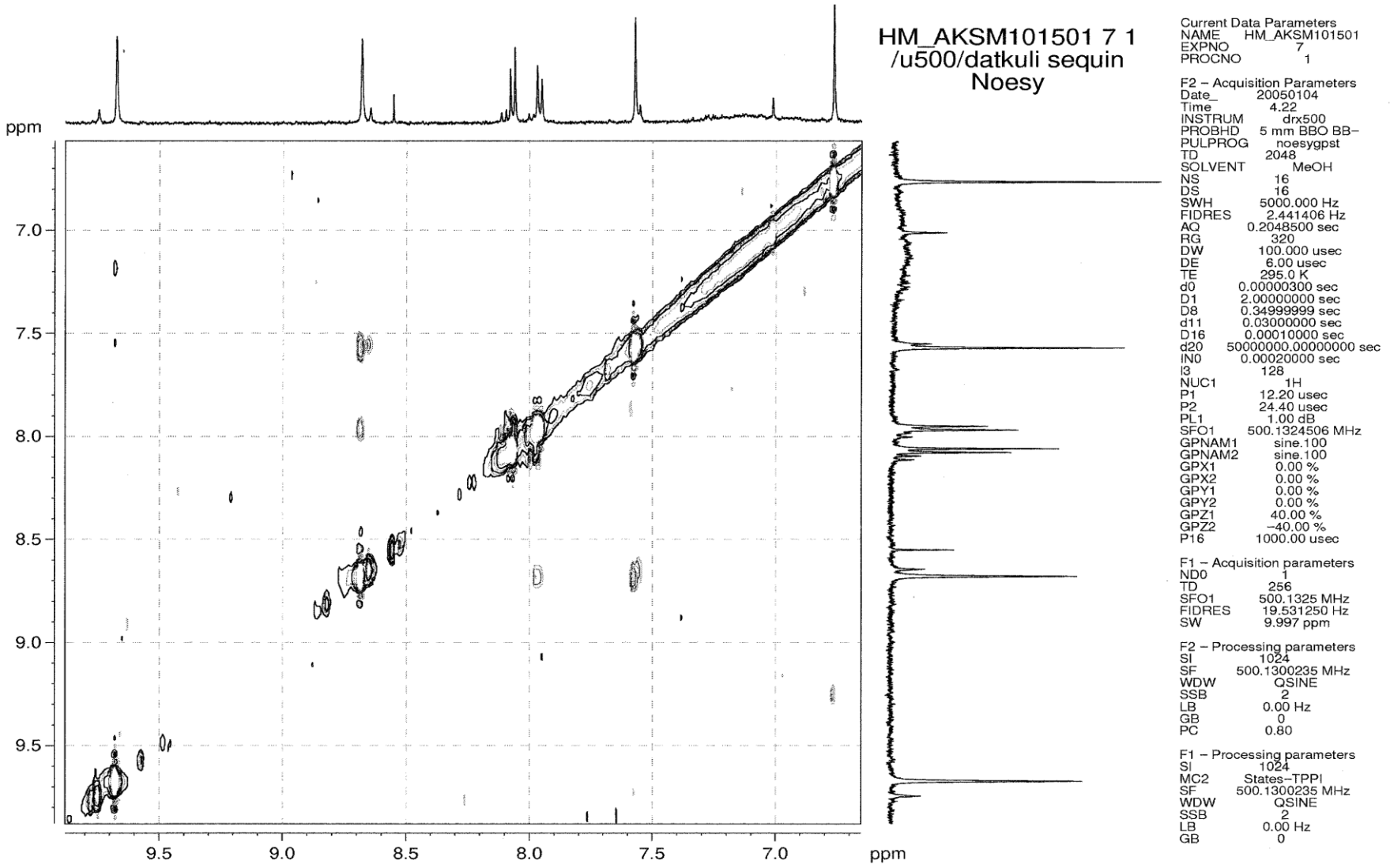
Appendix 5e: HMBC spectrum of jatrorrhizine (**83**)



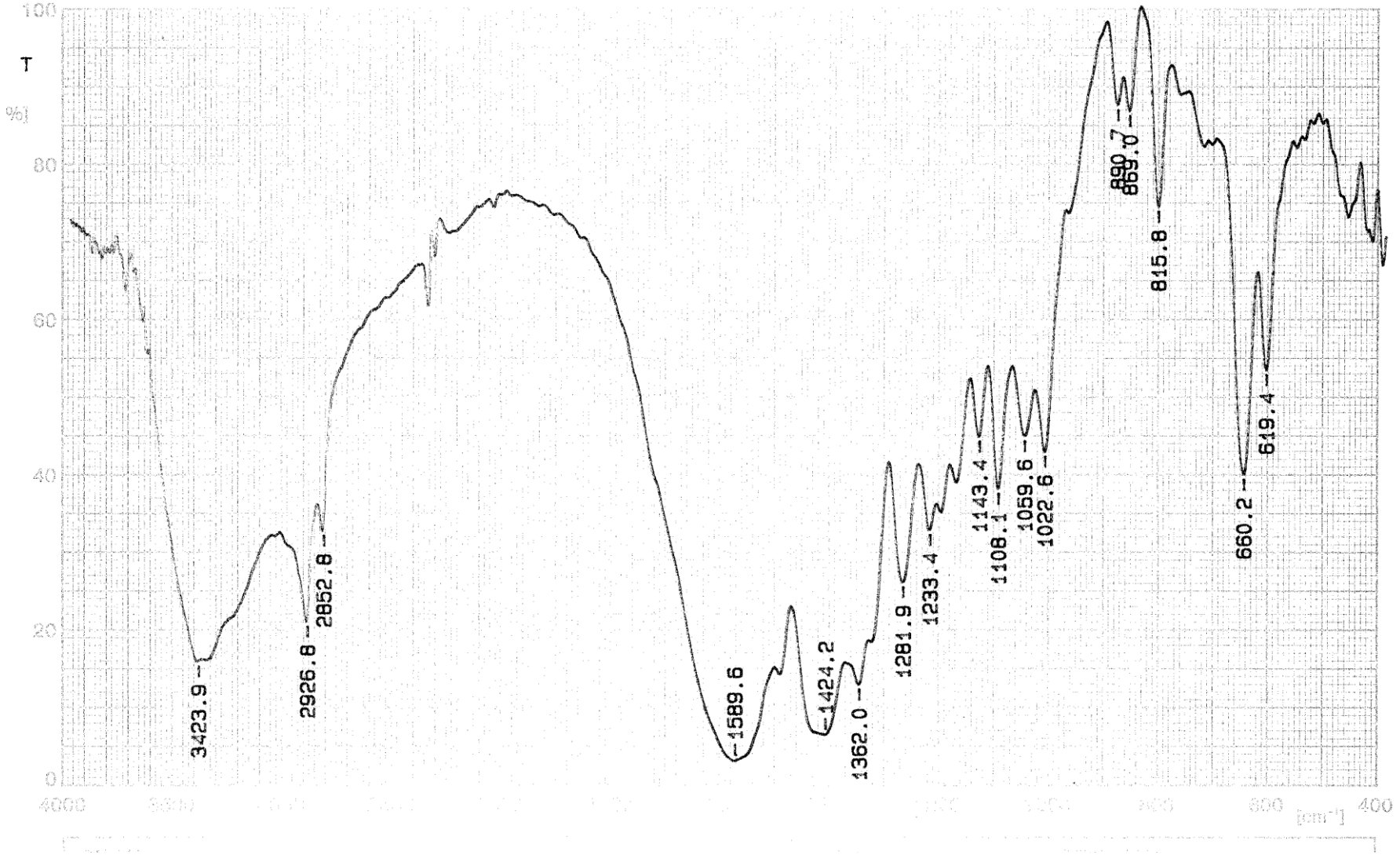
Appendix 5f (i): NOESY spectrum of jatrorrhizine (**83**)



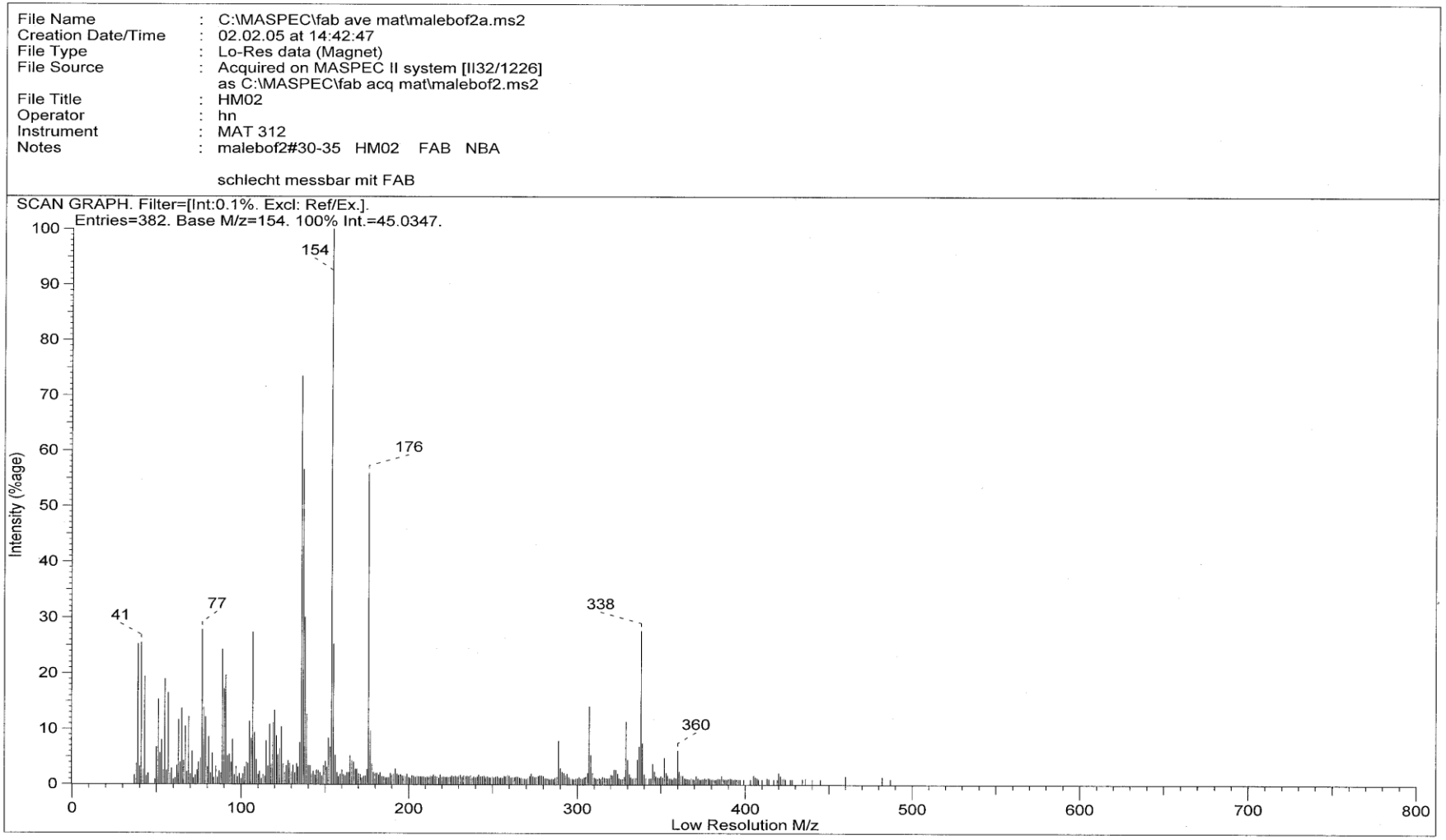
Appendix 5f (ii): NOESY spectrum of jatrorrhizine (**83**)



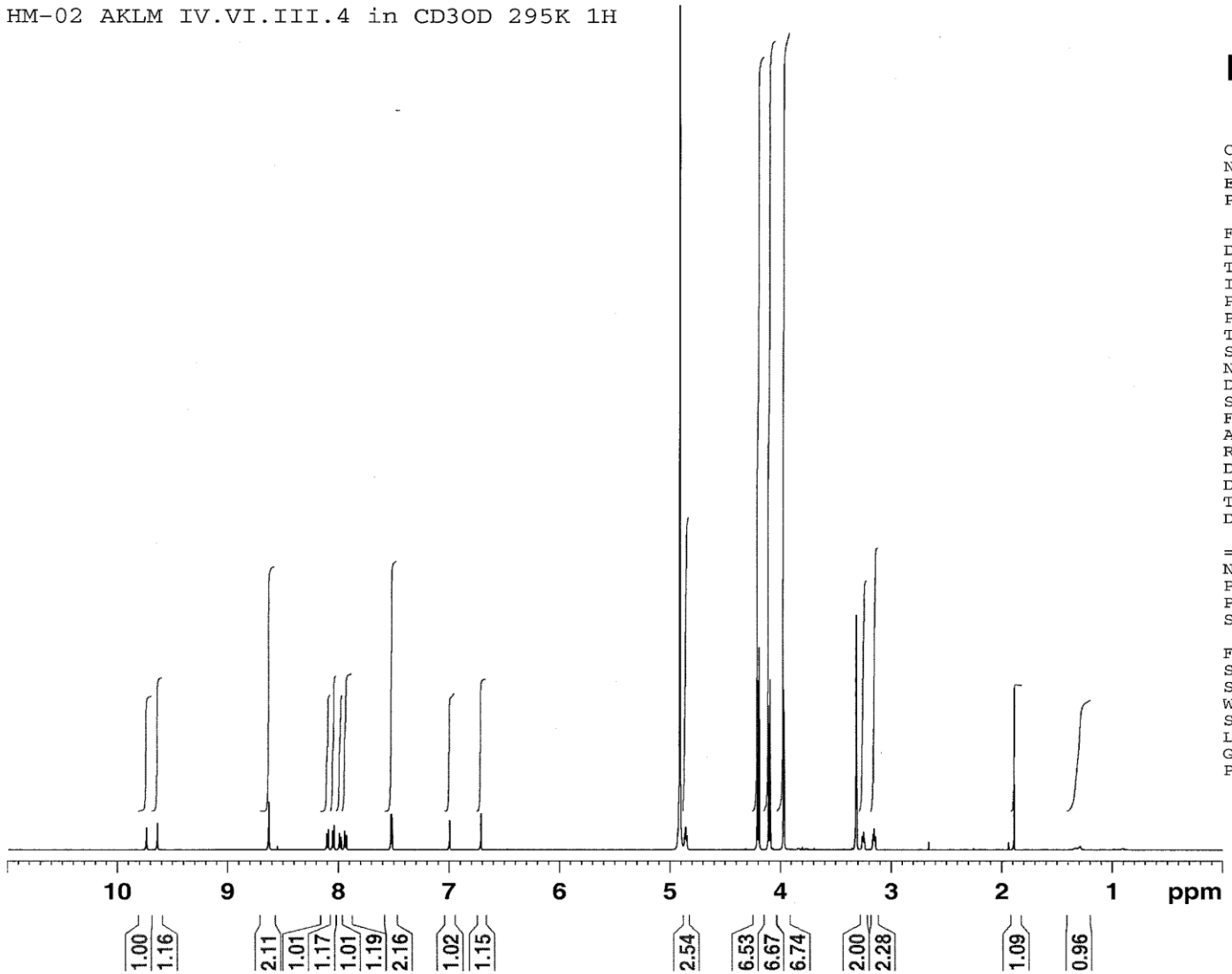
Appendix 5g: IR spectrum of jatrorrhizine (**83**)



Appendix 5h: MS spectrum of jatrorrhizine (**83**)



Appendix 6a: ^{1}H NMR spectrum of a mixture of jatrorrhizine (**83**) and columbamine (**130**)



BRUKER

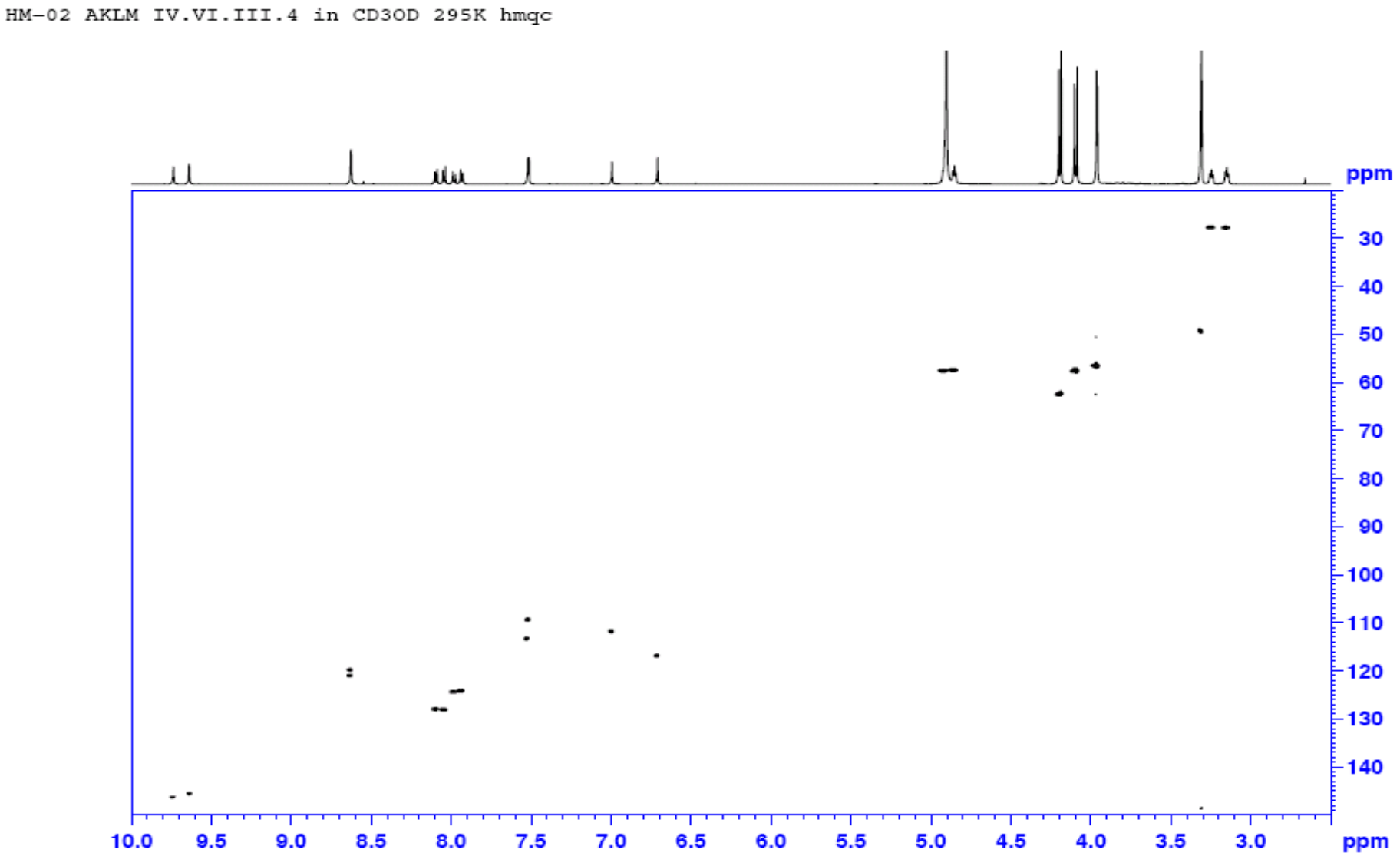
Current Data Parameters
NAME HM-02
EXPNO 1
PROCNO 1

F2 - Acquisition Parameters
Date_ 20061013
Time 16.03
INSTRUM drx600
PROBHD 5 mm Multinucl
PULPROG zg
TD 43102
SOLVENT MeOD
NS 32
DS 4
SWH 6613.757 Hz
FIDRES 0.153444 Hz
AQ 3.2585611 sec
RG 1024
DW 75.600 usec
DE 12.50 usec
TE 295.0 K
D1 1.00000000 sec

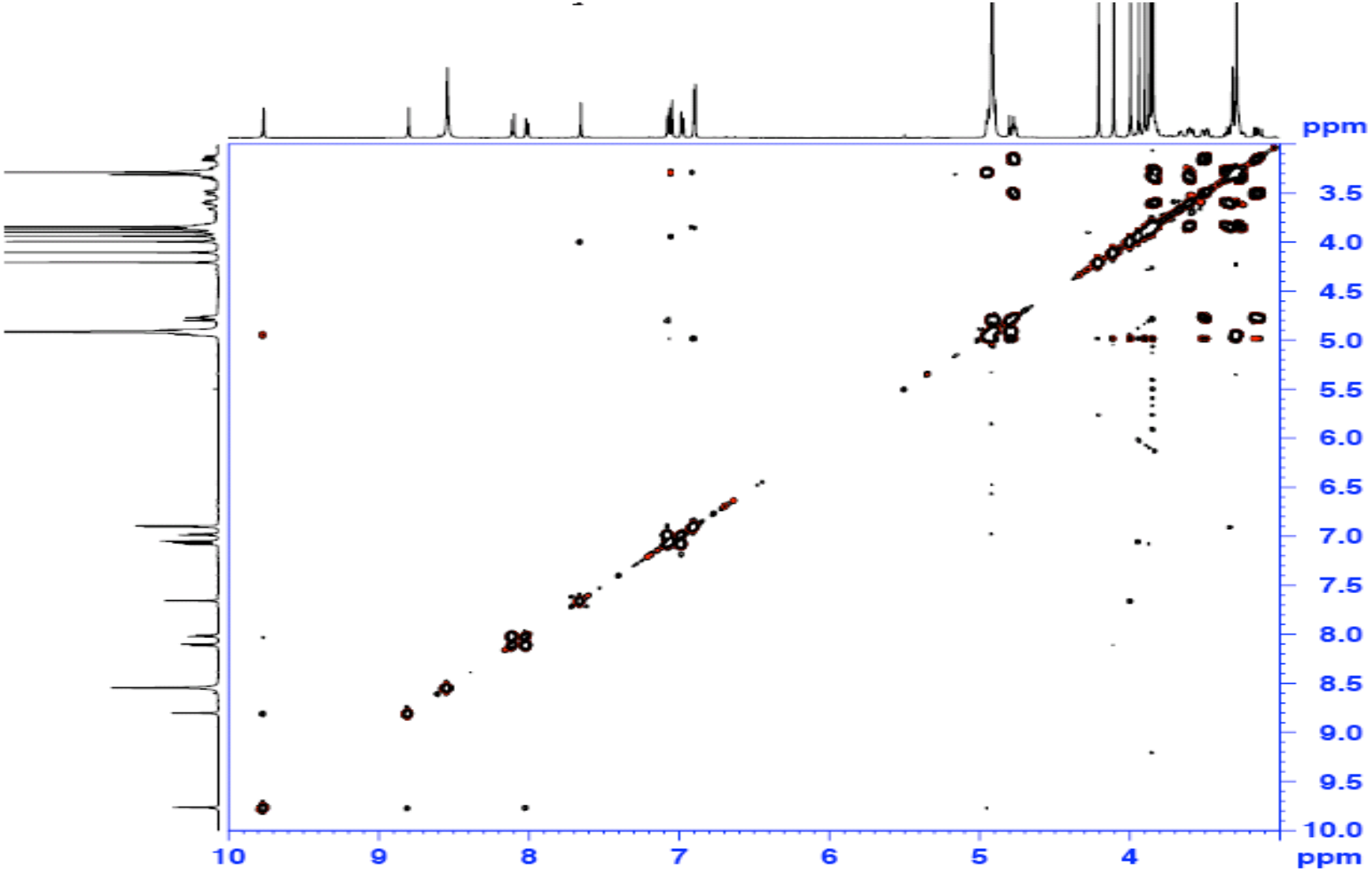
======== CHANNEL f1 ========
NUC1 1H
P1 3.00 usec
PL1 -3.00 dB
SFO1 600.1333007 MHz

F2 - Processing parameters
SI 131072
SF 600.1300142 MHz
WDW no
SSB 0
LB 0.00 Hz
GB 0
PC 1.00

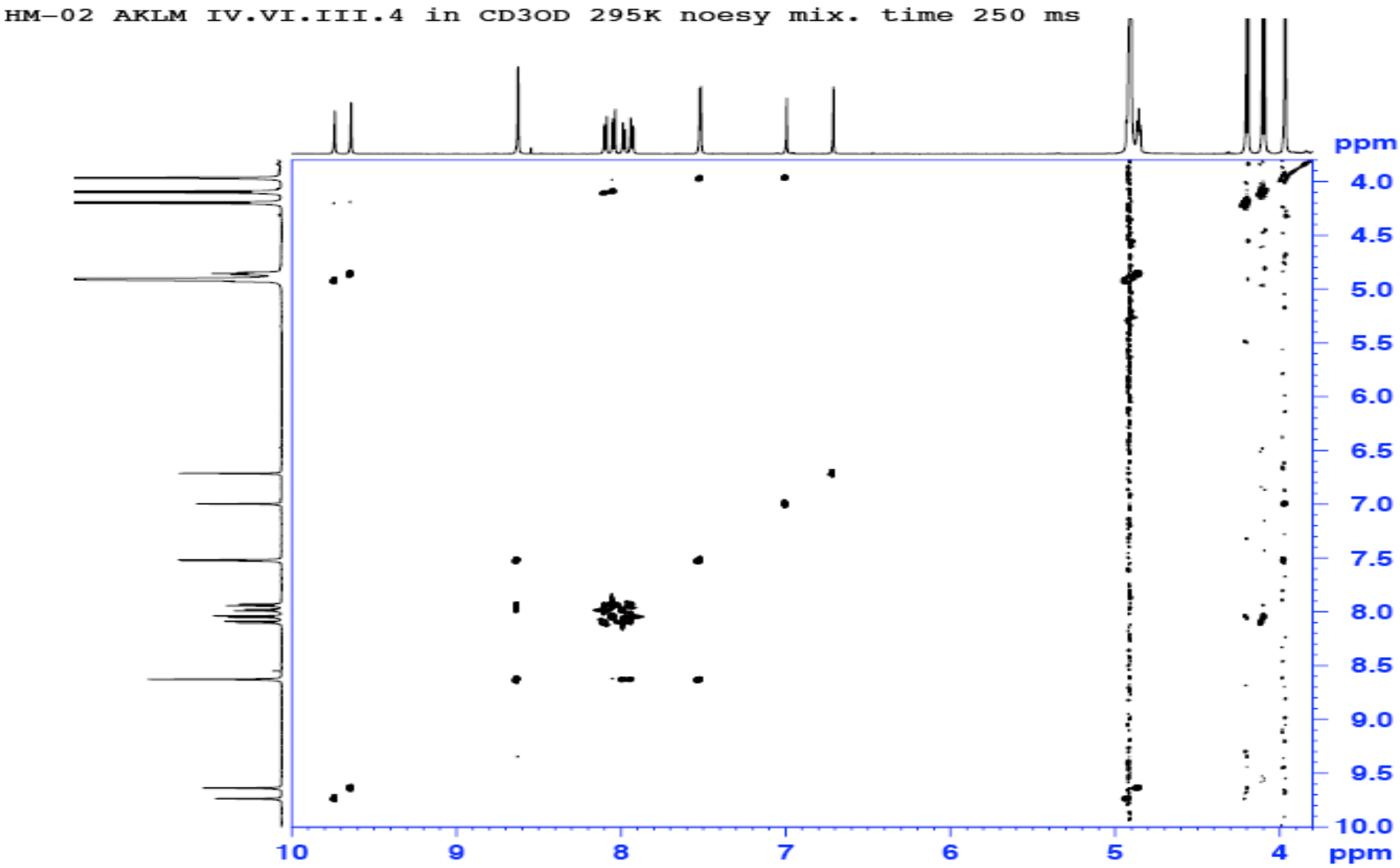
Appendix 6b: HMQC spectrum of a mixture of jatrorrhizine (**83**) and columbamine (**130**)



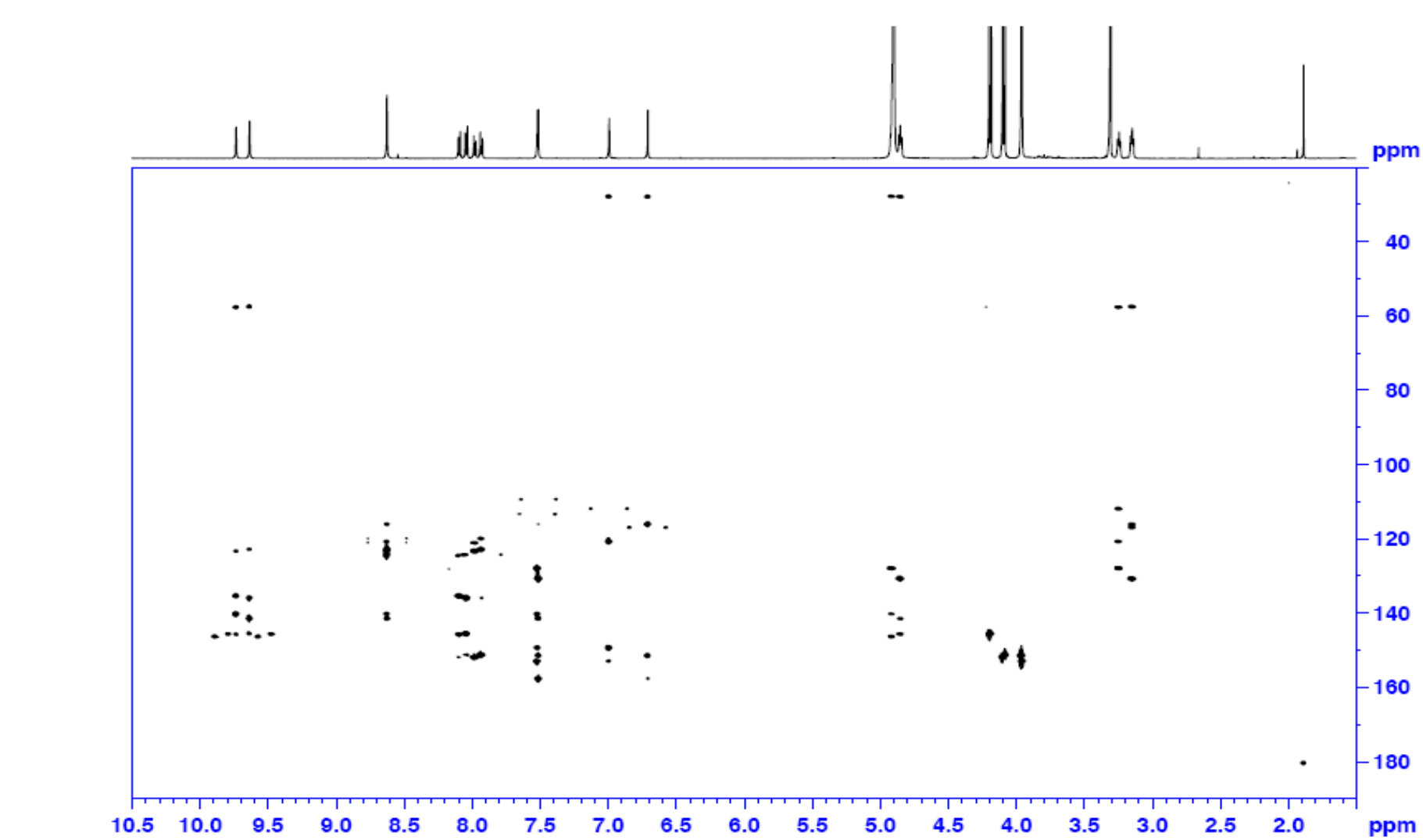
Appendix 6c: COSY spectrum of a mixture of jatrorrhizine (**83**) and columbamine (**130**)



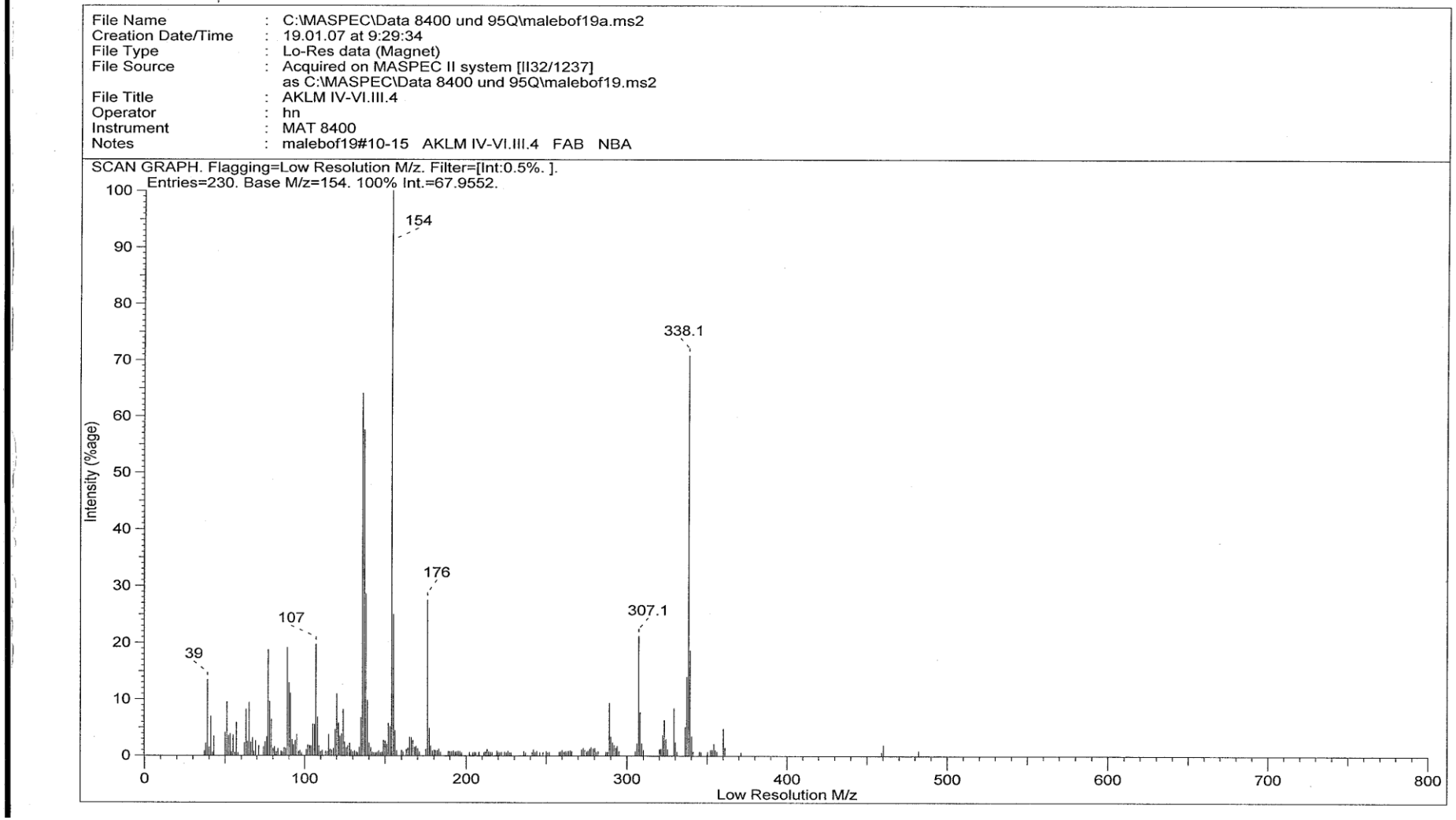
Appendix 6d: NOESY spectrum of a mixture of jatrorrhizine (**83**) and columbamine (**130**)



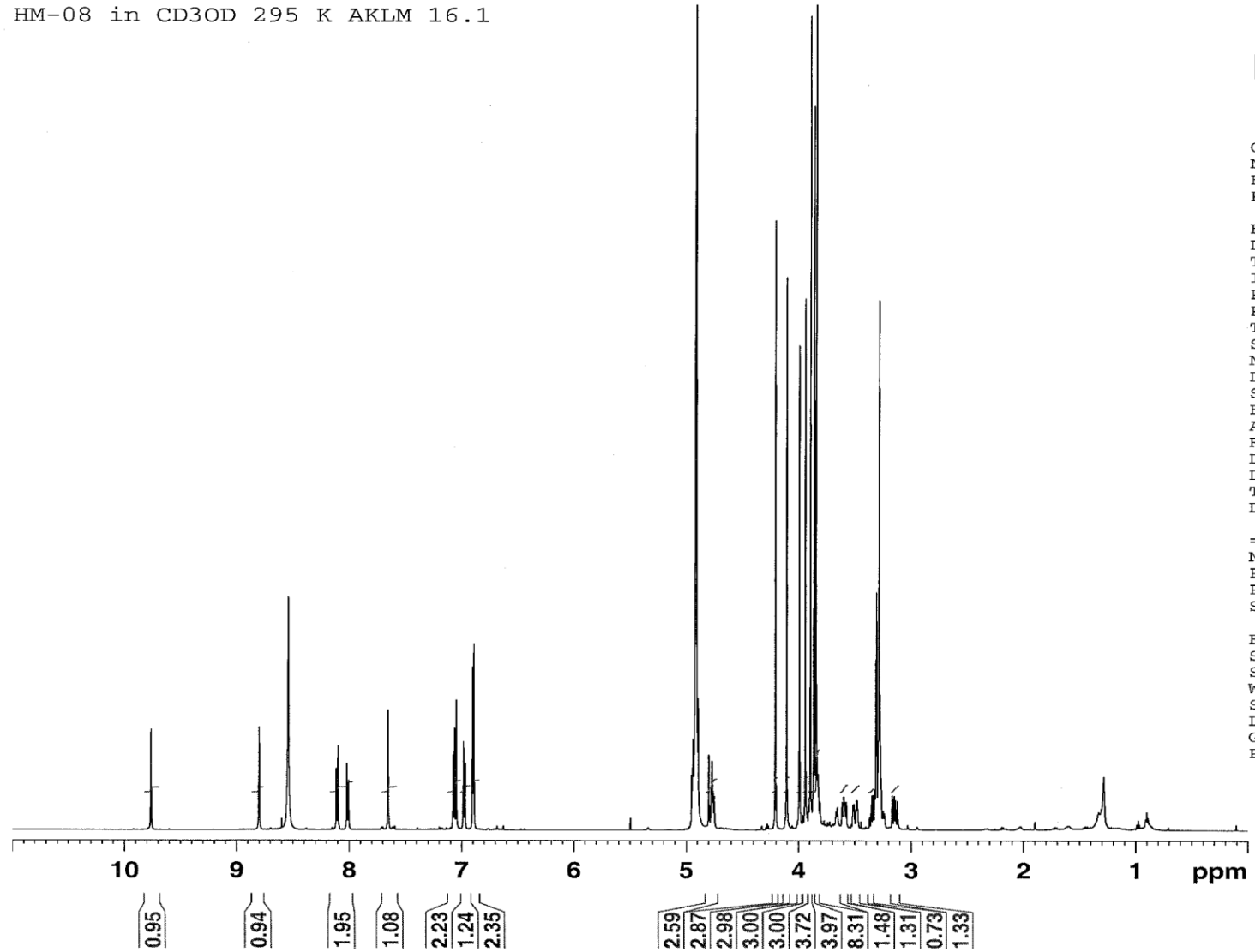
Appendix 6e: HMBC spectrum of a mixture of jatrorrhizine (**83**) and columbamine (**130**)



Appendix 6f: MS spectrum of a mixture of jatrorrhizine (**83**) and columbamine (**130**)



Appendix 7a: ^{1}H NMR spectrum of a mixture of palmatine (**82**) and (−) - tetrahydropalmatine (**131**)



BRUKER

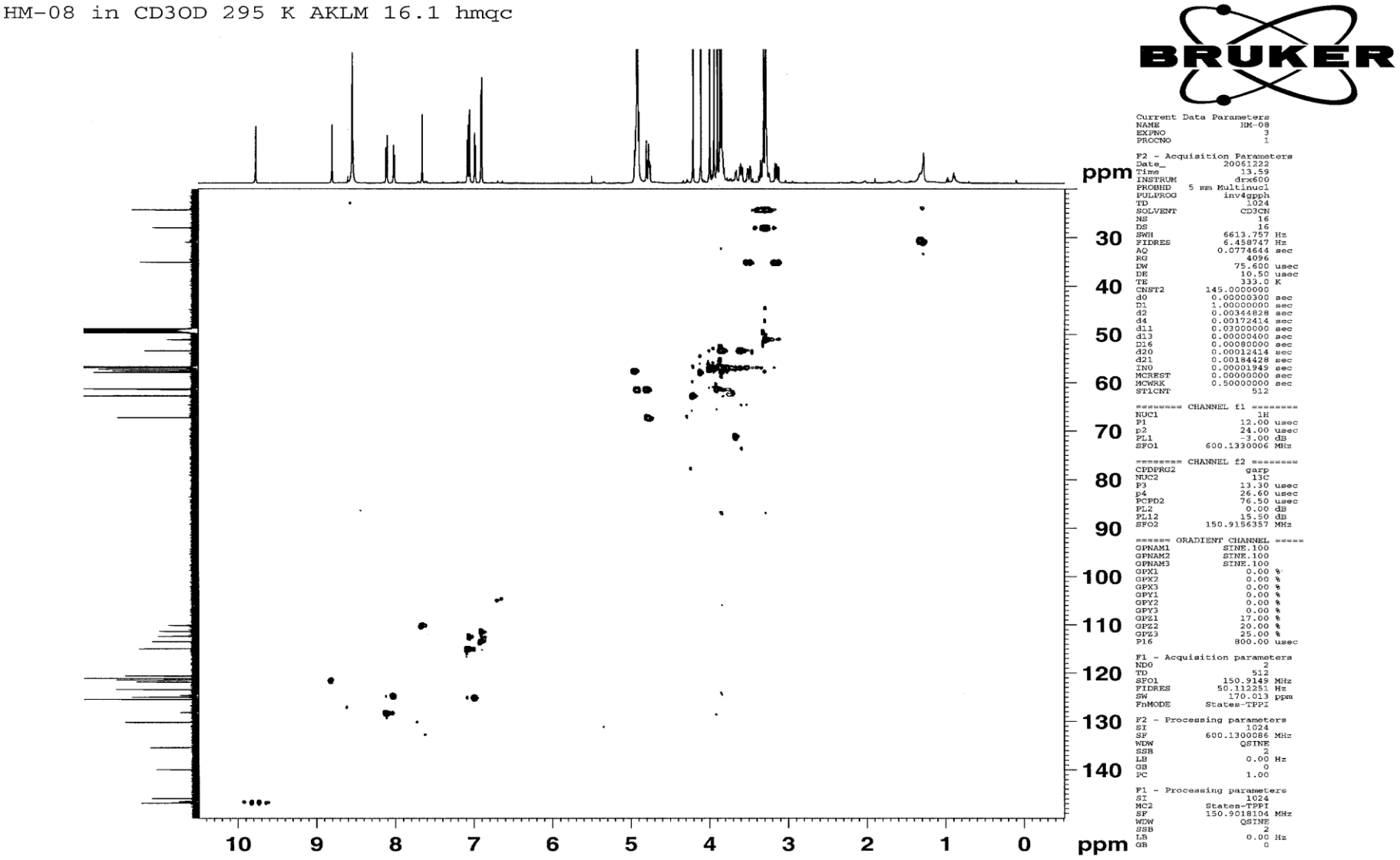
Current Data Parameters
NAME HM-08
EXPNO 1
PROCNO 1

F2 - Acquisition Parameters
Date_ 20061222
Time 12.40
INSTRUM drx600
PROBHD 5 mm Multinucl
PULPROG zg
TD 52908
SOLVENT MeOD
NS 32
DS 4
SWH 13227.514 Hz
FIDRES 0.250010 Hz
AQ 1.9999723 sec
RG 400
DW 37.800 usec
DE 12.50 usec
TE 295.0 K
D1 1.50000000 sec

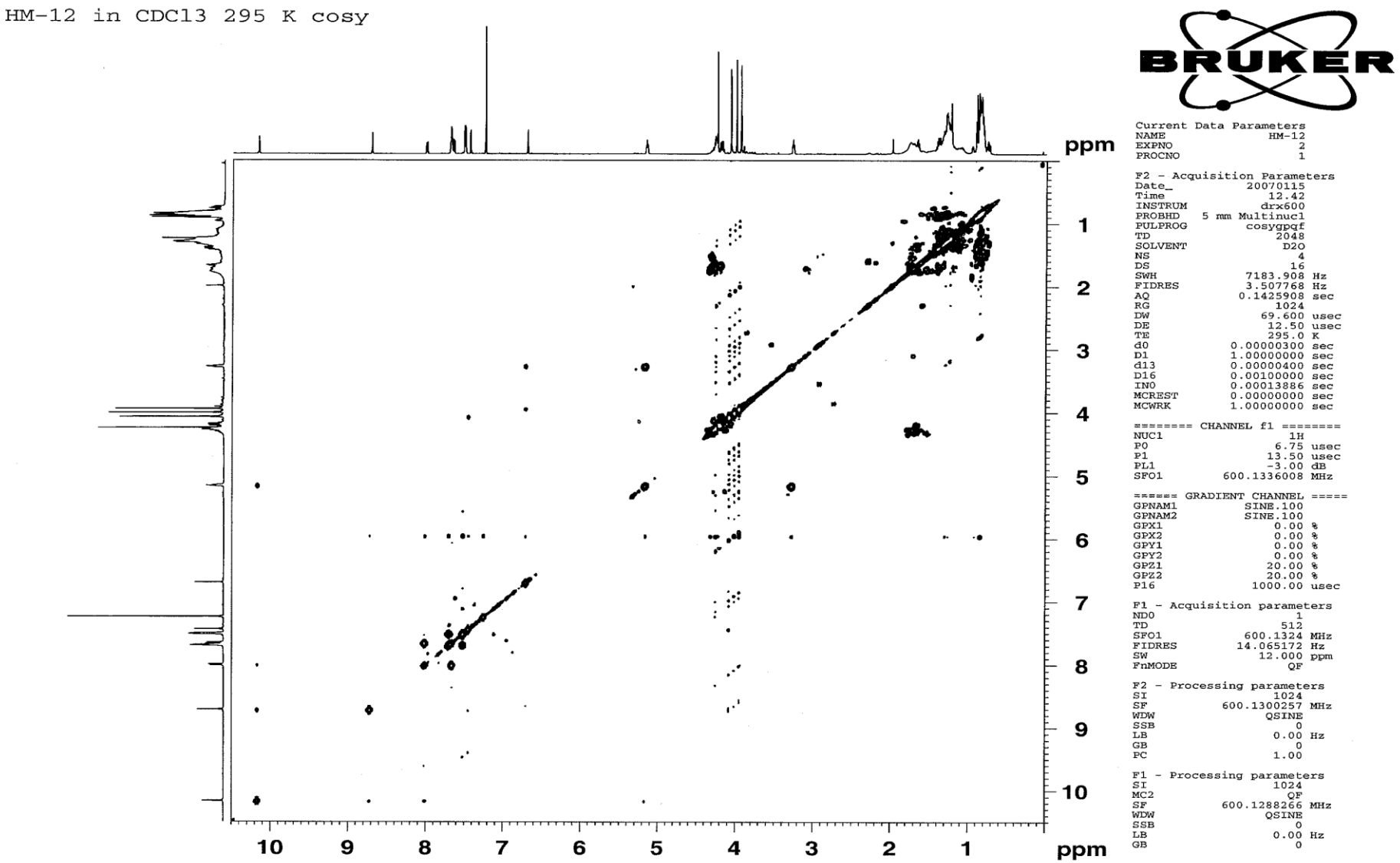
======== CHANNEL f1 ========
NUC1 1H
P1 3.00 usec
PL1 -3.00 dB
SFO1 600.1328529 MHz

F2 - Processing parameters
SI 131072
SF 600.1300140 MHz
WDW EM
SSB 0
LB 0.20 Hz
GB 0
PC 1.00

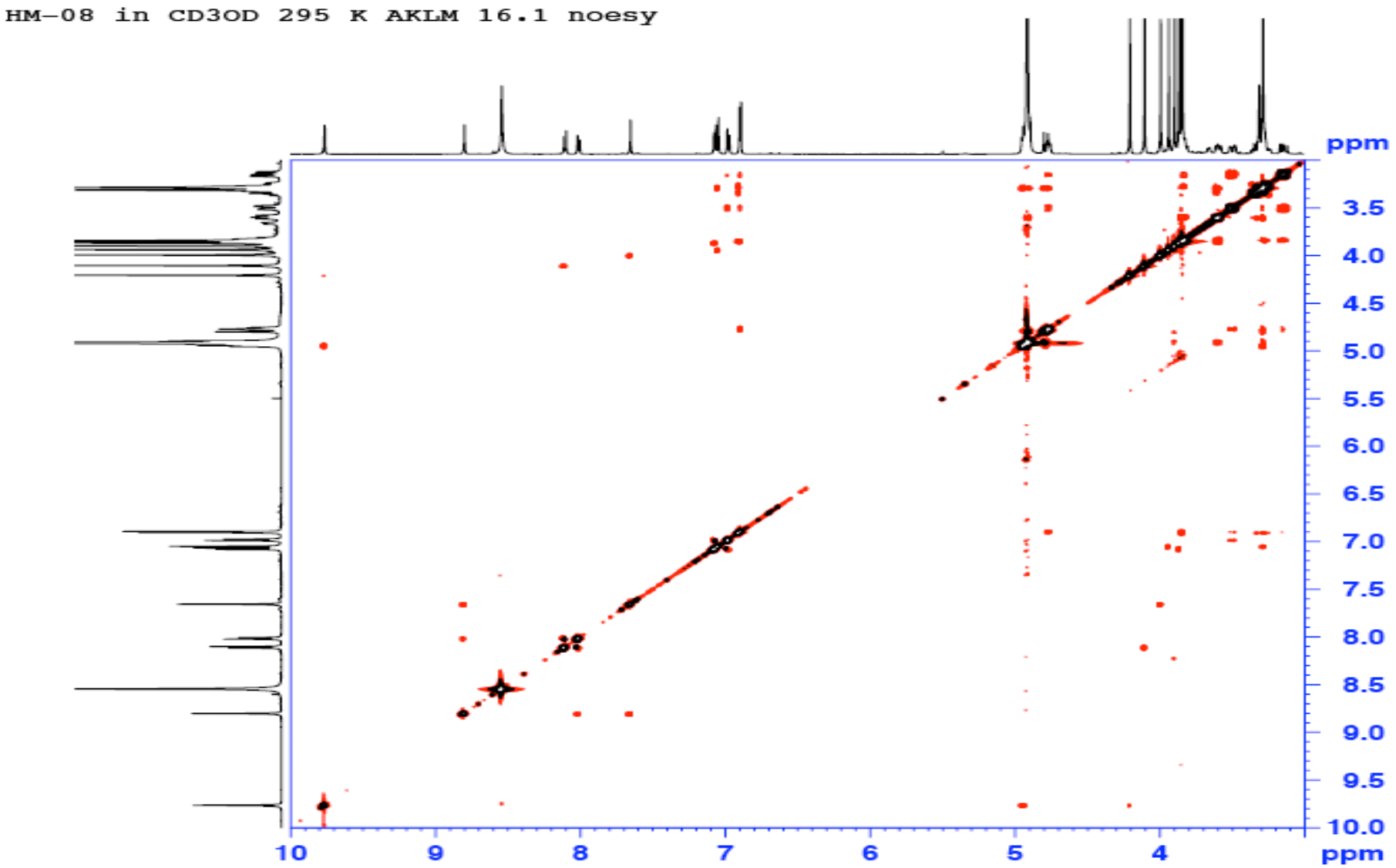
Appendix 7b: HMQC spectrum of a mixture of palmatine (**82**) and (−) - tetrahydropalmatine (**131**)



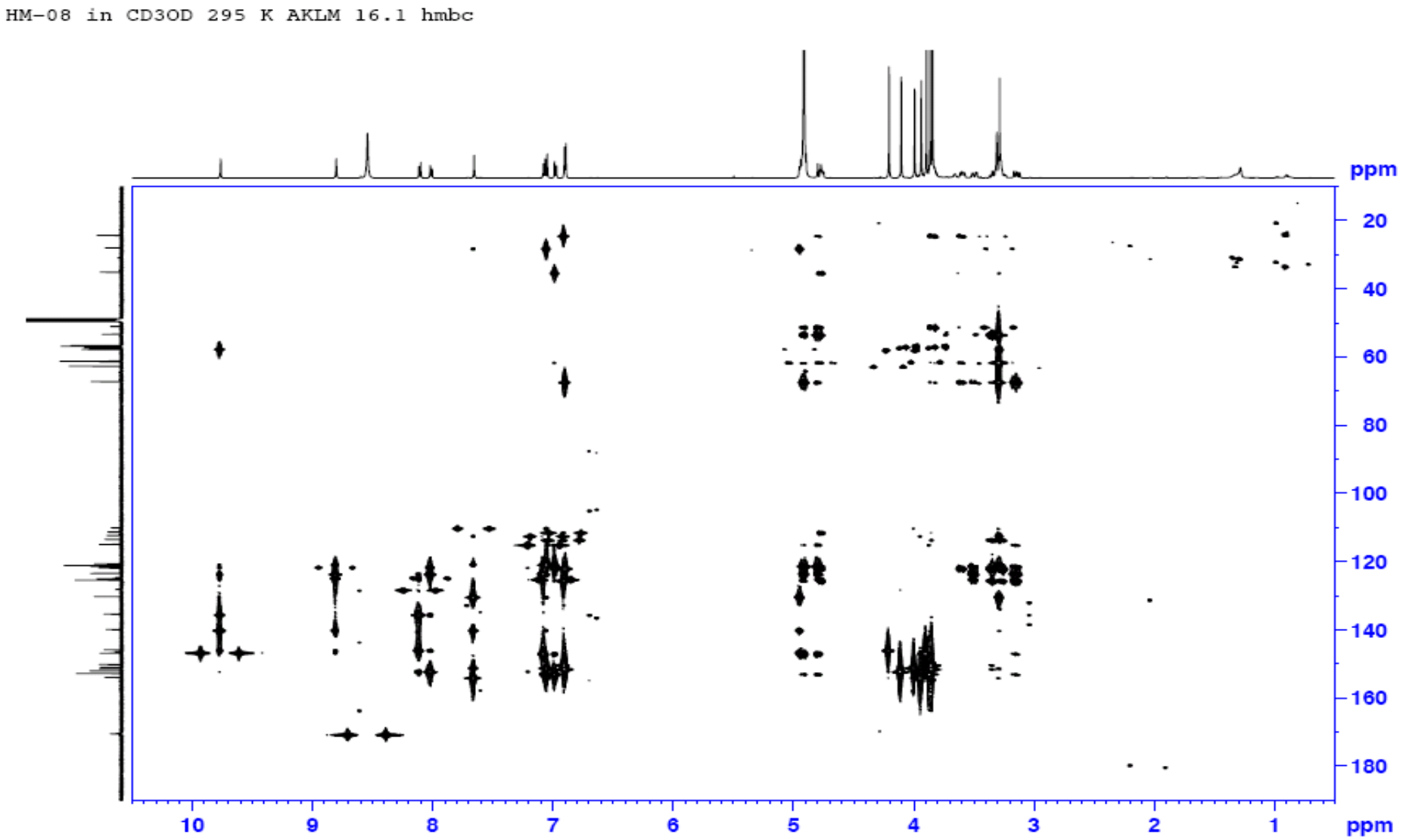
Appendix 7c: HMQC spectrum of a mixture of palmatine (**82**) and (−) - tetrahydropalmatine (**131**)



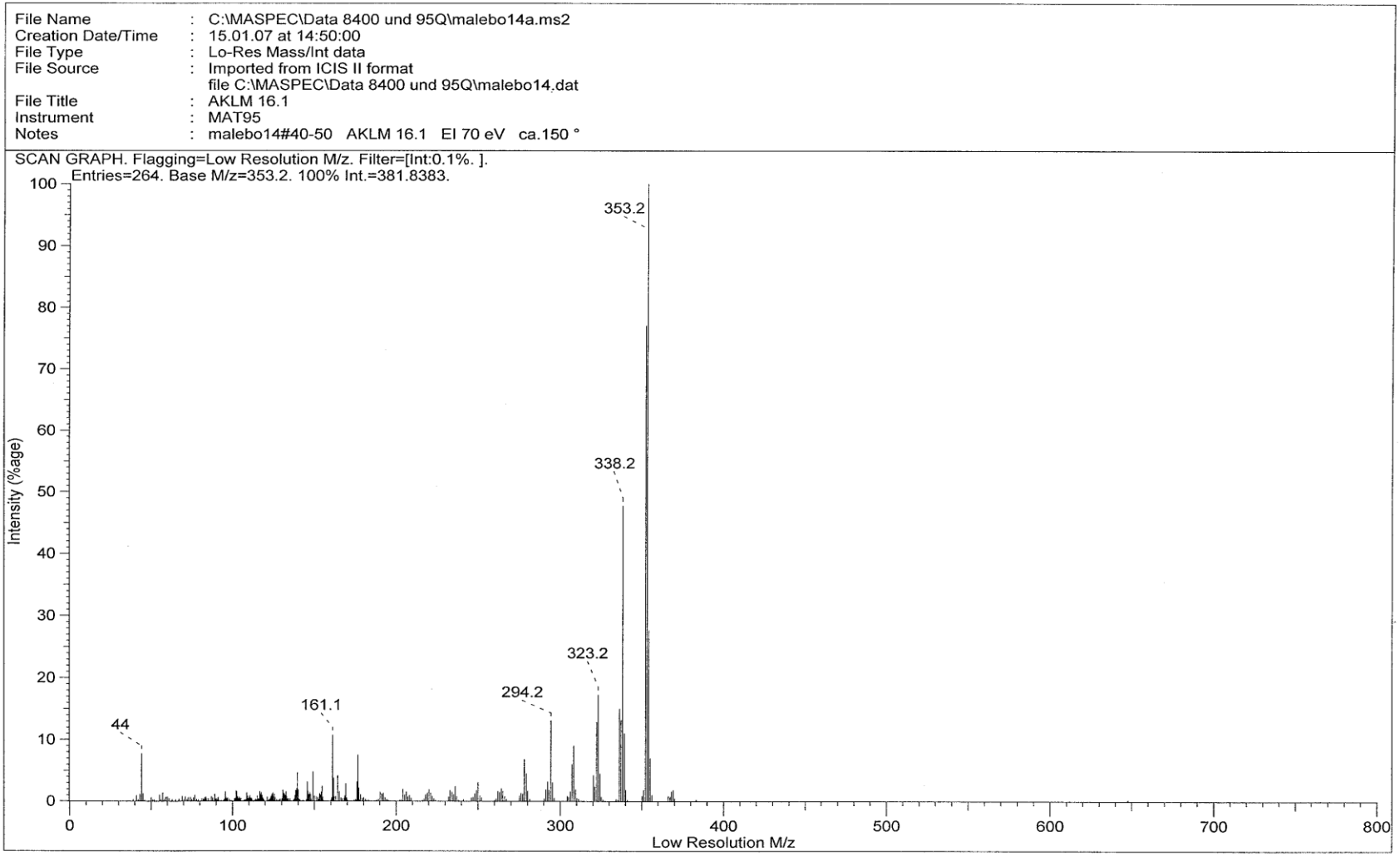
Appendix 7d: NOESY spectrum of a mixture of palmatine (**82**) and (−) - tetrahydropalmatine (**131**)



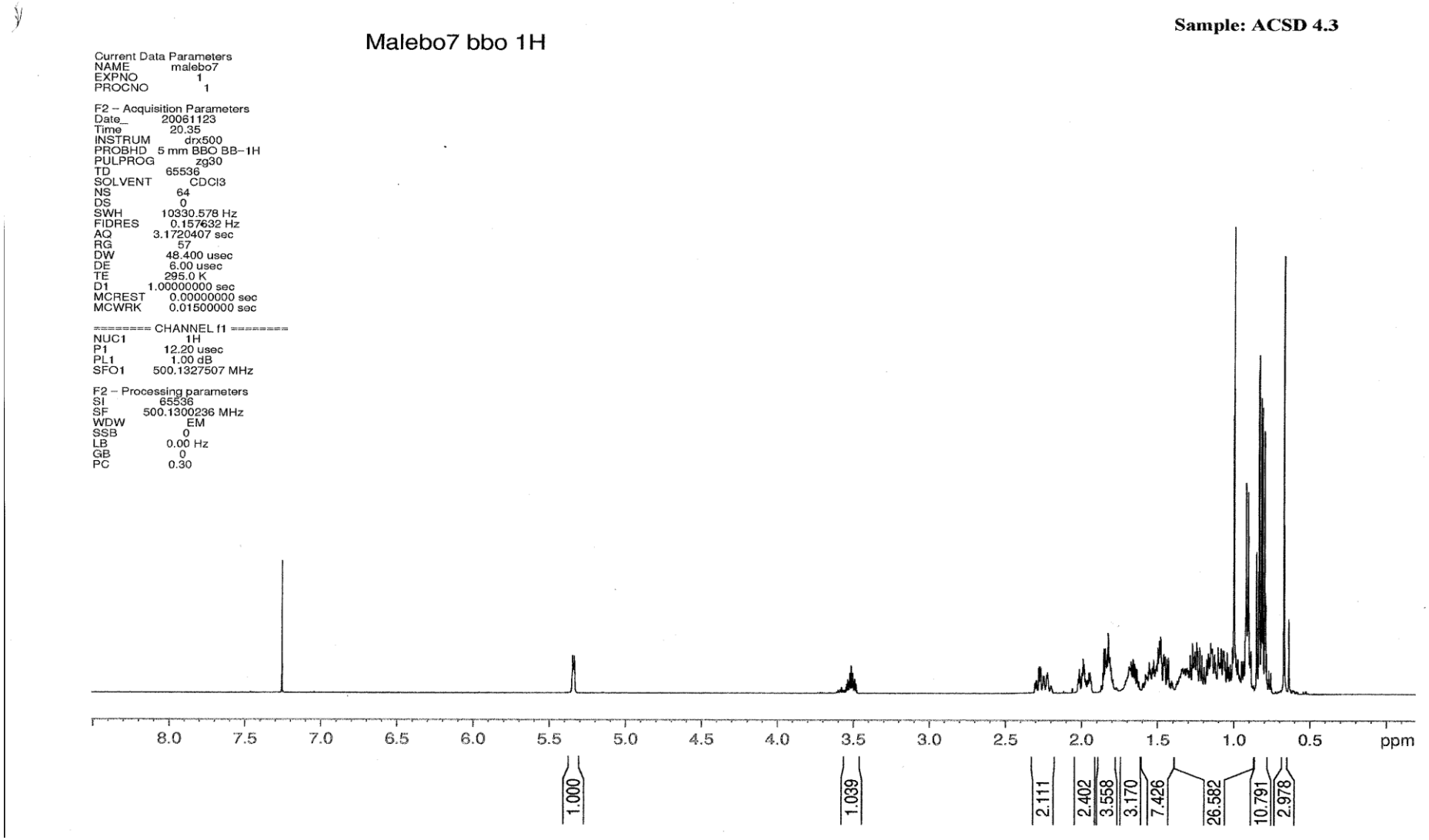
Appendix 7e: HMBC spectrum of a mixture of palmatine (**82**) and (−) - tetrahydropalmatine (**131**)



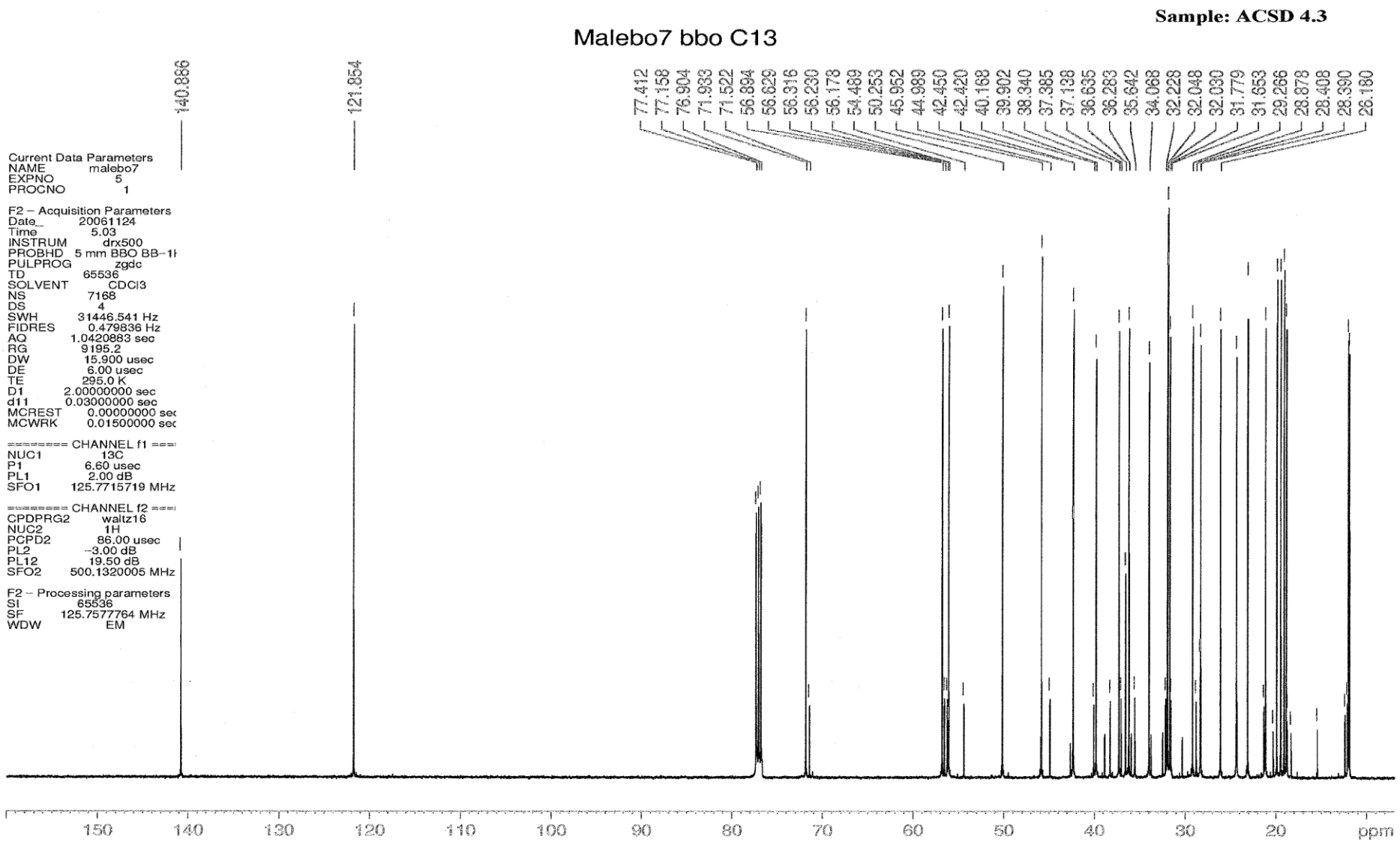
Appendix 7f: MS spectrum of a mixture of palmatine (**82**) and (−) - tetrahydropalmatine (**131**)



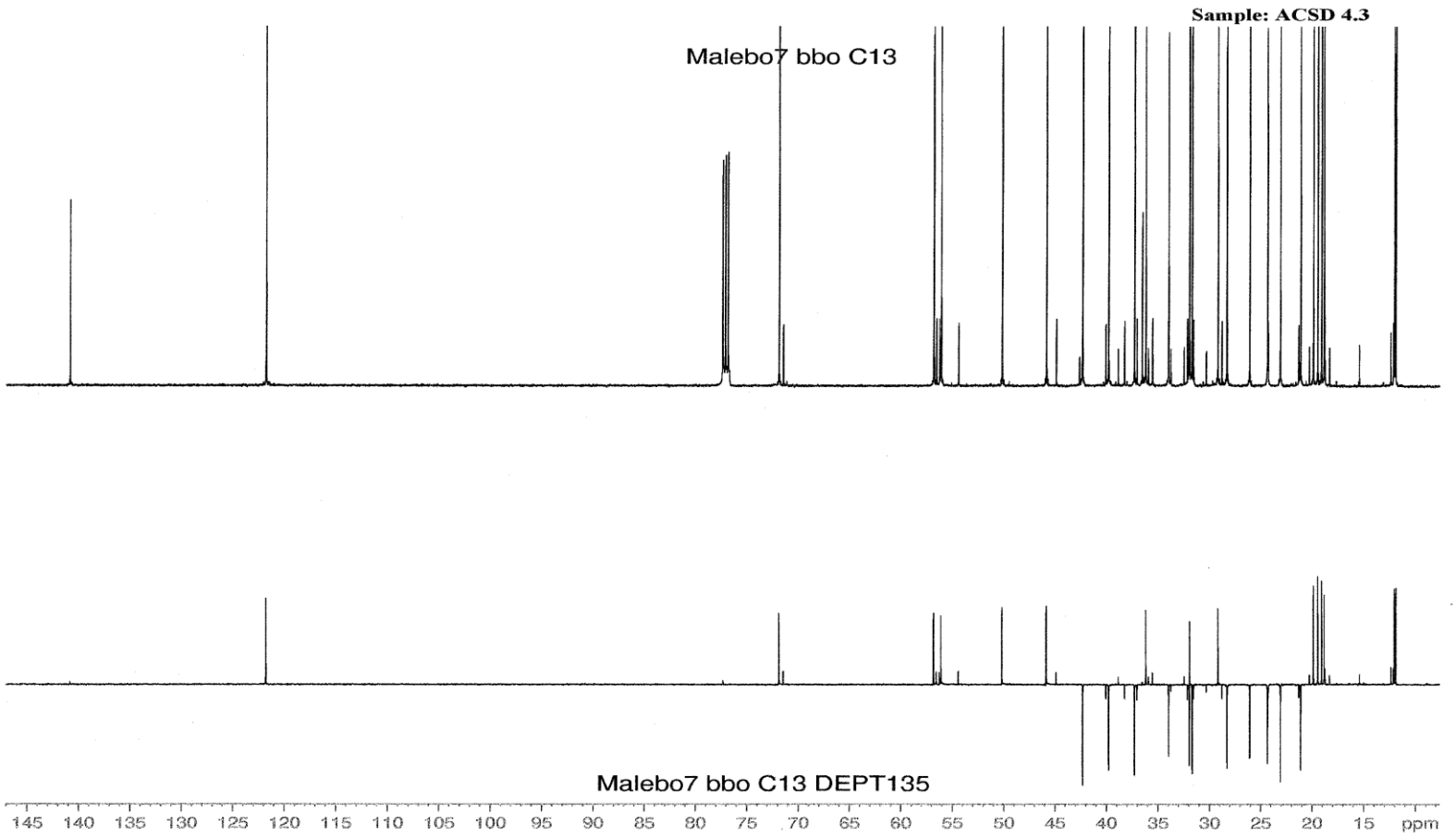
Appendix 8a: ^{1}H NMR spectrum of β-sitosterol (**132**)



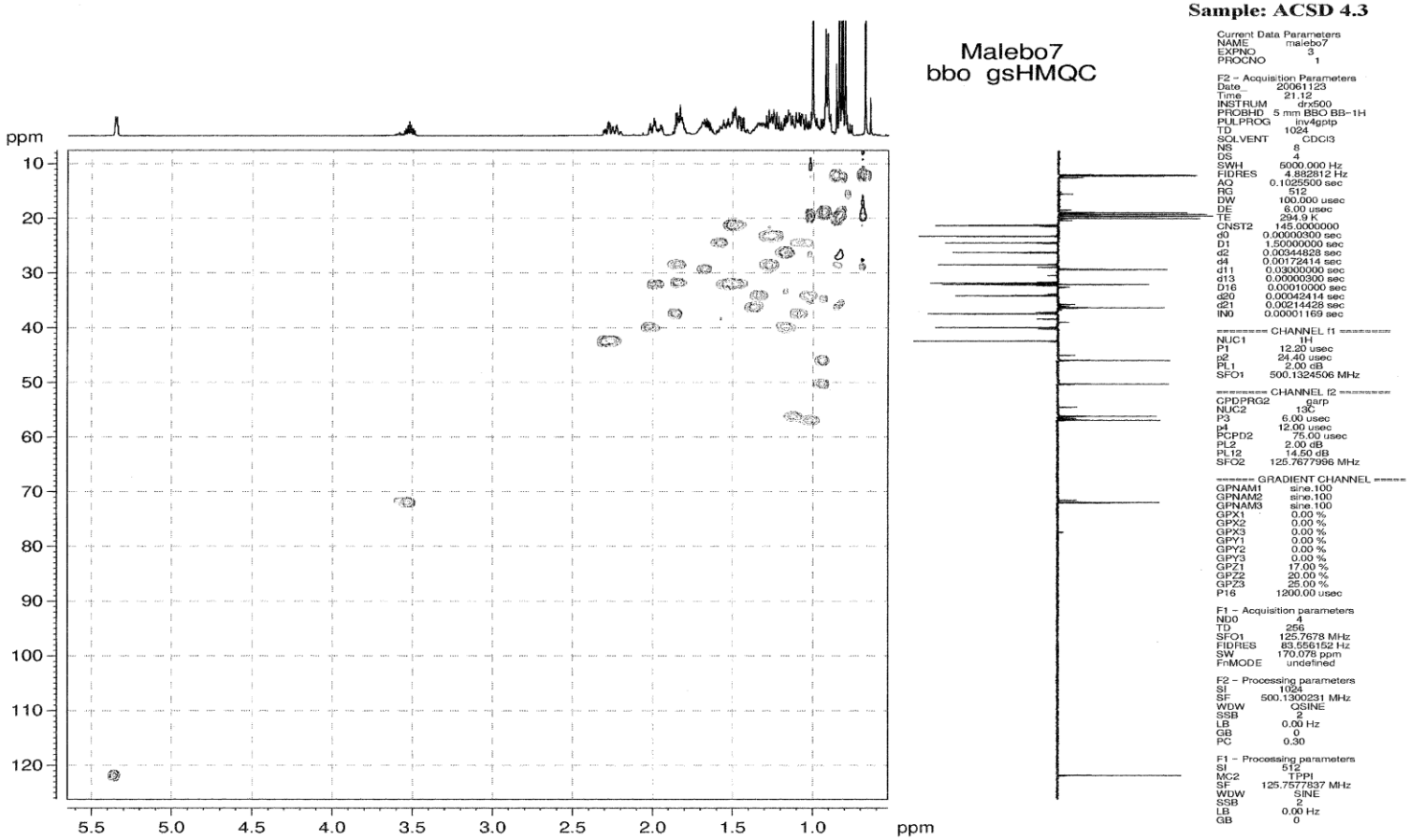
Appendix 8b: ^{13}C NMR spectrum of β-sitosterol (**132**)



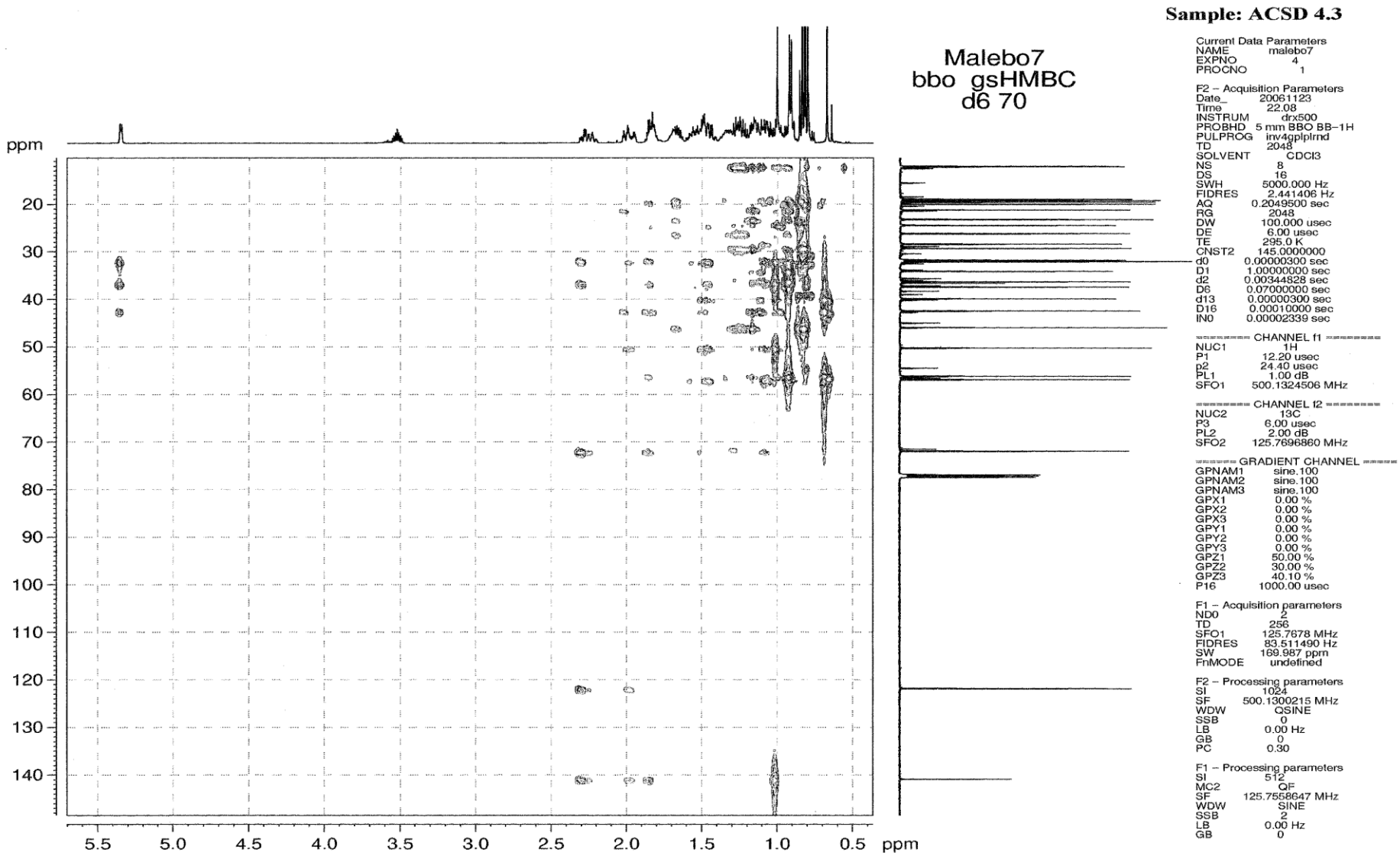
Appendix 8c: DEPT 135 spectrum of β-sitosterol (**132**)



Appendix 8d: HMQC spectrum of β-sitosterol (**132**)



Appendix 8e: HMBC spectrum of β-sitosterol (**132**)



Sample: ACSD 4.3

Current Data Parameters
NAME malebo7
EXPNO 4
PROCNO 1

F2 – Acquisition Parameters
Date_ 20061123
Time 22.08
INSTRUM drx500
PROBHD 5 mm BBO BB–1H
PULPROG inv4gplplrnd
TD 2048
SOLVENT CDCl3
NS 8
DS 16
SWH 5000.000 Hz
FIDRES 2.441406 Hz
AQ 0.2049500 sec
RG 2048
DW 100.000 usec
DE 6.00 usec
TE 295.0 K
CNST2 145.0000000
d0 0.00000300 sec
D1 1.00000000 sec
d2 0.00344828 sec
D6 0.07000000 sec
d13 0.00000300 sec
D16 0.00010000 sec
IN0 0.00002339 sec

======== CHANNEL f1 ========
NUC1 1H
P1 12.20 usec
p2 24.40 usec
PL1 1.00 dB
SFO1 500.1324506 MHz

======== CHANNEL f2 ========
NUC2 13C
P3 6.00 usec
PL2 2.00 dB
SFO2 125.7696860 MHz

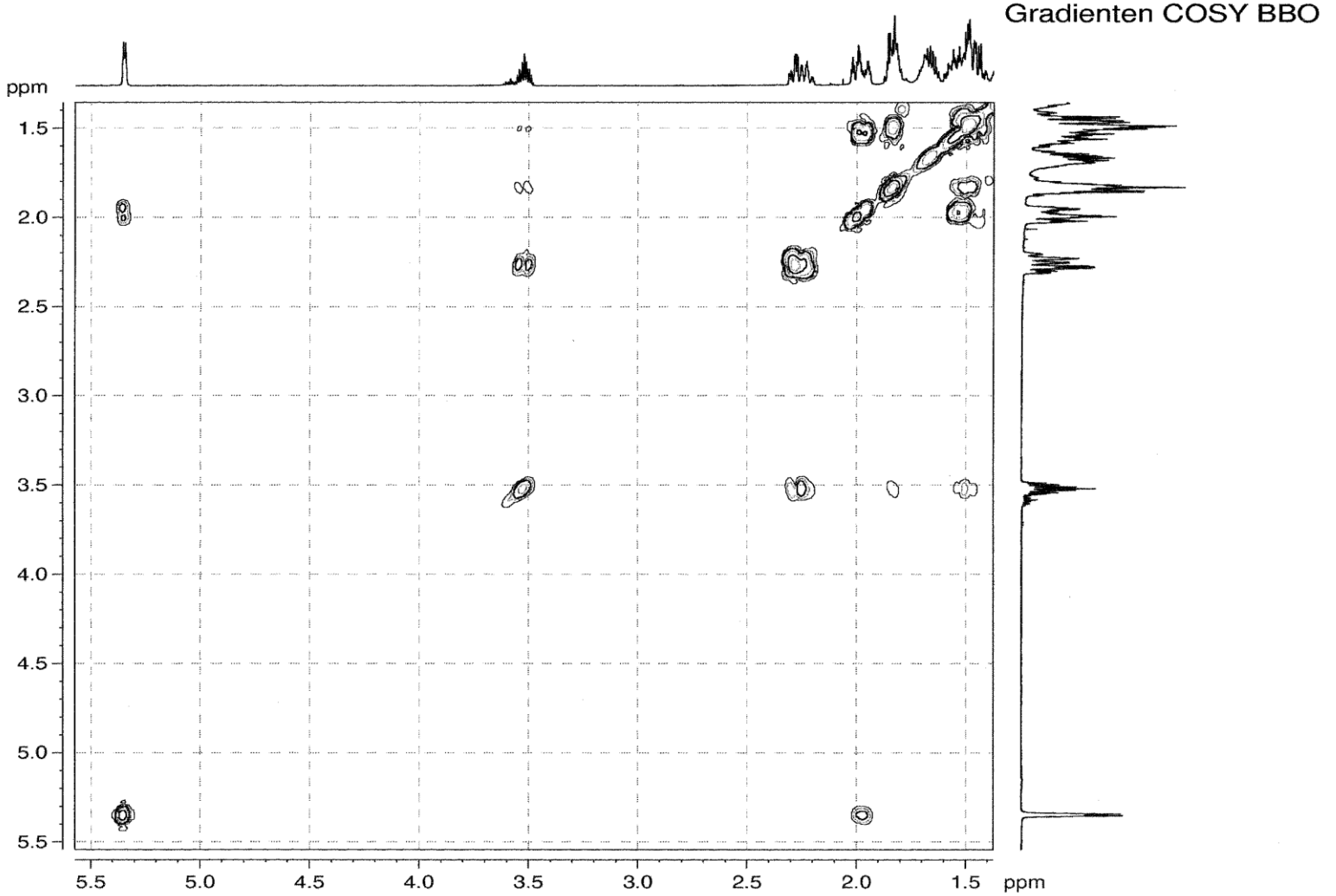
====== GRADIENT CHANNEL =====
GPNAM1 sine.100
GPNAM2 sine.100
GPNAM3 sine.100
GPX1 0.00 %
GPX2 0.00 %
GPX3 0.00 %
GPY1 0.00 %
GPY2 0.00 %
GPY3 0.00 %
GPZ1 50.00 %
GPZ2 30.00 %
GPZ3 40.10 %
P16 1000.00 usec

F1 – Acquisition parameters
ND0 2
TD 256
SFO1 125.7678 MHz
FIDRES 83.511490 Hz
SW 169.987 ppm
FnMODE undefined

F2 – Processing parameters
SI 1024
SF 500.1300215 MHz
WDW QSINE
SSB 0
LB 0.00 Hz
GB 0
PC 0.30

F1 – Processing parameters
SI 512
MC2 QF
SF 125.7558647 MHz
WDW SINE
SSB 2
LB 0.00 Hz
GB 0

Appendix 8f: COSY spectrum of β-sitosterol (**132**)



Sample: ACSD 4.3

Current Data Parameters
NAME malebo7
EXPNO 2
PROCNO 1

F2 – Acquisition Parameters
Date_ 20061123
Time 20.36
INSTRUM drx500
PROBHD 5 mm BBO BB-1H
PULPROG cosygp
TD 1024
SOLVENT CDCl3
NS 4
DS 8
SWH 5000.000 Hz
FIDRES 4.882812 Hz
AQ 0.1025500 sec
RG 28
DW 100.000 usec
DE 6.00 usec
TE 295.0 K
d0 0.00000300 sec
D1 2.00000000 sec
d13 0.00000300 sec
D16 0.00100000 sec
IN0 0.00020000 sec

======== CHANNEL f1 ========
NUC1 1H
P0 6.00 usec
P1 12.20 usec
PL1 1.00 dB
SFO1 500.1324506 MHz

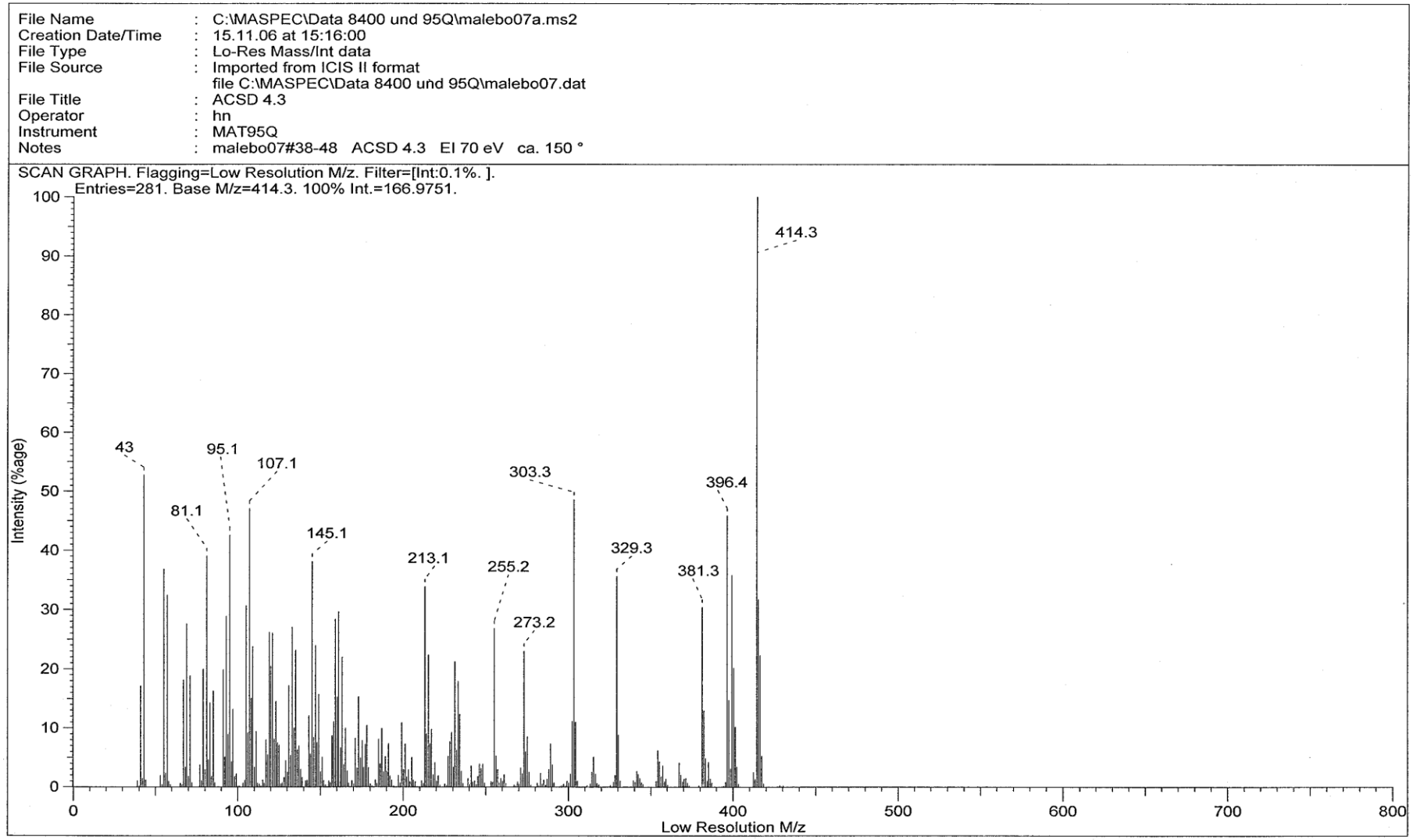
===== GRADIENT CHANNEL =====
GPNAM1 SINE.100kk
GPNAM2 SINE.100kk
GPX1 0.00 %
GPX2 0.00 %
GPY1 0.00 %
GPY2 0.00 %
GPZ1 10.00 %
GPZ2 10.00 %
P16 1000.00 usec

F1 – Acquisition parameters
ND0 1
TD 256
SFO1 500.1328 MHz
FIDRES 19.531250 Hz
SW 9.997 ppm
FnMODE undefined

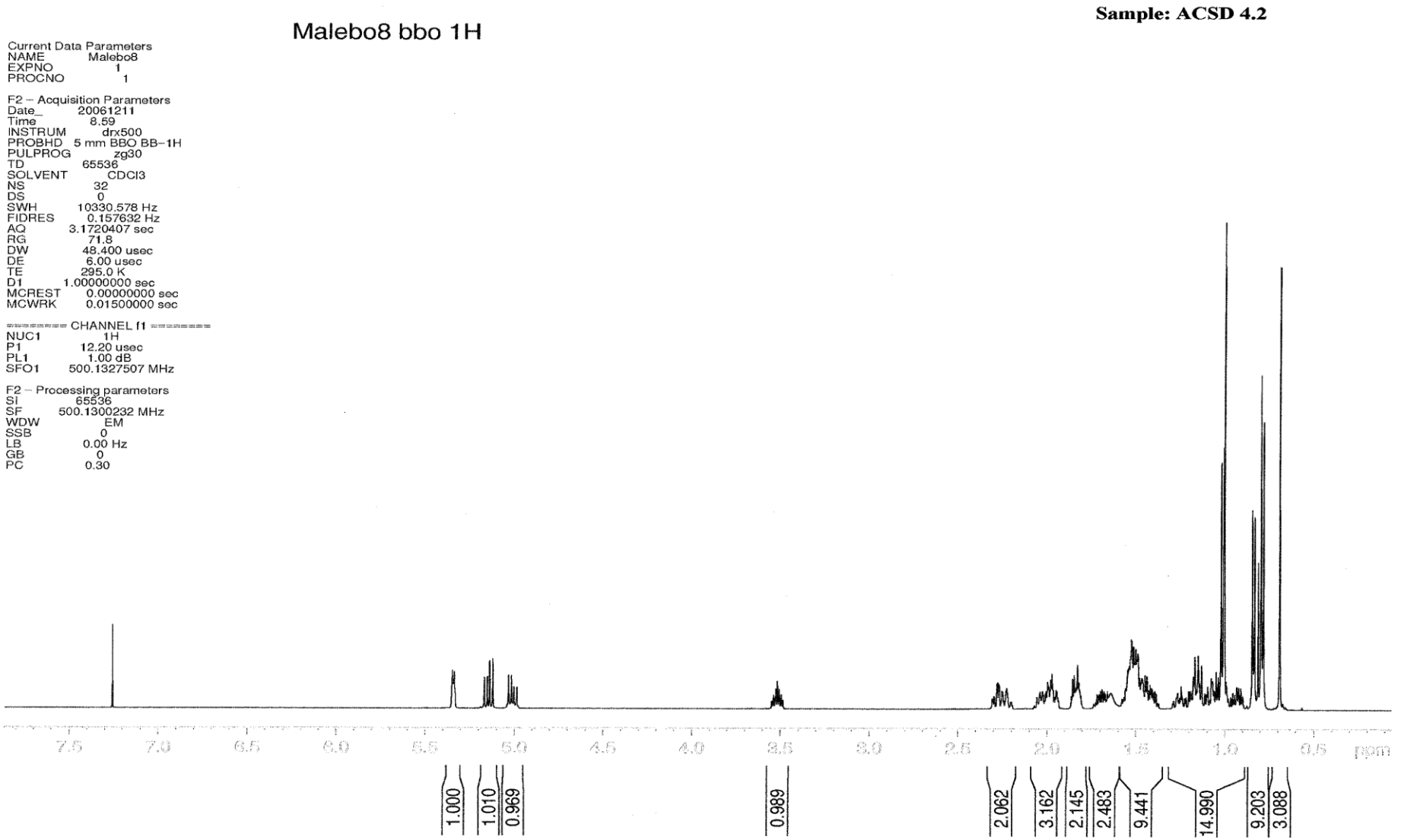
F2 – Processing parameters
SI 1024
SF 500.1300230 MHz
WDW SINE
SSB 0
LB 0.00 Hz
GB 0
PC 0.30

F1 – Processing parameters
SI 1024
MC2 QF
SF 500.1303215 MHz
WDW SINE
SSB 0
LB 0.00 Hz
GB 0

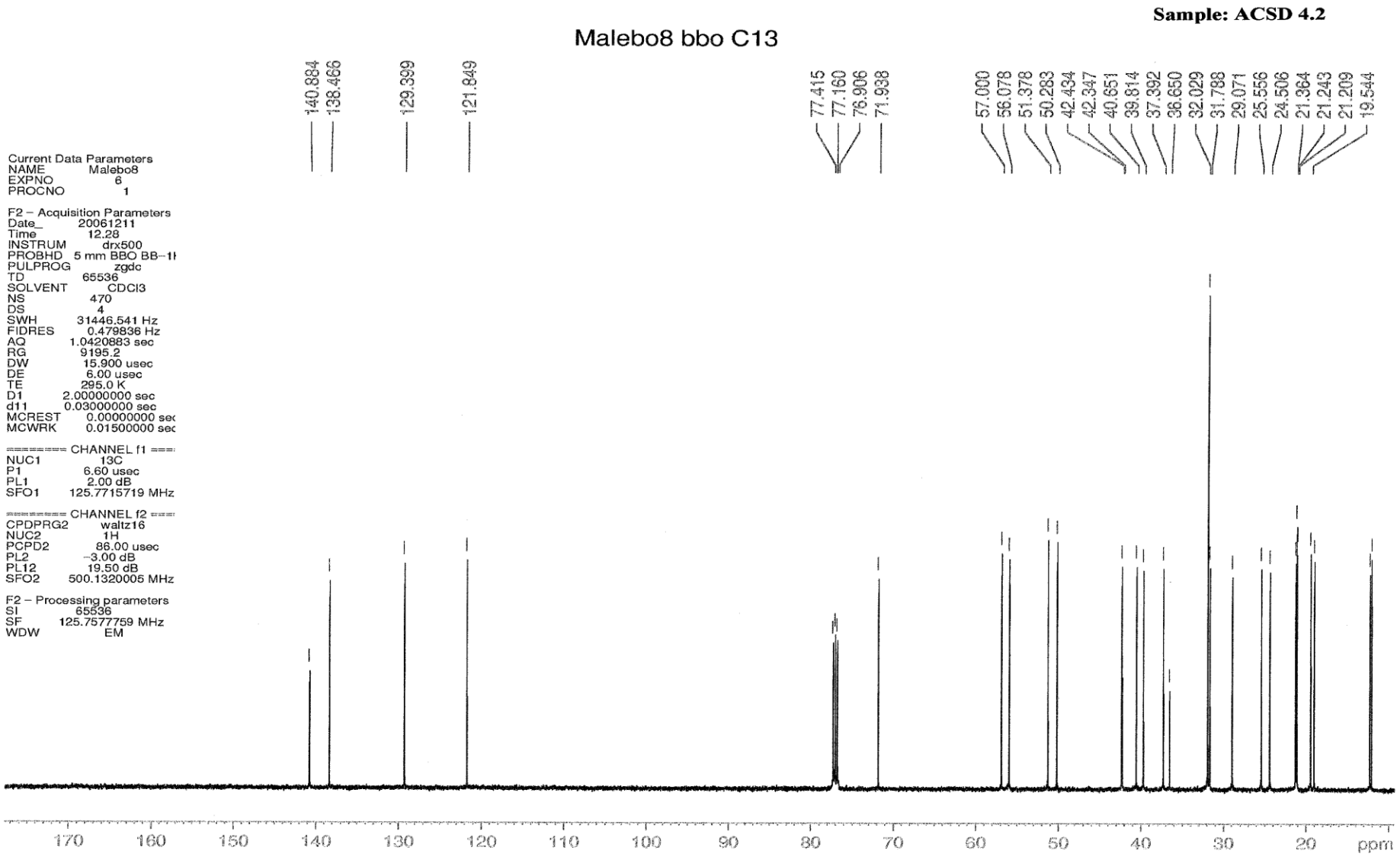
Appendix 8f: COSY spectrum of β-sitosterol (**132**)



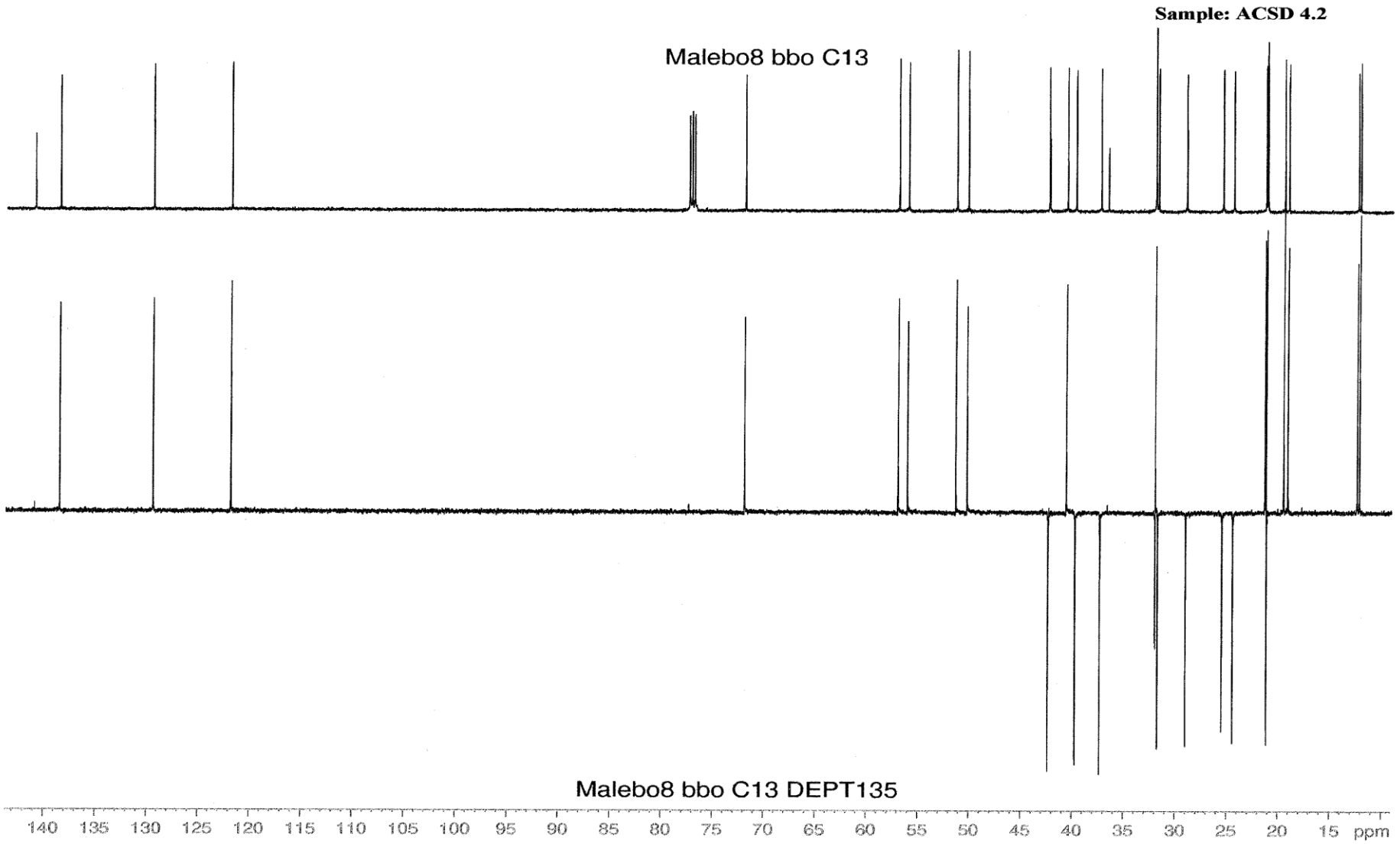
Appendix 9a: ^{1}H NMR spectrum of stigmasterol (**133**)



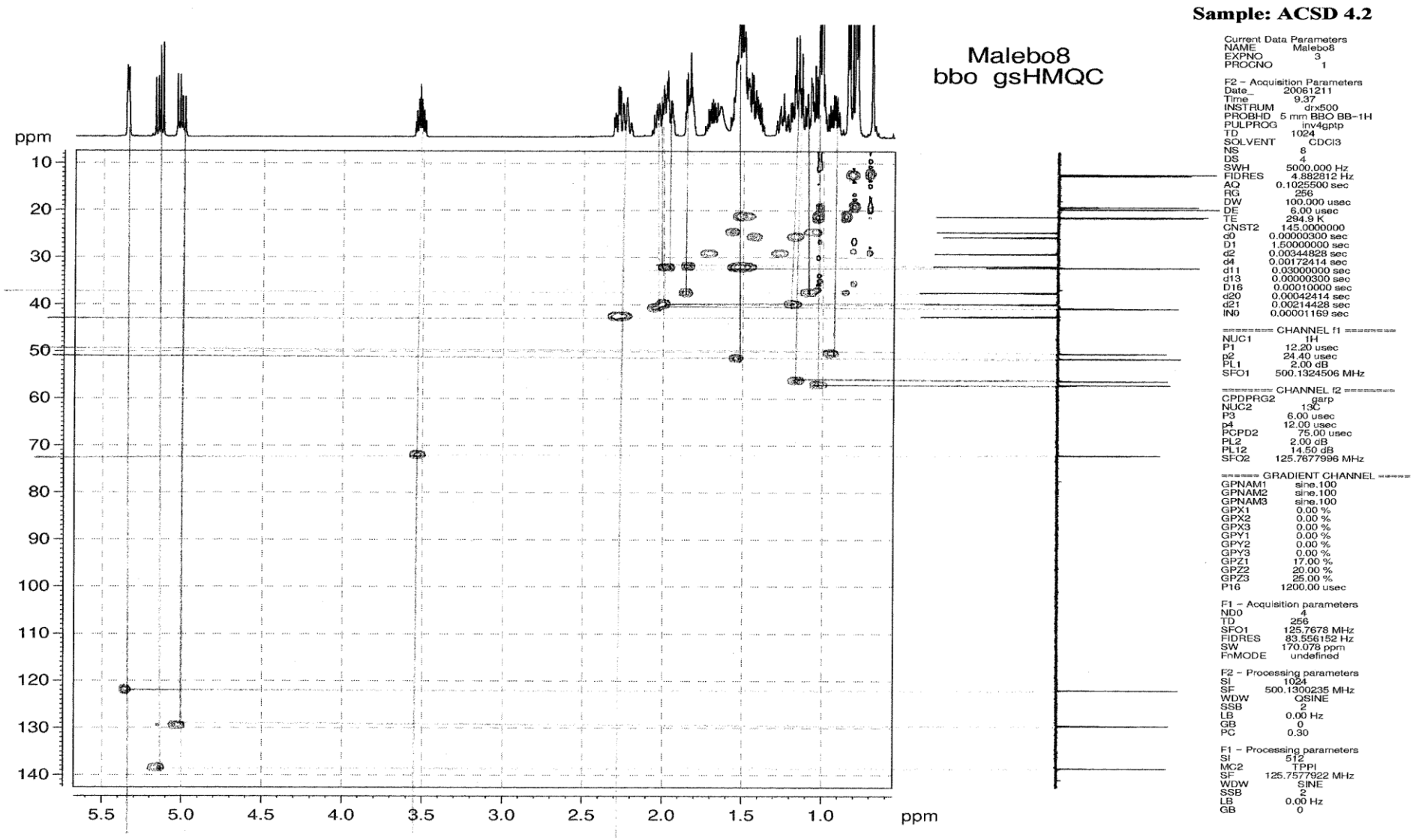
Appendix 9b: ^{13}C NMR spectrum of stigmasterol (**133**)



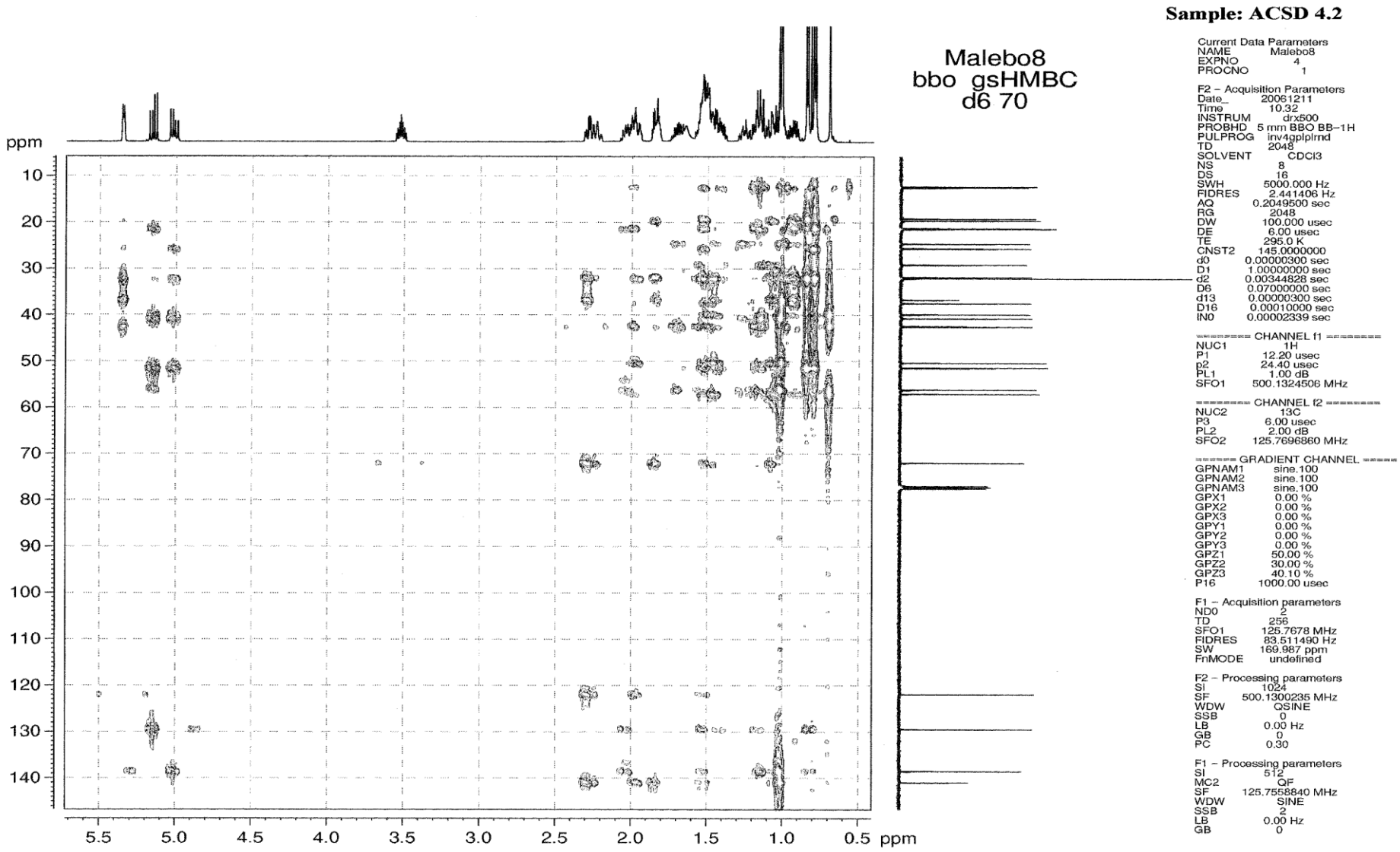
Appendix 9c: DEPT 135 spectrum of stigmasterol (**133**)



Appendix 9d: HMQC spectrum of stigmasterol (**133**)



Appendix 9e: HMBC spectrum of stigmasterol (**133**)



Sample: ACSD 4.2

Current Data Parameters
NAME Malebo8
EXPNO 4
PROCNO 1

F2 – Acquisition Parameters
Date_ 20061211
Time 10.32
INSTRUM drx500
PROBHD 5 mm BBO BB–1H
PULPROG inv4gplplrnd
TD 2048
SOLVENT CDCl3
NS 8
DS 16
SWH 5000.000 Hz
FIDRES 2.441406 Hz
AQ 0.2049500 sec
RG 2048
DW 100.000 usec
DE 6.00 usec
TE 295.0 K
CNST2 145.0000000
d0 0.00000300 sec
D1 1.00000000 sec
d2 0.00344828 sec
D6 0.07000000 sec
d13 0.00000300 sec
D16 0.00010000 sec
IN0 0.00002339 sec

======== CHANNEL f1 ========
NUC1 1H
P1 12.20 usec
p2 24.40 usec
PL1 1.00 dB
SFO1 500.1324506 MHz

======== CHANNEL f2 ========
NUC2 13C
P3 6.00 usec
PL2 2.00 dB
SFO2 125.7696860 MHz

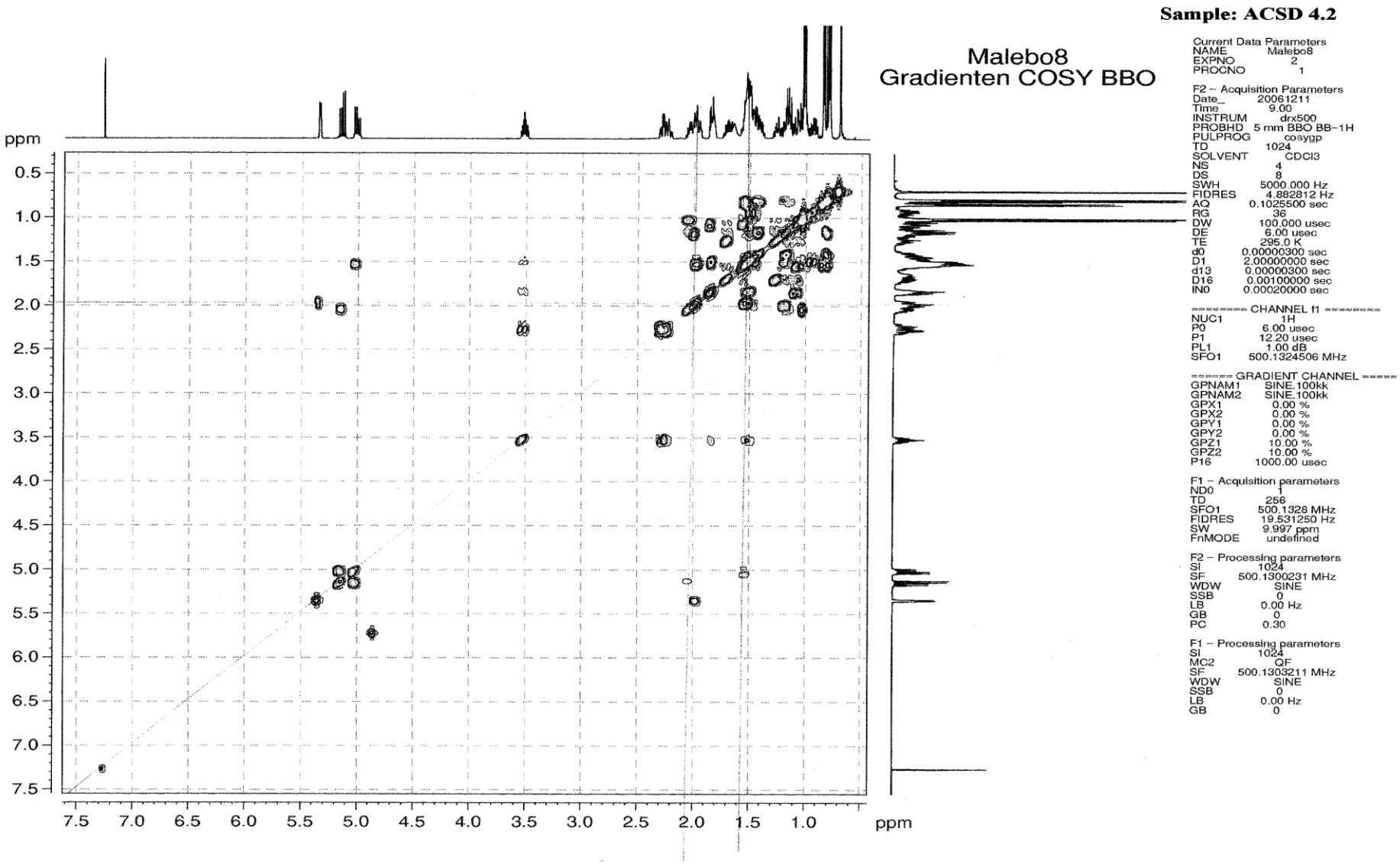
====== GRADIENT CHANNEL =====
GPNAM1 sine.100
GPNAM2 sine.100
GPNAM3 sine.100
GPX1 0.00 %
GPX2 0.00 %
GPX3 0.00 %
GPY1 0.00 %
GPY2 0.00 %
GPY3 0.00 %
GPZ1 50.00 %
GPZ2 30.00 %
GPZ3 40.10 %
P16 1000.00 usec

F1 – Acquisition parameters
ND0 2
TD 256
SFO1 125.7678 MHz
FIDRES 83.511490 Hz
SW 169.987 ppm
FnMODE undefined

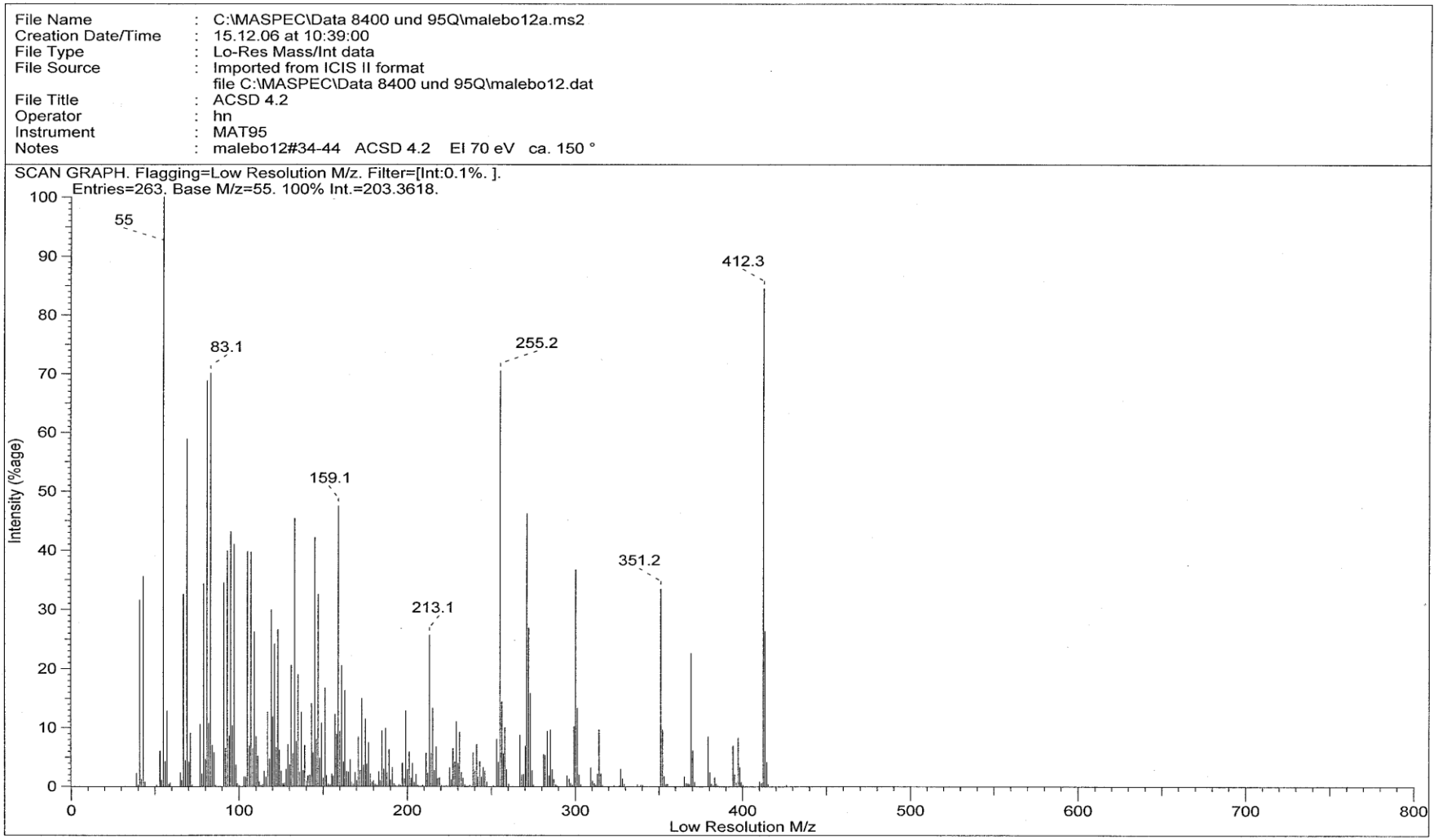
F2 – Processing parameters
SI 1024
SF 500.1300235 MHz
WDW QSINE
SSB 0
LB 0.00 Hz
GB 0
PC 0.30

F1 – Processing parameters
SI 512
MC2 QF
SF 125.7558840 MHz
WDW SINE
SSB 2
LB 0.00 Hz
GB 0

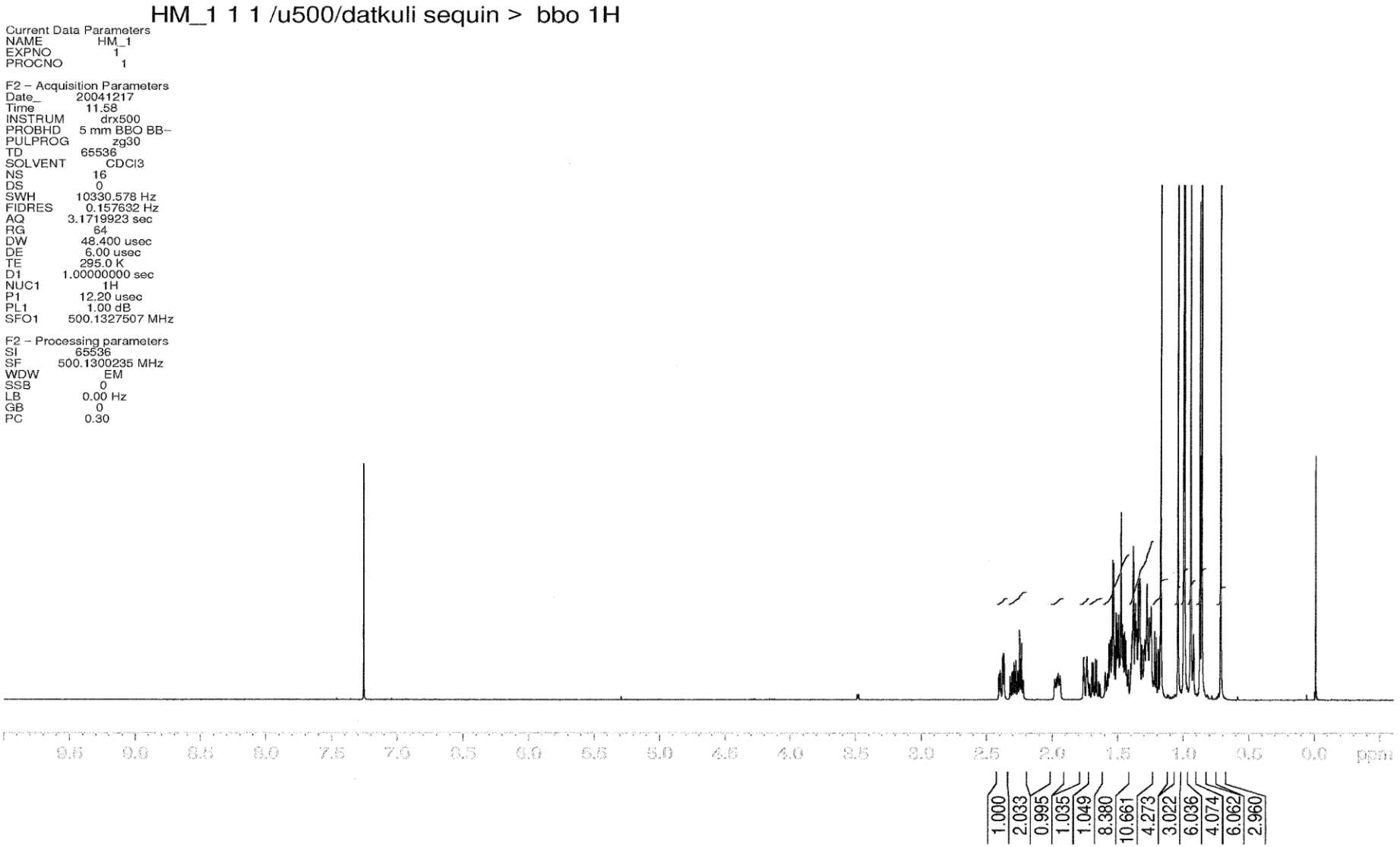
Appendix 9f: COSY spectrum of stigmasterol (**133**)



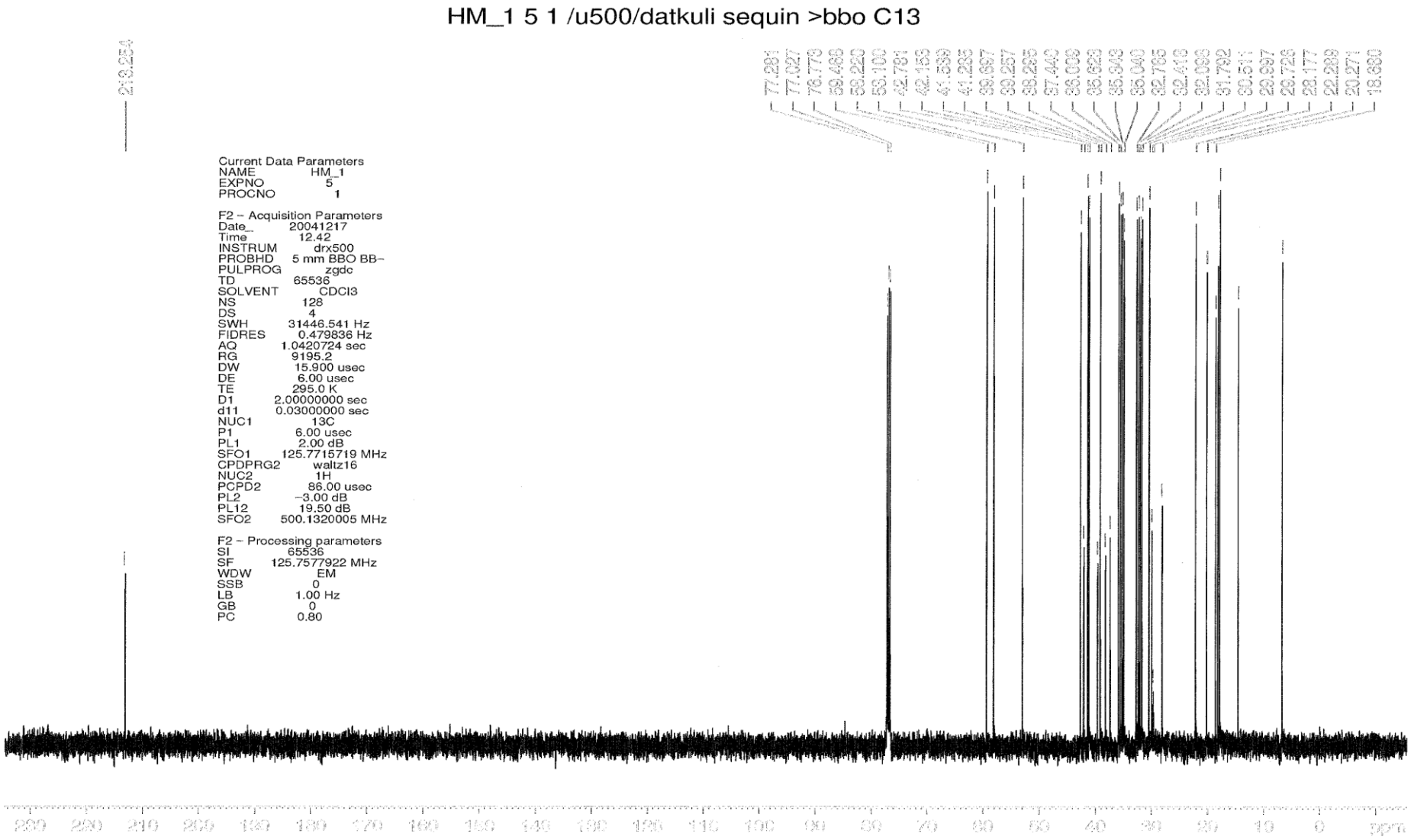
Appendix 9g: MS spectrum of stigmasterol (**133**)



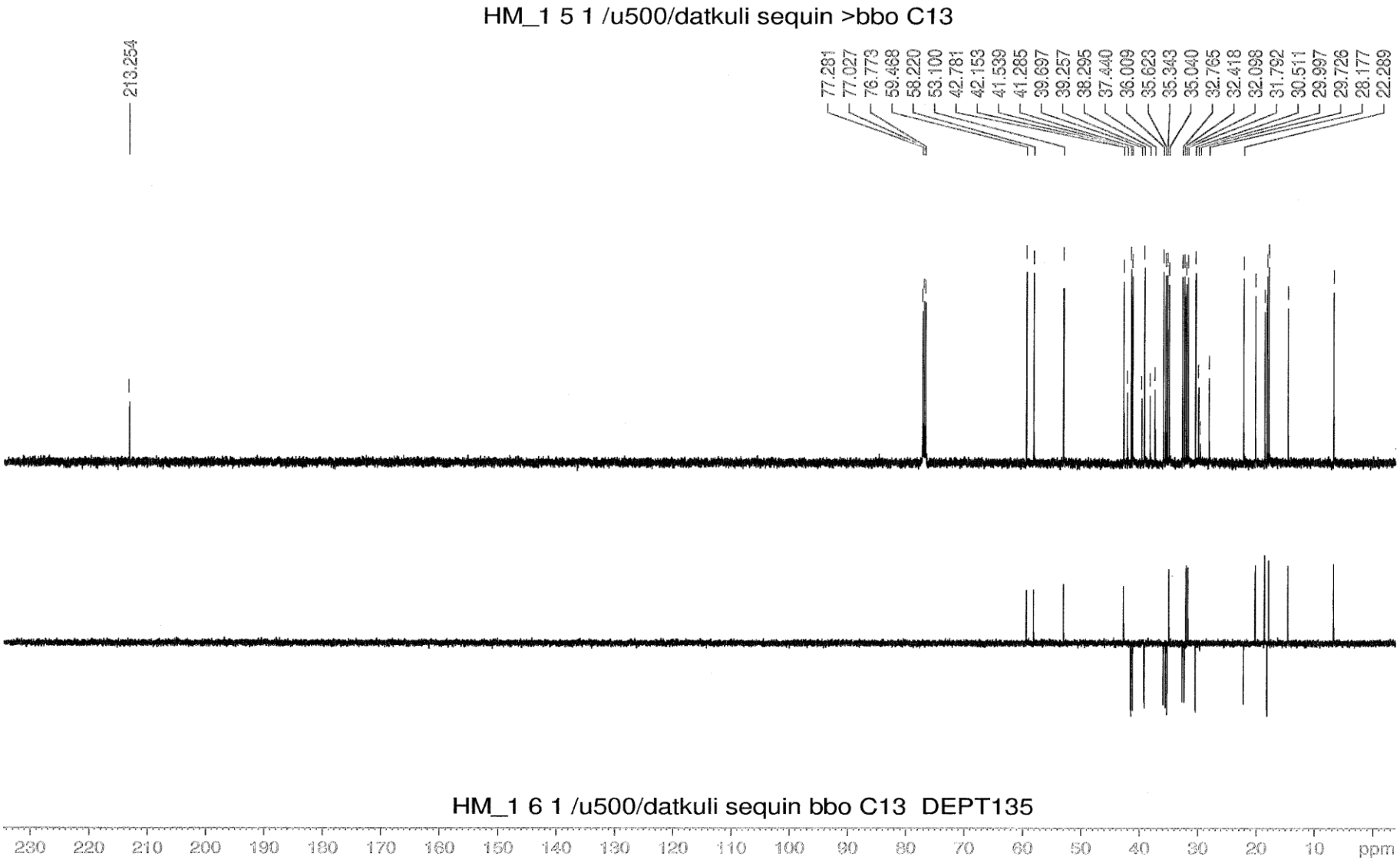
Appendix 10a: ^{1}H NMR spectrum of friedelin (**134**)



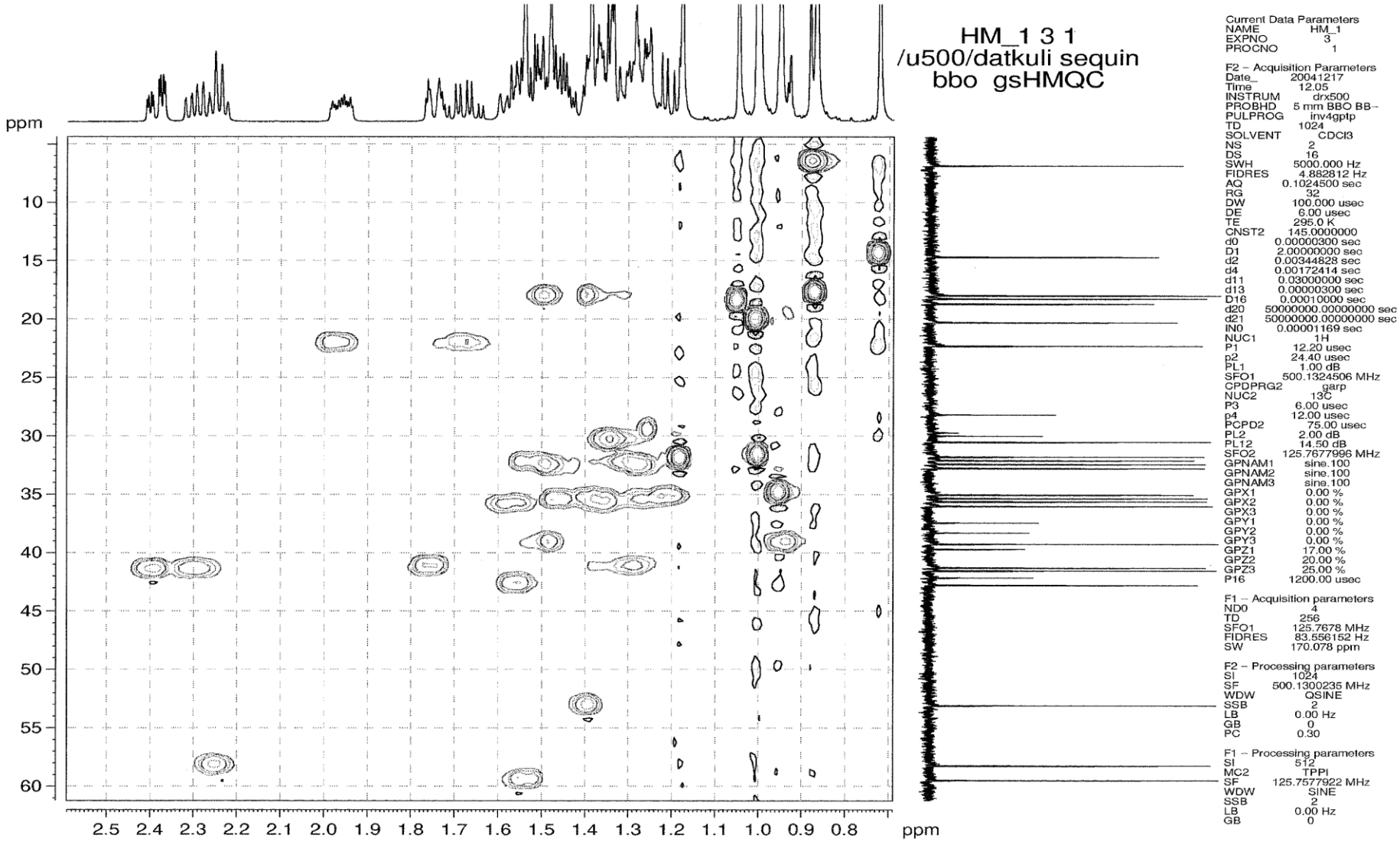
Appendix 10b: ^{13}C NMR spectrum of friedelin (**134**)



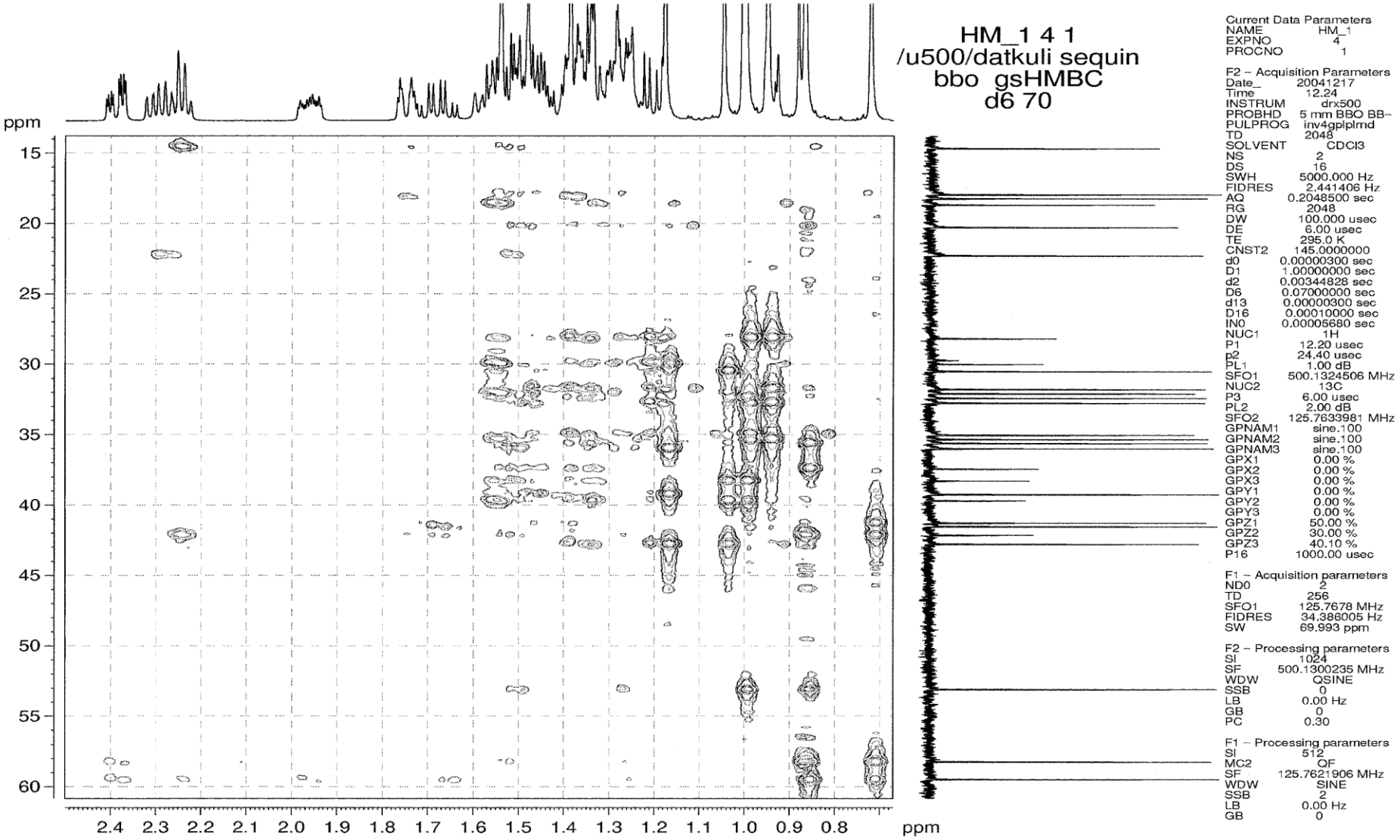
Appendix 10c: DEPT 135 spectrum of friedelin (**134**)



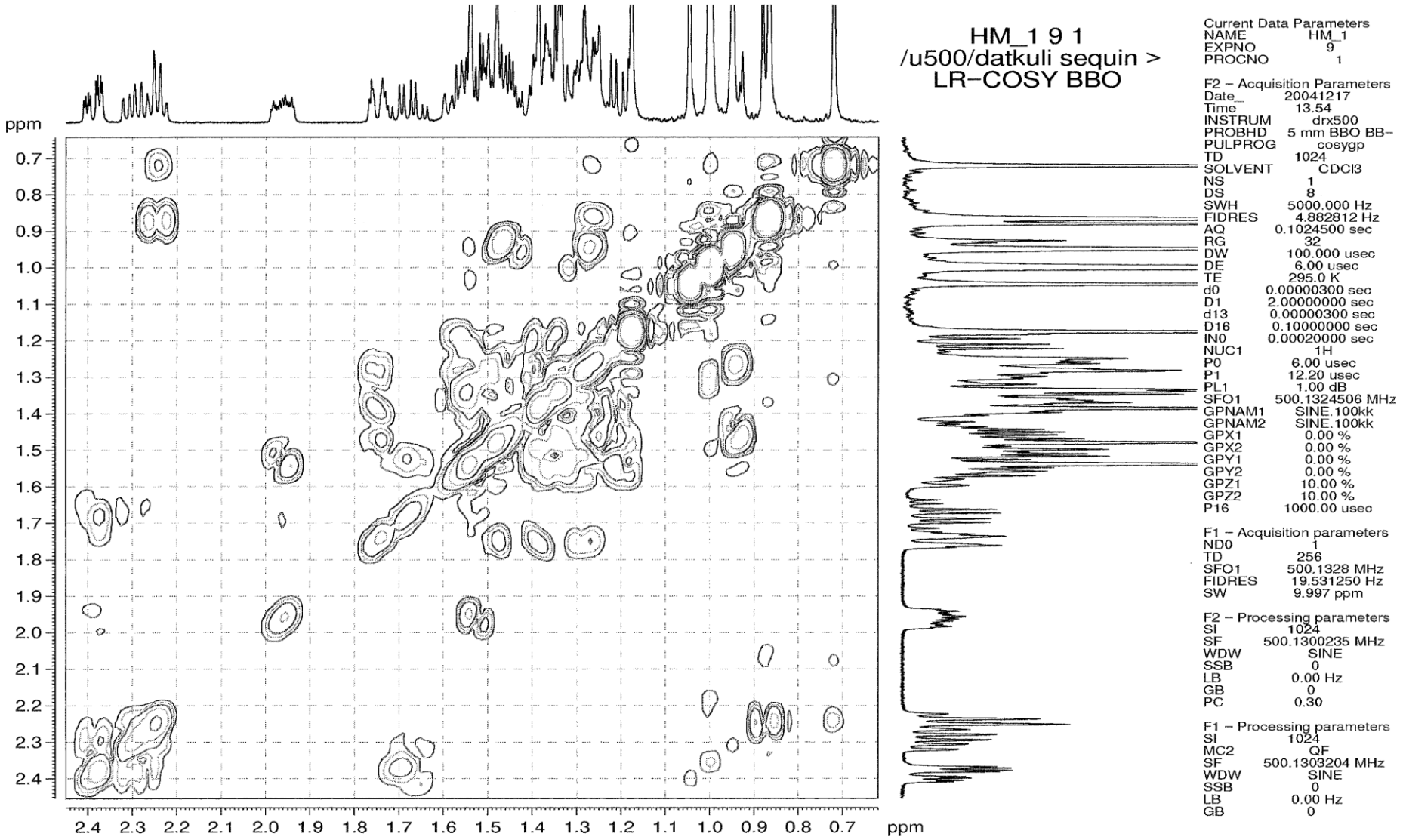
Appendix 10d: HMQC spectrum of friedelin (**134**)



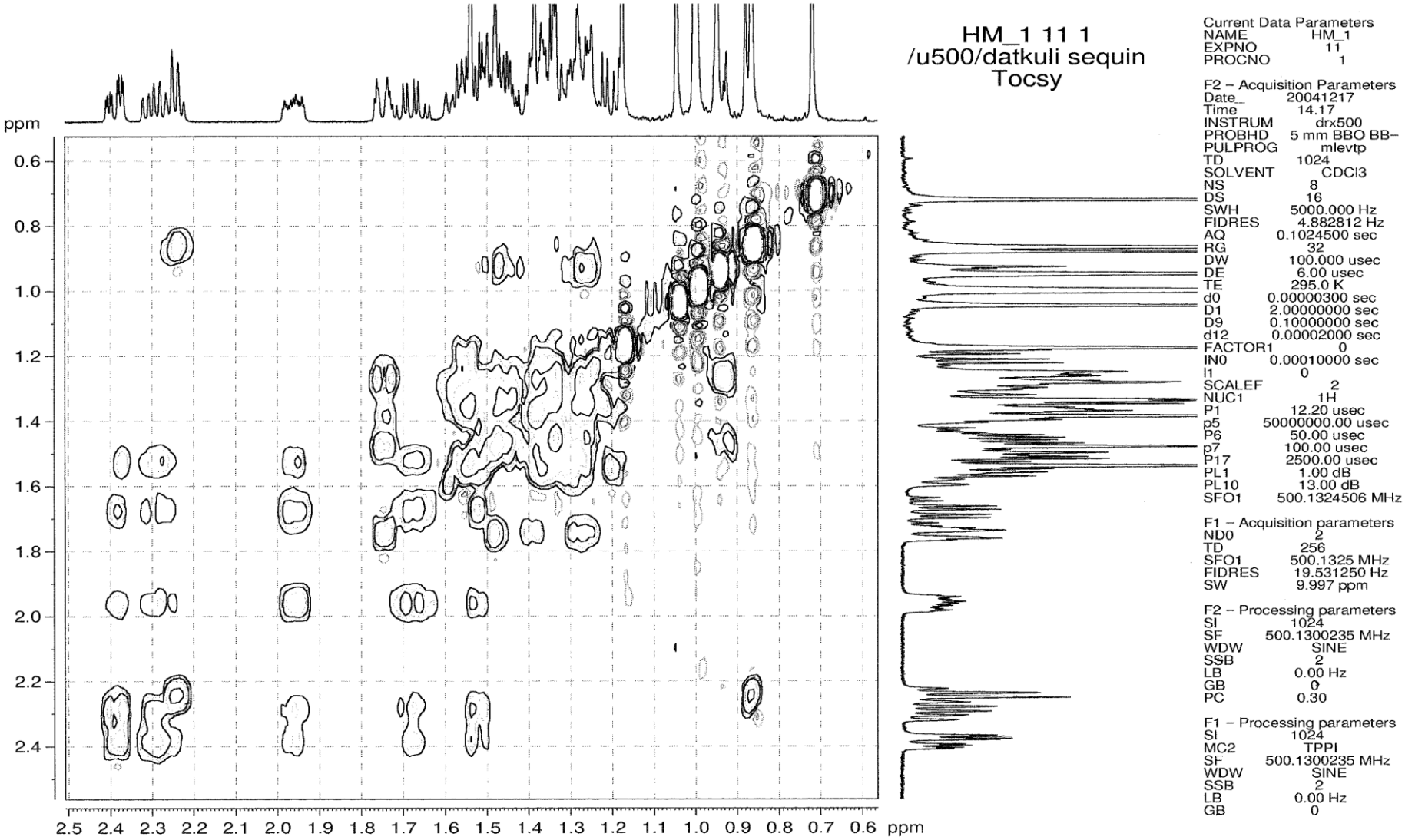
Appendix 10e: HMBC spectrum of friedelin (**134**)



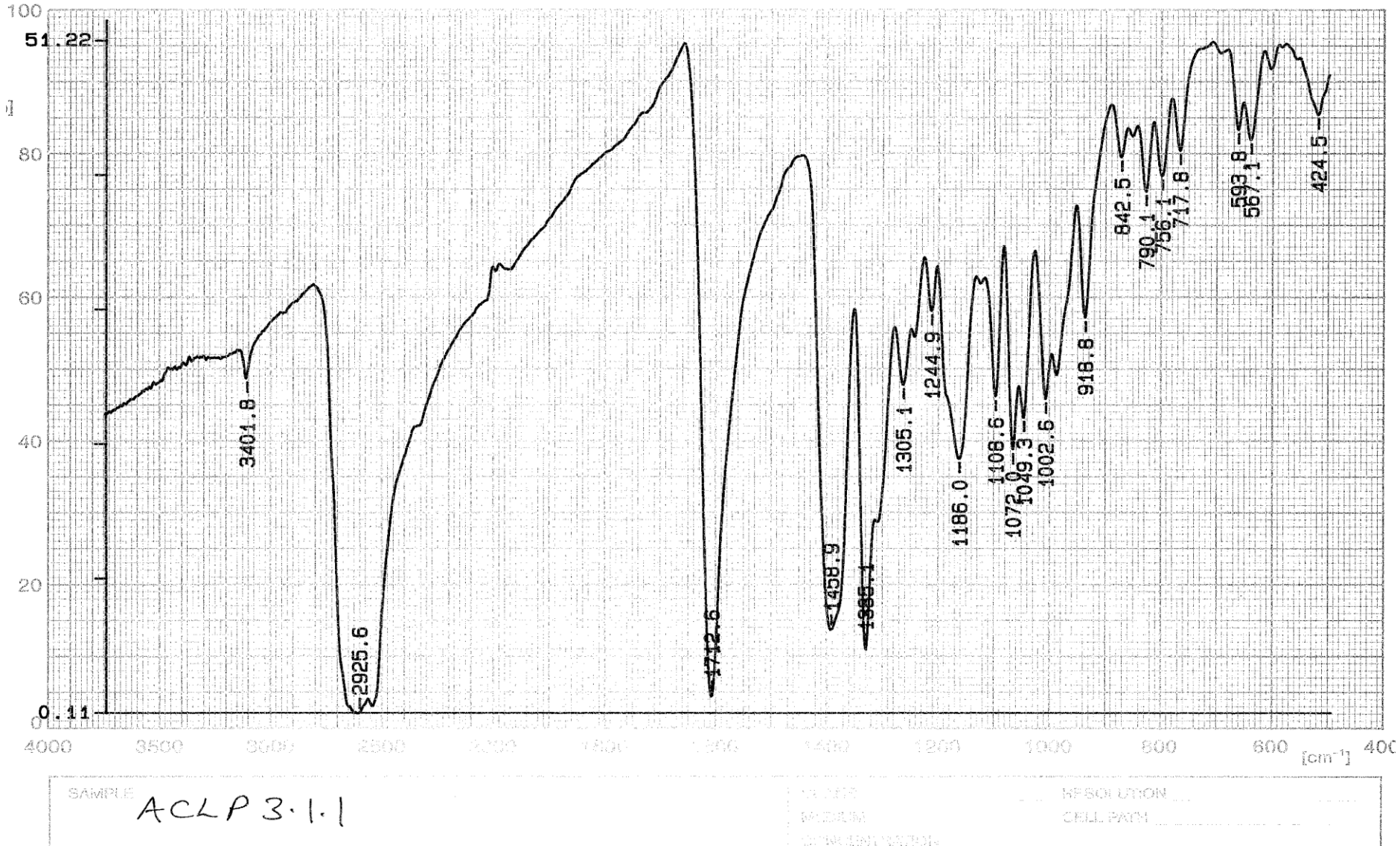
Appendix 10f: COSY spectrum of friedelin (**134**)



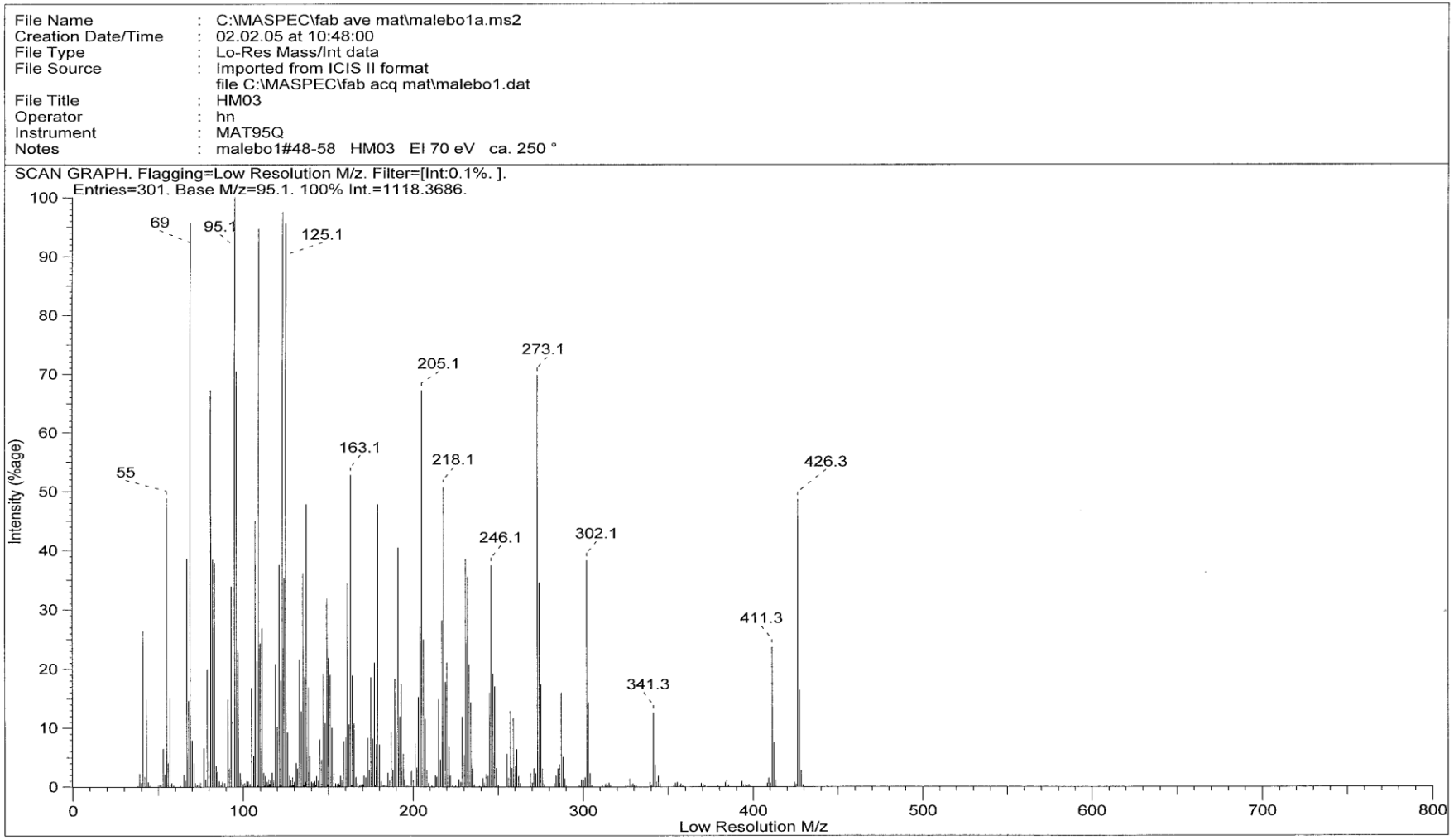
Appendix 10g: TOCSY spectrum of friedelin (**134**)



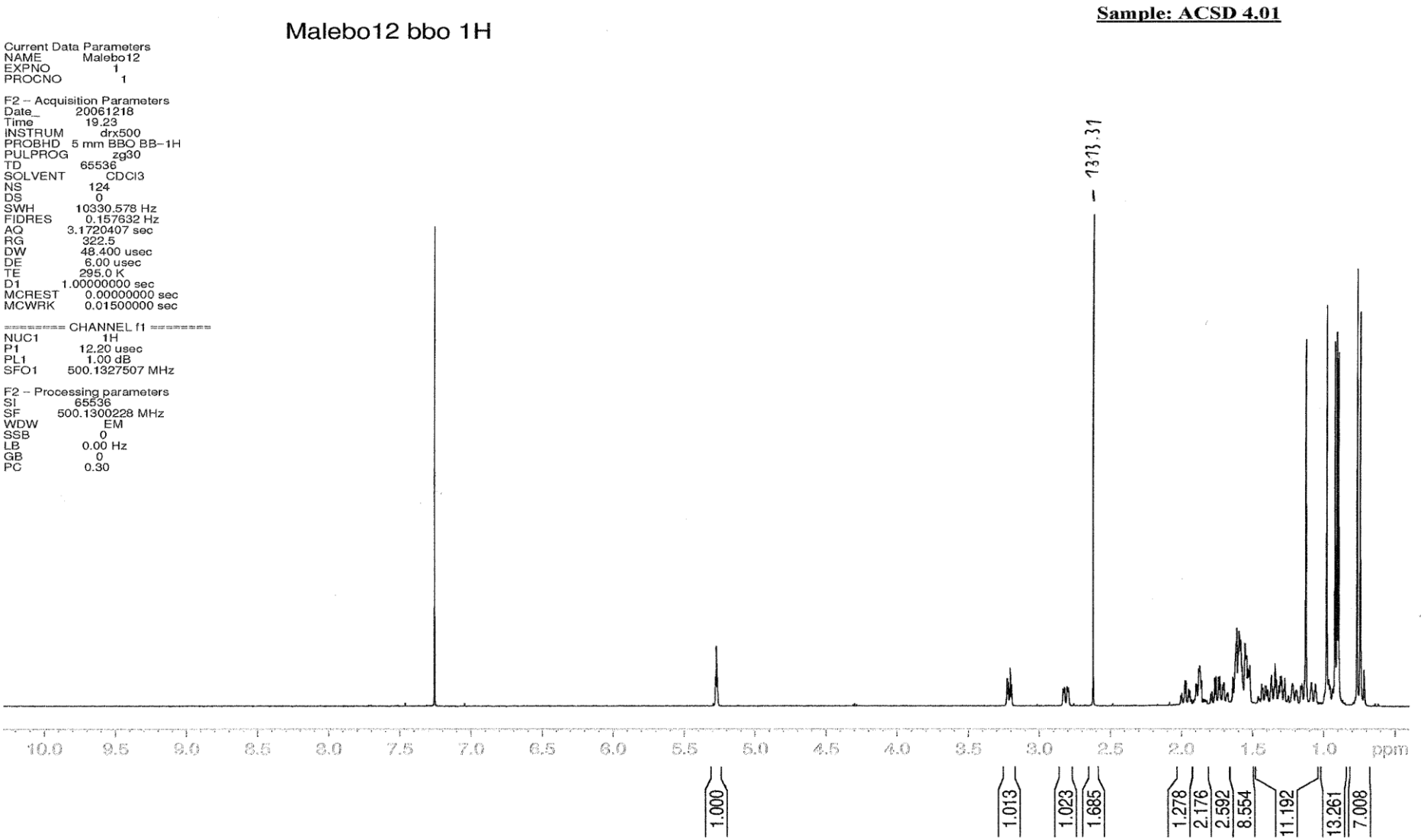
Appendix 10h: IR spectrum of friedelin (**134**)



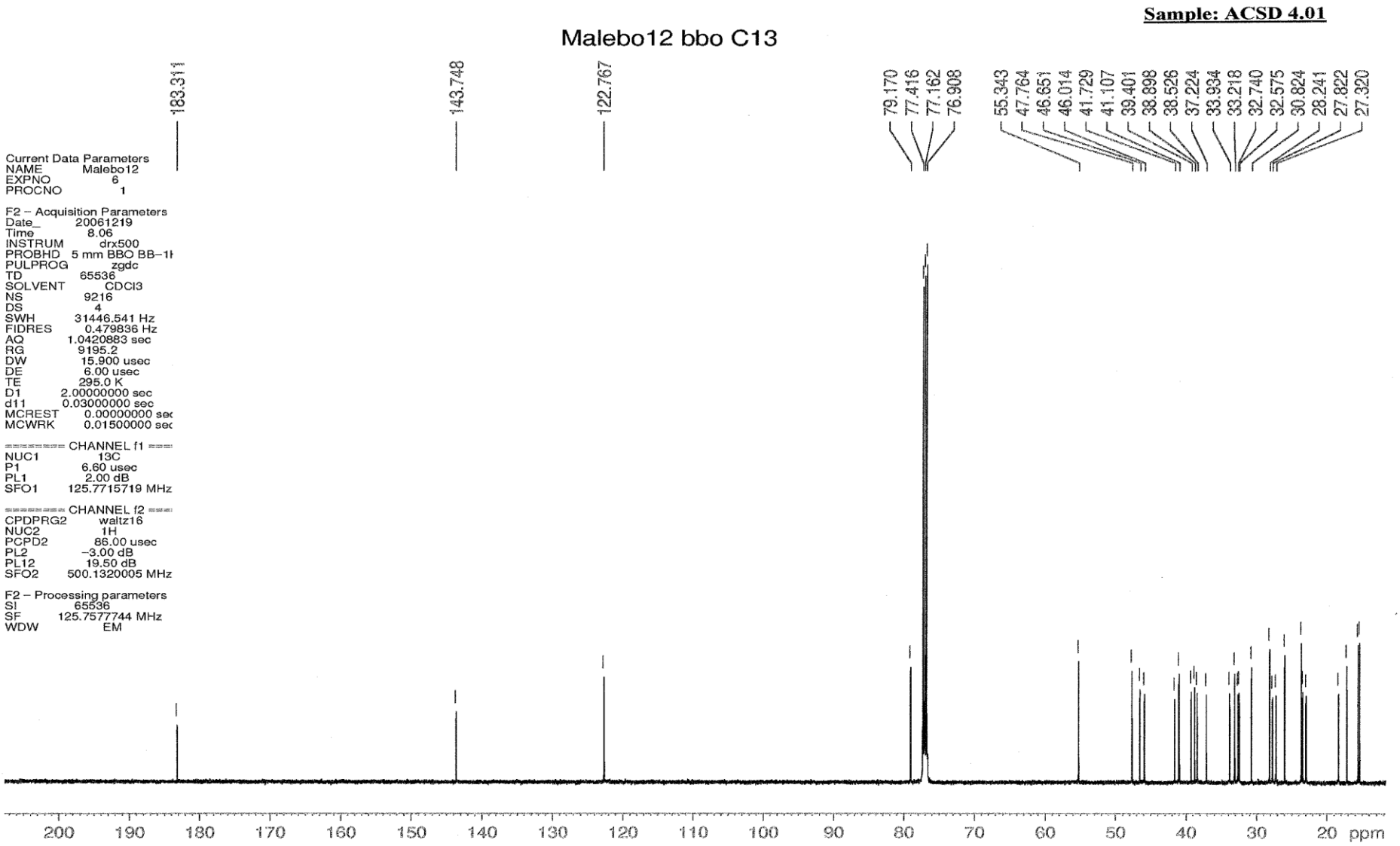
Appendix 10i: MS spectrum of friedelin (**134**)



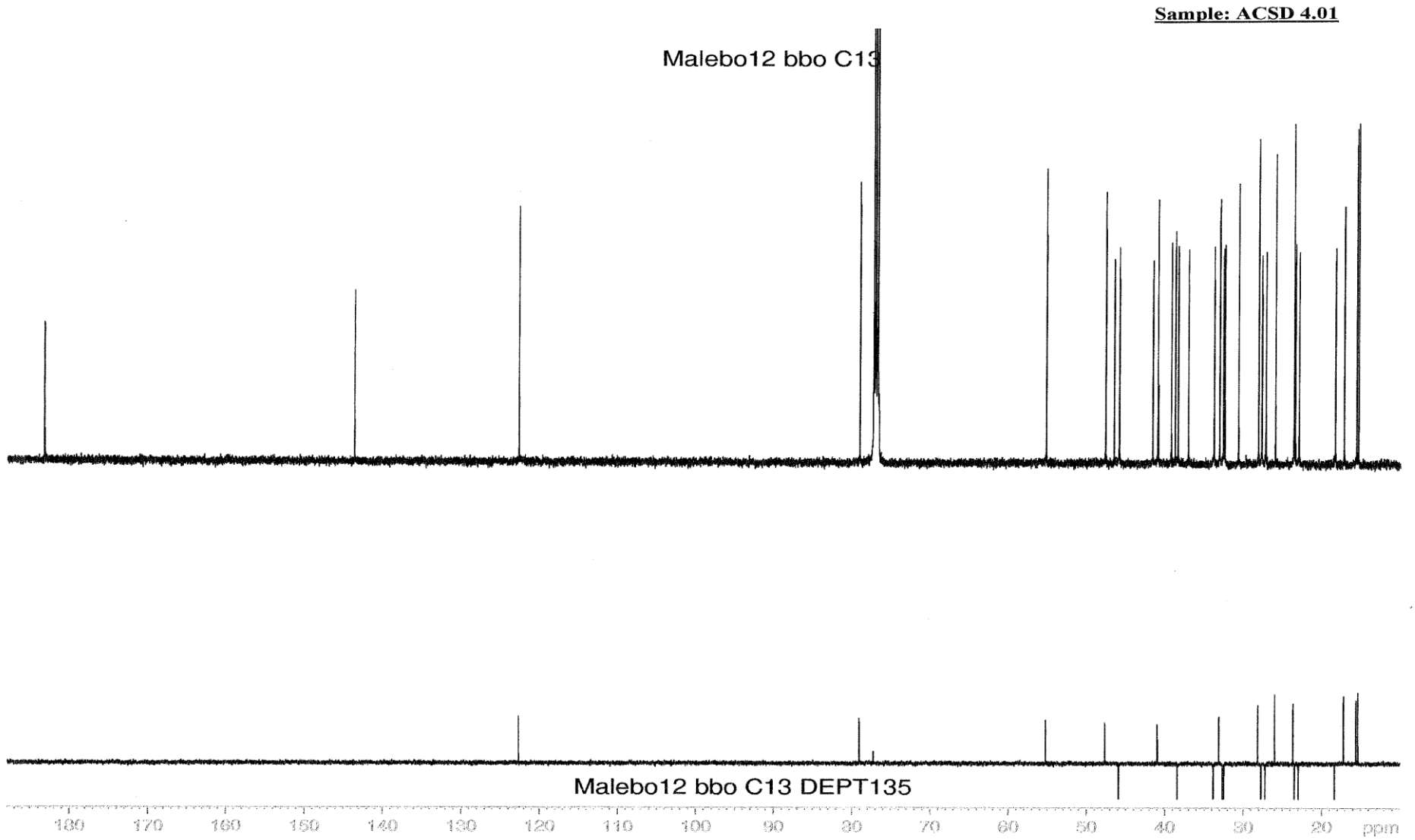
Appendix 11a: ^{1}H NMR spectrum of oleanolic acid (**124**)



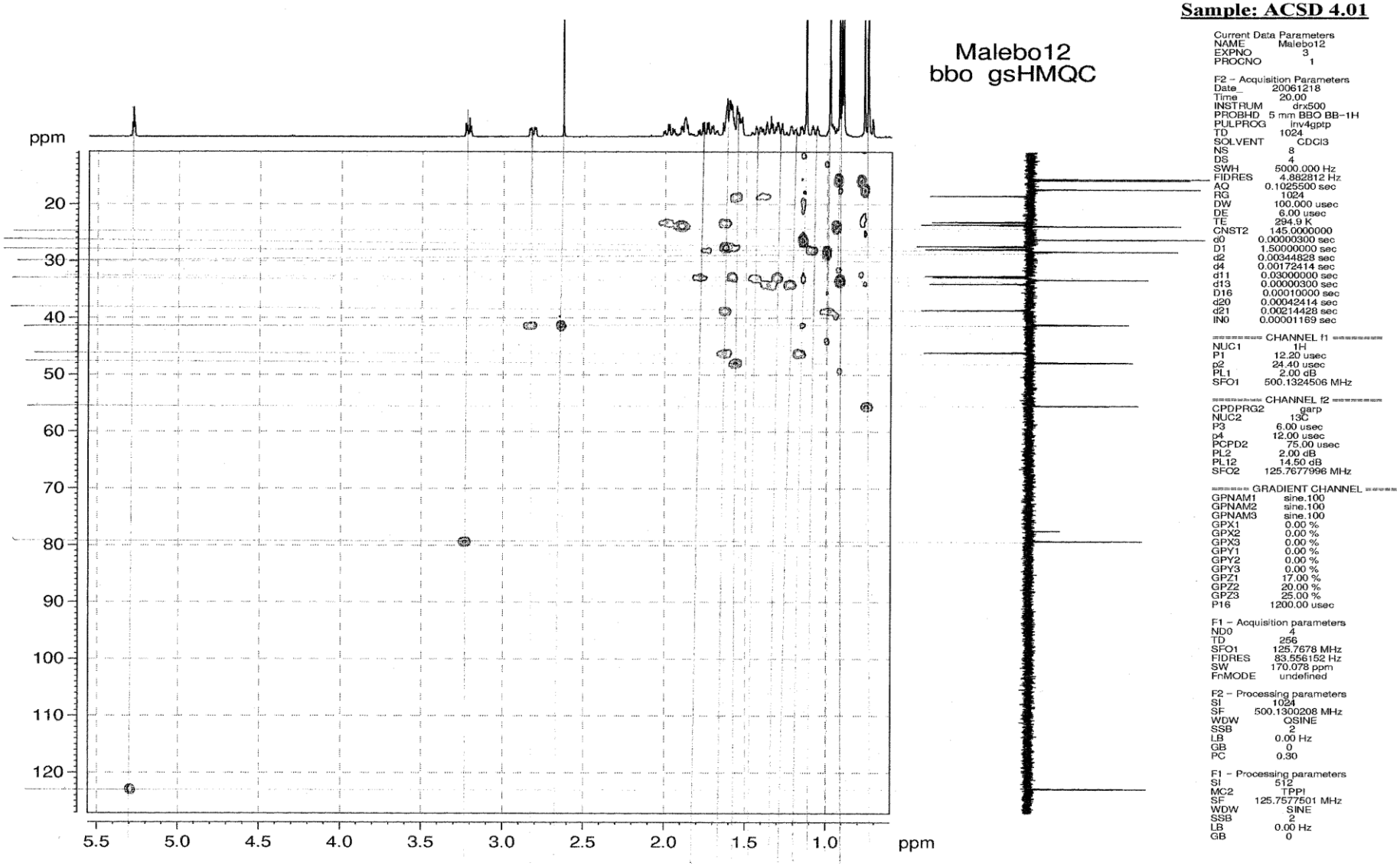
Appendix 11b: ^{13}C NMR spectrum of oleanolic acid (**124**)



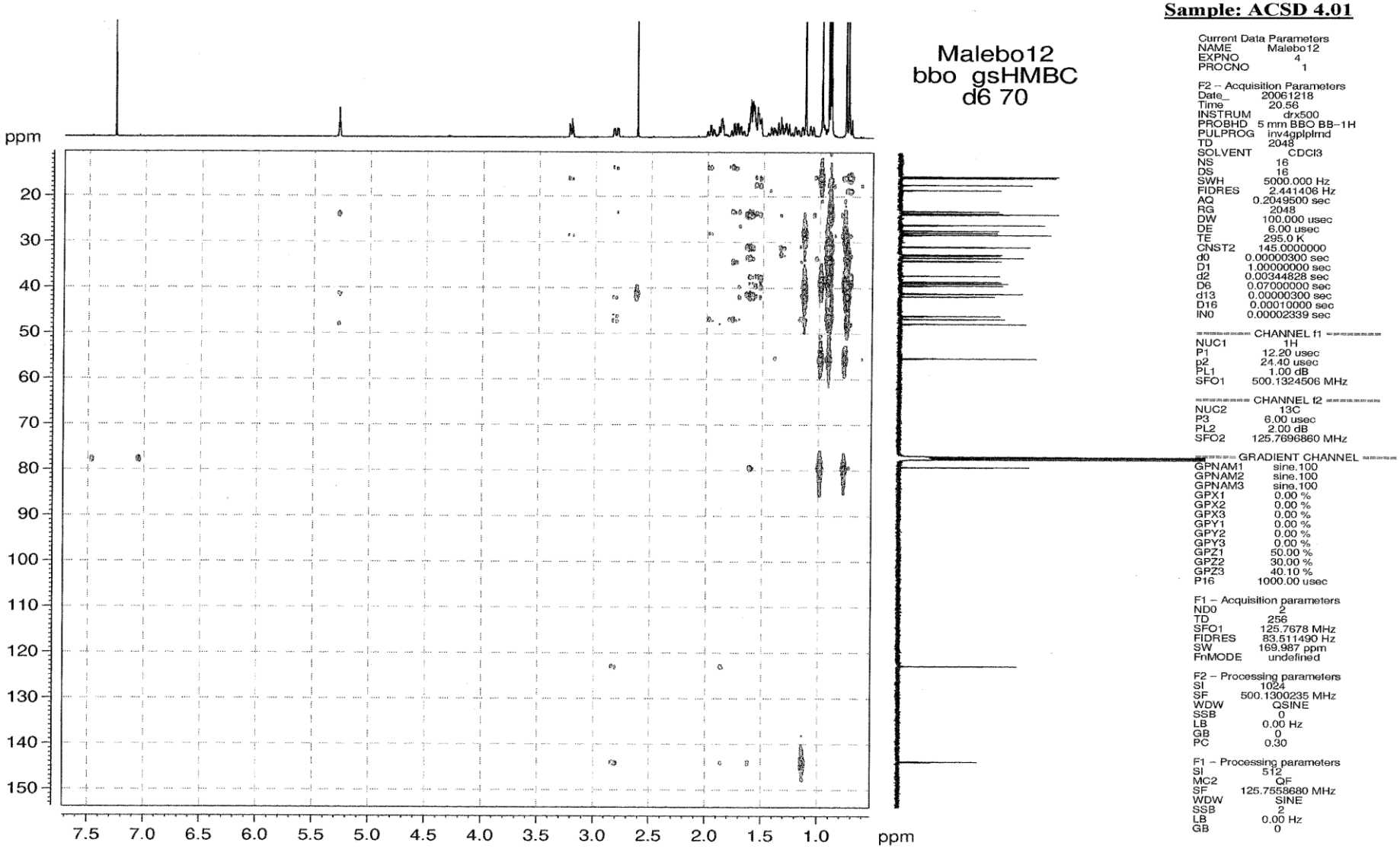
Appendix 11c: DEPT 135 spectrum of oleanolic acid (**124**)



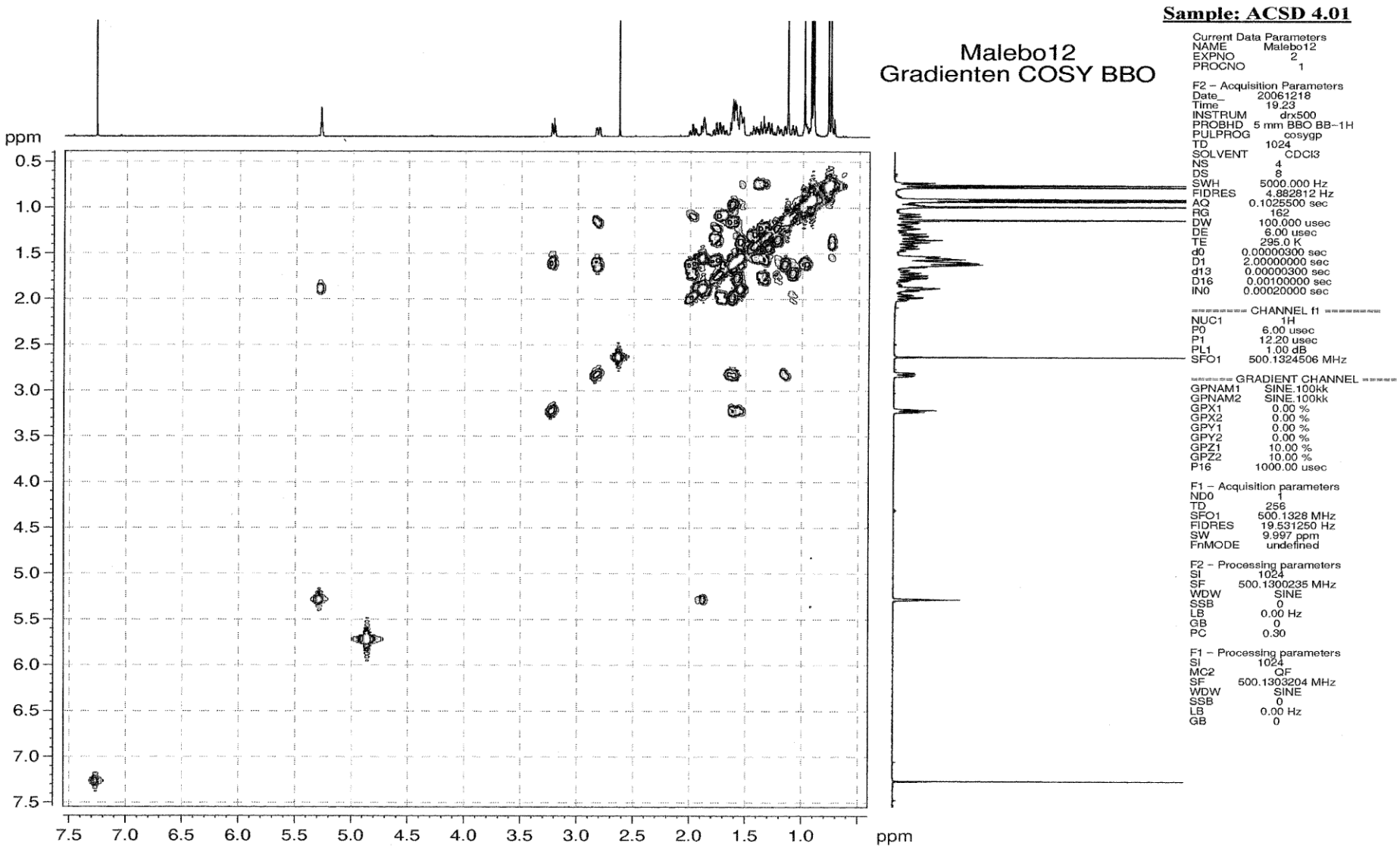
Appendix 11d: HMQC spectrum of oleanolic acid (**124**)



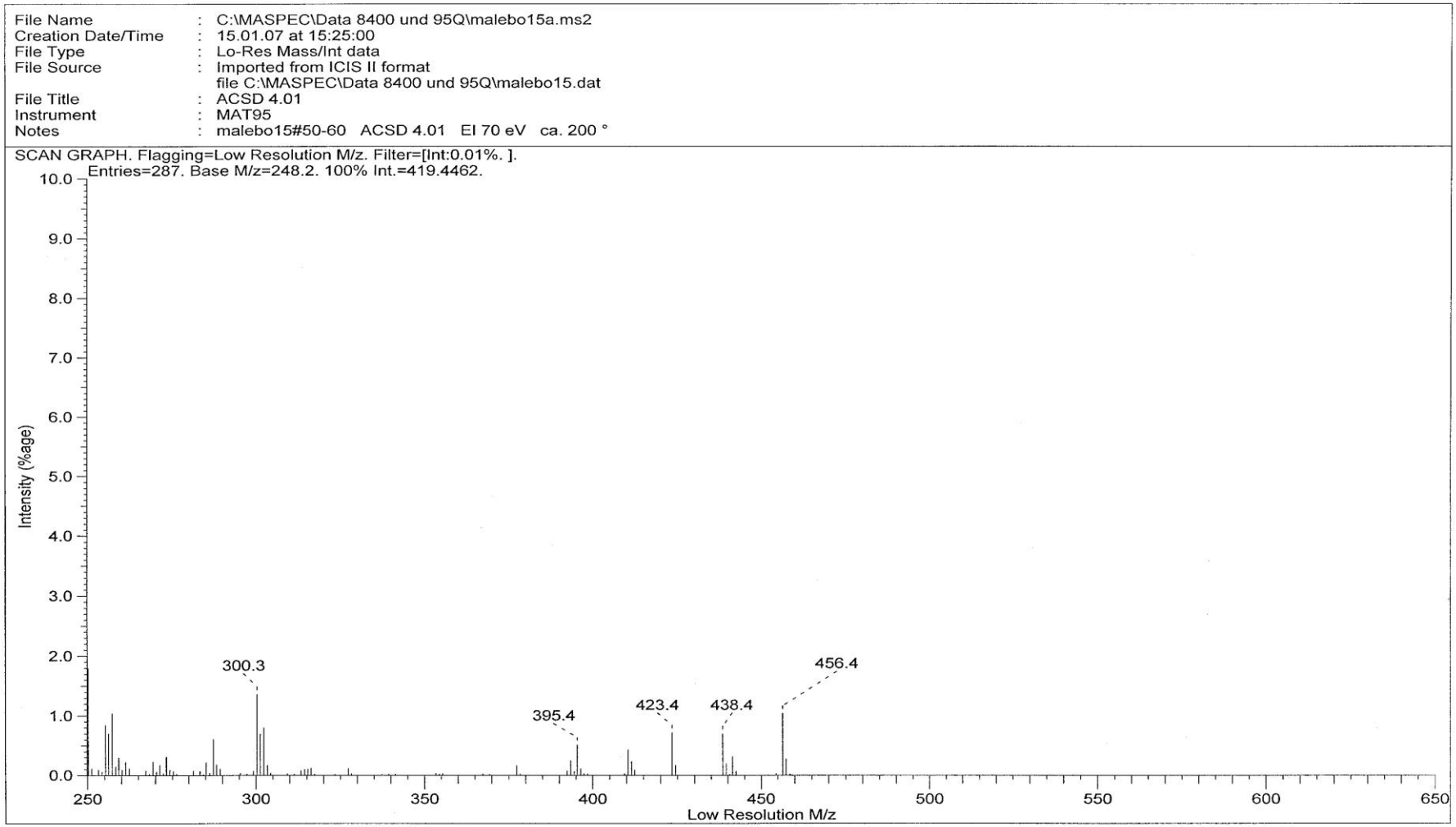
Appendix 11e: HMBC spectrum of oleanolic acid (**124**)



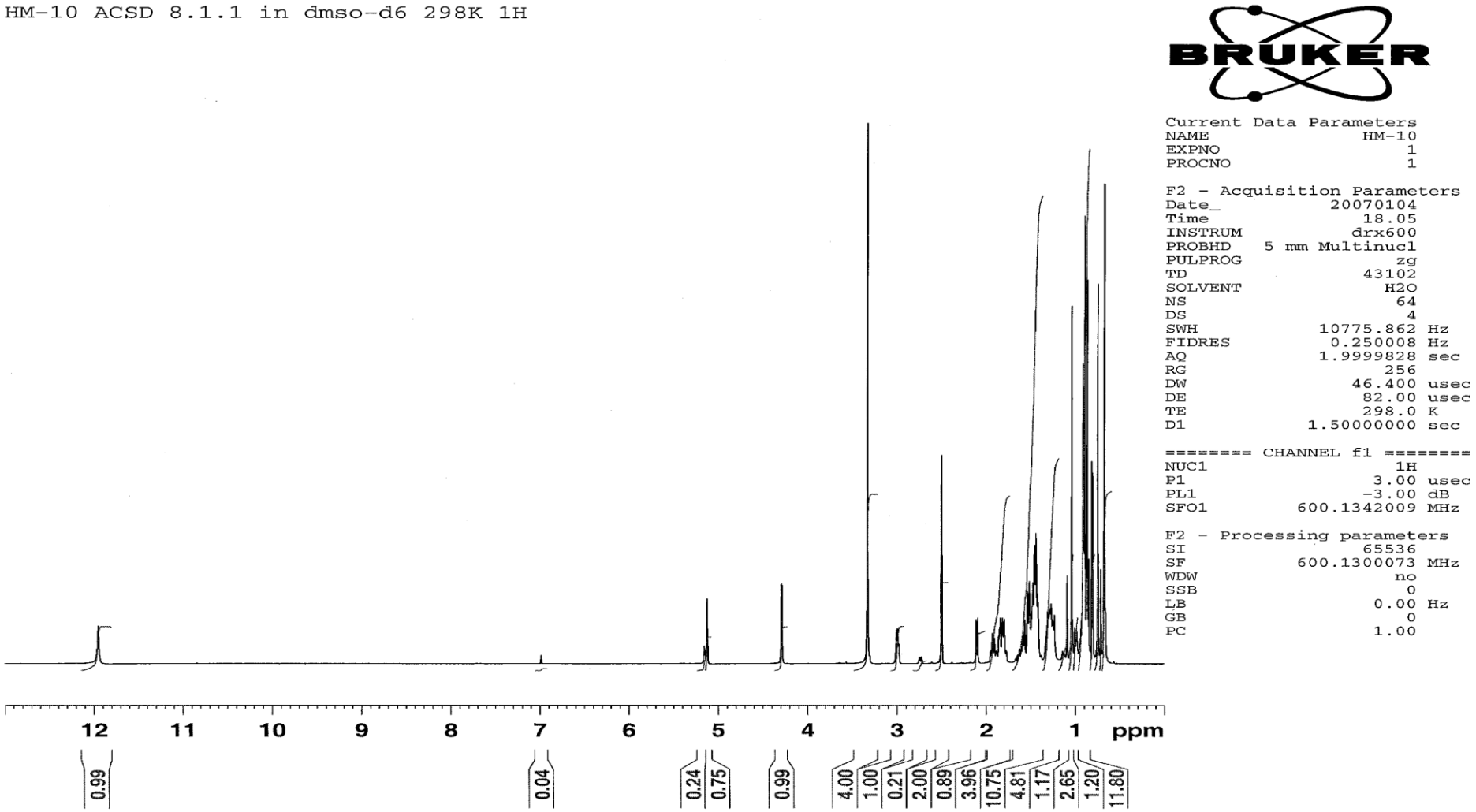
Appendix 11f: COSY spectrum of oleanolic acid (**124**)



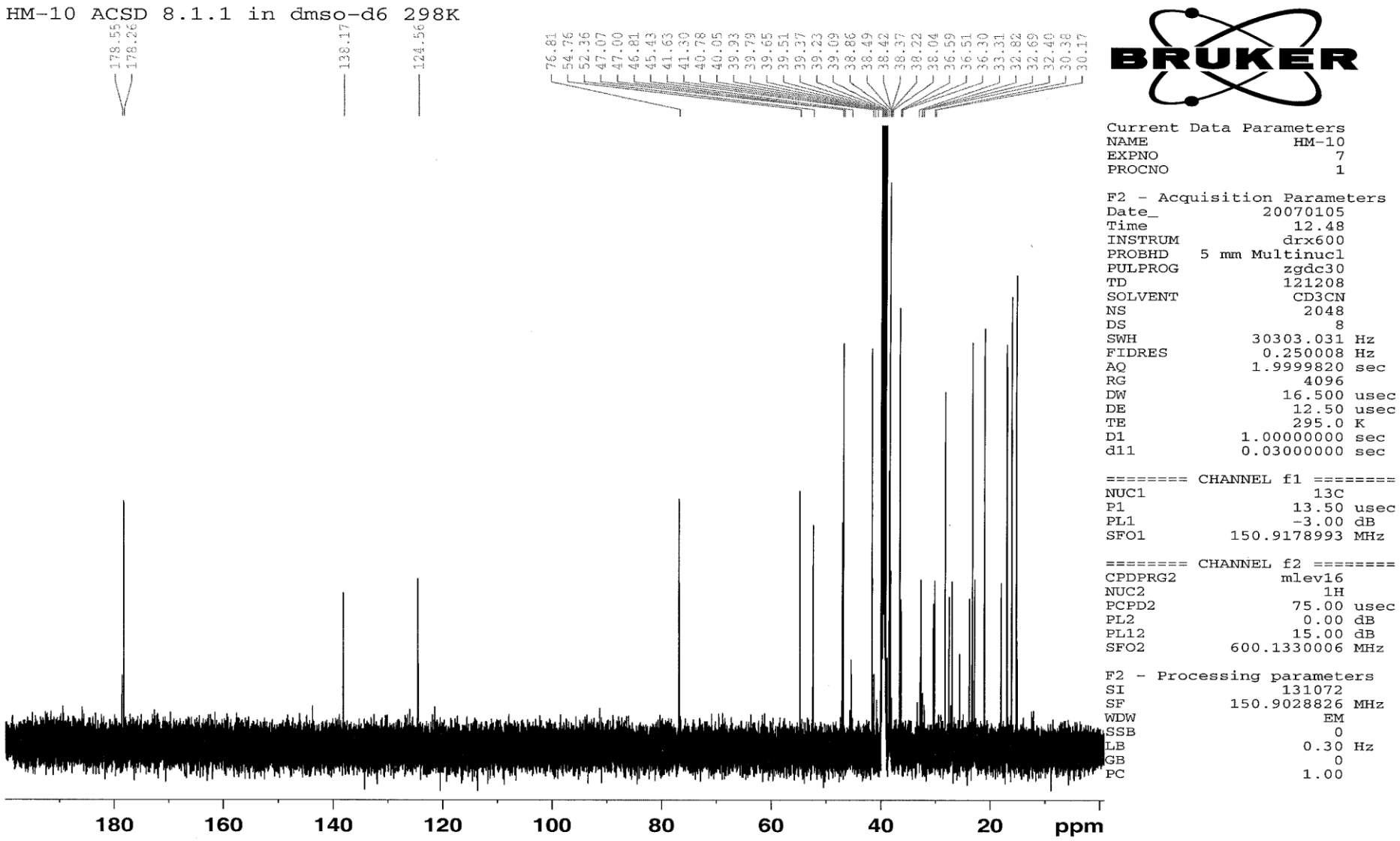
Appendix 11g: MS spectrum of oleanolic acid (**124**)



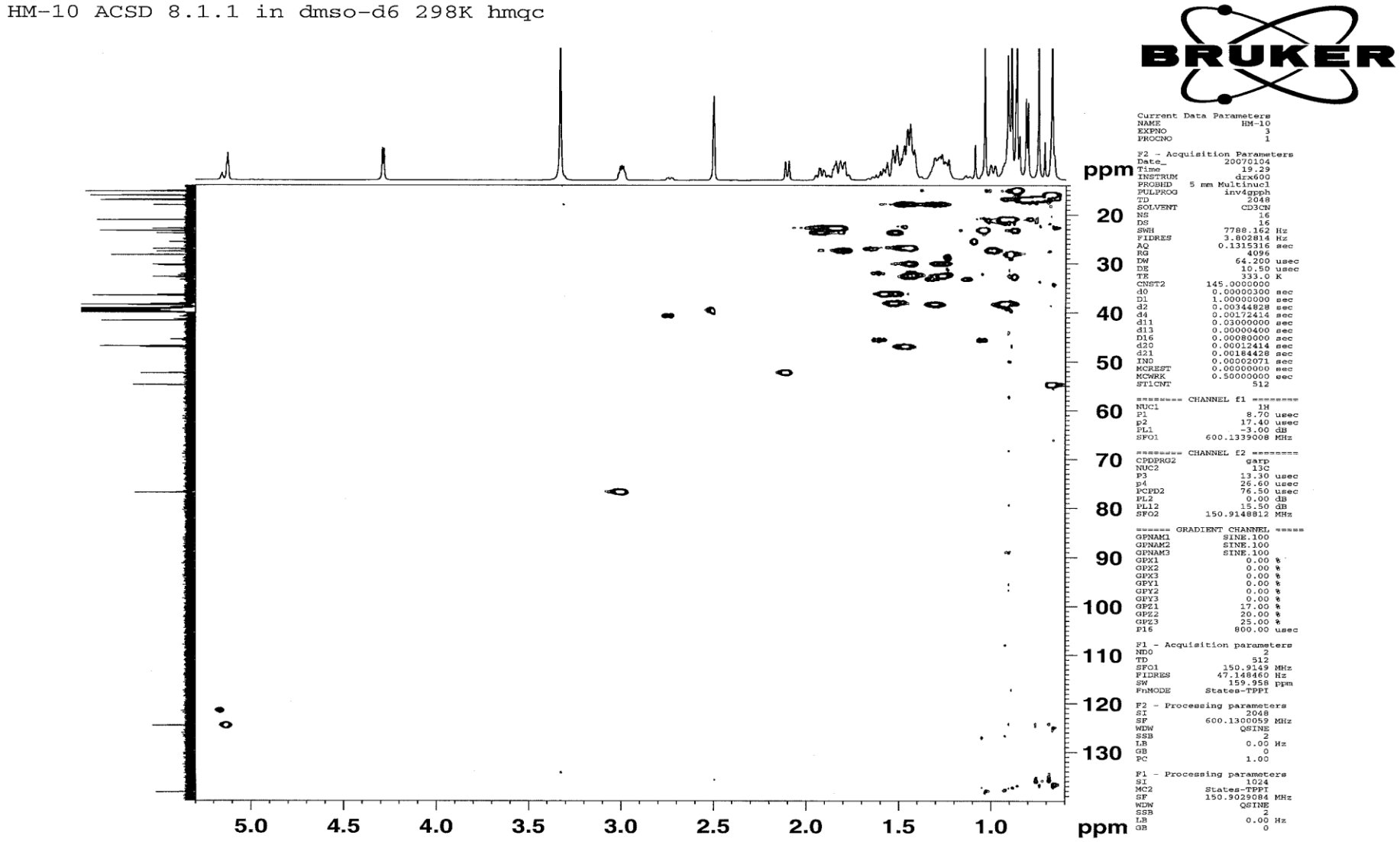
Appendix 12a: ^{1}H NMR spectrum of ursolic acid (**123**)



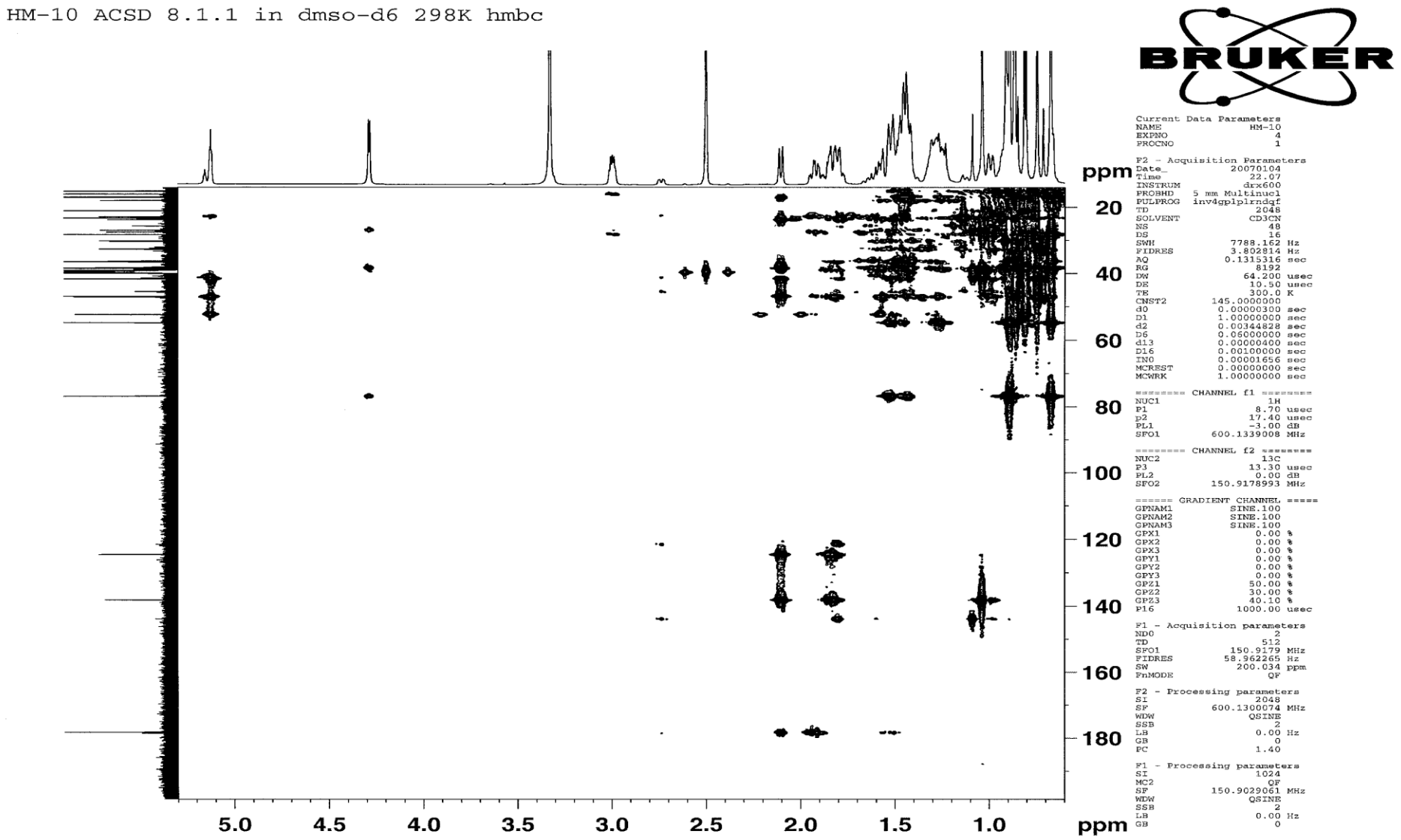
Appendix 12b: ^{13}C NMR spectrum of ursolic acid (**123**)



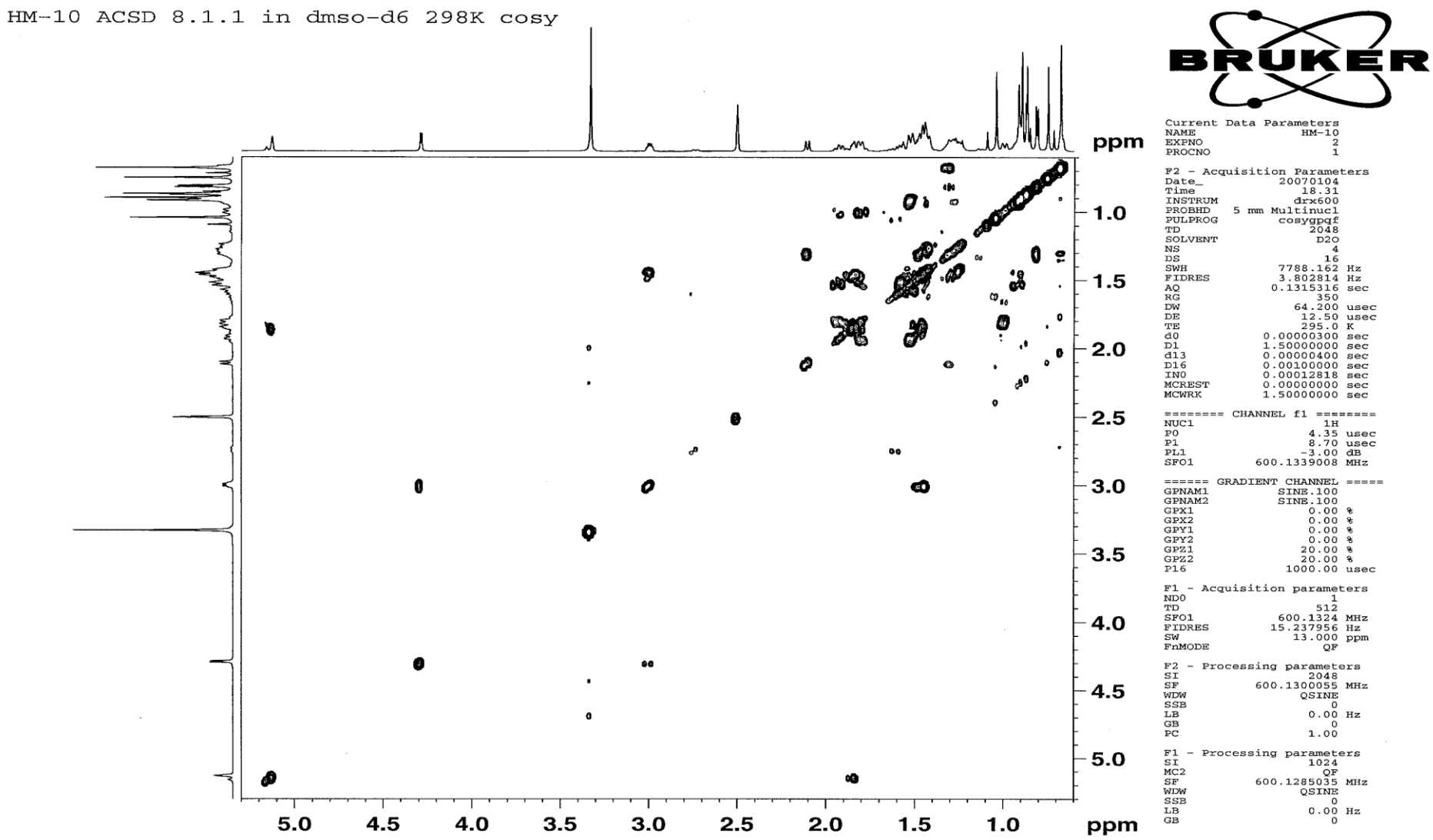
Appendix 12c: HMQC spectrum of ursolic acid (**123**)



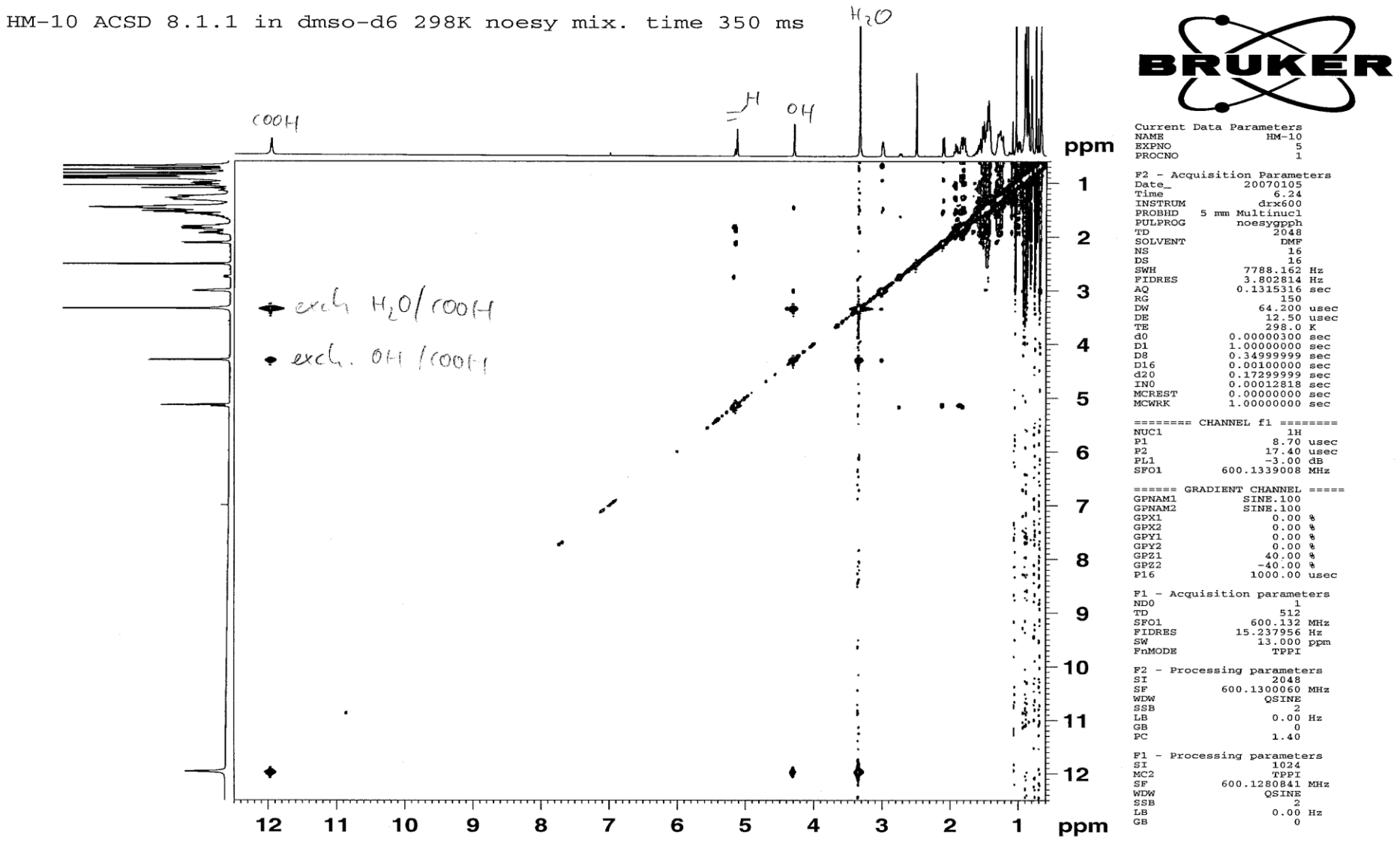
Appendix 12d: HMBC spectrum of ursolic acid (**123**)



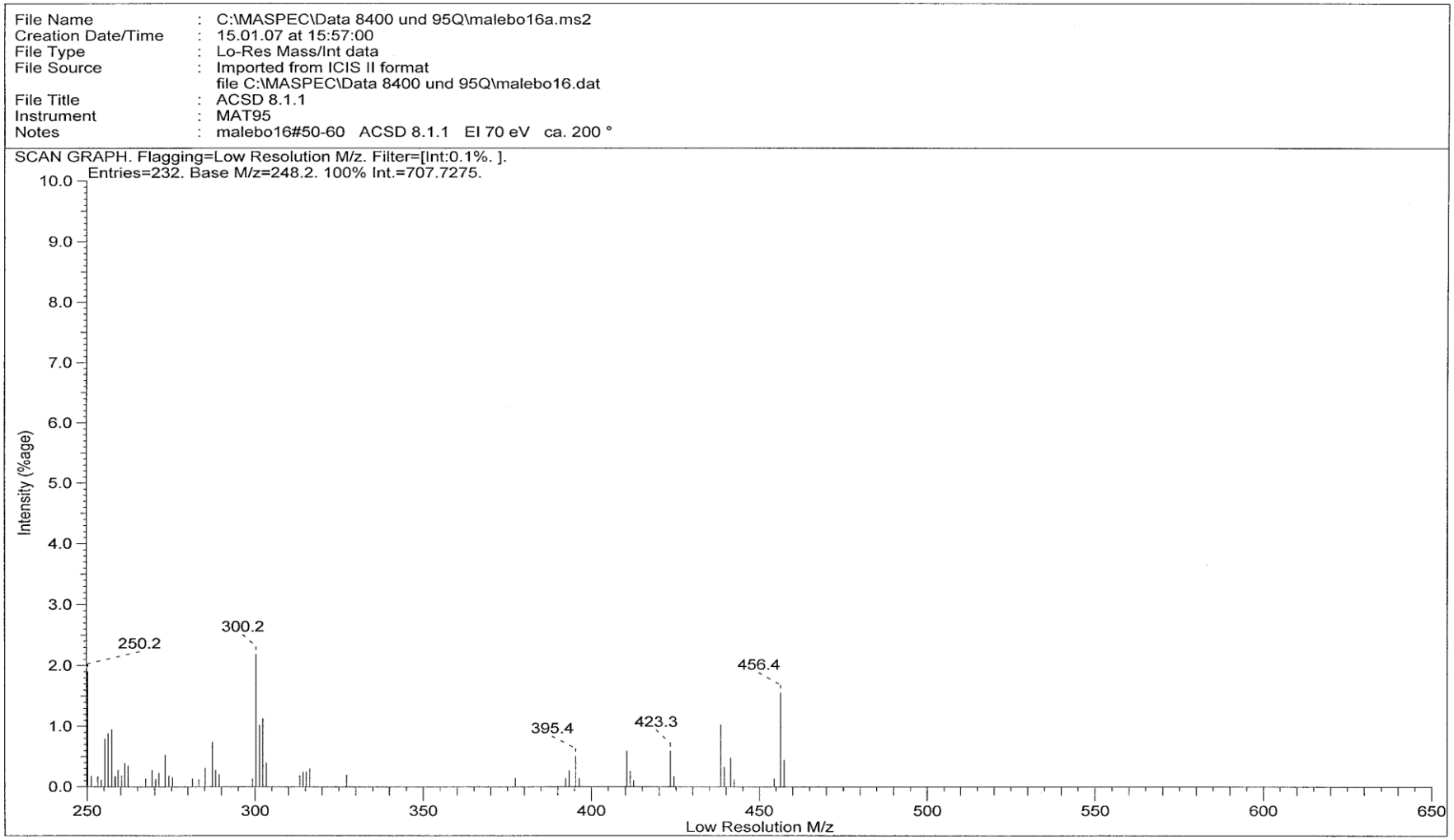
Appendix 12e: COSY spectrum of ursolic acid (**123**)



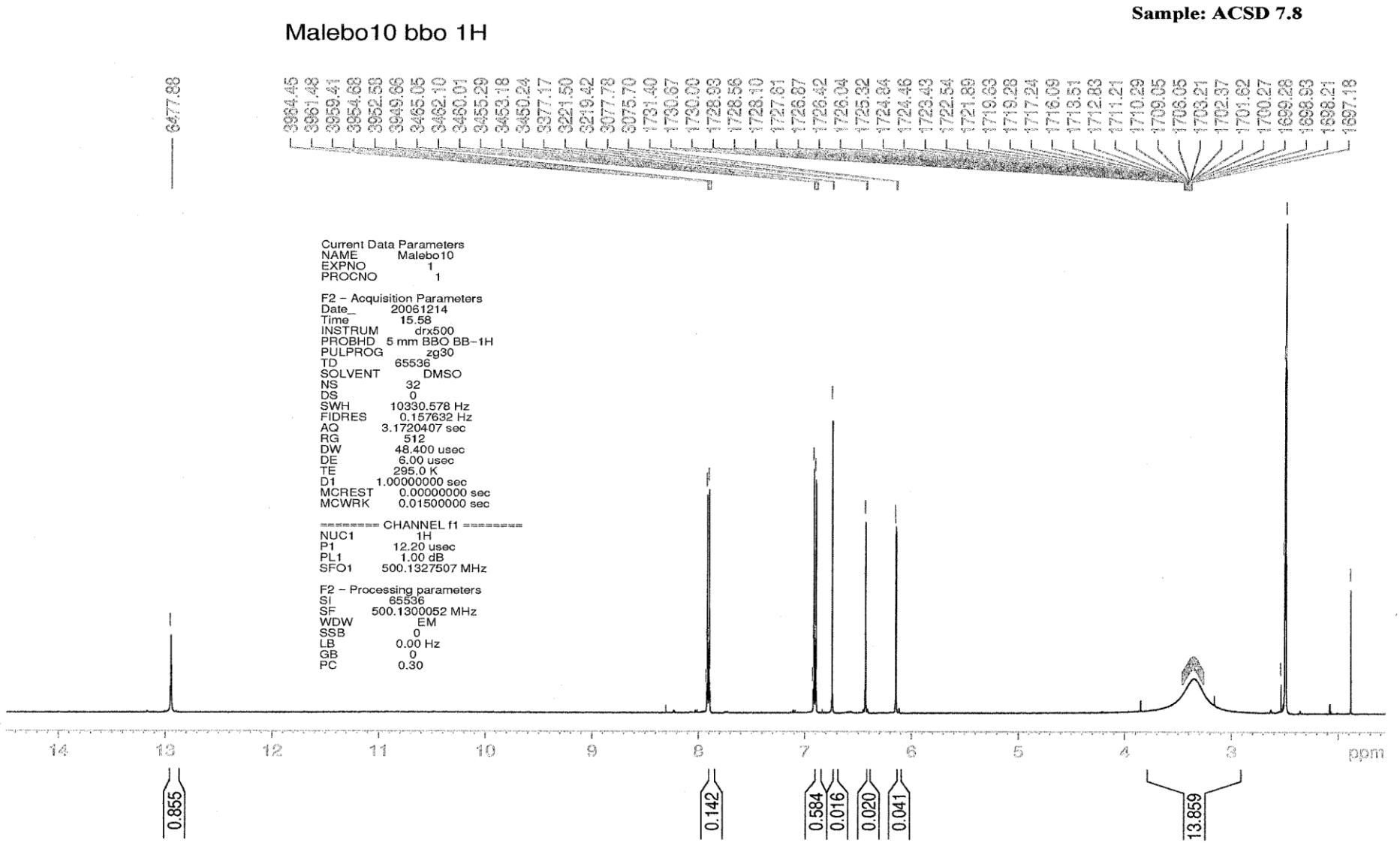
Appendix 12f: NOESY spectrum of ursolic acid (**123**)



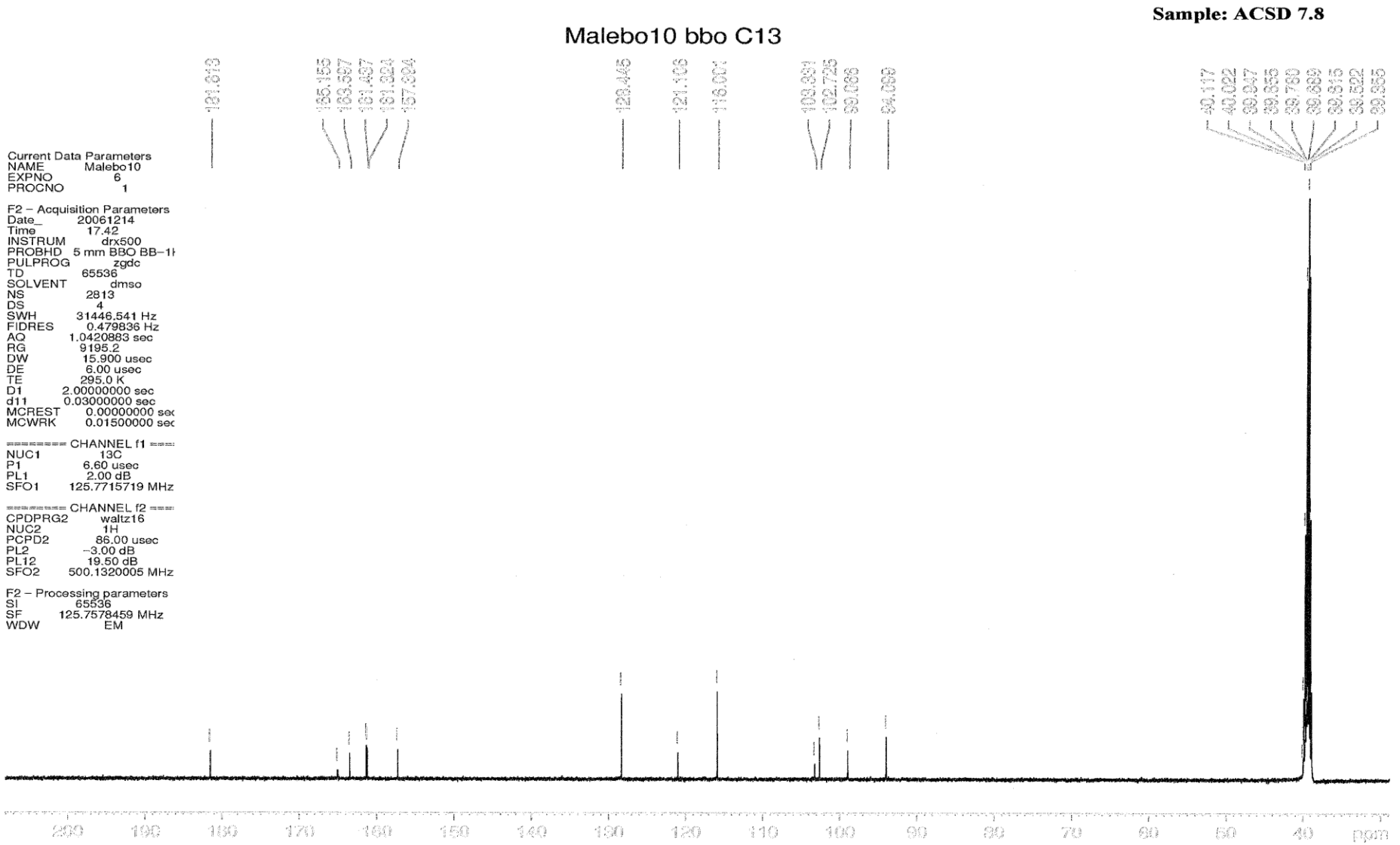
Appendix 12g: MS spectrum of ursolic acid (**123**)



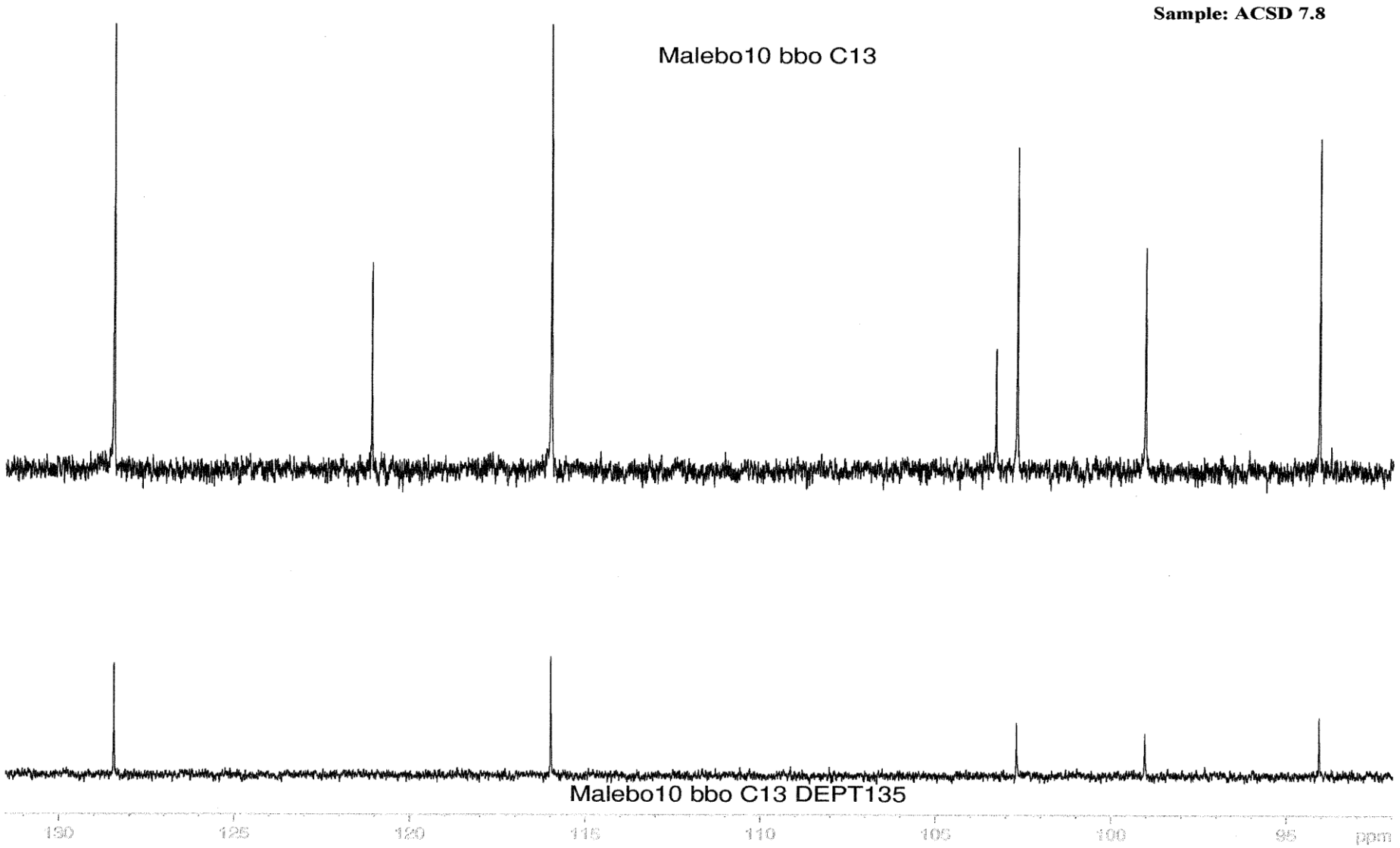
Appendix 13a: ^{1}H NMR spectrum of apigenin (**135**)



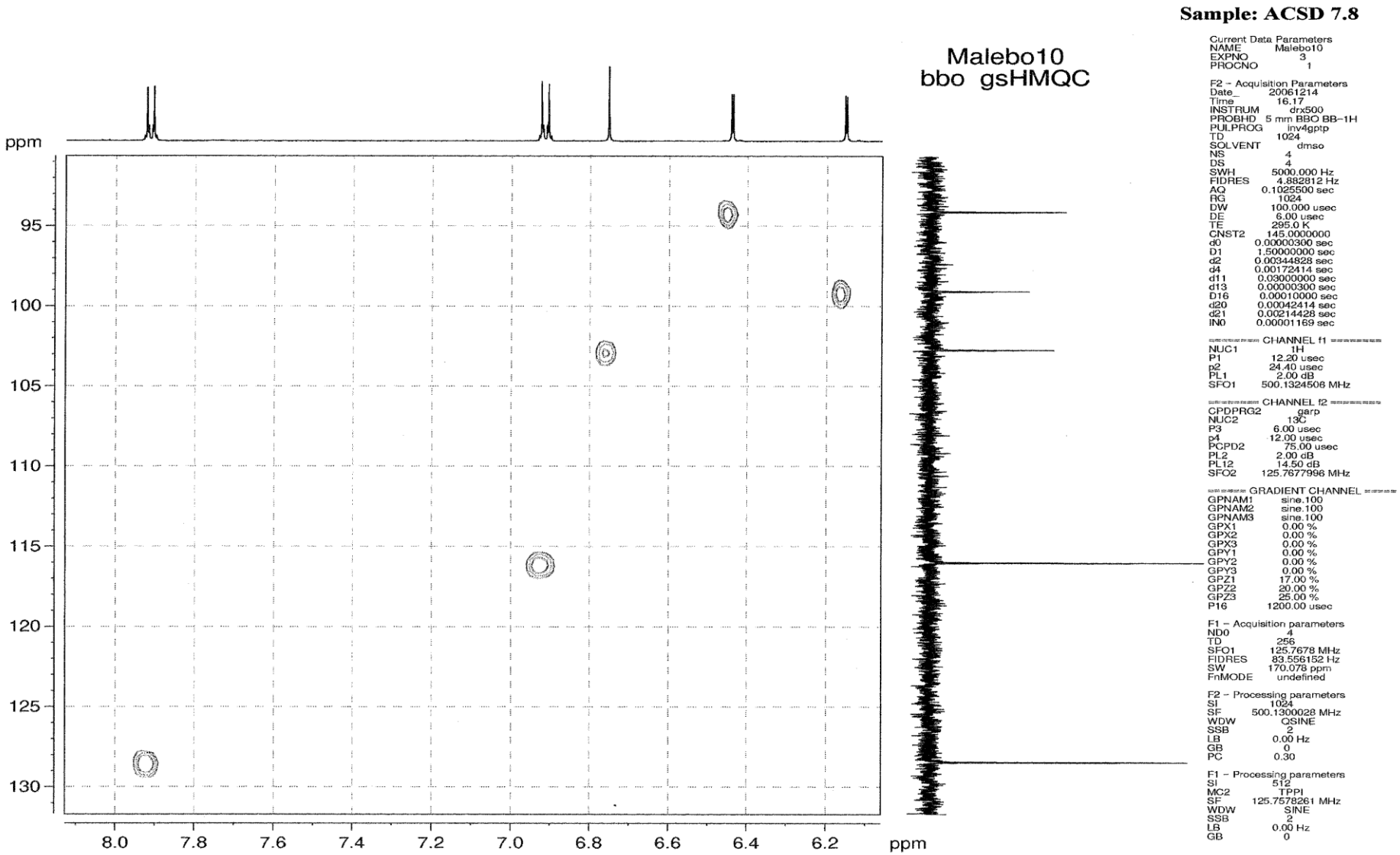
Appendix 13b: ^{13}C NMR spectrum of apigenin (**135**)



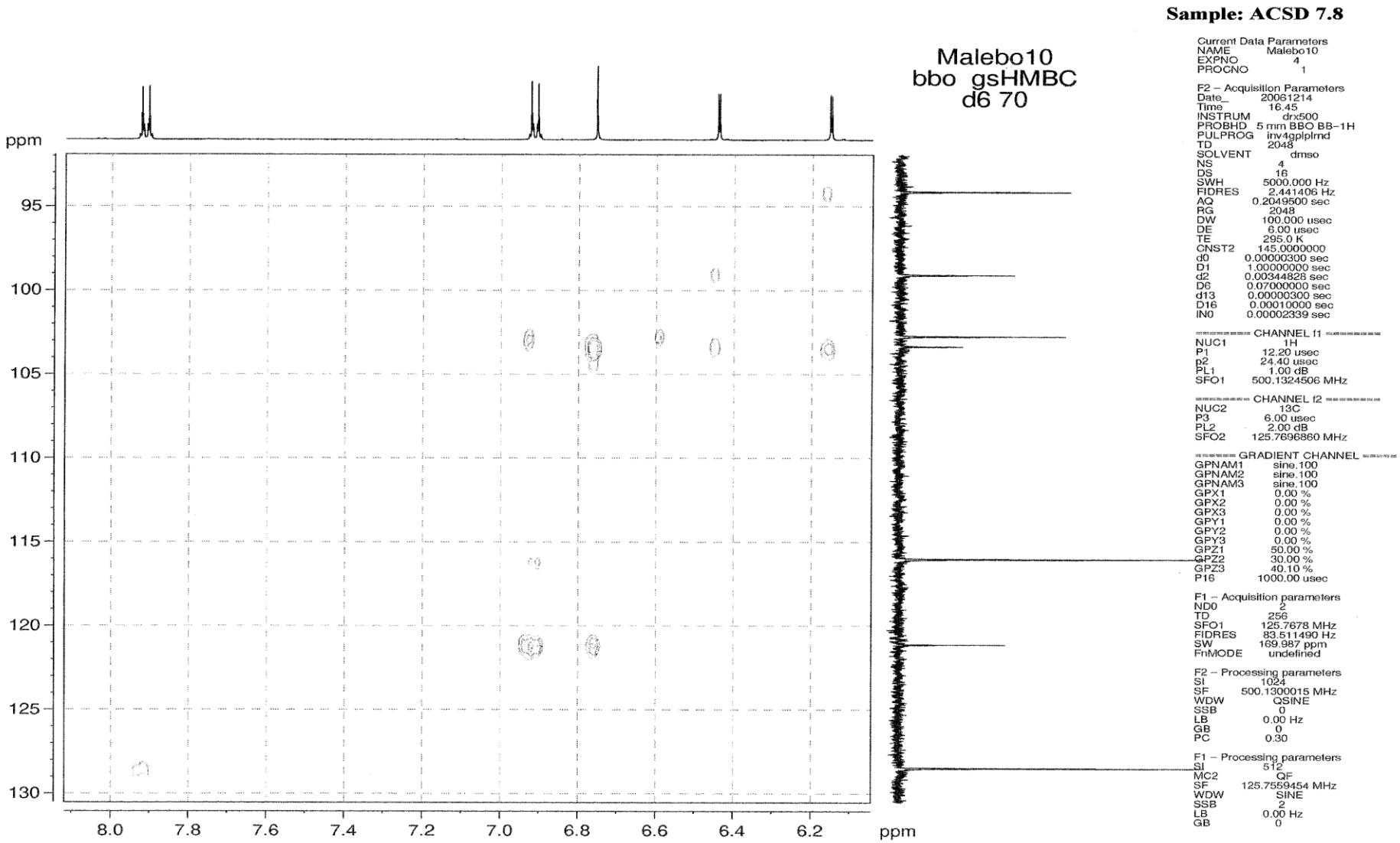
Appendix 13c: DEPT 135 spectrum of apigenin (**135**)



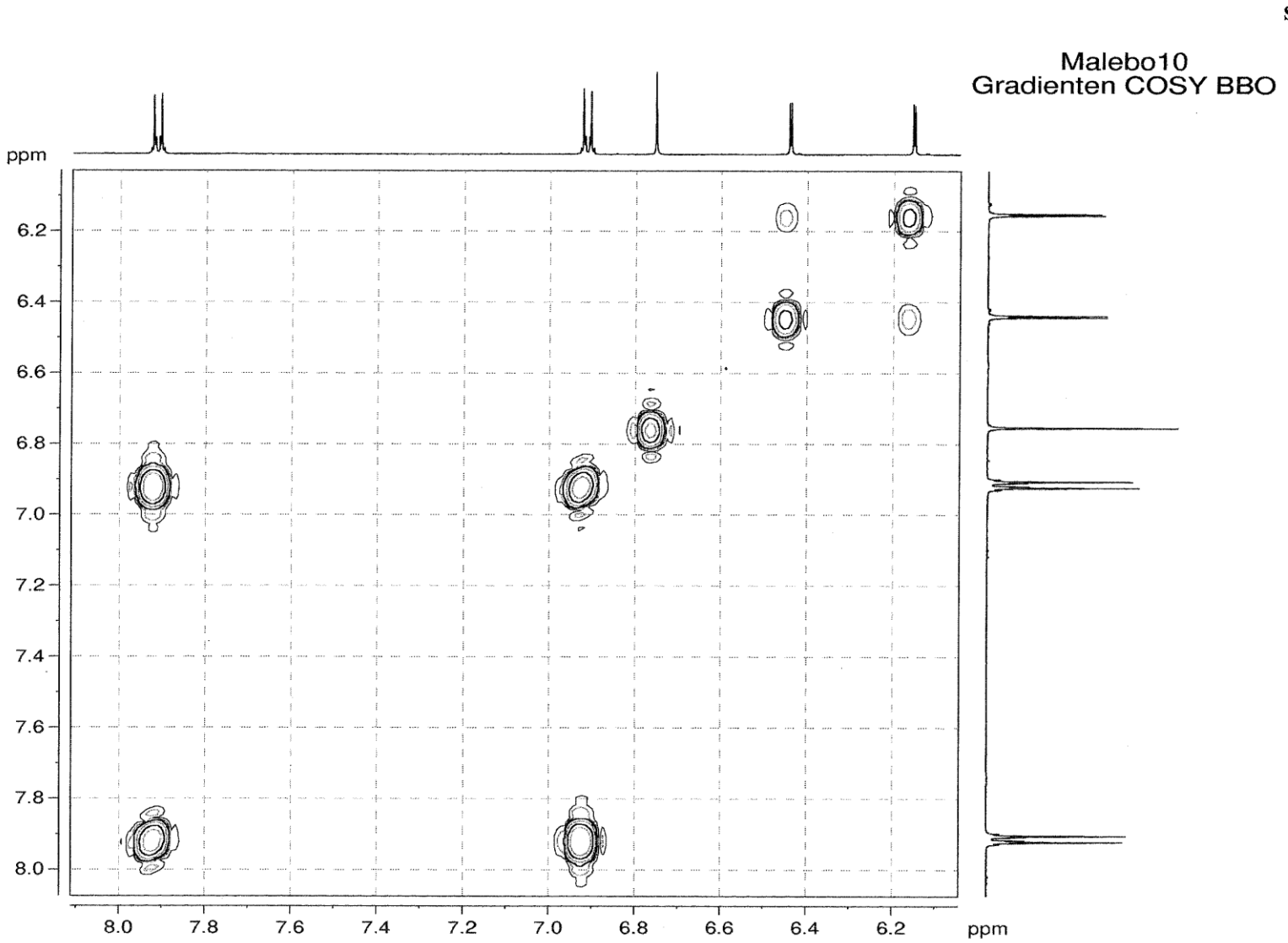
Appendix 13d: HMQC spectrum of apigenin (**135**)



Appendix 13e: HMBC spectrum of apigenin (**135**)



Appendix 13f: COSY spectrum of apigenin (**135**)



Sample: ACSD 7.8

Current Data Parameters
NAME Malebo10
EXPNO 2
PROCNO 1

F2 – Acquisition Parameters
Date_ 20061214
Time 15.58
INSTRUM drx500
PROBHD 5 mm BBO BB–1H
PULPROG cosygp
TD 1024
SOLVENT DMSO
NS 2
DS 8
SWH 5000.000 Hz
FIDRES 4.882812 Hz
AQ 0.1025500 sec
RG 256
DW 100.000 usec
DE 6.00 usec
TE 295.0 K
d0 0.00000300 sec
D1 2.00000000 sec
d13 0.00000300 sec
D16 0.00100000 sec
IN0 0.00020000 sec

======== CHANNEL f1 ========
NUC1 1H
P0 6.00 usec
P1 12.20 usec
PL1 1.00 dB
SFO1 500.1324506 MHz

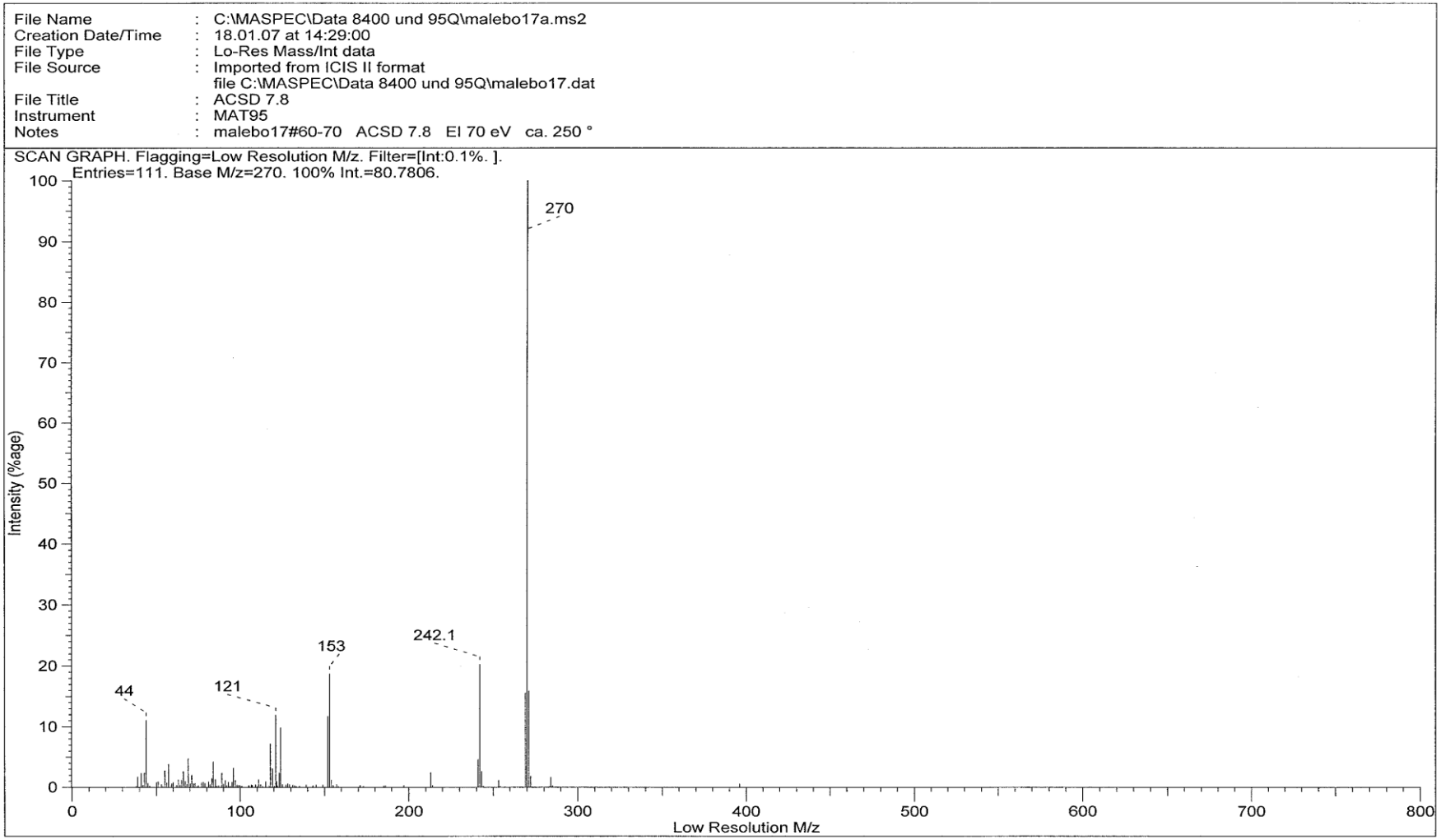
====== GRADIENT CHANNEL =====
GPNAM1 SINE.100kk
GPNAM2 SINE.100kk
GPX1 0.00 %
GPX2 0.00 %
GPY1 0.00 %
GPY2 0.00 %
GPZ1 10.00 %
GPZ2 10.00 %
P16 1000.00 usec

F1 – Acquisition parameters
ND0 1
TD 256
SFO1 500.1328 MHz
FIDRES 19.531250 Hz
SW 9.997 ppm
FnMODE undefined

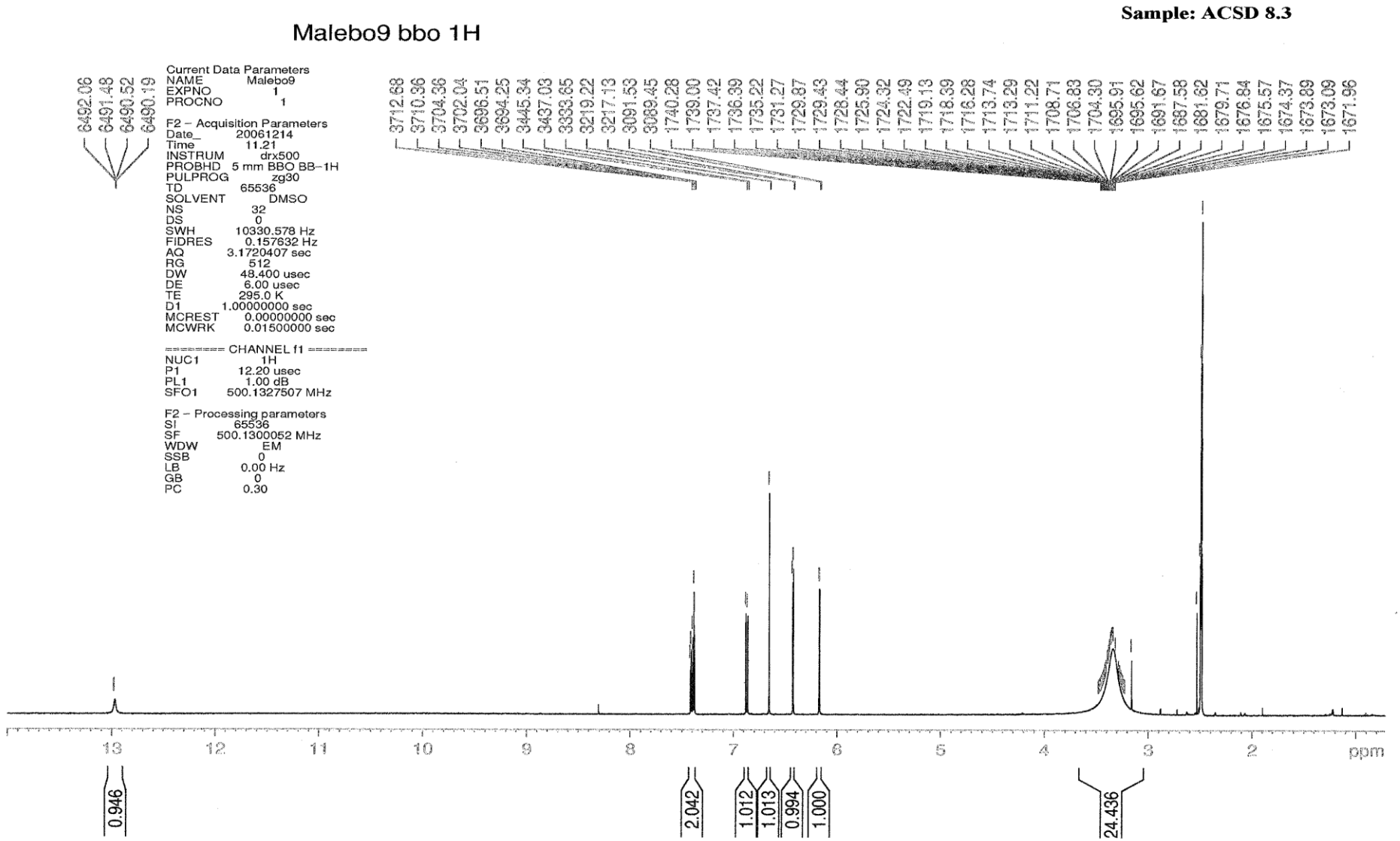
F2 – Processing parameters
SI 1024
SF 500.1300011 MHz
WDW SINE
SSB 0
LB 0.00 Hz
GB 0
PC 0.30

F1 – Processing parameters
SI 1024
MC2 QF
SF 500.1303015 MHz
WDW SINE
SSB 0
LB 0.00 Hz
GB 0

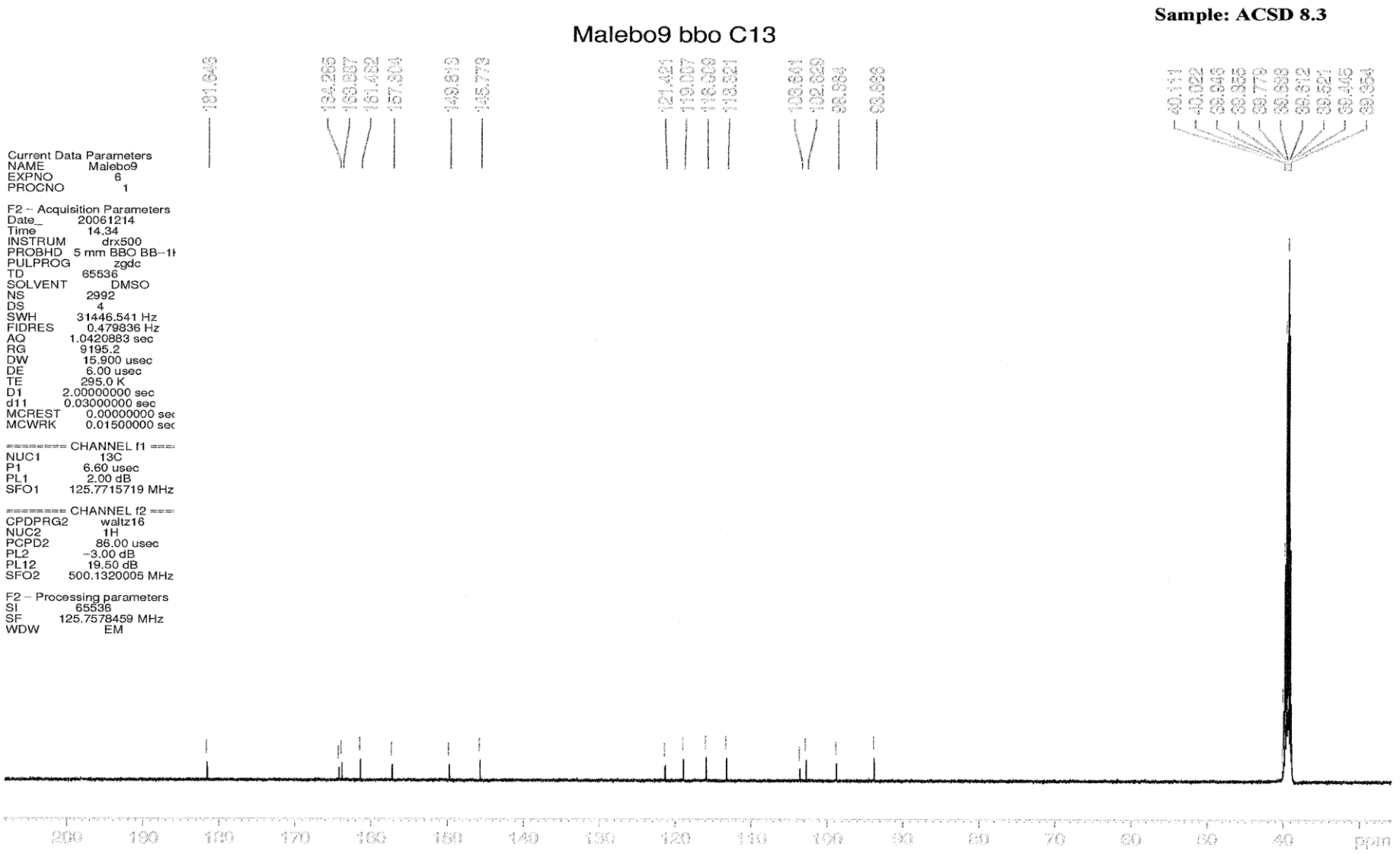
Appendix 13g: MS spectrum of apigenin (**135**)



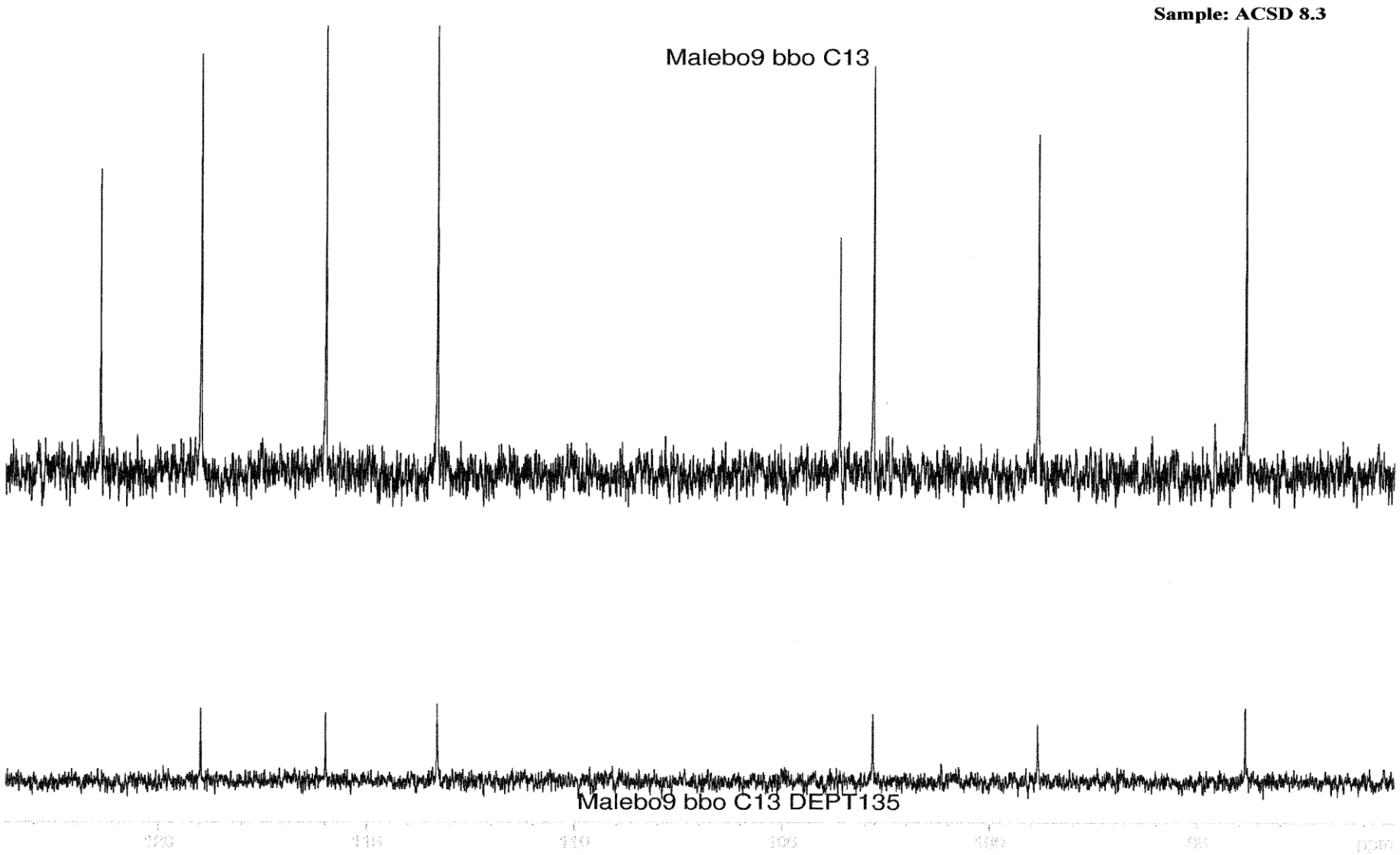
Appendix 14a: ^{1}H NMR spectrum of luteolin (**136**)



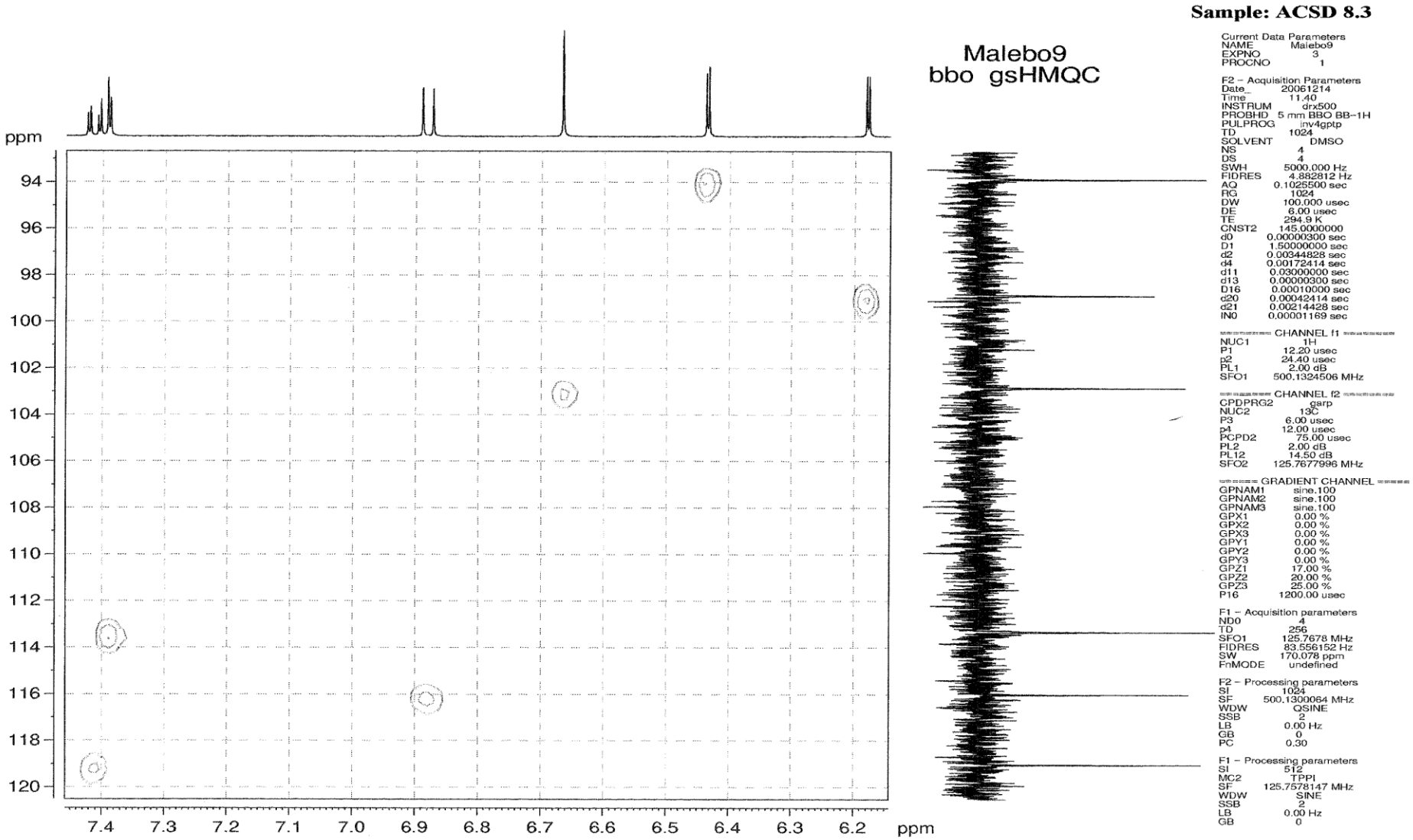
Appendix 14b: ^{13}C NMR spectrum of luteolin (**136**)



Appendix 14c: DEPT 135 spectrum of luteolin (**136**)



Appendix 14d: HMQC spectrum of luteolin (**136**)



Sample: ACSD 8.3

Current Data Parameters
NAME Malebo9
EXPNO 3
PROCNO 1

F2 – Acquisition Parameters
Date_ 20061214
Time 11.40
INSTRUM drx500
PROBHD 5 mm BBO BB–1H
PULPROG inv4gptp
TD 1024
SOLVENT DMSO
NS 4
DS 4
SWH 5000.000 Hz
FIDRES 4.882812 Hz
AQ 0.1025500 sec
RG 1024
DW 100.000 usec
DE 6.00 usec
TE 294.9 K
CNST2 145.0000000
d0 0.00000300 sec
D1 1.50000000 sec
d2 0.00344828 sec
d4 0.00172414 sec
d11 0.03000000 sec
d13 0.00000300 sec
D16 0.00010000 sec
d20 0.00042414 sec
d21 0.00214428 sec
IN0 0.00001169 sec

======== CHANNEL f1 ========
NUC1 1H
P1 12.20 usec
p2 24.40 usec
PL1 2.00 dB
SFO1 500.1324506 MHz

======== CHANNEL f2 ========
CPDPRG2 garp
NUC2 13C
P3 6.00 usec
p4 12.00 usec
PCPD2 75.00 usec
PL2 2.00 dB
PL12 14.50 dB
SFO2 125.7677996 MHz

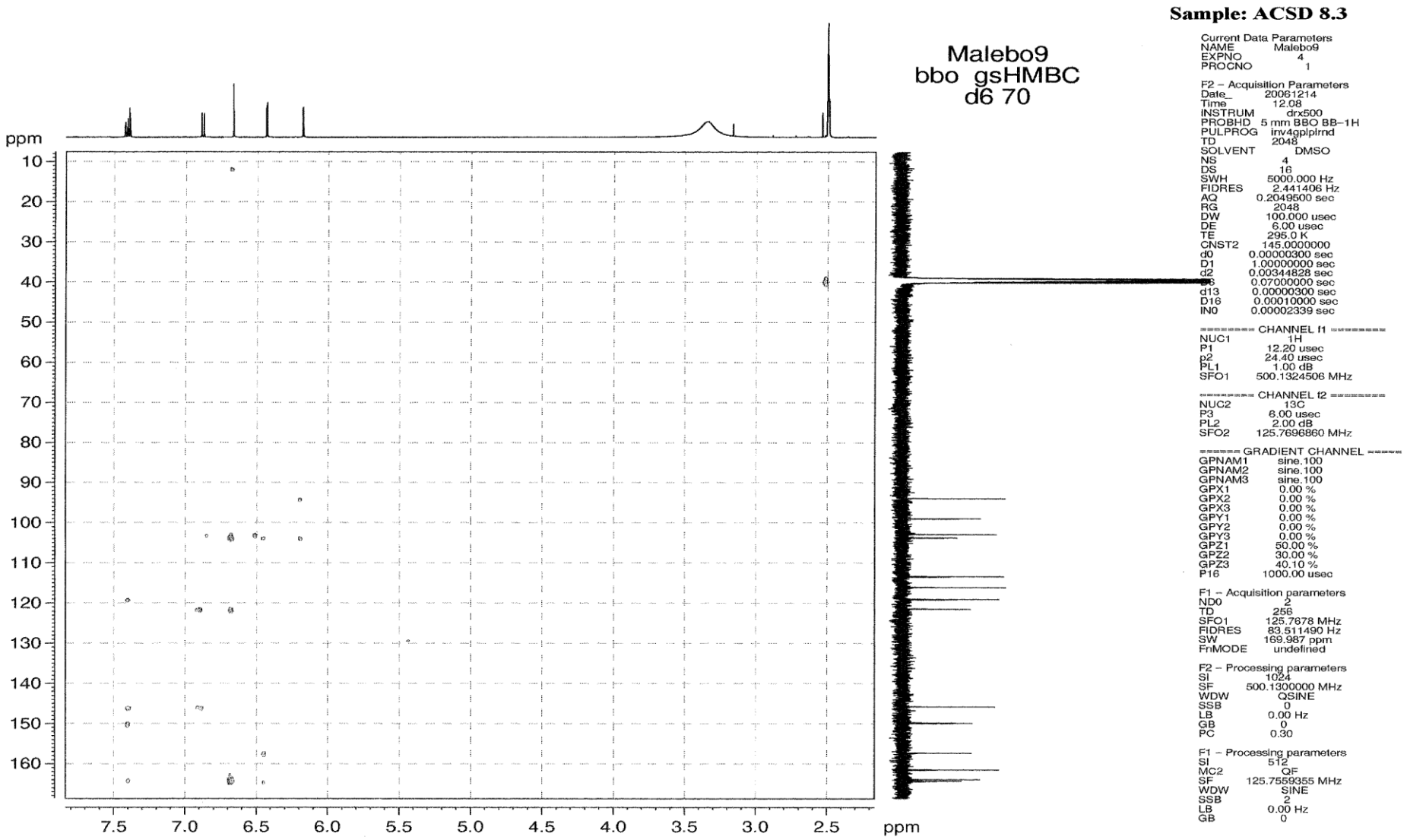
======= GRADIENT CHANNEL =====
GPNAM1 sine.100
GPNAM2 sine.100
GPNAM3 sine.100
GPX1 0.00 %
GPX2 0.00 %
GPX3 0.00 %
GPY1 0.00 %
GPY2 0.00 %
GPY3 0.00 %
GPZ1 17.00 %
GPZ2 20.00 %
GPZ3 25.00 %
P16 1200.00 usec

F1 – Acquisition parameters
ND0 4
TD 256
SFO1 125.7678 MHz
FIDRES 83.556152 Hz
SW 170.078 ppm
FnMODE undefined

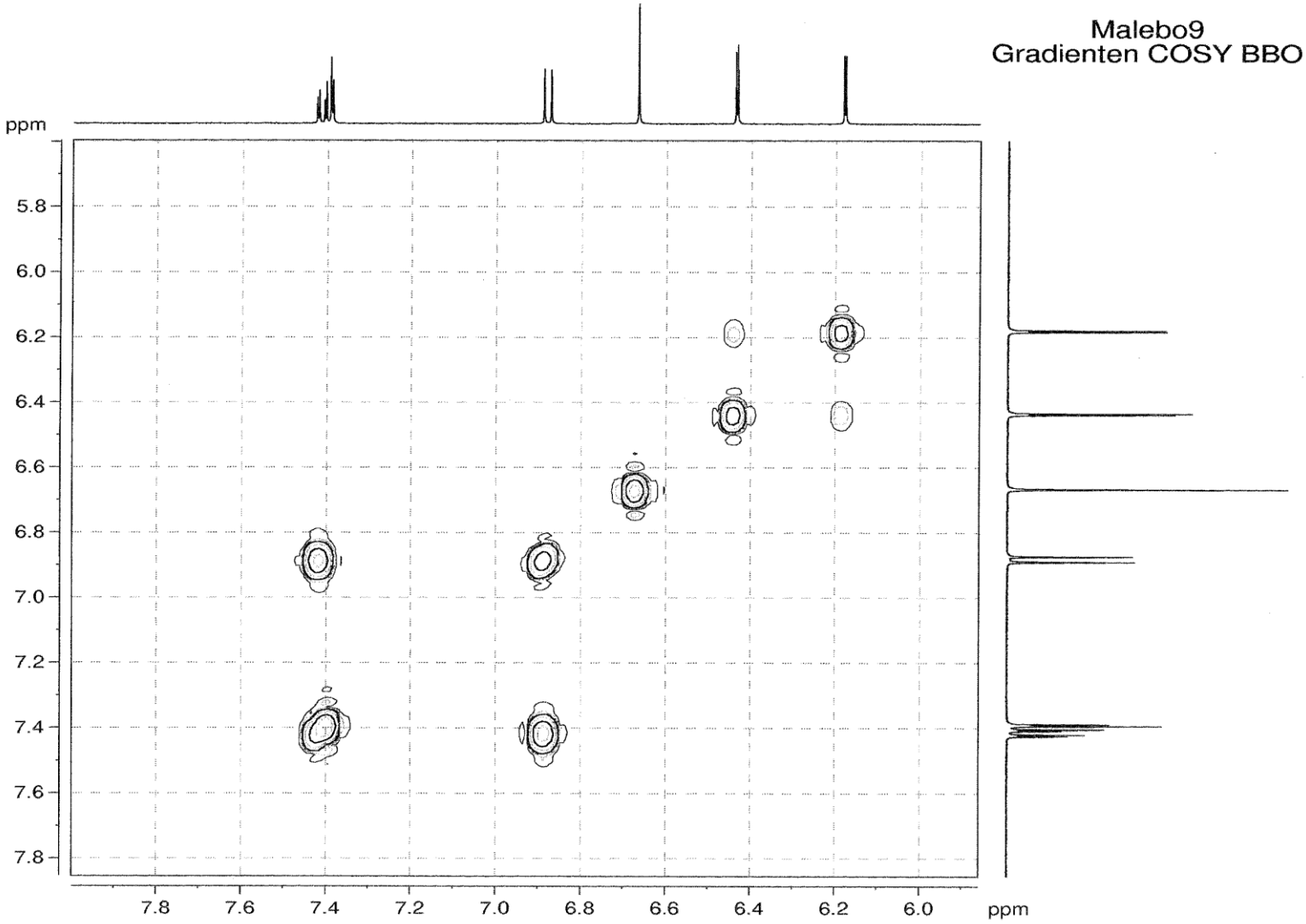
F2 – Processing parameters
SI 1024
SF 500.1300064 MHz
WDW QSINE
SSB 2
LB 0.00 Hz
GB 0
PC 0.30

F1 – Processing parameters
SI 512
MC2 TPPI
SF 125.7578147 MHz
WDW SINE
SSB 2
LB 0.00 Hz
GB 0

Appendix 14e: HMBC spectrum of luteolin (**136**)



Appendix 14f: COSY spectrum of luteolin (**136**)



Sample: ACSD 8.3

Current Data Parameters
NAME Malebo9
EXPNO 2
PROCNO 1

F2 – Acquisition Parameters
Date_ 20061214
Time 11.21
INSTRUM drx500
PROBHD 5 mm BBO BB–1H
PULPROG cosygp
TD 1024
SOLVENT DMSO
NS 2
DS 8
SWH 5000.000 Hz
FIDRES 4.882812 Hz
AQ 0.1025500 sec
RG 256
DW 100.000 usec
DE 6.00 usec
TE 295.0 K
d0 0.00000300 sec
D1 2.00000000 sec
d13 0.00000300 sec
D16 0.00100000 sec
IN0 0.00020000 sec

======== CHANNEL f1 ========
NUC1 1H
P0 6.00 usec
P1 12.20 usec
PL1 1.00 dB
SFO1 500.1324506 MHz

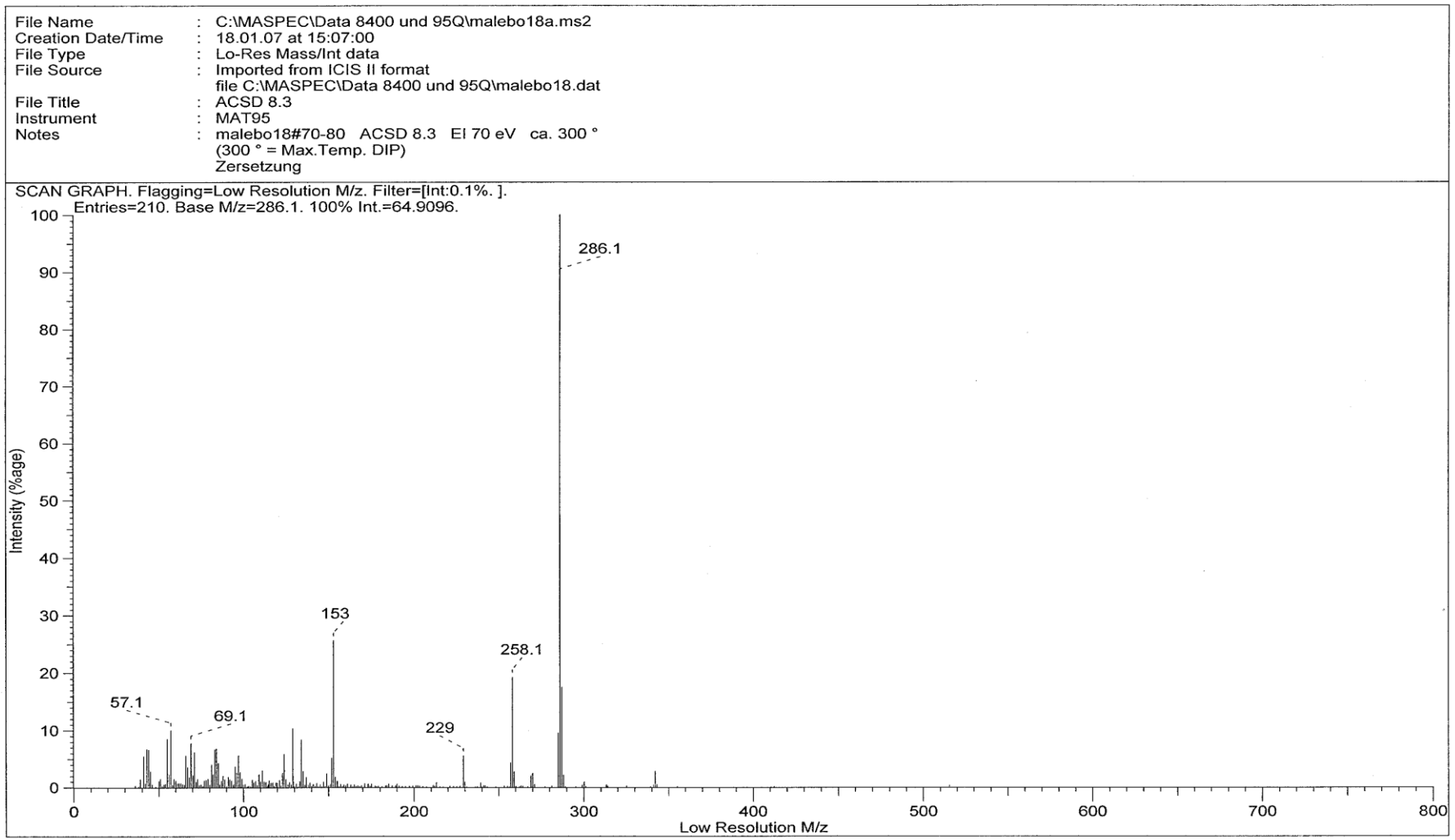
====== GRADIENT CHANNEL =====
GPNAM1 SINE.100kk
GPNAM2 SINE.100kk
GPX1 0.00 %
GPX2 0.00 %
GPY1 0.00 %
GPY2 0.00 %
GPZ1 10.00 %
GPZ2 10.00 %
P16 1000.00 usec

F1 – Acquisition parameters
ND0 1
TD 256
SFO1 500.1328 MHz
FIDRES 19.531250 Hz
SW 9.997 ppm
FnMODE undefined

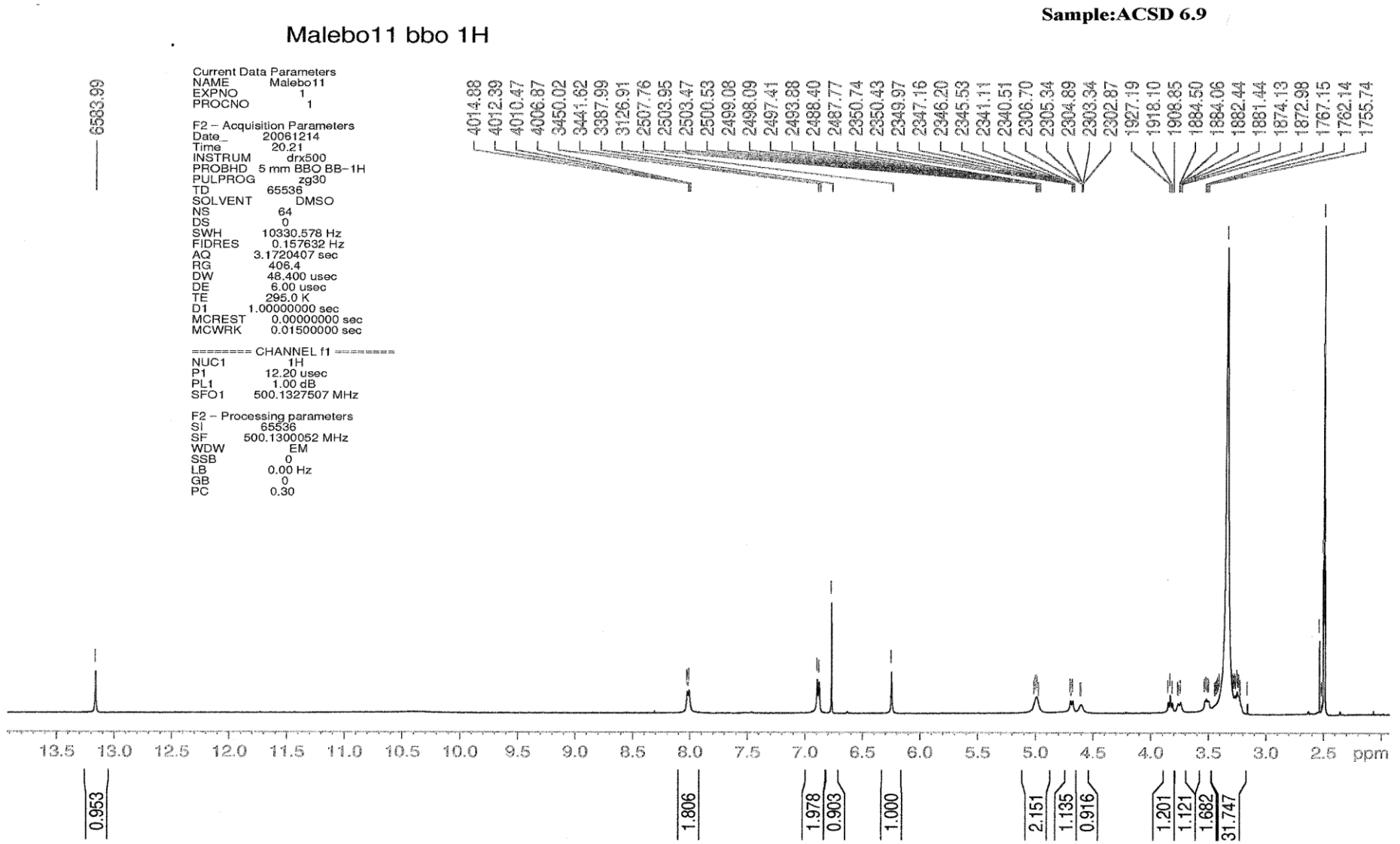
F2 – Processing parameters
SI 1024
SF 500.1300034 MHz
WDW SINE
SSB 0
LB 0.00 Hz
GB 0
PC 0.30

F1 – Processing parameters
SI 1024
MC2 QF
SF 500.1303023 MHz
WDW SINE
SSB 0
LB 0.00 Hz
GB 0

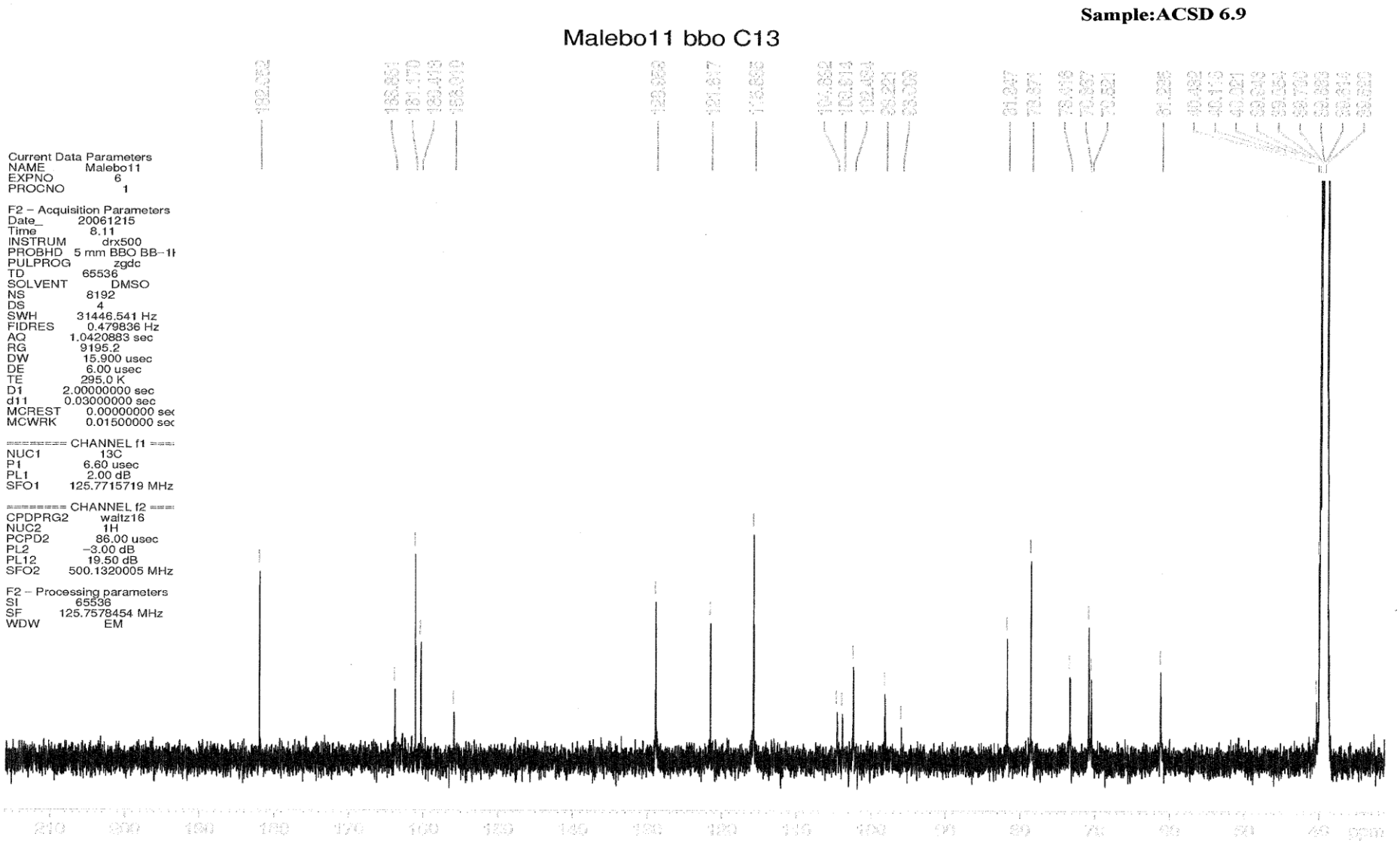
Appendix 14g: MS spectrum of luteolin (**136**)



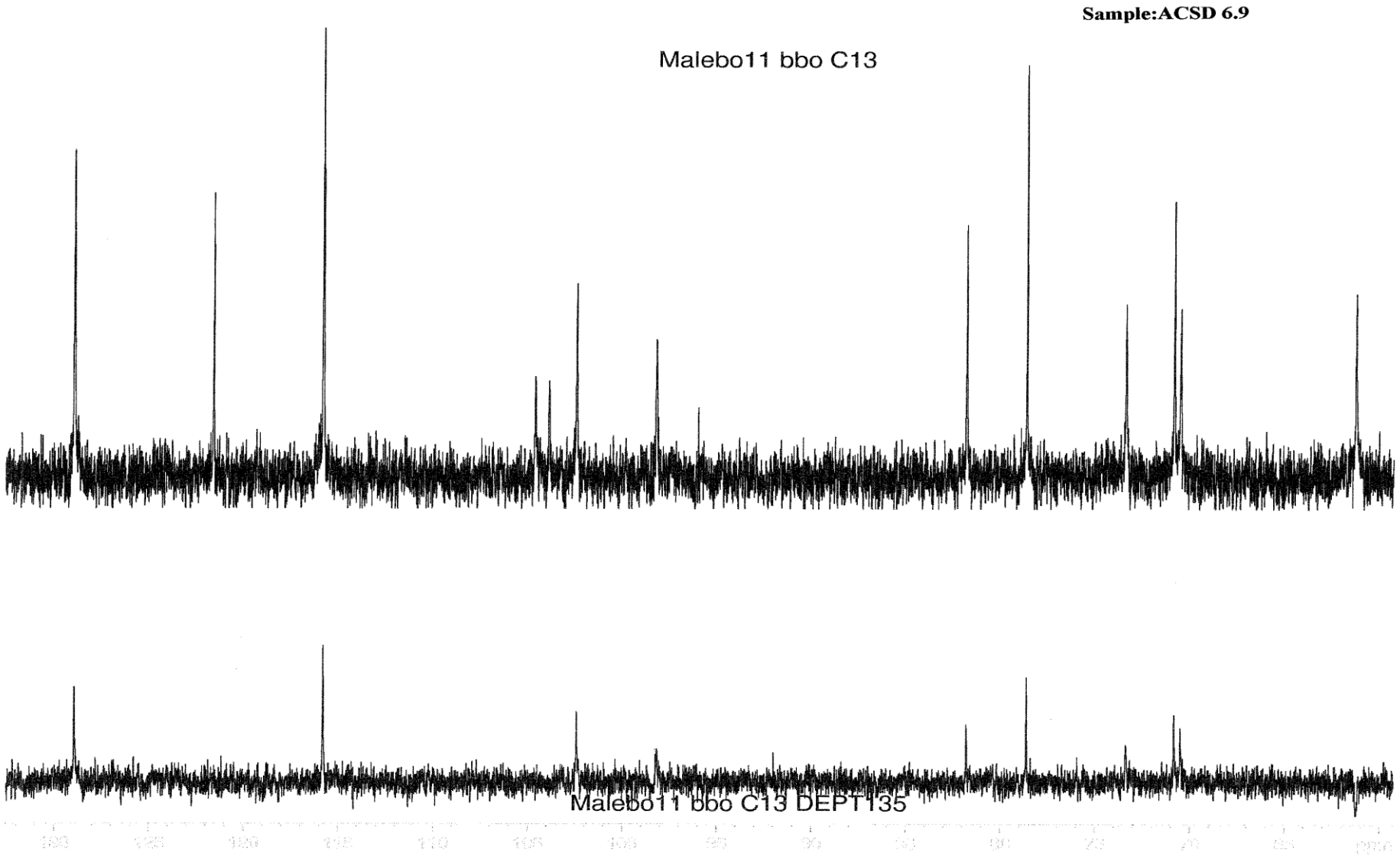
Appendix 15a: ^{1}H NMR spectrum of vitexin (**137**)



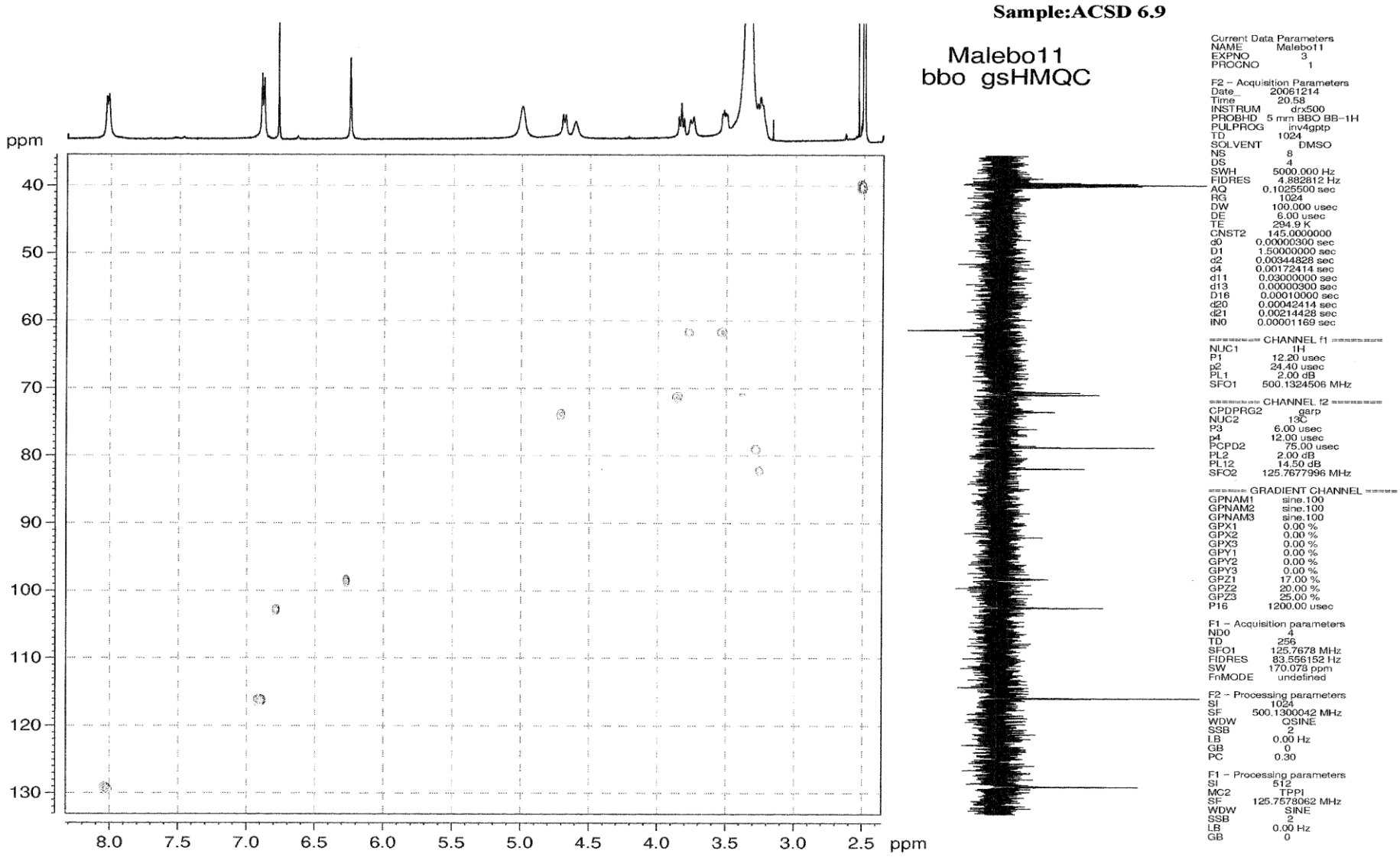
Appendix 15b: ^{13}C NMR spectrum of vitexin (**137**)



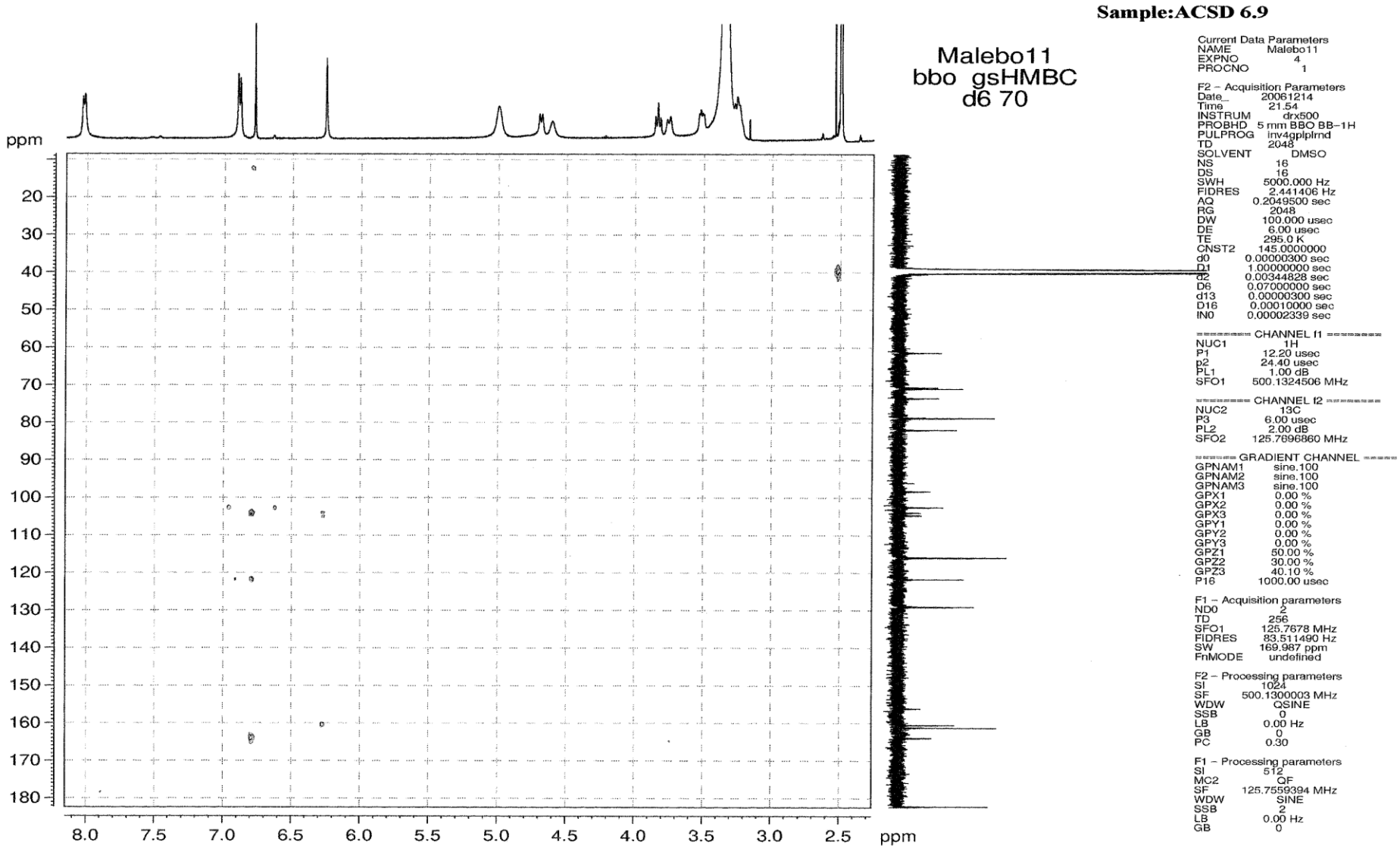
Appendix 15c: DEPT 135 spectrum of vitexin (**137**)



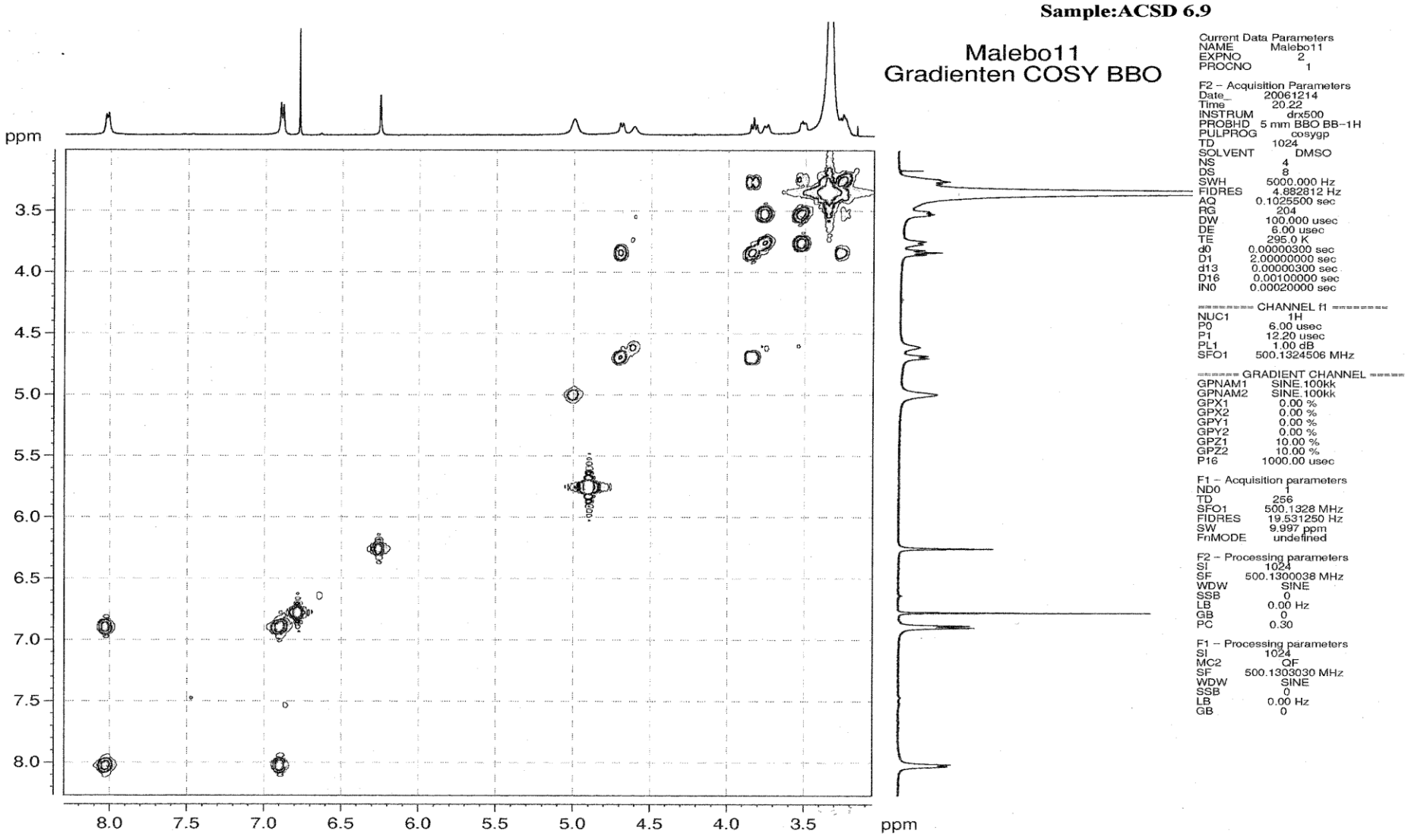
Appendix 15d: HMQC spectrum of vitexin (**137**)



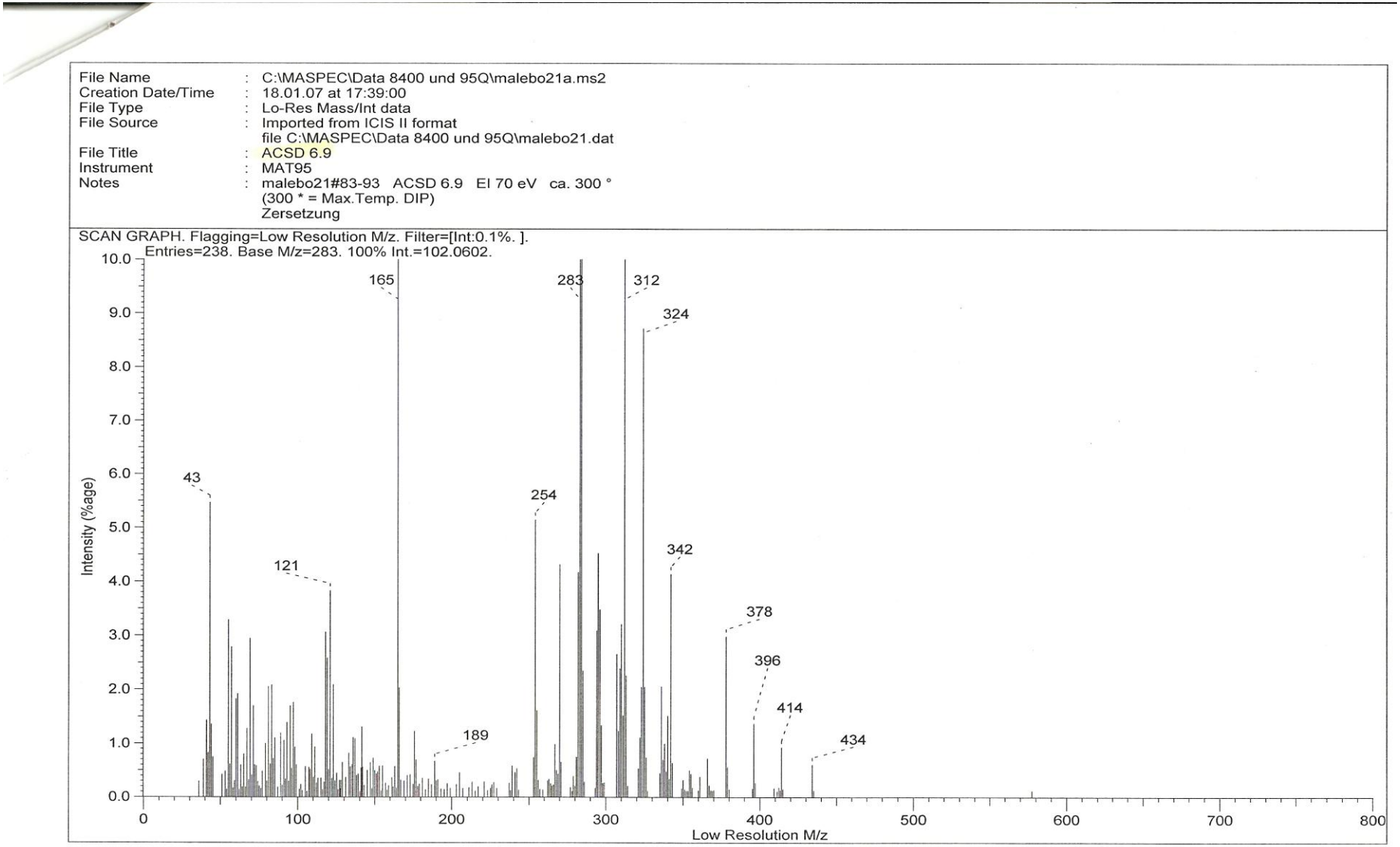
Appendix 15e: HMBC spectrum of vitexin (**137**)



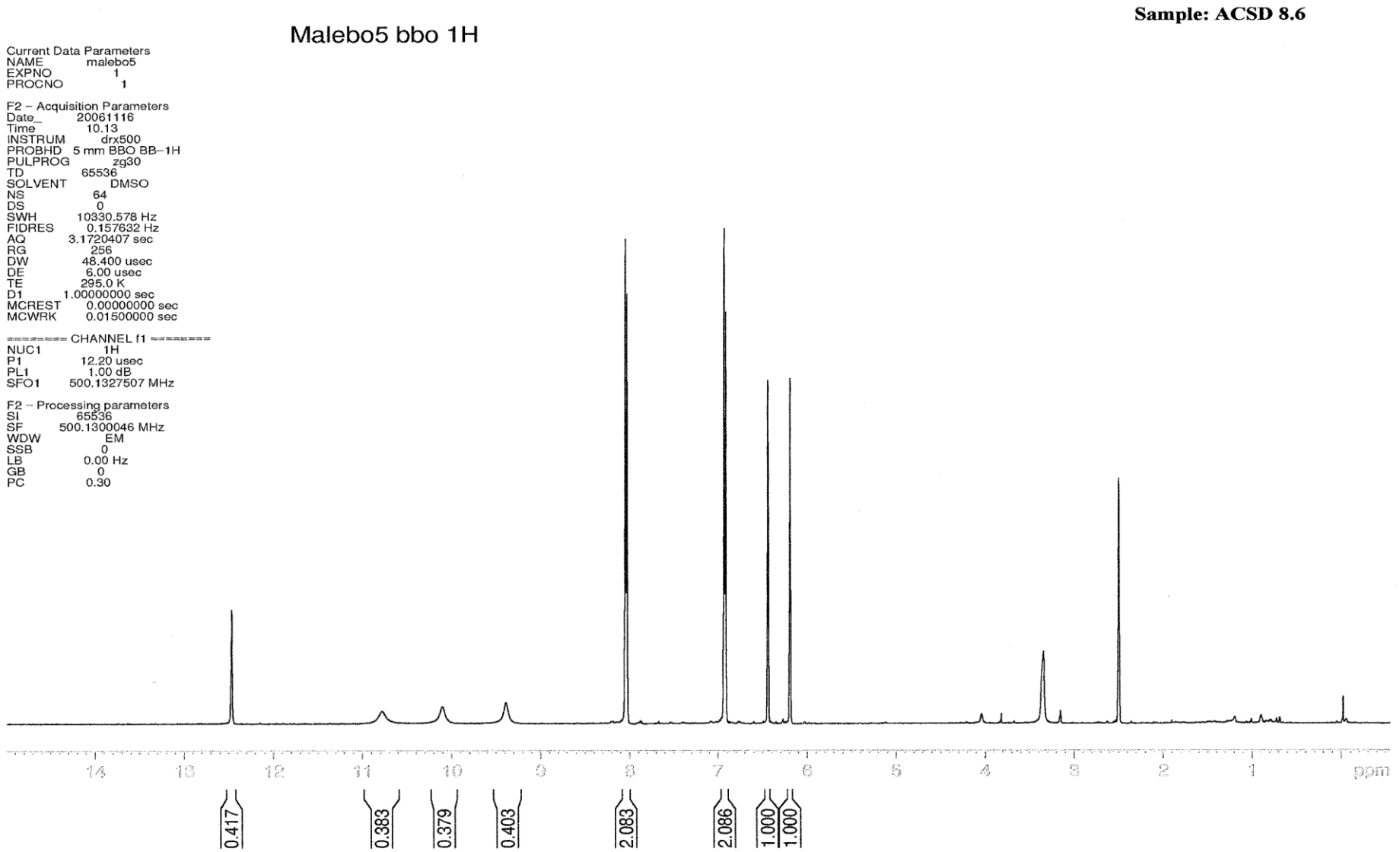
Appendix 15f: COSY spectrum of vitexin (**137**)



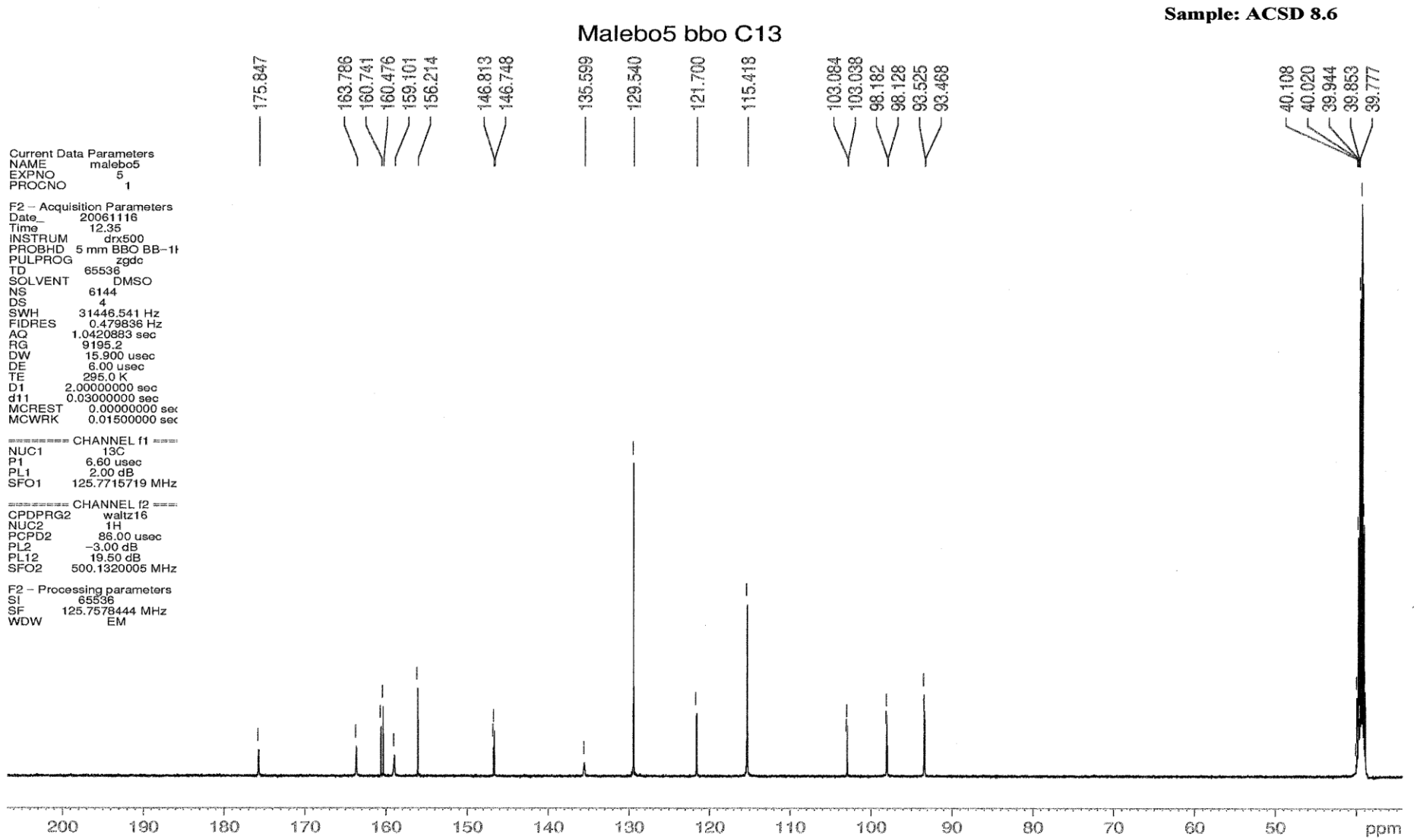
Appendix 15g: MS spectrum of vitexin (**137**)



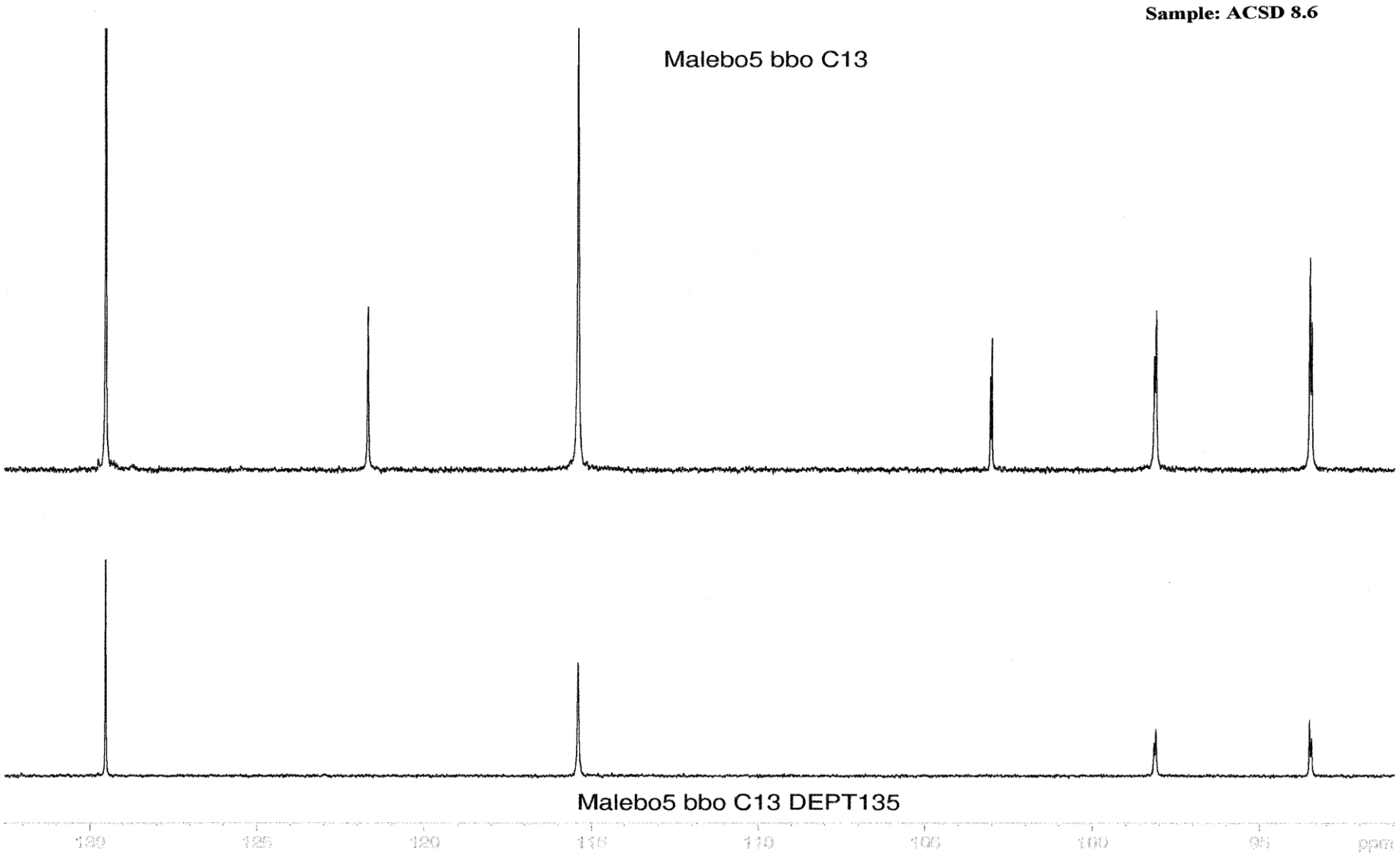
Appendix 16a: ^{1}H NMR spectrum of kaempferol (**138**)



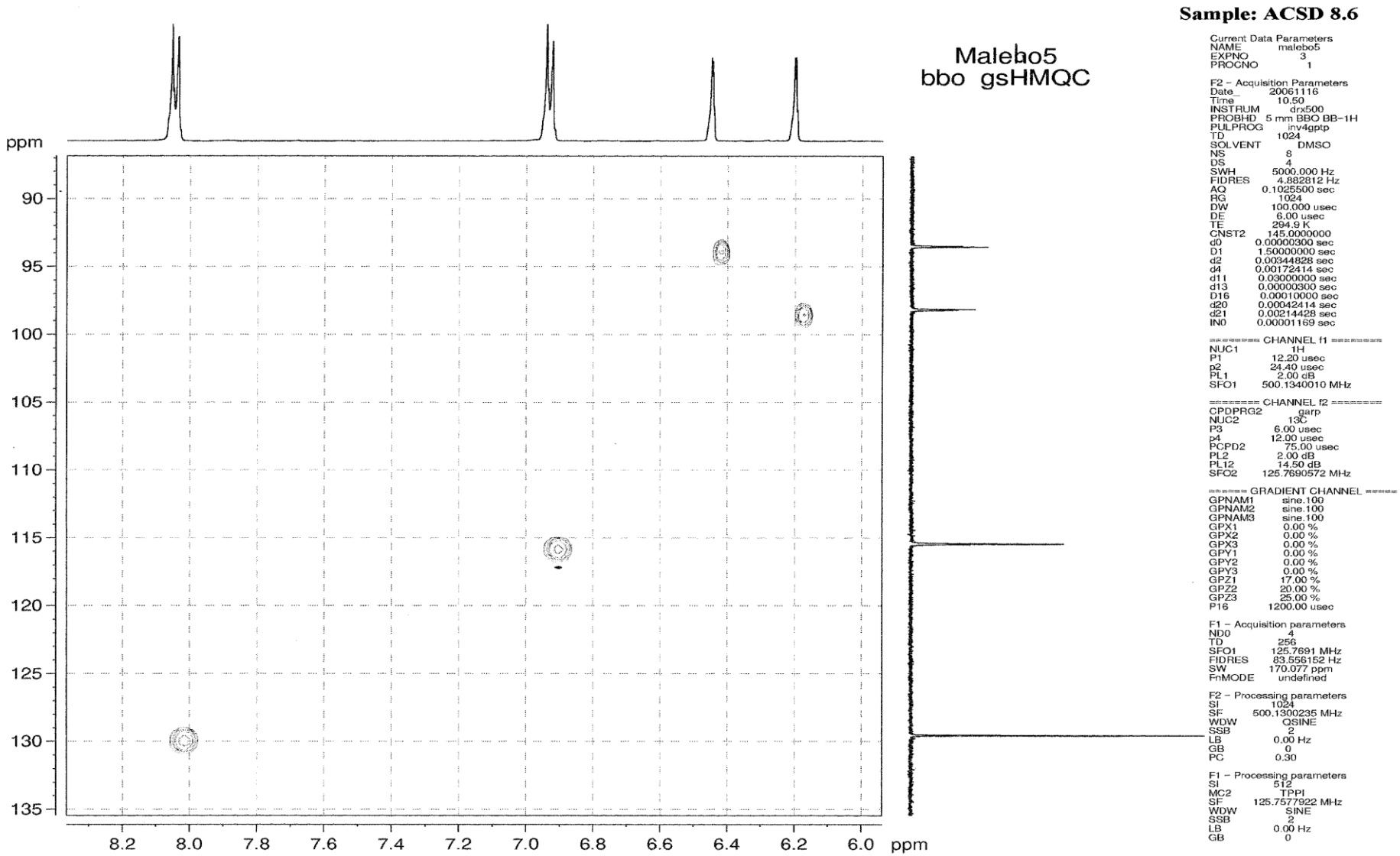
Appendix 16b: ^{13}C NMR spectrum of kaempferol (**138**)



Appendix 16c: DEPT 135 spectrum of kaempferol (**138**)



Appendix 16d: HMQC spectrum of kaempferol (**138**)



Sample: ACSD 8.6

Current Data Parameters
NAME malebo5
EXPNO 3
PROCNO 1

F2 – Acquisition Parameters
Date_ 20061116
Time 10.50
INSTRUM drx500
PROBHD 5 mm BBO BB-1H
PULPROG inv4gptp
TD 1024
SOLVENT DMSO
NS 8
DS 4
SWH 5000.000 Hz
FIDRES 4.882812 Hz
AQ 0.1025500 sec
RG 1024
DW 100.000 usec
DE 6.00 usec
TE 294.9 K
CNST2 145.0000000
d0 0.00000300 sec
D1 1.50000000 sec
d2 0.00344828 sec
d4 0.00172414 sec
d11 0.03000000 sec
d13 0.00000300 sec
D16 0.00010000 sec
d20 0.00042414 sec
d21 0.00214428 sec
IN0 0.00001169 sec

======== CHANNEL f1 ========
NUC1 1H
P1 12.20 usec
p2 24.40 usec
PL1 2.00 dB
SFO1 500.1340010 MHz

======== CHANNEL f2 ========
CPDPRG2 garp
NUC2 13C
P3 6.00 usec
p4 12.00 usec
PCPD2 75.00 usec
PL2 2.00 dB
PL12 14.50 dB
SFO2 125.7690572 MHz

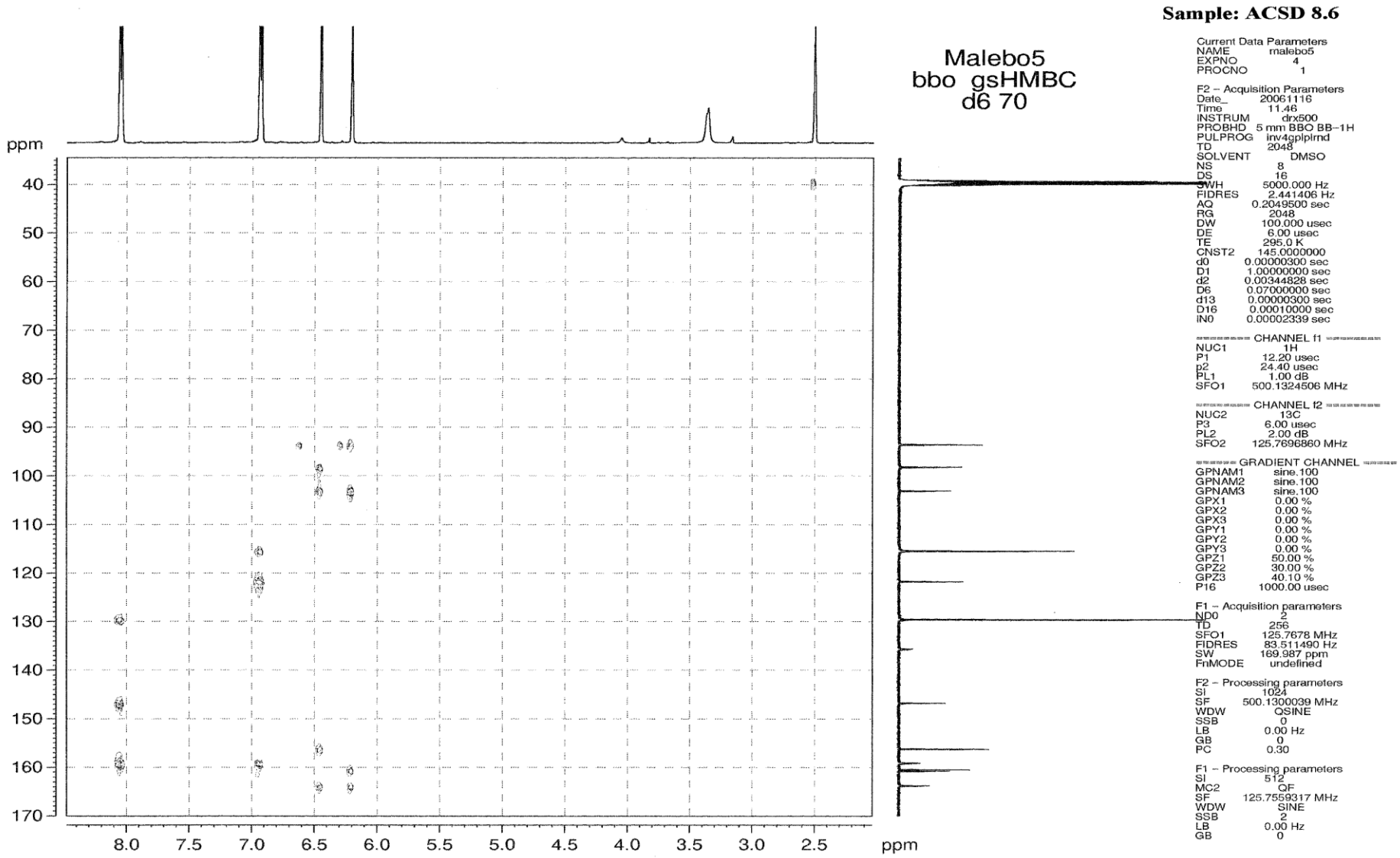
====== GRADIENT CHANNEL =====
GPNAM1 sine.100
GPNAM2 sine.100
GPNAM3 sine.100
GPX1 0.00 %
GPX2 0.00 %
GPX3 0.00 %
GPY1 0.00 %
GPY2 0.00 %
GPY3 0.00 %
GPZ1 17.00 %
GPZ2 20.00 %
GPZ3 25.00 %
P16 1200.00 usec

F1 – Acquisition parameters
ND0 4
TD 256
SFO1 125.7691 MHz
FIDRES 83.556152 Hz
SW 170.077 ppm
FnMODE undefined

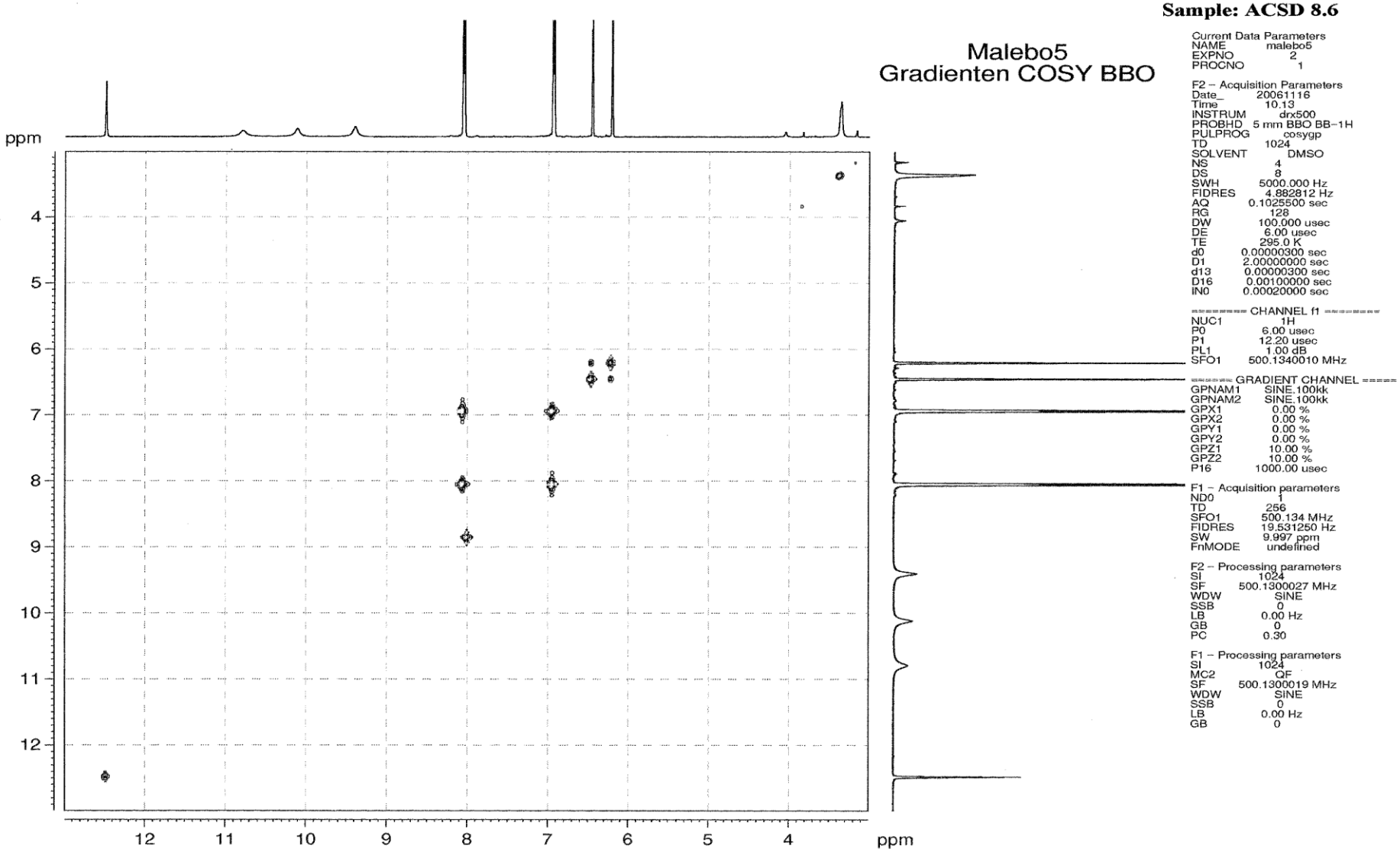
F2 – Processing parameters
SI 1024
SF 500.1300235 MHz
WDW QSINE
SSB 2
LB 0.00 Hz
GB 0
PC 0.30

F1 – Processing parameters
SI 512
MC2 TPPI
SF 125.7577922 MHz
WDW SINE
SSB 2
LB 0.00 Hz
GB 0

Appendix 16e: HMBC spectrum of kaempferol (**138**)



Appendix 16f: COSY spectrum of kaempferol (**138**)



Sample: ACSD 8.6

Current Data Parameters
NAME malebo5
EXPNO 2
PROCNO 1

F2 – Acquisition Parameters
Date_ 20061116
Time 10.13
INSTRUM drx500
PROBHD 5 mm BBO BB-1H
PULPROG cosygp
TD 1024
SOLVENT DMSO
NS 4
DS 8
SWH 5000.000 Hz
FIDRES 4.882812 Hz
AQ 0.1025500 sec
RG 128
DW 100.000 usec
DE 6.00 usec
TE 295.0 K
d0 0.00000300 sec
D1 2.00000000 sec
d13 0.00000300 sec
D16 0.00100000 sec
IN0 0.00020000 sec

========== CHANNEL f1 ==========
NUC1 1H
P0 6.00 usec
P1 12.20 usec
PL1 1.00 dB
SFO1 500.1340010 MHz

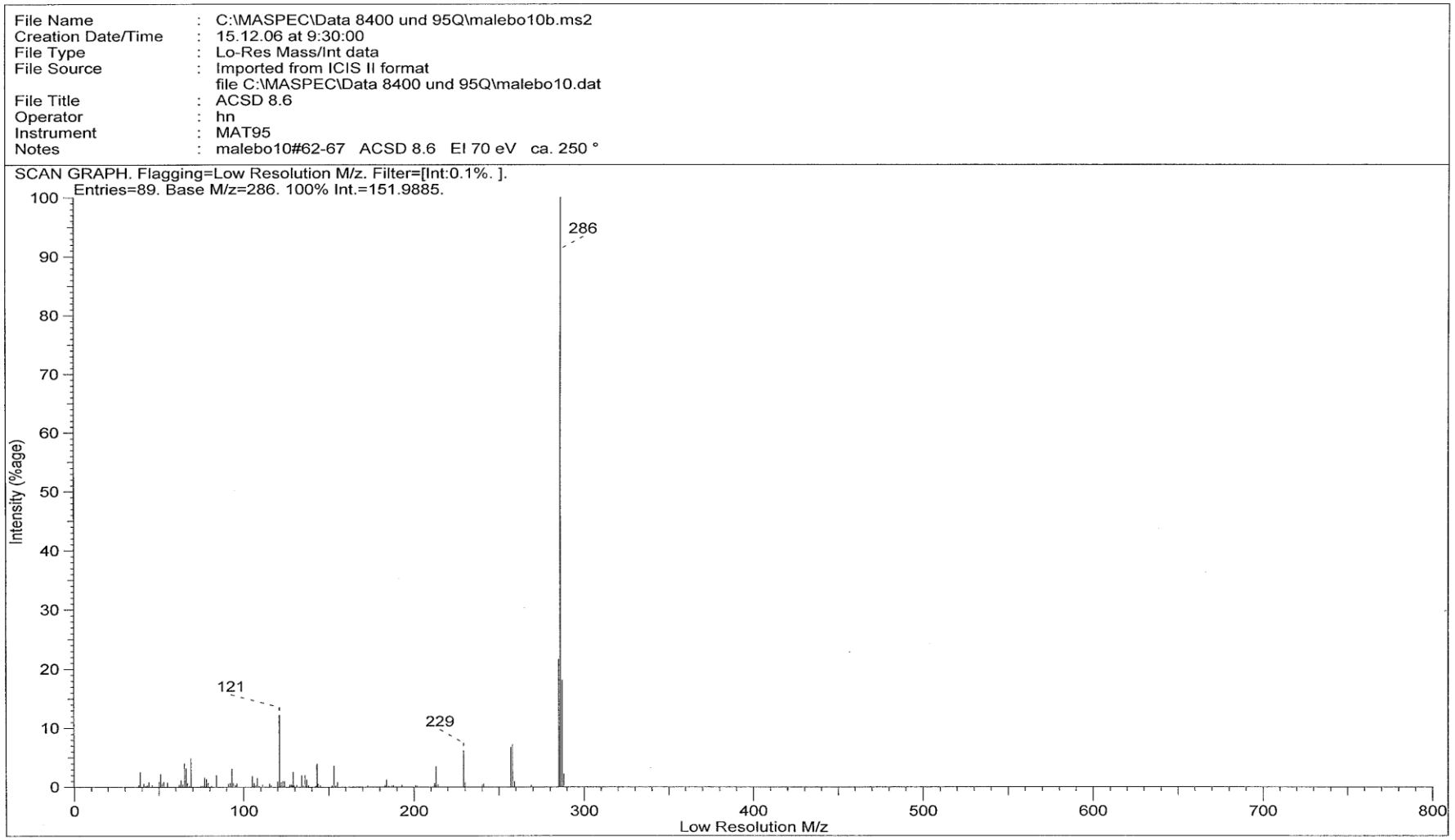
====== GRADIENT CHANNEL =====
GPNAM1 SINE.100kk
GPNAM2 SINE.100kk
GPX1 0.00 %
GPX2 0.00 %
GPY1 0.00 %
GPY2 0.00 %
GPZ1 10.00 %
GPZ2 10.00 %
P16 1000.00 usec

F1 – Acquisition parameters
ND0 1
TD 256
SFO1 500.134 MHz
FIDRES 19.531250 Hz
SW 9.997 ppm
FnMODE undefined

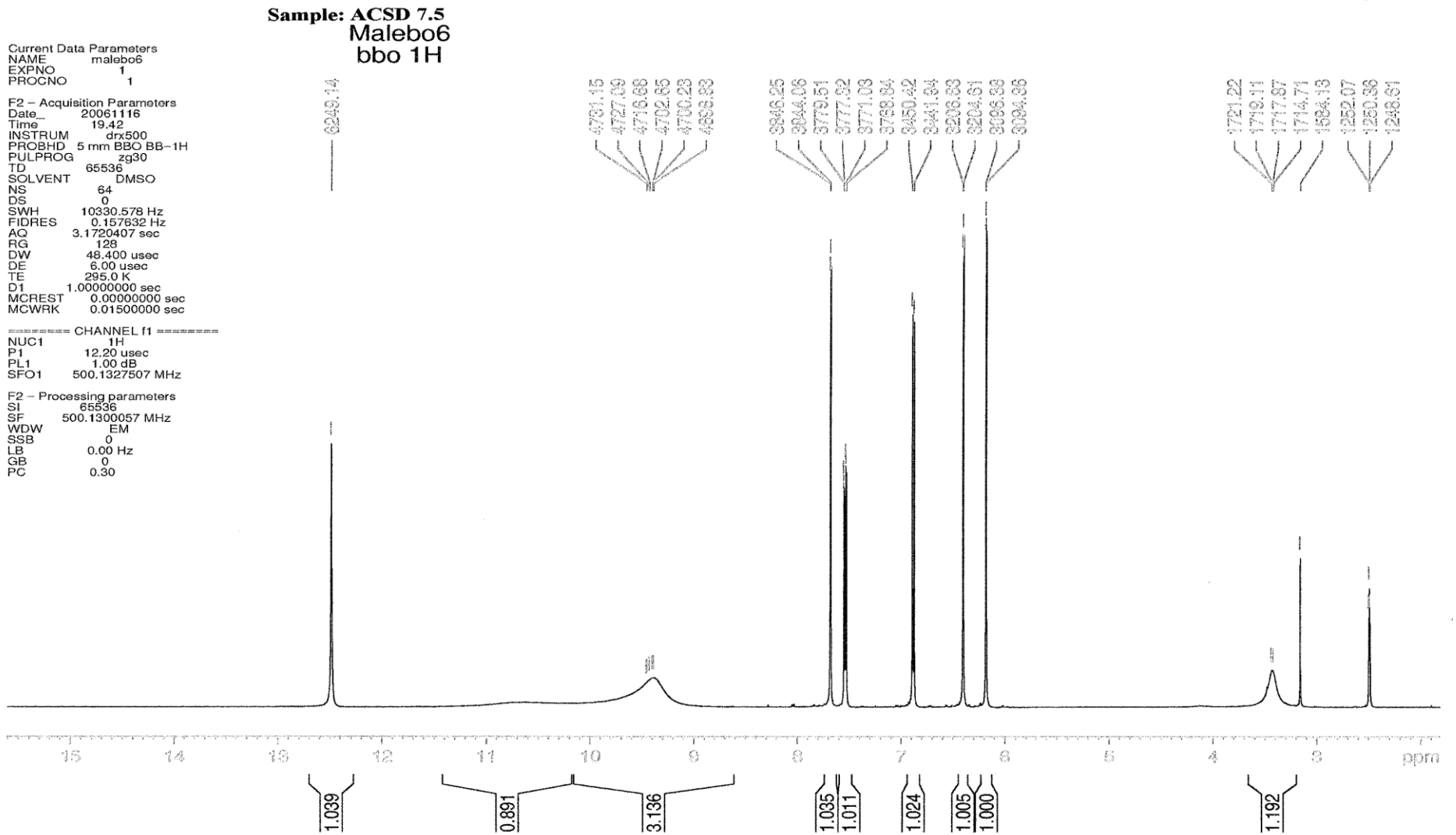
F2 – Processing parameters
SI 1024
SF 500.1300027 MHz
WDW SINE
SSB 0
LB 0.00 Hz
GB 0
PC 0.30

F1 – Processing parameters
SI 1024
MC2 QF
SF 500.1300019 MHz
WDW SINE
SSB 0
LB 0.00 Hz
GB 0

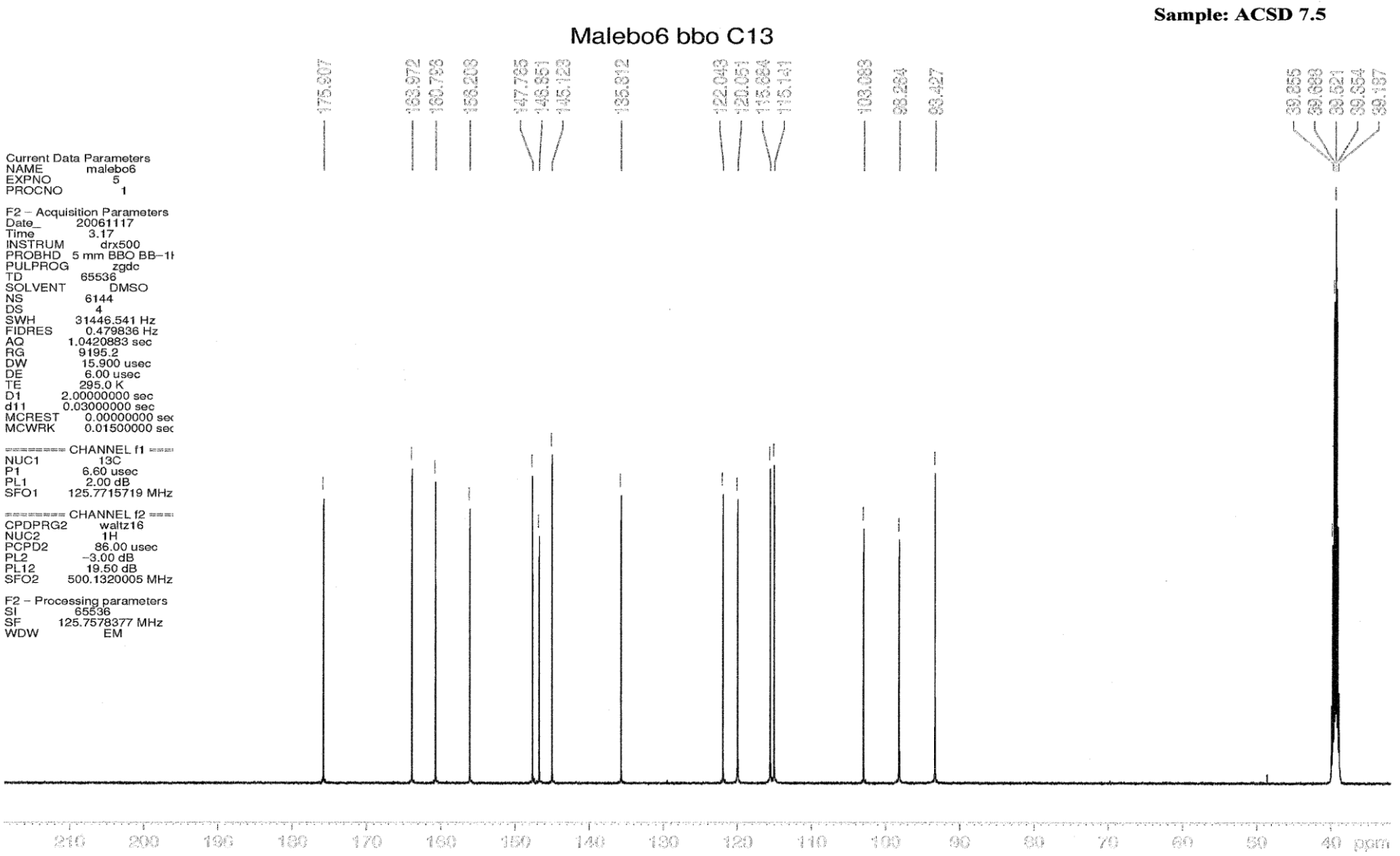
Appendix 16g: MS spectrum of kaempferol (**138**)



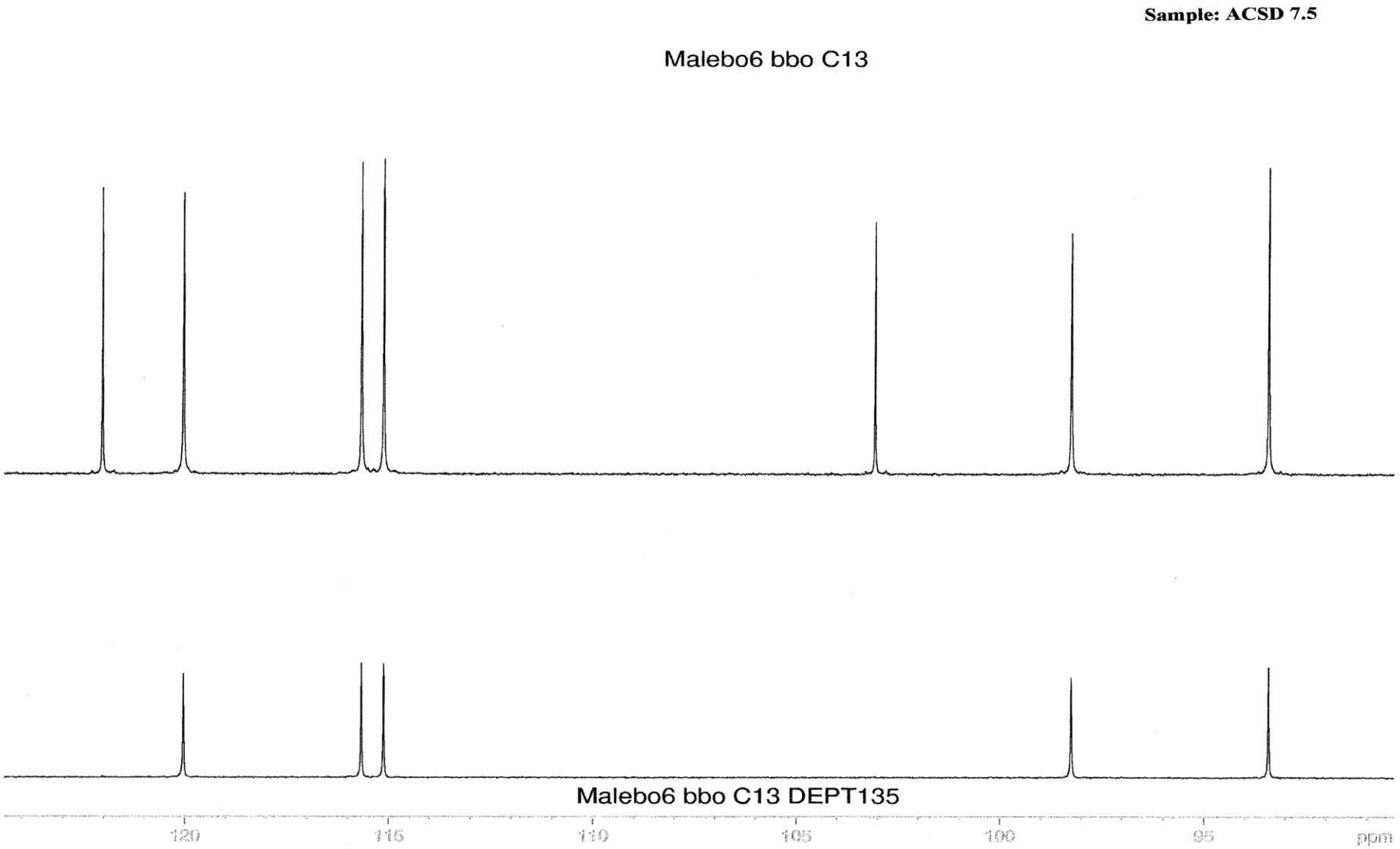
Appendix 17a: ^{1}H NMR spectrum of quercetin (**139**)



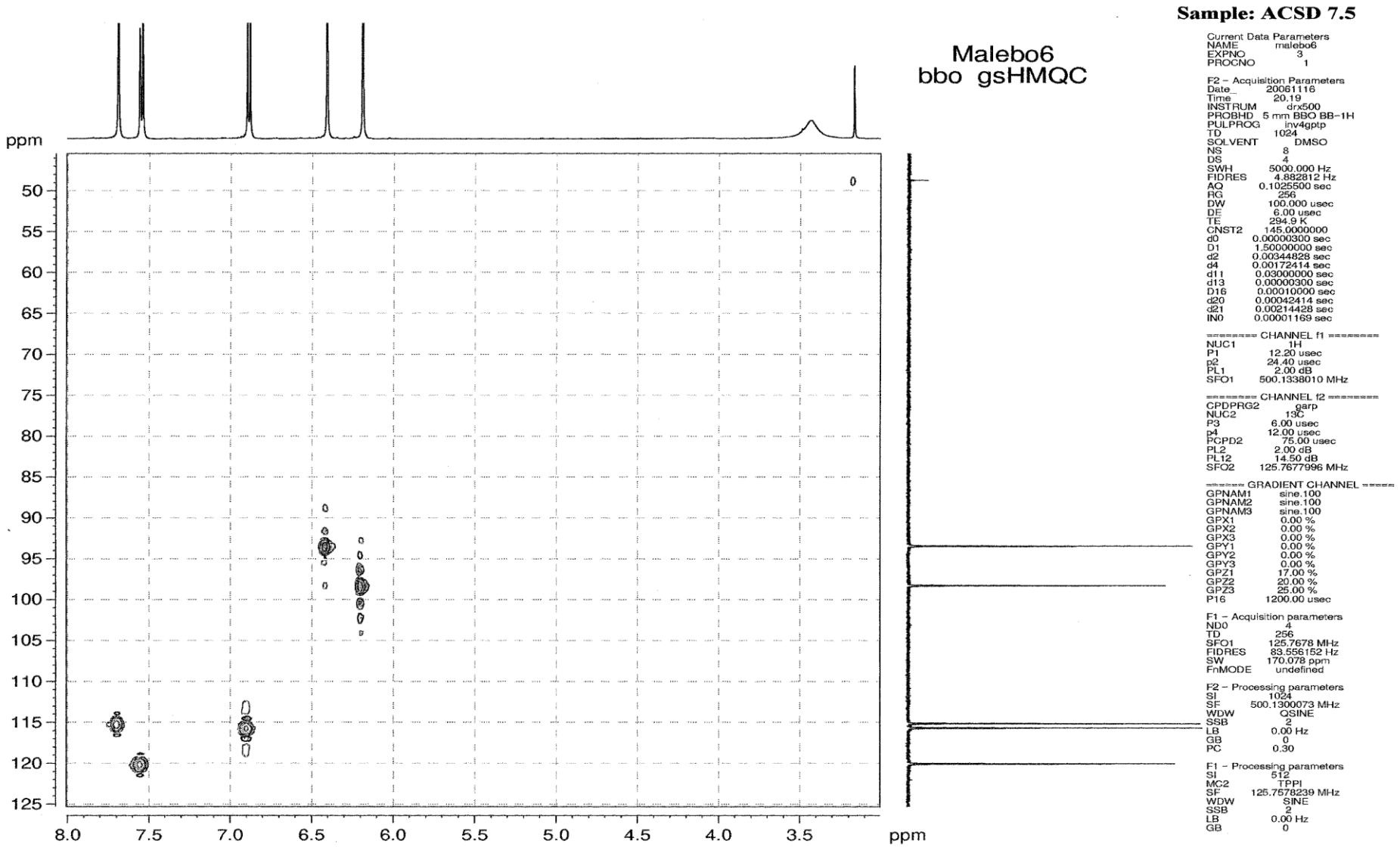
Appendix 17b: ^{13}C NMR spectrum of quercetin (**139**)



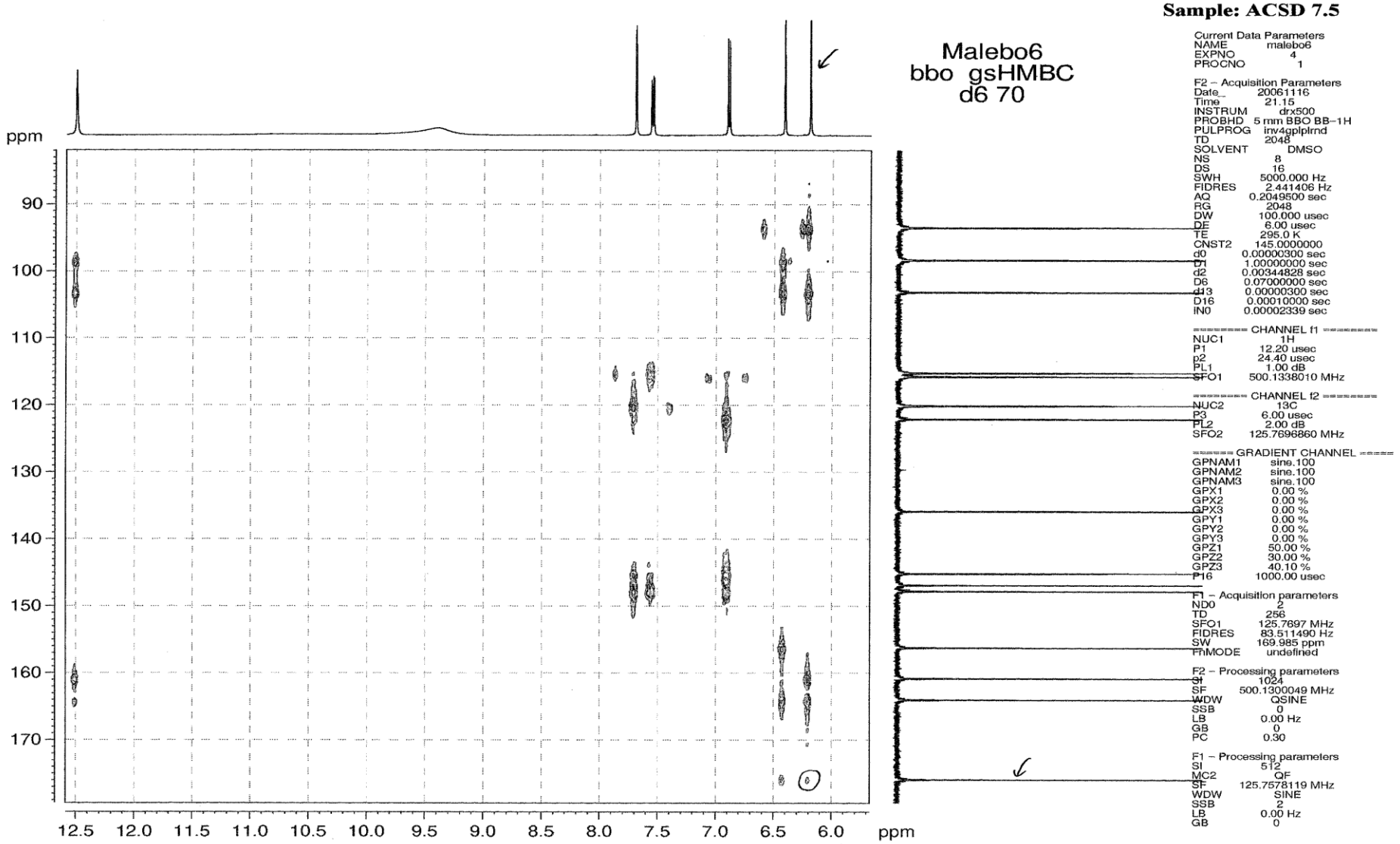
Appendix 17c: DEPT 135 spectrum of quercetin (**139**)



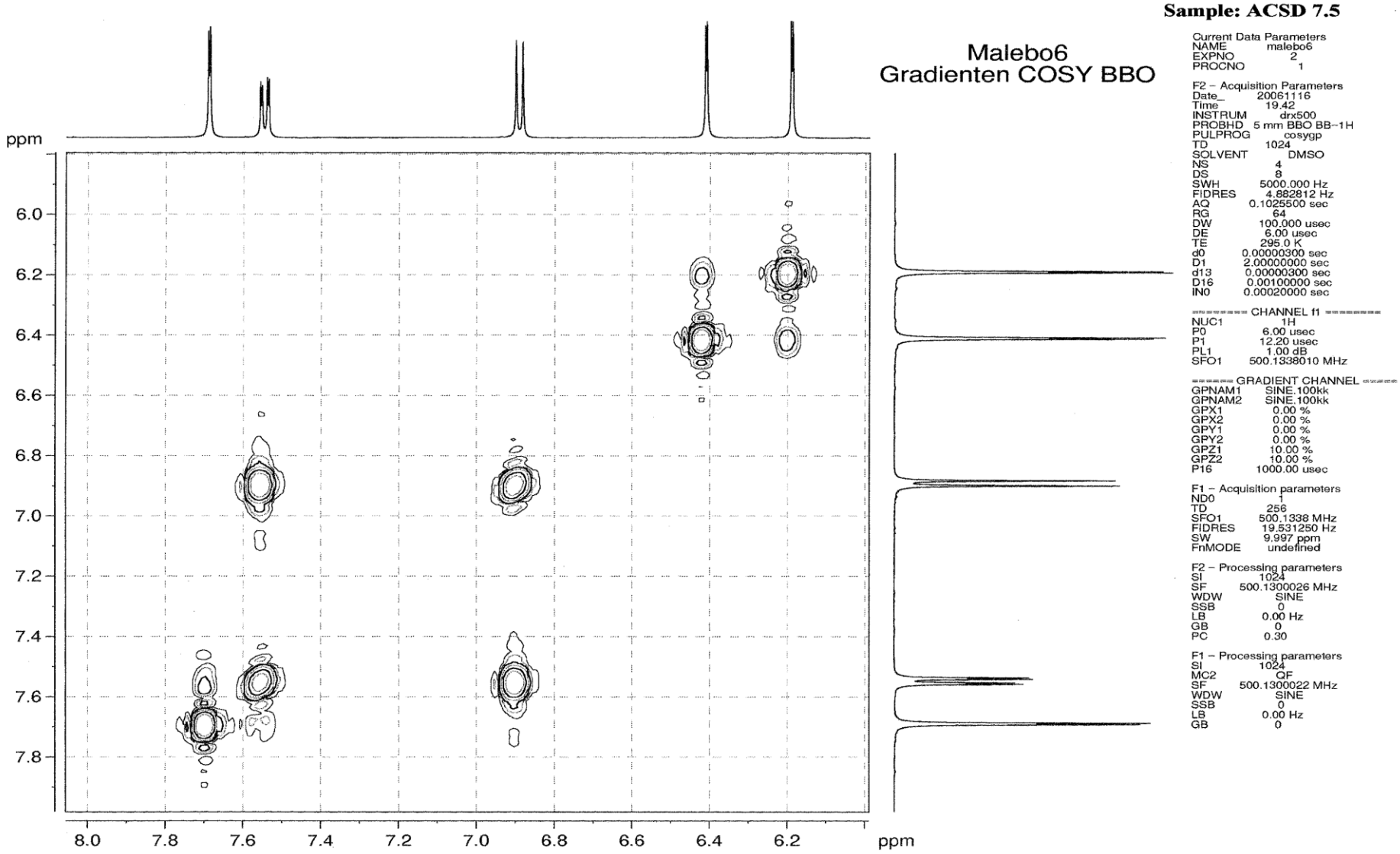
Appendix 17d: HMQC spectrum of quercetin (**139**)



Appendix 17e: HMBC spectrum of quercetin (**139**)



Appendix 17f: HMBC spectrum of quercetin (**139**)



Sample: ACSD 7.5

Current Data Parameters
NAME malebo6
EXPNO 2
PROCNO 1

F2 – Acquisition Parameters
Date_ 20061116
Time 19.42
INSTRUM drx500
PROBHD 5 mm BBO BB-1H
PULPROG cosygp
TD 1024
SOLVENT DMSO
NS 4
DS 8
SWH 5000.000 Hz
FIDRES 4.882812 Hz
AQ 0.1025500 sec
RG 64
DW 100.000 usec
DE 6.00 usec
TE 295.0 K
d0 0.00000300 sec
D1 2.00000000 sec
d13 0.00000300 sec
D16 0.00100000 sec
IN0 0.00020000 sec

========== CHANNEL f1 ==========
NUC1 1H
P0 6.00 usec
P1 12.20 usec
PL1 1.00 dB
SFO1 500.1338010 MHz

======= GRADIENT CHANNEL =======
GPNAM1 SINE.100kk
GPNAM2 SINE.100kk
GPX1 0.00 %
GPX2 0.00 %
GPY1 0.00 %
GPY2 0.00 %
GPZ1 10.00 %
GPZ2 10.00 %
P16 1000.00 usec

F1 – Acquisition parameters
ND0 1
TD 256
SFO1 500.1338 MHz
FIDRES 19.531250 Hz
SW 9.997 ppm
FnMODE undefined

F2 – Processing parameters
SI 1024
SF 500.1300026 MHz
WDW SINE
SSB 0
LB 0.00 Hz
GB 0
PC 0.30

F1 – Processing parameters
SI 1024
MC2 QF
SF 500.1300022 MHz
WDW SINE
SSB 0
LB 0.00 Hz
GB 0

Appendix 17g: MS spectrum of quercetin (**139**)

